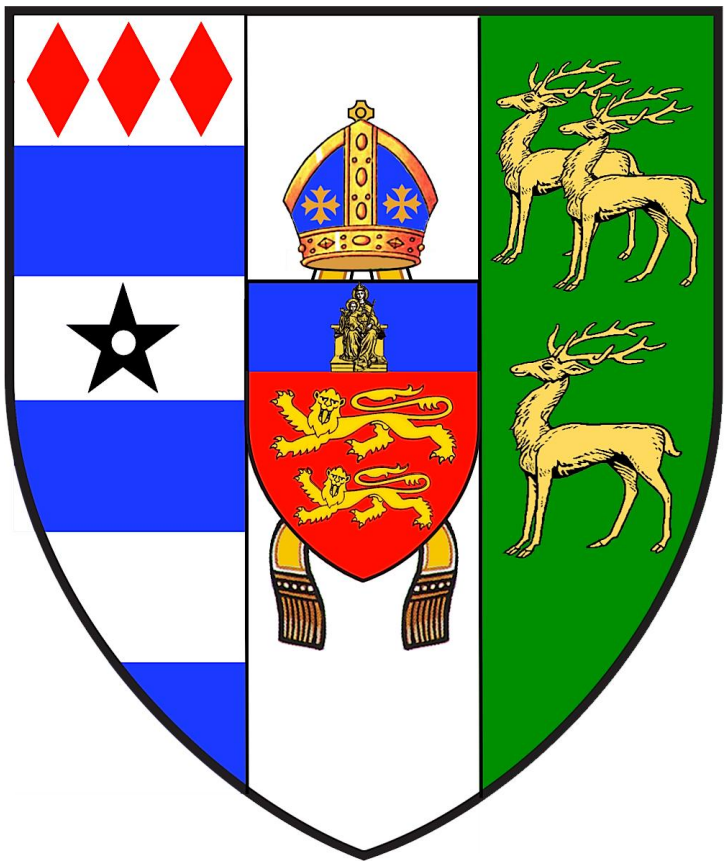
Investigation of T cell populations in coeliac disease and intestinal transplantation using functional, transcriptomic, and T cell receptor repertoire analysis approaches

---

Dr Michael Edward Barnaby FitzPatrick

Lincoln College, Oxford



Written submission to be considered for Doctor of Philosophy in Clinical Medicine

Supervisors:

Professor Paul Klenerman and Dr Elizabeth Soilleux

Acknowledgements

First, I would like to thank my supervisors, Professors Paul Klenerman and Elizabeth Soilleux. Liz did so much to support my application for fellowship funding, and I will be forever grateful for her faith in me, and for giving me the opportunity to step into research. Paul has been a source of great encouragement, sage advice, and support, and I could not have asked for a better research group to be a part of. It is a great privilege to have supervisors who believe in you, particularly when you are struggling to believe in yourself.

I thank my many collaborators in this work - Nicholas Provine, Lucy Garner, Agne Antanavicuite, Mel Dunstan, Riccardo Ferreira, Philip Allan, Tim Ambrose, Kate Powell, and Helen Ferry in particular. The supportive, collegiate nature of these collaborations has improved both the research, and the experience of delivering it.

I thank all the members of Paul's research group who are the best of colleagues, and have become good friends. Their advice, suggestions, technical assistance, support, and good humour has been invaluable. In particular, I thank Nick Provine for all his guidance, advice, and support. I thank Ali Amini, Lucy Garner, and Sarah Sasson for many productive discussions about T cell biology; I have learnt a great deal from you. I thank Kate Lynch and Steph Slevin for their technical advice, training, and excellent bench banter. I thank Dr Helen Ferry for cell sorting, and for answering myriad questions about flow cytometry, and Vinny Cheung and James Chivenga for help with sample collection. In the wider TGU, I thank Drs Hannah Chen, Dominik Aschenbrenner, Chantal Hargreaves, and Sumeet Panday for technical advice. I acknowledge the Wellcome Trust Centre for Human Genetics for sequencing services. I thank the Oxford-Celgene Fellowship programme and the BRC for financial support, and Peter Schafer from Celgene Corporation for is advice and encouragement.

Within the Translational Gastroenterology Unit, I thank Dr Carolina Arancibia and Professor Simon Travis for their advice and support. I also wish to thank the late Professor Satish Keshav for his wise counsel, kind words, unequivocal support, and sharp intellect. I miss our conversations about T cells, CCR9, and paneth cells, as well as politics, wine, travel, history, and art, greatly.

I thank my friends, colleagues, and family, without whose support I wouldn't have been able to complete my research. In particular, I thank my three sons: their beautiful souls, filled with the mindfulness and ever-present joy of childhood, have kept me grounded on this long road. Finally, I thank Rebecca: my wife, my love, my rock, my morning star. Thank you for keeping me true, and providing much-needed perspective when I had temporarily misplaced it.

A note on the COVID-19 pandemic

At the start of my research, a friend told me that much of the key work for a doctoral thesis is completed in the last year. By that time, the research questions are focused, the student's understanding of the field is more mature, and their technical and analytical abilities are well-developed, meaning that they are at their most productive.

The COVID-19 pandemic has disrupted all our lives, and much global scientific research, with people's personal and professional plans torn asunder. My own situation is less difficult than many colleagues find themselves in, but the pandemic has disrupted my work substantially. Several experiments planned for the Spring, designed to tie together particular themes in the research (especially chapter 4, and to a lesser extent chapter 5), have not been able to proceed as planned. As a physician, I returned to the wards during the COVID-19 peak, work made all the more arduous due to living away from my family just after the birth of my third son at the end of March. It has not been the end to the doctoral programme that I had hoped for.

In particular, additional flow cytometry and functional experiments on CD8+ duodenal IELs were not possible between February and the time of writing. These experiments would have provided greater statistical power for the final analyses, and were designed to tie together the TCR repertoire and sequencing approaches which precede them. These analyses will be performed in due course, and I hope the frustratingly incomplete nature of those analyses can be set aside by the examiners.

Finally, it is in times of difficulty that the mettle of one's friends and colleagues is tested. I could not ask for more supportive supervisors and colleagues, particularly Paul Klenerman and Nick Provine, who provided me with much-needed support and perspective as I approached writing a thesis during a global pandemic while home-schooling my sons. Thank you.

Attribution of collaborative work

Much of the research in this thesis has been collaborative in nature and, in my opinion, the strength and impact of the research is all the better for it. For me, science is a team sport, and collaboration is hugely important, particularly for physician-scientists. It is working with inspirational, like-minded, driven colleagues that makes science such an engaging and satisfying area of academia. I have learnt a great deal from those with whom I have worked, and learnt much about how to drive forward collaborative research.

In particular, while I have been fully involved in the analysis and interpretation of the single-cell RNAseq datasets in Chapters 4, 5, and 6, I have not performed the data processing in R and Python, although I have made every effort to understand the processes involved. For Chapter 4, I am indebted to Nicholas Provine for his tuition in molecular biology techniques. For Chapters 4 and 5, I am indebted to Dr Agne Antanavicuite, with whom I collaborated in the analysis of single-cell RNA sequencing datasets. I am also indebted to Dr Riccardo Ferriera, with whom some of the single-cell RNAseq library preparation was performed. For Chapter 6, I am indebted to Drs Nicholas Provine and Lucy Garner, with whom I collaborated in the single-cell RNAseq library preparation and analysis of the datasets. Some of the flow cytometry experiments were also performed in collaboration with Dr Nicholas Provine, and the three of us are co-authors of the manuscript of this work, currently under review. I have stated at the start of each chapter in more detail where experiments and analyses were performed in collaboration.

Table of contents

Acknowledgements *2*

A note on the COVID-19 pandemic *3*

Attribution of collaborative work *4*

Abstract: *9*

Glossary: *11*

Chapter 1: Introduction *14*

1.1 Clinical and immunological aspects of coeliac disease **14**

1.1.1 Clinical aspects of coeliac disease 14

1.1.1.1 Epidemiology 14

1.1.1.2 Clinical presentation 15

1.1.1.3 Diagnosis 16

1.1.1.4 Treatment 18

1.1.1.5 Refractory CD and enteropathy-associated T cell lymphoma 19

1.1.1.6 Novel diagnostic and therapeutic approaches 21

1.1.2 Immunological aspects of coeliac disease 22

1.1.2.1 Coeliac disease genetics 23

1.1.2.2 The gluten-specific CD4+ T cell 24

1.1.2.3 The molecular basis of the gluten-specific adaptive immune response 25

1.1.2.4 Plasma cells, antigen presentation, and CD-associated antibodies 25

1.1.2.5 CD8+ T cells in coeliac disease 26

1.1.2.6 γδ T cells in coeliac disease 28

1.1.2.7 Putative triggers for coeliac disease development 30

1.1.3 Conclusions 32

1.2 Biology of γδ T cells in humans **33**

1.2.1 Vδ2+ T cells in humans 37

1.2.1.1 The Vδ2+ T cell development and the Vδ2+Vγ9+ TCR 38

1.2.1.2 Vδ2+ T cells in human disease 39

1.2.1.3 Vδ2+ T cell function and phenotype 40

1.2.1.4 Phenotypic and functional heterogeneity of Vδ2+ T cells 40

1.2.1.5 Vδ2+ T cells and the wider innate-like T cell family 41

1.2.2 Non-Vδ2 γδ T cells 42

1.2.2.1 Non-Vδ2+ T cell phenotype 43

1.2.2.2 Non-Vδ2 T cells in human disease 44

1.2.3 Conclusions 44

1.3 Tissue-resident memory T cells **46**

1.3.1 Characteristics of T_{RM} cells in mice and humans 46

1.3.2 Heterogeneity in T_{RM} cells 50

1.3.3 T_{RM} cells in human disease 51

1.3.3.1 T_{RM} cells in infection 51

1.3.3.2 T_{RM} cells in malignancy 53

1.3.3.3 T_{RM} cells in autoimmunity 53

1.3.3.4 T_{RM} cells in GI autoimmunity: IBD and coeliac disease 54

1.3.3.5 T_{RM} cells in transplantation 56

1.3.4 Conclusions and key questions 57

1.4 Thesis questions and hypotheses **58**

Chapter 2: Materials and methods *59*

2.1 Identification and consent of donors **59**

2.2 Isolation of peripheral blood mononuclear cells (PBMCs) 59
2.3 Collection of intestinal biopsy tissue 60
2.4 Dissociation of intestinal biopsy tissue 60
2.5 Cryopreservation of intestinal biopsy tissue 61
2.6 Ex vivo stimulation assays 61
2.6.1 Cytokine and HMB-PP stimulation assays 61
2.6.2 Plate-bound CD3 stimulation assays 62
2.6.3 All-trans retinoic acid (ATRA) stimulation 62
2.6.4 Cellular proliferation assay 62
2.7 Flow cytometry 63
2.7.1 Surface staining 63
2.7.2 Intracellular and intranuclear staining 63
2.7.3 Sample barcoding for flow cytometry using cellular dyes 64
2.7.4 HLA allele congenic cell tracking 64
2.7.5 Data acquisition and instruments 64
2.8 Cell sorting 65
2.9 Enzymatic digestion on cell surface markers (Chapter 3) 65
2.10 Chip cytometry 66
2.11 Molecular biology techniques 67
2.11.1 Nucleic acid extraction 67
2.11.2 HLA-DQ genotyping 67
2.11.3 Whole transcriptome amplification 68
2.11.4 Quantitative RT-PCR 69
2.11.5 Bulk RNA sequencing 69
2.11.6 Single-cell RNA sequencing using the 10x Genomics platform 69
2.11.7 Plate-based single-cell RNA sequencing 70
2.11.8 Combined targeted single-cell RNA sequencing and surface protein quantification using the BD Rhapsody platform 70
2.11.9 Bulk TCR repertoire sequencing 71
2.12 Analysis 72
2.12.1 Graphs, statistics, and flow cytometry analysis 72
2.12.2 Bulk TCR repertoire analysis 73
2.12.3 Bulk RNA-Seq Analysis 73
2.12.4 10x genomics scRNAseq analysis (Chapters 1-3) 75
2.12.5 BD Rhapsody scRNAseq analysis (Chapter 3) 78
2.12.6 scRNAseq data analysis (Chapter 4) 79
2.12.7 Single cell classification 80
2.12.8 Weighted Gene Correlation Network Analysis 82
2.12.9 Gene Ontology and Pathway Enrichment Analyses 82
2.12.10 Transcriptional data integration with published datasets 83
2.12.11 Antibodies and key reagents 84
Chapter 3: Method development 88
3.1 Introduction 88
3.2 Effect of tissue digestion methods on surface marker immunophenotyping 89
3.3 Optimisation of cell sorting and TCR repertoire sequencing 95
3.4 Comparison of fresh and cryopreserved intestinal immune cells for scRNAseq 104
3.5 Figures 110

Chapter 4: Characterisation of CD8+ and γδ T cells in coeliac disease using TCR repertoire sequencing, RNA sequencing, and flow cytometry 123

4.1 Acknowledgement of contributions 123

4.2 Introduction 123

4.3 Peripheral and mucosal T cell populations in coeliac disease 128

4.3.1 Non-Vδ2 γδ T cells are increased in the gut, but not blood, in coeliac disease 128

4.3.2 Non-Vδ2 γδ T cells do not respond to combinatorial cytokine stimulation 129

4.4 TCR repertoire sequencing of mucosal CD8+ and γδ T cells 130

4.4.1 Descriptive statistics of TCR repertoire cohort 131

4.4.2 The γδ T cell repertoire 132

4.4.3 The CD8+ TCR repertoire 136

4.5 RNA sequencing of mucosal CD8+ and γδ T cells 140

4.6 Single-cell RNA sequencing of intestinal CD8+ and γδ T cells in coeliac disease 146

4.7 Flow cytometric evaluation of intestinal T cells in coeliac disease 154

4.8 Discussion 157

4.9 Figures 165

Chapter 5: Investigating peripheral γδ T cell populations in health and coeliac disease ..204

5.1 Introduction 204

5.2 Phenotypic heterogeneity of peripheral γδ T cells 209

5.2.1 Technical considerations 210

5.3 Single cell RNA sequencing of human circulating γδ T cells and conventional CD8+ T cells 217

5.3.1 Vδ2+ T cells display a transcriptional spectrum of effector function 219

5.3.2 Non-Vδ2 γδ T cells 226

5.3.3 Interim conclusions 227

5.4 Single-cell functional heterogeneity of γδ T cells 228

5.4.1 Vδ2+ T cells form a spectrum of effector function 229

5.4.2 Vδ2+ and MAIT cell responses to cytokine and TCR stimulation 230

5.4.3 Non-Vδ2 T cells show transcriptional heterogeneity in CD27hi naive populations 232

5.4.4 Non-Vδ2 T cells show NK-like responses to stimulation 233

5.5 Phenotypic and functional characterisation of Vδ2+ T cells 233

5.6 Investigation of CCR9 expression on non-Vδ2 T cells 238

5.7 Discussion 241

5.8 Figures 250

Chapter 6: Characterisation of tissue resident memory populations using intestinal transplantation as a model system 282

6.1 Acknowledgement of contributions 282

6.2 Introduction 282

6.2.1 Identification of T_{RM} cells 283

6.2.2 Intestinal transplantation as a model for T_{RM} cell study 284

6.3 Results 285

6.4 Discussion 296

6.5 Figures..... 302

Chapter 7: Discussion 316

7.1 CD8+ and γδ T cells in CD..... 316

7.2 Insights into γδ T cell and innate-like T cell biology..... 318

7.3 Transcriptional heterogeneity of human CD8+ T_{RM} cells..... 321

7.4 Common themes: rebellious T cells, and the nature of immune cell heterogeneity..... 324

7.5 Future work..... 326

List of Publications 328

Supplementary Figures and Tables 329

References.....368

Abstract:

Coeliac disease (CD) is caused by an adaptive immune response to gluten, however the gluten-specific CD4+ T cell response is insufficient to cause tissue damage in isolation. CD8+ intra-epithelial T cells (IELs) mediate epithelial cell damage in CD, which is thought to occur in a TCR-independent manner, while the role of γδ IELs, which are increased in CD, remains enigmatic. I sought to investigate CD8+ and γδ T cell populations in CD.

After optimisation of intestinal tissue dissociation, TCR repertoire sequencing (TCRseq) and single-cell RNA sequencing (scRNAseq) (**Chapter 3**), I examined intestinal CD8+ and γδ T cells in CD using flow cytometry, bulk and single-cell RNAseq, and TCRseq (**Chapter 4**). I confirmed previously reported changes in γδ TCR repertoires in CD, and identified perturbations in the CD8+ TCR repertoire, including enrichment of TRBV28-expressing clonotypes in CD. Bulk and scRNAseq approaches identified an activated, cytotoxic, highly regulated, tissue-resident population of CD8+ T cells associated with CD, which were associated with these TRBV28 clonotypes, consistent with a TCR-driven CD8+ T cell process involved in CD pathogenesis.

This work on CD led further research in two directions, examining the wider landscape of human γδ T cells and their relationships to other innate-like T cells, and exploring CD8+ T cell heterogeneity in tissue resident populations in the human gut.

First, I examined transcriptional, phenotypic, and functional heterogeneity in human γδ T cells (**Chapter 5**). scRNAseq and flow cytometry of circulating γδ T cells revealed a Vδ2+ γδ T cell effector spectrum, from an innate-like, cytokine-responsive CD26bright population to a highly cytotoxic GPR56+ population. CD26bright Vδ2+ T cells were highly similar to MAIT cells, in transcriptional profile, phenotype, and function, in particular in their IFNγ- and IL-26-dominated response to

cytokine stimulation. In addition, unexpected heterogeneity within naive non-Vδ2 T cell populations was identified, including a SOX4+ subset that expressed the gut-homing chemokine receptor CCR9.

Second, I used intestinal transplantation as a model to study tissue resident memory (T_{RM}) CD8+ T cells in the small intestine (**Chapter 6**). scRNAseq identified two transcriptionally distinct subsets of *bona fide* CD8+ T_{RM} cells in the human gut, differing in their expression of cytotoxic molecules, chemokine receptors, and integrins. Further flow cytometry and functional assays demonstrated that these populations differed in phenotype and function.

In sum, I have explored CD8+ and γδ T cell biology in coeliac disease, health, and intestinal transplantation. The work raises questions about the nature of classification systems of cell types in immunology, and the shared and distinct features of unconventional and innate-like T cells.

Glossary:

AA	Amino acid
ACD	Active coeliac disease
ADCC	Antibody-dependent cell-mediated cytotoxicity
ANOVA	Analysis of variance
ATRA	All-trans-retinoic acid
BSA	Bovine Serum Albumin
CCL25	Chemokine (C-C motif) ligand 25
CCR9	C-C chemokine receptor 9
CD	Coeliac disease
CMV	Cytomegalovirus
CrD	Crohn's disease
CTFR	CellTrace Far Red®
CTV	CellTrace Violet®
DC	Dendritic cell
DEG	Differentially expressed gene
DNA	Deoxyribonucleic acid
DTT	1,4- Dithiothreitol
EATL	Enteropathy-associated T-cell lymphoma
EBV	Epstein-Barr virus
EDTA	Ethylenediaminetetraacetic acid
FACS	Flow assisted cell sorting
FC	Fold change
FCS	Foetal calf serum
FDR	False discovery rate
FFPE	Formalin-fixed, paraffin-embedded
FMO	Fluorescence minus one control
FSC-A/H	Forward Scatter-Area/Height
GALT	Gut associated lymphoid tissue
GEM	Gel Bead-In-Emulsion
GFD	Gluten-free diet
GWAS	Genome-wide Association Study
HC	Healthy control subject
HEPES	4-(2-hyroxyethyl)piperazine-1-ethanesulfonic acid
HIV	Human immunodeficiency virus
HLA	Human leucocyte antigen
HMB-PP	(E)-4-hydroxy- 3-methyl-but-2-enyl pyrophosphate
HSV	Herpes simplex virus
IBD	Inflammatory bowel disease
IEL	Intra-epithelial lymphocyte
IFN-α	Interferon-α
IFN-γ	Interferon-γ

IL-	Interleukin
IL	Intestinal lymphocyte
IPP	Isopentyl pyrophosphate
IQR	Interquartile range
ITGA4	Gene encoding α4-integrin
ITGAE	Gene encoding αE-integrin (CD103)
ITGB2	Gene encoding β2-integrin (CD18)
ITGB7	Gene encoding β7-integrin
IU	International units
KO	Knock-out (murine model)
LAG-3	Lymphocyte activating gene-3
LCMV	Lymphocytic choriomeningitis virus
LFA-1	Lymphocyte function-associated antigen 1 (αL/β2 integrin heterodimer)
LLD	Lower limit of detection
LLN	Lower limit of normal
LPL	Lamina propria lymphocyte
MACS	Magnetic assisted cell sorting
MAdCAM-1	Mucosal Addressin Cellular Adhesion Molecule-1
MAIT	Mucosal-associated invariant T-cell
MFI	Median fluorescence intensity
MHC	Major histocompatibility complex
MR1	MHC-like protein 1
N.S.	Not significant
NGS	Next generation sequencing
NK	Natural killer
Non-Vδ2 T cell	Gamma delta T cell not expressing Vδ2/Vγ9 TCR (this includes Vδ2+Vγ9- T cells)
NRCD	Non-responsive coeliac disease
pAg	Phosphoantigen
PBMC	Peripheral blood mononuclear cells
PBS	Dulbecco's phosphate buffered saline
PCR	Polymerase chain reaction
PE	Phycoerythrin
PHA	Phytohaemagglutinin
PMA	Phorbol 12-myristate 13-acetate
RAG-1	Recombinase activation gene-1
RCD	Refractory coeliac disease
RNA	Ribonucleic acid
RNAseq	RNA sequencing
RPMI-1640	Roswell Park Memorial Institute-1640
scRNAseq	Single-cell RNA sequencing
SEM	Standard error of the mean
SI	Small intestine
SSC-A/H	Side Scatter-Area/Height

TCD	Treated coeliac disease
T_{CM}	Central memory T cells
TCR	T-cell receptor
TCRseq	TCR repertoire sequencing
TECK	Thymus expressed chemokine (CCL25)
T_E	Early effector T cells
T_{EM}	Effector memory T cells
T_{EMRA}	Terminal effector memory T cells
TGU	Translational Gastroenterology Unit
Th	T-helper
T_N	Naïve T-cells
TNF-α	Tumour necrosis factor-alpha
TRAIL	TNF-related apoptosis-inducing ligand
T_{reg}	T-regulatory
T_{RM}	Tissue-resident T cell
tSNE	t-Distributed Stochastic Neighbour Embedding
UC	Ulcerative colitis
ULN	Upper limit of normal
UMAP	Uniform Manifold Approximation and Projection
VA	Villous atrophy
Vδ1+ T cell	Gamma delta T cell expressing Vδ1 TCR chain
Vδ2+ T cell	Gamma delta T cell expressing Vδ2/Vγ9 TCR
WTCHG	Wellcome Trust Centre for Human Genetics (Oxford)

Chapter 1: Introduction

1.1 Clinical and immunological aspects of coeliac disease

Coeliac disease (CD) is a common, immune-mediated condition where dietary gluten induces inflammation and mucosal damage in the small intestine. This damage leads to troublesome symptoms, malabsorption, and nutrient deficiencies, as well as complications including osteoporosis and cancer. CD has no cure, although can be effectively treated with dietary exclusion of gluten.

I will briefly discuss the epidemiology, presentation, diagnosis, treatment, and complications of CD. I will then provide an overview of the current understanding of the immunology of CD, and discuss several unanswered questions regarding its biology.

1.1.1 Clinical aspects of coeliac disease

1.1.1.1 Epidemiology

Coeliac disease is found worldwide, with a seroprevalence of 1.1-1.8%, and biopsy-confirmed prevalence of 0.4-0.8% (Singh et al., 2018). Regional variation, with high prevalence in Scandinavia, may be due to underlying genetic factors or dietary patterns, but comparisons between countries are confounded due to differences in diagnostic testing(King et al., 2020).

Multiple studies suggest that CD incidence and prevalence increased in the late 20th century(King et al., 2020). Comparisons of current and historical data are fraught with potential confounders, as

diagnostic criteria, along with physician practices and patient behaviour, change over time. Despite these challenges, epidemiological studies indicate a 2- to 5-fold increase in CD in this period(Catassi et al., 2010; Dydensborg et al., 2011; Riddle et al., 2012; West et al., 2014). Importantly, there is evidence that this represents a genuine underlying increase in CD incidence based on historical serum from US servicemen(Rubio Tapia et al., 2009).

The drivers for this increase remain unclear. The 'Swedish epidemic', a marked increase in childhood CD incidence in the 1980s and 1990s, has been attributed to changes in infant feeding practices(Myléus et al., 2009). Other postulated factors contributing to altered risk of CD include antibiotics in the first year of life(Kemppainen et al., 2017; Mårild et al., 2013), diverse microbial exposure in childhood(Kondrashova et al., 2009), probiotics(Uusitalo et al., 2019), season of birth, latitude(Unalp-Arida et al., 2017), childhood infection (particularly enteric viral exposure)(Lindfors et al., 2020; Myléus et al., 2012), and mode of birth delivery(Koletzko et al., 2018; Mårild et al., 2012), although robust evidence is lacking, and data are often conflicting. Recent data suggest that CD incidence is now stablising in the countries with highest CD prevalence(Kivelä et al., 2015; Namatovu et al., 2014), suggesting CD may be undergoing an autoimmune transition from low to high prevalence in industrialised societies, as seen for inflammatory bowel disease (IBD) (Ng et al., 2017).

1.1.1.2 Clinical presentation

The traditional presentation of CD was with childhood malabsorption. This 'classical CD' is characterised by diarrhoea, steatorrhoea, weight loss, and growth failure, along with the sequelae of nutritional deficiencies. While still seen in paediatric populations, is uncommon in adults(Ludvigsson et al., 2012). 'Non-classical CD' is more typical, with patients often presenting with symptoms similar to irritable bowel syndrome (IBS) (Ludvigsson et al., 2014). Constitutional symptoms of malaise, tiredness, and 'brain-fog' are also common, while an increasing proportion of adults present asymptomatically.

Patients with CD often have vitamin or mineral deficiencies at presentation, including iron, folate, vitamin B12 and vitamin D. CD is associated with osteoporosis, likely mediated through reduced calcium adsorption, which confers a risk of major fracture in older patients(Heikkilä et al., 2015). A panoply of other extra-intestinal manifestations have been linked with either coeliac disease or gluten(Leffler et al., 2015).

1.1.1.3 Diagnosis

Gold-standard diagnosis of CD relies on three criteria: compatible symptoms, serology, and duodenal biopsy, with none alone diagnostic of CD. Despite the strong association with HLA type and CD, the frequency of HLA-DQ2/DQ8 haplotypes in the population (30-40%) makes HLA-typing a poor diagnostic test, except to exclude CD. The clinical presentation of CD is often protean, with substantial overlap with IBD, IBS, gastrointestinal malignancy, and food intolerance. Moreover, the need for life-long restrictive dietary change, and the challenge of retrospective diagnosis once on a gluten-free diet (GFD), make accurate diagnosis important to avoid iatrogenic harm.

CD serology - the detection of endomysial (EMA), IgA anti-tissue transglutaminase (TTG), or anti-deaminated gliadin peptide (DGP) antibodies - has transformed CD diagnosis. Most patients with CD are positive for IgA-TTG antibodies, with IgG-DGP useful in those with selective IgA deficiency(Ludvigsson et al., 2014). EMA is less sensitive but may be more specific for CD. For adults, serology is generally used to screen patients with compatible symptoms before endoscopic biopsy. Anti-gliadin antibodies (AGA) are neither sensitive nor specific for CD, although they can be used to investigate suspected gluten-induced ataxia(Hadjivassiliou et al., 2015; Schiepatti et al., 2020).

Diagnostic criteria based solely on serology have been developed for paediatric patients, which show high positive and negative predictive values in prospective trials(Wolf et al., 2017), and have reduced

the need for endoscopy in children(Husby et al., 2012). While serological diagnosis is not formally advocated in adults, and lacks prospective evidence of diagnostic accuracy(Penny et al., 2020), temporary guidelines in the COVID-19 pandemic for serological diagnosis in adults will move practice away from endoscopy(British Society of Gastroenterology, 2020). However, one concern is that not all serological tests are created equal, with substantial differences in sensitivity and dynamic range of commercial kits(Egner et al., 2012).

The histological hallmarks of CD are villous atrophy (VA), crypt hypertrophy, and intraepithelial lymphocytosis, typically reported using the Marsh-Oberhuber scheme(Marsh, 1992; Oberhuber et al., 1999), although morphometric analyses quantifying villous height and crypt depth may be more accurate in clinical trials(Taavela et al., 2013). Histological changes are most clearly assessed in the second part of the duodenum and beyond, although a small proportion of patients only have histological changes in the duodenal bulb(Kurien et al., 2012; Mooney et al., 2016).

Histological diagnosis of CD faces two challenges: the non-specific nature of VA, and the subjectivity of histological assessment. Villous atrophy is a common consequence of multiple disease processes, including drug reactions, infection, inflammatory and autoimmune disease, hypersensitivity, and malignancy(Aziz et al., 2017). While most alternative causes are easily excluded by detailed history and simple investigations, a proportion of patients with seronegative villous atrophy (SNVA) pose a diagnostic dilemma. Seronegative CD does exist, accounting for a third of SNVA(Aziz et al., 2017), although is probably less common than previously thought(Ludvigsson et al., 2014).

Histological assessment is subjective, and can be complicated due to technical factors. Histopathologist scoring of the Marsh-Oberhuber classification shows only moderate intra-observer variability (Kappa = 0.5), although differences in final diagnosis between pathologists is less common (4-25%)(Arguelles-Grande et al., 2012; Mubarak et al., 2011; Wolf et al., 2017). Diagnostic

discrepancies are exacerbated when samples are of poor technical quality, due to biopsy size or number, crush artifact, or the plane of sectioning. This last factor can generate pronounced artefact, leading to under- or over-estimation of villous atrophy, emphasising the importance of interpretation by expert histopathologists(Taavela et al., 2013). However, most patients will have positive serology, compatible symptoms and histological changes, allowing a confident positive diagnosis.

1.1.1.4 Treatment

Following the description of classical CD by Samuel Gee in the 19th Century, a number of (often extreme) restriction diets were used to treat CD(Losowsky, 2008), some with positive results(Haas, 1924). The key observation linking gluten to CD was made by Willem Karel Dicke, a dutch physician, in the mid-20th century. He hypothesised a link between wheat and CD in the pre-war period(van Berge Henegouwen and C. J. Mulder, 1993), and went on to conduct meticulous experiments demonstrating that the alcohol-soluble protein fraction of wheat (gliadin) triggered diarrhoea and steatorrhoea in children with CD(Kamer et al., 1953). This observation led to the current standard of care, the gluten-free diet (GFD).

A GFD is the mainstay of CD treatment. Gluten includes wheat storage proteins (gliadins), as well as those from barley (hordeins) and rye (secalins). Uncontaminated oats are safe for consumption for most patients(Janatuinen et al., 2000), although some may be truly sensitive to oats(Arentz Hansen et al., 2004; Lundin et al., 2003). Exclusion of gluten must be strict to induce mucosal healing; the tolerable amount of gluten is between 10-50 mg/day(Akobeng and Thomas, 2008). The near-ubiquitous use of wheat flour in processed food, combined with the ease of cross-contamination, make the diet challenging to follow, and patients benefit from expert dietetic advice. While GFD improves symptoms, quality of life, and mucosal histology, it is expensive, and burdensome to follow(Ludvigsson et al., 2014).

However, recent studies indicate that complete histological normalisation is uncommon with a GFD, with persistent intra-epithelial lymphocytosis and mild reduction in villous height most common despite overall improvement in villous atrophy(Daveson et al., 2020). Whether this represents true ongoing inflammation, or an immunological 'scar' of altered and increased IEL populations despite treatment, is unclear.

1.1.1.5 Refractory CD and enteropathy-associated T cell lymphoma

In some patients, symptoms of CD and villous atrophy persist despite a strict GFD, a condition described as refractory coeliac disease (RCD). RCD is rare, with incidence less than 1%, and perhaps as low as 0.05%, of those with CD(Eigner et al., 2016; van Gils et al., 2015). Risk factors, apart from known CD, include HLA-DQ2 homozygosity, female sex, and increasing age. Observational studies suggest that RCD may be becoming rarer, although this may be a 'denominator problem' as mild presentations of CD are increasingly recognised(Eigner et al., 2016).

In some patients, the clinical, biochemical, and histological changes of RCD are indistinguishable from ongoing active coeliac disease, despite gluten exclusion. This is termed RCDI, and may be related to high sensitivity to trace quantities of gluten, or ongoing T cell activation independent of antigen. Patients with RCDI have a good long-term prognosis.

However, in a small number of patients, aberrant lineage negative intra-epithelial lymphocyte (IEL) populations undergo clonal expansion, carrying clonal TCRγ rearrangements, and taking on a characteristic phenotype with absent surface CD3, but ongoing intracellular CD3 expression. This is termed RCDII, and can be considered a lymphoma *in situ*. The ongoing inflammation and villous atrophy leads to malabsorption, abdominal pain, diarrhoea and weight loss. It can progress to enteropathy-associated T-cell lymphoma (EATL), a rare malignancy with a poor prognosis.

Diagnosis of RCDII is challenging. Conventional immunohistochemistry does not allow clear distinction between the aberrant, pre-malignant IEL population from the IELs seen in active CD or RCDI. TCRγ clonality studies of duodenal biopsies can may a monoclonal TCRγ peak, however in active CD the presence of oligoclonal T cell clones can produce a false-positive pseudo-clonal peak (Celli et al., 2019; Cellier et al., 1998; Goerres et al., 2003). Dual immunohistochemistry staining for CD3 and CD8 may show an increased IEL population of CD3+CD8- T cells(Patey-Mariaud de Serre et al., 2001)(H. Liu et al., 2010), however, false positive and negative tests do occur(Celli et al., 2019; van Gils et al., 2015; van Wanrooij et al., 2010). Flow cytometry of duodenal IELs, staining for surface and intracellular CD3, identifies the aberrant T cell populations in RCDII, and may be a more sensitive and specific test than TCRγ clonality testing(van Wanrooij et al., 2010; Verbeek et al., 2008). However this approach is only available in specialist centres. Recently, immunohistochemical staining for the NK receptor NKp46 has shown promise to diagnose RCDII(Cheminant et al., 2019). These different techniques have not been prospectively compared, and a combination of clinical features, TCRγ clonality studies, and either IHC or flow cytometry is required for diagnosis.

The evidence for RCD treatments is poor, relying on observational studies in small cohorts. For RCD I, strict GFD and nutritional support are the mainstays of treatment. For those with ongoing symptoms and severe villous atrophy, topical and systemic corticosteroids and thiopurines can be used, with good responses in unblinded trials and observational studies(Goerres et al., 2003). Anti-TNFα therapy, 5-ASA, and ciclosporin have also been used(Costantino et al., 2008; van Gils et al., 2015). Despite the limited evidence base for therapeutics, RCDI has an excellent prognosis, with a 5-year survival greater than 90%(Malamut et al., 2009).

RCDII carries an awful prognosis, with most patients developing EATL within 3 years of diagnosis, and a 5-year survival of approximately 50%(Malamut et al., 2009; Nasr et al., 2015). Data on the efficacy

of steroid and immunomodulator use in RCDII is conflicting, with early reports of minimal efficacy with prednisolone and azathioprine, but more recent studies of budesonide showing potential benefit(Goerres et al., 2003; Mukewar et al., 2017; Nasr et al., 2015). Additional therapies include cladribine, cyclosporin, and chemotherapy followed by autologous stem cell transplantation(Al-Toma et al., 2006; Tack, 2011; Tack et al., 2011). A recent trial of anti-IL-15 therapy in RCDII proved disappointing(Cellier et al., 2019).

Enteropathy-associated T cell lymphoma is an aggressive small-bowel malignancy with a dismal prognosis, with a 5-year survival less than 20% despite treatment. Surgery, systemic chemotherapy, and ASCT have all been used to treat EATL, with poor results(Gale et al., 2000; van de Water et al., 2010).

1.1.1.6 Novel diagnostic and therapeutic approaches

The limited diagnostic and therapeutic armamentarium for CD poses a challenge in clinical practice. Diagnosis is challenging in some patients, particularly those with seronegative disease, or who embark on a GFD beforehand. A GFD is burdensome and disliked by patients, and may not be as effective as previously thought in controlling intestinal inflammation(Daveson et al., 2020). For those for whom GFD is ineffective, either due to inability to adequately exclude gluten from their diet or due to RCD type I, therapy with steroids and immunosuppressants has a poor evidence base and may well cause more harm than good. Finally, for the rare patients who develop RCD type II or EATL, treatments are generally ineffective, and prognosis poor.

Our improved understanding of CD immunopathology have led to novel diagnostic and therapeutic strategies which are undergoing development (recently reviewed in Christophersen et al., 2019b). Novel diagnostics may incorporate TCR repertoire analysis, including identification of public TCR sequences of CD-specific CD4+ T cells. These activated, gut-homing disease-specific CD4+ T cells can

also be identified using tetramer staining(Christophersen et al., 2014; Sarna et al., 2018a). The clinical utility of these techniques will depend on whether they are effective in individuals on a GFD. Recent work elucidating the role of gluten-specific CD4+ T cell-derived IL-2 in mediating early symptoms of gluten challenge such as nausea, has led to the possibility of short-term gluten challenge and IL-2 response as a novel diagnostic(Goel et al., 2019; Tye-Din et al., 2019). This would certainly be preferable to current gluten challenges required to induce antibody formation and histological changes, which can take between 2 and 8 weeks(Leffler et al., 2013; Sarna et al., 2018b).

Novel therapeutics are in development targeting each stage of the immunopathology of CD (Caio et al., 2020). One major challenge in for CD treatments is the need for excellent safety profiles from any treatment, given the safety of a GFD, and the fact that untreated CD is not associated with high morbidity or mortality. A suite of therapies targeting gluten are in development, including those seeking to reduce the immunogenicity of gluten peptides in wheat, in degrading ingested gluten before it reaches the small intestine, or seeking to block its deamidation by TG2. However, the first agent targeting gluten degradation was not successful in clinical trials, and it remains unclear if any upstream strategy targeting ingested gluten can provide sufficient degradation to prevent stimulation of the sensitive adaptive immune response(Murray et al., 2017).

A number of strategies that seek to tolerise or delete antigen-specific CD4+ T cells are also in development(Christophersen et al., 2019b). Given our knowledge of the CD4+ T cell response, and the antigen and HLA interactions that underpin it, this strategy is attractive. However, the first agent that entered clinical trials of efficacy, a vaccine of immunogenic gluten peptides, did not meet its primary endpoint(Mitchell and Garg, 2019; Truitt and Anderson, 2019). This raises a question about whether other tolerising strategies will be effective in CD.

1.1.2 Immunological aspects of coeliac disease

1.1.2.1 Coeliac disease genetics

There is a striking link between CD and other autoimmune conditions; 15% of CD patients go onto develop other autoimmune disorders and 5% of patients with type 1 diabetes develop CD(Cosnes et al., 2008). This link suggests shared genetic mechanisms for autoimmunity. There is a strong association between CD and the MHC, specifically the HLA-DQ locus. Over 90% of CD patients possess HLA-DQ2.5, either encoded in *cis* confirmation by the DR3DQ2 haplotype, or *trans* in DR5DQ7/DR7DQ2 heterozygotes(Sollid et al., 1989). Most other CD patients express HLA-DQ2.2 or HLA-DQ8 molecules, which confer a lower risk of disease, while rare cases of CD associated with HLA-DQ2.3, HLA-DQ7.5, and HLA-DQ8.5 are reported(Sollid et al., 2012).

HLA loci contribute about 40% of the genetic risk for CD, with genome-wide association studies (GWAS) identifying over 40 other loci that contribute to susceptibility(Dubois et al., 2010; Ricaño-Ponce et al., 2019; Trynka et al., 2011; Withoff et al., 2016). Many of these variants are common, each conferring a small change in risk(Abadie et al., 2011). Many are also associated with other autoimmune diseases, including primary sclerosing cholangitis, multiple sclerosis, juvenile arthritis, ulcerative colitis, type 1 diabetes, and alopecia areata, suggesting shared pathways which alter the balance between host defence and autoimmunity(Farh et al., 2015). One challenge of translating insights gained from GWAS to understanding CD pathogenesis is that most CD-associated SNPs localise to non-protein coding parts of the genome, and are thought to exert their effects through promoter and enhancer sequences, as well as regulatory RNAs(Withoff et al., 2016). Much work is still needed to unpick these complex interactions, and the cell types in which such SNPs exert their effects.

1.1.2.2 The gluten-specific CD4+ T cell

Gluten epitope specific CD4+ T cells are found in the intestine of patients with CD(Lundin, 1993), but not in the mucosa of subjects without disease(Molberg et al., 2003). These stimulatory gluten epitopes are presented by HLA-DQ2 (DQ2.5 or DQ2.2) or HLA-DQ8 molecules, the CD-associated HLA types. Individuals without CD who possess the HLA-DQ2.5 haplotype do not seem to mount a gluten-specific immune response(Christophersen et al., 2016). This is intriguing as the default response to oral antigen is tolerogenic, with the induction of regulatory T (Treg) cells, and suggests that the adaptive immune system is not exposed to gluten in unaffected individuals with the susceptible HLA type.

Gluten-specific CD4+ T cells exhibit a Th1 phenotype, and express IFNγ and IL-21 on antigen stimulation, pro-inflammatory cytokines enriched in the mucosa in CD(Bodd et al., 2010; Lundin, 1993). This Th1 phenotype indicates that priming intestinal dendritic cells have taken on a pro-inflammatory phenotype, possibly due to polarisation following enteric viral exposure (discussed in detail below) (Bouziat et al., 2017). These mucosal gluten-specific CD4+ T cells are long-lived, with clonotypes persisting for decades despite treatment with a gluten-free diet(Risnes et al., 2018). The persistence of these clonotypes may be maintained by ongoing, low-level gluten exposure, or by other survival mechanisms as seen in T_{RM} cells.

Gluten-specific CD4+ T cells in the blood and gut exhibit a characteristic phenotype, including the expression of several markers of both activation and negative regulation, such as CD38, CD161, CD28, HLA-DR and OX40, CD39, and PD-1(Christophersen et al., 2019a). Intriguingly, CD4+ T cells exhibiting a similar phenotype are seen in other autoimmune diseases, raising the possibility that this phenotype could identify antigen-specific T cells in other conditions.

1.1.2.3 The molecular basis of the gluten-specific adaptive immune response

The molecular interactions between gluten and predisposing HLA molecules that underpin the development of CD have been elucidated over the past two decades(Abadie et al., 2011). These interactions depend on the physicochemical properties of gluten peptides, and the properties of HLA molecules and TCRs.

The gluten epitopes that CD4+ T cells recognise are mainly not native gluten peptides, but ones which have undergone enzymatic modification (deamidation). Gluten peptides are rich in proline and glutamine residues, which renders them resistant to proteolysis(Shan et al., 2002). These gluten peptides are substrates for the enzyme tissue transglutaminase 2 (TG2), which deamidates glutamine residues to negatively-charged glutamate, particularly at Q-X-P amino acid motifs within the gluten peptide. HLA-DQ2.5 and HLA-DQ8 molecules possess positively-charged pockets which therefore preferentially bind to peptides with such negatively-charged residues.

HLA-DQ2.5 and HLA-DQ8 presentation of these deamidated gluten peptides activate gluten-specific CD4+ T cells with a characteristic TCR repertoire. Around 90% of CD patients carry HLA-DQ2.5, with DQ2.5glia-α1-specific TCRs showing skewed V gene usage (TRAV4/TRBV20-1/TRBV29-1), and DQ2.5glia-α2-specific TCRs enriched for TRAV26-1/TRBV7.2, with a key arginine residue in CDR3β, which is required for gliadin epitope binding(Petersen et al., 2014). HLA-DQ8glia-α1-specific TCRs also show skewed V gene usage (TRAV26-2/TRBV9-1) (Broughton et al., 2012).

1.1.2.4 Plasma cells, antigen presentation, and CD-associated antibodies

Antibodies directed against TTG and DGP are found in most patients with active CD, and wane with GFD treatment. Even in patients with seronegative CD, such antibodies can often be detected in the mucosa(Salmi et al., 2006). The plasma cells are enriched in the mucosa in CD, of which at least 10%

are TG2-specific and possess a highly restricted BCR repertoire(Di Niro et al., 2012). Recent murine work has shown that TG2-specific B cells develop in the presence or absence of TG2 expression, with no evidence of clonal deletion or anergy in the presence of TG2, suggesting that naive TG2-specific B cells do not encounter TG2 in their development, and that self-tolerance is not mediated at the B-cell level, but through the absence of T cell help(M Fleur du Pré et al., 2019).

The initially surprising association between an adaptive immune response to gluten and the presence of anti-tissue transglutaminase 2 (TG2) antibodies has been unraveled in recent years. Tissue transglutaminase 2 (TG2) plays a key role in coeliac pathogenesis through its deamidation of gluten peptides, which renders them immunogenic. Enterocytes express TG2(Arike et al., 2020), and enterocyte lysates contain catalytically active TG2, which would allow TG2 from shed enterocytes to come in contact with luminal gluten peptides(Iversen et al., 2020). TG2-gliadin complexes would then come into contact with B cells in Peyer's patches, allowing uptake of this protein complex and presentation of gliadin peptides by TG2-specific B cells to gluten-specific CD4+ T cells, which has been demonstrated *in vitro* (Iversen et al., 2020).

In addition plasma cells are the major APC population that presents gluten epitopes on MHC Class II in the gut(Høydahl et al., 2019). These gluten-presenting plasma cells express TG2-specific BCR, as well as co-stimulatory molecules that would enable T cell activation. Recent work has demonstrated that mucosal plasma cells in CD can express IL-15, as well as its receptor, which raises the possibility of IL-15 trans-presentation and plasma cell-T cell crosstalk in coeliac disease(Snir et al., 2019).

1.1.2.5 CD8+ T cells in coeliac disease

The CD4+ T cell response does not, in isolation, lead to villous atrophy, either in murine models, or patients with potential CD(Bouziat et al., 2017; de Kauwe et al., 2009; M F Du Pré et al., 2011). Early work highlighted the role of intra-epithelial CD8+ T cells, which are increased in CD(Selby et al.,

1983). These cytotoxic CD8+ IELs, expressing a αβTCR, are thought to mediate epithelial cell damage in CD, driven by tissue alarmins, in particular IL-15(Abadie and Jabri, 2014; Jabri and Abadie, 2015; Maiuri et al., 2000). Both IL-15 and IFNβ induce widespread transcriptional and epigenetic changes on CD8+ IELs *in vitro*, which induce genes associated with antiviral responses, T cell activation, and cytotoxicity(Zorro et al., 2020).

TCR-independent processes, mediated by NK cell receptors (NKRs), are thought to play the major role in CD8+ T IEL cytotoxicity in CD. The activating NKRs, NKG2D and NKG2C/CD94, are upregulated on IELs in CD via increased IL-15 exposure, while their ligands, HLA-E and MICA, show increased expression on epithelial cells(Meresse et al., 2004; 2006). The observation that these activating NK receptors are not upregulated in either potential or treated CD supports their role in CD-related tissue damage(Hüe et al., 2004).

This NK-like activity may be promoted by type 1 interferon, which is increased in the small intestine in CD(Monteleone, 2001), likely from dendritic cells(Di Sabatino et al., 2007), as well as by CD4+ T cell-derived IL-21(Kasaian et al., 2002; Leonard and Spolski, 2005). The gluten-specific CD4+ T cell response may also directly lead to the upregulation of the ligands of these NKRs, in particular HLA-E and MICA, via IFNγ(Perera et al., 2007). As CD8+ T IELs also produce IFNγ in CD(Olaussen et al., 2002), it may be that CD8+ IEL activation itself leads to the induction of their own non-classical MHC ligands on epithelial cells.

The hypothesis that CD8+ TCR-dependent processes are not required for tissue damage in coeliac disease is supported by a recently described murine model, where humanised mice expressing the HLA-DQ8 molecule, in combination with constitutive over-expression of IL-15 in the lamina propria and epithelium, leads to gluten-related villous atrophy(Abadie et al., 2020). However, the failure of recent clinical trials of anti-IL-15 therapy for CD suggests the model of IL-15-driven IEL cytotoxicity is

incomplete(Lähdeaho et al., 2019). There is also circumstantial evidence that CD8+ T IELs may play a TCR-dependent role in CD. Gluten-specific, class I HLA-restricted CD8+ T cells from CD patients have been described, with cytotoxic and pro-inflammatory functionality *in vitro*(Gianfrani et al., 2003; Mazzarella et al., 2008; Picascia et al., 2017). Activating NK receptor expression by CD8+ T IELs is linked to their TCR clonotype, suggesting a link between antigen specificity and functional role in CD(Jabri et al., 2002). In addition, activated, gut-homing CD8+ T cells in the circulation increase in proportion following gluten challenge(Han et al., 2013), in a manner analogous to gluten-specific CD4+ T cells(Anderson et al., 2000; Raki et al., 2007). The hypothesis that TCR-dependent processes may be relevant to the CD8+ T cell response in coeliac disease is examined in more detail in Chapter 4.

1.1.2.6 γδ T cells in coeliac disease

The intra-epithelial lymphocytosis seen in CD is formed not just of CD8+ T cells, but also γδ T cells. This was first recognised over 30 years ago(Halstensen et al., 1989), and numerous further studies have confirmed the increase in γδ T IELs in CD(Arranz et al., 1994; Bernardo et al., 2008; Bhagat et al., 2008; Calleja et al., 2011; Camarero et al., 2000; Dunne et al., 2013; Fernández-Bañares et al., 2014; Montalvillo et al., 2015; Remes-Troche et al., 2007; Sánchez-Castañon et al., 2016). This increase is particularly striking, given that γδ T cell frequencies do not increase in other inflammatory intestinal diseases(Catalan-Serra et al., 2017). In contrast to CD4+ and CD8+ T cells, the γδ T cells in the epithelium remain elevated on a GFD. Despite these profound changes in the gut, studies have not shown consistent changes in circulating γδ T cells in CD.

The TCR repertoire of γδ T cells in health and disease are not well understood, particularly within tissue. In the colon and healthy small bowel, γδ T cells most commonly express TRDV1- or TRDV3-containing TCRs(Chowers et al., 1994; Holtmeier et al., 1995). There is more diversity in their TRGV usage, skewed towards TRGV4, with the most common population in the gut expressing a Vδ1+Vγ4+

TCR (Di Marco Barros et al., 2016; Eggesbø et al., 2019; Mayassi et al., 2019), a subset that responds to epithelial cell BTNL3 via super antigen-like binding to Vγ4 TCR (Willcox et al., 2019).

In active CD, TRDV1 and TRDV3-expressing γδ T cells are increased in the mucosa(Deusch et al., 1991; Dunne et al., 2013; Falk et al., 2008). There is a reduction in the proportion of TRGV4-expressing γδ T cells, with a concomitant increase in the proportion expressing TRGV2 or TRGV3(Eggesbø et al., 2019; Mayassi et al., 2019). In both health and CD, the CDR3γ repertoires in the small intestine contain public sequences, although these public sequences are not CD-specific, and display near-germline sequences, so are probably generated by chance(Eggesbø et al., 2019). There is contradictory evidence of the presence of CD-associated CDR3 motifs. Activated, gut-homing γδ T cells in the blood following gluten challenge show enrichment of particular CDR3δ motifs(Han et al., 2013), while a pro-inflammatory, IFNγ-producing Vδ1+ population bearing a particular CDR3γ motif has been identified in the duodenal mucosa(Mayassi et al., 2019). While these results are suggestive of antigen-specific clonotypes in CD, other studies have not replicated these findings, while TCR repertoire diversity in the mucosa paradoxically increases in CD(Eggesbø et al., 2019; Mayassi et al., 2019). These contradictory observations may point to fundamental differences in γδ T cell behaviour, in particular their ingress to inflamed tissue.

Despite recognition of the association between CD and γδ T cells for over 30 years, their role in CD remains unclear. While intestinal γδ T IELs show pro-inflammatory IFNγ production following gluten challenge(Mayassi et al., 2019), and gut-derived γδ T cell lines can respond to gluten stimulation *ex vivo*(Steenholt et al., 2017), it remains unclear if direct responses to gluten by γδ T cells play a role in CD. Vδ1+ γδ T IELs display altered phenotype in coeliac disease, with a loss of an NK-like population expressing NKp44 and NKp46(Mayassi et al., 2019). In parallel, these Vδ1+ γδ T IELs demonstrate changes in gene expression, with down regulation of gene sets associated with tissue repair and NK function, and up regulation of gene sets associated with TCR signalling and cytokine production.

These data would be consistent with the loss of an NK-like natural IEL γδ T cell population with tissue repair properties, and their replacement with a pro-inflammatory population of γδ T cells that contribute to inflammation. However, in vitro work has shown that γδ T IELs can suppress cytotoxic T IELs via TGF-β production in response to enterocyte-derived HLA-E, suggesting a regulatory role in disease(Bhagat et al., 2008).

In sum, while the association between CD and γδ T cells is clear, their role in pathogenesis remains opaque. Previous work indicates the potential for complex pro-inflammatory and regulatory/tissue repair roles in coeliac disease, although whether this is gluten-driven, TCR-mediated, or a cytokine-mediated bystander effect remains unclear.

1.1.2.7 Putative triggers for coeliac disease development

As I have described, coeliac disease is driven by two distinct T cell populations: HLA-DQ2/8-restricted gluten-specific CD4+ T cells which produce pro inflammatory cytokines in an antigen-dependent manner, and cytotoxic CD8+ T IELs which directly drive epithelial cell damage in a TCR-independent manner. However, neither process is inevitable in individuals with CD-risk HLA alleles, and the two processes can be uncoupled, as seen in potential and refractory CD, as well as murine models. The triggers for the development of CD autoimmunity, and for epithelial cell damage, are key unknowns in our understanding of CD.

Epithelial stress, perhaps mediated via infection (particularly viral infection), is a long-standing hypothesis for what triggers CD(Lerner et al., 2017; Setty et al., 2015). The development of CD has previously been associated with infection with adenovirus(Kagnoff, 1984), enterovirus(Kahrs et al., 2019; Lindfors et al., 2020), reovirus(Tai et al., 2005), hepatitis C (albeit in the context of IFN-α therapy) (Bourlière et al., 2001; Cammarota et al., 2000), and rotavirus(Stene et al., 2006), amongst others(Lerner et al., 2017). In addition to an epidemiological association between CD and rotavirus

infection, intriguing evidence links the European rollout of rotavirus vaccination with reduced CD incidence(de Hoog et al., 2018). However, the mechanisms by which viral infection could lead to persistent loss of tolerance to dietary antigen have remained unclear until recently.

A recent study demonstrated that infection with an enterotropic strain of orthoreovirus (reovirus type 1 lang) can induce a Th1 inflammatory immune response to dietary antigen in murine models(Bouziat et al., 2017). This is mediated by changes in mesenteric LN dendritic cells (mLN DCs) in an IRF1-dependent manner, and IRF1 expression is increased in intestinal mucosa in CD(Salvati et al., 2003). These inflammatory mLN DCs prime antigen-specific CD4+ T cells to assume a pro-inflammatory phenotype, and suppress the development of tolerogenic peripheral Tregs. Intriguingly, this same viral-induced loss of tolerance to dietary antigen is seen after infection with murine norovirus strain CW3, despite being a distinct virus family (*Caliciviridae* vs *Reoviridae*) with a different structure (positive sense RNA vs double-stranded RNA) (Bouziat et al., 2018). It is therefore likely that different viral infections can induce similar host defense pathways (including those mediated by type 1 interferon), leading to differential capacity to induce loss of tolerance to dietary antigen. This may explain the lack of robust association between reovirus type 1 Lang serology and CD in humans(Bouziat et al., 2017), as multiple pathogens may be responsible for loss of tolerance. This finding may also explain prior associations with IFN-α therapy and CD (Bourlière et al., 2001; Cammarota et al., 2000).

Therefore, we can posit a model where viral (and perhaps other pathogen) infection can induce a loss of dietary tolerance in genetically predisposed individuals. It is unclear if infection can only induce this loss of tolerance in a particular window in development, or whether repeated infections lead to an increased risk on each subsequent exposure. It is also intriguing to speculate whether other risk factors associated with coeliac disease - birth delivery method, probiotic and antibiotic exposure, the hygiene hypothesis, and latitude(Kemppainen et al., 2017; Koletzko et al., 2018;

Kondrashova et al., 2009; Mårild et al., 2013; 2012; Unalp-Arida et al., 2017; Uusitalo et al., 2019) - mediate their effect via altered risk of viral infections during susceptible periods.

1.1.3 Conclusions

Arguably we know more about the pathogenesis of coeliac disease than about any other immune-mediated process, in particular understanding the culprit antigen, and the molecular mechanisms by which it causes disease. However, despite this understanding, recent therapeutic trials targeting gluten degradation, gluten-specific CD4+ T cell tolerance, and IL-15-driven CD8+ T IEL cytotoxicity have not been successful(Cellier et al., 2019; Lähdeaho et al., 2019; Mitchell and Garg, 2019; Murray et al., 2017; Truitt and R. P. Anderson, 2019). The disappointing results of the Nexvax2 peptide vaccine suggest that tolerogenic mechanisms seen in peripheral immune responses may be different in the intestinal mucosa, perhaps due to the characteristics of tissue-resident T cell populations. Similarly, the failure of anti-IL-15 therapy to reduce IEL numbers or improve villous atrophy suggests that the drivers of the CD8+ T cell response are more complex *in vivo*, and that additional, redundant mechanisms maintain inflammation in the epithelial compartment.

In addition, much remains unclear about the triggers for CD autoimmunity and epithelial stress that are posited to lead to CD. While epidemiological data and murine studies indicate a role for viral infection, it remains unclear how this translates to CD development in humans, and how this could lead to preventative or therapeutic strategies. Repeated enteric viral infection is the norm through childhood, and specific viruses linked to CD (e.g. rotavirus, enterovirus, and reovirus) are commonly-encountered pathogens. Moreover, the increased incidence of CD in the developed world, despite the reduced number of enteric viral infections in those societies, points to a more complex interaction between viral infection and host defense that triggers CD.

Addressing these unanswered questions about the pathogenesis of CD may provide direct benefits in terms of diagnostic, therapeutic, and preventative strategies for CD. Moreover, the understanding of coeliac disease may provide insights into other inflammatory and autoimmune diseases, within the gut and beyond.

1.2 Biology of γδ T cells in humans

The gamma-delta (γδ) T lymphocytes form a subset of unconventional T cells, a diverse family that recognise antigen without presentation by MHC molecules(Godfrey et al., 2015). While γδ T cells constitute only 1-5% of the circulating lymphocytes in humans, they are more common in barrier tissues. γδ T cells display features of both adaptive and innate immune cells, and can have both direct, cytotoxic effector functions, as well as indirect actions via cytokine and chemokine-mediated activation of other immune cell types. They have pleiotropic roles in mediating inflammatory processes, direct clearance of pathogens, tissue stress responses, and tissue homeostasis. This review will focus on the development, TCR repertoire, function, and heterogeneity of γδ T cells in humans, as well as shared aspects of their biology with other innate-like T cell subsets. Murine γδ T cell biology will not be covered in detail, as mice lack the phosphoantigen (pAg) responsive Vδ2+ T cell subset which became a particular focus of my research (Chapter 5).

A note on nomenclature

In the late 1980s, two competing nomenclatures for TRGV genes were in use. Unfortunately this continues to cause confusion, in particular because the γ-chain of the semi-invariant Vδ2+ T cell subset is referred to as either Vγ9 or Vγ2 by the Lefranc and Strauss nomenclature

respectively(LeFranc et al., 1986; Strauss et al., 1987). Within this thesis, either the Lefranc or IMGT designations are used(LeFranc, 2011).

Table 1-1: TRGV nomenclature.

Lefranc (LeFranc et al., 1986)	Strauss (Strauss et al., 1987)	IMGT (LeFranc, 2011)
Vγ1	*Vγ1.1*	*TRGV1*
Vγ2	**Vγ1.2**	**TRGV2**
Vγ3	**Vγ1.3**	**TRGV3**
Vγ4	**Vγ1.4**	**TRGV4**
Vγ5	**Vγ1.5**	**TRGV5**
Vγ5p	*Vγ1.5*	*TRGV5P*
Vγ6	*Vγ1.6*	*TRGV6*
Vγ7	*Vγ1.7*	*TRGV7*
Vγ8	**Vγ1.8**	**TRGV8**
Vγ9	**Vγ2**	**TRGV9**
Vγ10	*Vγ3*	*TRGV10*
Vγ11	*Vγ4*	*TRGV11*

IMGT, ImMunoGeneTics information system®. Genes in **bold** are functional genes. Genes in *italic* are non-functional/pseudogenes.

Evolution of γδ T cells

In humans, three groups of lymphocytes with rearranged, hyper-variable receptors make up the adaptive immune system: the antibody-producing B cells, and two populations of T cells expressing either αβ or γδ TCR. It is striking to note that this division of immunological labour has been conserved since the origins of jawed vertebrates, over 400 million years ago(Hirano et al., 2013; Rast et al., 1997). Such long-lived evolutionary conservation indicates that γδ T cells provide non-redundant immunological functions and consequent survival advantages.

γδ T cells in humans

There are two major subsets of human γδ T cells, identified by their TRDV chain use. Most circulating γδ T cells are ***Vδ2+ T cells***, and express a semi-invariant Vδ2+Vγ9+ TCR, which is stimulated by

microbial and endogenous phosphoantigen (pAg). This allows Vδ2+ T cells to respond to bacterial or parasitic infection, as well as stressed infected or malignant cells.

In contrast, non-Vδ2Vγ9 γδ T cells display fundamentally different characteristics. I will use the term ***non-Vδ2 T cells*** to describe these cells, although the recent identification of a small population of Vδ2+Vγ9- T cells that behave in a manner similar to other non-Vδ2 T cells complicates the already challenging γδ nomenclature(Davey et al., 2018b). Non-Vδ2 T cells are more common at mucosal sites and predominate in the gut. Few ligands have been well-characterised, but those that have are diverse and include stress-induced self-antigens and some lipid molecules presented on CD1c or CD1d(Roy et al., 2016; Vermijlen et al., 2018). Non-Vδ2 T cells display a biology much more analogous to adaptive conventional T cells, in contrast to the innate-like biology of their Vδ2+ counterparts, and have roles in CMV responses, tumour surveillance, and immune regulation. Putative subsets of Vδ2+ and non-Vδ2 T cells, as defined by TCR usage and function, are described in Table 1-2.

Table 1-2: Human γδ T cell subsets defined by TCR repertoire (modified from Fichtner et al., 2020)

Subset	TCRγ repertoire	TCRδ repertoire	Location and function	Reference
Adult Vδ2Vγ9+	Semi-invariant TRGV9/TRGJP 14aa CDR3γ length Small number of N additions	TRDV2/TRDJ1 Private, diverse CDR3δ Longer CDR3δ lengths	pAg reactive Post-natal thymic origin Polyclonal expansion	(Papadopoulou et al., 2019) (Willcox et al., 2018)
Foetal Vδ2Vγ9+	Semi-invariant TRGV9/TRGJP 14aa CDR3γ length Small number of P additions	TRDV2/TRDJ3 Private and shared CDR3δ Shorter CDR3δ lengths	pAg reactive Pre-natal thymic origin Extra-thymic post-natal polyclonal expansion	(Papadopoulou et al., 2019) (Willcox et al., 2018) (Fichtner et al., 2020)
Vδ1+	Diverse and private TRGV usage	Private TRDV1 usage	Predominant non-Vδ2+ subset in blood Common in tissue Clonal expansion in CMV infection	(Hunter et al., 2018) (Ravens et al., 2017)
Vδ3+	Diverse and private TRGV usage	Private TRDV3 usage	Clonal expansion post HCV Vδ3+Vγ8+ responds to annexin A2	(Marlin et al., 2017) (Davey et al., 2017) (Ravens et al., 2018)
Vδ2+Vγ9-	Diverse and private TRGV usage	TRDV2	Clonal expansion in CMV infection Liver-infiltrating phenotype	(Davey et al., 2018a) (Davey et al., 2018b)
Vδ1+Vγ4+	Public TRGV4	Private TRDV1	Clonal expansion Intestinal IEL population Population lost in coeliac disease BTNL3-restricted	(Mayassi et al., 2019) (Eggesbø et al., 2019) (Willcox et al., 2019)
Foetal Vγ8+	TRGV8/TRGJP1 Public CDR3γ Short CDR3γ	TRDV1 or TRDV2 Public CDR3δ Short CDR3δ	Only present in foetal life CMV-responsive Lin 28b modulated	(Tieppo et al., 2019) (Vermijlen et al., 2010)

1.2.1 Vδ2+ T cells in humans

Human Vδ2+ T cells are uniquely activated by non-peptide pAg, of both exogenous and endogenous origin. Pathogens, including *Plasmodium falciparum*, many bacteria, and *Toxoplasma gondii*, synthesise (E)-4-hydroxy- 3-methyl-but-2-enyl pyrophosphate (HMB-PP), an intermediate in isoprenoid biosynthesis, which is a highly potent exogenous ligand(Deroost and Langhorne, 2018; Howard et al., 2018; Vermijlen et al., 2018). In addition, Vδ2+ T cells are also activated by isopentyl pyrophosphate (IPP), which accumulates in malignant or stressed eukaryotic cells(Gober et al., 2003), or after exposure to aminobisphosphonates(Thompson et al., 2006).

Butyrophilin 3 receptors (BTN3) play a key role in pAg sensing and Vδ2+ T cell activation, but do not act as conventional antigen-presenting molecules. BTN3A proteins are unrelated to MHC molecules, and instead contain Ig-like extracellular domains similar to the B7 protein superfamily. In humans, hominoids and Old World monkeys, there are 3 BTN3 genes: BTN3A1, BTN3A2, and BTN3A3(Afrache et al., 2017). BTN3A1 possesses a cytoplasmic histidine-containing B30.2 domain which binds pAg directly, and induces a conformational change in both cytoplasmic and extracellular domains(Gu et al., 2017; Harly et al., 2012). BTN3A1 is necessary but not sufficient for Vδ2+ T cell activation by pAg, and BTN2A1 is also required. BTN2A1 interacts with BTN3A1, with their cytoplasmic domains in close proximity. While the BTN3A1 molecule interacts with the δ-chain CDR2 and the γ-chain CDR3 and is required for pAg sensing, the BTN2A1 molecule interacts with the side of the TCRγ chain, distinct from the CDRs, and it is this combined interaction that leads to Vδ2+ T cell TCR stimulation(Rigau et al., 2020).

At one point, pAg-responsive Vδ2 T cells were thought to be restricted to primates. However, several species of placental mammals possess both Vδ2 ,Vγ9, and BTN3 orthologues(Fichtner et al., 2018; Karunakaran et al., 2014), and the alpaca (*Vicugna pacos*) possesses circulating γδ T cells

which respond and proliferate to pAg(Fichtner et al., 2020b). This suggests the origin of this pAg-sensing subset much older, with secondary loss in some mammalian lineages, including the rodents.

1.2.1.1 Vδ2+ T cell development and the Vδ2+Vγ9+ TCR

Murine γδ T cell populations emerge as pre-expanded effector cells, and migrate to specific tissues. Of particular interest, these tissue-specific populations have predefined oligoclonal TCR repertoires using specific TRGV genes; for instance, intestinal IELs in mice express the Vγ7 chain, skin epidermal γδ T cells express the Vγ5 chain, and other V gene usage is associated with differential functionality(Hartwig et al., 2015; Murphy et al., 2014; Ramírez-Valle et al., 2015; Sheridan et al., 2013).

There is emerging evidence that human γδ T cells emerge in developmental waves with some analogies to mice(Fichtner et al., 2020c). Vδ2+ T cells appear early in foetal life, before 20 weeks' gestation, and remain the dominant subset until the third trimester(Dimova et al., 2015). These foetal γδ T cells are pre-programmed to respond to pAg, produce IFNγ on stimulation, possess an effector phenotype as seen in post-natal Vδ2+ T cells, with hypothesised roles against congenital infection(Cairo et al., 2013; Papadopoulou et al., 2019).

The semi-invariant Vδ2+Vγ9+ TCR expresses a γ-chain formed of the TRGV9 and TRGJP segments. The chain is predominantly germline encoded, with a homogeneous CDR3γ length and similar sequence, and a broadly public repertoire in both foetal and post-natal life(Dimova et al., 2015; Willcox et al., 2018). There are subtle differences in foetal and adult Vδ2+ T cells. Foetal Vδ2+ T cells have few N additions, but some short palindromic repeats, and the TRDV2 segment preferentially with TRDJ3. In contrast, the post-natal Vδ2+ T cells have more N additions in their junctional regions, and the TRDV2 segment typically pairs with TRDJ1(Fichtner et al., 2020a; Papadopoulou et al., 2019). It remains unclear if these differences alter their functional responses to pAg. This indicates that

their development is distinct, and that the adult Vδ2+ T cell population is derived from the small Vδ2+ thymocyte population, rather than from extra-thymic expansion of foetal-derived Vδ2+ T cells.

1.2.1.2 Vδ2+ T cells in human disease

Vδ2+ T cells provide defense against pAg-producing pathogens, including malaria(Deroost and Langhorne, 2018; Howard et al., 2018), bacterial infection(Caccamo et al., 2011), toxoplasmosis(Vermijlen et al., 2018), and tuberculosis(Kabelitz et al., 1991). However, Vδ2+ T cells also exhibit antiviral functionality, including against influenza, dengue virus, and HIV(Juno and Kent, 2020; Qin et al., 2012; Tsai et al., 2015). γδ T cells are considered attractive candidates for cellular immunotherapies to control HIV infection. Vδ2+ T cells kill HIV-infected cells, elite viral controllers have higher circulating Vδ2+ T cell frequencies, and Vδ2+ T cells may play a role in protection against infection(Juno and Kent, 2020). The manner of infected cell recognition, the particular receptors most relevant to direct cytotoxicity, and the role of antibody-dependent cytotoxicity remains incompletely understood. This may be via endogenous pAg production by stressed infected cells(Jameson et al., 2010), or TCR-independent signalling mediated by combinatorial cytokine stimulation in a manner analogous to MAIT cells(Tsai et al., 2015).

While cancer cells can accumulate the endogenous pAg IPP, the role of Vδ2+ T cells in anti-tumour responses is unclear(Raverdeau et al., 2019). However, their capacity for cytotoxicity, and the ability to expand and activate cells *ex vivo* using aminobisphosphonates, make them an attractive substrate for cellular therapies for cancer(Hoeres et al., 2018; Pauza et al., 2018). Vδ2+ T cells may also have a role in autoimmunity(Kenna et al., 2012; C. T. Nguyen et al., 2019).

1.2.1.3 Vδ2+ T cell function and phenotype

Vδ2+ T cells have potent cytotoxic function, mediated both through the release of cytotoxic molecules, such as granzymes and perforin, and via expressed ligands for apoptosis-inducing receptors on target cells. Cytotoxic function can be TCR-dependent, or triggered via NK receptors such as NKG2D (Rincon-Orozco et al., 2005). Vδ2+ T cells can express CD16, which identifies a highly cytotoxic population that can kill target cells via antibody-dependent cellular toxicity (ADCC) (Angelini et al., 2004). Vδ2+ T cells also exhibit remarkable plasticity in their cytokine responses to stimuli, based on their microenvironment(Kabelitz and He, 2012; Patil et al., 2016; Vermijlen et al., 2007).

While activation can induce HLA Class II molecule expression on most T cells, Vδ2+ T cells possess antigen presenting functions typically associated with professional APCs(Brandes et al., 2005; Himoudi et al., 2012; Y. Wu et al., 2009). Vδ2+ T cells can phagocytose, degrade, and process extracellular debris and viral material, and present antigen both to CD4+ T cells and cross-present to CD8+ αβ T cells in an HLA Class I-dependent manner. These characteristics, along with their inherent cytotoxicity, make Vδ2+ T cells attractive candidates for anti-cancer cellular therapies.

1.2.1.4 Phenotypic and functional heterogeneity of Vδ2+ T cells

Several classification systems which identify putative Vδ2+ subsets have been proposed to explain this phenotypic and functional heterogeneity(Dieli et al., 2003; Ryan et al., 2016; Wistuba-Hamprecht et al., 2015; Wragg et al., 2020). These subsets differ in their proliferative capacity, response to TCR stimulation, cytotoxic granule production, chemokine and cytokine receptor expression, and cytotoxicity(Ryan et al., 2016; Wragg et al., 2020). Differences in gene expression between putative subsets have also been described. However, to what extent these competing classification systems describe the underlying heterogeneity within Vδ2+ T cell populations remains

unclear; indeed whether this heterogeneity is best conceptualised as discrete cell subsets, a phenotypic spectrum, or functional plasticity is unknown(Kabelitz and He, 2012). Understanding Vδ2+ T cell heterogeneity is of particular interest given their potential in oncological therapy, where phenotypes are associated with different cytotoxic potential may explain lacklustre results from early trials(Hoeres et al., 2018; Pauza et al., 2018).

1.2.1.5 Vδ2+ T cells and the wider innate-like T cell family

In humans, a group of innate-like T cell subsets possess the capacity for activation independent of TCR ligation, a characteristic not shared by most conventional T cells(Godfrey et al., 2015; Provine and Klenerman, 2020). In particular, mucosal-associated invariant T (MAIT) cells, the most common innate-like T cell subset in humans, can be activated by combinatorial cytokine stimulation, with the invariant natural killer T (iNKT) cells also showing this capacity(Ussher et al., 2013; van Wilgenburg et al., 2016). Vδ2+ T cells also share this property, and are found at similar frequency to MAIT cells(Provine et al., 2018; Tsai et al., 2015). This TCR-independent stimulation requires at least two cytokines; stimulation with IL-12 plus IL-15 or IL-18 results in robust IFNγ production(van Wilgenburg et al., 2016).

These three T cell populations share several characteristics (Table 1-3) (Godfrey et al., 2015; Provine and Klenerman, 2020). First, they all express a semi-invariant TCR. Second, they respond to small molecule pathogen or endogenous metabolites. Third, those metabolites are not presented on a conventional MHC molecule, mediated instead by an MHC-like or Ig-like molecule. Fourth, these subsets are present *in utero*, where they possess an effector phenotype despite no prenatal exposure to bacterial metabolites. Fifth, these populations share transcriptional and phenotypic characteristics, including expression of the transcription factor ZBTB16, the C-type lectin-like molecule CD161, and a transcriptional programme that is associated with CD161 expression. The overlapping transcriptional, phenotypic, and functional characteristics of these innate-like T cell

suggests that they may play partially redundant roles in host defense, which is supported by the recent description of MR1 deficiency (and therefore MAIT cell deficiency) in humans associated with a compensatory increase in Vδ2+ T cell frequencies(Godfrey et al., 2015; Howson et al., 2020).

Table 1-3: Characteristics innate-like T cells (Vδ2+ T cells, MAIT cells, and iNKT cells) in comparison to non-Vδ2 γδ T cells.

	Non-Vδ2 γδ T cells	Vδ2+ γδ T cells	MAIT cells	iNKT cells
TCR	Diverse	Semi-invariant: Vδ2+Vγ9+	Semi-invariant: Vα7.2/Jα33 Vβ2/13	Semi-invariant: Vα24/Jα18 Vβ11
TCR repertoire	Private	Public	Public	Public
Antigen	Diverse (CMV, EPCR, ULBP, MICA)	Phosphoantigen (HMB-PP/IPP)	5-OP-RU (and other riboflavin metabolites)	α-GalCer
Target molecule	Various (CD1a, CD1c, CD1d, BTNLs)	BTN3A1/BTN2A1	MR1	CD1d
Development	Post-natal selection	Foetal	Foetal	Foetal
Rapid effector function	+	+++	+++	+++
Response to cytokine stim	-	+++	+++	++

1.2.2 Non-Vδ2 γδ T cells

Non-Vδ2 T cells possess a fundamentally different biology from Vδ2+ T cells(Davey et al., 2018a). Non-Vδ2 T cells are less common in blood, but enriched in tissue, particularly mucosal barrier sites. While the striking association of TCR sequence and mucosal site seen in mice is not mirrored in

humans, some associations between TCR V gene usage and tissue are seen. Vγ4+ populations are enriched in the healthy gut(Willcox et al., 2019), while Vδ2+Vγ9- T cells favour the liver(Davey et al., 2018b).

In contrast to Vδ2+ T cells, non-Vδ2 T cells possess a remarkably diverse TCR repertoire and ligands. Several of these ligands facilitate the recognition of cellular stress, including annexin A2(Marlin et al., 2017) and the epithelial protein C receptor(Willcox et al., 2012), as well as the MHC Class I chain-related (MIC) proteins A and B(B. Xu et al., 2011), and endogenous glycolipids presented on CD1 molecules(Bai et al., 2012; Luoma et al., 2013). Some non-Vδ2 T cell populations also interact with butyrophilin-like (BTNL) molecules. Human Vγ4+ T cells bind to a BTNL3/BTNL8 heterodimer, and tissue-specific BTNL expression may shape γδ T cell repertoires in different organ compartments(Di Marco Barros et al., 2016; Willcox et al., 2019).

Individual non-Vδ2 T cell TCRs possess the capacity to recognise multiple ligands, often in atypical ways that do not involve the CDR3 region, or the binding site of the ligand. For instance the Vγ4+ T cell clone that binds EPCR in a CDR3-dependent manner can also respond to BTNL3-8 heterodimers in a super-antigen-like, CDR3-independent manner(Willcox et al., 2019).

In sum, non-Vδ2 T cell TCR ligands are incompletely understood, and challenge the assumed conventions of TCR recognition. However, the recognition of cellular stress seems to be central to their role.

1.2.2.1 Non-Vδ2 T cell phenotype

Non-Vδ2 T cells display an adaptive immunobiology much more akin to conventional T cells, albeit without MHC restriction. The foetal TCR repertoire is highly diverse, with cells exhibiting a naive CD27hi phenotype, with expression of lymphoid-homing molecules (CCR7 and CD62L) and high proliferative capacity(Davey et al., 2017). This develops into a highly focused TCR repertoire in most,

but not all, adults (partly related to CMV exposure), a transition associated with a memory CD27lo/neg phenotype which expresses cytotoxic granzymes and perforins, responds robustly to TCR stimulation, and expresses tissue-homing chemokine receptors.

1.2.2.2 Non-Vδ2 T cells in human disease

The immunological role of non-Vδ2 T cells is best understood in CMV infection. Both Vδ1+ and Vδ3+ T cells increase in the blood following CMV infection(Davey et al., 2017; Déchanet et al., 1999), associated with clonotypic focusing of the TCR repertoire, expansion of a few dominant clones, and accompanying phenotypic change from a CD27hi naive to CD27lo/neg memory phenotype(Davey et al., 2017). This, in combination with changes to the TCR repertoire and *in vitro* evidence of TCR-dependant γδ T cell expansion upon CMV exposure, is consistent with an *in vivo* antigen-driven TCR-mediated selection and expansion of non-Vδ2 γδ T cells in CMV infection(Déchanet et al., 1999).

Non-Vδ2 T cells may also have a role in other infections(Fenoglio et al., 2009), haematopoetic-stem-cell transplantation(Hirokawa et al., 2000), and anti-tumour responses(Mikulak et al., 2019; P. Wu et al., 2014). Indeed a γδ T cell gene signature identified in multiple tumour types is associated with patient survival, suggesting that they play a key role in the intra-tumoral environment(Gentles et al., 2015).

1.2.3 Conclusions

Our understanding of the biology of γδ T cells in humans, and their role in disease, is incomplete, with their study made harder by the lack of an analogous pAg-sensing Vδ2+ T cell population in mice, and the non-MHC-restricted diverse ligands of the non-Vδ2 T cell subset. However, mounting evidence points to their importance in infection and malignancy.

Two important questions remain unanswered for Vδ2+ T cells. First, their phenotypic and functional heterogeneity, as well as the underlying genetic control of such heterogeneity, is incompletely understood. This may have implications for our understanding of Vδ2+ T cell function in infectious disease *in vivo*, and cellular therapies for cancer. Second, the increasing recognition of analogous functionality between Vδ2+ T cells and other innate-like T cells raises questions about their degree of transcriptional and functional similarity, and to what extent these cell types possess analogous, or even redundant, role in humans.

Much of the fundamental biology of non-Vδ2 T cells in humans remains unanswered, most notably their antigens/ligands. In addition, questions remain about the tissue-homing and retention pathways involved in non-Vδ2+ T cell populations found in tissues, including in the gut, and their functional roles in those tissues.

1.3 Tissue-resident memory T cells

The development of long-term immunological memory is the key role of the adaptive immune system. Classically, initial antigen challenge of naive T cells in secondary lymphoid organs leads to the development of effector T (T_E) cells, short-lived populations which down-regulate markers facilitating lymph node entry, and instead express addressins that permit access to peripheral tissues. Following antigen clearance, this population undergoes contraction, with the simultaneous development of a central memory T (T_{CM}) cell population of long-lived cells which express lymph node-homing molecules, and have high proliferative capacity, and an effector memory T (T_{EM}) cell population with low proliferative capacity, which continue to patrol peripheral tissues.

These populations were classically believed to form the core of long-term cellular immunological memory. However, in the last two decades it has become clear that T_E cells can develop into another long-lived subset, tissue-resident memory T (T_{RM}) cells. T_{RM} cells are a subset of long-lived T cells that reside in tissue and do not recirculate, acting as localised sentinels of the adaptive immune system, with memory of prior antigen exposure (Mackay and Kallies, 2017; Szabo et al., 2019).
I will briefly discuss the key characteristics of T_{RM} cells identified from murine studies, the challenges of research on human T_{RM} cells, transcriptional and phenotypic heterogeneity of T_{RM} cells, and the emerging evidence of T_{RM} involvement in human disease, including autoimmunity, coeliac disease, and intestinal transplantation.

1.3.1 Characteristics of T_{RM} cells in mice and humans

The very nature of T_{RM} cells - a commitment to residence in a particular tissue without recirculation - creates challenges to their study. Several techniques in mice have been used to uncover the fundamental biology of *bona fide* murine T_{RM} cells. This includes transplantation or parabiosis between congenic strains(Gebhardt et al., 2009; Jiang et al., 2012), and intravascular labelling of

circulating cells(Steinert et al., 2015), methods which allow the identification of definitely resident T cells. In humans, the study of T_{RM} cells provides a particular challenge, as the experimental murine tools of parabiosis and intravascular labelling are clearly not available. However, organ transplantation can be used as a fortuitous natural experiment for the study of tissue residency. Donor and recipient immune cell populations can be studied where HLA- or sex-mismatch between donor and recipient exists. Such studies have shown convincing evidence for the persistence of donor-origin T cells for years following skin(Lian et al., 2014), lung(Snyder et al., 2019), kidney(de Leur et al., 2019), and intestinal transplantation(Bartolomé-Casado et al., 2019; Zuber et al., 2016).

T_{RM} cells possess a phenotype that precludes their recirculation in blood vessels or lymphatics. Endothelial cells produce sphingosine-1-phosphate (S1P), a chemoattractant which promotes tissue egress(Mandala, 2002). T_{RM} cells downregulate S1P receptors (via the transcription factor Krueppel-like factor 2 (KLF2), and direct antagonism by CD69) (Mackay et al., 2015a; Skon et al., 2013), and do not express L-selectin (CD62L) and CCR7, lymph node-homing molecules(Mackay et al., 2013). This phenotype effectively traps the cell in the tissue by removing the physiological mechanisms for tissue egress.

Murine models have provided insight into the process of acquisition of a T_{RM} phenotype. This requires a particular local cytokine milieu, including tumour growth factor β (TGFβ) and IL-15, which contribute to T_{RM} development in the lung, skin, and intestine(Mackay et al., 2013). T_{RM} cells develop from early KLRG1- effector T_E cells, rather than mature or terminally differentiated T_{EM} cells or T_{CM} cells(Mackay et al., 2013; Milner et al., 2017). T_{RM} cells do not undergo the rapid contraction that T_{EM} populations do, although numbers of virus-specific T_{RM} cells in tissue do wane over time(Slütter et al., 2017).

Recent evidence indicates that T_{RM} cells may display greater phenotypic plasticity than was previously thought, and that both tissue egress, and differentiation into different memory subsets, may be possible in certain situations. Infection/reinfection studies indicate that after reinfection, some T_{RM} cells can exit tissue and generate a secondary memory subset with a T_{EM} phenotype(Behr et al., 2020).

The canonical markers of T_{RM} cells, identified from murine parabiosis studies initially, are CD69 and αE integrin (CD103). While CD69 is expressed on virtually all CD4+ and CD8+ T_{RM} cells in tissues, CD103 is only expressed on some CD8+ T_{RM} cells, and on the minority of CD4+ T_{RM} cells(Jiang et al., 2012; Kumar et al., 2017; Mackay et al., 2016; Turner et al., 2019). Other markers associated with T_{RM} cells include CD49a (*ITGA1*), CD101, PD-1, and CXCR6 (Cheuk et al., 2017; Kumar et al., 2017; Weisberg et al., 2019).

Despite this strong association between CD69 expression and residency, and the use of CD69 as a residency marker for identification of T_{RM} cells in most human studies, the functional role of CD69 in residency, and its use as a residency marker, has been questioned. CD69 is not required for the development of functional T_{RM} cells in mice (Shiow et al., 2006; Walsh et al., 2019). CD69 can be induced by cytokine stimulation(Freeman et al., 2012), and a proportion of CD69+ T cells in tissue are not resident, making CD69 a suboptimal residency marker (Beura et al., 2018; Sancho et al., 2005; Shiow et al., 2006). Moreover, CD69- cells are found in tissue, and it may be that CD69- T cells can be resident. Indeed, the persistence of CD69- donor-derived T cells in transplanted human lung for up to 12 months post-transplant indicates that the use of CD69 alone as a marker of residency may be flawed in some tissues(Snyder et al., 2019). Therefore, additional phenotypic markers to unequivocally identify CD103- T_{RM} populations are required.

From murine studies, a picture of key regulators of T_{RM} cell biology is emerging. T_{RM} cells display a distinct transcriptional program, with many elements conserved between tissues(Mackay et al., 2013). A specific transcriptional program, regulated by the TFs Hobit and Blimp-1, is shared not only by T_{RM} cells, but also other resident lymphocytes, including NK cells and NKT cells(Mackay et al., 2016). For the development of CD103+ CD8+ T_{RM} cells, the expression of the T-box TF Eomesodermin (Eomes) is effectively extinguished, facilitating effective TGFβ signalling, needed for T_{RM} development. T-bet, a TF homolog of Eomes, is down-regulated but its expression maintained, which is required for effective IL-15 sensing, which drives long-term survival in tissue(Mackay et al., 2015b). Several other TFs play key roles in mice: Runx3 is required T_{RM} development(Milner et al., 2017), Bhlhe40 plays roles in both T_{RM} development and functionality(C. Li et al., 2019), while the aryl hydrocarbon receptor supports T_{RM} cell maintenance(Zaid et al., 2014).

Human T_{RM} cells also share a common transcriptional profile, with some similarity to that of murine T_{RM} cells(Kumar et al., 2017). However differences do exist, including the expression of the key murine TF associated with residency, Hobit (human ortholog gene *ZNF683*), which has not been shown to be upregulated in human T_{RM} cells. As such, it is clear that murine studies alone cannot completely explain human T_{RM} development and function.

The potent pro-inflammatory and cytotoxic characteristics of T_{RM} cells are kept in check by co-inhibitory and co-stimulatory receptors, with CTLA4, ICOS, PDCD1, CD101, and several SLAM receptors identified in both human and murine T_{RM} gene sets(Kumar et al., 2017; Mackay et al., 2013). The expression of PD-1 by human TRM cells suggests that this population is carefully regulated to prevent inappropriate activation. The expression of immune checkpoints is routinely associated with T cell exhaustion or dysfunction, phenomena seen in the context of chronic (viral) infection and malignancy(Philip and Schietinger, 2019). However, T_{RM} cells remain polyfunctional effector cells and maintain their proliferative capacity, unlike exhausted populations. Moreover, it

remains unclear if the processes of exhaustion and dysfunction, or the converse process of memory inflation(Klenerman, 2018), occur in T_{RM} cells.

1.3.2 Heterogeneity in T_{RM} cells

Murine work has highlighted the existence of transcriptionally distinct intestinal T_{RM} cell populations. Two recent studies employing scRNAseq in the context of the murine LCMV Armstrong model of tissue residency, identified two transcriptionally distinct populations of small intestinal T_{RM} cells, with differences in transcription factor expression, phenotype, cytokine production, and persistence(Kurd et al., 2020; Milner et al., 2020). While a recent human study of *bona fide* lung T_{RM} cells following lung transplantation indicated transcriptional heterogeneity in a limited scRNAseq experiment, this has not been shown for intestinal T_{RM} cells(Snyder et al., 2019). Moreover, it is unclear whether any transcriptional heterogeneity in human T_{RM} cells corresponds to murine T_{RM} subsets, and if murine findings can be extrapolated to human studies.

Human T_{RM} cells demonstrate functional and phenotypic heterogeneity. In skin, CD8+ T_{RM} cells can be divided by CD49a (α1-integrin) and CD103 expression. CD49a+ T_{RM} cells secrete IFN-γ and produce perforin, while CD49a- populations have a Tc17 phenotype(Cheuk et al., 2017). CD103+ T_{RM} cells possess greater effector functionality, but reduced proliferative capacity to CD103- counterparts(Watanabe et al., 2015). Human T_{RM} cells with the ability to efflux fluorescent dyes (a characteristic of haematopoietic stem cells, mediated by their expression of ATP-binding cassette family multi drug transporters) show differences in phenotype, expression of the senescence marker CD57, and cytokine production compared to efflux-negative T_{RM} counterparts from the spleen(Kumar et al., 2018). Within the intestine, CD103+, CD103- KLRG1+ and CD103-KLRG1- CD8+ T_{RM} cells have been shown to differ in phenotype and cytokine production potential(Bartolomé-Casado et al., 2019). However, it remains unclear to what extent this phenotypic heterogeneity is due to underlying transcriptional variation.

1.3.3 T_{RM} cells in human disease

T_{RM} cells protect against repeated infection (bacterial and viral) and cancer progression in mice (Gebhardt et al., 2011; Schenkel et al., 2014). T_{RM} cells are potent cytokine producers upon repeat stimulation, proliferate when challenged, and act as sentinels in mucosal tissues, recruiting circulating populations to the inflamed tissue. These diverse roles in mouse models have triggered great interest in the role of human T_{RM} cells in these settings. I will review the key roles of human T_{RM} cells in disease, with limited reference to murine studies. It should be noted that in the following studies, human T_{RM} cells have been defined as cells which phenocopy murine T_{RM} cells (e.g. CD103+), and thus are inferred to be T_{RM} cells.

1.3.3.1 T_{RM} cells in infection

T_{RM} cells, resident at the front-line of immunological defence, and armed with rapid effector functions, are well-placed as sentinels against pathogens. As discussed earlier, two key characteristics of the T cell response to chronic infection - exhaustion and memory inflation - are not well-understood in the context of T_{RM} cells.

Viral infection

The roles of T_{RM} cells in mice and men are best understood in the context of viral infection. Lung T_{RM} cells have key roles in the immune response to influenza. Virus-specific T_{RM} cells are found in the human lung, and play a role in the acute infection(Koutsakos et al., 2019). Influenza-specific T_{RM} cells are potent producers of pro-inflammatory cytokines. Influenza-specific T_{RM} cells also accumulate in the lung following re-infection, although it remains unclear if T_{RM} cell populations decay over time in

humans, a process seen in mice(Slütter et al., 2017; Zens et al., 2016). These T_{RM} cell responses generate some cross-strain protection in mice, while in humans virus-specific T cells responses correlate with reduced symptoms during infection(Sridhar et al., 2019) and can also provide cross-strain protection in *ex vivo* studies(Koutsakos et al., 2019).

Similar to influenza, respiratory syncytial virus (RSV) induces virus-specific CD8+ T cells with a T_{RM} phenotype in the lung, which persist following infection, and correlate with reduced disease severity upon reinfection(Jozwik et al., 2019). Similar induction of virus-specific CD8+ T cells with a T_{RM} phenotype is seen in the female genital tract following HSV infection(Posavad et al., 2017; Zhu et al., 2007), in tonsillar tissue after EBV infection(Woodberry et al., 2005), in multiple tissues following CMV infection(Gordon et al., 2017), and in the liver after infection with hepatitis B and hepatitis C viruses (Pallett et al., 2017; Stelma et al., 2017). HIV-specific CD8+ T_{RM} cells are generated in mucosal tissue, including the intestine and female genital tract. Certain individuals are able to control HIV infection without antiviral therapy, and these elite controllers show increased numbers of CD8+ T_{RM} cells with potent cytokine responses in tissues including the intestine, suggesting T_{RM} cells play a key role in controlling viral replication(Kiniry et al., 2017).

Non-viral infection

T_{RM} cell responses to bacterial, fungal, and parasitic disease are less well-characterised, with few human studies in this field(Muruganandah et al., 2018). However, murine models have implicated T_{RM} cells in adaptive immune responses to pulmonary non-viral pathogens, including *Bordetella pertussis, Streptococcus pneumoniae*, and *Mycobacterium tuberculosis*, with evidence that these T_{RM} cells provide protection against repeat infection, or following vaccination(Hansen et al., 2018; Perdomo et al., 2016; Smith et al., 2017; Walrath et al., 2005; Wilk et al., 2017). T_{RM} cells also have roles in control of enteric infection, including *Yersinia pseudotuberculosis*(Bergsbaken and Bevan, 2015) and *Listeria monocytogenes*(Sheridan et al., 2014).

1.3.3.2 T_{RM} cells in malignancy

Tumour surveillance and the elimination of cells that have undergone malignant transformation is a key role of the immune system. Solid organ tumours are the predominant burden of human malignant disease, with many of the most common cancers developing at mucosal sites. Malignant tumours contain complex populations of immune cells, including penetrating tumour-infiltrating lymphocytes (TILs), the quantity of which is associated with improved prognosis(Rao et al., 2010). A proportion of penetrating CD8+ T cells have a T_{RM} phenotype and transcriptional profile(Milner et al., 2017). Moreover, the frequency of these T_{RM} TIL populations correlates with improved cancer survival(Djenidi et al., 2015; Webb et al., 2014).

The importance of CD103 (αE-integrin)-expressing T_{RM} TILs may be directly mediated by αEβ7-integrin expression. Integrins engage in complex, bidirectional signalling, with chemokine and TCR stimuli inducing conformational change in integrin heterodimers, facilitating their binding (inside-out signalling), while CD103 binding to its ligand, E-cadherin, can act as a TCR co-stimulus (outside-in signalling), and augment TCR-dependent cytotoxicity(Corgnac et al., 2018). T_{RM} TILs express co-inhibitory immune checkpoint molecules(Edwards et al., 2018), but, like T_{RM} cells in healthy tissues, these cells maintain their capability for cytokine production and cytotoxicity. The PD-1 expression of T_{RM} TILs may explain the efficacy of immunotherapy targeting the PD1-PDL1 axis(Ribas and Wolchok, 2018), with T_{RM} TILs proliferating soon after anti-PD-1 treatment(Edwards et al., 2018).

1.3.3.3 T_{RM} cells in autoimmunity

The presence of long-lived pro-inflammatory resident T cells in tissue raises the possibility that T_{RM} cells could drive autoimmune disorders. The expression of co-inhibitory molecules on T_{RM} cells suggests that their pro-inflammatory properties require careful control to maintain homeostasis, a

hypothesis supported by the role of T_{RM} cells in the inflammatory colitis induced following anti-PD-1 cancer therapy (Luoma et al., 2020). The understanding of the role of T_{RM} cells in autoimmunity is only just emerging, particularly in humans.

The role of T_{RM} cells in dermatological autoimmunity is best described. Psoriasis, an IL-17/IL-23-mediated autoimmune skin disease, characteristically causes inflammatory plaques, which remain the site of disease in future flares. This recurrence at a specific site, as well as experimental evidence that skin grafts from healed psoriatic lesions can transfer disease to RAG-deficient mice, suggest a role for resident T cells(Boyman et al., 2004; Ho and Kupper, 2019). Pro-inflammatory T_{RM} phenotype CD8+ T cell populations remain in the skin despite years of successful anti-TNF therapy(Cheuk et al., 2014).

T_{RM} cells also play a role in autoimmunity away from mucosal sites. T_{RM} phenotype CD8+ T cells predominate in multiple sclerosis lesions(Machado-Santos et al., 2018), and Rasmussen's encephalitis. Pancreatic T_{RM} phenotype CD8+ T cells are implicated in the insulinitic lesion in type 1 diabetes (Kuric et al., 2017; Weisberg et al., 2019).

1.3.3.4 T_{RM} cells in GI autoimmunity: IBD and coeliac disease

The GI tract is the mucosal site with greatest antigenic load from dietary antigens and commensal microbes. Localised T_{RM} responses to certain antigens may mediate autoimmunity. The antigenic triggers for inflammatory bowel disease (IBD) are not known, however a combination of dietary and microbial triggers, combined with polygenic risk factors, are likely to be the cause. One interesting phenomenon in both ulcerative colitis (UC) and Crohn's disease (CrD) is the persistence and recurrence of inflammation at specific sites. In UC, inflammation proceeds from rectum proximally along the colon, often with a sharp demarcation between inflamed and healthy tissue. While CrD can affect any part of the GI tract from mouth to anus, the pattern and location of inflammation

within a specific individual is typically stable over time. When treatments fail, inflammation returns in this segment, even after surgery.

In humans, CD103+ T_{RM} cells are increased in the intestinal mucosa in IBD, increase with duration of disease, and possess a pro-inflammatory phenotype(Zundler et al., 2019). Moreover, higher proportions of of T_{RM} cells in the tissue was associated with reduced disease-free survival. Murine studies indicate a causal relationship between T_{RM} cells and increased severity of disease in several IBD models. This role for T_{RM} cells in intestinal autoimmunity raises the possibility for therapeutics directed at resident populations. Indeed, the β7-integrin-targeting therapy etrolizumab, currently under investigation as a therapeutic in IBD, may mediate its effect through targeting T cell retention and residency, rather than through impeding ingress of T cells into tissue(Zundler et al., 2017).

Viewed through the prism of tissue residency, coeliac disease (CD) demonstrates features of an immune-mediated disorder driven, at least in part, by T_{RM} cells. First, the defined location of tissue inflammation and damage, confined to the proximal small intestine, would be consistent with T_{RM}-mediated disease. Second, ingested gluten leads to rapid immunological and symptomatic changes in patients with treated CD. Serum cytokine perturbations (particularly IL-2, IL-8, and IL-10) are detectable within two hours of gluten ingestion or gluten peptide injection, with gluten-specific CD4+ T cell-derived IL-2 strongly associated with patient-reported symptoms(Daveson et al., 2019; Truitt et al., 2019; Tye-Din et al., 2019). This rapid response is suggestive of a local tissue response to antigen exposure.

Third, key cell types involved in the pathogenesis of CD show the phenotype and functional characteristics of T_{RM} cells. Gluten-specific CD4+ T cells, the central player in CD pathogenesis, are enriched in intestinal tissue compared to blood by several orders of magnitude(Christophersen et al., 2014; Lundin, 1993; Risnes et al., 2018), and exhibit a CD4+ T_{RM} phenotype, with CD69, CD161,

and PD-1 expression(Bartolomé-Casado et al., 2020; Christophersen et al., 2019a). Remarkably, these disease-associated CD4+ T cell clones can persist in the gut for decades after diagnosis(Risnes et al., 2018). Although the role of γδ T cells in coeliac disease is not understood, CD results in a permanent reshaping of the γδ TCR repertoire, with these cells also exhibiting a T_{RM} phenotype(Mayassi et al., 2019).

Fourth, in the dynamic situation of gluten challenge, CD103+ CD38+ T cells (gluten-specific CD4+ T cells, as well as CD8+ and γδ+ T cell populations) rise dramatically in frequency 6 days after gluten challenge, consistent with previously resident cells mobilised following inflammation(Anderson et al., 2000; Han et al., 2013; Raki et al., 2007).

The understanding of how residency affects coeliac disease pathogenesis may not just be academic; it may have a bearing on potential therapeutic strategies. In particular, the discontinuation of a clinical trial of the gliadin peptide vaccination strategy (Nexvax2, ImmusanT), despite promising early results based on circulating T cell responses(Daveson et al., 2017; Truitt et al., 2019), suggests that peripheral and T_{RM} cells may differ in their response to tolerising therapies.

1.3.3.5 T_{RM} cells in transplantation

During organ transplantation, the donor immune populations within the graft are also transplanted. Persistent donor-derived T cells, unequivocal T_{RM} cells, have been found in solid organ transplant grafts for over a year post-transplantation, and provide the clearest evidence in humans for long-lived T_{RM} cells(Bartolomé-Casado et al., 2019; Snyder et al., 2019; Zuber et al., 2016).

Intestinal transplantation is an increasingly common treatment for intestinal failure. However, it confers substantial risks, with 50% of patients developing rejection and 10% graft vs host disease (GvHD) (Loo et al., 2017). Rejection is associated with a depletion of donor-derived T cells and an

infiltration of host-derived T cells, however, the role of donor-derived T_{RM} cells in rejection and GvHD is not well-explored(Zuber et al., 2016). Survival lags behind that of solid organ transplants and prevention and treatment of these complications constitutes an unmet need(Grant et al., 2014).

Intestinal transplantation offers an excellent opportunity to study intestinal T_{RM} cells, as donor-derived T cells persisting in the graft long-term by definition constitute a functionally-resident T_{RM} population. Moreover, intestinal transplants are often mismatched for Class I HLA, allowing discrimination of donor- and recipient-derived T cells by type-specific HLA antibodies in a manner analogous to tracking with congenic markers in mice(Lian et al., 2014; Zuber et al., 2016; 2015).

1.3.4 Conclusions and key questions

In the two decades since their first description, the importance of tissue-resident memory T cells in appropriate and effective immunological memory responses has been recognised, both in murine models and increasingly in human disease. While their role in infection is well-established, and their significance in cancer increasingly recognised, our understanding of what part T_{RM} cells play in autoimmunity is still in its infancy.

Despite our understanding of the distinct transcriptional, phenotypic, and functional characteristics of T_{RM} cells, much still remains unclear about their fundamental biology, particularly in humans, due to the challenges of identification of unequivocal T_{RM} populations. In particular, it remains unclear to what extent the development and transcriptional regulation of T_{RM} cells differs between mice and humans. The degree of transcriptional heterogeneity within T_{RM} populations also remains unclear, and what the implications of distinct T_{RM} cell subsets are in terms of function, proliferation, and longevity.

1.4 Thesis questions and hypotheses

My doctoral research sought to examine the role of CD8+ and γδ T cells in CD. In particular, I hypothesised that these populations may show perturbations in their TCR repertoires consistent with a TCR-dependent process. In addition, I hypothesised that intestinal CD8+ and γδ T cells would show transcriptional differences in health and disease, due to different roles in the immune response. In chapter 3, I focus on method development to achieve these aims, while in Chapter 4, I examine CD8+ and γδ T cells in CD using flow cytometry, bulk and single-cell RNA sequencing, and TCR repertoire sequencing.

The work on γδ T cells in CD led to an interest γδ T cell biology. I was particularly interested in the similarities and differences between some subsets of γδ T cells and MAIT cells. I hypothesised that Vδ2+ T cells showed unappreciated heterogeneity, with some populations sharing features with MAIT cells. In chapter 5, I examine the transcriptional, phenotypic, and functional heterogeneity of peripheral γδ T cells.

The clearly tissue resident phenotype of intestinal CD8+ and γδ T cells in CD led to a focus on intestinal T_{RM} cell biology in humans. My clinical interest in nutrition and intestinal transplantation led to a fortuitous collaboration with our clinical transplant team and a project to examine transcriptional, phenotypic, and functional heterogeneity within definitively-resident donor-derived T cells in the gut following intestinal transplantation, which is described in chapter 6.

Chapter 2: Materials and methods

2.1 Identification and consent of donors

Study subjects with suspected or diagnosed CD, and healthy controls, were identified via the Oxford University Hospitals NHS Foundation Trust (OUHFT) coeliac disease clinic or endoscopy service (Oxford, UK). Non-coeliac control study subjects were identified via the OUHFT endoscopy service. Intestinal transplant recipients were identified via the OUHFT transplantation service. Peripheral blood and intestinal biopsies were taken at the time of endoscopy under the study framework and consent of the Oxford Gastrointestinal Illnesses Biobank (REC Ref: 16/YH/0247). Peripheral blood was obtained from healthy donors, and healthy NHS blood donor leucocyte cones from NHS Blood and Transplant. Patient and sample characteristics are described in tables in each chapter.

2.2 Isolation of peripheral blood mononuclear cells (PBMCs)

Peripheral blood mononuclear cells (PBMCs) were extracted from whole blood or leucocyte cones via density gradient centrifugation. Briefly, peripheral blood was diluted 1:1 with Dulbecco's phosphate buffered saline without calcium or magnesium (PBS) and layered over Lymphoprep™ (Axis-Shield) before centrifugation (973 g for 30 minutes at 20^{o}C without brake). The mononuclear layer was retrieved and washed twice in PBS or R10 culture media (RPMI-1640 (Sigma-Aldrich), 10% foetal calf serum, 1% penicillin/streptomycin, 1% L-glutamine). Viable mononuclear cells stained with Trypan blue were counted manually by microscopy using a haemocytometer before downstream applications. If remnant red blood cells were present, they were lysed with Ammonium-Chloride-Potassium (ACK) solution for 2-3 minutes, then washed again in R10. Samples were cryopreserved in freezing medium (10% DMSO [Sigma-Aldrich], 90% FCS [Sigma-Aldrich]).

When needed, samples were thawed rapidly in a water bath (37°C), then washed twice in R10 before downstream use.

2.3 Collection of intestinal biopsy tissue

Intestinal biopsies were collected at endoscopy from duodenum, jejunum or ileum. Biopsies for intestinal lymphocyte extraction were immediately placed in sterile R10 media (as above) on ice for transportation.

2.4 Dissociation of intestinal biopsy tissue

For the extraction of total intestinal lymphocytes, biopsies were washed in R10, then placed in R10 containing 100 µg/ml DNAase I (Thermofisher Scientific) and 1mg/ml Collagenase D (Sigma-Aldrich). Biopsies were mechanically mixed using a gentle cycle on the GentleMACS™ Dissociator (Miltenyi Biotech), followed by incubation for 60 minutes in a shaking incubator (200 rpm, 37°C). Biopsies were vigorously dissociated using the GentleMACS™ Dissociator, strained through a 70 µm filter and washed 2-3 times with culture media or PBS. Depending on the downstream application and the degree of visible blood contamination, a red blood cell lysis step was performed using ACK as above. Viable mononuclear cells stained with Trypan blue were counted manually by microscopy using a haemocytometer before downstream applications.

For the extraction and separation of intraepithelial lymphocytes (IELs) and lamina propria lymphocytes (LPLs), biopsies were washed in culture media, then placed in 10 ml HBSS with 1 mM EDTA and 1 mM DTT (both Sigma-Aldrich) and placed in a shaking incubator (200 rpm, 37°C) for 15 minutes. Epithelial cells and IELs were strained through a 70 µm filter and washed 2-3 times with culture media or PBS. The remaining tissue from straining was washed again in culture media to

remove residual EDTA and DTT, before mechanical and enzymatic digestion with DNAse I/Collagenase D as above.

In experiments involving overnight culture and for some FACS sorting experiments, intestinal lymphocytes were purified by density gradient centrifugation. After DNAse/Collagenase D digestion as above, cells were washed, then suspended in 35% Percoll (GE Healthcare) and underlaid with 70% Percoll, before centrifugation at 700 g for 20 minutes at 20°C without brake. Intestinal lymphocytes were taken from the 35%/70% Percoll interface and washed once in PBS before downstream applications.

2.5 Cryopreservation of intestinal biopsy tissue

Small intestinal biopsies were collected at the time of endoscopy and transported in R10 (RPMI-1640 [Lonza] + 10% FCS [Sigma-Aldrich] + 1% penicillin/streptomycin [Sigma-Aldrich]), before cryopreservation in freezing medium (10% DMSO [Sigma-Aldrich], 90% FCS [Sigma-Aldrich]). This method preserves immune cell viability, surface marker expression, and function (Konnikova et al., 2018). When required, samples were rapidly thawed in a 37°C water bath and washed in 20 ml R10 before tissue dissociation.

For multiplex fluorescence chip cytometry, single intestinal biopsies were embedded in OCT cryo-embedding matrix (Thermo Fisher Scientific) then frozen in isopentane (Sigma-Aldrich) suspended over liquid nitrogen, and stored at -80°C until use.

2.6 Ex vivo stimulation assays

2.6.1 Cytokine and HMB-PP stimulation assays

Intestinal lymphocytes were extracted and purified by density gradient centrifugation as above. Up to $1x10^5$ intestinal mononuclear cells and $1x10^6$ PBMCs were plated in 96-well plates in complete media in the presence or absence of recombinant IL-12, IL-18, IL-15 (all R&D systems), or IFNα (Sigma), all at a final concentration of 50 ng/ml, or with (E)-1-Hydroxy-2-methyl-2-butenyl 4-pyrophosphate (HMB-PP; Sigma) at 1 nM. Cells were incubated for 20 hours at 37°C, 5% CO_2. In order to stain for intracellular cytokine production, Brefeldin A (5 μg/ml) and Monensin (2 μM) (both Biolegend) were added 4 hours before the end of incubation.

2.6.2 Plate-bound CD3 stimulation assays

For TCR stimulation assays, stimulation with plate-bound CD3 and soluble CD28 was performed. Anti-CD3 antibody (OKT3 clone; 2.5 μg/ml in D-PBS) was added to wells of uncoated MaxiSorp™ ELISA Plates (Biolegend), and incubated at 37°C for 2 hours. Wells were washed twice with D-PBS, before up to $1x10^5$ intestinal mononuclear cells or $1x10^6$ PBMCs were plated per well, along with anti-CD28 antibody at a final concentration of 1 μg/ml.

2.6.3 All-trans retinoic acid (ATRA) stimulation

Purified T cells were isolated from cryopreserved PBMCs through MACS negative selection with CD14- and CD19-conjugated magnetic beads (Miltenyi). The purified T cells ($1x10^6$/ml) were cultured in R10 media + 100 U/ml recombinant human IL-2 in 12-well plates with the following conditions: IL-2 alone; IL-2 plus plate-bound CD3 (3 μg/ml overnight) and soluble CD28 (1 mg/ml); IL-2 plus 100 nM ATRA; IL-2 plus CD3/28 plus 100 nM ATRA. Cells were incubated at 37°C and 5% CO2 for 7 days, with fresh culture media + IL-2 added after 72 hours.

2.6.4 Cellular proliferation assay

To assess cellular proliferation of Vδ2+ T cells in response to stimulation, PBMCs were stained with CellTrace™ Violet (Thermofisher Scientific) as per manufacturer's instructions. PBMCs were then stimulated for either four or seven days with cytokine, HMB-PP, or plate-bound CD3 as described above.

2.7 Flow cytometry

2.7.1 Surface staining

For surface marker staining, cells were stained in FACS buffer (PBS + 1 mM EDTA + 0.05% BSA) for 20-30 minutes at 4^{o}C, except for tetramers and antibodies for some chemokine receptors, which were stained at 37^{o}C. Surface antibodies and clones used are listed in Table 2-1. Fluorescence Minus One (FMO) controls were used for antigens of particular interest, or if needed for accurate gating.

2.7.2 Intracellular and intranuclear staining

For intracellular cytokine staining, after surface staining as above, cells were fixed and permeabilised in 100 µL Cytofix/Cytoperm solution for 20 minutes at 4^{o}C (BD Biosciences). Cells were then washed twice in Perm/Wash buffer (BD Biosciences). Intracellular staining was performed in 50 µl of Perm/Wash buffer (BD Biosciences) for 30 minutes at 4^{o}C.

Intranuclear transcription factor staining was performed following staining of surface markers as above. Cells were then fixed for 1 hour at room temperature using FoxP3 kit fixation buffer (ThermoFisher Scientific). Cells were then washed in FoxP3 kit wash buffer, then permeabilized for 1 hour at room temperature in FoxP3 kit wash buffer. Transcription factor antibodies were stained in 50 µl of FoxP3 kit Wash Buffer for 1 hour, again at room temperature, then washed in FoxP3 kit wash buffer, and resuspended in FACS buffer, before storage at 4^{o}C until acquisition.

2.7.3 Sample barcoding for flow cytometry using cellular dyes

In chapters 1 and 3, I used cellular dyes to perform multiplex flow cytometry. Once ready for staining, sample cells were washed, then resuspended in D-PBS at room temperature. Differing concentrations of CellTrace™ Violet or CellTrace™ Far Red cell dye (both Thermofisher Scientific) were added to the cells (CellTrace™ Violet 1μM, 200 nM, 40 nM and 0 nM; CellTrace™ Far Red 40 nM and 0 nM), and immediately vortexed to achieve rapid mixing. The cells were incubated at 37^{o}C for 20 minutes in the dark. After incubation, the sample was washed 3-4 times with R10, before samples were pooled for staining with antibodies for flow cytometry.

2.7.4 HLA allele congenic cell tracking

For identification of donor- and recipient-origin immune cells in blood and intestinal tissue, HLA allele congenic cell tracking was used. This uses HLA Class I mismatches between transplant donor and recipient to identify the cell origin, using fluorophore-conjugated antibodies to the relevant HLA Class I antigens. HLA typing information of transplant donors and recipients was accessed via OUHFT transplantation service and OUHFT tissue typing laboratory, from which potential mismatched HLA alleles were identified. Antibodies against HLA Class I antigens that were used for flow cytometry, FACS, and chip cytometry are listed in Table 2-1.

2.7.5 Data acquisition and instruments

After staining, cells were stored at 4^{o}C protected from light until data acquisition. Flow cytometry data were acquired on a BD LSRII flow cytometer , BD Fortessa flow cytometer (both BD Biosciences), or an Aurora spectral flow cytometer (Cytek).

2.8 Cell sorting

For fluorescence-activated cell sorting (FACS) samples were surface stained as above, with DAPI (Thermofisher Scientific) used as viability dye. FACS was performed on an AriaIII (BD Biosciences; 70 µm nozzle). Sort purity was assessed for each sort, and was >95%. Sorted cells were collected in D-PBS with 2% BSA before downstream use.

Magnetic activated cell sorting (MACS) was performed for B-cell and myeloid depletion before T cell culture with ATRA. A standard Pan T-cell microbead cocktail for T cell negative selection was not used, as this includes CD56 depletion, which is expressed by some γδ T cells. Briefly, $2x10^7$ PBMCs were incubated with CD14- and CD19-conjugated magnetic beads in MACS buffer (PBS, 0.5% BSA, 2 mM EDTA) for 15 minutes at 4°C. After washing and resuspension in MACS buffer, the stained cells were applied to a MACS LD column in a magnetic MACS separator. The flow-through was collected, washed, and used for downstream stimulation.

2.9 Effect of enzymatic digestion on cell surface markers (Chapter 3)

PBMCs ($8x10^8$) from 3 donors, isolated by density gradient centrifugation from leucocyte cones as above, were cultured for 20 hours in culture media (RPMI 1640 with 10% FBS and 1% Penicillin/Streptomycin) at 10^7 cells/ml at 37°C, 5% CO2, either unstimulated, or stimulated with low-dose phorbol myristate acetate (PMA)/ionomycin stimulation (5 ng/ml PMA, 500 mg/ml Ionomycin). After stimulation, cells were washed, then incubated for 1 hour in either culture media (Control), EDTA (1 mM) and DTT (1 mM) in Ca2+/Mg2+ free HBSS (EDTA/DTT - IEL extraction protocol), DNAse (100 µg/ml) and Collagenase A (1.5 mg/ml) in RPMI + 10% FBS (DNAse/Collagenase A - total IL or LPL extraction protocol) or DNAse (100 µg/ml) and Collagenase D (1 mg/ml) in RPMI +

(DNAse/Collagenase D - total intestinal lymphocyte (IL) or lamina propria lymphocyte (LPL) extraction protocol).

After incubation, cells were washed, then stained with differing concentrations of cell dye to barcode the cells for multiplex flow cytometry, as described above. After further washes, cells from the eight conditions for each donor were pooled. Samples from the three donors were stained with different fluorophore-conjugated CD3ε monoclonal antibody (CD3ε-FITC, UCHT1 Biolegend; CD3ε-BV711, UCHT1 Biolegend, CD3ε-BV785, OKT3 Biolegend) to barcode them for multiplex flow cytometry, in addition to other antibodies in the panel (CD4-BV650, OKT4 Biolegend; CD8α-PerCP-Cy5.5, SK1 Biolegend; Live-Dead-nearIR, Thermofisher). After further washes, all samples were pooled, and the mixed cells from the 24 samples (three donors each with eight conditions), were added to the 332 reconstituted, lyophilised, PE-conjugated antibodies of the LEGENDScreeen™ Human Cell Screening Kit along with 10 PE-conjugated isotype controls and fluorescence minus one (FMO) controls, per the manufacturer's instructions. Cells were fixed and stored at 4^{o}C in the dark until analysed. Acquisition on a BD LSRII flow cytometer using the high throughput sampler with appropriate single stain compensation controls.

I specifically sought to identify markers reduced in expression by exposure to the analysed extraction techniques. Therefore, markers where the MFI was reduced by more than 10% with the digestion condition were compared using a 1-tailed paired t-test.

2.10Chip cytometry

Chip cytometry was performed at the Peter Medawar building facility by Dr Kate Powell. Samples were frozen in OCT (as described above), cryosectioned onto coverslips and placed in cytometer chips (Zellsafe Tissue chips, Zellkraftwerk, Germany). Sections were fixed *in situ* at room

temperature for 10 minutes using 4% paraformaldehyde, then washed with 10 mL PBS. Non-specific binding was blocked by incubating in 5% goat serum (Thermo Fisher Scientific) in PBS for 1 hour at room temperature. Fluorophore-conjugated antibodies (see Table 2-1) were diluted for staining in PBS. Immunostaining was performed iteratively, with up to three antibodies conjugated to different fluorophores applied simultaneously. Fluorophores were then photo-bleached and additional antibodies applied to build up the panel (Hennig et al., 2009). Images were acquired using a Zellscanner One Chip cytometer (Zellkraftwerk) and ZellExplorer software.

2.11Molecular biology techniques

2.11.1Nucleic acid extraction

A Trizol nucleic acid extraction method was used to extract high purity RNA from low numbers of sorted lymphocyte populations, as previously described(Barnitz et al., 2013; Quigley et al., 2010), except that phase-lock gel tubes were replaced with standard 1.5ml Eppendorf tubes. Briefly, after sorting, cells were centrifuged (500 g, 5 minutes), resuspended in 1 ml Trizol, then frozen at -80^{o}C until RNA extraction. For RNA extraction samples were brought to room temperature, mixed with 200 µl chloroform and centrifuged at 12500 rpm for 5 minutes. 500 µl of the aqueous phase was taken and RNA extracted using the Agencourt RNAdvance Tissue Isolation kit, a bead-based RNA extraction protocol. RNA was assessed for concentration and purity using RNA Pico assay on a 2100 Bioanalyzer instrument (Agilent).

2.11.2HLA-DQ genotyping

HLA DQ2/DQ8 genotype status was determined using an RT-PCR method (AnDiaTec-Quidel, Germany). This kit tests for three HLA alleles: DQA1*05 and DQB1*02 (which encode the genotype DQ2) and DQB1*0302 (which encodes DQ8). In brief, genomic DNA was combined with HLA allele-specific primers and supplied amplification mix as per manufacturer's instructions, except that a

total reaction volume of 10 µl was used. A positive and negative control was used for each plate performed, as well as an internal control included in the amplification mix. RT-PCR was then performed using the following temperature protocol (95°C for 2min, 45 x (95°C for 10s, 58°C for 30s, 72°C for 30s), with signal detection following the 58°C step. HLA allele amplification was detected by FAM fluorescence, while internal control amplification was detected by VIC/HEX/JOE fluorescence.

2.11.3Whole transcriptome amplification

Whole transcriptome amplification was used to generate sufficient cDNA from small populations of sorted T cells for RT-PCR quantification of gene expression. This was performed using the Ovation® PicoSL WTA system v2 (Nugen), an approach using oligo dT primers and random primers for first strand synthesis, an approach designed to minimise 3' bias in transcriptome amplification, and which allows for standard RT-PCR primers to be used. The single primer isothermal amplification (SPIA) process is designed to preserve the stoichiometry of input material.

The kit was used in accordance with manufacturer's instructions. Briefly, high-quality RNA was isolated from sorted T cells using a Trizol-based approach, as described earlier. First strand cDNA is generated using random and oligo dT primers. The hybrid cDNA/mRNA molecule that is produced contains a specific RNA tag sequence (SPIA tag). After second cDNA generation, SPIA amplification using a DNA/RNA chimeric primer, DNA polymerase and RNase H allows rapid amplification of cDNA in an isothermal assay. This generates large quantities (>2 mg) of cDNA from as little as 500 pg input RNA. The cDNA product is then purified using QIAquick® PCR purification kit (Qiagen), with modifications to the protocol as detailed in the PicoSL instructions. Purified cDNA was quantified and assessed for quality using a Nanodrop spectrophotometer (Thermofisher Scientific), before downstream RT-PCR.

2.11.4Quantitative RT-PCR

For (quantitative) RT-PCR, cDNA was thawed on ice, diluted to appropriate starting concentration with nuclease-free water, and added to a thermocycler plate, with RT-PCR master mix (Taqman), and primers, to a total volume of 10 µl. Samples were mixed, then plates sealed and centrifuged briefly. Strict sterile technique was used throughout. Amplification and signal detection was performed in a CFX96 thermal cycler (Bio-Rad). Three housekeeping genes (HKGs), GAPDH, GUSB, and ACTB, were used in combination, with the mean of these results used as the HKG reference. Samples were run in duplicate with the mean of the duplicate results used. For samples where no amplification was detected during the cycle run, a Ct value of the total number of runs + 1 was used for calculation of expression relative to HKGs. Data were analysed using the 2^-ΔΔCt method(Livak and Schmittgen, 2001).

2.11.5Bulk RNA sequencing

Bulk RNA sequencing on low-input samples was performed using the Smart-seq2 protocol(Picelli et al., 2013; 2014) at the Oxford Genomics Centre (WTCHG, University of Oxford). Up to 10 ng RNA was used as the template from each sample for library generation. Barcoded samples were pooled, and External RNA Controls Consortium (ERCC) RNA (1:100,000) was added prior to 75bp paired-end sequencing on an Illumina HiSeq4000 instrument.

2.11.6Single-cell RNA sequencing using the 10x Genomics platform

Libraries were generated using 10x Genomics Chromium Single Cell V(D)J Reagents Kits (v1 Chemistry) as per manufacturer's instructions. Sorted cells suspended in PBS (plus 0.04% BSA) at a concentration of 1000 cells/µL were loaded into one lane of a Chromium controller. Library quality and quantity were assessed using a TapeStation (Agilent) and Qubit Fluorometer (Thermofisher Scientific). Libraries were sequenced on an Illumina HiSeq 4000 following manufacturer's

instructions. Library generation and sequencing were performed at the Oxford Genomics Centre (WTCHG, University of Oxford).

2.11.7 Plate-based single-cell RNA sequencing

Single cells were index-sorted into wells of 96-well plates (one cell/well) containing 2.3 µl lysis buffer (0.8% Triton X-100, 2U/µL RNase inhibitor). Smart-Seq2 libraries were generated following the published protocol (Picelli et al., 2014). External RNA Controls Consortium (ERCC) RNA (1:100,000) was added prior to sequencing. cDNA was pre-amplified by PCR (21 cycles). Libraries were sequenced on an Illumina HiSeq4000 with 75 bp paired-end reads. Library generation and sequencing were performed at the Oxford Genomics Centre (WTCHG, University of Oxford).

2.11.8 Combined targeted single-cell RNA sequencing and surface protein quantification using the BD Rhapsody platform

PBMCs from three donors were either rested, or stimulated for 20 hours with TCR stimulation - plate-bound CD3 (2.5 µg/ml) and soluble CD28 (1µg/ml) - or with combinatorial cytokine stimulation with IL-12 and IL-18 (both 50 ng/ml) as described previously. Following surface antibody staining, conventional CD4+ and CD8+ T cells, Vδ1+ and Vδ2+ γδ T cells, and MAIT cells were sorted by FACS. Sorted cells were resuspended in 50 µl PBS+2% FCS. Sorted populations from each donor (n=3; 12 populations/donor; approximately 5,000 cells/population) were incubated with different oligo-conjugated barcoding antibody from the sample multiplexing kit (BD Biosciences) for 15 min at room temperature. The 12 subsets from the same donor were washed 3 times (400 g, 5min at 4^{o}C) in cold sample buffer (BD Biosciences) to remove residual barcoding antibodies, then combined. The cells were then stained with a panel of 91 oligo-conjugated antibodies (BD Biosciences), as per manufacturer's directions. Samples were washed 3 times (400 g, 5min at 4^{o}C) in cold sample buffer, filtered through a 35 µm mesh strainer, and resuspended in 620 µl of cold sample buffer (40 cells/µl

for donors 1 and 2, 32 cells/µl for donor 3), with an intended capture rate 20,000 cells for donors 1 and 2, and 15,000 cells for donor 3. The cells were loaded on a BD Rhapsody cartridge (BD Biosciences) for single-cell capture (one cartridge/donor) as per manufacturer's instructions.

cDNA library preparation was performed with the Rhapsody Express single-cell analysis system (BD Biosciences), as per manufacturer's directions. Briefly, cDNA was amplified (PCR1 - 11 cycles) using the pre-designed Human T cell expression Panel (BD Biosciences), containing 259 primer pairs, in combination with a custom panel containing a further 306 primers pairs, targeting 286 different genes. The resulting PCR1 products were purified using AMPure XP magnetic beads (Beckman Coulter). mRNA and AbSeq/sample barcode products were separated using size-selection (bead ratios of 0.7X and 1.2X, respectively). Purified mRNA and sample barcode PCR1 products were amplified again (10 cycles), and the resulting PCR2 products purified by size selection (0.8X and 1.2X for the mRNA and sample barcode libraries, respectively). The concentration, size and integrity of the resulting PCR products was assessed using both Qubit (High Sensitivity dsDNA kit; Thermofisher Scientific) and a Tapestation (High Sensitivity D1000 screentape; Agilent). The final products were normalised to 2.5 ng/µl (mRNA) and 1.1 ng/µl (Sample tag and AbSeq) and underwent a final round of amplification (6 cycles) using indexes for Illumina sequencing to prepare the final libraries. Following purification based on size selection (0.7X and 0.8X for mRNA and sample barcoding/AbSeq libraries, respectively), final libraries were quantified using Qubit and Tapestation and pooled (29/69/2% mRNA/AbSeq/sample barcode ratio) to achieve a final concentration for sequencing of 5nM. Pooled libraries were spiked with 15% PhiX control DNA to increase sequence complexity and sequenced (150bp paired-end) on a NovaSeq sequencer (Illumina).

2.11.9 Bulk TCR repertoire sequencing

Bulk TCR repertoire sequencing was performed using the amplicon-rescued multiplex (ARM)-PCR method (iRepertoire, Inc., USA). This method performs an initial first-round RT-PCR with TCR V and C

gene-specific primers for the relevant TCR chain, followed by further amplification steps with universal primers for the exponential phase of amplification. This method is designed to provide quantitative, deep sequencing of the TCR repertoire, with minimal bias.

Library generation was performed in-house following manufacturer's instructions, except for performing the library generation in 96-well plates. In brief, high-quality RNA, enzyme mix, and barcoded primer reaction mix were combined and mixed in a clean hood on ice, before a combined RT-PCR and initial amplification step in the thermal cycler using the low-input protocol. The PCR product was then cleaned up and purified using solid phase reverse immobilisation (SPRI) beads and ethanol washes, then eluted in water. This product was then combined with enzyme mix and universal primers for the second amplification step. The final product was cleaned up and purified again using SPRI beads, and eluted in water. The quality, size distribution, concentration, and presence of contaminating primer dimers of the final product was assessed using several QC steps, including identification of a clear band of appropriate size on agarose gel electrophoresis, a spectral photometer (Nanodrop, Thermofisher Scientific), and the Bioanalyser DNA 1000 assay using a 2100 Bioanalyzer instrument (Agilent). Libraries were quantified using the KAPA Library Quantification Kit (Roche) on a CFX96 Thermal Cycler instrument (Bio-Rad) before equimolar pooling. A PhiX library spike-in was added (10%) due to the low diversity of the TCR library, before 300bp paired-end sequencing on a Illumina MiSeq instrument at the Oxford Genomics Centre (WTCHG,University of Oxford).

2.12Analysis

2.12.1Graphs, statistics, and flow cytometry analysis

All statistical analyses and graphs, except transcriptional data, were performed using Prism Software v8 (GraphPad, USA). Specific statistical tests are described in relevant figure legends. All data are

presented as mean +/- SEM unless stated otherwise. Heatmaps and Principal Component Analysis (PCA) plots were created using ClustVis(Metsalu and Vilo, 2015) or Heatmapper(Babicki et al., 2016).

Flow cytometry data were analysed using FlowJo v9.9.5 and v10.6.1 (FlowJo, LLC). For phenotypic analysis of rare cell subsets, populations with fewer than 10 cells were excluded.

2.12.2 Bulk TCR repertoire analysis

Data processing of TCR repertoire libraries was performed using the iRepertoire analysis pipeline. In brief, reads were demultiplexed based on the 6-N molecular barcode associated with the sample. Low quality reads were trimmed (removing anything with a Phred score of less than 30), and R1 and R2 reads were overlapped and stitched. Only stitched reads where identity within the overlapped portions was 100% were included in downstream analysis. Reads were then mapped to the IMGT database, and only reads that map to reference sequences and contain canonical CDR3 motifs were included for further analysis. Finally, a number of filters (see irepertoire.com/irweb-technical-notes) were applied to remove sequencing artefacts, PCR artefacts, insertion, deletion, and substitution errors, and low frequency (n=1) reads.

Initial data analysis was performed using the iRweb data analysis platform (iRepertoire, Inc., USA). Additional analysis and generation of plots was performed using SeeTCR (friedmanlab.weizmann.ac.il/SeeTCR), Heatmaper(Babicki et al., 2016), Clustvis(Metsalu and Vilo, 2015), IMGT/JunctionAnalysis(Monod et al., 2004), and iceLogo(Colaert et al., 2009).

2.12.3 Bulk RNA-Seq Analysis

Data processing for these experiments was performed in collaboration with Dr Agne Antanaviciute. Raw sequence reads were quality checked using FastQC software(Andrews, 2010). Cutadapt(Martin,

2011) software was used to trim poor-quality bases (<20 Phred Score) and Illumina universal adapter sequences from raw reads before alignment.

The human hg38 reference genome analysis set was obtained from the University of California Santa Cruz (UCSC) ftp site(Kuhn et al., 2013). The reference genome was indexed using STAR aligner(Dobin et al., 2012) and sequenced reads were then aligned to this reference, using the following parameters:

```
STAR --runMode alignReads --genomeDir $genome --runThreadN 5 --readFilesIn $read1 $read2 \
 --outFilterMismatchNoverLmax 0.1 --outFileNamePrefix $prefix --outSAMtype BAM
SortedByCoordinate \
 --outFilterMultimapNmax 50 \
 --outFilterMatchNminOverLread 0.75 \
 --outFilterScoreMinOverLread 0.5 \
 --outSAMattributes All \
 --outFilterMatchNmin 10 \
 --outFilterMismatchNmax 10 \
 --outReadsUnmapped Fastx \
--readFilesCommand zcat \
```

Samtools(H. Li et al., 2009) were used to merge, sort and index alignment bam files and to compute alignment statistics for alignment QC. Picard tools (Wysoker, A; 2013) was used to mark duplicate sequences as an additional quality control step. Raw gene expression counts were summarized with featureCounts(Liao et al., 2013), with multi-mapping reads counted as fractions of all mapped loci. The MultiQC tool(Ewels et al., 2016) was used to aggregate quality metrics. Sample quality metrics and raw read counts were imported into R for further processing. The DESeq2(Love et al., 2014) R package was used to estimate library size factors, normalize counts and perform differential expression analyses. Benjamini–Hochberg multiple testing correction was used to compute FDR, and genes were considered significantly differentially expressed at <5% FDR. Principal component analysis was performed in base R, with normalized DESeq2 variance-stabilized transformation expression as input. Correlation significance between principial components and variables of interest were computed in R using Kruskal-Wallis test for categorical variables and Spearman's correlation

for continuous variables. Gene set enrichment analysis was performed with GSEA (version 4.0.3, BROAD Institute) (Subramanian et al., 2005).

2.12.4 10x genomics scRNAseq analysis (Chapters 3-5)

Data processing for these experiments was performed in collaboration with Dr Agne Antanaviciute. Human hg38 reference genome analysis set was downloaded from the University of California Santa Cruz (UCSC) ftp site(R. M. Kuhn et al., 2013). Human hg38 reference genome Ensembl gene annotations were obtained using the UCSC Table Browser Tool(Karolchik, 2004).For each sequenced scRNAseq pool, Cellranger software from 10× Genomics (https://support.10xgenomics.com/single-cell-gene-expression/software/downloads/latest) was used to process, align and summarize unique molecular identifier (UMI) counts against hg38 human reference genome.

UMI counts matrices were imported into R for further processing. R package Seurat(Satija et al., 2015) was used for subsequent analyses. First, poor quality droplets were filtered out based on total UMI counts (< 500) and percentage of mitochondrial content in each cell (> 8%). Substantial batch effects were observed and corrected using liger(Welch et al., 2019) algorithm. Briefly, data were normalised for total expression across each cell, scaled and variable genes selected within each sample separately with the following parameters: var.thresh=0.1, alpha.thresh=0.99, tol = 1e-04; then final variable genes were taken as a union of all variable genes across samples. Integration parameters were estimated using 'suggestK' and 'suggestLambda' functions, integrative non-negative matrix factorisation was carried out using estimated parameters (k=30, lambda=5) and factor loadings were quantile aligned. Aligned factors were used as input for UMAP algorithm to generate visualisations, with the following parameters: min_dist =0.01, spread =2 and n_neighbours = 30. Integrated data were converted into a Seurat object for further analysis.

Differential gene expression analyses were carried out using R package MAST(Finak et al., 2015), in each case blocking for gene detection rate and batch covariates. Trajectory analyses were carried out using Monocle 3(X. Qiu et al., 2017), with batch-corrected data (as described above) used as input. Cells were clustered (k=50, reduction_method="UMAP") and a disjoint principal graph was learnt for each partition. Starting point of the pseudotime trajectory was specified manually.

TCR Analysis

TCR αβ clonotypes were assembled using 10x Cellranger VDJ pipeline from targeted libraries. In order to assemble γδ TCR chains from these cells, we first extracted all read 2 sequences into individual fastq files for each passing QC cell from BAM alignment files. Aligned reads were filtered to remove reads mapping to a feature where the majority of other reads with that UMI did not (tag xf 2) and only adapter and TSO-trimmed part of the sequences were retained. Tracer pipeline (Stubbington et al., 2016) was then used to assemble TCR alpha, beta, gamma and delta chains for all cells. The results from cells within each individual sample were then pooled to determine consensus shared clonotypes and cells were annotated with a given clonotype, if assembled. TCR delta chains were successfully assembled in 12-828 cells per sample, while successful assemblies of gamma chains were very rare (between 14-283 cells with assembly per sample) likely due to lower overall expression of this chain, akin to the alpha chain, and as a result, paired gamma-delta assemblies were rarer still (up to 62 total cells per sample). Thus, we excluded gamma chain assemblies from subsequent downstream analyses due to low number of assemblies.

VDJ chain usage analyses were performed using VDJtools(Shugay et al., 2015), with the single cell clonotype frequencies substituted for read frequencies (a proxy for cell frequencies in bulk TCR analyses) in the analyses. Cluster sharing of clonotypes considered only clonotypes shared by cells from the same donor. UpsetR R package(Conway et al., 2017) was used to visualise cluster shared clonotype intersections.

Transcription Factor Module Analysis

R package "SCENIC" workflow was used to detect active transcription factor modules using transcriptional profiles of single cells from 10x data. Normalized single cell gene expression matrix was first filtered to exclude all genes detected in fewer than 20 total cells. The RcisTarget database containing transcription factor motif scores for gene promoters and around transcription start sites for hg38 human reference genome were downloaded from (https://resources.aertslab.org/cistarget/databases/homo_sapiens/hg38/refseq_r80/mc9nr/gene_based/) and the expression matrix was further filtered to only include genes available in the RcisTarget database. The remaining genes were used to compute a gene-gene correlation matrix for co-expression module detection using random forest based GENIE3 algorithm(Huynh-Thu et al., 2010) and R package 'SCENIC'(Aibar et al., 2017) was used to perform transcription factor network analysis to detect co-expression modules enriched for target genes of each candidate TF from RcisTarget database. AUCell package was used to compute a score for each TF module in each individual cell as follows. First, for each cell single cell gene expression matrix was used to compute gene expression rankings using "AUCell_buildRankings" function with default parameters.

Downstream targets of identified TF modules were assembled as gene sets and then used to score each cell, where for each gene set and each cell, area under the curve (AUC) value was computed ("AUCell_calcAUC" function) based on gene expression rankings, where AUC value represents the fraction of genes within the top ranking genes for each cell that are defined as part of the pathway gene set. In order to identify differential TF module activities, we compared individual module AUC score distributions in single cells using generalised linear models. For each TF module, we fit a generalised linear model with the formula of 'AUC ~ Condition + Gene Detection Rate + Donor' to single cell data. Gene detection rate was included as an additional covariate, as we observed that AUC values are highly correlated individual cell library size. Condition coefficients and model p-

values (corrected using Benjamini-Hochberg multiple testing correction) were then used to prioritise condition or cluster-specific enriched (positive coefficients) or underrepresented (negative coefficient) module TF module activities.

To visualise expression of all detected human TFs, we first downloaded a TF list from Lambert et al(Lambert et al., 2018) and filtered it to keep only genes annotated as TFs by consensus and at least minimally expressed within our 10x dataset. Expression patterns were visualised as mean, scaled expression level per cluster using hierarchical clustering analysis and heatmaps. To visualise distribution of expression patterns along pseudotime, we first divided all cells into 80 bins based on their position along pseudotime, as cell distribution along pseudotime is not uniform. Then, for each gene we fit a loess curve of pseudotime ~ expression and used the curve fits along pseudotime as input for hierarchical clustering of genes and visualisation via heatmaps.

2.12.5 BD Rhapsody scRNAseq analysis (Chapter 5)

Data processing for these experiments was performed in collaboration with Dr Agne Antanaviciute. Raw data were processed using BDR single cell analysis system. UMI count matrices were imported in R and Seurat R package was used for further analysis. mRNA data were normalised to total cell counts and natural log transformed, adding a pseudocount of 1, while antibody-based counts were normalised using centered log ratio transform. Variable feature selection was carried out in Seurat for cells in each reaction and a union of the features was taken. Data were then merged and as batch effects were minimal, simple linear regression was used to correct the selected feature set for batch variables. Scaled, batch-corrected data were then used as input for principal component analysis. The first 14 principial components were found to account for the majority of variability in the data and were used as input for Louvain clustering analysis (resolution=0.7) and visualisation using UMAP. Differential expression analyses were carried out as before.

To compare targeted single cell RNAseq data, we split 10x data into ADGR1-like cells and MAIT-like cells. We subset BDR data to retain only VD2 cells at rest, and performed normalisation, scaling and clustering analysis of this subset as described above. We then used factor analysis to align the two datasets (in Seurat, as implemented via functions FindTransferAnchors and TransferData) and generate a probability matrix for each VD2 cell of the likelihood it represents the expression profile of ADGR1-like or MAIT-like reference cells.

2.12.6 scRNAseq data analysis (Chapter 6)

Data processing for these experiments was performed in collaboration with Dr Lucy Garner.

Droplet-based (10x Genomics) scRNAseq data analysis

FastQ generation, read alignment, barcode counting and UMI counting were performed using the Cell Ranger pipeline v2.2.0. Downstream processing steps were performed using Seurat v2.3.4 (Butler et al., 2018; Stuart et al., 2019). Briefly, TCR and BCR genes, and genes expressed in fewer than 10 cells, were removed. Cells with < 3,460 UMIs (local minimum of the UMI distribution to the left of the mode UMI count), < 500 genes, and > 10,000 UMIs, > 2,500 genes, and/or > 10% mitochondrial reads were removed (Supplementary Fig. 2A). Variable genes were identified using M3Drop (Andrews et al., 2018). Data were log normalised and scaled, with cell-cell variation due to UMI counts, percent mitochondrial reads, and S and G2M cell cycle scores regressed out. The top 10 principal components (PCs) were used as input for graph-based clustering (0.4 resolution), as determined by visual inspection of the scree plot. Clusters were visualised by tSNE. Differential gene expression analysis between clusters was performed using the Wilcoxon Rank Sum test (FindMarkers function with default parameters).

Plate-based (Smart-Seq2) scRNAseq data analysis

Reads were trimmed to remove contaminating adapter and oligo-dT primer sequences using Trimmomatic v0.36 (Bolger et al., 2014). Trimmed reads were aligned to the human genome (hg38 assembly) plus added ERCC "spike-in" sequences using STAR v2.5.3a (--outFilterMismatchNoverLmax 0.04 --outFilterType BySJout --outMultimapperOrder Random) (Dobin et al., 2012). Alignments were filtered using Samtools v1.6 (H. Li et al., 2009) to retain only primary alignments and properly paired reads. Ensembl gene counts were generated using featureCounts v1.6.0 (-C -B -p) (Liao et al., 2014). Poor quality cells that fit one or more of the following criteria were removed from the analysis (Supplementary Fig. 2G-I): small log-library size (< 3 median absolute deviations (MADs) below the median), low percentage of uniquely mapped reads (< 55%), low gene count (< 3 MADs below the median), high percentage of ERCCs (> 37.5%), or high mitochondrial read fraction (> 6%). Outlier cells with a large library size or high gene count (potential doublets) were also removed. Genes with "undetectable" expression were removed (gene defined as "detectable" if at least 5 read counts in two cells), along with TCR (and BCR) genes. Log normalised expression values were generated using the normalize function from scater v1.10.1 (D. J. McCarthy et al., 2017) with cell-specific size factors calculated using scran v1.12.1 (Lun et al., 2016). Feature selection was performed using M3Drop v3.10.4 (FDR < 0.01) (Andrews et al., 2018) and the expression matrix subset to retain only the selected genes. Clustering analysis was performed using SC3 v1.12.0 (Kiselev et al., 2017). Clusters were visualised by UMAP generated using the top 30 PCs (McInnes et al., 2018). Differential gene expression analysis was performed using DEsingle v1.2.1 (Miao et al., 2018) (FDR < 0.05).

2.12.7Single cell classification

In the BD Rhapsody dataset, to classify stimulated cells, which could not be sorted due to internalisation of cell surface receptors in response to stimulation, into VD1, VD2, Tconv and MAIT cells, we trained a random forest classifier using unstimulated cells. First, we split all unstimulated cells into training and testing datasets. Training dataset was composed by randomly sampling 300 cells per donor per class to generate a balanced training dataset composed of 900 VD1, VD2, Tconv

and MAIT cells respectively, for a total of 3600 training cells. The remaining cells (7,148 total across all groups and donors) were used to generate an independent testing dataset.

As input training features, we compiled all mRNA and protein expression profiles, together with cell donor and molecule detection rates per cell. We removed antibody tag read-outs for TCR segments from the training dataset, as while these features are highly discriminative in at rest cells, they may confound the predictor in stimulated cells. Then, we performed backwards feature selection on the dataset, where least important features are eliminated sequentially until a subset of predictors is found that produces the most accurate model. The selected features were then used as input to train the final model using the training data set of at rest cells, generating a random forest model of 1,000 random decision trees. Next, we classified the at rest testing data in order to assess the performance of the classifier. We carried out area-under-the-ROC-curve (AUC) analysis, converting the class labels of the multi-class classifier into binary for each class separately, and using the multi-class prediction probabilities to calculate performance metrics. For each class, high AUC values were achieved (> .98) and subsequently the model was then used to predict cell types of stimulated cells, assigning a class label to each cell based on the highest class probability.

The models were trained and assessed in R, using packages randomForest (version 4.6-14), caret (version 6.0-85) (M. Kuhn, 2008) and ROCR (version 1.0-7) (Sing et al., 2005).

Using a similar procedure as described above, we trained a random forest model to classify single cells as CD8 or Gamma-Delta cells. As input training data, we used data from one donor where CD8 and Gamma-delta cells were sorted and processed separately. We split this training data into 1/3 testing and 2/3 training sets and used recursive feature selection to select predictive features as before. A final random forest model was then trained and performance assessed using AUC analysis on the hold out testing data set. The model was then used to classify cells from pooled CD8 and Gamma-Delta samples. The accuracy of the classifications was confirmed visually in each case by

examining the expression distribution of Gamma-Delta and Alpha-Beta TCR gene segments, as well as CD8A and CD8B.

2.12.8Weighted Gene Correlation Network Analysis

WGCNA analysis for bulk and single cell data was carried out in R using WGCNA package(Langfelder and Horvath, 2008). Briefly, single cell counts were first imputed using scimpute(W. V. Li and J. J. Li, 2018), with dropout threshold set to 0.5. The data were then filtered to keep only genes which were expressed in more than 50 cells in the original, unimputed data. A signed network was then constructed by first estimating the soft power parameters (power=8) and used to compute a pairwise adjacency matrix, from which a topological overlap matrix was calculated. Genes were then clustered using hierarchical clustering (linkage =" average") and dynamic hydrid tree cut method (parameters: minModuleSize=20, deepSplit=2) was used to partition the genes into modules.

2.12.9Gene Ontology and Pathway Enrichment Analyses

Gene Ontology and pathway enrichment analyses were performed using the 'clusterProfiler' R package(Yu et al., 2012). Annotation Dbi R package "org.Hs.eg.db" was used to map gene identifiers. In each case, all expressed/detected genes were used as a background control and gene sets were tested for over-representation in cluster markers or differentially expressed genes by computing enrichment p-values ('enricher' R function, default parameters) from the hypergeometric distribution of total genes in the background gene set, the number of genes within background that are annotated with the gene set, the size of the gene set and the number of genes within cluster marker/differentially expressed genes list annotated with the gene set. Hypergeometric p-value was adjusted in each case for multiple testing using Benjamini-Hochberg correction as before. The results were visualized as dot plots and emap plots using 'clusterProfiler', 'enrichPlot' and 'ggplot2' R packages.

2.12.10 Transcriptional data integration with published datasets

In chapter 4, for comparison of the T_{RM} gene sets with an external non-transplant human dataset (J. C. Martin et al., 2019), the web-based graphical interface for the data was used (https://scdissector.org/martin). Ileum T cell clusters with high expression of CD8A and CD8B, and low expression of CD4, were chosen for analysis. Consensus DEGs between populations 1 and 2 identified in both scRNAseq datasets (Figure 3D) were examined, with hierarchical analysis of the expression of genes performed.

In chapter 4, For Gene Set Enrichment Analysis (GSEA) within DEGs between murine intestinal TRM cell clusters post-LCMV infection (Kurd et al., 2020), a gene set associated with population 2/CD103- T_{RM} cells identified in this study was created. This included all genes differentially expressed in either experiment, and showing congruent direction of fold change in both experiments. These genes were converted to murine orthologues using DAVID Bioinformatics Resources 6.7 (https://david.ncifcrf.gov/)(D. W. Huang et al., 2008) and Mouse Genome Database (MGD) at the Mouse Genome Informatics website (http://www.informatics.jax.org). GSEA was performed using GSEAv4.0.3 (https://www.gsea-msigdb.org/gsea) (Subramanian et al., 2005).

2.12.11 Antibodies and key reagents

Table 2-1: Antibodies and key reagents used for experimental work.

REAGENT or RESOURCE	SOURCE	IDENTIFIER
Antibodies		
Anti-human CCL4 (clone D21-1351) BV421	BD Biosciences	Cat# 562900
Anti-human CCR6 (clone G034E3) FITC	Biolegend	Cat# 353411
Anti-human CCR7 (clone G043H7) PE-Dazzle	Biolegend	Cat# 353235
Anti-human CCR9 (clone L053E8) APC	Biolegend	Cat# 358907
Anti-human CCR9 (clone L053E8) PE	Biolegend	Cat# 358903
Anti-human CCR9 (clone L053E8) PE-Cy7	Biolegend	Cat# 358909
Anti-human CCR9 (clone REA469)	Miltenyi	Cat# 130-107-169
Anti-human CD103 (clone Ber-ACT8) APC-Cy7	Biolegend	Cat# 350227
Anti-human CD103 (clone Ber-ACT8) BV421	Biolegend	Cat# 350213
Anti-human CD103 (clone Ber-ACT8) PE	Biolegend	Cat# 350205
Anti-human CD127 (clone A019D5) BV650	Biolegend	Cat# 351325
Anti-human CD127 (clone REA614) PE	Miltenyi	Cat# 130-113-976
Anti-human CD16 (clone 3G8) AF700	Biolegend	Cat# 302025
Anti-human CD16 (clone 3G8) PE-Dazzle	Biolegend	Cat# 302053
Anti-human CD161 (clone 191B8) APC	Miltenyi	Cat# 130-113-591
Anti-human CD161 (clone 191B8) FITC	Miltenyi	Cat# 130-113-592
Anti-human CD161 (clone 191B8) PE	Miltenyi	Cat# 130-092-677
Anti-human CD18 (clone 7E4) PE	Beckman	Cat# IM157OU
Anti-human CD18 (clone L130) BUV563	BD Biosciences	Cat# 749441
Anti-human CD26 (clone BA5b) APC	Biolegend	Cat# 302709
Anti-human CD26 (clone BA5b) PE-Cy7	Biolegend	Cat# 302713
Anti-human CD27 (clone M-T271) BV421	Biolegend	Cat# 356417
Anti-human CD27 (clone M-T271) BV510	Biolegend	Cat# 356420
Anti-human CD28 (clone CD28.2) APC/FIre	Biolegend	Cat# 302951
Anti-human CD28 (clone CD28.2) BV421	Biolegend	Cat# 302929
Anti-human CD3 (clone OKT3) BV785	Biolegend	Cat# 317329
Anti-human CD3 (clone UCHT1) AF700	Biolegend	Cat# 300423
Anti-human CD3 (clone UCHT1) PerCP	Biolegend	Cat# 300427
Anti-human CD4 (clone OKT4) BV650	Biolegend	Cat# 317435
Anti-human CD4 (clone RPA-T4) PerCP	Biolegend	Cat# 300527
Anti-human CD4 (clone SK3) BUV805	BD Biosciences	Cat# 612888
Anti-human CD45 (clone HI30) FITC	Biolegend	Cat# 304038
Anti-human CD45RA (clone HI100) BV785	Biolegend	Cat# 304139
Anti-human CD45RA (clone HI100) BV785	Biolegend	Cat# 304139
Anti-human CD69 (clone FN50) BUV395	BD Biosciences	Cat# 564364

Anti-human CD69 (clone FN50) PE-Dazzle	Biolegend	Cat# 310941
Anti-human CD7 (clone M-T701) BB700	BD Biosciences	Cat# 566489
Anti-human CD8 (clone RPA-T8) AF532	Thermofisher Scientific	Cat# 58-0088-42
Anti-human CD8 (clone SK1) AF700	Biolegend	Cat# 344723
Anti-human CD8 (clone SK1) FITC	Biolegend	Cat# 344704
Anti-human CX3CR1 (clone 2A9-1) APC	Biolegend	Cat# 341609
Anti-human CXCR6 (clone K041E5) PE-Dazzle	Biolegend	Cat# 356015
Anti-human GPR56 (clone REA467) PE	Miltenyi	Cat# 130-106-975
Anti-human GPR56 (clone REA467) VB FITC	Miltenyi	Cat# 130-106-915
Anti-human Granzyme A (clone CB9) FITC	Biolegend	Cat# 507204
Anti-human Granzyme B (clone GB11) BV510	BD Biosciences	Cat# 563388
Anti-human Granzyme K (clone GM26E7) PE	Biolegend	Cat# 370511
Anti-human Granzyme K (clone GM26E7) PE-Cy7	Biolegend	Cat# 370515
Anti-human Helios (clone 22F6) FITC	Biolegend	Cat# 137204
Anti-human Histone H3 (clone 17H2L9) AF488	Invitogen	Cat# MA702023
Anti-human HLA-A2 (clone BB7.2) PE	Biolegend	Cat# 343306
Anti-human HLA-A3 (clone GAP.A3) PE	Thermofisher Scientific	Cat# 12-5754-41
Anti-human Hobit (clone Sanquin-Hobit/1) AF647	BD Biosciences	Cat# 566250
Anti-human IFN-γ (clone B27) BV750	BD Biosciences	Cat# 566357
Anti-human IL-10 (clone JES3-9D7) APC	Biolegend	Cat# 501409
Anti-human IL-17A (clone BL168) BV711	Biolegend	Cat# 512327
Anti-human IL-18Ra (clone 70625)	R&D	Cat# FAB840G-025
Anti-human IL-2 (clone MQ1-17H12) PE-Dazzle	Biolegend	Cat# 500343
Anti-human IL-26 (clone 510414) PE	R&D	Cat# IC13751P
Anti-human Ki-67 (clone B56) BV480	BD Biosciences	Cat# 566172
Anti-human KLRG1 (clone REA261) VioBlue	Miltenyi	Cat# 130-123-526
Anti-human KLRG1 (clone SA231A2) PE	Biolegend	Cat# 367711
Anti-human LAG3 (clone C9B7W) PE-Cy7	Biolegend	Cat# 125225
Anti-human NKG2C (clone REA205) VB515	Miltenyi	Cat# 130-120-105
Anti-human NKp30 (clone AF29-4D12) PE-Cy7	Miltenyi	Cat# 130-124-455
Anti-human pan Cytokeratin (clone C-11) FITC	GeneTex	Cat# GTX11212
Anti-human PD-1 (clone EH12.2H7) PE-Dazzle	Biolegend	Cat# 329939
Anti-human Perforin (clone dG9) PE-Cy7	Biolegend	Cat# 308125
Anti-human PLZF (clone R17-809) PE-Dazzle	BD Biosciences	Cat# 565738
Anti-human RORγt (clone Q21-559) PE	BD Biosciences	Cat# 563081
Anti-human Tbet (clone O4-46) BV786	BD Biosciences	Cat# 564141
Anti-human TIGIT (clone MBSA43) PCPe710	Thermofisher Scientific	Cat# 46-9500-42
Anti-human Tim3 (clone 344823) APC	R&D	Cat# FAB2365A

Anti-human TNF-α (clone OKT3) BV650	Biolegend	Cat# 502935
Anti-human Vα7.2 (clone 3C10) BV605	Biolegend	Cat# 351719
Anti-human Vβ3/TRBV28 (clone JOVI.3) PE	BD Biosciences	Cat# 566432
Anti-human Vγ9 (clone B3) APC	Biolegend	Cat# 331309
Anti-human Vδ2 (clone B6) BV711	Biolegend	Cat# 331411
Anti-human β7-integrin (clone FIB504) PerCP5.5	Biolegend	Cat# 321219
Anti-human γδTCR (clone 11F2) FITC	Miltenyi	Cat# 130-114-029
Anti-human γδTCR (clone 11F2) VioBlue	Miltenyi	Cat# 130-113-507
Anti-human γδTCR (clone 5A6.E9) PE	Thermofisher Scientific	Cat# MHGD04
LEGENDScreen™ Lyophilized An□body Panel	Biolegend	Cat# 700001

REAGENT or RESOURCE	**SOURCE**	**IDENTIFIER**
Cell Dyes		
Near-IR Live-Dead amine-reactive dye	Thermofisher Scientific	Cat# L10119
Zombie Yellow™ Fixable Viability dye	Biolegend	Cat# 423103
CellTrace™ Violet Cell Proliferation Kit	Thermofisher Scientific	Cat# C34557
CellTrace™ Far Red Cell Proliferation Kit	Thermofisher Scientific	Cat# C34564

REAGENT or RESOURCE	**SOURCE**	**IDENTIFIER**
Other reagents		
DNase I	Roche/ Merck	Cat# 11284932001
PerColl	GE Healthcare/ Merck	Cat# GE17-0891-01
LymphoPrep	Axis Shield	Cat# 07851
Cytofix/cytoperm kit	BD Biosciences	Cat# 554714
Cytofix	BD Biosciences	Cat# 554655
DAPI (4',6-Diamidino-2-Phenylindole, Dihydrochloride)	ThermoFisher scientific	Cat# D1306
Brilliant Stain Buffer Plus	BD Biosciences	Cat# 566385
MACS® Separation columns (size LS)	Miltenyi	Cat# 130-042-401
MACS® Separation columns (size LD)	Miltenyi	Cat# 130-042-901
Cell Activation cocktail (without Brefeldin A)	Biolegend	Cat# 423301
Brefeldin A	Biolegend	Cat# 420601
Monensin	Biolegend	Cat# 420701
Zellsafe Tissue chips	Zellkraftwerk GmbH	Cat# 28050606/02-010
gentleMACS C tubes	Miltenyi	Cat# 130-093-237

TaqMan Fast Advanced Master Mix	Life Technologies	Cat# 433182
RNAdvance Tissue RNA isolation kit	Agencourt/ Beckman Coulter	Cat# A32649
HLA-DQ (Celiac disease) RT-PCR kit	AnDiaTec	Cat# 936100
DNeasy Blood and Tissue DNA isolation kit	Qiagen	Cat# 69504
QIAquick® PCR purification kit	Qiagen	Cat# 28104

Chapter 3: Method development

3.1 Introduction

The initial aims of my research were focused on phenotypic, transcriptional, and TCR repertoire analysis of tissue-derived T cell populations in CD. Several required methods were, at the time, not well-established in the research group, and I sought to optimise and validate these methods.

First, isolation of intestinal T cell populations, both from the lamina propria and epithelium, was an important method to achieve my research aims. I examined how intestinal lymphocyte isolation protocols affected surface marker expression.

Second, I planned to perform TCR repertoire sequencing on intestinal T cell populations. After choosing a particular approach to suit the research aims, I examined the performance of the method using the input material planned for the study, including low cell numbers of sorted T cell populations from the intestine. I also assessed the validity of this bulk-sequencing approach, in particular the method's ability to semi-proportionally represent TCR chain usage in the sample material.

Finally, it became clear during the first single-cell RNA sequencing (scRNAseq) experiments that I performed (Chapters 4 & 5) that scRNAseq was particularly sensitive to batch effects. Therefore, I evaluated the validity of using frozen intestinal biopsies for the extraction of intestinal T cells, both for flow cytometry and scRNAseq.

In this chapter, I will briefly outline the methods discussed, the rationale for particular experimental approaches in my work, and the validation work that I performed on T cells.

3.2 Effect of tissue digestion methods on surface marker immunophenotyping

Introduction: Biases and challenges of tissue digestion methods

Multiparameter flow cytometry, mass cytometry by time of flight (CyTOF), and cellular indexing of transcriptomes and epitopes by sequencing (CITE-seq) are powerful tools for the identification and phenotyping of immune cell subsets from mucosal sites and tumour tissue(Spitzer and Nolan, 2016; Stoeckius et al., 2017). Such techniques require the preparation of a single-cell suspension from tissue, using enzymatic, chemical, and mechanical methods. In gastrointestinal research, proteases, particularly collagenases in combination with DNAse, are used for tissue digestion to extract lamina propria lymphocytes (LPLs). EDTA and DTT, chelating and reducing agents respectively, are used for separation of the epithelium and extraction of intraepithelial lymphocytes (IELs) (Madrigal et al., 1993; Schreurs et al., 2017).

However, exposure to these chemicals and enzymes can alter surface marker expression through epitope change by enzymatic protein cleavage or distortion of tertiary structures. DTT alters the detection of a number of important immunological markers in humans(Loppow et al., 2000; D. Qiu and W. C. Tan, 1999; Van Damme et al., 2000). Several tissue digestion enzymes also alter detection of immunological surface markers, with different enzymes and types of collagenases varying in their effects on surface marker detection (Abuzakouk et al., 1996; Autengruber et al., 2012; Ford et al., 1996; Grange et al., 2011; W. M. C. Mulder et al., 1994; C. Shen et al., 2015). In addition, tissue digestion protocols have the potential to alter T cell function, such as proliferative capacity in response to stimulation(Autengruber et al., 2012; Grange et al., 2011).

With the advent of high-parameter immuno-phenotyping techniques, data to help researchers predict the effects of tissue dissociation on surface markers, and to design experiments accordingly,

are lacking(Spitzer and Nolan, 2016). Such data could help guide experimental optimisation and potentially prevent erroneous conclusions from technical error.

When starting my research, two enzymatic digestion techniques for intestinal immune cell isolation were in common use in the laboratory. I chose to evaluate the effect of these two tissue digestion protocols, as well as of IEL isolation with EDTA/DTT, on T cell surface markers (Table 3-1). I examined the effects of these protocols on the detection of immune cell surface markers detected by a standard set of 332 PE-conjugated antibodies (LEGENDScreen™, Biolegend) on T cells from peripheral blood, and used cellular barcoding to multiplex samples for antibody staining and cytometry analysis to control for technical noise(Krutzik et al., 2001; Krutzik and Nolan, 2006). I identified a number of immune cell surface markers altered by these digestion protocols, which have implications for experimental optimisation and design when studying tissue-derived immune cells.

Table 3-1: Tissue digestion protocols for intraepithelial lymphocytes (IELs) and lamina propria lymphocytes (LPLs) examined in this study.

Protocol	Chemical/Enzyme	Concentration	Conditions
IEL extraction	**EDTA** (Sigma-Aldrich) **DTT** (Sigma-Aldrich)	1 mM 1 mM	Ca^{2+}/Mg^{2+} free HBSS for 1 hour at 37°C
LPL extraction (DNAse/Coll A)	**Collagenase A** (Roche) **DNAse I** (Thermofisher)	1.5 mg/ml 100 µg/ml	RPMI with 10% FBS for 1 hour at 37°C
LPL extraction (DNAse/Coll D)	**Collagenase D** (Sigma-Aldrich) **DNAse I** (Thermofisher)	1 mg/ml 100 µg/ml	RPMI with 10% FBS for 1 hour at 37°C

IEL, intra-epithelial lymphocyte; LPL, lamina propria lymphocyte.

Results

Using the LEGENDScreen® antibody panel, the expression of 332 surface markers were examined on stimulated and unstimulated T cells from three donors exposed to three gastrointestinal tissue dissociation conditions (EDTA/DTT, Collagenase A/DNase, and Collagenase D/DNase) or to complete media as a control (Fig. 3-1A). The 24 sample conditions were barcoded using three fluorophore-conjugated anti-CD3 antibodies and varying concentrations of cell dyes to allow for multiplex flow cytometry, which in order to minimize batch effects and technical variation in data acquisition on the cytometer.

Live, singlet lymphocytes were gated and the 24 cell populations were deconvoluted (Fig. 3-1B-D). Representative histograms and dot plots from a single donor for all 332 antibodies are displayed in Supplementary Fig. 3-1. Surface markers that were not expressed on T cells in either the unstimulated or stimulated conditions were excluded from further analysis (Supplementary Fig. 3-1, marked §), leaving 230 markers for analysis.

To determine the impact of chemical/enzymatic treatment on surface marker expression, the MFI of each marker on each treated sample was compared to the control condition for each donor. Representative analysis for expression of CD4 is shown in Fig. 3-1E. Finally, the MFI of each treated condition was compared to the control in a paired manner for the three donors. MFI was chosen as the most appropriate measure to detect differences expression of surface markers with symmetrical, skewed and bimodal distributions. In total, extraction protocols significantly reduced the expression of 71 markers by at least 10%. While the relative reduction in MFI for most surface markers was less than 30%, 31 markers were reduced by more than 30%, 20 markers were reduced by more than 50% and nine markers by more than 70% (Table 3-2).

EDTA/DTT exposure had the most widespread effect on surface marker expression, with the MFI of 44 surface markers significantly reduced by more than 10% (Fig. 3-2, left column). The surface expression of CD2, CD11a, CD49d, CD38, CD103 and β7 integrin was reduced by the greatest magnitude following EDTA/DTT treatment, consistent with previous reports (Loppow et al., 2000; D. Qiu and W. C. Tan, 1999; Van Damme et al., 2000).

Collagenase A/DNase treatment also had a considerable impact on marker expression, and reduced MFI of 37 surface markers by more than 10% (Fig. 3-2, middle column), including CD25 and IL-6Rα. Collagenase D/DNAse had the smallest effect, only reducing the MFI of four surface markers by more than 10% (Fig. 3-2, right column). Of these, only the expression of the W4A5 epitope, a marker of mesenchymal stem cells and neuronal cell progenitors, was significantly reduced by Collagenase D/DNase treatment but not by the other two treatment conditions.

Table 3-2: Surface markers with reduced expression after enzymatic or chemical exposure (% reduction in MFI compared to control)

% Reduction	EDTA/DTT	DNAse/Collagenase A	DNAse/Collagenase D
>70%	CD6	CD99	
	CD102	CD162	
	CD132	CD196	
	CD245		
	BTLA		
	Notch 2		
50%-70%	CD27	CD87	
	CD87	CD183	
	CD97	CD205 (DEC-205)	
	Integrin β7	C3AR	
	Notch 1	DR3 (TRAMP)	
		LAP	
30%-50%	CD1d	CD109	
	CD2	CD154	
	CD38	CD270 (HVEM)	
	CD48	CD352 (NTB-A)	
	CD137 (4-1BB)	BTLA	
	CD150 (SLAM)	GARP (LRRC32)	
	CD218a (IL-18Ra)	Notch 1	
10%-30%	CD5	CD4	CD140b
	CD11a	CD25	Galectin-9
	CD18	CD27	MSC & NPC (W4A5)
	CD20	CD31	TCR Vβ8
	CD49d	CD44	
	CD49e	CD45RB	
	CD49f	CD46	
	CD50 (ICAM-3)	CD62L	
	CD58	CD94	
	CD93	CD97	
	CD100	CD100	
	CD103	CD102	
	CD105	CD108	
	CD124	CD126 (IL-6Ra)	
	CD127 (IL-7Ra)	CD132	
	CD134	CD137L (4-1BB L)	
	CD140b	CD138	
	CD141	CD229 (Ly-9)	
	CD156c (ADAM-10)	Galectin-9	
	CD184 (CXCR4)	Notch 2	
	CD221 (IGF-1R)	TCR Vβ8	
	CD231 (TALLA)		
	CD262 (DR5)		
	CD266 (Fn14)		
	Galectin-9		
	TCR Vβ8		

Several of the affected antibodies have particular relevance to gastrointestinal research. The gut-homing integrins CD103 (αEβ7 integrin) and β7 integrin are both affected by EDTA/DTT and have key roles in lymphocyte trafficking to the intestine, as well as tissue residency. CD102 (ICAM-2), also reduced by EDTA/DTT, may also have a role in lymphocyte recirculation(Berlin et al., 1993). Several cytokine and chemokine receptors are also affected by these enzymatic and chemical protocols, including IL-18Ra, IL-7Ra, IL-6Ra, CD183 (CXCR3), CD25 and CD132. EDTA/DTT and Collagenase A also reduce antibody binding to BTLA, an co-inhibitory receptor on lymphocytes with similarities to PD-1 and CTLA-4, while EDTA/DTT reduces CD97, both with relevance to oncological research(Safaee et al., 2013; N. Watanabe et al., 2003). EDTA/DTT and Collagenase A reduce CD27, which has particular relevance for phenotyping γδ T cells and B cells(Davey et al., 1AD; De Rosa et al., 2004; Wei et al., 2011). These results corroborate similar findings on the effects of Collagenase II in the intestinal mucosa of non-human primates using the same human antibody clone(C. Shen et al., 2015). As γδ T cells are common in the gut, and are increased in the mucosa in some gastrointestinal diseases such as coeliac disease, previous work describing their phenotype in the gut may require validation using methods that avoid these reagents(Dunne et al., 2013).

Conclusions and implications for experimental design

In summary, three routinely used protocols for the isolation of gut-derived immune cells reduced the detection of phenotypic surface markers. EDTA/DTT, used to isolate intraepithelial lymphocytes, and Collagenase A/DNase, used to isolate lamina propria lymphocytes (LPLs), both interfered with the detection of a considerable number of markers. By contrast, Collagenase D/DNase treatment, also used to isolate LPLs, had minimal effects on the detection of T cell-associated markers.
Based on these data, I chose to use Collagenase D/DNAse for the extraction of intestinal T cells whenever possible. Where separation of IELs with EDTA/DTT was required, I ensured that the relevant markers for that particular experiment were not affected. These data provide a resource for researchers designing experiments requiring tissue dissociation.

3.3 Optimisation of cell sorting and TCR repertoire sequencing

Introduction: The adaptive immune system and T cell receptor

The vertebrate adaptive immune system arose nearly 500 million years ago in the early jawed fish, a step-change in immunological defence that required two major evolutionary events: the emergence of recombination-activating gene (RAG)-mediated gene rearrangement, and whole genome duplication allowing creation of paralogous genes that would form the T cell receptor (TCR), B cell receptor (BCR), and major histocompatibility complex (MHC) gene regions(Flajnik and Kasahara, 2009; Rast et al., 1997). The adaptive immune system possesses three key properties: it is highly diverse, the resultant immunological response is highly specific, and it allows the development of immunological 'memory', allowing rapid recall responses to antigens encountered previously.

The properties of the adaptive immune system are due to the ability of vertebrates to generate lymphocytes with rearranged, hyper-variable receptors. Humans have three groups of such lymphocytes; the antibody-producing B cells expressing a BCR, and two groups of T cells expressing either an αβ or γδ TCR. These heterodimeric receptors are generated by variable-(diversity)-joining (V(D)J) rearrangement (as well as somatic hypermutation in B cells, which is not discussed further).

In developing thymocytes in the thymus, V, D, and J gene segments (only V and J gene segments for TRA and TRG chains) are stochastically chosen and combined, with palindromic sequences (P nucleotides) and non-templated nucleotides (N nucleotides) added at the junctions between V(D)J regions by the enzyme terminal deoxynucleotidyl transferase (TdT). The hypervariable region of 40-60bp spanning the V(D)J junction is called the complementarity determining region 3 (CDR3), which directly interacts with peptide-MHC binding (in conventional T cells) and is, for all practical intents and purposes, unique to that TCR and clone. This generates an extraordinary level of potential TCR diversity (in the order of 10^{20} receptors), which is honed down by the process of positive selection (elimination of T cells with insufficient affinity for MHC), and negative selection (elimination of self-

reactive T cells). The resultant naive T cell repertoire is highly diverse (estimated 10^{13} TCRs in the naive repertoire(Laydon et al., 2015)), specific to particular antigens, and self-tolerant.

Following thymic egress, the TCR repertoire is not static, but is sculpted by antigen encounter and immunological events throughout life. The encounter of a naive T cell with its cognate MHC-presented antigen on an antigen-presenting cell will, assuming appropriate co-stimulatory signals, lead to clonal expansion and the generation of effector T cells with that TCR. Following antigen/pathogen clearance, this effector population contracts, leaving a small, but long-lived, memory population that provide long-term immunological memory and can respond rapidly to recurrent antigen exposure. Therefore, the TCR repertoire is in constant flux, shaped by new T cell output, constant antigen exposure, and ageing(Boyd et al., 2013). When considering the immunopathology of human diseases, understanding the changes in this TCR repertoire, and how this links to disease states, is of great importance, and a focus for current research.

TCR repertoire sequencing methods

TCR repertoire sequencing (TCR-seq) requires amplification and sequencing of the recombined TCR gene sequence, specifically over the CDR3 region, a process enabled at scale through the advent of next-generation sequencing (NGS) technologies. Ideally, a TCR-seq method would provide the precise paired sequences of every rearranged TCR in a sample, along with their exact frequency. However, there are a number of biological and methodological aspects of TCR-seq that introduce imperfection and bias in this process.

First, additional complexity to interpretation of TCR-seq data is the coexpression of duplicate chains within a single T cell. Due to allelic exclusion mechanisms, a single T cell can only possess one β-chain, however cells can possess and express multiple α-chains, both at the DNA, RNA, and protein

level. In addition, αβ T cells can possess a rearranged TRG chain, which can also be expressed at the RNA level. αβ T cells cannot express TRD chains, as this locus is excised during TRA recombination.

The choice of source material for TCR-seq - DNA or RNA - is of importance. DNA is easily extracted and suitable for long-term storage. Moreover, as there are two loci for each TCR subunit, the number of template molecules is proportional to the number of starting cells. However, for PCR amplification, multiple V/J gene primers are required, which will vary in efficiency of annealing and amplification, and can lead to bias in PCR amplification of particular genes. Analysis of DNA-based TCR-seq datasets requires the exclusion of recombined TCR genes that would not have been expressed or functional, including sequences with stop codons and those with pseudogene rearrangements. In addition, as almost all extracted DNA from a sample is irrelevant for TCR-seq, initial sample quantity may need to be larger.

In contrast, RNA-based sequencing can provide broader coverage of the TCR repertoire as there will be a greater proportion of TCR template molecules in the sample. Amplification may not generate the same PCR amplification biases to DNA as described above. In addition, as RNA contains the final spliced TCR transcript, there is no noise from incomplete DNA VDJ-recombination products. However, as TCR transcript expression may vary between T cells, copy number may not be proportional to cell count.

TCR-seq is susceptible to sequencing errors that are introduced during NGS sequencing methods, irrespective of template material. While single nucleotide substitutions are rare (in the order of 1 in 1000 for Illumina sequencing(Fox et al., 2014)), when these fall within the CDR3 it can be effectively impossible to distinguish this sequence from a true, rare clone. Such duplicate sequences take the form of erroneous very low frequency clonotypes that are near-identical at the nucleic acid level to a true high frequency clone(Woodsworth et al., 2013). Removal of low quality sequences is important

(frequency of single nucleotide substitutions rapidly diminishes with increasing phred score), but only partially mitigates against this phenomenon(Nguyen et al., 2011). Inclusion of unique molecular identifiers (UMIs) can allow for near-complete correction, but is not used in several commercial and in-house approaches(Rosati et al., 2017). Bioinformatic strategies for error mitigation can be applied (removing all low frequency clonotypes, or collapsing highly similar sequences into one clonotype) however, both may also remove true low-frequency clonotypes from the data. However, while sequencing is undoubtedly a source of error in TCR-seq data, this affects only around 1% of sequences(Nguyen et al., 2011), and if technical and sequencing conditions are controlled, the rate of error between samples will be similar, allowing valid comparisons between samples and conditions.

Another important choice in approach is between bulk and single-cell TCR-seq approaches(De Simone et al., 2018). Importantly, single-cell approaches allow the identification of paired TCR sequences, the more straightforward exclusion of sequencing error, and precise knowledge of clonotype frequency. Although bulk sequencing methods allowing paired TCR sequences have been described(Howie et al., 2015), in general bulk approaches do not allow the identification of paired sequences, while clonotype frequency must be estimated by number of sequencing reads. The principal limitation of single-cell TCR-seq approaches is the practical and financial limitations in the number of cells that can be sequenced. While plate-based and droplet-based TCR-seq approaches can sequence the repertoire of 100s to 1000s of cells, bulk sequencing methods allow the sequencing of potentially 100,000s to millions of cells.

In summary, TCR-seq can provide important insights into the role of adaptive immunity in human disease. However, there is no ‘gold standard’ method for TCR-seq, with rapidly-evolving technologies, each with their own advantages and disadvantages. As such, the choice of method should be determined by the experimental question.

Rationale for TCR repertoire sequencing strategy

The primary aim for TCR-seq in my experimental plan was for the comparison of CD8+ and γδ T cell TCR repertoires from the intestinal mucosa between health and coeliac disease. I estimated that sorted cell numbers from intestinal biopsies would be in the order of 10^4-10^5 cells from each patient, so a bulk sequencing approach was chosen, several of which were available at the time (Table 3-3).

Table 3-3: Characteristics of potential bulk TCR repertoire sequencing approaches.

Company	Source material	RNA/cDNA quantity required	Available as kit?	Library preparation method	Chains	Cost
BGI (Shenzhen, China)	gDNA RNA	500ng RNA	Service	Multiplex PCR (V/C gene primers)	TRA, TRB	£££
Adaptive Biotechnologies (Seattle, USA)	gDNA cDNA	1µg cDNA	Service/ Kit (TRB only)	Multiplex PCR (V/J gene primers)	TRA, TRB, TRG, TRD	££££
iRepertoire (Huntsville, USA)	gDNA RNA	50ng RNA 10ng RNA if high-quality	Service/ Kit (all chains)	Multiplex PCR (V/J gene primers)	TRA, TRB, TRG, TRD	££
Clonotech/Takara (Mountain View, USA)	RNA	10ng RNA	Kit	5' RACE	TRA, TRB	££
Invivoscribe	gDNA	50ng DNA	Kit/Service	Multiplex PCR (V/J gene primers)	TRB, TRD	£££

5'RACE, rapid amplification of 5' complementary DNA ends.

Several TCRseq approaches either lacked validated primers for TRG or TRD, or do not include TRG or TRD in kits or services, which narrowed choice of approach. Due to estimated cell number, the starting nucleic acid concentration for library preparation was likely to be low. I also sought a kit that could be used in-house, as I would be able to trial using smaller cell numbers and starting RNA concentrations, and perform validation on the assay.

Based on these factors, I chose an RNA-based kit from iRepertoire (Huntsville, USA). This kit was affordable for the scale of experiment that I intended to perform. The iRepertoire method uses a amplicon-rescued multiplex PCR (arm-PCR), a method using multiplexed inner and outer primers for first strand synthesis during reverse transcription(Chunlin Wang et al., 2010). This is intended to improve reaction sensitivity, for if secondary RNA structures interfere with inner primer binding, the outer primer will generate target template for the inner primer to bind in the first PCR round. The first PCR round adds a shared tag sequence which is the target for communal primer binding during amplification in the subsequent PCR round. This method has been used successfully in studies involving both αβ and γδ T cells, and from samples from the intestine(Davey et al., 2018b; 2017; J. Wu et al., 2018).

The library preparation allows for relatively high throughput, in terms of sample number, and is validated for use down to 10ng of starting RNA (if high-quality). Primers are available for all four TCR genes, and sample barcodes allow multiplexing of samples for sequencing, controlling to some extent for sequencing error. The company also provide a standardised data processing pipeline for TCR repertoire analysis, which includes bioinformatic filters to remove sequence errors introduced during PCR amplification and sequencing. However, the approach lacks UMIs.

Optimisation of cell-sorting of intestinal T cells

I planned to perform bulk TCR repertoire sequencing of sorted populations of intestinal T cells in coeliac disease. The advantage of bulk TCR repertoire sequencing was the ability to sequence many more cells than would be possible or affordable using single-cell techniques. Therefore, I wished to optimise the strategy for sorting T cells from intestinal biopsy samples.

After optimisation of tissue digestion techniques, including evaluation of the effect of chemical and enzymatic tissue dissociation methods on surface marker phenotype, I evaluated sorting methods to maximise cell number, and a sorting panel to accurately identify CD4+ and CD8+ αβ T cells and γδ+ T cells. This is of particular importance with TRG sequencing, as αβ T cells can express a rearranged TRG transcript, which can confound TRG repertoire analysis if there is αβ T cell contamination.

Using a simplified flow cytometry panel, I identified live intestinal T cells as CD45+CD3+ singlet lymphocytes (Fig. 3-3A). αβ and γδ T cell populations were then distinguished, using the 11F2 γδ-TCR clone which identifies all γδ T cells (not just Vδ2+ T cells), and co-staining for αβ-TCR(Wistuba-Hamprecht et al., 2014). This provided confidence that I could sort all γδ T cells in the gut, without loss of any populations based on inadequate staining.

Intestinal biopsy tissue dissociations contain cellular debris, which can promote cell clumping, leading to temporary blocks of FACS sorters, lost material and reduced sorted cell yields. I tested two methods for reducing this problem: use of EGTA and DNAse I in the sorting medium to lyse free DNA and reduce clumping, or density gradient centrifugation using Percoll (see methods). I compared the sorted cell yield using these two methods, with samples (n=3) divided in two and sorting performed using each method. Sorted cell yield was higher using Percoll density gradient centrifugation for all three samples (Fig. 3-3B), and this method was adopted thereafter. Sorted cell numbers varied substantially (10^3-10^5 cells) between subjects, dependent on cell type and disease state, with greater numbers of all cell types seen in active coeliac disease (Fig. 3-3C).

Optimisation and validation of TCR repertoire sequencing (TCRseq) using amplicon rescued multiplex (arm)-PCR

Following the optimisation of tissue digestion protocols and cell sorting strategies, I optimised RNA extraction, and downstream TCR repertoire sequencing. Due to low input cell numbers, extraction of high quality RNA was not straightforward, with standard column-based kits providing inconsistent results, both in terms of quantity and quality. Instead I used a Trizol-based technique, optimised for low-input cell number samples(Barnitz et al., 2013; Quigley et al., 2010). This provided reliable, high-quality RNA in the 5-50 ng range from sorted T cells (Fig. 3-4A,B).

Then, I developed the use of a bulk TCR repertoire library amplification approach using this RNA. The recommended input RNA quantity for this assay is >50 ng, or >10 ng can be used if high-quality. As my samples would in general be in the 5-50 ng range, this underlined the importance of high-quality RNA extraction techniques. First, I generated libraries from sorted intestinal T cells from three subjects, with input cell numbers ranging from 926 to 79,000 cells. Library generation was successful for all samples, with a single major product generated with an estimated size between 470-545bp, and library concentration greater than 10 ng/µl (Fig. 3-4C,D). An optional clean-up step removed some smaller products and was therefore used thereafter(Fig. 3-4D).

RNA-based bulk TCR sequencing, prone to PCR duplicates and unequal amplification of different products, may not generate a library which is proportional to the input sample TCR repertoire. I sought to evaluate whether this iRepertoire method would provide semi-proportional representation of an underlying TCR repertoire, and whether very small input populations of cells could be detected in the final sample. To test this, I performed a spike-in experiment of varying proportions of cell types with known semi-invariant TCR chain usage. I chose to test the TRA and TRG kits for this approach. To test the TRA kit, I sorted varying proportions (0.025%-100%) of MAIT

cells (identified by CD161 and Vα7.2, the invariant α-chain) into samples of Vα7.2- CD8+ T cells. TRAV1-2 clonotypes consistent with MAIT cell TCR sequences were detected in samples down to 0.025% MAIT cell frequency (50 cells), with semi-proportional increases in the proportion of TRAV1-2 clonotypes with increasing MAIT cell input frequency (Fig. 3-4E). The TRG kit was tested in an analogous manner, sorting Vδ2+ T cells (stained with the B1 clone, which stains Vδ2+Vγ9+ T cells only). The Vγ9 TCR is used by non-Vδ2+ populations also; despite this I saw semi-proportional increases in the proportion of TRGV9 clonotypes with increasing Vδ2+ T cell input frequency (Fig. 3-4F).

Conclusions and implications for experimental design

In summary, I developed strategies for isolating and sorting live intestinal T cell subsets from intestinal mucosal biopsies, with confident identification of αβ and γδ T cell populations. I used Trizol-based RNA extraction approach to extract high-quality RNA from sorted intestinal T cells. Using this RNA, I optimised a bulk TCR repertoire library generation approach for low input samples, and confirmed that this method could produce libraries from low cell number samples, and would provide semi-proportional representation of T cell populations in the samples. Based on these data, I elected to proceed with this method for the evaluation of TCR repertoires of intestinal T cell populations in coeliac disease.

3.4 Comparison of fresh and cryopreserved intestinal immune cells for scRNAseq

Introduction

Single-cell transcriptional profiling of immune cells within the tissue is of great importance to understanding immune-mediated disease processes. However, isolation of immune cell populations from fresh tissue must be performed quickly, is time-consuming, and can be technically challenging. Single-cell RNA sequencing (scRNAseq) is highly prone to batch effects, predominantly due to technical variations introduced at the time of tissue processing, cell sorting, cell capture, library generation, and sequencing(Chen et al., 2018). Even with careful design and unique molecular identifiers to limit amplification bias, such batch effects can severely hamper data interpretation(Tung et al., 2016). This is of particular importance in experiments where the number of study subjects is low, and examination of inter-sample differences (e.g. related to disease), rather than intra-sample differences (e.g. related to cell type), are being examined.

To reduce technical variation and consequent batch effects, preparing and analysing multiple samples in parallel is desirable. However there are substantial logistical barriers to parallel sample processing in studies of human tissue. For gastrointestinal procedures, study subjects are likely to be attending for endoscopic procedures on different days, with the precise time of sample collection often unpredictable. Tissue dissociation, cell sorting, single-cell capture, and library preparation may require specific laboratory equipment that is not available at all times. scRNAseq remains expensive, and therefore the number of study subjects that can be included in an analysis is often low.

A recent paper described the successful cryopreservation of human intestinal tissue for up to six months, which preserved the phenotype and function of intestinal immune cell subsets(Konnikova et al., 2018). My first scRNAseq experiments (in particular Chapter 4) had incorporated blood and

tissue samples that had not been generated in parallel. This introduced batch effects which severely limited the interpretation of inter-sample variation in the context of disease. Therefore, I sought to evaluate whether scRNAseq of intestinal immune populations from cryopreserved intestinal biopsies was possible, and whether relevant intra- and inter-sample variability was comparable to those from fresh intestinal biopsies.

Key Questions:

- Are immune cell subsets isolated in cryopreserved intestinal biopsies?
- Can immune cell subsets isolated in cryopreserved intestinal biopsies be used for scRNAseq?
- What is the effect of cryopreservation on single-cell transcriptional profiles?
- Can relevant intra- and inter-sample variability be detected in scRNAseq data from cryopreserved intestinal cells?

Intestinal biopsy freezing preserves lymphocyte populations

I sought to evaluate the effect of cryopreservation of intestinal biopsy samples on cell population number and transcriptional profile, in particular the effect on lymphocyte populations. I collected intestinal biopsy samples from three patients, two with coeliac disease (one active CD, one treated CD). The samples were either processed fresh, or frozen using a modification of a recently-published approach(Konnikova et al., 2018). In brief, intestinal biopsies were immersed in 1 ml of 90% FCS, 10% DMSO, before controlled freezing (-1^{o}C/minute) to -80^{o}C. After 7-14 days, samples were rapidly thawed in a water bath then washed in R10 medium, before tissue dissociation. Samples were then divided for either flow cytometry or scRNAseq(Fig. 3-5A).

Lymphoid and myeloid populations were quantified by flow cytometry. Lymphoid populations dominated in the small intestine (Fig. 3-5B,C). Myeloid cell numbers were reduced after freezing, although were still present, while lymphoid populations were similar in number between fresh and

frozen samples (Fig. 3-5C,D). The CD4+, CD8+, and double negative (DN - predominantly γδ T cells) populations within CD3+ T cells were maintained following freezing (Fig. 3-5E), as were CD25+ CD4+ T cells (a surrogate for regulatory T cells) and CD56+ T cells (a surrogate for NKT cells)(Fig. 3-5F).

Effects of cryopreservation on single-cell transcriptional profiling of immune cells

To evaluate the effects of intestinal biopsy freezing on scRNAseq of intestinal immune cells, I performed 5' scRNAseq on sorted CD45+ T cells derived from either fresh or frozen intestinal biopsies (Fig. 3-5A). Due to the experimental design, fresh and frozen samples were run on different cell capture chips. Unfortunately due to a cell capture chip failure, one sample from the subject with active coeliac disease could not be sequenced and was removed from the analysis, leaving one healthy control and one treated CD subject. Cell number and reads per cell were down-sampled to the level of the lowest sample to allow accurate comparison between samples.

Intestinal CD45+ cells formed 12 transcriptionally distinct clusters, including conventional and innate-like T cells, γδ T cells, B cells, plasma cells, and a small myeloid population (Fig. 3-6A). Fresh and frozen samples broadly co-clustered without batch correction (Fig. 3-6B). Cells from fresh and frozen samples differed in cell cycle transcriptional characteristics, with frozen cells showing a greater G1 cell cycle score (Fig. 3-6C). The proportion of T cell populations were preserved in frozen samples, although myeloid and mast cell populations were reduced (Fig. 3-6D).

Several scRNAseq quality parameters were compared between fresh and frozen samples. Frozen samples showed an increased percentage of ribosomal transcripts per cell compared to fresh samples, however the percentage of ribosomal transcripts remained low (<0.5%)(Fig. 3-6E). Both the unique molecular identifier (UMI) count per cell, and the percentage of mitochondrial transcripts, were similar between fresh and frozen samples(Fig. 3-6F,G).

The effects of freezing on gene expression were then examined. Transcriptional variation in the dataset was predominantly determined by the effect of cell type/cluster, with differences from either disease status or cell storage status having much smaller effects (Fig. 3-7A). However, freezing did have a consistent effect on transcriptional profiles, best assessed in the populations with the greatest number of cells for purposes of statistical power. CD4+ and CD8+ T cells showed similar changes in response to freezing, with changes in expression of transcripts encoding ribosomal proteins and some cytosolic and lysosomal enzymes (Fig. 3-7B). These transcriptional changes were seen across other clusters/cell types also, with global, rather than cluster-specific, changes in expression seen between fresh and frozen cells (Fig. 3-7C).

A key question for this experiment was to assess whether cryopreservation compromised the ability of scRNAseq to identify cell-types or disease-specific transcriptional signals. First, I compared the cluster marker genes identified in fresh and frozen cell clusters. Cluster marker genes identified between fresh and frozen samples were highly correlated, indicating that cell-type and cluster characteristics are conserved with freezing (Fig. 3-7D). Second, I compared differentially expressed genes between disease states (healthy control vs treated coeliac disease). Due to low cell number limiting statistical power, this was performed for CD4+ and CD8+ T cell clusters only. Differentially expressed genes between disease states found in the fresh and cryopreserved samples were highly correlated in both CD4+ and CD8+ T cell clusters. This indicated that disease-relevant gene expression differences are conserved with freezing (Fig. 3-7E).

Conclusions and implications for the project

In summary, cryopreservation of intestinal biopsy samples preserves the frequency of lymphoid populations, although may reduce myeloid cell numbers. Single-cell RNA sequencing of CD45+ populations from frozen intestinal biopsies is technically possible and again preserves lymphoid populations. While cryopreserved samples do display subtle changes in transcriptional profile, cell

cycle genes, and ribosomal RNA content, these changes are a small source of transcriptional variation, and do not compromise the ability to resolve transcriptionally distinct cell clusters, or detect transcriptional differences between samples.

This experiment was designed to assess whether I should switch to cryopreservation of intestinal biopsy samples, in particular for scRNAseq of intestinal T cell populations. Based on these data, I chose to use cryopreservation, which was used both for flow cytometry and scRNAseq experiments in Chapter 4 (Characterisation of tissue resident memory CD8 populations using intestinal transplantation as a model system). Cryopreservation will also form the basis of further single-cell sequencing experiments in the lab.

There are several limitations to evaluation of cryopreservation and scRNAseq, and the degree of reassurance it can provide about cryopreservation in the wider context. First, cryopreservation does reduce myeloid cell populations, and may alter other cell types that were not included in this study, such as epithelial or stromal cells. However, previous work has shown that epithelial cells can be preserved with this method, and epithelial stem cells retain their ability to form intestinal organoids, suggesting these findings could be extrapolated to other cell types(Konnikova et al., 2018). Second, while I sought to identify major subsets of T cells, it remains unclear if subtypes of B cells, NK cells, or myeloid cells are disproportionally affected by cryopreservation. Third, cryopreservation does alter the transcriptional profile and cell cycle state of immune cells, albeit in a global manner, with no evidence that this compromised underlying intra-sample or inter-sample biological signals. However, it remains possible that particular biological signals could be missed due to changes from cryopreservation.

Cryopreservation with 10% DMSO and 90% FCS was used as this is standard for PBMC cryopreservation in our lab, and on the results of a recent study(Konnikova et al., 2018). However,

equivalent viability of recovered mucosal immune cell populations has been shown using various cryopreservation media(Hughes et al., 2016). Moreover, commercial serum-free products for cryopreservation may show equivalent qualities, based on studies of peripheral and cord blood(Nicoud et al., 2012). In addition, the absence of serum could reduce batch-to-batch variability, with potential benefits in studies of long duration.

In conclusion, scRNAseq of immune populations isolated from cryopreserved intestinal biopsies is technically feasible, with intra- and inter-sample biological variation being preserved, despite some transcriptional changes associated with freezing. Therefore, for experiments in Chapter 4 I used cryopreserved intestinal biopsies for both flow cytometry and scRNAseq experiments.

3.5 Figures

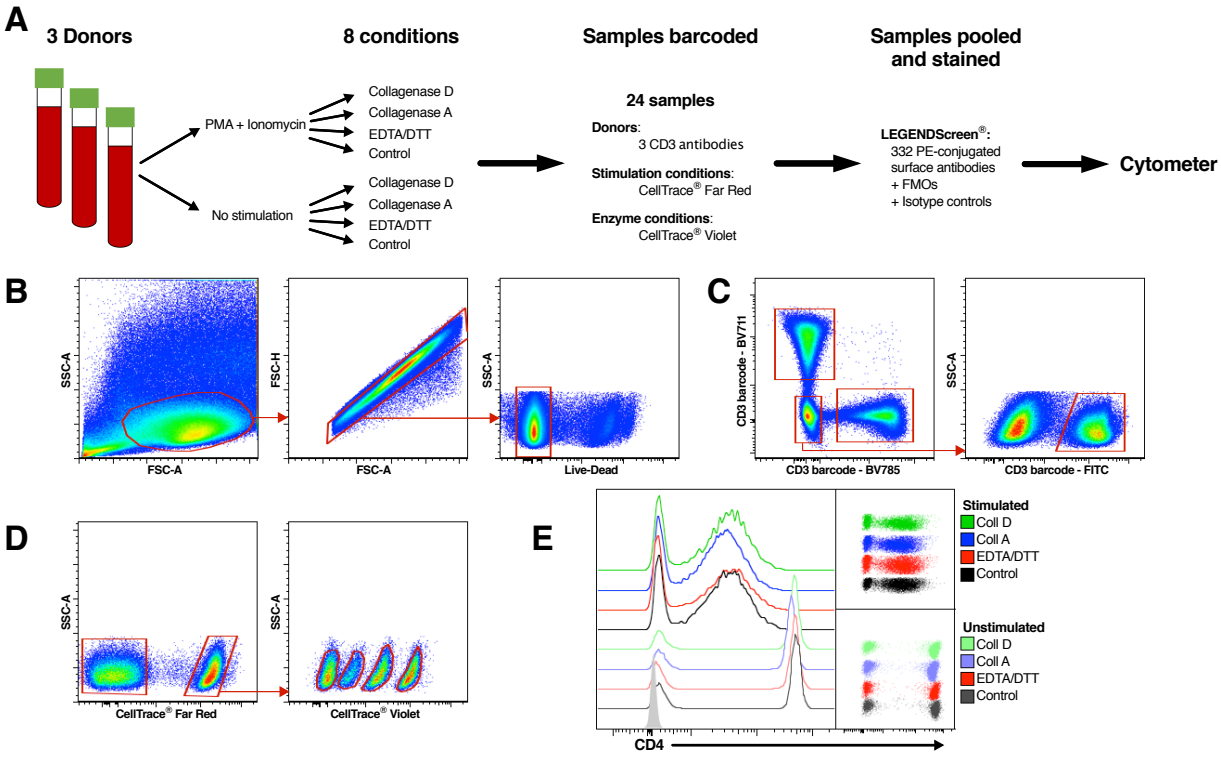
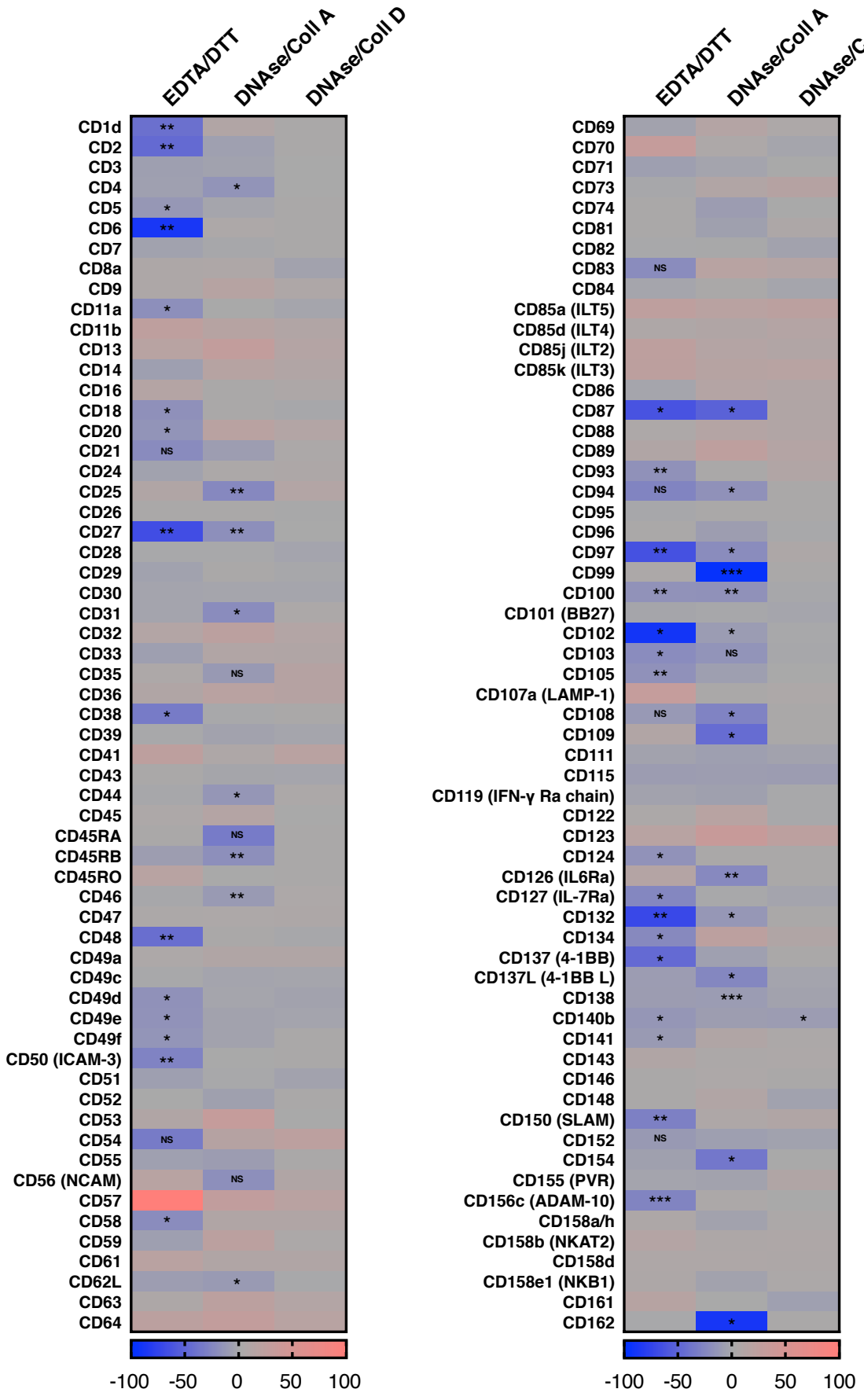


Figure 3-1: Schematic diagram of experiment and gating strategy.

(A) 8x10^8 PBMCs from three donors, either unstimulated or stimulated with PMA/Ionomycin, were incubated with one of three tissue digestion protocols (EDTA/DTT, DNAse/Collagenase A, DNAse/Collagenase D) or control (complete media). The 24 samples/conditions were barcoded for multiplex flow cytometry with three different fluorophore-conjugated CD3 antibodies and varying concentrations of two cell dyes, before staining with the antibody panel and 332 PE-conjugated surface markers. (B) Live, singlet lymphocytes were identified. (C) Samples from the three donors were deconvoluted by gating on the respective CD3 antibody. (D) Stimulated and unstimulated samples and the four tissue digestion conditions were deconvoluted by gating on populations stained with CellTrace Far Red and CellTrace Violet respectively. (E) Histograms and dot plots for all conditions were created (CD4 as example; see Supplemental Fig. 3-1 for representative plots of all markers).


EDTA/DTT
DNAse/CoII A
DNAse/CoII D
CD1d
CD2
CD3
CD4
CD5
CD6
CD7
CD8a
CD9
CD11a
CD11b
CD13
CD14
CD16
CD18
CD20
CD21
CD24
CD25
CD26
CD27
CD28
CD29
CD30
CD31
CD32
CD33
CD35
CD36
CD38
CD39
CD41
CD43
CD44
CD45
CD45RA
CD45RB
CD45RO
CD46
CD47
CD48
CD49a
CD49c
CD49d
CD49e
CD49f
CD50 (ICAM-3)
CD51
CD52
CD53
CD54
CD55
CD56 (NCAM)
CD57
CD58
CD59
CD61
CD62L
CD63
CD64
-100 -50 0 50 100
EDTA/DTT
DNAse/CoII A
DNAse/CoII D
CD69
CD70
CD71
CD73
CD74
CD81
CD82
CD83
CD84
CD85a (ILT5)
CD85d (ILT4)
CD85j (ILT2)
CD85k (ILT3)
CD86
CD87
CD88
CD89
CD93
CD94
CD95
CD96
CD97
CD99
CD100
CD101 (BB27)
CD102
CD103
CD105
CD107a (LAMP-1)
CD108
CD109
CD111
CD115
CD119 (IFN-γ Ra chain)
CD122
CD123
CD124
CD126 (IL6Ra)
CD127 (IL-7Ra)
CD132
CD134
CD137 (4-1BB)
CD137L (4-1BB L)
CD138
CD140b
CD141
CD143
CD146
CD148
CD150 (SLAM)
CD152
CD154
CD155 (PVR)
CD156c (ADAM-10)
CD158a/h
CD158b (NKAT2)
CD158d
CD158e1 (NKB1)
CD161
CD162
-100 -50 0 50 100

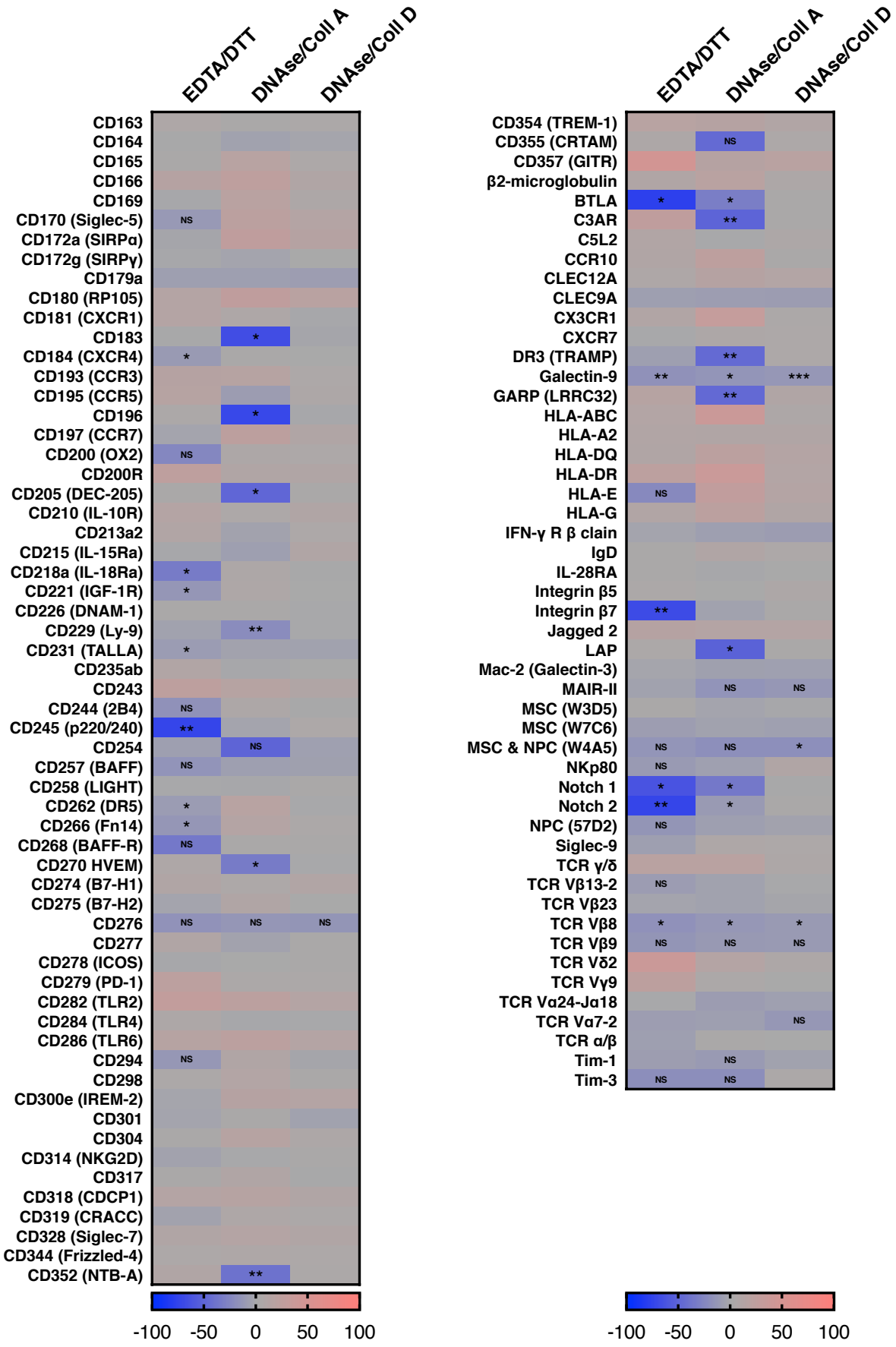

EDTA/DTT
DNAse/Coll A
DNAse/Coll D
CD163
CD164
CD165
CD166
CD169
CD170 (Siglec-5)
CD172a (SIRPα)
CD172g (SIRPγ)
CD179a
CD180 (RP105)
CD181 (CXCR1)
CD183
CD184 (CXCR4)
CD193 (CCR3)
CD195 (CCR5)
CD196
CD197 (CCR7)
CD200 (OX2)
CD200R
CD205 (DEC-205)
CD210 (IL-10R)
CD213a2
CD215 (IL-15Ra)
CD218a (IL-18Ra)
CD221 (IGF-1R)
CD226 (DNAM-1)
CD229 (Ly-9)
CD231 (TALLA)
CD235ab
CD243
CD244 (2B4)
CD245 (p220/240)
CD254
CD257 (BAFF)
CD258 (LIGHT)
CD262 (DR5)
CD266 (Fn14)
CD268 (BAFF-R)
CD270 HVEM)
CD274 (B7-H1)
CD275 (B7-H2)
CD276
CD277
CD278 (ICOS)
CD279 (PD-1)
CD282 (TLR2)
CD284 (TLR4)
CD286 (TLR6)
CD294
CD298
CD300e (IREM-2)
CD301
CD304
CD314 (NKG2D)
CD317
CD318 (CDCP1)
CD319 (CRACC)
CD328 (Siglec-7)
CD344 (Frizzled-4)
CD352 (NTB-A)
-100 -50 0 50 100
EDTA/DTT
DNAse/Coll A
DNAse/Coll D
CD354 (TREM-1)
CD355 (CRTAM)
CD357 (GITR)
β2-microglobulin
BTLA
C3AR
C5L2
CCR10
CLEC12A
CLEC9A
CX3CR1
CXCR7
DR3 (TRAMP)
Galectin-9
GARP (LRRC32)
HLA-ABC
HLA-A2
HLA-DQ
HLA-DR
HLA-E
HLA-G
IFN-γ R β clain
IgD
IL-28RA
Integrin β5
Integrin β7
Jagged 2
LAP
Mac-2 (Galectin-3)
MAIR-II
MSC (W3D5)
MSC (W7C6)
MSC & NPC (W4A5)
NKp80
Notch 1
Notch 2
NPC (57D2)
Siglec-9
TCR γ/δ
TCR Vβ13-2
TCR Vβ23
TCR Vβ8
TCR Vβ9
TCR Vδ2
TCR Vγ9
TCR Vα24-Jα18
TCR Vα7-2
TCR α/β
Tim-1
Tim-3
-100 -50 0 50 100

Figure 3-2: Effect of T cell tissue extraction methods on surface marker detection.
Relative mean fluorescence intensity (MFI) of surface markers expressed on circulating T cells incubated with 1mM EDTA & DTT for 30 minutes (EDTA/DTT), DNAse I and Collagenase A for 1 hour (DNAse/Coll A), or DNAse I and Collagenase D for 1 hour (DNAse/Coll D), compared to incubation in complete media (N=3). Markers were detected using a panel of 332 PE-conjugated antibodies (LEGENDScreen™, Biolegend); full method details are found on p66 in Chapter 2. For markers with MFI reduced by greater than 10% compared to complete media, a 1-tailed t-test was performed. *, $P<0.05$; **, $P<0.01$; ***, $P<0.001$; NS, not significant.

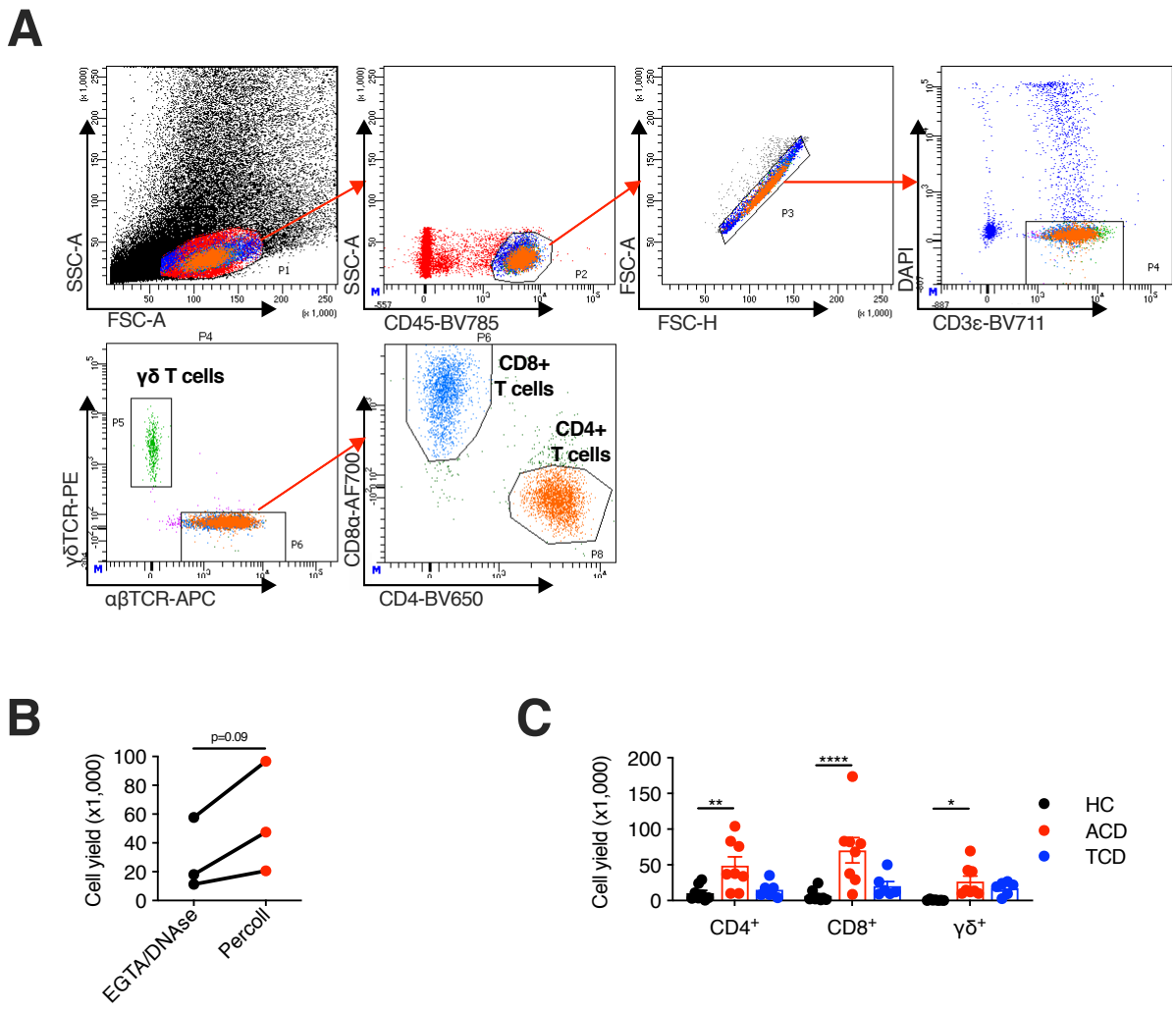


Figure 3-3: Optimisation of sorting strategy

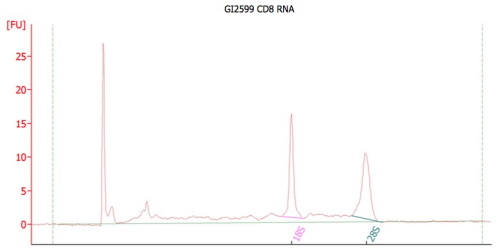
(A) Representative gating strategy for FACS-sorting of intestinal T cell subsets (CD4+, CD8+ and γδ+).

(B) Comparison of FACS-sorted cell yield with intestinal T cell samples pre-treated with EGTA/DNAse, or treated with density gradient (Percoll) separation (n=3).

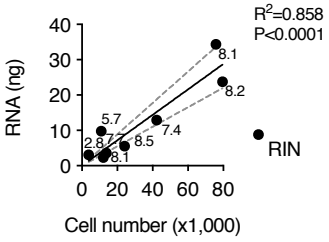
(C) Comparison of FACS-sorted cell yields between healthy control (HC), active coeliac disease (ACD), and treated coeliac disease (TCD) intestinal T cell samples.

2-way ANOVA with comparison between HC and ACD samples for each cell population. *, P<0.05; **, P<0.01; ***, P<0.001.

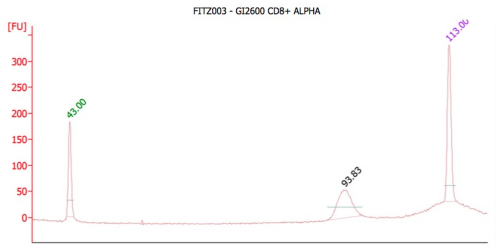
A


GI2599 CD8 RNA
[FU]
25
20
15
10
5
0
18S
28S

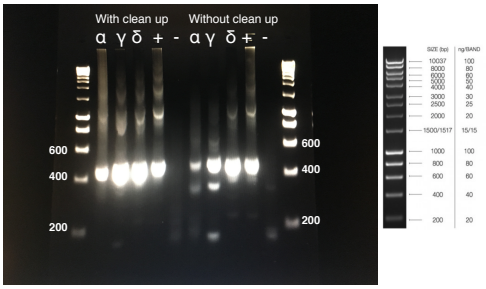
B


R2=0.858
P<0.0001
RIN
RNA (ng)
40
30
20
10
0
0 20 40 60 80
Cell number (x1,000)
8.1
8.2
5.7
7.4
8.5
8.1

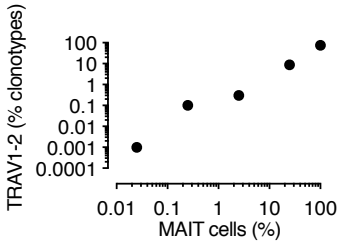
C


FITZ003 - GI2600 CD8+ ALPHA
[FU]
300
250
200
150
100
50
0
43.00
97.83
113.0u

D


With clean up
Without clean up
α γ δ + - α γ δ + -
600
400
200
600
400
200

E


TRAV1-2 (% clonotypes)
100
10
1
0.1
0.01
0.001
0.0001
0.01 0.1 1 10 100
MAIT cells (%)

F

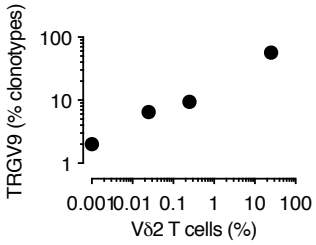

TRGV9 (% clonotypes)
100
10
1
0.001 0.01 0.1 1 10 100
Vδ2 T cells (%)

Figure 3-4: Optimisation of low-input RNA extraction and downstream bulk TCR-repertoire sequencing

(A) Representative Agilent Bioanalyser RNA assay of RNA extracted from sorted intestinal T cells using low-input Trizol-based method.

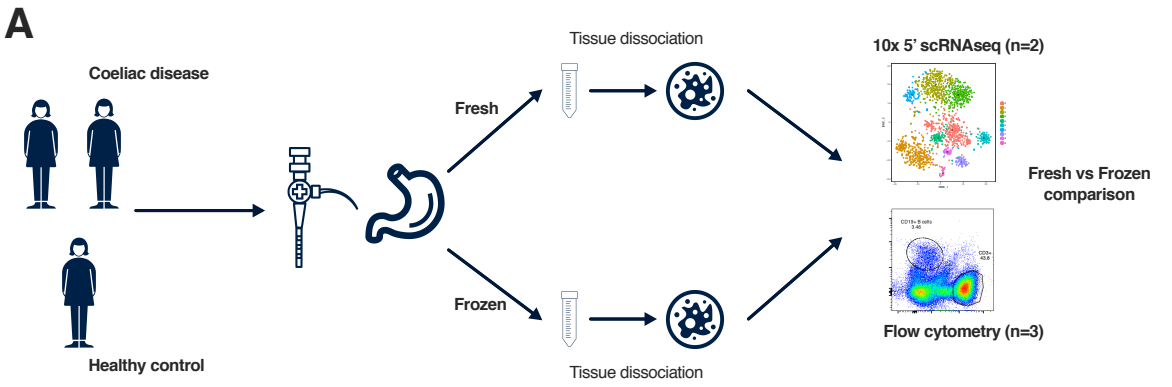
(B) Scatter plot of RNA yield from sorted intestinal T cells compared to input sorted-cell number. RNA Integrity Number (RIN) calculated from Agilent Bioanalyser assay is indicated next to each datum.

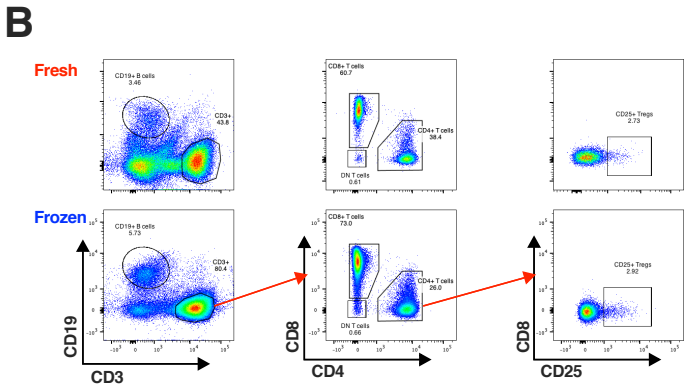
(C) Representative Agilent Bioanalyser DNA assay of TCR repertoire library generated by iRepertoire arm-PCR method.

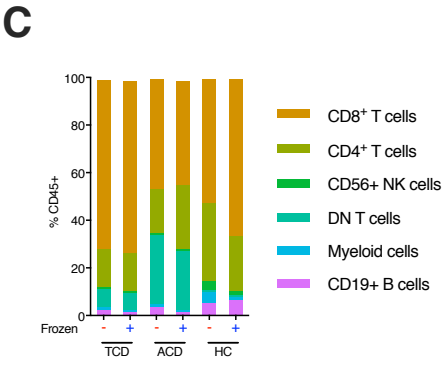
(D) DNA gel electrophoresis of TCR repertoire libraries generated by iRepertoire arm-PCR method TRA (α), TRG (γ), and TRD(δ) libraries are indicated, either with or without optional library clean-up step.

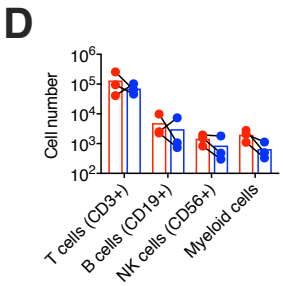
(E) Proportion of TRA clonotypes expressing TRAV1-2 in iRepertoire-generated libraries from CD8+ T cell samples with differing proportions of MAIT (Vα7.2+CD161++) cells in sample.

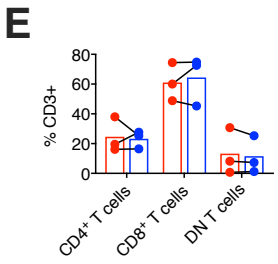
(F) Proportion of TRG clonotypes expressing TRGV9 in iRepertoire-generated libraries from γδ T cell samples with differing proportions of Vδ2+Vγ9+ (Vδ2+ (clone B1)) cells in sample.


A
Coeliac disease
Healthy control
Fresh
Frozen
Tissue dissociation
Tissue dissociation
10x 5' scRNAseq (n=2)
Fresh vs Frozen comparison
Flow cytometry (n=3)


B
Fresh
Frozen
CD19
CD3
CD8
CD4
CD8
CD25


C
% CD45+
Frozen
TCD
ACD
HC
CD8+ T cells
CD4+ T cells
CD56+ NK cells
DN T cells
Myeloid cells
CD19+ B cells


D
Cell number
T cells (CD3+)
B cells (CD19+)
NK cells (CD56+)
Myeloid cells


E
% CD3+
CD4+ T cells
CD8+ T cells
DN T cells

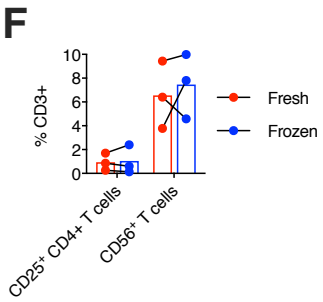

F
% CD3+
Fresh
Frozen
CD25+ CD4+ T cells
CD56+ T cells

Figure 3-5: Effect of cryopreservation on isolation of viable intestinal CD45+ cells

(A) Schematic diagram of the experimental design.

(B) Representative flow cytometry plots for identification of CD19+ B cells, CD3+ T cells, CD4+ and CD8+ T cells, and CD25+ CD4+ T cells isolated from fresh and cryopreserved intestinal biopsies.

(C) Proportion of total viable intestinal CD45+ cells isolated either with or without cryopreservation from different immune cell subsets, from three donors. HC, healthy control; ACD, active coeliac disease; TCD, treated coeliac disease.

(D) Number of viable intestinal cells isolated either with or without cryopreservation from different immune cell subsets (n=3). Fresh, red; Cryopreservation, blue.

(E) Intestinal CD4+, CD8+, and double negative (DN) T cell subsets as a proportion of total T cells, categorised as with or without cryopreservation (n=3). Fresh, red; Cryopreservation, blue.

(F) Intestinal CD4+CD25+, and CD56+ T cell subsets as a proportion of total T cells, categorised as with or without cryopreservation (n=3). Fresh, red; Cryopreservation, blue. Lines connect samples from the same study subject.

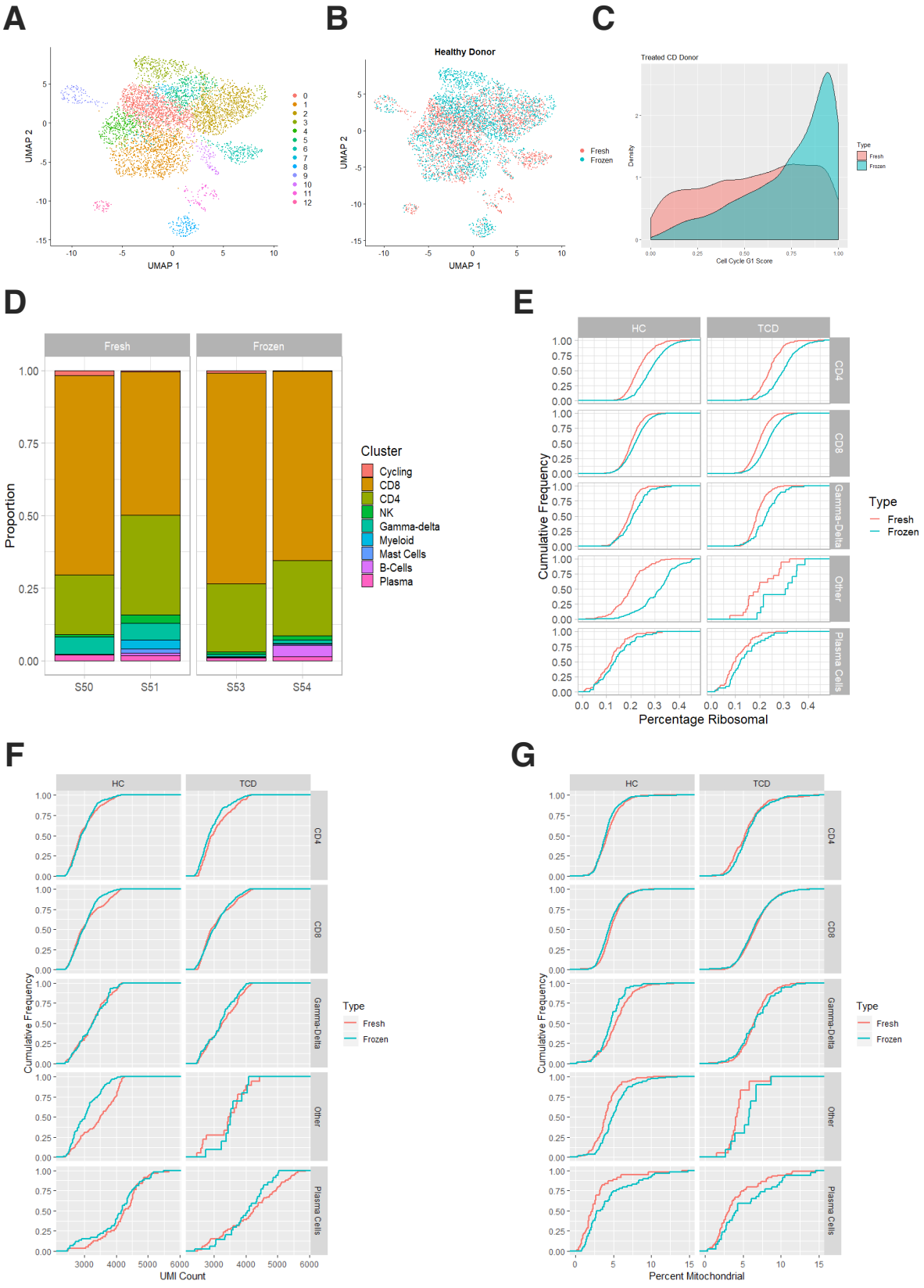

A
B
C
UMAP 2
UMAP 1
0
1
2
3
4
5
6
7
8
9
10
11
12
Healthy Donor
Fresh
Frozen
Treated CD Donor
Density
Cell Cycle G1 Score
Type
D
Fresh
Frozen
Proportion
S50
S51
S53
S54
Cluster
Cycling
CD8
CD4
NK
Gamma-delta
Myeloid
Mast Cells
B-Cells
Plasma
E
HC
TCD
CD4
CD8
Gamma-Delta
Other
Plasma Cells
Cumulative Frequency
Percentage Ribosomal
Type
Fresh
Frozen
F
UMI Count
G
Percent Mitochondrial

Figure 3-6: Effect of cryopreservation on single-cell RNA sequencing quality metrics

UMAP plot of viable CD45+ cells isolated from a single healthy subject, with (A) transcriptionally distinct clusters identified, and with (B) cells isolated fresh or from cryopreserved biopsies identified. (C) Cell cycle G1 score of cells isolated from fresh or from cryopreserved biopsies, categorised by fresh (red) or cryopreserved (blue) biopsy source.

(D) Proportion of total viable intestinal CD45+ cells isolated either with or without cryopreservation from different clusters of putative immune cell subsets, from two donors. HC, healthy control; TCD, treated coeliac disease.

(E) Percentage of ribosomal RNA in CD45+ cells from two donors, categorised by fresh (red) or cryopreserved (blue) biopsy source. HC, healthy control; TCD, treated coeliac disease.

(F) Unique molecular identifier (UMI) count per cell in CD45+ cells from two donors, categorised by fresh (red) or cryopreserved (blue) biopsy source. HC, healthy control; TCD, treated coeliac disease.

(G) Percentage of mitochondrial RNA in CD45+ cells from two donors, categorised by fresh (red) or cryopreserved (blue) biopsy source. HC, healthy control; TCD, treated coeliac disease.

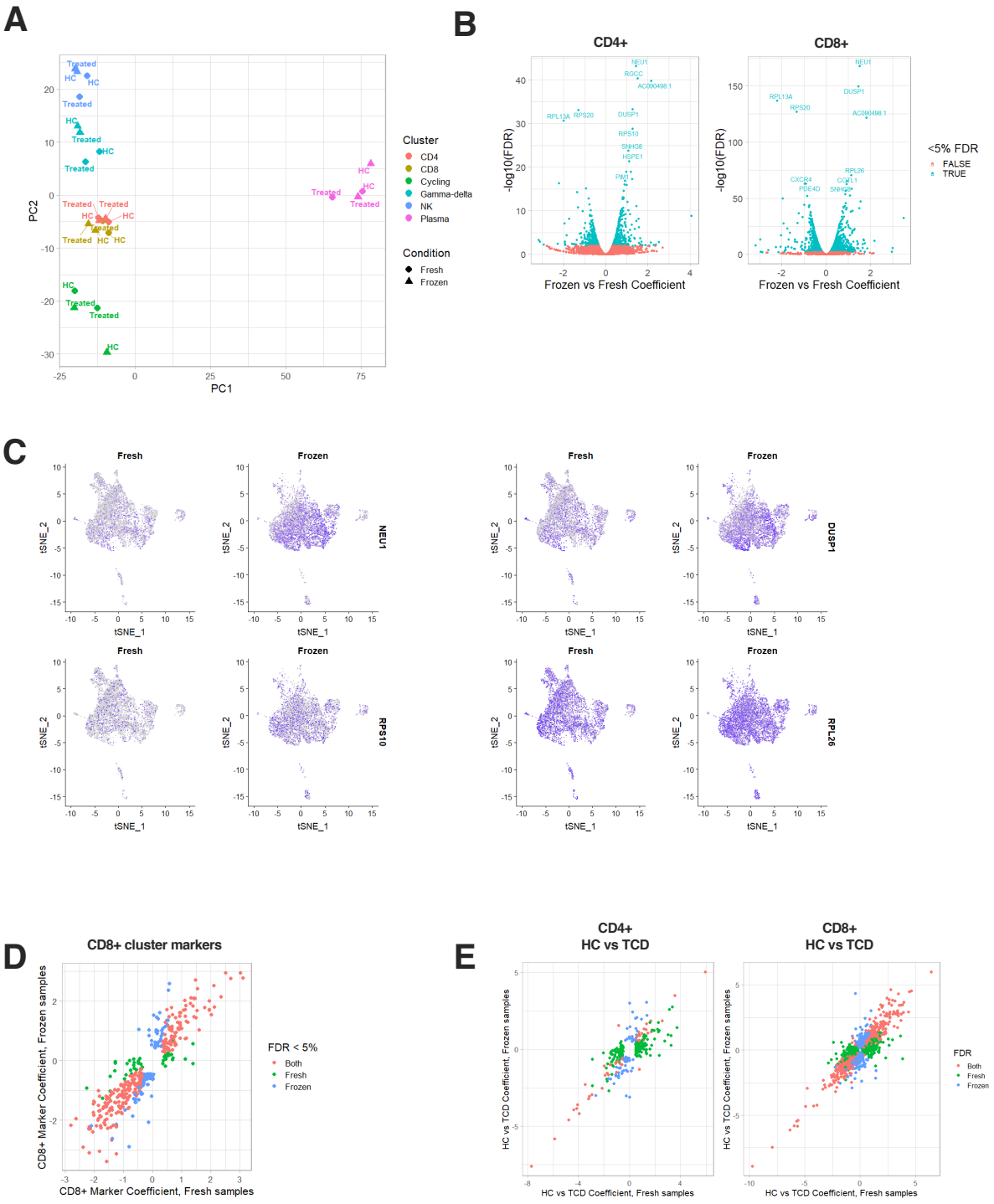

A
PC2
PC1
Cluster
CD4
CD8
Cycling
Gamma-delta
NK
Plasma
Condition
Fresh
Frozen
B
CD4+
CD8+
-log10(FDR)
Frozen vs Fresh Coefficient
<5% FDR
FALSE
TRUE
C
Fresh
Frozen
tSNE_1
tSNE_2
NEU1
DUSP1
RPS10
RPL26
D
CD8+ cluster markers
CD8+ Marker Coefficient, Frozen samples
CD8+ Marker Coefficient, Fresh samples
FDR < 5%
Both
Fresh
Frozen
E
CD4+
HC vs TCD
CD8+
HC vs TCD
HC vs TCD Coefficient, Frozen samples
HC vs TCD Coefficient, Fresh samples
FDR

Figure 3-7: Effect of cryopreservation on transcriptional profiles of intestinal CD45+ cells

(A) PCA plot of heterogeneity between pseudobulk transcriptional profiles (amalgamated from the transcriptional profiles of all cells in the cluster) of intestinal CD45+ cell clusters, categorised by disease status (healthy control, HC; treated coeliac disease, treated), and prior cryopreservation of intestinal biopsies (fresh, diamonds; frozen, triangles). Small clusters of less common CD45+ populations were removed from the analysis.

(B) Volcano plots of differentially expressed genes between cells isolated from cryopreserved (frozen) and fresh intestinal biopsies within CD4+ and CD8+ T cell clusters. Highly variable genes are labelled.

(C) UMAP of cells from both subjects combined, overlaid with genes most differentially expressed between fresh and cryopreserved intestinal biopsies (*NEU1, DUSP1, RPS10, RPL26*).

(D) Correlation of the CD8+ cluster marker coefficient (corrected fold change between the CD8+ cluster cells and all other cells) from fresh samples (x-axis) and cryopreserved samples (y-axis). Red, genes differentially expressed in both experiments; green, genes differentially expressed in fresh samples only; blue, genes differentially expressed in cryopreserved samples only.

(E) Correlation of the coefficient between treated coeliac disease and healthy control cells (corrected fold change between TCD cells and HC cells) from fresh samples (x-axis) and cryopreserved samples (y-axis) in CD4+ and CD8+ T cell clusters (left and right respectively). Red, genes differentially expressed in both experiments; green, genes differentially expressed in fresh samples only; blue, genes differentially expressed in cryopreserved samples only.

Chapter 4: Characterisation of CD8+ and γδ T cells in coeliac disease using TCR repertoire sequencing, RNA sequencing, and flow cytometry

4.1 Acknowledgement of contributions

Library preparation for single-cell RNA sequencing was performed in collaboration with Dr Melanie Dunstan and Dr Riccardo Ferreira. Single cell RNA sequencing data analysis was performed in collaboration with Dr Agne Antanavicuite, who generated some of the plots used in Figures 2-12 to 2-18. Part of this work (*ex vivo* cytokine stimulations of intestinal T cells) has previously been published(Provine et al., 2018), and Figure 4-2 is adapted from the data used for publication.

4.2 Introduction

The striking association of CD with HLA-DQ alleles(Sollid et al., 1989), as well as the discovery of HLA-DQ2.5-restricted, gluten-specific CD4+ T cells (Lundin, 1993), established, by the mid-1990s, that the gluten-specific CD4+ T cell was the key player in the development of CD. In the following two decades, the molecular basis of how gluten peptides - protected from degradation by virtue of their proline-rich structure, and altered by the ubiquitous enzyme tissue transglutaminase 2(Qiao et al., 2011; 2014) – interact with HLA-DQ molecules and their cognate TCR has been uncovered. This has provided a level of understanding of CD immunopathology beyond that in any other autoimmune disease (as discussed in the introduction).

However, most individuals possessing HLA-DQ alleles associated with CD do not develop the disease, indicating that this risk factor, while necessary, is not sufficient for the development of CD. In addition, a fraction of individuals with CD-risk HLA alleles develop a state of potential CD, where gluten-specific CD4+ T cells are present with serum and tissue TG2 IgA detectable, however with no evidence of epithelial damage or villous atrophy. Humanized murine models of CD also show that a gluten-specific CD4+ T cell response in isolation is not sufficient to cause intestinal damage, due to appropriate regulatory CD4+ T cell responses(Black et al., 2002; M F Du Pré et al., 2011). These observations indicate that there are additional genetic and environmental factors required to trigger coeliac disease autoimmunity, and that this autoimmunity can be prevented from causing mucosal damage through regulatory mechanisms. These processes beyond the CD4+ T cell gluten-specific response in CD are not well understood, nor are the cellular players that drive it.

Two such putative players in the immunological orchestra are those most enriched at the site of CD inflammation and villous atrophy: the CD8+ and γδ+ T cells that crowd the inflamed intra-epithelial compartment in CD(Halstensen et al., 1989; Kutlu et al., 1993; Selby et al., 1983). CD8+ T IELs (expressing an αβTCR) are thought to be the proximate cause of intestinal cell damage, through cytolysis of epithelial cells. This is thought to be mediated by NKG2C-CD94 and NKG2D, which are upregulated on CD8+ T IELs in CD, while their ligands MICA and HLA-E are upregulated on target epithelial cells(Meresse et al., 2006; 2004). The presence of IL-15 can 'arm' such NKG2D-expressing IELs to mediate cytolysis of target cells in a TCR independent manner *in vitro*(Meresse et al., 2004), while NKG2C can mediate IEL proliferation *in vitro*(Meresse et al., 2006), theoretically freeing these T cells from TCR-mediated control of proliferation and cytotoxicity. The recent development of a promising murine model of coeliac disease (a HLA-DQ8-expressing transgenic mouse with over-expression of IL-15 in both lamina propria and epithelial compartments), where both gluten-peptide autoimmunity and villous atrophy are seen, provides additional evidence that TCR-dependent CD8+ T cell function is not required in coeliac disease(Abadie et al., 2020). However, it remains unclear if

these NKR signals, in combination with IL-15, are sufficient to induce epithelial cell death and villous atrophy in humans *in vivo*.

There are several lines of evidence that suggest a potential role for TCR-dependent processes in the CD8+ T cell response in coeliac disease. CD8+ T cell lines isolated from CD patients have been shown to recognise gliadin peptides in a Class I HLA-restricted manner(Gianfrani et al., 2003; Mazzarella et al., 2008; Picascia et al., 2017). Such responses can, *in vitro*, induce IFNγ production and cytotoxicity against epithelial cell lines, although their involvement *in vivo* remains unclear. While early reports of HLA Class I associations with CD were likely due to linkage disequilibrium with the HLA-DQ locus, recent work performing fine mapping of the MHC associations with CD identified additional genetic risk beyond previously identified associations, including with HLA Class I alleles(Gutierrez-Achury et al., 2015). Gluten-specific CD4+ T cells increase substantially in the circulation following gluten challenge(R. P. Anderson et al., 2000; Raki et al., 2007). A similar phenomenon involving CD8+ T cells has been noted, with an increased proportion of activated, gut-homing CD8+ T cells following gluten challenge(Han et al., 2013). Of note, these populations showed skewed, oligoclonal TCR repertoires, suggesting that this may represent an antigen-specific population. In sum, there is circumstantial evidence that HLA Class I-restricted gluten-specific CD8+ T cell responses are, at least theoretically, a potential player in coeliac disease pathogenesis.

While the increased number and proportion of γδ T cells in the mucosa in coeliac disease has been recognised for over 30 years(Halstensen et al., 1989), the reason for this increase, and the role of γδ T cells in coeliac disease immunopathology, remains unclear. Intestinal γδ T cells express cytotoxic molecules in coeliac disease, and can produce pro-inflammatory mediators including IFN-γ in vitro. Recent work has shown that coeliac disease reshapes the Vδ1+ T cell TCR repertoire, with a permanent loss of BTNL3-8-reactive NKp46+ γδ T cells from the mucosa, and an increase in IFN-γ producing populations(Mayassi et al., 2019). This is associated with a change in transcriptional

profile, with changes in NK receptors and associated genes, as well as genes associated with tissue repair. This change from an NK-like population is supported by reduced CD56 expression on mucosal γδ T cells in coeliac disease(Dunne et al., 2013). This suggests that a specific population of γδ T cells enter the tissue in response to coeliac disease inflammation, usurping the natural IEL populations previously present, and taking up a tissue-resident phenotype with pro-inflammatory and chemoattractant roles.

Whether γδ T cells respond directly to gluten in the mucosa remains unclear. Following gluten challenge in subjects with treated coeliac disease, Vδ1+ T cells demonstrated enhanced production of IFN-γ in *ex vivo* assays(Mayassi et al., 2019). Moreover, *in vitro* stimulations of gut-derived T cell lines with gluten have shown proliferation of γδ T cells(Steenholt et al., 2017). However, this evidence does not discriminate between direct stimulation of γδ T cells by gluten, or indirect stimulation, for instance via cytokine mediators, from gluten-specific CD4+ T cells. Similar to CD8+ T cells, activated, gut-homing γδ T cells markedly increase in the circulation following gluten challenge, with a clonotypically focused TCR repertoire and enrichment of particular CDR3δ motifs, suggestive of an antigen-specific process(Han et al., 2013). Recent studies of the intestinal TCR repertoire of γδ T cells have shown changes in V-gene usage, potentially related to altered BTNL3/8 expression by epithelial cells, however evidence for antigen-specific CDR3 motif enrichment is contradictory(Eggesbø et al., 2019; Mayassi et al., 2019).

Finally, a potential regulatory role for γδ T cells has been postulated, in contradiction with the evidence above of their pro-inflammatory role. In particular, in vitro studies show that NKG2A+ γδ T IELs can suppress the activation of cytotoxic T lymphocytes (IFN-γ and granzyme-B expression) via TGF-β, mediated via enterocyte-expressed HLA-E(Bhagat et al., 2008). This suggests that intestinal γδ T cell populations may have complex pro-inflammatory and regulatory roles in coeliac disease.

In summary, CD8+ T IELs are thought to be the foot soldiers of the coeliac immune response, commanded ultimately by the adaptive CD4+ T cell immune response to induce epithelial cell death via innate-like NK receptors and cytokines alone. However, there remains uncertainty about whether adaptive, TCR-dependent mechanisms are also at play, which may explain why the CD4+ T cell gluten-specific response is not sufficient alone to induce villous atrophy. The uncertainties regarding the roles of γδ T IELs are more profound, and it remains unclear if they possess an analogous role to CD8+ T IELs, play a separate part in coeliac disease pathogenesis, or are merely increased as a bystander effect.

My research in this chapter sought to examine the role of CD8+ and γδ T cells in coeliac disease. I hypothesised that:

- Intestinal CD8+ and γδ T cell TCR repertoires are perturbed in CD, suggestive of a TCR-dependent role in coeliac disease pathogenesis.
- Intestinal CD8+ and γδ T cells show differing transcriptional responses to CD, indicative of potentially different roles in the immune response.

I performed flow cytometry, bulk and single-cell RNA sequencing, and TCR repertoire sequencing to examine CD8+ and γδ T cells in the gut in coeliac disease.

4.3 Peripheral and mucosal T cell populations in coeliac disease

4.3.1 Non-Vδ2 γδ T cells are increased in the gut, but not blood, in coeliac disease

I performed flow cytometry on PBMCs, intraepithelial lymphocytes (IELs), and lamina propria lymphocytes (LPLs) to compare the proportion of particular T cell subsets in health and coeliac disease. Within peripheral blood there was no change in the proportion of CD4+, CD8+, and γδ T cells between health and CD (Fig. 4-1A). There was also no difference in the proportion of Vδ1+, Vδ2+, or Vδ1/2- γδ T cells between health and CD.

Within the IEL compartment there was a striking increase in the proportion of γδ T cells, from 4% of total CD3+ T cells in healthy controls to 24% in ACD(Fig. 4-1A). This increased proportion of γδ T cells persisted in TCD (40%). This increase was entirely confined to Vδ1+ and Vδ1/2- γδ T cell subsets, with no increase in the Vδ2+ T cell population. The proportion of γδ T cells in the lamina propria was substantially lower than that in the IEL compartment, both validating the efficacy of IEL/LPL separation, and indicating that the increase of Vδ1+ and Vδ1/2- γδ T cells in coeliac disease is localised to the epithelium.

A previous study reported a reduction in circulating γδ T cell and MAIT cell subsets in adult individuals with CD(Dunne et al., 2013), however, this small first cohort had not replicated this finding. I analysed the proportion of circulating γδ T and MAIT cells in a second cohort of individuals with and without CD. There was no difference in the proportion of total γδ T cells, Vδ2+ T cells, or non-Vδ2 T cells between health and coeliac disease (Fig. 4-1B). Non-Vδ2 T cells can be categorised into CD27hi and CD27lo/neg subsets, with naive and memory characteristics(Davey et al., 2018a; 2017). There was no difference in the proportion of CD27lo/neg (memory) non-Vδ2 T cells between

health and coeliac disease (Fig. 4-1C). Finally, there was no difference in MAIT cell frequency between health and coeliac disease (Fig. 4-1D).

In sum, while there are profound changes to the IEL T cell compartment in coeliac disease, these changes are highly localised, with no evidence of a systemic disturbance in γδ T cells, CD8+ T cells, or MAIT cells with coeliac disease.

4.3.2 Non-Vδ2 γδ T cells do not respond to combinatorial cytokine stimulation

Some populations of γδ T cells show pro-inflammatory responses to combinatorial cytokine stimulation, including IL-12, IL-15, and IL-18, in a manner analogous to MAIT cells(Fergusson et al., 2014; Sattler et al., 2015; van Wilgenburg et al., 2016). IL-15 is increased in the mucosa in active coeliac disease(Abadie and Jabri, 2014; Jabri and Abadie, 2015; Maiuri et al., 2000), and CD is has been associated with variants associated with the genes *IL18R1* and *IL18RAP*, which encode the IL18 receptor(Lindfors et al., 2019; Withoff et al., 2016). I hypothesised that non-Vδ2 T cell populations in the gut respond to combinatorial cytokine stimulation with pro-inflammatory cytokine release, particularly IFNγ.

To test this hypothesis, I performed *ex vivo* stimulation of PBMCs and intestinal-derived T cells with combinatorial cytokine (IL-12 + IL-18). CD161 expression, which is linked to innate-like T cell cytokine responses(Fergusson et al., 2014), was expressed on almost all Vδ2+ T cells in blood, while Vδ1+ T cells expressed CD161 at lower levels, akin to conventional T cells (Fig. 4-2A). In the duodenum, Vδ2+ T cells again expressed higher levels of CD161 than Vδ1+ counterparts (Fig. 4-2B). Vδ1+ T cells expressed lower levels of the IL18 receptor (IL18Rα) in both the blood and intestine (Fig. 4-2C).

On combinatorial cytokine stimulation, MAIT cells responded with IFNγ production, both in blood and intestinal tissue. Vδ2+ T cells showed analogous responses to MAIT cells in tissue and blood. However, Vδ1+ T cells, the population increased in proportion in coeliac disease, showed negligible responses to combinatorial cytokine stimulation in both blood and intestine(Fig. 4-2D,E; published in (Provine et al., 2018)).

These results indicate that Vδ1+ T cells in the blood and intestine do not show the innate-like pro-inflammatory responses to combinatorial cytokine stimulation that MAIT cells and Vδ2+ T cells demonstrate. Therefore cytokine-mediated activation of Vδ1+ T cells in the epithelium is unlikely to be relevant in coeliac disease.

4.4 TCR repertoire sequencing of mucosal CD8+ and γδ T cells

I sought to examine mucosal CD8+ and γδ T cell populations in coeliac disease in more detail. While the TCR repertoire of CD-related CD4+ T cell populations has been the focus of extensive study, at the time of starting this work there was a paucity of studies applying NGS TCR repertoire techniques to CD8+ and γδ T cells in the gut in CD. I performed bulk TCR repertoire sequencing of mucosal CD8+ and γδ T cells using an RNA-based approach. Development, optimisation, and validation of the approach is included in Chapter 3. Two important studies of the TCR repertoire of mucosal γδ T cells have since been published, and my results are discussed with reference to them(Eggesbø et al., 2019; Mayassi et al., 2019).

4.4.1 Descriptive statistics of TCR repertoire cohort

Twenty subjects with and without coeliac disease undergoing upper gastrointestinal endoscopy were included (characteristics in Table 4-1). The mean age of study subjects was 36.5 years, ranging from 17 to 68 years old. There was no age difference between disease groups. Seventeen of the twenty patients were female, consistent with the known female preponderance of CD. Disease status was ascertained based on clinical parameters, positive coeliac serology (TTG or EMA), histology report, HLA genotype, and response to treatment.

Only subjects with Marsh 3 duodenal villous atrophy, a positive TTG ten times the upper limit of normal, and who were currently consuming gluten in their diet were included in the active coeliac disease (ACD) cohort. Subjects in the treated coeliac disease (TCD) cohort had to have previously met the criteria for active coeliac disease, must be following a gluten-free diet, have had a reduction in TTG titre, and have an improved in duodenal histology to Marsh 0 or Marsh 1. Healthy control patients must have no clinical suspicion of coeliac disease, no endoscopic or histological evidence of villous atrophy, and/or a negative TTG antibody. Subjects in the ACD cohort had a median TTG titre of 867 (range 356-1621), and all had Marsh 3 duodenal villous atrophy. Subjects in the TCD cohort had a median TTG titre of 17 (range 0-296; ULN = 20), with two subjects having a Marsh score of 0, and three subjects a Marsh score of 1.

The maximum number of cells were sorted by FACS from each intestinal sample, which meant that cell number varied between individuals and cell populations. The distribution of cell number was not normally distributed. The median number of cells sorted was 38,155 CD8+ T cells (range 2,423-173,712) and 9,918 γδ T cells (range 626-69,651). There was no significant difference in sorted CD8 T cell numbers between disease cohorts, however γδ T cell numbers were lower in the non-coeliac cohort (2,815 cells in HC, vs 12,087 in TCD and 19,295 in ACD).

Table 4-1. Demographics of the TCRseq patient cohort

Biobank ID	Diagnosis	Age	Gender	TTG	EMA	Histology	HLA type
2484	HC	63	F	ND	ND	Normal	ND
2547	ACD	19	F	356	+	Marsh 3	ND
2600	ACD	26	F	867	+	Marsh 3	ND
2751	TCD	30	F	16	-	Marsh 1	DQ2
2750	ACD	33	F	831	+	Marsh 3	DQ2
2797	ACD	45	F	1301	+	Marsh 3	DQ2
2798	ACD	27	F	789	+	Marsh 3	DQ2
2799	TCD	41	M	296	-	Marsh 1	DQ2
2801	HC	23	M	ND	ND	Normal	NEG
2790	TCD	30	F	17	-	Marsh 1	DQ2
2894	ACD	20	F	1621	+	Marsh 3	DQ2
2898	TCD	57	M	0	-	Normal	DQ2
2899	ACD	62	F	879	+	Marsh 3	DQ2
2900	TCD	60	F	83	-	Normal	DQ8
2874	HC	33	F	ND	ND	Normal	DQ2
3187	HC	25	F	ND	ND	Normal	NEG
3369	HC	25	F	0	-	Normal	NEG
3370	HC	26	F	ND	ND	Normal	DQ8
3372	HC	68	F	0	-	Normal	DQ2
3374	HC	17	F	0	-	Normal	DQ8

ACD, active coeliac disease; HC, healthy control; Pot CD, potential coeliac disease; TCD, treated coeliac disease; TTG, anti-tissue transglutaminase 2 antibodies; EMA, anti-endomysial antibodies; ND, not done.

4.4.2 The γδ T cell repertoire

Diversity and TCR gene usage

In total, 313,140 γδ T cells from 20 subjects were sorted for RNA-based bulk TCR repertoire sequencing. The number of unique TRG and TRD CDR3 sequences was higher in active CD (Fig. 4-3A). This may be explained by the increased sorted cell number in active CD. D50, Diversity Index, Shannon entropy, and proportion of reads from the top 10 clones did not differ between HC and CD subjects. However, given variable cell numbers in different samples, and the use of an RNA-based, non-UMI method, true changes in diversity may not be detected, and cannot simply be corrected using statistical techniques. However, the most common clonotypes in HC subjects accounted for a greater proportion of the total reads in the repertoire compared to active CD subjects, suggestive of higher repertoire diversity in active CD, consistent with prior work (Fig. 4-3B-D) (Eggesbø et al.,

2019). The distribution of the number of N/P additions to the CDR3 sequence did not differ between conditions (Fig. 4-3E,F).

The TRDV repertoire was dominated by TRDV1 gene usage, accounting for over half of unique CDR3 sequences, and approximately 40% of reads. TRDV3 gene usage accounted for approximately 30% of CDR3 sequences and reads (Fig. 4-4A,B). The proportion of these gene segments was not affected by disease state. TRDV2 gene usage was also common, representing approximately 20% of CDR3 sequences and reads. This was surprising, as the canonical Vδ2+Vγ9+ T cell population is uncommon in the gut, and accounted for less than 1% of all T IELs in HC and ACD subjects by flow cytometry (Fig. 4-1A). However, recent work showed that the commonly used Vδ2 antibody clone (B1) only identifies Vδ2+Vγ9+ T cells, missing cells using TRDV2 with a different TRGV gene(Davey et al., 2018b). These Vδ2+Vγ9- cells have a phenotype more similar to non-Vδ2 T cells and are found in tissue (the liver). These results indicate that the Vδ2+Vγ9- T cells may also be common in the gut. Clonotypes using TRDV4-TRDV8 genes were uncommon, accounting for less than 10% of CDR3 sequences in total. The proportion of clonotypes using TRDV8 was reduced in TCD vs healthy controls. However, this effect was not seen between ACD and healthy controls, and was small in magnitude, suggesting that it may not represent a biologically relevant effect. The TRDJ repertoire was almost entirely dominated by TRDJ1 gene usage, representing over 90% of CDR3 sequences and reads (Fig. 4-4B).

TRGV gene showed perturbations between health and CD. TRGV4 usage, which accounted for 51% of CDR3 sequences and 40% of reads in HC subjects, was reduced to 24% and 22% of CDR3 sequences in active and treated CD respectively (Fig. 4-4C,D) . Of note, the TRGV3 gene segment use increased from 5% in HC to 17% and 20% in ACD and TCD respectively. The TRGJ repertoire was similar in health and disease (Fig. 4-4D).

This marked difference in TRGV repertoire in disease is particularly interesting, as it persisted in treated coeliac disease, suggesting a permanent perturbation of the γδ TCR repertoire in context of disease, irrespective of active inflammation. Two recent publications of Vδ1+ γδ T cell repertoires in the gut in health and coeliac disease have shown similar findings(Eggesbø et al., 2019; Mayassi et al., 2019). This provides validity to the experimental approach, particularly given the use of a different TCR repertoire library generation approaches in these studies. This provides reassurance that the sorting, RNA extraction, library preparation, and analysis methods are robust, and are able to detect biologically relevant perturbations in the TCR repertoire.

CDR3 length and sequence sharing

Recent work has hypothesised that γδ T cells play a TCR-dependent role in coeliac disease(Han et al., 2013; Mayassi et al., 2019). To explore this hypothesis, I examined CDR3 length, clonal sharing, and previously identified putative disease-specific sequence motifs in the TRD and TRG repertoire.

While CDR3γ length did not vary by disease state (Fig. 4-5A), CDR3δ length differed, with longer CDR3 sequences in active and treated CD compared to healthy controls(median 17 vs 16 AAs, $p<0.001$), in keeping with prior work(Mayassi et al., 2019)(Fig. 4-5B). CDR3δ sequence sharing was rare, with less than 1% of the 34,720 individual clonotypes shared between subjects. The number of clonotypes shared between HC samples was small. However, several pairs of ACD subjects showed considerable clonotype sharing, with the highest sharing between ACD samples (Fig. 4-5C).

I then examined CDR3 sequences shared only between ACD samples (and not found in HC samples), and compared them to shared HC sequences. 207 sequences were shared between two or more ACD samples, compared to 21 samples shared between HC samples (Fig. 4-5D). Shared HC sequences showed a shorter CDR3 length than the overall HC CDR3 length (median 12 AAs vs 16 AAs). The short CDR3 length of shared HC sequences is consistent with non-specific sequence

sharing through near-germline sequences. Conversely, shared ACD sequences were longer than private sequences (median 18 AAs vs 17 AAs), which is not consistent with non-specific sequence sharing.

CDR3γ and CDR3δ motif analysis

Disease-specific CDR3 motifs provide evidence for a TCR-driven, potentially antigen-specific role of T cell populations. Han and colleagues (Han et al., 2013) showed that activated, gut-homing (CD38+CD103+) γδ T cells increase in frequency in the blood in patients with CD after a gluten challenge, and that these populations show enrichment in particular TRDV1 CDR3 motifs: CxxxxxPxLGD and CxxxxxxxxYWGI.

I examined the use of these motifs in TRDV clonotypes. I used two definitions of the motifs from Han *et al.*: the first agnostic of motif position in the CDR3 sequence, the second, more strict definition including the distance of the motif from the TRDV cysteine residue. The CxxxxxPxLGD motif was enriched in active CD clonotypes compared to controls in all TRDV clonotypes (0.08% vs 0.87%; Fig. 4-5E), with a similar effect size when examined in TRDV1 clonotypes alone (0.14% vs 1.04%; Fig. 4-5F). The CxxxxxxxxYWGI motif was also enriched in ACD clonotypes in all TRDV clonotypes (1.02% vs 2.48%; Fig. 4-5G), and when examining TRDV1 alone (1.53% vs 4.17%; Fig. 4-5H).

Mayassi and colleagues also reported an increase in 'H-J1' motif use in TRGV sequences in active CD TCR repertoires, where a histidine CDR3 residue at one end of the CDR3 joins onto a TRGJ1 sequence(Mayassi et al., 2019). This finding was restricted to TRDV1 repertoires. The γδTCR duodenal repertoires I generated were from total duodenal γδ T cells rather than Vδ1+ T cells, however Vδ1+ T cells do constitute the majority of the γδ T cells in the duodenum (Fig. 4-1A). Therefore I examined the H-J1 motif use in the dataset. Histidine residues within three AAs of the germline-encoded 'KKLF' J-gene sequence were counted as H-J1 motifs (i.e. HKKLF, H*KKLF,

H**KKLF). Using this definition, there was no enrichment of the H-J1 motif in active or treated coeliac disease compared to controls(Fig. 4-5I).

Interim conclusion

The differences in CDR3δ length in active CD, in particular in shared clonotypes, is suggestive of disease-specific alterations in the TCR repertoire. The enrichment of CDR3δ motifs, as first reported by Han *et al.* (Han et al., 2013), is in contrast with data from two recent publications(Eggesbø et al., 2019; Mayassi et al., 2019). However, in those works, there was a numerical enrichment in these motifs, albeit not statistically significant. The high number of samples with no motifs detected in previous studies may mean that the prior lack of statistical difference was due to low cell number per sample.

The absence of enrichment of the H-J1 motif is in contrast to Mayassi et al., but in agreement with Eggesbø et al., who used a single-cell TCR-seq approach. Importantly, the original report identified the H-J1 motif in Vδ1+ T cells, whereas my dataset includes all duodenal γδ T cells. Therefore it is possible that a Vδ1-specific enrichment of the H-J1 motif could be present, but the effect obscured by non-Vδ1 TCRs. However, Vδ1+ T cells make up two-thirds of duodenal γδ T cells in coeliac disease (Fig 2-1A), which would make it likely that an effect would be detected, even in a mixed sample.

In sum, these data provide support for the presence of specific TRDV CDR3δ motif enrichments in CD, as first described in gut-homing populations in the blood following gluten challenge. However, no evidence for the CDR3γ H-J1 motif is found.

4.4.3 The CD8+ TCR repertoire

*The CD8+ TCR*β *repertoire is altered in coeliac disease*

In total, 1,068,814 CD8+ T cells from 20 subjects were sorted for RNA-based bulk TCR repertoire sequencing. Comparison of TRBV gene usage showed a striking enrichment in the proportion of clonotypes expressing TRBV28 in active and treated CD compared to healthy controls, while other TRBV gene usage was similar (Fig. 4-6A). Indeed, hierarchical clustering of samples by clonotype TRBV gene usage was able to partially separate coeliac and non-coeliac samples, which was not attributable to histological severity or HLA DQ status alone (Fig. 4-6B). TRBV28 gene usage was increased in all clonotypes in ACD and TCD compared to controls (Fig. 4-6C - left). Sequencing error in non-UMI controlled bulk sequencing approaches can generate low-frequency erroneous sequences (as discussed in chapter 3), however this difference in TRBV28 gene usage persisted when examining just the top 100 most common clonotypes (Fig. 4-6C - right). TRBV28 clonotypes in CD samples showed diverse combination with TRBJ genes, albeit with a slight differences in the repertoire compared to non-TRBV28 clonotypes (Fig. 4-6D).

I compared amino acid usage in the CDR3 sequence of TRBV28 and non-TRBV28 clonotypes in coeliac disease samples. There was an enrichment in leucine residues in TRBV28 CDR3 sequences (Fig. 4-6E,F). There is a germ-line encoded leucine residue in the TRBV28 gene which contributes to the CDR3 sequence. However CDR3 positional motif analysis between TRBV28 and non-TRBV28 CDR3 sequences showed that leucine residues were enriched in TRBV28 CDR3 sequences at positions 4, 5, and 6 following the germline-encoded cysteine, rather than at a single position (Fig. 4-6G). Junctional analysis of a sample of leucine-containing TRBV28 sequences from CD samples showed that 50% of examined sequences contained a non-germline encoded leucine residues at positions 4,5, or 6.

TRBV28 gene usage in other intestinal inflammatory disorders

One hypothesis for the increased TRBV28 gene usage in the CD8+ TCR repertoire in coeliac disease is that this represents a gut-specific, but not disease-specific, response to inflammation. To test this

hypothesis, I examined two intestinal inflammatory disorders with known perturbations of CD8+ populations: ulcerative colitis and immunotherapy-related adverse event (irAE) colitis.

First, I generated TRB TCR libraries from RNA extracted from colonic mucosal biopsies from patients with ulcerative colitis, irAE colitis, and controls (n=24, RNA samples kindly provided by Sarah Sasson and Oliver Brain). TRB libraries were successfully generated from 21 samples. There was no difference in TRBV gene usage between conditions (Fig. 4-7A), and specifically no signal for an increase in TRBV28 gene usage (Fig. 4-7B).

Second, I analysed the usage of TRBV28 in colonic mucosal CD8+ T cells from subjects with and without ulcerative colitis from a published scRNAseq dataset which included paired CD8+ TCR clonotypes(Corridoni et al., 2020). TRBV28+ CD8+ T cells formed between 5-15% of the colonic CD8+ T cell population in this study. There was no difference in the mean proportion of clonotypes containing TRBV28 (10.1% controls, 7.1% ulcerative colitis; Fig. 4-7C).

While this analysis of total colonic mucosal RNA will be partially compromised by the inclusion of CD4+ T cell-derived clonotypes, the absence of any signal for increased TRBV28 in these two conditions, and the support of the reanalysed single-cell RNAseq data, provides evidence that this is not a non-specific generalised response of the intestinal TCR repertoire to inflammation, and is either specific to the small intestine, to coeliac disease, or both.

Interim conclusion

TRBV28 clonotypes are increased in the CD8+ T cell repertoire in the intestinal mucosa in coeliac disease. This increase persists in treated coeliac disease, similar to the perturbations in the TRGV repertoire of mucosal γδ T cells. CD-associated TRBV28 clonotypes are largely private and have diverse TRBJ gene usage, which suggests that this is not a semi-invariant T cell population.

Moreover, there are some non-germline encoded CDR3 sequence similarities, which suggest that this may represent an antigen-driven expansion.

4.5 RNA sequencing of mucosal CD8+ and γδ T cells

Description of RNAseq cohort and dataset

To examine the transcriptional changes in CD in CD8+ and γδ+ T cells, I performed bulk RNAseq of sorted IEL populations from 12 subjects. CD8+ αβ T cells, Vδ1+ T cells, and Vδ1/2- γδ T IELs were sorted by FACS, before low-input RNA extraction. RNAseq library preparation was performed with the SMARTSeq2 protocol. All samples were successfully sequenced. Two samples (γδ T cell samples from a single individual) with the lowest number of cells (<1,000) were of low technical quality and were therefore removed from the analysis.

4 subjects had active coeliac disease, with Marsh 3 villous atrophy on duodenal biopsy. 3 non-coeliac controls with histologically normal duodenal biopsies and no clinical suspicion of coeliac disease were included, as well as 3 subjects with treated coeliac disease (on GFD>6 months, TTG<2xULN, normal duodenal biopsies. 2 individuals with potential CD were included (low-positive TTG <10xULN, with negative EMA and normal duodenal biopsies). Subject characteristics are included in Table 4-2.

Table 4-2. Demographics of the RNAseq patient cohort

ID	Category	Sex	TTG	EMA	Histology
2602	ACD	F	1642	+	Marsh 3
2967	ACD	F	770	+	Marsh 3
3007	ACD	M	909	+	Marsh 3
3010	ACD	M	ND	+	Marsh 3
2993	HC	F	-	-	Normal
2604	HC	F	-	-	ND
3014	HC	F	ND	ND	Normal
2603	Pot CD	M	47	-	Normal
2285	Pot CD	F	23	-	Normal
2966	TCD	F	7.6	-	Normal
2969	TCD	M	25	-	Normal
3009	TCD	F	30	-	Normal

ACD, active coeliac disease; HC, healthy control; Pot CD, potential coeliac disease; TCD, treated coeliac disease; TTG, anti-tissue transglutaminase 2 antibodies; EMA, anti-endomysial antibodies; ND, not done.

Intestinal Vδ1+ and Vδ1/2- γδ T cells are transcriptionally similar

Vδ1+ T cells form the majority of non-Vδ2 γδ T cells in the circulation and human tissue, and therefore have been the main population studied. Recently, non-Vδ2 T cells have been shown to have an adaptive yet unconventional biology, in contrast to Vδ2+ T cells, and suggests that Vδ1+ and Vδ1-/2- T cell populations share similar characteristics(Davey et al., 2017). Recent bulk RNA sequencing of intestinal γδ T cells in coeliac disease focused solely on Vδ1+ T cells(Mayassi and Jabri, 2018). It remains unclear if the perturbations seen in Vδ1+ T cells in CD are mirrored in the Vδ1-/2- T cell population, or whether their transcriptional changes differ by V-gene usage. I hypothesised that intestinal Vδ1+ and Vδ1-/2- T cell populations are transcriptionally similar.

I examined the transcriptional profiles of Vδ1+ and Vδ1-/2- T cell populations in the dataset. On principal component analysis (PCA), the first principal component (PC1) was dominated by the effect of disease (Fig. 4-8A), while PC2 aligned to biological sex of the study subjects (Fig. 4-8B). Vδ1+ and Vδ1/2- populations showed highly similar transcriptional profiles. On PCA, Vδ1+ and Vδ1/2- γδ T cells did not separate based on examination of PCs 1-6 (Fig. 4-8C). Differential expression analysis identified only 26 Ensembl transcripts that differed between the two populations (Fig. 4-8D). Seven of these transcripts were TCR genes, with Vδ1+ T cells expressing higher levels of *TRDV1* and *TRDJ1*, while Vδ1/2- T cells expressed higher *TRDV3*, *TRAV14/DV4, TRAV29/DV5*, and *TRAV38/DV8*. The remaining differentially expressed genes either showed very low absolute expression, or only slight differences between the two populations, with no genes of relevance to T cell function or coeliac disease differentially expressed.

In sum, Vδ1+ and Vδ1/2- T IELs show negligible differences in transcriptional profiles, and can, for the purposes of bulk RNAseq, be considered part of the same population. Therefore, for further analysis these two populations were combined, and are referred to as γδ T cells below (although they exclude Vδ2+Vγ9+ T cells due to the sorting strategy).

CD8+ and γδ+ T IELs in coeliac disease

I examined the transcriptional profiles of CD8+ and γδ+ T cells isolated from duodenal epithelium from healthy controls, and subjects with active, treated, and potential CD. PCA of samples showed that PC1 divided CD8+ and γδ+ T cell populations, while PC2 divided ACD from all other conditions(Fig. 4-9A,B). Treated coeliac disease samples predominantly clustered with the healthy control and potential CD samples.

Comparison between CD8+ T cell samples from HC and active CD subjects showed up-regulation of cytotoxic molecules including *GZMA*, *GZMB*, and *PRF1*, as well as NK-receptors (*NCR1*, and *NCR2*) and KIR molecules (*KIR2DL1, KIR2DL4, KIR3DL2*) (Fig. 4-9C). CD8+ T cells in ACD also up-regulated co-inhibitory receptors including *HAVCR2*, *TIGIT*, and *TNFRSF9*, as well as *ENTPD1* (encoding CD39) which exerts immuno-modulatory effects via extracellular ATP degradation.

CD8+ T cells in ACD expressed higher levels of the transcription factors (TFs) *IKZF2* (encoding Helios) and basic leucine zipper transcription factor, ATF-like (*BATF*). BATF is linked to Tc17 function, gut-homing molecule expression, and T cell exhaustion(Quigley et al., 2010; Chuanwu Wang et al., 2013). CD8+ T cells also up-regulated *LAYN*, which encodes layilin, a C-type lectin domain-containing glycoprotein. Layilin has recently been shown to be highly expressed in a population of phenotypically exhausted, yet cytotoxic tumour-infiltrating lymphocytes, where it mediated anti-tumour immunity via enhancement of LFA-1 activation(Mahuron et al., 2020). The increased expression of *ITGAE* and *MKI67* by CD8+ T cells in ACD is suggestive of proliferation of a tissue resident population.

The γδ T cells in ACD showed a combination of shared and distinct responses with their CD8+ counterparts (Fig. 4-9D-F). Similar to CD8+ T cells, the γδ T cells up-regulated *BATF* and *TNFRSF9*, as

well as class II MHC and the aryl hydrocarbon receptor repressor (*AHRR*), and down-regulated the Fc gamma receptor genes *FCGR3A* and *FCGR3A* (Fig. 4-9E). However, γδ T cells did not show the same up-regulation of cytotoxic molecules and KIR molecules as seen in the CD8+ T cells, and displayed differences in co-inhibitory molecule up-regulation, with γδ T cells showing greater upregulation of *PDCD1* (Fig. 4-9F).

Gene set enrichment analysis

To further investigate these shared and distinct transcriptional changes between CD8+ and γδ T cells in coeliac disease, I performed gene set enrichment analysis (GSEA) on differentially expressed genes between health and active CD for each of the cell populations(Subramanian et al., 2005). While γδ T cells showed enrichment for TCR activation genes as previously reported (Mayassi et al., 2019), no enrichment was seen for CD8+ T cells (Fig. 4-10A). Both populations showed reduced expression of a tissue repair gene set(Linehan et al., 2018) in active coeliac disease, with reduced expression of *TNF*, *TGFB1*, and *AREG* (Fig. 4-10B,C).

CD8+ and γδ T cells showed opposing changes in NK cell-related genes (Fig. 4-10D,E). CD8+ T cells showed enrichment of this gene set, with increases in cytotoxic molecules and KIR molecules. In contrast, γδ T cells showed reduced expression of this gene set, driven by reduced expression of *NCR1*, *NCR2*, *GZMK*, and *TYROBP*, consistent with prior work(Mayassi et al., 2019). CD8+ and γδ T cells also differed in their expression of cell adhesion molecules. γδ T cells showed enrichment of the KEGG cell adhesion molecule gene set, while CD8+ T cells showed no enrichment (Fig. 4-10F). This was driven predominantly by differential baseline expression of *ICOS*, *ICAM2*, *NCAM1*, and *PDCD1* between the two subsets (Fig. 4-10G).

Increased expression of multiple co-inhibitory molecules and the TF *BATF* by CD8+ T cells in ACD could be consistent with an exhausted phenotype, however gene sets associated with exhaustion

were not enriched in CD8+ T cells in ACD (Fig. 4-10H), suggesting that while these populations may be highly regulated, they may not be functionally exhausted.

In sum, comparison of gene and gene set expression changes in coeliac disease between CD8+ and γδ T cells indicates that these populations differ in their response. In active coeliac disease, CD8+ T cells show a cytotoxic, NK-like phenotype, with evidence of tissue residency and proliferation. Their expression of co-inhibitory receptors and TFs indicate that they are highly regulated, but not exhausted.

TRBV28 gene usage is associated with CD in CD8+ T cells

Of note, the *TRBV28* transcript was identified in the RNAseq dataset as a differentially expressed gene in differential expression analysis of CD8+ T IELs between health and active CD(Fig. 4-9C). *TRBV28* was the only TRBV gene differentially expressed between health and CD, indicating that this was not a generalised phenomenon of increased TCR gene transcript levels in active CD (Fig. 4-11A). Comparison between the four clinical states indicated that *TRBV28* gene expression was high in both active and treated coeliac disease compared to non-coeliac controls, in concordance with the TCR repertoire sequencing results (Fig. 4-11A - right). Potential CD, defined as individuals with raised tissue transglutaminase serology titres with normal histological findings on duodenal biopsy, showed transcript levels similar to healthy controls.

To gain insight into potential transcriptional and phenotypic characteristics of CD8+ T cells expressing TRBV28, I sought to examine which genes were correlated with *TRBV28* in the dataset. Weighted correlation network analysis (WGCNA), a technique to identify clusters (modules) of highly correlated genes, was used for this purpose(Langfelder and Horvath, 2008). The transcriptome of CD8+ T IELs in the samples was clustered into linked gene modules (Fig. 4-11B), and the modules containing *TRBV28* were examined (a broader, merged module of 542 genes, or a smaller, more

specific unmerged module of 81 genes; Fig. 4-11C). The expression of both these modules segregated the active and treated CD samples from healthy controls and potential CD samples (Fig. 4-11C). The unmerged (81 gene) TRBV28-associated module showed enrichment of several GO terms (Fig. 4-11D), driven by a suite of genes upregulated in active CD, including *ENTPD1*, *KIR2DL4*, *LAYN*, *IKZF2*, and *KIR3DL1* (Fig. 4-11E). In particular, GO terms related to regulation of immune and leukocyte responses, as well as those related to NK cell functions, were enriched in this gene module(Fig. 4-11F).

In sum, *TRBV28* expression is significantly increased in active and treated coeliac disease, with no other TRBV genes altered. *TRBV28* gene expression is correlated with a gene module associated with the regulation of immune response, and of NK cell function.

4.6 Single-cell RNA sequencing of intestinal CD8+ and γδ T cells in coeliac disease

Dataset description and cluster identification

Single-cell RNA sequencing (scRNAseq) and TCR sequencing (scTCR-seq) were performed on sorted duodenal γδ and CD8+ T cells from four paediatric subjects, three with coeliac disease (CD). After sequencing and quality filtering, 5,552 cells were analysed (Fig. 4-12A).

Cells formed 14 transcriptionally distinct clusters (Fig. 4-12B,C). A description of cell clusters, including their gene and TF expression characteristics, is given in Table 2-3. A small population of CD4+ expressing cells were assumed to be contaminants from cells sorting, and were excluded from the analysis. Hierarchical clustering indicated two broad groupings of clusters, with *CXCR6*-expressing clusters grouping together, and IL7R and GZMK expressing clusters grouping separately (Supplementary Fig. 4-1A). Of note, *CXCR6* is part of a core transcriptional signature of human tissue resident memory T (T_{RM}) cells, seen across tissues in humans(Kumar et al., 2017).

I compared the relative proportions of each cluster between the three coeliac disease samples and one healthy control sample (Fig. 4-12D,E). Cells from CXCR6+ clusters formed a greater proportion of total cells in the coeliac samples, while activated CCL3+CCL4+ cells were more common in the control sample. However, the limited sample number limits further analysis of differential expression, and the differences in proportion remain speculative.

One striking finding was that γδ T cells were distributed throughout the clusters, and did not form transcriptionally distinct clusters of their own (Supplementary Fig. 4-1B). This suggests that these different lineages of T cells take on similar transcriptional states, and presumably functional roles, in

the intestinal mucosa. The one notable exception for this was the FCER1G+ cluster, which was highly overrepresented for γδ T cells in the tissue (Supplementary Fig. 4-1C). This effector population expressed cytotoxic molecules such as *GZMA*, as well as *ENTPD1* and *CD160*. In addition, this population expressed a number of molecules suggestive of NK-like functionality, including *FCER1G* and *KIR2DL4*. This suggests that while CD8+ and γδ T cells predominantly share similar functional niches in the intestine, there is a particular NK-like phenotype dominated by γδ T cells.

Table 4-3. Cluster annotations, with cluster-defining genes and transcription factors.

Name	Genes of note	TFs and TF modules	Comments
MKI67+	*MKI67*		Mixed population of actively dividing cells.
LEF1	*CCR7, SELL*	*LEF1, TCF7,*	Putative naïve, predominantly CD8+ T cell population
CXCR6+	*GZMA, ITGAE, CXCR6++, ENTPD1, HAVCR2, TIGIT, LAYN, NKG7*	*BATF, PRDM1, IKZF3, RORA*	Possible increased proportion in coeliac disease.
CXCR6+ #2	*GZMA, ITGAE, CXCR6, ENTPD1, HAVCR2, TIGIT, LAYN, KIR2DL4,*	*BATF, PRDM1, CREM*	Population highly related to CXCR6+ cluster
CXCR6+ #3	*GZMA, ITGAE, CXCR6, ENTPD1, HAVCR2, TIGIT, LAYN,*	*IKZF2, PRDM1*	Population highly related to CXCR6+IKZF2+ cluster
CXCR6+ IKZF2+	*GZMA, ITGAE, CXCR6, ENTPD1, HAVCR2, TIGIT, LAYN, KIR2DL4, KLRC2, TNFRSF9*	*IKZF2++, PRDM1, ARID5B*	
Intermed.		*REL*	Small population closely related to IL7R+CXCL16+ cluster
CCL3+CCL4+	*IFNG, CCL4, CCL3, CD160, CXCL16, CD69*	*JUN, NR4A1, EGR2*	Activated cytokine- and chemokine-producing population
IL7R+	*CCR6, IL7R, AHNAK*	*KLF6, RUNX3, FOS*	Clonal overlap with circulating CD8+ T cells
IL7R+ CXCL16+	*IL7R, CXCL16,*	*RUNX3, CREM, STST4, SATB1*	Clonal overlap with circulating CD8+ T cells
GZMK+	*FGFBP2, GZMK, CXCR4*	*KLF6, RUNX3, IRF7, RARA, FOS, JUN*	Clonal overlap with circulating CD8+ T cells
XCL1/2+	*IL7R, XCL1, XCL2,*	*RUNX3, IRF7, NR4A2, NR4A3*	
FCER1G+	*FCER1G, GZMA++, KIR2DL4, ENTPD1, TNFRSF18*	*IRF4, IRF7, CREM*	Increased proportion of γδ T cells.

TCR analysis

TCR clonotypes from αβ T cells were examined for clonotype sharing between clusters, and the degree of clonal expansion within clusters. Clonotype sharing between clusters was seen, with TCR clonotypes shared between neighbouring clusters (Fig. 4-13A). CXCR6+ and IKZF2+ clusters shared multiple clonotypes, with IL7R+ clusters also sharing clonotypes, with less sharing between CXCR6+ and IL7R+ clusters. The degree of clonal expansion differed between clusters (Fig. 4-13B,C). As expected, the LEF1+ cluster showed minimal clonal expansion. CXCR6+ and IL7R+CXCL16+ clusters showed the highest levels of clonal expansion.

Clonal expansion also differed based on TRBV gene usage. TRBV28 clonotypes were more clonally expanded than non-TRBV28 clonotypes in all three coeliac disease subjects (Fig. 4-13D). This was not seen in the healthy control subject. Moreover, expanded TRBV28 clonotypes were not evenly distributed between clusters. The most expanded TRBV28 clonotypes (quintiles 1 and 2) were highly localised to CXCR6+ and IKZF2+ clusters, with few expanded TRBV28 clonotypes in the IL7R+ clusters (Fig. 4-13E).

PBMC-derived CD8+ T cells from three of the subjects were also sequenced as part of a related project (see Chapter 5 for details of the dataset). The overlap of CD8+ αβ T cell clonotypes between the blood and gut was examined. Most intestinal clonotypes were not found in the sequenced peripheral blood TCR repertoire. The degree of clonal sharing with blood was not equal between clusters (Supplementary Fig. 4-1D,E). The greatest degree of sharing with blood was from the related IL7R+CXCL16+, IL7R+, GZMK+, and XCL1/2+ clusters. In contrast, the four related CXCR6+ and IKZF2+ clusters showed negligible overlap with circulating TCR clonotypes. This would be consistent with the first group of clusters representing a non-resident effector CD8+ population, while the second group of clusters representing a tissue-resident memory T (T_{RM}) cell population. Despite the frequency and clonal expansion of TRBV28+ clonotypes in intestinal CD8+ T cell populations, only

four cells expressing a TRBV28 clonotype were shared with the peripheral blood, none of which were from the CXCR6+ group of clusters (Supplementary Fig. 4-1F). Intestinal TRBV28+ clonotypes, while showing increased clonality, showed a diversity of TRA chain pairings (Supplementary Fig. 4-2A).

In sum, there are multiple clusters showing clonal expansion, with clonotype sharing mainly with a group of CXCR6+ clusters and also within a group of IL7R and GZMK+ clusters. TRBV28 clonotypes may be more clonally expanded than non-TRBV28 clonotypes, with expanded TRBV28 clonotypes highly restricted to CXCR6+ clusters. CXCR6+ clusters, and TRBV28+ clonotypes, show minimal clonal sharing with peripheral blood CD8+ clonotypes, consistent with a tissue resident population.

Detailed characterisation of CXCR6+ populations in coeliac disease

CXCR6+ clusters showed enrichment of clonally expanded TRBV28 clonotypes, the same V-gene usage associated with CD in the TCR-seq and bulk RNAseq datasets. Therefore, I examined the CXCR6+ clusters in greater detail. These CXCR6+ clusters expressed high levels of cytotoxic molecules, including *GZMA* and *GZMB*, as well as the NK receptors *NCR1* (NKp46) and *NCR3* (NKp30) (Fig. 4-14A).

CXCR6+ clusters also expressed high levels of *ITGAE* (αE integrin) and *CXCR6*, consistent with a tissue resident, and potentially IEL population (Fig. 4-14B). I examined the expression of a previously-published gene set associated with human tissue residency in the intestinal T cell clusters (Supplementary Fig. 4-2B) (Kumar et al., 2017). CXCR6+ clusters in my dataset expressed high levels of *ITGAE*, *CXCR6*, and *KCNK5*, and low levels of *SELL*, *S1PR1*, *KLF2*, and *KLF3*, consistent with a tissue resident population. In contrast, LEF1+, IL7R+, and GZMK+ clusters expressed higher levels of *S1PR1, SELL, KLF2*, and *KLF3*, suggesting that these populations may not be resident.

The CXCR6+ clusters expressed higher levels of *BATF*, *IKZF2*, and *LAYN* (Fig. 4-14B). As discussed earlier, BATF and LAYN are associated with highly regulated or exhausted T cell phenotypes(Mahuron et al., 2020; Quigley et al., 2010). In keeping with a highly regulated or exhausted phenotype, these clusters expressed higher levels of *HAVCR2* (encoding Tim3) and *TIGIT*, although *PDCD1* expression was similar to other clusters (Fig. 4-14C). However, CXCR6+ clusters expressed higher levels of *IFNG* and *IL26*, suggesting that these CXCR6+ clusters retain cytokine-producing capacity and are not functionally exhausted (Fig. 4-14D). Analysis of enriched GO terms and pathways showed that these clusters were enriched for GO terms related to TCR signalling, T cell proliferation and activation, cell-cell adhesion, and cytolysis, suggesting that indeed these are functional, and not exhausted populations (Fig. 4-14E and Supplementary Fig. 4-2C).

Single cell expression of curated gene sets showed increased expression of gene sets related to PD-1 and CTLA4 signalling, as well as CD28 family co-stimulation, in CXCR6+ clusters (Fig. 4-15A-C). The CXCR6+ clusters also showed increased expression of TCR signalling pathway genes, and of gene sets related to cellular defence and cell surface receptor signalling (Fig. 4-15D-F).

CXCR6+ clusters expressed high levels of numerous molecules associated with co-inhibitory functions (Supplementary Fig. 4-3A), reminiscent of IEL and mucosal CD8+ T cells populations identified in other studies, including those recently described in the colon(Corridoni et al., 2020). The similarity of clusters in this dataset and the previous study were compared. CD8+ T cells in CXCR6+ clusters showed most similarity to IL26+ and IEL clusters identified in colonic tissue (Supplementary Fig. 4-3B-E).

In sum, the CXCR6+ cluster group possess a tissue resident, highly regulated phenotype, with co-inhibitory molecule expression, expression of cytotoxic molecules and pro-inflammatory cytokines, and NK receptors.

Transcriptional regulation of intestinal CD8+ and γδ T cells in coeliac disease

I examined the expression of a curated lists of transcription factors (TFs) in the clusters (Fig. 4-16A) (Lambert et al., 2018). As expected, LEF1+ clusters also expressed the TF *TCF7*. CXCR6+ clusters expressed a group of TFs, including *BATF* and *IKZF2* as already discussed, and *PRDM1, IKZF3, RORA, STAT3*, and *ARID5B*. Of note, PRDM1 is a key transcription factor in tissue residency(Behr et al., 2019; Mackay et al., 2016).

The expression of TF modules (gene sets predicted to be regulated by a particular TF(Aibar et al., 2017; Van de Sande et al., 2020)) in the intestinal T cell clusters was examined. The 10 TF modules most highly enriched in each cluster were plotted (Fig. 4-16B). This divided clusters into two groups, each displaying a different set of putative transcription factor networks. Again CXCR6+ clusters were enriched for TF modules for BATF, HIVEP1, IKZF2, STAT2 and STAT3, RUNX1, TRPS1, and PRDM1 (Fig. 4-16C). IL7R and GZMK+ clusters showed higher expression of TF modules for RUNX3 and RARA.

Differential gene expression between health and disease

Interpretation of cluster-specific differentially expressed genes in the context of active coeliac disease was limited by the single healthy control subject in the experiment. Therefore, instead of interpreting the disease-related transcriptional changes in the single cell data in isolation, I compared the differentially expressed genes from bulk RNAseq of sorted CD8+ T IELs performed earlier to the cluster-specific differentially expressed genes (DEGs) in coeliac disease.

The CXCR6+ clusters showed congruent changes in transcriptional profile to the bulk RNAseq signature. This was most clearly seen in the CXCR6+ cluster, due to the higher number of cells, with strong concordance in differentially expressed genes between health and coeliac disease(Fig. 4-17A).

Genes up-regulated in active coeliac disease in the bulk RNAseq dataset and CXCR6+ scRNAseq dataset included co-inhibitory molecules (*ENTPD1, HAVCR2, TNFRSF9, TNFRSF18, TIGIT*), cytotoxic molecules and NK receptors (*GZMB, PRF1, KIR2DL4*), markers of tissue residency (*ITGAE*), and genes associated with highly regulated and exhausted populations (*BATF, LAYN*) (Fig. 4-17 B). In contrast, these genes were not upregulated in IL7R+ and GZMK+ clusters, which instead show increased expression of genes involved in cytokine and interferon responses (Fig. 4-17C).

In sum, CXCR6+ clusters show similar changes in gene expression in coeliac disease as seen in bulk CD8+ RNAseq signatures. This suggests that CXCR6+ clusters are likely to be driving the overall CD8+ T cell transcriptional changes in coeliac disease, through changes in their transcriptional profile (as well as possibly increased cell number) in active disease. This provides strong circumstantial evidence that these populations play an active role in coeliac disease immunopathology.

Pseudotime analysis of intestinal CD8+ and γδ T cell populations

Pseudotime analysis was performed on the gut-derived T cell populations, which formed a transcriptional spectrum (Fig. 4-18A). The LEF1+ cluster, followed by GZMK+ and IL7R+ clusters, dominated one end, with CXCR6+ and proliferating clusters at the other end of the pseudotime spectrum (Fig. 4-18B). While the degree of clonal expansion did not vary along pseudotime (Fig. 4-18C), GZMK+ and IL7R+ clusters at one pole of pseudotime showed the highest degree of overlap with peripheral blood clonotypes (Fig. 4-18D). At the other pole of the spectrum were the CXCR6+ clusters, which showed minimal overlap with peripheral blood clonotypes (Fig. 4-18D), and were enriched for TRBV28-expressing clonotypes (Fig. 4-18E).

Genes associated with cytotoxic function and tissue residency increased in expression with pseudotime (Fig. 4-18F). In addition, genes encoding co-inhibitory molecules, and the transcription factors associated with their expression, increased in expression along pseudotime (Fig. 4-18G).

Finally, several TF gene modules associated with CXCR6+ clusters increased in expression along pseudotime (Fig. 4-18H)

In sum, the pseudotime trajectory is suggestive of a pathway of residency differentiation, with early tissue-colonising populations, shared with blood, giving way to oligoclonal tissue resident memory populations with high expression of cytotoxic, and co-inhibitory molecules, and increased TRBV28-containing clonotype usage.

4.7 Flow cytometric evaluation of intestinal T cells in coeliac disease

Validation of JOVI.3 (TRBV28-specific) antibody clone

A commercial antibody (JOVI.3 clone), directed against TRBV28 (also known as Vβ3) is available. The antibody produced clear staining of cells at 1:200 concentration with standard surface staining protocols. TRBV28+ CD3+ T cells from frozen PBMCs were sorted from a single donor, before low input RNA extraction, and generation and sequencing of TRA and TRB TCR repertoire libraries. In the TRB repertoire, 97.3% of total reads were of TRBV28 clonotypes, accounting for 95.1% of unique CDR3 clonotypes (Fig. 4-19A). The repertoire showed a broad use of TRBJ segments, and demonstrated considerable diversity, without dominance from a single clonotype (Fig. 4-19B,C). The TRA repertoire was oligoclonal, however it did demonstrate a broad use of different TRAV segments (Fig. 4-19D). These findings indicate that the JOVI-3 antibody identifies TRBV28-expressing clonotypes with minimal contamination, that TRBV28-expressing T cells in the peripheral blood are not a single clonal population, and do not have TCR repertoire characteristics of a semi-invariant T cell population.

Expression and cell phenotype of TRBV28+ CD8+ T cells in coeliac disease

The scRNAseq dataset had shown minimal clonal sharing of TRBV28 clonotypes between intestinal and circulating populations. However, the majority of the peripheral blood CD8+ T cells in this dataset were naive, as the subjects were children and adolescents, limiting the proportion of the effector T cell repertoire sequenced. Moreover, I hypothesised that if there was clonotype sharing of coeliac-related TRBV28 clonotypes between blood and intestine, these cells would have an effector memory, gut-homing phenotype, as seen in prior studies post-gluten challenge(Han et al., 2013). Such populations represent a small fraction of total circulating CD8+ T cells.

I sought to examine whether TRBV28+ CD8+ T cells were enriched in effector memory and gut-homing compartments in individuals with CD. I performed flow cytometry of cryopreserved PBMCs from healthy donors and individuals with active and treated CD (Fig. 4-20A).

First, as a control, I analysed the proportion of total CD3+ T cells expressing TRBV28. As expected, was no difference in TRBV28 expression in total CD3+ T cells between HC and CD subjects (Fig. 4-20B). There was also no difference in TRBV28 TCR usage in total CD8+ T cells, which includes naive and central memory populations. However, TRBV28 expression was higher on effector memory (T_{EM}) CD8+ T cells (Fig. 4-20C)

I went on to identify putative gut-homing populations of CD8+ T cells based on integrin and chemokine receptor expression (Fig. 4-20D). β7-integrin forms heterodimeric receptors with both α4- and αE-integrin, which are involved in lymphocyte homing to intestinal mucosa, and in tissue residency, while the chemokine receptor CCR9 is also involved in lymphocyte entry to intestinal mucosa(Habtezion et al., 2019). I examined these markers on CD8+ T cells and examined TRBV28+ expression on these sub-populations. TRBV28 expression was higher on β7-integrin+ CD8+ T cells, and CD103+ CD8+ T cells in subjects with coeliac disease, while CCR9+ CD8+ T cells showed a

difference of smaller magnitude which was not statistically significant (Fig. 4-20E). These differences were present in individuals with both active and treated coeliac disease (Fig. 4-20F).

Next I examined the phenotype and TRBV28 expression on intestinal T cells in health and coeliac disease. Due to the current COVID-19 pandemic, these experiments have not been completed, and the sample numbers remain small, so statistical analysis was not performed on an incomplete dataset.

I examined phenotypic characteristics of CD8+ and γδ T cells in the intestinal mucosa. CD8+ and γδ T cell populations showed higher Ki67 expression in active coeliac disease (Fig. 4-21A,B), and possessed a tissue-resident phenotype (Fig. 4-21C,D), in concordance with the transcriptional findings. CD8+ T cells showed increased expression of Helios (encoded by IKZF2) in active and treated CD, while γδ T cells showed high baseline expression of Helios (Fig. 4-21E,F). Expression of NK receptors and molecules NKG2C and NKp30 was lost from γδ T cells in active and treated CD (Fig. 4-21G,H), consistent with prior work examining NKp44 and NKp46 expression(Mayassi et al., 2019).

CD8+ T cells showed low expression of the co-inhibitory molecules PD-1, TIGIT, and Tim3 in healthy samples. Expression was higher in active and treated coeliac disease, with increased most striking in TIGIT and Tim3, in concordance with the transcriptional data (Fig. 4-21I). CD8+ T cell co-expression of one or more co-inhibitory molecule increased in active and treated coeliac disease (Fig. 4-21J). In contrast, γδ T cells showed high baseline expression of TIGIT and Tim3, which was not changed in coeliac disease, and with similarly high levels of co-inhibitory molecule co-expression in health and CD (Fig. 4-21K,L).

I examined TRBV28 expression by intestinal CD8+ T cells. As a control, I examined TRBV28 expression on intestinal CD4+ T cells, which showed no difference between health and CD, as expected (Fig. 4-

21M). The mean proportion of intestinal CD8+ T cells expressing TRBV28 in active CD was 18.4% compared to 2.5% in control patients (p=0.22), with two active CD samples showing strikingly high expression (Fig. 4-21N). For two subjects, intestinal and peripheral blood samples were available from the same day. For both samples, TRBV28 expression was higher on duodenal T cells, compared to matched circulating T_{EM} CD8+ T cells (Fig. 4-21O).

These early data support the phenotypic changes of CD8+ and γδ T cells in CD, as suggested by the transcriptional data. TRBV28 expression is higher in gut-homing, effector memory populations in the blood in active and treated coeliac disease, and may be higher in intestinal CD8+ T cell populations also.

4.8 Discussion

Summary of results

In this chapter I examined CD8+ and γδ T cells in coeliac disease using multiple transcriptomic approaches. Non-Vδ2 γδ T cells are strikingly enriched in the mucosa in active and treated coeliac disease. Vδ1+ and Vδ1/2- γδ T cells show very similar transcriptional profiles, with no evidence that these populations differ in their role in health or disease. γδTCR repertoires are perturbed in coeliac disease, with altered V-gene usage, CDR3 length, clonal sharing, and enrichment of particular CDR3 motifs.

CD8+ and γδ T cells show both shared and distinct transcriptional changes in response to coeliac disease, partly related to differences in their profiles in health. CD8+ T cells also show striking alteration of their TCR repertoire, with increased usage of TRBV28 in active and treated CD. These TRBV28 clonotypes are expanded but largely private, with diverse TRBJ and TRAV/J gene usage, but with differences in CDR3 amino acid usage. TRBV28 clonotype usage is associated with CXCR6-

expressing populations, which possess a tissue resident, cytotoxic, and pro-inflammatory profile, with high expression of co-inhibitory receptors.

Discussion with reference to the literature

γδ T cells can be divided into Vδ2+ and non-Vδ2 subsets. Vδ2+ populations are most common in blood, express a semi-invariant Vδ2Vγ9 TCR that responds to pAg stimulation, and possess an innate-like phenotype akin to iNKT and MAIT cells. The majority of non-Vδ2 γδ T cells express the Vδ1 chain, and most work has focused on this Vδ1+ subset. Vδ1+ T cells are enriched in tissue and at mucosal barriers, and demonstrate an adaptive, albeit unconventional, biology(Davey et al., 2018a; 2017). When Vδ1/2- γδ T cells (which predominantly express the Vδ3 chain) have been included in these studies, their biology aligns to their Vδ1+ counterparts(Davey et al., 2018b; Hunter et al., 2018). This work indicates that Vδ1+ and Vδ1/2- γδ T cells are strikingly transcriptionally similar in the intestinal mucosa in health and coeliac disease, and should be considered to form a single population.

Previous work examining the transcriptional changes of intestinal γδ T cells in CD focused solely on the Vδ1+ subset(Mayassi et al., 2019). This work recapitulated several key findings: the loss of NK receptors and an NK-like phenotype in active coeliac disease, reduced expression of genes associated with tissue repair, and increased expression of gene sets associated with TCR signaling and activation. Two studies have recently described perturbations in the γδ T cell TCR repertoire, with loss of TRGV4 clonotypes, with compensatory increases in TRGV3(Eggesbø et al., 2019; Mayassi et al., 2019). My work also found this reduction in TRGV4 and increase in TRGV3 gene use in active and treated coeliac disease, and that the difference is present when examining total γδ T cells, rather than just Vδ1+ T cells. These congruent results from three studies, using different TCR repertoire sequencing approaches, provide robust evidence for a permanent reshaping of the γδ T cell repertoire in the epithelium in coeliac disease.

Potential coeliac-related γδ T cell CDR3δ motifs in the blood following gluten challenge have been previously reported(Han et al., 2013), however, studies examining the use of these motifs in Vδ1+ IEL TCR repertoires have shown conflicting results. Mayassi and colleagues detected YWGI motifs in 8/15 CD samples and 1/8 and control samples, and PxLGD motifs in 4/15 CD and 0/15 control samples, although these were not statistically significant differences(Mayassi et al., 2019). Eggesbø and colleagues also did not detect enrichment of these motifs(Eggesbø et al., 2019). In contrast, my analysis showed enrichment of both motifs, particularly when motifs in a particular CDR3 position were analysed. In contrast, the TRGV H-J1 motif enrichment reported by Mayassi and colleagues was not replicated in my work, nor was it in a recent study of single-cell paired TCR repertoires(Eggesbø et al., 2019).

The total cell number used to generate the repertoire may be a key determinant in the detection of uncommon disease-associated CDR3 motifs. The single-cell paired approach of Eggesbø and colleagues allows for TRG and TRD pairing and precise identification of clonal expansion, however the study included sequences of only 3,325 cells from 20 subjects. Mayassi and colleagues performed bulk RNA-based TCR sequencing on 64,085 γδ T cells from 23 subjects. In comparison this work sequenced 313,140 cells from 20 subjects. The discordant results between this work and other recent studies suggest that detection of disease-specific motifs through TCR repertoire analysis approaches is challenging, both related to technical aspects of amplification and sequencing, and the number of cells sequenced.

The replication of previous findings in the γδ T cell repertoire provided me with reassurance that the methodological approach I had chosen was able to detect disease-related perturbations in the TCR repertoire. The finding of preferential use of TRBV28 in CD8+ T cell clonotypes in coeliac disease was unexpected, as the cytotoxic role of CD8+ T IELs in coeliac disease is thought to be TCR-

independent(Jabri and Sollid, 2017). However, within the analyses I have performed, this finding seems to be robust. As well as TRBV28 preferential use in total and most common clonotypes in the TCR-seq dataset, TRBV28 is the only TRBV gene differentially expressed in the RNAseq dataset, with both experiments showing enrichment of TRBV28 in active and treated coeliac disease, analogous to the TRGV repertoire changes in γδ T cells Moreover, the clonal expansion of TRBV28 clonotypes in the scRNAseq dataset, along with their enrichment in the CXCR6+ clusters that seem most associated with active disease, provides further supportive evidence that this is a real effect.

The increased expression of TRBV28 by β7- and αE-integrin expressing CD8+ T cells in the circulation of patients with coeliac disease was an unexpected finding, particularly given the tissue-resident phenotype of intestinal CD8+ T cell clusters containing TRBV28 clonotypes in the single-cell data. However, mounting evidence suggests that tissue resident T cell populations may not be as restricted as was thought, and can, in certain circumstances, re-enter the circulation(Fonseca et al., 2020; Gratz and Campbell, 2020).

It is known that gluten challenge induces an increase in activated, gut-homing T cells in the peripheral circulation, both gluten-specific CD4+ T cells, and populations of CD8+ T cells(R. P. Anderson, 2005; R. P. Anderson et al., 2000; Han et al., 2013). In the steady state, gluten-specific CD4+ T cells can be detected at low levels in the circulation and are enriched in coeliac disease, with these cells displaying a distinct phenotype, including the expression of gut-homing integrins(Christophersen et al., 2019a). Indeed the detection of β7-integrin expressing gluten-specific CD4+ T cells shows promise as a novel diagnostic for coeliac disease, even in individuals treated with a gluten-free diet(Sarna et al., 2018b; 2018a). It may be that the enrichment of TRBV28 in these CD8+ T cell populations represents an analogous process, potentially the mobilisation of T_{RM} cells, and trans-differentiation into T_{EM} populations(Fonseca et al., 2020).

This work has not investigated the antigen-specificity of TRBV28 clonotypes, or indeed restriction to a particular MHC or MHC-like molecule. Cytotoxic gluten-specific CD8+ T cell clones have been described *in vitro*(Gianfrani et al., 2003; Mazzarella et al., 2008).Recent fine mapping of the MHC region has suggested HLA-B*08:01 and HLA-B*39:06 is an additional risk factor for coeliac disease, over and above the effect of linkage disequilibrium with HLA class II DQ genes(Gutierrez-Achury et al., 2015), while HLA-B*0801-restricted CD8+ T cells from CD patients can respond to gliadin peptides(Picascia et al., 2017). However, there is little evidence that gluten-specific CD8+ T cell responses play a role in coeliac disease immunopathology *in vivo*. Assuming the association with TRBV28 CD8+ T cells and coeliac disease is correct, there are several possible theories that could explain their role. These theories are discussed in more detail in the thesis discussion, along with possible experimental approaches to explore these theories.

Intestinal CXCR6+ CD8+ T cell clusters showed high levels of expression of multiple co-inhibitory molecules, with increased expression in CD. Such markers, along with the expression of the transcription factor BATF, are associated with T cell exhaustion - a functional state defined by loss of cytokine production, cytotoxicity, and proliferation, eventually predisposing to cell deletion(Quigley et al., 2010). However, as exhaustion is a functional state, not a purely phenotypic one, the expression of these markers does not confirm that these populations are exhausted, and indeed there are several lines of evidence to indicate that they are not, in fact, exhausted. First, transcriptional changes seen in exhaustion can overlap with other cell states, for instance memory inflation(Marchi et al., 2019). Second, GSEA of exhaustion-related gene sets did not demonstrate enrichment CD8+ T cells in CD. Third, the expression of cytotoxic molecules, pro-inflammatory cytokines, and Ki67/*MKI67* by these clusters suggests that these are functional, cytotoxic, and proliferating cell populations, and therefore not functionally exhausted. Fourth, BATF has pleiotropic roles, including the regulation of gut-homing chemokine receptors and integrins, and its expression in these clusters may be related to this role(Chuanwu Wang et al., 2013). Finally, layilin (encoded by

LAYN), which is expressed by these CXCR6+ clusters, has been shown to have a role in preserving cytotoxic function in phenotypically 'exhausted' tumour infiltrating lymphocytes(Mahuron et al., 2020), and a similar process may be occurring here.

The transcriptional similarity between the CXCR6+ clusters in the small bowel in coeliac disease, and recently described IL26+ CD8+ T cell populations in the colon in ulcerative colitis, suggests that there may be common pathways of T cell activation in these locations (Corridoni et al., 2020). While the structure, function, dietary antigen load, and microbial exposure in the proximal small bowel and colon differ markedly, it may be that these sites share immunological niches in the context of inflammation, even in different disease processes.

Strengths and limitations

The pros and cons of different TCR sequencing approaches are discussed in some detail in Chapter 3. In short, while this bulk approach facilitated sequencing of relatively small cell number samples, used a reliable library preparation method, was affordable, allowed sequencing of αβ and γδ T cell TCR repertoires, and has been used in previous published studies of αβ and γδ T cells, the method, and my experimental design, had several drawbacks. The lack of unique molecular identifiers meant that PCR-duplicates and sequencing error could not be eliminated. Using a bulk, rather than single-cell, approach meant that paired TCR clonotypes could not be identified. Finally, the deliberate choice to sort as many cells as possible for each sample meant that samples were of different sizes, and made interpretation of diversity parameters challenging. However, the identification of previously reported changes to the TRGV repertoire in coeliac disease, along with the validation work I performed, provide reassurance that the approach is able to identify biologically relevant perturbations in TCR repertoires.

HLA typing of patients is not performed routinely on patients in our gastroenterology service and was not planned prospectively in this study. Sufficient DNA was extracted from sorted cell populations for DQ2/DQ8 PCR-based typing, however, given the unexpected findings of CD8+ TCR repertoire perturbations in CD, full typing including of Class I HLA, would be useful, and will be planned for future prospective experiments.

The scRNAseq experiments were originally planned to only include active coeliac disease subjects, with an additional healthy control subject added later. Samples were processed fresh, and on separate occasions, creating substantial batch effects. Both the limited number of control samples and the batch effect correction limit interpretation of health vs disease comparisons from this dataset, and I have tried to avoid over interpretation of the data through comparison to the larger and better controlled bulk RNAseq dataset. This experience led to testing frozen intestinal biopsy preparation for scRNAseq (as described earlier), and future experiments will use cryopreserved samples.

Finally the COVID-19 pandemic has prevented completion of planned flow cytometry experiments of intestinal CD8+ T cells to validate the findings of the transcriptomic work. Additional samples are needed to allow firm conclusions to be drawn from these experiments, and the analyses deliberately avoid statistical testing on an incomplete dataset.

Conclusion

In conclusion, I have examined CD8+ and γδ T cells in coeliac disease using RNAseq, scRNAseq, and TCR repertoire sequencing approaches. I have delineated shared and distinct transcriptional changes in these populations in CD, recapitulated previously reported perturbations in the γδ T cell TCR repertoire, and identified preferential TRBV28 gene usage in CD8+ T cells in coeliac disease, associated with a cytotoxic, tissue resident, and highly regulated cell phenotype.

The findings from this chapter spurred further research in two separate directions. First, the striking differences in how γδ T cell populations with differing TRDV-gene usage behave in coeliac disease led me to explore transcriptional, phenotypic, and functional heterogeneity in γδ T cells (Chapter 3). Second, the possible involvement of a tissue-resident CD8+ cell population in coeliac disease pathogenesis drove my interest in tissue residency, and led to a study of CD8+ T cell residency in the context of intestinal transplantation (Chapter 4).

4.9 Figures

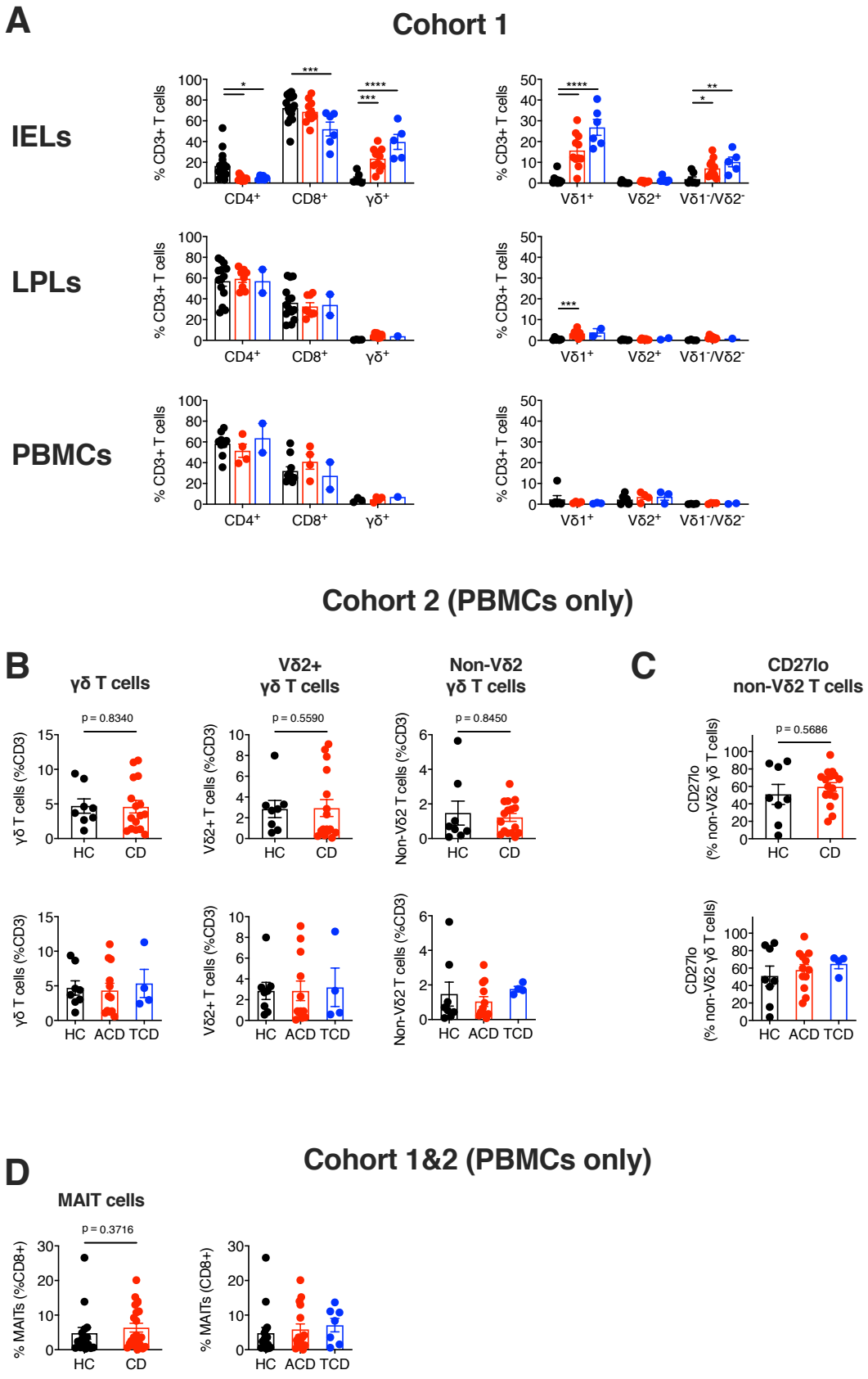

A
Cohort 1
IELs
LPLs
PBMCs
% CD3+ T cells
CD4+
CD8+
γδ+
Vδ1+
Vδ2+
Vδ1-/Vδ2-
Cohort 2 (PBMCs only)
B
γδ T cells
Vδ2+ γδ T cells
Non-Vδ2 γδ T cells
p = 0.8340
p = 0.5590
p = 0.8450
γδ T cells (%CD3)
Vδ2+ T cells (%CD3)
Non-Vδ2 T cells (%CD3)
HC
CD
ACD
TCD
C
CD27lo non-Vδ2 T cells
p = 0.5686
CD27lo (% non-Vδ2 γδ T cells)
D
Cohort 1&2 (PBMCs only)
MAIT cells
p = 0.3716
% MAITs (%CD8+)
% MAITs (CD8+)

Figure 4-1. Proportion of T cell subsets in intestinal mucosa and blood in coeliac disease

(A) Proportion (%total CD3+ T cells) of CD4+, CD8+, and γδ+ T cells (left) and Vδ1+, Vδ2+, and Vδ1/2- γδ T cells (right) in the intestinal epithelium (n=33), lamina propria(n=24), and peripheral blood(n=16) in a cohort of subjects with and without coeliac disease. Healthy control (HC), black; active coeliac disease (ACD), red; treated coeliac disease (TCD), blue.
(B) Proportion (%total CD3+ T cells) of γδ+ T cells Vδ2+, and non-Vδ2 γδ T cells in the peripheral blood(n=24) in a cohort of subjects with and without coeliac disease. Top row: Healthy control, black; coeliac disease, red. Bottom row: Healthy control, black; Active coeliac disease, red; treated coeliac disease, blue.
(C) Proportion of non-Vδ2 γδ+ T cells with a CD27lo (memory) phenotype in the peripheral blood(n=24) in a cohort of subjects with and without coeliac disease. Top row: Healthy control, black; coeliac disease, red. Bottom row: Healthy control, black; Active coeliac disease, red; treated coeliac disease, blue.
(D) Proportion (%total CD8+ T cells) of MAIT cells (CD8+CD161++Vα7.2+,) in the peripheral blood(n=33) in a cohort of subjects with and without coeliac disease. Top row: Healthy control, black; coeliac disease, red. Bottom row: Healthy control, black; Active coeliac disease, red; treated coeliac disease, blue.
(A & B) 2-way ANOVA with Holm-Sidak's multiple comparisons test. (C & D) Mann-Whitney test. *, $P \leq 0.05$; **, $P \leq 0.01$; ***, $P \leq 0.001$; ****, $P \leq 0.0001$.

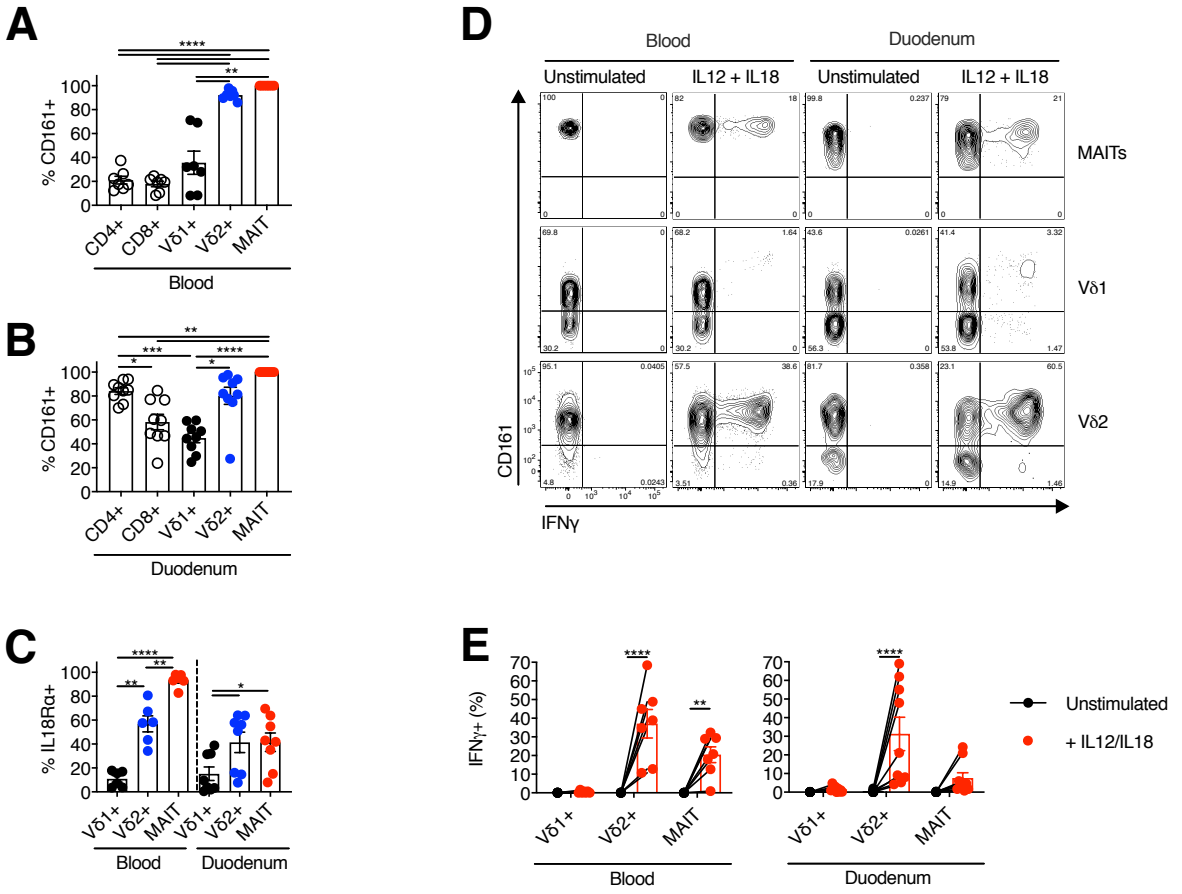


Figure 4-2. MAIT and γδ T cell responses to combinatorial cytokine stimulation in blood and intestine.

(A) Proportion of circulating CD4+, CD8+, MAIT, Vδ1+, and Vδ2+ T cells expressing CD161 (n=7).

(B) Proportion of intestinal CD4+, CD8+, MAIT, Vδ1+, and Vδ2+ T cells expressing CD161 (n=9).

(C) Proportion of MAIT, Vδ1+, and Vδ2+ T cells expressing IL18Rα in the circulation (n=6) and intestine (n=8).

Representative flow cytometry plots (D) and grouped averages (E) of IFNγ production by MAIT, Vδ1+, and Vδ2+ T cells with or without IL-12 + IL-18 stimulation in the circulation (n=7) and intestine (n=9). Black, unstimulated; Red, stimulated. Lines connect samples from the same study subject. (A-C) 1-way ANOVA with Tukey's multiple comparisons test. (E) 2-way ANOVA with Sidak's multiple comparisons test. *, P ≤ 0.05; **, P ≤ 0.01; ***, P ≤ 0.001; ****, P ≤ 0.0001.

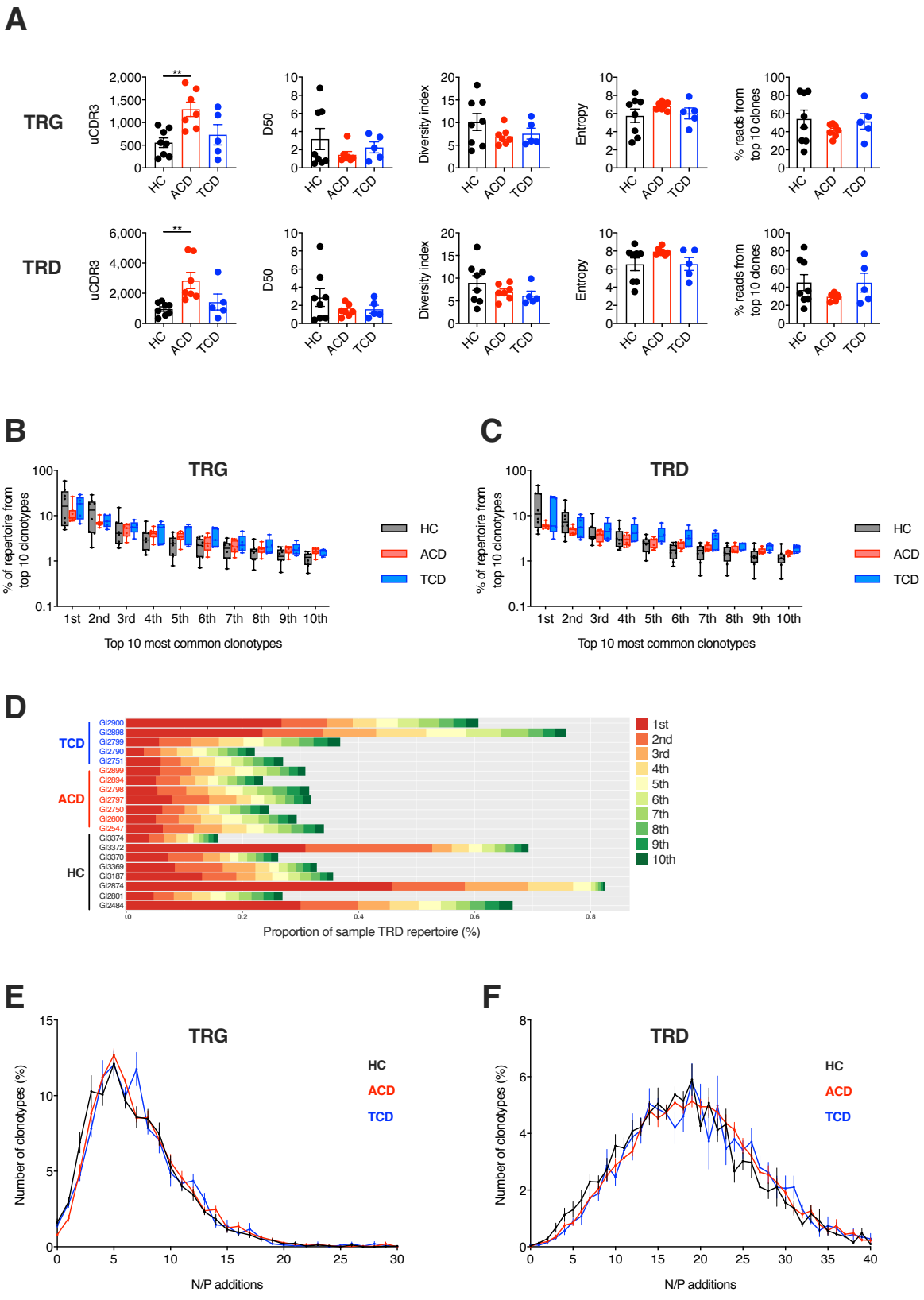

A
TRG
TRD
uCDR3
D50
Diversity index
Entropy
% reads from top 10 clones
HC
ACD
TCD
**
B
TRG
% of repertoire from top 10 clonotypes
Top 10 most common clonotypes
1st 2nd 3rd 4th 5th 6th 7th 8th 9th 10th
C
TRD
D
TCD
ACD
HC
Proportion of sample TRD repertoire (%)
1st
2nd
3rd
4th
5th
6th
7th
8th
9th
10th
E
TRG
Number of clonotypes (%)
N/P additions
F
TRD

Figure 4-3. Diversity of intestinal γδ T cell TCR repertoires.

(A) Diversity metrics of TCR-γ and TCR-δ repertoires of sorted duodenal γδ T cells in health and coeliac disease (n=20). From left to right: uCDR3, number of unique CDR3 clonotypes; D50, percentage of clonotypes that constitute 50% of the total number of reads; Diversity index; Shannon entropy; % of reads contributed by the top 10 most common clones. Healthy control (HC), black; active coeliac disease (ACD), red; treated coeliac disease (TCD), blue.
Percentage of the total number of reads contributed by each of the top ten clonotypes for TCR-γ (B) and TCR-δ (C) repertoires of sorted duodenal γδ T cells in health and coeliac disease (n=20). Box and whiskers plot showing median +/- IQR +/- range. Healthy control, black; active coeliac disease, red; treated coeliac disease, blue.
(D) Proportion of the total number of reads contributed by each of the top ten clonotypes TCR-δ repertoires for individual samples of sorted duodenal γδ T cells in health and coeliac disease (n=20).
(E & F) Number of N/P additions to CDR3 nucleotide sequences of TCR-γ (E) and TCR-δ (F) clonotypes from sorted duodenal γδ T cells in health and coeliac disease (mean +/- SEM). Healthy control (HC), black; active coeliac disease (ACD), red; treated coeliac disease (TCD), blue (n=20).
(A) Mann-Whitney test. **, $P \leq 0.01$.

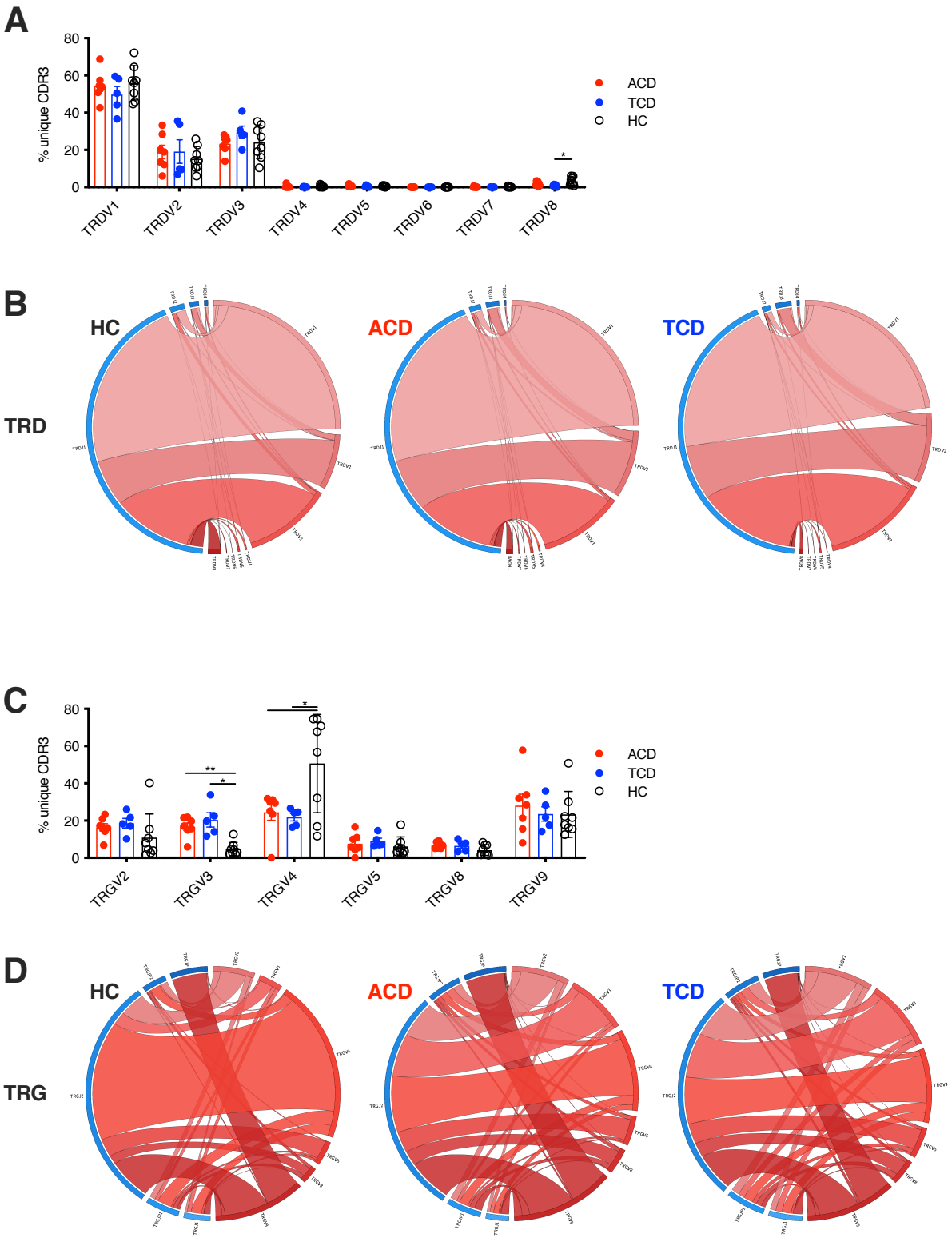

A
% unique CDR3
80
60
40
20
0
TRDV1
TRDV2
TRDV3
TRDV4
TRDV5
TRDV6
TRDV7
TRDV8
*
ACD
TCD
HC
B
TRD
HC
ACD
TCD
C
% unique CDR3
80
60
40
20
0
TRGV2
TRGV3
TRGV4
TRGV5
TRGV8
TRGV9
**
*
*
ACD
TCD
HC
D
TRG
HC
ACD
TCD

Figure 4-4. TRG and TRD gene usage of intestinal γδ T cell TCR repertoires.

(A) TRDV gene usage of unique CDR3 clonotypes of intestinal γδ T cells in health and coeliac disease (n=20). Healthy control, black; active coeliac disease, red; treated coeliac disease, blue.

(B) Circos (chord) plots showing TRDV/TRDJ paired gene usage of unique CDR3 clonotypes of intestinal γδ T cells in health and coeliac disease.

(C) TRGV gene usage of unique CDR3 clonotypes of intestinal γδ T cells in health and coeliac disease (n=20). Healthy control, black; active coeliac disease, red; treated coeliac disease, blue.

(D) Circos (chord) plots showing TRGV/TRGJ paired gene usage of unique CDR3 clonotypes of intestinal γδ T cells in health and coeliac disease.

(A & C) 2-way ANOVA with Holm-Sidak's multiple comparisons test. *, $P \leq 0.05$; **, $P \leq 0.01$.

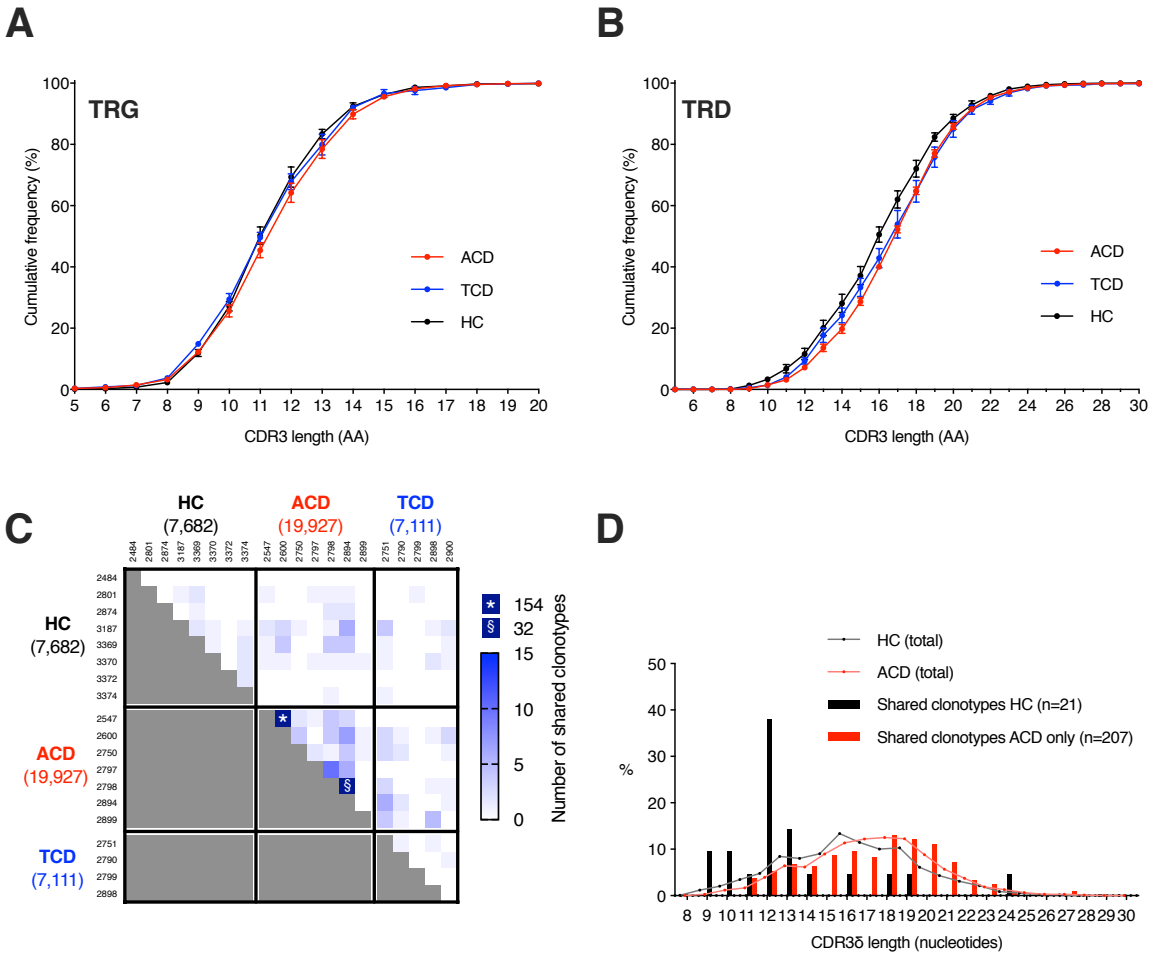

A
TRG
Cumulative frequency (%)
CDR3 length (AA)
ACD
TCD
HC
B
TRD
Cumulative frequency (%)
CDR3 length (AA)
ACD
TCD
HC
C
HC (7,682)
ACD (19,927)
TCD (7,111)
Number of shared clonotypes
154
32
15
10
5
0
D
HC (total)
ACD (total)
Shared clonotypes HC (n=21)
Shared clonotypes ACD only (n=207)
%
CDR3δ length (nucleotides)
E
PxLGD - all TRDV
CxxxxxPxLGD - all TRDV
% uCDR3
p=0.09
**
HC
ACD
TCD
F
PxLGD - TRDV1
CxxxxxPxLGD - TRDV1
% uCDR3
p=0.08
G
YWGI - all TRDV
CxxxxxxxxYWGI - all TRDV
% uCDR3
*
**
H
YWGI - TRDV1
CxxxxxxxxYWGI - TRDV1
% uCDR3
p=0.07
***
I
H-J1 - all TRDV
% uCDR3
n=166

Figure 4-5. CDR3 length, clonal sharing, and coeliac-related motif frequency in intestinal γδ T cell TCR repertoires.

Cumulative frequency of CDR3 length of TRG (A) and TRD (B) clonotypes of intestinal γδ T cells in health and coeliac disease (n=20). Healthy control, black; active coeliac disease, red; treated coeliac disease, blue.
(C) Sharing of TRD clonotypes between study subjects with or without coeliac disease, displayed as a heatmap.
(D) CDR3 length of total TRD clonotypes in health and active coeliac disease (black and red lines respectively, and CDR3 length of clonotypes shared between HC and ACD subjects (black and red bars respectively).
(E-I) Frequency of reported putative coeliac-related CDR3δ motifs in health and coeliac disease.
(E) Frequency of the PxLGD CDR3δ motif in all TRDV intestinal clonotypes, either located anywhere in the CDR3 sequence (left), or defined by its position from the V-gene cysteine residue (right).
(F) Frequency of the PxLGD CDR3δ motif in TRDV1 intestinal clonotypes only, either located anywhere in the CDR3 sequence (left), or defined by its position from the V-gene cysteine residue (right).
(G) Frequency of the YWGI CDR3δ motif in all TRDV intestinal clonotypes, either located anywhere in the CDR3 sequence (left), or defined by its position from the V-gene cysteine residue (right).
(H) Frequency of the YWGI CDR3δ motif in TRDV1 intestinal clonotypes only, either located anywhere in the CDR3 sequence (left), or defined by its position from the V-gene cysteine residue (right).
(I) Frequency of the H-J1 CDR3δ motif in all TRDV intestinal clonotypes.
(E-I) Mann-Whitney test. *, $P \leq 0.05$; **, $P \leq 0.01$; ***, $P \leq 0.001$; ****, $P \leq 0.0001$.

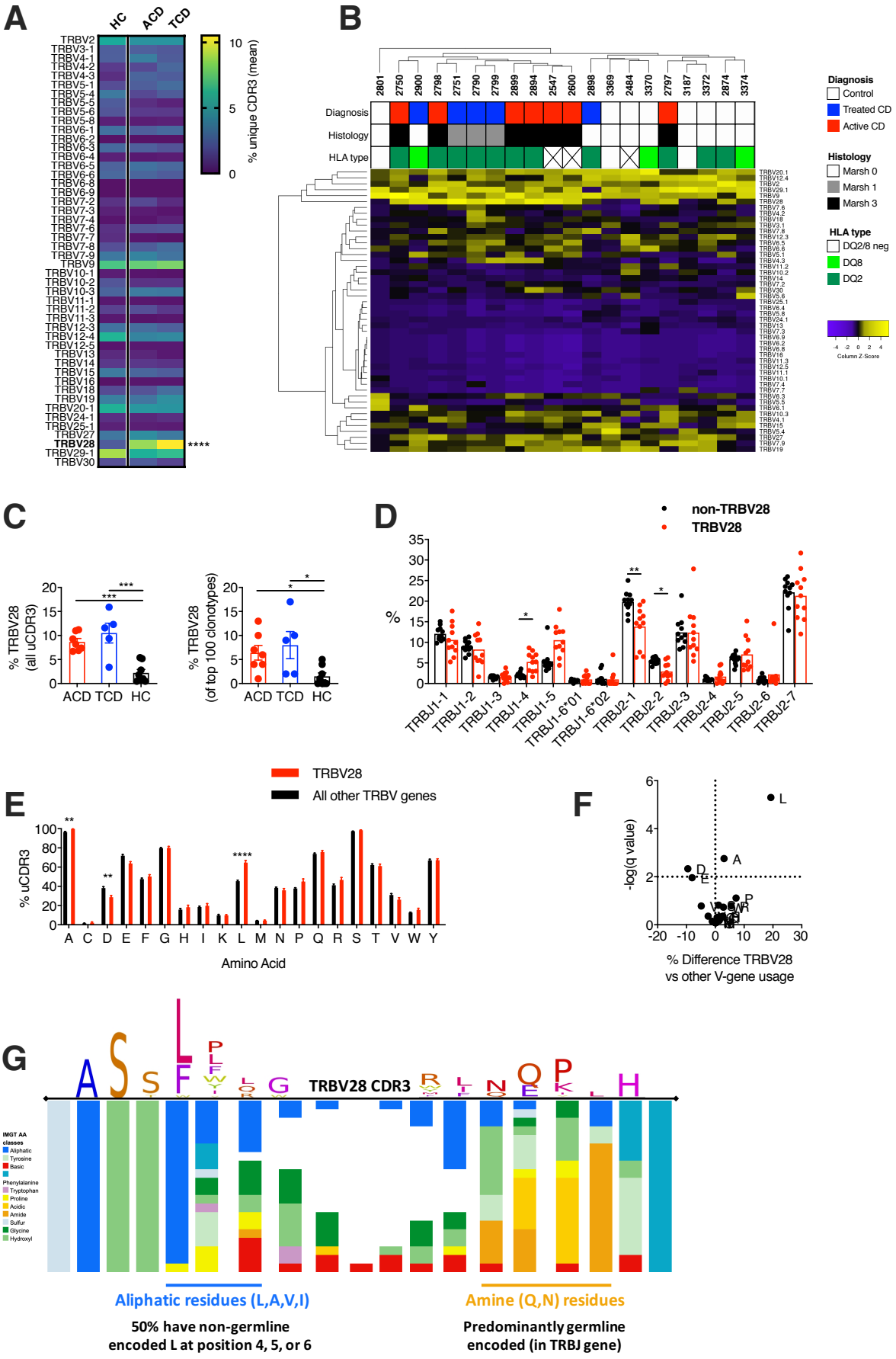

A
HC
ACD
TCD
% unique CDR3 (mean)
10
5
0
TRBV28
****
B
Diagnosis
Histology
HLA type
Control
Treated CD
Active CD
Marsh 0
Marsh 1
Marsh 3
DQ2/8 neg
DQ8
DQ2
Column Z-Score
C
% TRBV28 (all uCDR3)
% TRBV28 (of top 100 clonotypes)
ACD TCD HC
D
non-TRBV28
TRBV28
%
TRBJ1-1
TRBJ1-2
TRBJ1-3
TRBJ1-4
TRBJ1-5
TRBJ1-6*01
TRBJ1-6*02
TRBJ2-1
TRBJ2-2
TRBJ2-3
TRBJ2-4
TRBJ2-5
TRBJ2-6
TRBJ2-7
E
TRBV28
All other TRBV genes
% uCDR3
A C D E F G H I K L M N P Q R S T V W Y
Amino Acid
F
-log(q value)
% Difference TRBV28
vs other V-gene usage
G
TRBV28 CDR3
IMGT AA classes
Aliphatic
Tyrosine
Basic
Phenylalanine
Tryptophan
Proline
Acidic
Amide
Sulfur
Glycine
Hydroxyl
Aliphatic residues (L,A,V,I)
50% have non-germline encoded L at position 4, 5, or 6
Amine (Q,N) residues
Predominantly germline encoded (in TRBJ gene)

Figure 4-6. TRBV28 gene usage in intestinal CD8+ T cell TCR repertoires.

(A) TRBV gene usage by unique CDR3 clonotypes in intestinal CD8+ T cell TCR repertoires in health and coeliac disease.

(B) Hierarchical clustering of samples by TRBV gene usage (n=20). Coeliac disease status, histological severity of villous atrophy, and HLA DQ2/DQ8 status are indicated.

(C) Proportion of unique CDR3β clonotypes (left) and proportion of top 100 most common clonotypes (right) using the TRBV28 V-gene in health and coeliac disease (n=20). Healthy control, black; active coeliac disease, red; treated coeliac disease, blue.

(D) TRBJ gene usage by TRBV28 (red) and non-TRBV28 (black) clonotypes in intestinal CD8+ T cell TCR repertoires in coeliac disease (n=12).

(E) Amino acid usage within CDR3 sequences of TRBV28 (red) and non-TRBV28 (black) clonotypes in intestinal CD8+ T cell TCR repertoires in coeliac disease (n=12).

(F) Volcano plot of the difference in amino acid usage between TRBV28 and non-TRBV28 clonotypes.

(G) CDR3 positional and junctional analysis of TRBV28 clonotypes in coeliac disease. Letters indicate enrichment of amino acids in the first and last 7 CDR3 positions in TRBV28 clonotypes compared to non-TRBV28 clonotypes (iceLogo). Stacked plots show amino acid class use within the CDR3 of TRBV28 clonotypes in coeliac disease (IMGT Junction Analysis).

(A,D) 2-way ANOVA with Holm-Sidak's multiple comparisons test. (C) 1-way ANOVA with Holm-Sidak's multiple comparisons test. (E,F) Multiple t-tests with Benjamini, Krieger, and Yetutieli two-stage step up control of multiple comparisons with FDR<0.01. *, $P \leq 0.05$; **, $P \leq 0.01$; ***, $P \leq 0.001$; ****, $P \leq 0.0001$.

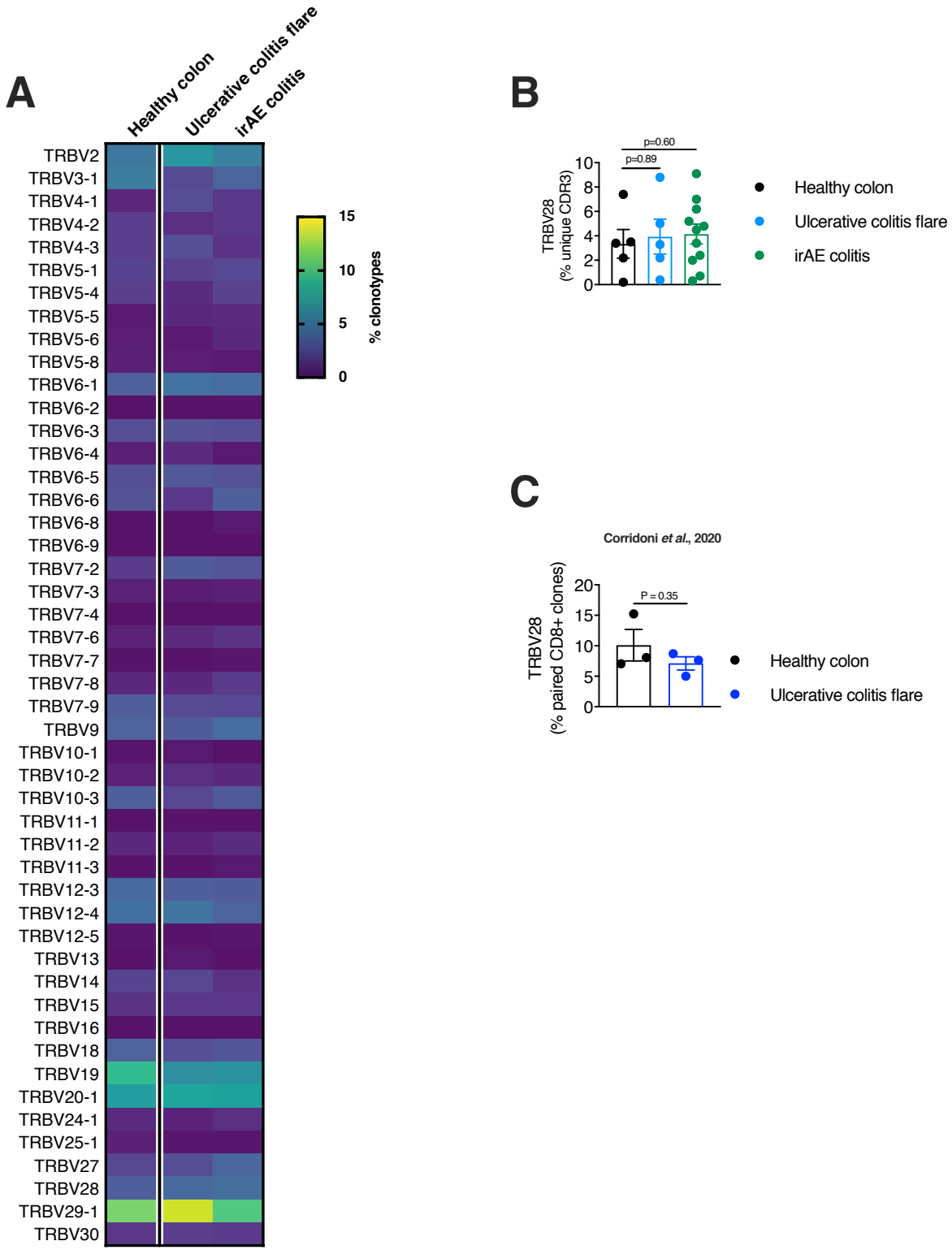

A
Healthy colon
Ulcerative colitis flare
irAE colitis
TRBV2
TRBV3-1
TRBV4-1
TRBV4-2
TRBV4-3
TRBV5-1
TRBV5-4
TRBV5-5
TRBV5-6
TRBV5-8
TRBV6-1
TRBV6-2
TRBV6-3
TRBV6-4
TRBV6-5
TRBV6-6
TRBV6-8
TRBV6-9
TRBV7-2
TRBV7-3
TRBV7-4
TRBV7-6
TRBV7-7
TRBV7-8
TRBV7-9
TRBV9
TRBV10-1
TRBV10-2
TRBV10-3
TRBV11-1
TRBV11-2
TRBV11-3
TRBV12-3
TRBV12-4
TRBV12-5
TRBV13
TRBV14
TRBV15
TRBV16
TRBV18
TRBV19
TRBV20-1
TRBV24-1
TRBV25-1
TRBV27
TRBV28
TRBV29-1
TRBV30
15
10
5
0
% clonotypes
B
p=0.60
p=0.89
TRBV28
(% unique CDR3)
10
8
6
4
2
0
Healthy colon
Ulcerative colitis flare
irAE colitis
C
Corridoni et al., 2020
TRBV28
(% paired CD8+ clones)
P = 0.35
20
15
10
5
0
Healthy colon
Ulcerative colitis flare

Figure 4-7. TRBV28 gene usage in other inflammatory intestinal conditions.

(A) Heatmap of TRBV gene usage by unique CDR3 clonotypes in intestinal mucosa TCR repertoires in health, active ulcerative colitis, and immunotherapy-related adverse event (irAE) colitis.
(B) Proportion of unique CDR3β clonotypes using the TRBV28 V-gene in health (black), active ulcerative colitis (blue), and irAE colitis (green) (n=21).
(C) Proportion of unique paired CD8+ clonotypes using the TRBV28 V-gene in health (black) and active ulcerative colitis (blue) (n=6). Data from (Corridoni et al., 2020).
(B) 1-way ANOVA with Holm-Sidak's multiple comparisons test. (C) Mann-Whitney test.

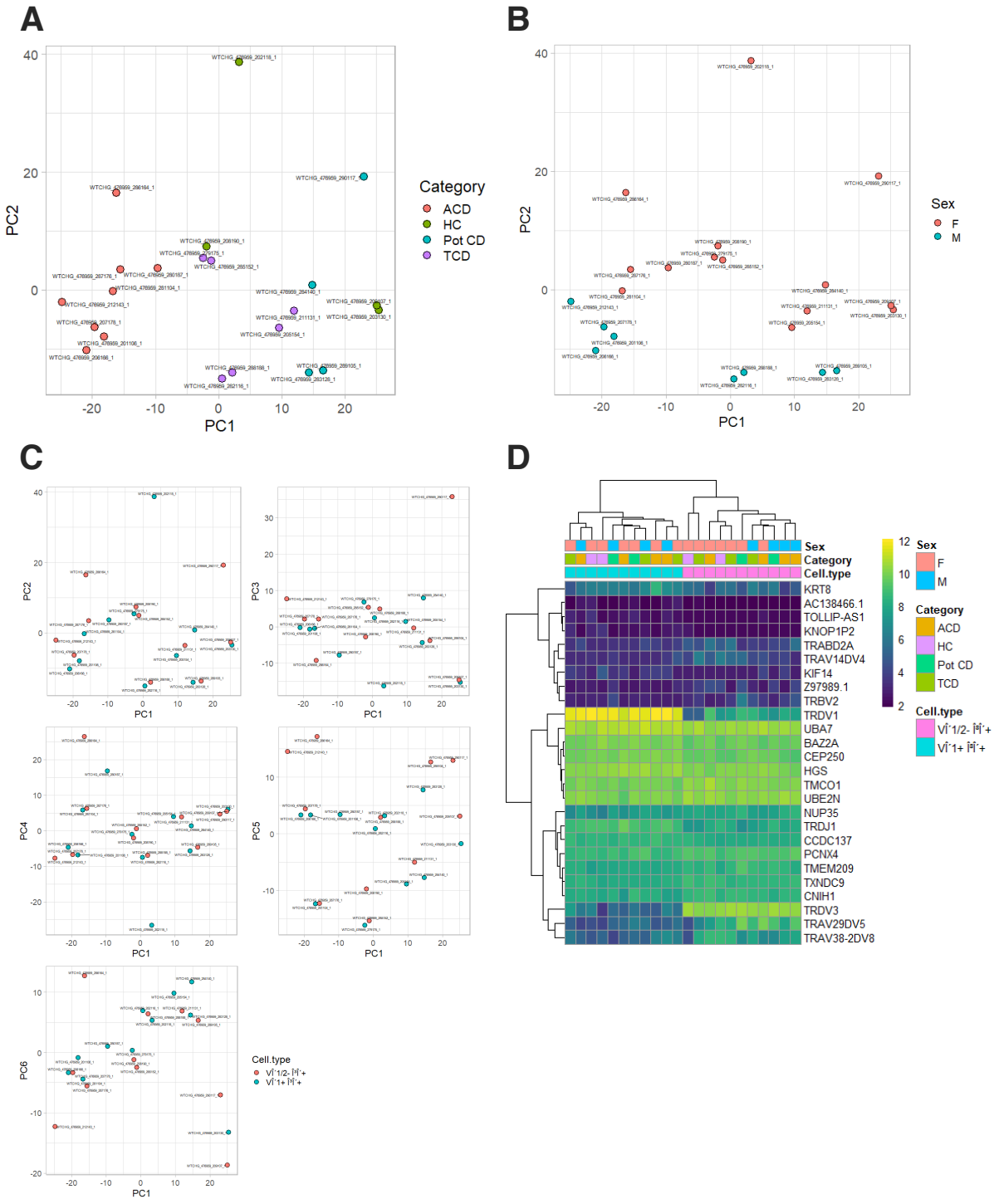

A
B
C
D
PC1
PC2
PC3
PC4
PC5
PC6
Category
ACD
HC
Pot CD
TCD
Sex
F
M
Cell.type
Vî¨1/2- Îº¨+
Vî¨1+ Îº¨+
KRT8
AC138466.1
TOLLIP-AS1
KNOP1P2
TRABD2A
TRAV14DV4
KIF14
Z97989.1
TRBV2
TRDV1
UBA7
BAZ2A
CEP250
HGS
TMCO1
UBE2N
NUP35
TRDJ1
CCDC137
PCNX4
TMEM209
TXNDC9
CNIH1
TRDV3
TRAV29DV5
TRAV38-2DV8

Figure 4-8. Transcriptional profiles of Vδ1+ and Vδ1/2- γδ T IELs.

Comparison of the bulk RNAseq transcriptional profiles of Vδ1+ and Vδ1/2- γδ T cells isolated from intestinal epithelium in health and coeliac disease.

(A & B) Principal component analysis (PCA) of transcriptional profiles of Vδ1+ and Vδ1/2- γδ T IELs displaying PCs 1 and 2, coloured by disease status (A) and subject sex (B), Active coeliac disease, ACD; healthy control, HC; potential coeliac disease, Pot CD; treated coeliac disease, TCD.

(C) Principal component analysis (PCA) of transcriptional profiles of Vδ1+ and Vδ1/2- γδ T IELs displaying PCs 1-6, coloured by cell type.

(D) Heatmap of normalised expression of differentially expressed genes between Vδ1+ and Vδ1/2- γδ T IELs.

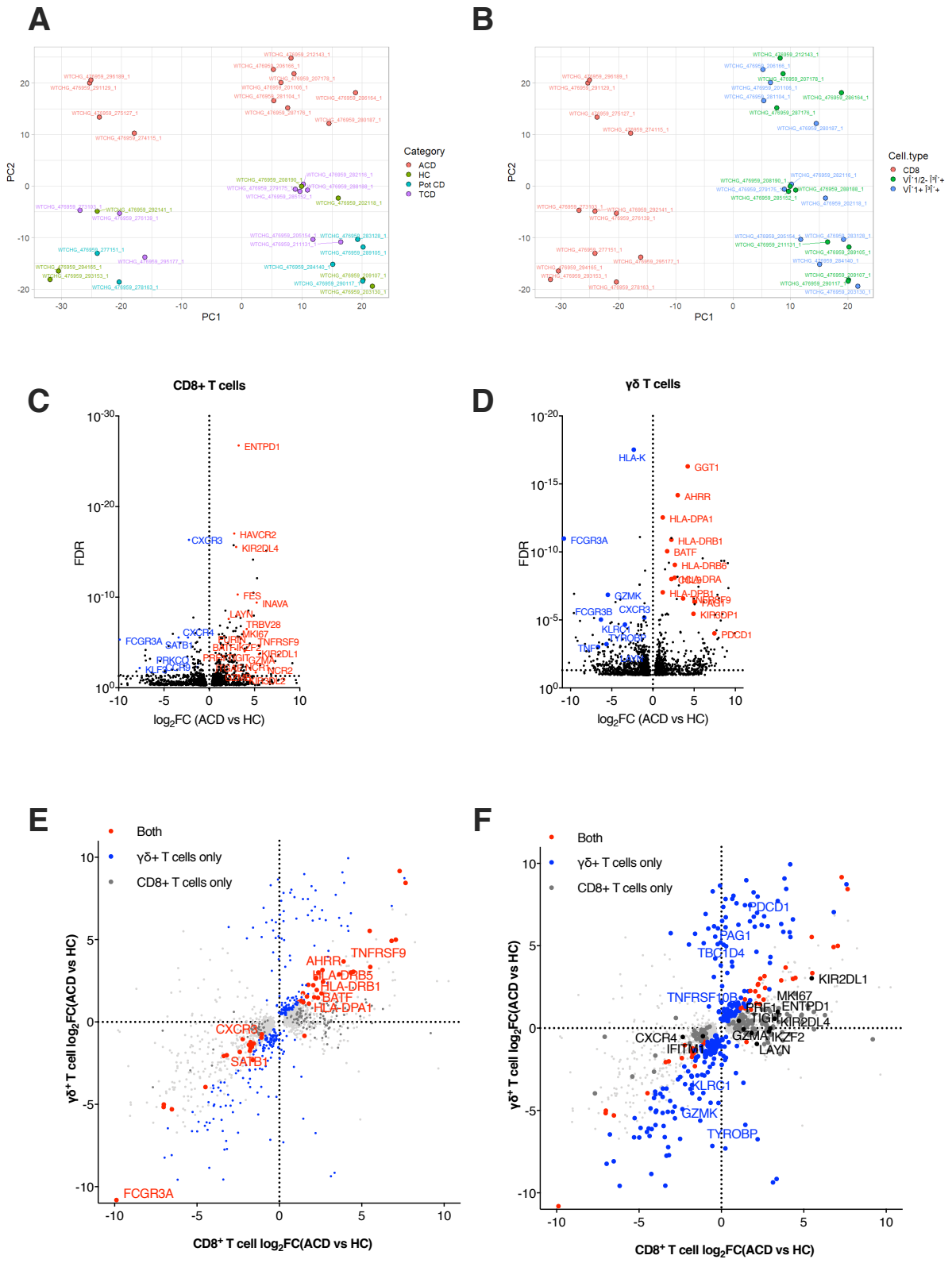

A
PC2
PC1
Category
ACD
HC
Pot CD
TCD
B
PC2
PC1
Cell.type
CD8
Vδ1/2- γδ+
Vδ1+ γδ+
C
CD8+ T cells
FDR
log2FC (ACD vs HC)
ENTPD1
HAVCR2
CXCR3
KIR2DL4
FES
INAVA
LAYN
TRBV28
MKI67
CXCR4
FCGR3A
SATB1
TNFRSF9
KIR2DL1
PRKCQ
GZMK
KLRC1
D
γδ T cells
FDR
log2FC (ACD vs HC)
HLA-K
GGT1
AHRR
HLA-DPA1
FCGR3A
HLA-DRB1
BATF
HLA-DRB5
HLA-DRA
GZMK
FCGR3B
CXCR3
KLRC1
TYROBP
PDCD1
E
Both
γδ+ T cells only
CD8+ T cells only
γδ+ T cell log2FC(ACD vs HC)
CD8+ T cell log2FC(ACD vs HC)
TNFRSF9
AHRR
HLA-DRB5
HLA-DRB1
BATF
HLA-DPA1
CXCR3
SATB1
FCGR3A
F
Both
γδ+ T cells only
CD8+ T cells only
γδ+ T cell log2FC(ACD vs HC)
CD8+ T cell log2FC(ACD vs HC)
PDCD1
PAG1
TBC1D4
KIR2DL1
MKI67
ENTPD1
KIR2DL4
CXCR4
IKZF2
LAYN
KLRC1
GZMK
TYROBP

Figure 4-9. Transcriptional changes between health and coeliac disease in CD8+ and γδ T IELs.
Comparison of the bulk RNAseq transcriptional profiles of CD8+ and γδ T cells isolated from intestinal epithelium in health and coeliac disease.
(A & B) Principal component analysis (PCA) of transcriptional profiles of CD8+ and γδ T IELs displaying PCs 1 and 2, coloured by disease status (A) and cell type (B), Active coeliac disease, ACD; healthy control, HC; potential coeliac disease, Pot CD; treated coeliac disease, TCD.
(C & D) Volcano plot of differentially expressed genes between HC and ACD disease states in CD8+ T cells (C) and γδ T cells (D). Selected differentially expressed genes are marked: up-regulated in CD (red), Down-regulated in CD (blue).
(E & F) Scatter plot of log_2(Fold change) (log_2FC) between ACD and HC samples for CD8+ T cells (x-axis) and γδ T cells (y-axis). Selected differentially expressed genes are marked: differentially expressed in both cell types (red; left); differentially expressed in either CD8+ (black) or γδ (blue) T cells (right).

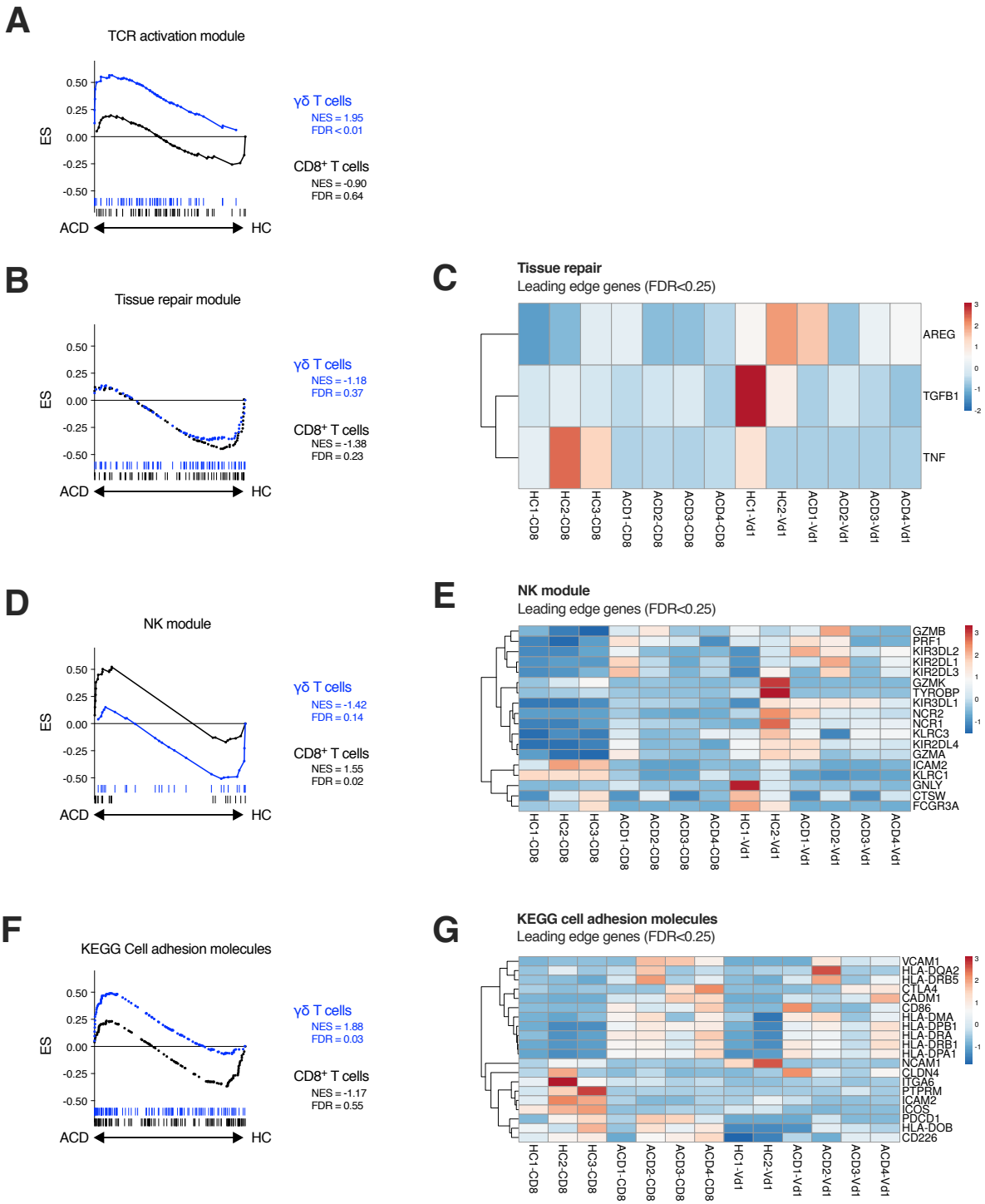

A
TCR activation module
ES
0.50
0.25
0.00
-0.25
-0.50
ACD
HC
γδ T cells
NES = 1.95
FDR < 0.01
CD8+ T cells
NES = -0.90
FDR = 0.64
B
Tissue repair module
γδ T cells
NES = -1.18
FDR = 0.37
CD8+ T cells
NES = -1.38
FDR = 0.23
C
Tissue repair
Leading edge genes (FDR<0.25)
AREG
TGFB1
TNF
HC1-CD8
HC2-CD8
HC3-CD8
ACD1-CD8
ACD2-CD8
ACD3-CD8
ACD4-CD8
HC1-Vd1
HC2-Vd1
ACD1-Vd1
ACD2-Vd1
ACD3-Vd1
ACD4-Vd1
D
NK module
γδ T cells
NES = -1.42
FDR = 0.14
CD8+ T cells
NES = 1.55
FDR = 0.02
E
NK module
Leading edge genes (FDR<0.25)
GZMB
PRF1
KIR3DL2
KIR2DL1
KIR2DL3
GZMK
TYROBP
KIR3DL1
NCR2
NCR1
KLRC3
KIR2DL4
GZMA
ICAM2
KLRC1
GNLY
CTSW
FCGR3A
F
KEGG Cell adhesion molecules
γδ T cells
NES = 1.88
FDR = 0.03
CD8+ T cells
NES = -1.17
FDR = 0.55
G
KEGG cell adhesion molecules
Leading edge genes (FDR<0.25)
VCAM1
HLA-DQA2
HLA-DRB5
CTLA4
CADM1
CD86
HLA-DMA
HLA-DPB1
HLA-DRA
HLA-DRB1
HLA-DPA1
NCAM1
CLDN4
ITGA6
PTPRM
ICAM2
ICOS
PDCD1
HLA-DOB
CD226
H
Gene set
NES
FDR
GSE9650 - Effector vs Exhausted CD8 T cell - DOWN
-1.06
1.0
GSE9650 - Effector vs Exhausted CD8 T cell - UP
-0.94
1.0
GSE41867 - D15 Effector vs D30 exhausted CD8 T cell - DOWN
-0.92
0.91
GSE41867 - D15 Effector vs D30 exhausted CD8 T cell - UP
-0.70
0.98
ACD
HC
Gene rank

Figure 4-10. Gene set enrichment health and coeliac disease in CD8+ and γδ T IELs.

Gene set enrichment analysis (GSEA) of pre-ranked differentially expressed genes between health and active coeliac disease in intestinal CD8+ and γδ T cells.

(A) Enrichment of a TCR activation module gene set. CD8+ T cells, black; γδ T cells, blue.

(B) Enrichment of a tissue repair module gene set. CD8+ T cells, black; γδ T cells, blue.

(C) Heatmap of expression of tissue repair module leading edge genes from (B), which were differentially expressed in either cell type with FDR<0.25.

(D) Enrichment of a NK-related module gene set. CD8+ T cells, black; γδ T cells, blue.

(E) Heatmap of expression of NK-related module leading edge genes from (D), which were differentially expressed in either cell type with FDR<0.25.

(F) Enrichment of the KEGG cell adhesion molecule gene set. CD8+ T cells, black; γδ T cells, blue.

(G) Heatmap of expression of KEGG cell adhesion molecule leading edge genes from (F), which were differentially expressed in either cell type with FDR<0.25.

(H) GSEA of T cell exhaustion-related gene sets in differential gene expression between ACD and HC samples of CD8+ T cells. NES, Normalised enrichment score; FDR, False discovery rate.

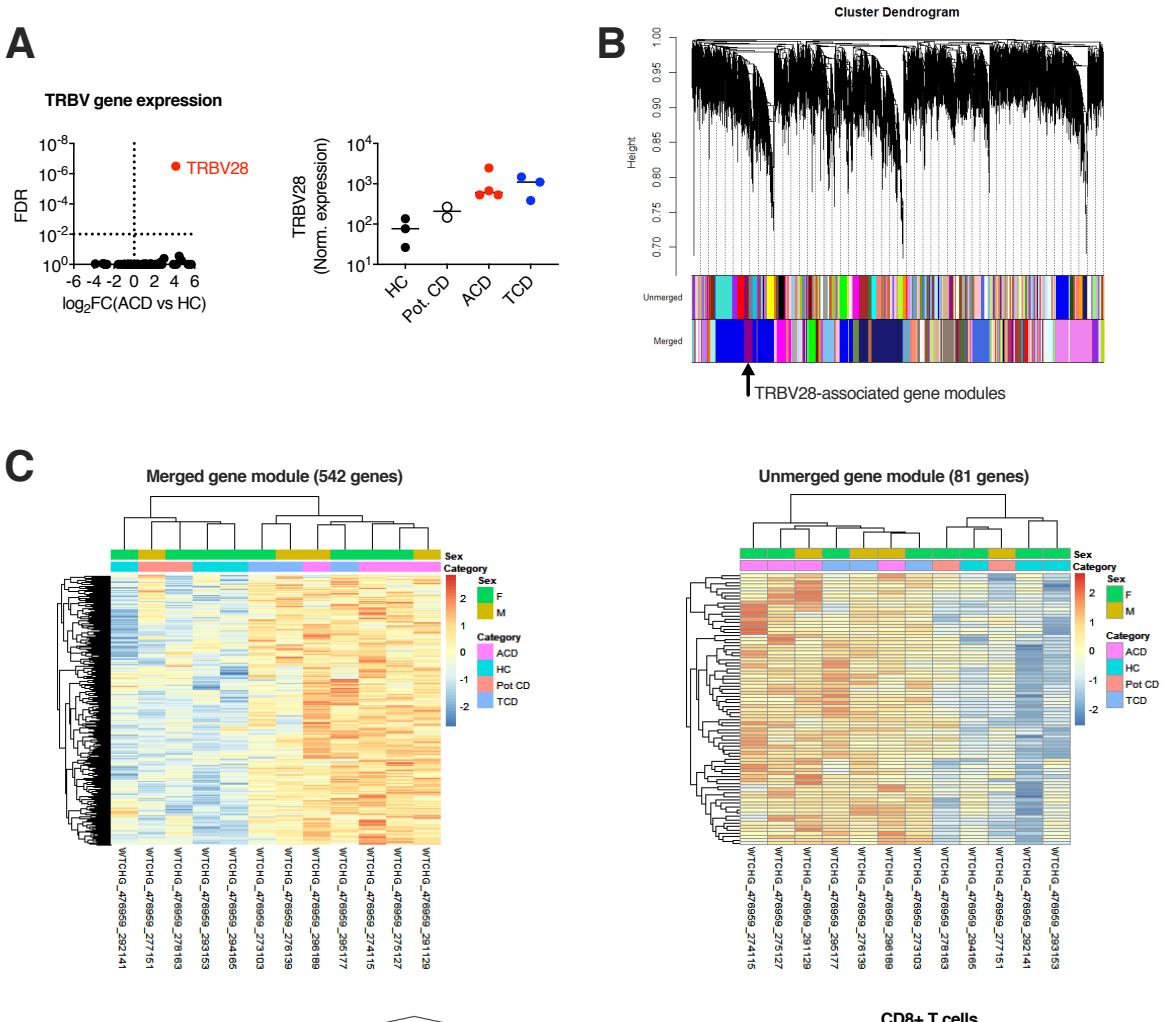

A
TRBV gene expression
FDR
TRBV28
log2FC(ACD vs HC)
TRBV28 (Norm. expression)
HC
Pot. CD
ACD
TCD
B
Cluster Dendrogram
Height
Unmerged
Merged
TRBV28-associated gene modules
C
Merged gene module (542 genes)
Unmerged gene module (81 genes)
Sex
Category
F
M
ACD
HC
Pot CD
TCD
D
biological_process
biological regulation
response to stimulus
immune system process
regulation of biological process
response to stress
immune response
regulation of response to stimulus
positive regulation of biological process
regulation of immune system process
defense response
adaptive immune response
regulation of response to stress
positive regulation of response to stimulus
regulation of immune response
positive regulation of immune system process
regulation of immune effector process
cellular defense response
regulation of cell killing
regulation of defense response
positive regulation of immune response
positive regulation of immune process
regulation of leukocyte mediated immunity
positive regulation of defense response
regulation of innate immune response
regulation of lymphocyte mediated immunity
positive regulation of leukocyte mediated immunity
regulation of leukocyte mediated cytotoxicity
positive regulation of innate immune response
regulation of natural killer cell mediated immunity
positive regulation of lymphocyte mediated immunity
regulation of natural killer cell mediated cytotoxicity
positive regulation of natural killer cell mediated immunity
E
CD8+ T cells
FDR
log2FC (ACD vs HC)
ENTPD1
KIR2DL4
LILRB2
LAYN
TRBV28
ADAM28
IKZF3
S1PR3
PTGFRN
KIR3DL1
F
GO:0050896 - response to stimulus
GO:0006968 - cellular defense response
GO:0050776 - regulation of immune response
GO:0006955 - immune response
GO:0031341 - regulation of cell killing
GO:0002717 - positive regulation of natural killer cell mediated immunity
GO:0001910 - regulation of leukocyte mediated cytotoxicity
GO:0002376 - immune system process
GO:0002250 - adaptive immune response
GO:0002715 - regulation of natural killer cell mediated immunity
GO:0042269 - regulation of natural killer cell mediated cytotoxicity
log(P value)

Figure 4-11. Analysis of TRBV28 and related gene sets in transcriptional profiles of CD8+ T IELs in coeliac disease.

(A) Volcano plot of expression of TRBV gene transcripts between healthy controls and active coeliac disease (left). Normalised expression of TRBV28 transcripts in health and coeliac disease (n=12; right). Healthy control, HC; potential CD, Pot. CD; active coeliac disease, ACD; treated coeliac disease, TCD.

(B) Cluster dendrogram output from WCGNA analysis showing unmerged and merged gene modules that co-correlate in the dataset.

(C) Heatmap of expression of merged (left) and unmerged (right) gene modules containing TRBV28 by CD8+ T cells in health and coeliac disease. Disease status and subject sex are indicated.

(D) Biological process GO term plot showing networks of gene sets enriched in the unmerged TRBV28-associated gene module. GO terms in yellow are enriched in the module.

(E) Volcano plot of differentially expressed genes between HC and ACD disease states in CD8+ T cells. Selected differentially expressed genes that are part of the TRBV28-associated gene module are markers in red.

(F) GO terms enriched in the unmerged TRBV28-associated gene module.

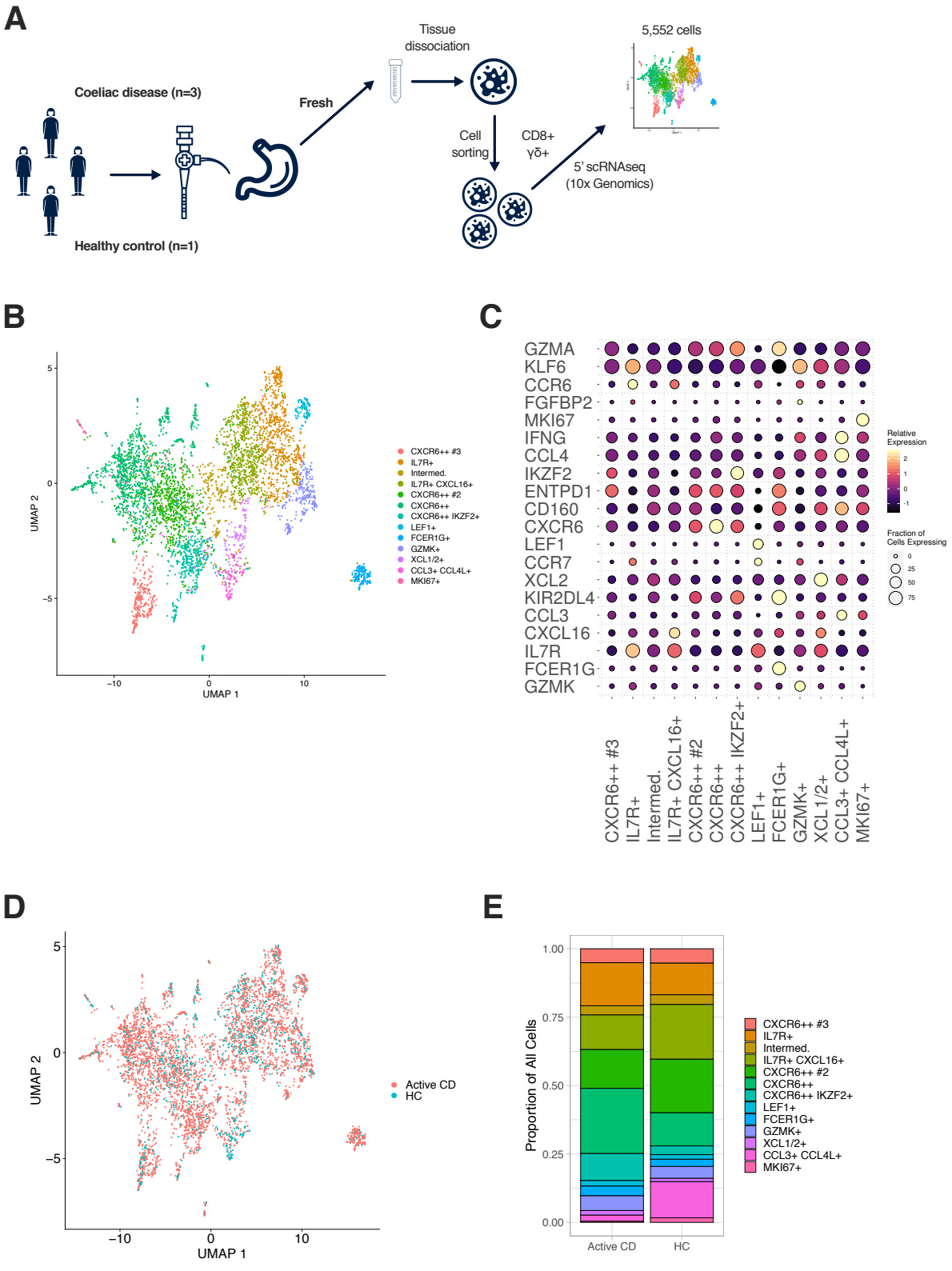

A
Coeliac disease (n=3)
Healthy control (n=1)
Fresh
Tissue dissociation
Cell sorting
CD8+ γδ+
5' scRNAseq (10x Genomics)
5,552 cells
B
UMAP 1
UMAP 2
CXCR6++ #3
IL7R+
Intermed.
IL7R+ CXCL16+
CXCR6++ #2
CXCR6++
CXCR6++ IKZF2+
LEF1+
FCER1G+
GZMK+
XCL1/2+
CCL3+ CCL4L+
MKI67+
C
GZMA
KLF6
CCR6
FGFBP2
MKI67
IFNG
CCL4
IKZF2
ENTPD1
CD160
CXCR6
LEF1
CCR7
XCL2
KIR2DL4
CCL3
CXCL16
IL7R
FCER1G
GZMK
Relative Expression
Fraction of Cells Expressing
D
UMAP 1
UMAP 2
Active CD
HC
E
Proportion of All Cells
Active CD
HC

Figure 4-12. The single-cell transcriptional landscape of intestinal CD8+ and γδ T cells in coeliac disease.

(A) Schematic diagram of scRNAseq experiment to characterise transcriptional heterogeneity of intestinal CD8+ and γδ T cells using 5' scRNAseq (10x Genomics). Study subject and cells numbers are indicated.

(B) UMAP plot of 5,552 intestinal CD8+ and γδ+ T cells from four donor subjects. 13 transcriptionally distinct clusters are identified (a small population of CD4+ T cells was removed).

(C) Bubble plot of key gene identifiers for the clusters identified in the dataset. Bubble size indicates the proportion of cells in which the gene is present. Colour intensity indicates the expression level of the gene in cells in that cluster.

(D) UMAP plot with subject disease status illustrated.

(E) Proportion of total cells forming each cluster in healthy and coeliac disease subjects.

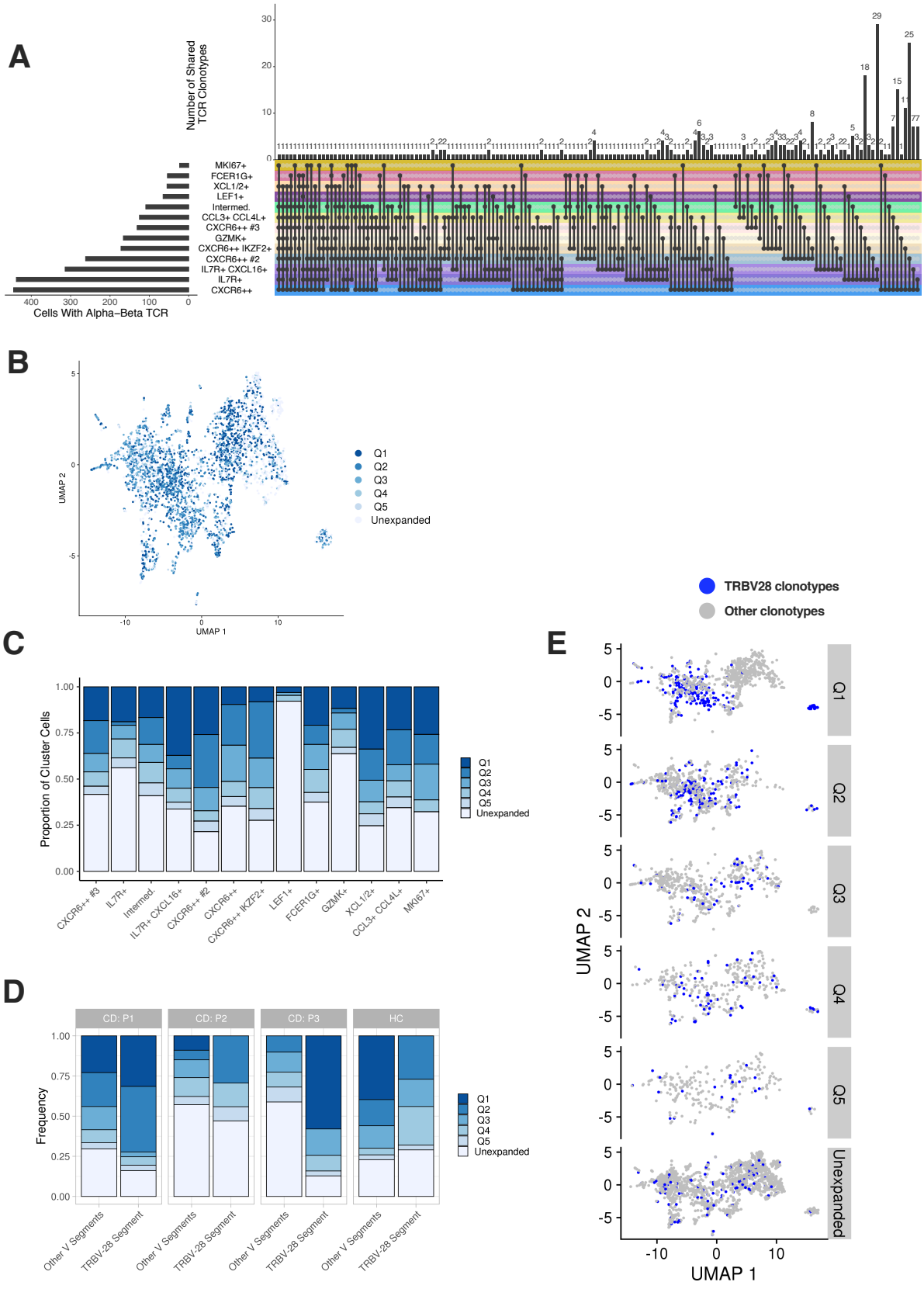

A
Number of Shared TCR Clonotypes
MKI67+
FCER1G+
XCL1/2+
LEF1+
Intermed.
CCL3+ CCL4L+
CXCR6++ #3
GZMK+
CXCR6++ IKZF2+
CXCR6++ #2
IL7R+ CXCL16+
IL7R+
CXCR6++
Cells With Alpha−Beta TCR
B
UMAP 2
UMAP 1
Q1
Q2
Q3
Q4
Q5
Unexpanded
C
Proportion of Cluster Cells
D
Frequency
CD: P1
CD: P2
CD: P3
HC
Other V Segments
TRBV-28 Segment
E
TRBV28 clonotypes
Other clonotypes
UMAP 2
UMAP 1

Figure 4-13. Clonotype sharing and clonal expansion in intestinal CD8+ T cells.

(A) Upset plot displaying shared CD8+ αβ TCR clonotypes between clusters, with shared clonotypes visualized as an 'interaction', indicated by a black circle joined by black lines. Bars above indicate the total number of shared TCR clonotypes for that interaction. Bars to left indicate number of clonotypes in the cluster. Cluster intersections with no shared TCR clonotypes are not shown.

(B) UMAP plot with degree of clonal expansion indicated. Quintiles of clonal expansion are indicated, with Q1 the most clonally expanded cells.

(C) Proportion of cells within each cluster that are clonally expanded. Quintiles of clonal expansion are indicated.

(D) Proportion of cells within TRBV28 and non-TRBV28 clonotypes that are clonally expanded in each study subject. Quintiles of clonal expansion are indicated.

(E) UMAP plots showing cells in each quintile of clonal expansion. TRBV28 clonotypes are indicated in blue.

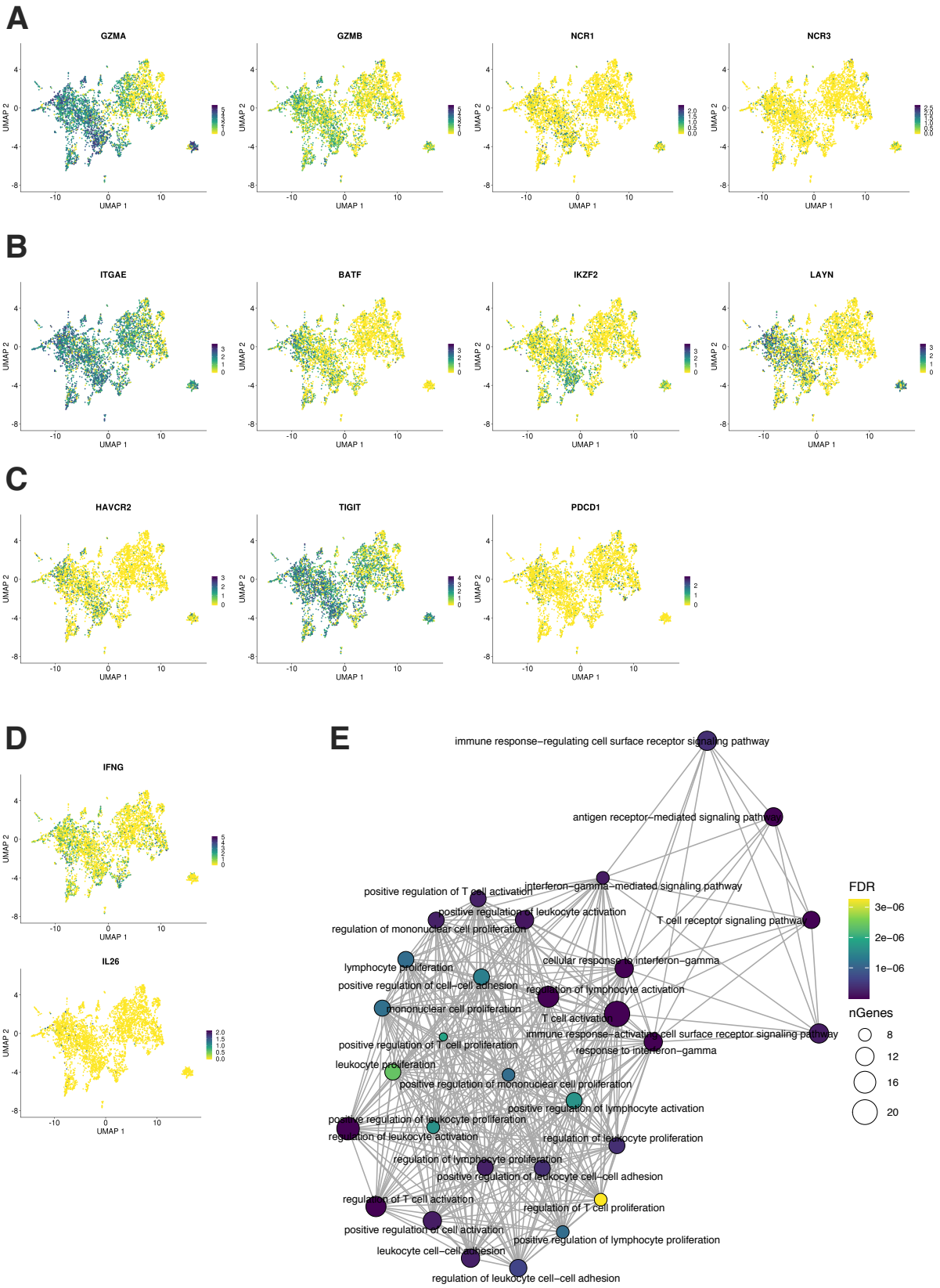

A
GZMA
GZMB
NCR1
NCR3
B
ITGAE
BATF
IKZF2
LAYN
C
HAVCR2
TIGIT
PDCD1
D
IFNG
IL26
E
immune response−regulating cell surface receptor signaling pathway
antigen receptor−mediated signaling pathway
interferon−gamma−mediated signaling pathway
positive regulation of T cell activation
positive regulation of leukocyte activation
regulation of mononuclear cell proliferation
T cell receptor signaling pathway
lymphocyte proliferation
cellular response to interferon−gamma
positive regulation of cell−cell adhesion
regulation of lymphocyte activation
mononuclear cell proliferation
T cell activation
immune response−activating cell surface receptor signaling pathway
positive regulation of T cell proliferation
response to interferon−gamma
leukocyte proliferation
positive regulation of mononuclear cell proliferation
positive regulation of lymphocyte activation
positive regulation of leukocyte proliferation
regulation of leukocyte activation
regulation of leukocyte proliferation
regulation of lymphocyte proliferation
positive regulation of leukocyte cell−cell adhesion
regulation of T cell activation
regulation of T cell proliferation
positive regulation of cell activation
positive regulation of lymphocyte proliferation
leukocyte cell−cell adhesion
regulation of leukocyte cell−cell adhesion
FDR
3e−06
2e−06
1e−06
nGenes
8
12
16
20

Figure 4-14. Gene expression of CXCR6+ intestinal T cell clusters.

(A) UMAP plot of intestinal CD8+ and γδ T cells overlaid with the expression of the genes *GZMA*, *GZMB*, *NCR1*, and *NCR3*.

(B) UMAP plot of intestinal CD8+ and γδ T cells overlaid with the expression of the genes *ITGAE*, *BATF*, *IKZF2*, and *LAYN*.

(C) UMAP plot of intestinal CD8+ and γδ T cells overlaid with the expression of the genes *HAVCR2*, *TIGIT*, and *PDCD1*.

(D) UMAP plot of intestinal CD8+ and γδ T cells overlaid with the expression of the genes *IFNG* and *IL26*.

(E) GO terms enriched in the CXCR6+ cluster in active CD. Overlap in genes within GO terms is shown by proximity and connecting lines.

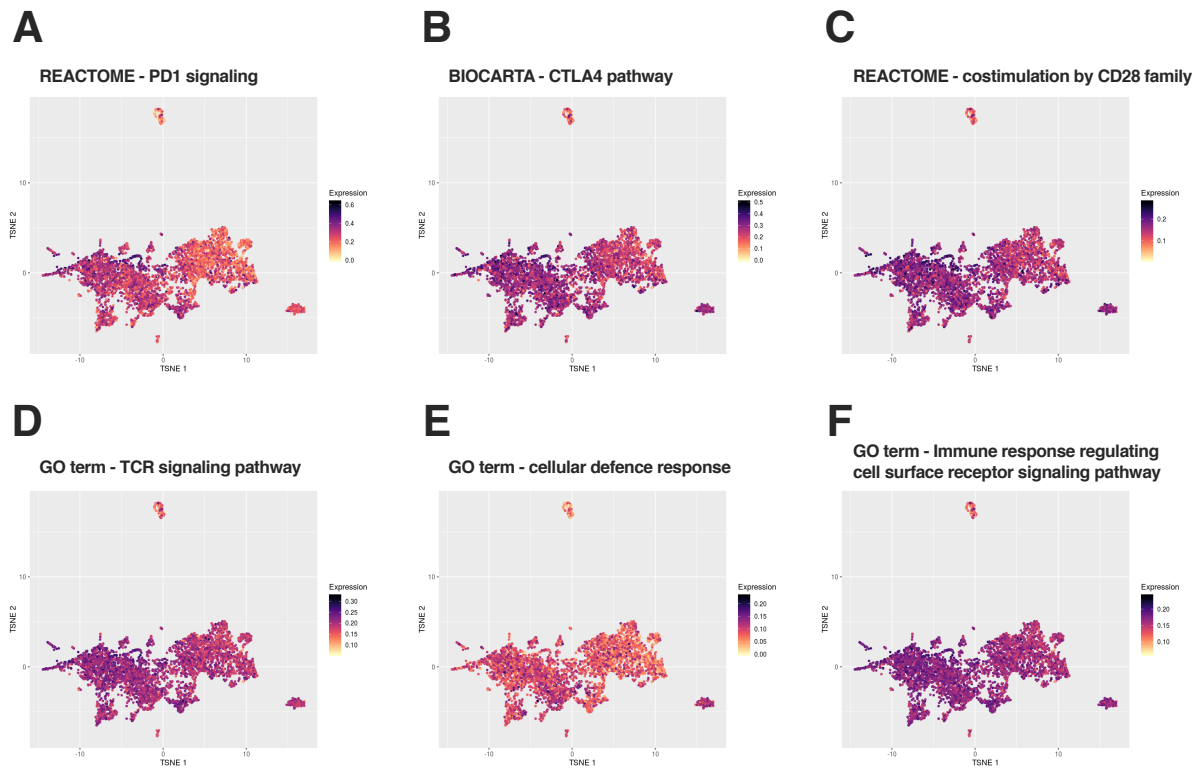


Figure 4-15. Gene pathway expression in CXCR6+ intestinal T cell clusters.

UMAP plot of intestinal CD8+ and γδ T cells overlaid with the single-cell expression of the following gene sets that were enriched in CXCR6+ clusters: REACTOME PD1 signaling (A), BIOCARTA CTLA4 pathway (B), REACTOME costimulation by CD28 family (C), GO TCR signaling pathway (D), GO cellular defence response (E), and GO immune response regulating cell surface receptor signaling pathway (F).

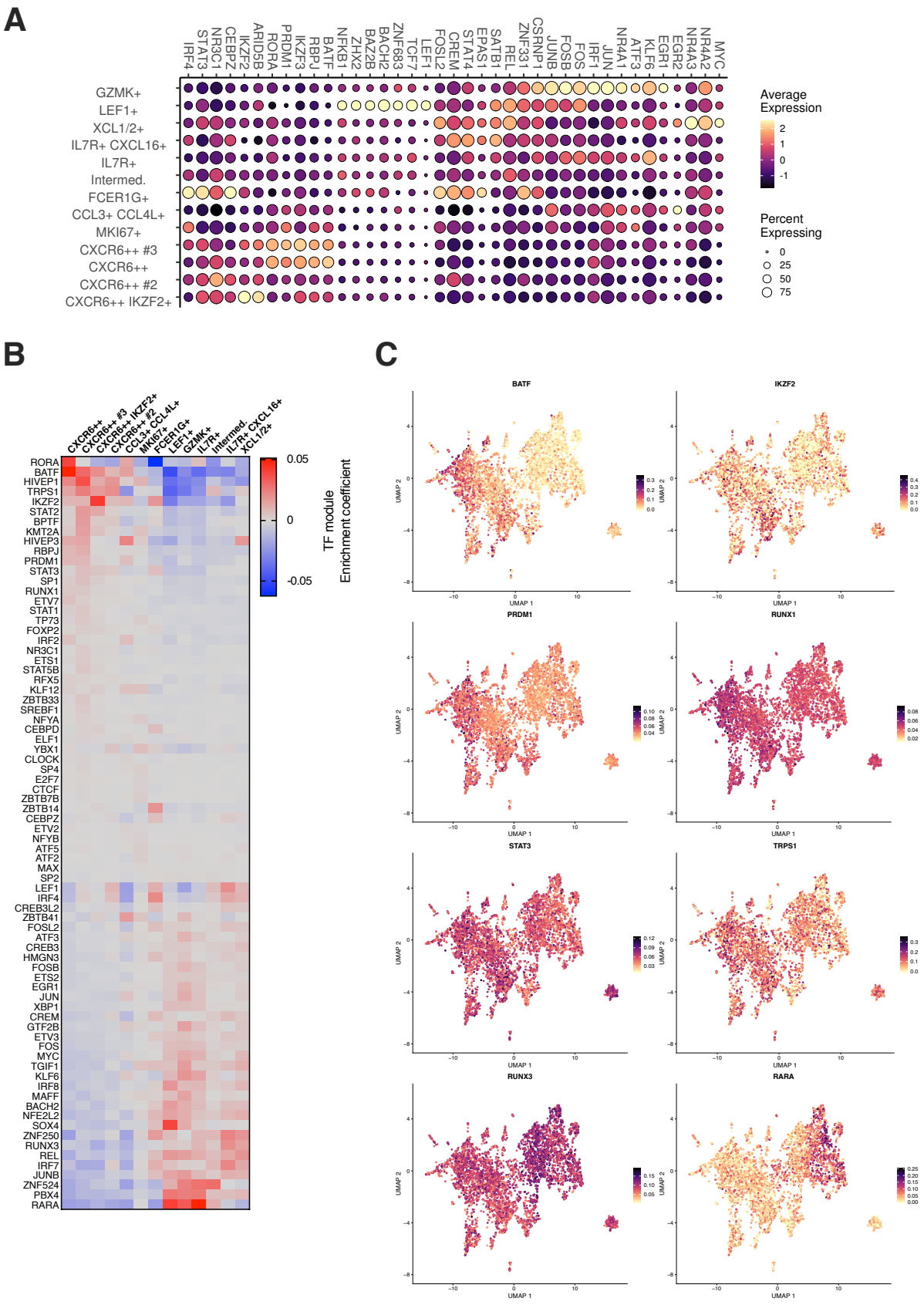

A
IRF4
STAT3
NR3C1
CEBPZ
IKZF2
ARID5B
RORA
PRDM1
IKZF3
RBPJ
BATF
NFKB1
ZHX2
BACH2
BAZ2B
ZNF683
TCF7
LEF1
FOSL2
CREM
STAT4
EPAS1
SATB1
REL
ZNF331
CSRNP1
JUNB
FOSB
FOS
IRF1
JUN
NR4A1
ATF3
KLF6
EGR1
EGR2
NR4A3
NR4A2
MYC
GZMK+
LEF1+
XCL1/2+
IL7R+ CXCL16+
IL7R+
Intermed.
FCER1G+
CCL3+ CCL4L+
MKI67+
CXCR6++ #3
CXCR6++
CXCR6++ #2
CXCR6++ IKZF2+
Average Expression
2
1
0
-1
Percent Expressing
0
25
50
75
B
CXCR6++
CXCR6++ #3
CXCR6++ IKZF2+
CXCR6++ #2
CCL3+ CCL4L+
MKI67+
FCER1G+
LEF1+
GZMK+
IL7R+
Intermed.
IL7R+ CXCL16+
XCL1/2+
RORA
BATF
HIVEP1
TRPS1
IKZF2
STAT2
BPTF
KMT2A
HIVEP3
RBPJ
PRDM1
STAT3
SP1
RUNX1
ETV7
STAT1
TP73
FOXP2
IRF2
NR3C1
ETS1
STAT5B
RFX5
KLF12
ZBTB33
SREBF1
NFYA
CEBPD
ELF1
YBX1
CLOCK
SP4
E2F7
CTCF
ZBTB7B
ZBTB14
CEBPZ
ETV2
NFYB
ATF5
ATF2
MAX
SP2
LEF1
IRF4
CREB3L2
ZBTB41
FOSL2
ATF3
CREB3
HMGN3
FOSB
ETS2
EGR1
JUN
XBP1
CREM
GTF2B
ETV3
FOS
MYC
TGIF1
KLF6
IRF8
MAFF
BACH2
NFE2L2
SOX4
ZNF250
RUNX3
REL
IRF7
JUNB
ZNF524
PBX4
RARA
0.05
0
-0.05
TF module Enrichment coefficient
C
BATF
IKZF2
PRDM1
RUNX1
STAT3
TRPS1
RUNX3
RARA
UMAP 1
UMAP 2

Figure 4-16: Transcriptional regulation of intestinal CD8+ and γδ T cells

(A) Bubble plot of transcription factors identified as cluster-specific markers. Bubble size indicates the proportion of cells in which the gene is present. Transcription factors identified from Lambert et al., 2018.

(B) Heatmap of expression of TF modules (gene sets proposed to be regulated by a particular TF) in intestinal CD8+ and γδ T cell clusters.

(C) UMAP plot of intestinal CD8+ and γδ T cells overlaid with the expression of TF modules of interest.

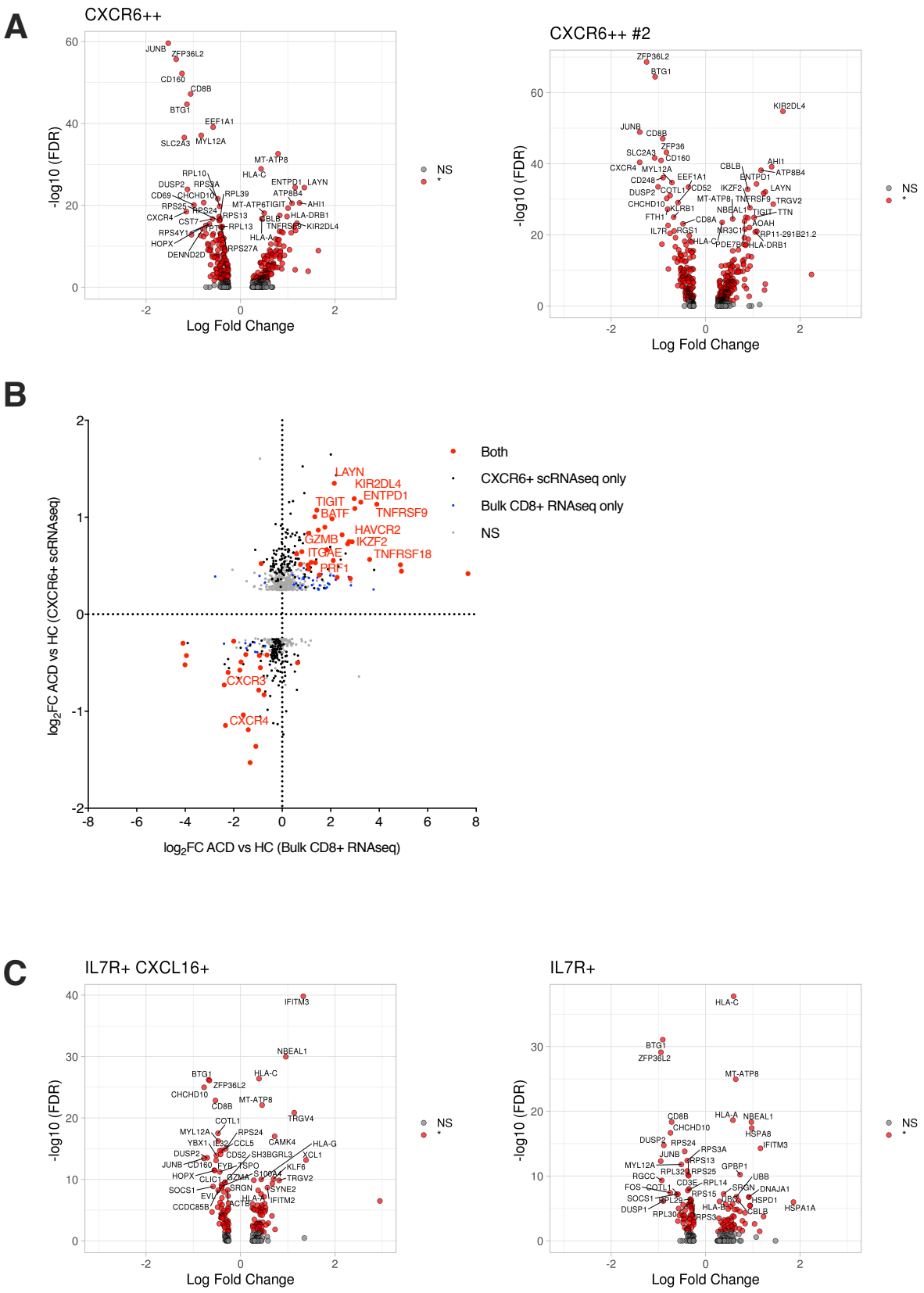

A
CXCR6++
-log10 (FDR)
Log Fold Change
NS
*
CXCR6++ #2
-log10 (FDR)
Log Fold Change
NS
*
B
log2FC ACD vs HC (CXCR6+ scRNAseq)
log2FC ACD vs HC (Bulk CD8+ RNAseq)
Both
CXCR6+ scRNAseq only
Bulk CD8+ RNAseq only
NS
LAYN
KIR2DL4
ENTPD1
TIGIT
BATF
TNFRSF9
HAVCR2
GZMB
IKZF2
ITGAE
TNFRSF18
PRF1
CXCR3
CXCR4
C
IL7R+ CXCL16+
-log10 (FDR)
Log Fold Change
NS
*
IL7R+
-log10 (FDR)
Log Fold Change
NS
*

Figure 4-17. Cluster-specific differential gene expression of CD8+ T cells between health and coeliac disease.

(A) Volcano plots of differentially expressed genes between health and active coeliac disease in CD8+ T cells in the CXCR6++ cluster (left) and CXCR6++ #2 cluster (right).

(B) Scatter plot of log2FC of genes between health and active coeliac disease in the bulk CD8+ T cell RNAseq dataset (x-axis) and in the CD8+ T cell CXCR6++ cluster from the scRNAseq dataset (y-axis). Genes differentially expressed in both datasets are marked in red.

(C) Volcano plots of differentially expressed genes between health and active coeliac disease in the CD8+ T cells in the IL7R+CXCL16+ cluster (left) and IL7R+ cluster (right).

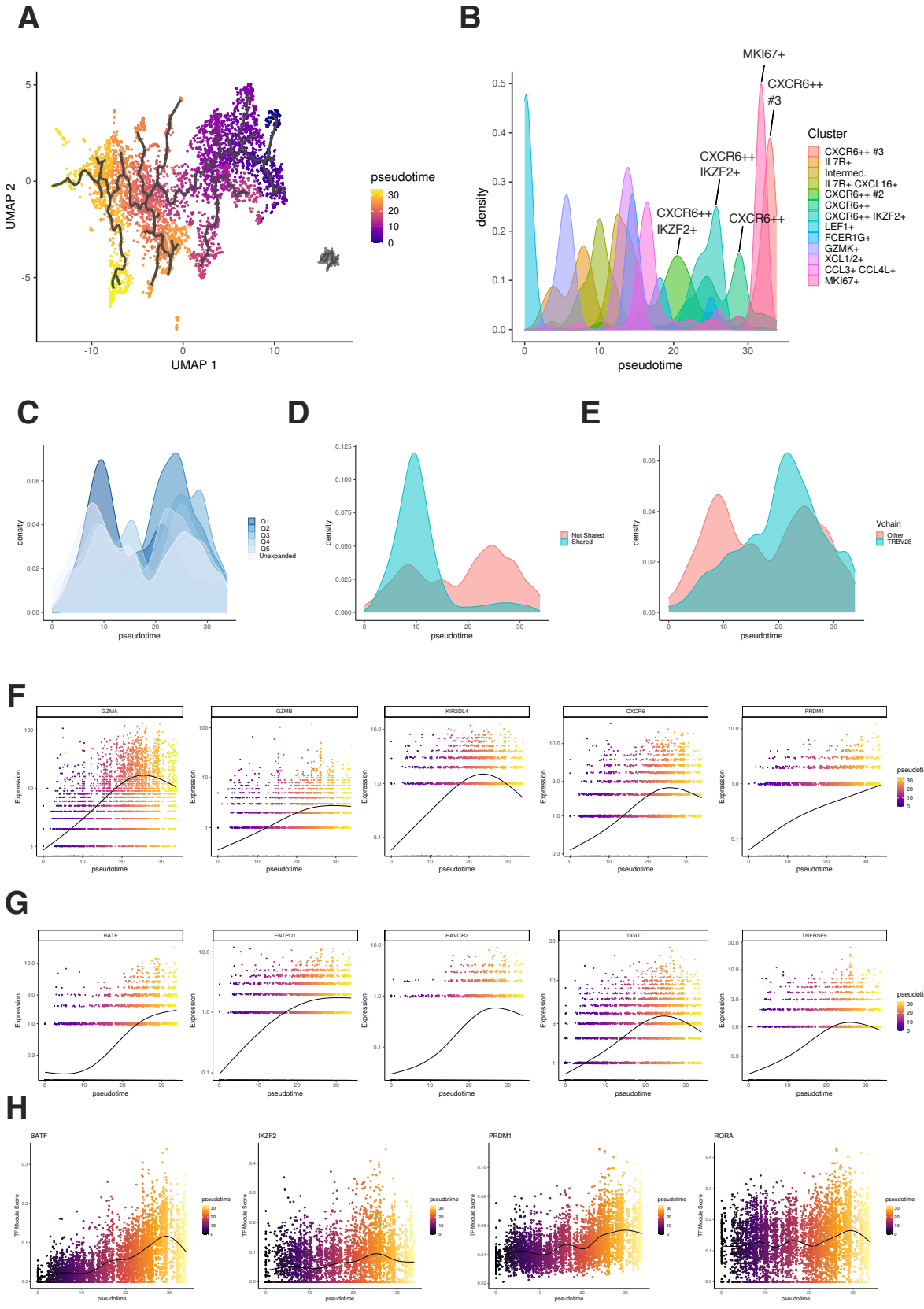

A
UMAP 2
UMAP 1
pseudotime
30
20
10
0
B
density
pseudotime
MKI67+
CXCR6++ #3
CXCR6++ IKZF2+
CXCR6++ IKZF2+
CXCR6++
Cluster
CXCR6++ #3
IL7R+
Intermed.
IL7R+ CXCL16+
CXCR6++ #2
CXCR6++
CXCR6++ IKZF2+
LEF1+
FCER1G+
GZMK+
XCL1/2+
CCL3+ CCL4L+
MKI67+
C
density
pseudotime
Q1
Q2
Q3
Q4
Q5
Unexpanded
D
density
pseudotime
Not Shared
Shared
E
density
pseudotime
Vchain
Other
TRBV28
F
GZMA
GZMB
KIR2DL4
CXCR6
PRDM1
Expression
pseudotime
pseudotime
G
BATF
ENTPD1
HAVCR2
TIGIT
TNFRSF9
Expression
pseudotime
pseudotime
H
BATF
IKZF2
PRDM1
RORA
TF Module Score
pseudotime
pseudotime

Figure 4-18. Pseudotime analysis reveals CXCR6+ clusters form a tissue-resident, cytotoxic, highly regulated population.

(A) Pseudotime trajectory of gene expression of Vδ2+ γδ+ T cells, coloured by pseudotime axis.

(B) Density of identified clusters along pseudotime.

(C) TCR clonality density of cells along pseudotime. Unexpanded, clonotype detected in 2 or fewer cells. Q1-5 represent quintiles of expanded clonotypes, with Q1 the top 20% most expanded clonotypes.

(D) Density distribution of TCR clones shared (blue) or not shared (red) with PBMC samples.

(E) Density distribution of TCR clones expressing TRBV28 (blue) or other V-genes (red).

(F) Single-cell gene expression along pseudotime of selected genes related to cytotoxicity and tissue residency.

(G) Single-cell gene expression along pseudotime of selected genes related to T cell regulation and co-inhibition.

(H) Single-cell expression along pseudotime of selected transcription factor modules which increase with pseudotime.

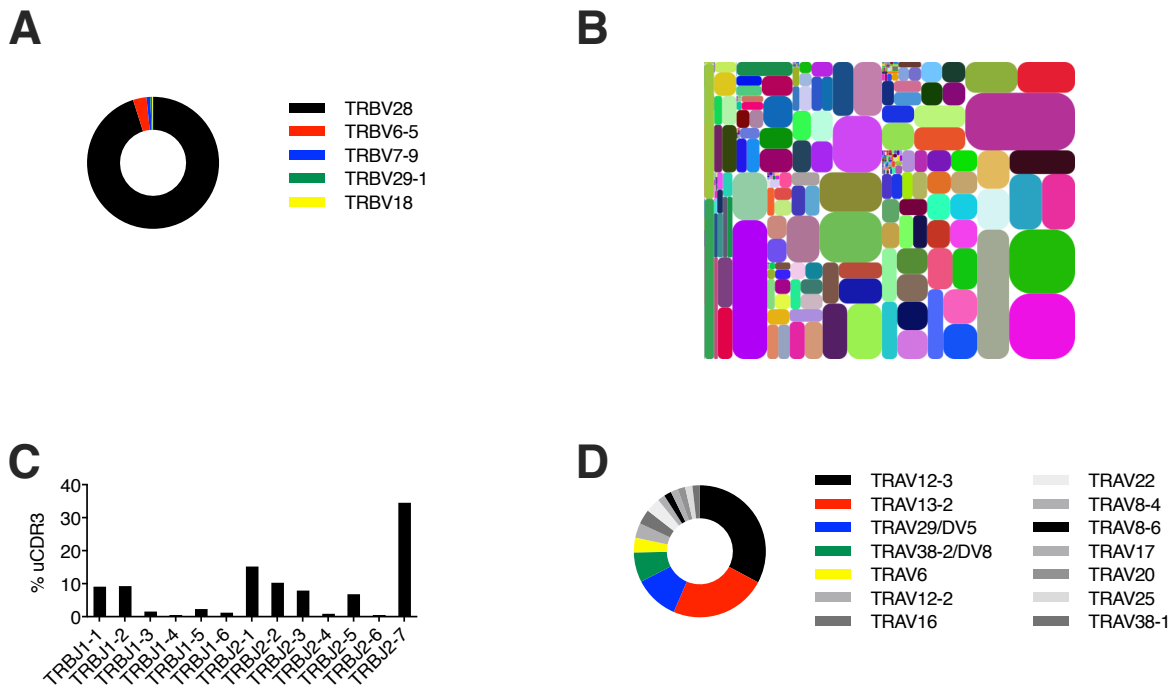


Figure 4-19. Validation of JOVI.3 (TRBV28) antibody using TCR sequencing.

(A) TRBV gene usage (proportion of unique CDR3 clonotypes) of sorted CD3+ JOVI.3+ T cells. TRBV genes not detected in the repertoire are not listed.

(B) Tree map of clonotypes of sorted CD3+ JOVI.3+ T cells. Each spot represents a unique clonotype, with the size of each spot proportional to the number of reads.

(C) TRBJ gene usage of TRBV28 clonotypes from sorted CD3+ JOVI.3+ T cells.

(D) TRAV gene usage (proportion of unique CDR3 clonotypes) of sorted CD3+ JOVI.3+ T cells. TRAV genes not detected in the repertoire are not listed.

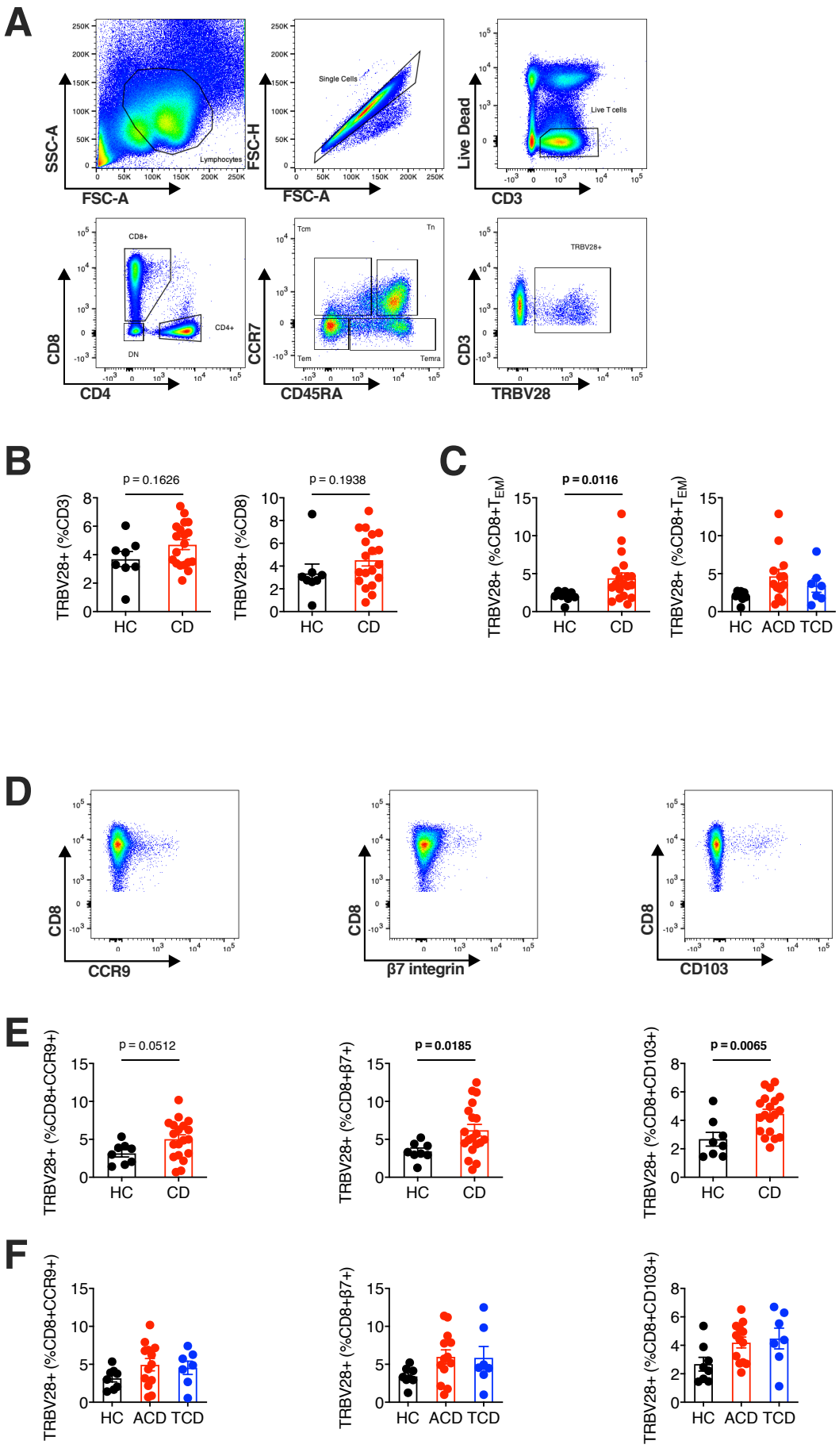

A
SSC-A
FSC-A
Lymphocytes
FSC-H
FSC-A
Single Cells
Live Dead
CD3
Live T cells
CD8
CD4
CD8+
CD4+
DN
CCR7
CD45RA
Tcm
Tn
Tem
Temra
CD3
TRBV28
TRBV28+
B
TRBV28+ (%CD3)
p = 0.1626
HC
CD
TRBV28+ (%CD8)
p = 0.1938
HC
CD
C
TRBV28+ (%CD8+TEM)
p = 0.0116
HC
CD
TRBV28+ (%CD8+TEM)
HC
ACD
TCD
D
CD8
CCR9
CD8
β7 integrin
CD8
CD103
E
TRBV28+ (%CD8+CCR9+)
p = 0.0512
HC
CD
TRBV28+ (%CD8+β7+)
p = 0.0185
HC
CD
TRBV28+ (%CD8+CD103+)
p = 0.0065
HC
CD
F
TRBV28+ (%CD8+CCR9+)
HC
ACD
TCD
TRBV28+ (%CD8+β7+)
HC
ACD
TCD
TRBV28+ (%CD8+CD103+)
HC
ACD
TCD

Figure 4-20. Surface expression of TRBV28 detected by flow cytometry is increased on effector memory and gut-homing CD8+ T cells in blood in coeliac disease.

(A) Representative flow cytometry plots and gating strategy.

(B) TRBV28 expression by total CD3+ T cells (left) and total CD8+ T cells (right) in peripheral blood in health and coeliac disease. Healthy controls, black; coeliac disease, red (n=30).

(C) TRBV28 expression by effector memory CD8+ T cells in peripheral blood, categorised by health and coeliac disease (left), and by health, active and treated coeliac disease (right) (n=30).

(D) Representative plots of staining for CCR9, β7-integrin, and CD103.

(E,F) TRBV28 expression by CCR9+ (left), β7-integrin+ (middle), and CD103+ (right) CD8+ T cells in peripheral blood, categorised by health and coeliac disease (E), and by health, active and treated coeliac disease (F) (n=30).

(B,C,E) Mann-Whitney test.

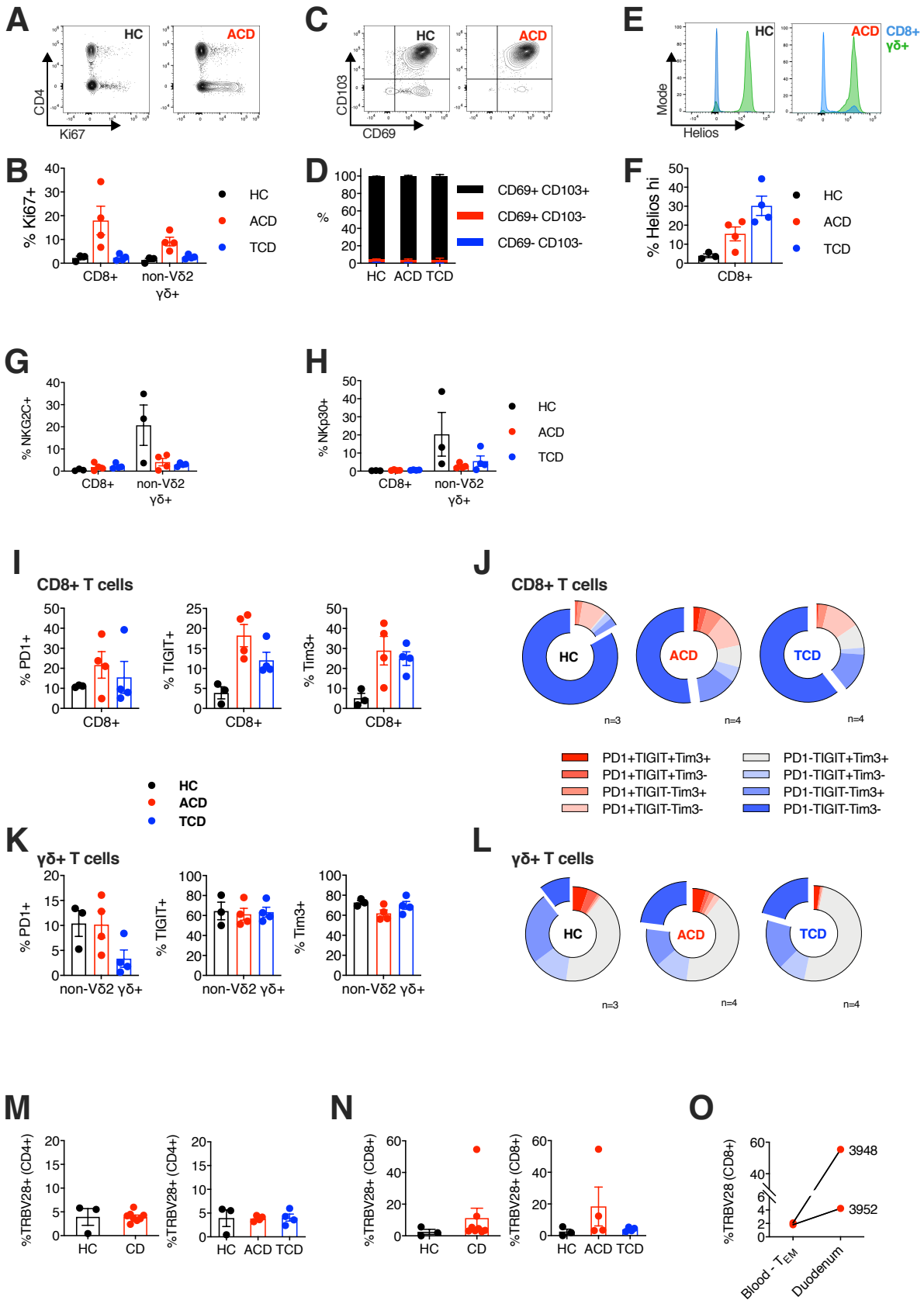

A
HC
ACD
CD4
Ki67
C
HC
ACD
CD103
CD69
E
HC
ACD
CD8+
γδ+
Mode
Helios
B
% Ki67+
HC
ACD
TCD
CD8+
non-Vδ2 γδ+
D
%
CD69+ CD103+
CD69+ CD103-
CD69- CD103-
HC ACD TCD
F
% Helios hi
HC
ACD
TCD
CD8+
G
% NKG2C+
CD8+
non-Vδ2 γδ+
H
% NKp30+
HC
ACD
TCD
CD8+
non-Vδ2 γδ+
I
CD8+ T cells
% PD1+
% TIGIT+
% Tim3+
CD8+
HC
ACD
TCD
J
CD8+ T cells
HC
ACD
TCD
n=3
n=4
n=4
PD1+TIGIT+Tim3+
PD1+TIGIT+Tim3-
PD1+TIGIT-Tim3+
PD1+TIGIT-Tim3-
PD1-TIGIT+Tim3+
PD1-TIGIT+Tim3-
PD1-TIGIT-Tim3+
PD1-TIGIT-Tim3-
K
γδ+ T cells
% PD1+
% TIGIT+
% Tim3+
non-Vδ2 γδ+
L
γδ+ T cells
HC
ACD
TCD
n=3
n=4
n=4
M
%TRBV28+ (CD4+)
HC
CD
HC ACD TCD
N
%TRBV28+ (CD8+)
HC
CD
HC ACD TCD
O
%TRBV28 (CD8+)
3948
3952
Blood - TEM
Duodenum

Figure 4-21. Phenotype and TRBV28 expression of intestinal T cells.

Representative plots (A) and grouped averages (B) of Ki-67 expression by intestinal CD8+ and non-Vδ2 γδ T cells, categorised by disease. Healthy control, black; active coeliac disease, red; treated coeliac disease, blue.

Representative plots (C) and stacked plots of grouped averages (D) of CD69 and CD103 co-expression by intestinal CD8+ T cells, categorised by disease.

(E) Representative plots of intranuclear Helios expression by intestinal CD8+ (blue) and non-Vδ2 γδ (green) T cells.

(F) Grouped averages of intranuclear Helios expression by intestinal CD8+ T cells, categorised by disease. Healthy control, black; active coeliac disease, red; treated coeliac disease, blue.

Grouped averages of NKG2C (G) and NKp30 (H) expression by intestinal CD8+ and non-Vδ2 γδ T cells, categorised by disease. Healthy control, black; active coeliac disease, red; treated coeliac disease, blue.

(I) Grouped averages of PD1, TIGIT, and Tim3 expression by intestinal CD8+ T cells, categorised by disease. Healthy control, black; active coeliac disease, red; treated coeliac disease, blue.

(J) Proportion of intestinal CD8+ T cells co-expressing the co-inhibitory molecules PD1, TIGIT, and Tim3, categorised by disease.

(K) Grouped averages of PD1, TIGIT, and Tim3 expression by intestinal γδ T cells, categorised by disease. Healthy control, black; active coeliac disease, red; treated coeliac disease, blue.

(L) Proportion of intestinal γδ T cells co-expressing the co-inhibitory molecules PD1, TIGIT, and Tim3, categorised by disease.

(M) TRBV28 expression by intestinal CD4+ T cells, categorised by health and coeliac disease (left), and by health, active and treated coeliac disease (right).

(N) TRBV28 expression by intestinal CD8+ T cells, categorised by health and coeliac disease (left), and by health, active and treated coeliac disease (right).

(O) TRBV28 expression by synchronously collected intestinal CD8+ T cells and peripheral CD8+ T_{EM} cells from two individuals with coeliac disease. Black lines connect samples collected from the same individual.

Chapter 5: Investigating peripheral γδ T cell populations in health and coeliac disease

5.1 Introduction

Overview

The findings from chapter 4, which had examined the changes in the TCR repertoire and transcriptional profile of mucosal T cells in coeliac disease, had demonstrated the profound changes in the γδ T cell population associated with CD. γδ T cells are increased in the mucosa in active CD, and this persists despite treatment with a gluten-free diet. The TCR repertoire of the mucosal γδ T cell compartment is permanently altered by coeliac disease, and there are changes in their transcriptional profile during active inflammation.

One striking finding is that these changes were restricted to non-Vδ2 γδ T cells. Both Vδ1+ and Vδ1/2- γδ T cells were increased in coeliac disease, and demonstrated near-identical transcriptional changes in the mucosa in response to active coeliac disease. In contrast, the Vδ2+ T cell population does not feature in the CD immune response. This difference between γδ T cell subsets in coeliac disease led me to explore in more detail the phenotypic differences of γδ T cell subsets in a wider context.

Vδ2+ and non-Vδ2 γδ T cells

γδ T cells, unconventional adaptive lymphocytes conserved since the origins of vertebrate evolution(Hirano et al., 2013; Rast et al., 1997), recognise non-peptide antigens and are not restricted by major histocompatibility complex (MHC) molecules(Godfrey et al., 2015). The role of this multifunctional population in human disease is increasingly recognised, including in infection

(CMV(Kallemeijn et al., 2017; Khairallah et al., 2017), HIV(Juno and Kent, 2020), malaria(Dantzler and Jagannathan, 2018; Deroost and Langhorne, 2018; Howard et al., 2018; Hviid et al., 2019), tuberculosis(Y. Li et al., 2019; Zhang et al., 2006), and influenza(Qin et al., 2012; Sant et al., 2019; Xue et al., 2017)), autoimmunity (IBD(Catalan-Serra et al., 2017; N. E. McCarthy and Eberl, 2018; Tyler et al., 2017), rheumatological disease (C. T. Nguyen et al., 2019; Venken et al., 2018)), tumour responses and cancer cell-based therapeutics(Fisher and J. Anderson, 2018; Gentles et al., 2015; D. Wu et al., 2017).

Due to their phenotypic and functional features that cross the boundary between adaptive and innate immunity, they are frequently classified together with the archetypal innate-like T cells: the mucosal-associated invariant T (MAIT) cells and the invariant natural-killer T (iNKT) cells(Godfrey et al., 2015). However, it is now recognised that there are two broad types of γδ T cells in humans, Vδ2Vγ9+ (hereafter Vδ2+) and non-Vδ2Vγ9 T cells (hereafter non-Vδ2, although they include a small population of Vδ2+Vγ9- cells(Davey et al., 2018b)).

Vδ2+ T cells express a semi-invariant Vδ2Vγ9 TCR, respond to small molecule phosphoantigens (pAgs) of microbial (4-hydroxy- 3-methyl-but-2-enyl pyrophosphate; HMBPP) or endogenous (isopentyl pyrophosphate; IPP) origin in a butyrophilin-like molecule-dependent manner(Karunakaran et al., 2020; Vantourout et al., 2018), and share phenotypic and functional features with innate-like T cells(Provine et al., 2018). Non-Vδ2 T cells display greater TCR diversity, respond to heterogeneous TCR ligands(Marlin et al., 2017; Willcox et al., 2012), and possess many features of conventional adaptive T cells(Davey et al., 2018a; 2017).

Vδ2+ T cells are often compared with the innate-like MAIT cells due to shared phenotypic and functional characteristics, however our understanding of the comparative function of these cell populations is incomplete. MAIT cells respond to combinatorial cytokine expression with robust IFN-

γ expression(Ussher et al., 2013), with implications for antiviral immunity (van Wilgenburg et al., 2016) and vaccine responses (Provine et al., 2019). Vδ2+ γδ T cells can respond in a similar manner(Provine et al., 2018; Tsai et al., 2015; Wragg et al., 2020), however the heterogeneity of the cytokine response by Vδ2+ γδ T cells has not been explored at the single-cell level. Moreover, the transcriptional responses of MAIT cells to cytokine and TCR stimulation have recently been delineated(Lamichhane et al., 2019; Leng et al., 2019), which includes distinct effector functions including tissue repair, but it is unclear if Vδ2+ T cells show similar responses.

Heterogeneity in human γδ T cells

In order to understand the role of γδ T cells in human disease, and how their responses could be modified for disease treatment, it is important to understand of the development and heterogeneity of these unconventional T cells. In particular, understanding of γδ T cell heterogeneity has implications for cell-based cancer immunotherapy using γδ T cells, which have proved of limited efficacy to date(Hoeres et al., 2018; Pauza et al., 2018).

Vδ2+ γδ T cells exhibit pleiotropic functions, and multiple systems for classifying putative subsets of Vδ2+ T cells have been proposed. Several classification systems use variations on memory markers that are used for the identification of conventional T cell memory subsets, including CD45RA and CD27 (4 subsets) (Dieli et al., 2003), and CD27, CD28, CD45RA, CD16 (16 possible combinations with 8 commonly found in study subjects) (Wistuba-Hamprecht et al., 2015)). However, this assumes some degree of analogous progression of memory development in γδ T cells as in conventional T cells.

This assumption is challenged by a number of characteristics of Vδ2+ T cells that do not follow this expected progression. First, many 'T_{EMRA}' Vδ2+ T cells expressing CD45RA maintain considerable proliferative capacity, and the frequency of these subsets does not change with age(Wistuba-

Hamprecht et al., 2015; W. Xu et al., 2019). Second, Vδ2+ T cells demonstrate a degree of resistance to senescence, for while CD57+ Vδ2 T cells do show diminished proliferative capacity, the proportion of CD57+ Vδ2 T cells does not increase with age. Third, Vδ2+ memory subsets do not show the expected changes in telomere shortening and DNA damage repair responses which are seen in CD8+ and non-Vδ2 γδ T cell populations(W. Xu et al., 2019).

Other Vδ2+ T cell classification systems have used markers tied to specific functions, including CD16(Angelini et al., 2004), CCR6(Caccamo et al., 2011), CD26/CD94(Wragg et al., 2020), or combinations thereof (CCR7, CD27, CD28, CD16) (Ryan et al., 2016).

Similarly, non-Vδ2 T cells can be divided into CD27hi naive and CD27lo/neg memory populations based on CD27/CD45RA expression, however transcriptional heterogeneity within and between these two broad populations remains undefined(Davey et al., 2017; Hunter et al., 2018).

Despite the use of these multiple classification systems, the transcriptional and functional heterogeneity of γδ T cells, which any subset classification seeks to represent, remains unclear. While transcriptional differences of four bulk-sorted Vδ2+ T cell populations (based on CCR7, CD27, CD28, and CD16 expression) have been defined, how these relate to single-cell transcriptional heterogeneity agnostic to pre-existing classifications is unclear.

Single-cell RNA sequencing (scRNAseq) is a powerful tool for identification of transcriptionally distinct states or subsets within cell populations. There are few datasets that have focused on transcriptional heterogeneity in γδ T cells. Pizzolatto and colleagues examined γδ T cell single-cell transcriptomes from PBMCs, tumour-infiltrating lymphocytes, and sorted populations. They described key transcriptional differences between non-Vδ2 and Vδ2+ subsets, and examined potential maturation trajectories using pseudo temporal reconstruction, however single cell

transcriptional heterogeneity within Vδ2+ and non-Vδ2 T cell population was not examined(Pizzolato et al., 2019).

Bulk transcriptional profiling of innate-like and conventional T cell populations demonstrated a gradient of an innate-like T cell transcriptional profile, with Vδ2 T cells enriched for this innate-like signature, similar to iNKT cells and MAIT cells(Gutierrez-Arcelus et al., 2019). However, the limited single-cell RNAseq of innate-like T cells demonstrated Vδ2+ T cells formed clusters with both MAIT and iNKT cells, and with a population of CD8+ and Vδ1+ T cells, suggesting considerable transcriptional heterogeneity within the Vδ2+ T cell population.

In sum, the single cell transcriptional, phenotypic, and functional heterogeneity of γδ T cells is incompletely understood. It remains unclear how the currently suggested surface marker identifiers of γδ T cell subsets align with this transcriptional heterogeneity, and whether superior markers to define subsets exist.

Key questions

- Do the surface marker phenotypes of Vδ2+ and non-Vδ2 γδ T cells align to those of known conventional T cell memory subsets?
- What is the transcriptional heterogeneity of circulating γδ T cells, and how does it compare to conventional T cell counterparts?
- What is the functional heterogeneity of circulating γδ T cells?
- What are the shared and distinct transcriptional and functional features of innate-like Vδ2+ T cells and MAIT cells?

First, I examined surface marker expression on Vδ2+ and non-Vδ2 γδ T cells, and their subsets identified by CD27 and CD45RA expression, in comparison to conventional CD8+ T cells. Then, to

establish a more comprehensive 'atlas' of human γδ T cells, I examined the transcriptional and functional heterogeneity of γδ T cells using two single-cell approaches, including in the steady state and in response to stimulation. Finally, using putative markers of γδ T cell subsets identified from sequencing data, I confirmed phenotypic and functional findings using flow cytometry and *ex vivo* stimulation.

5.2 Phenotypic heterogeneity of peripheral γδ T cells

Rationale for experimental design

Non-Vδ2 γδ T cells have recently been shown to possess characteristics similar to adaptive conventional CD8+ T cells, with a naive CD27hi population, and a effector memory CD27lo/neg population(Davey et al., 2017; Hunter et al., 2018). However, a systematic examination of their surface molecule expression and phenotype has not been performed. I hypothesised that surface marker expression would be similar between the naive and memory non-Vδ2 and CD8+ T cell populations. I further hypothesised that the memory subsets of Vδ2+ T cells would show similarities in surface marker expression to their conventional T cell counterparts.

To test this hypothesis, I examined the surface marker expression on PBMC-derived T cell populations and memory subsets from four blood donors. This was performed using a 332-plex PE-conjugated antibody flow cytometry assay, with cells from each donor barcoded using different concentrations of CellTrace Violet^{TM} (CTV) cell dye, allowing sample multiplexing in each well (Fig. 5-1A). Cells were gated on singlet, live lymphocytes, before identification of T cells from the four donors using CD3 and CTV. Vδ2+, Vδ1+ and Vδ1-2- γδ T cells are then identified, as well as conventional CD8+ T cells (Fig. 5-1B). Memory subsets were determined by CD27 and CD45RA

expression, in line with previously published gating strategies (Fig. 5-1C) (Davey et al., 2017; Dieli et al., 2003).

5.2.1 Technical considerations

Cell concentration from each donor was predicted to give greater than 1000 naive and memory CD8+ T cells per sample per well, and greater than 200 Vδ2+ and non-Vδ2 T cells per sample per well. Naive CD8+ T cell and memory CD8+ T cell samples contained adequate cell numbers for complete analysis, with a median of 2760 cells (range 456-12050) and 5575 cells (range 335-8017) respectively (Fig. 5-1D,E). Most γδ T cell samples also contained adequate cell numbers, with a median of 620 Vδ2+ T cells (range 78-2129) and 703 non-Vδ2 T cells (range 52-1430). Low γδ T cell numbers (less than 200) were confined to a single donor. I elected to include this sample in the analysis of non-Vδ2 memory subsets and total Vδ2+ T cells, as expression patterns for particular cell types were broadly congruent with the other 3 samples. Cell numbers from this donor within Vδ2+ memory subsets were very small(<20 cells/subset), and were therefore removed.

The panel design, limited by the spectral effects of CTV cell dye and the intention to minimise spectral interference with PE (on which markers of interest were conjugated), resulted in data spread between PE and CD27-BV605. As such, for PE-conjugated markers which were particularly bright, the memory population gates were less clear-cut. However, gating was possible, and markers with known expression patterns on naive and memory CD8+ T cell populations demonstrated the expected profile.

Fluorescence minus one (FMO) controls were included on each plate of the Legendscreen kit and were used to draw the %PE positive gate. Isotype controls were included for all antibodies in the Legendscreen panel. Two isotype controls, Rat IgM and Mouse IgG3, showed staining to

conventional T cells and both conventional and γδ T cells respectively. However, the respective antibodies using these formats (SSEA-3 Rat IgM, and SSEA-4, CD167a, and CD255 Ms IgG3) showed minimal expression on all subsets as expected, indicating that the non-specific staining of the isotype control was not leading to staining artefact, and so the markers were not removed from the analysis. The pan-γδ TCR clone 11F2 (Miltenyi Biotec), used in the panel to identify non-Vδ2 γδ T cells, is a recombinant human IgG1 antibody, and can cross-react with antibodies targeting the BCR or Ig light chain. All Ig chain antibodies were removed. Antibodies targeting specific TCR V genes were used to check appropriate staining of cell populations, however they were not used in further analyses.

Vδ1+ and Vδ1-/2- γδ T cells share a surface marker expression phenotype

Non-Vδ2 T cells are formed of Vδ1+ and Vδ1-/2- populations (predominantly expressing a Vδ3 TCR). Vδ1+ T cells are more common than Vδ1-/2- T cells in the blood, and have been more extensively studied in respect to their adaptive phenotype and biology. I examined the surface protein expression between Vδ1+ and Vδ1-/2- T cells in the sample to examine the phenotypic similarity these populations.

Hierarchical clustering analysis of surface marker expression (% positive cells) showed that these two populations clustered together, predominantly by donor, and separately from Vδ2+ and conventional CD8+ T cells(Supplemental Fig. 5-1A). Vδ1+ and Vδ1-/2- T cell surface marker expression (% positive) was highly correlated(R^2=0.98, p<0.0001), despite the stochasticity that would be expected from the low cell number in some samples(Supplemental Fig. 5-1B). The strength of correlation was considerably higher than that seen between Vδ2- T cells and either Vδ2+ T cells or conventional CD8+ subsets (Supplemental Fig. 5-1C) This indicates that circulating Vδ1+ and Vδ1-2- T cells possess highly similar surface molecule expression, consistent with them sharing phenotypic and biological characteristics. Therefore, for the rest of the analysis, Vδ1+ and Vδ1-2- γδ T cells were grouped as non-Vδ2 T cells.

CD27hi and CD27lo/neg non-Vδ2 γδ T cells possess naive and effector phenotypes respectively

I compared the surface protein expression of CD27hi and CD27lo/neg non-Vδ2- T cells to naive and memory conventional T cells using hierarchical clustering and PCA analysis. Markers with near-ubiquitous expression (>95% positive cells on all samples) or minimal expression (<2% positive cells on all samples) were removed before clustering, leaving 167 surface markers for analysis. Naive CD8+ T cells clustered with CD27hi Vδ2- γδ T cells, with memory CD8+ T cells and CD27lo/neg Vδ2- γδ T cells clustering together (Fig. 5-2A-B).

I then examined the expression of a curated list of T cell differentiation markers(Mahnke et al., 2013; van den Broek et al., 2018). Some similarities of expression were seen, with CCR7, CD62L, and CD28 expression highest on naive CD8+ and CD27hi Vδ2- T cells, and CD122 (IL-2/IL-15 receptor), CD57 (a senescence marker), and CD161 showing low expression on those populations(Fig. 5-2C). However, several differentiation markers did not show this congruence. CCR7 showed ubiquitous expression on naive CD8+ T cells, but was not expressed on approximately a quarter of CD27hi non-Vδ2 T cells. CD31, expressed by CD4+ recent thymic emigrants and naive CD8+ T cells, showed similar expression on CD27hi and CD27lo/neg populations(van den Broek et al., 2018). CD95 (the Fas receptor) was not expressed on naive CD8+ cells as expected, but showed high expression on both CD27hi and CD27lo/neg non-Vδ2 T cells. Similarly, the CD27hi non-Vδ2 T cells expressed similar levels of PD-1 to their CD27lo/neg counterparts. This expression pattern is consistent with the hypothesis CD27hi and CD27lo/neg populations are analogous to naive and memory conventional CD8+ T cell populations. However, the differences suggest that the CD27hi non-Vδ2 population is heterogeneous, and may consist of multiple subsets.

I compared the CD27hi and CD27lo/neg Vδ2- T cells to their conventional naive and memory CD8+ T cell counterparts. Non-Vδ2 T cells differed from their conventional counterparts in their expression

of chemokine receptors and tissue homing molecules, expression of regulators of immune response, complement and cytokine receptors, molecules associated with innate-like T cell function, and natural killer (NK) cell function (Fig. 5-2D).

Non-Vδ2 T cells expressed lower levels of the chemokine receptor CXCR1, while CD27lo/neg non-Vδ2- T cells almost universally expressed the fractalkine receptor CX3CR1 and ICAM-1 (CD54). B- and T-lymphocyte attenuator (BTLA) and CD150 (SLAM) expression was lower on CD27lo/neg non-Vδ2 T cells than CD8+ counterparts, while conversely, CD244 (2B4, a SLAM family immunoregulatory receptor) and PD-1 were expressed on a higher proportion of CD27hi non-Vδ2 T cells than on naive CD8+ T cells. CD38, the ectoenzyme that is expressed at high levels on naive conventional T cells (and is also a marker of activation on memory populations), was expressed at low levels on CD27hi Vδ2- T cells, similar to memory populations. CD35 (complement receptor type 1) and CD55 (decay accelerating factor), both complement receptors with roles in T cell regulation, were expressed on a lower proportion of CD27lo/neg Vδ2- T cells compared to conventional CD8+ memory T cells.

CD27lo/neg non-Vδ2 T cells expressed low levels of CD127 (IL-7Rα) compared to conventional memory CD8+ T cells. The low CD127 expression on CD27lo/neg non-Vδ2 T cells was confirmed in a second cohort (Supplementary Fig. 5-2A), and was not associated with a regulatory T cell phenotype, determined by CD25 or FoxP3 expression (Supplementary Fig. 5-2B,C).

CD243 (multidrug resistance protein 1, MDR1) and CD172g (signal regulatory protein gamma, SIRPG) showed differential expression between conventional and non-Vδ2 T cells, in a manner suggestive of a more innate-like profile based on previous transcriptomic studies(Fergusson et al., 2014). In keeping with some degree of innate-like function, a proportion of CD27lo/neg non-Vδ2 T cells expressed surface molecules typically shared with NK cells, including CD56, and the cytotoxicity receptors NKp80, NKp44, NKp46, CD94, and natural killer cell Ig-like receptor NKAT2

(KIR2DL2/L3)(Fig. 5-2D). The co-expression of CD56, NKAT2, and NKp80 by CD27lo/neg non-Vδ2 T cells was validated in a second cohort(Supplementary Fig. 5-2D-E).

In summary, CD27hi and CD27lo/neg non-Vδ2 T cells possess broadly analogous phenotypes to conventional naive and memory CD8+ T cell populations respectively, albeit with potential heterogeneity in the CD27hi non-Vδ2 population. In addition, non-Vδ2 T cells express a different pattern of tissue-homing molecules and regulators of immune function, which may indicate different processes are involved in tissue localisation and triggering of the immune response. Finally, while recent evidence has provided evidence of the adaptive properties of non-Vδ2 T cells, the striking expression of a number of NK cell cytotoxicity receptors indicates that these cells may have the capacity for innate-like cytotoxic functionality.

Putative subsets of Vδ2+ T cells defined by CD27/CD45RA exhibit effector-memory phenotypes

CD27 and CD45RA also define putative memory subsets of Vδ2+ T cells. These subsets have been correlated with differences in proliferative capacity, cytokine production, and cytotoxicity, as described earlier. I hypothesised that the CD27+CD45RA+ Vδ2+ T cells would cluster with the naive non-Vδ2 and conventional CD8+ T cells, while the effector populations would demonstrate differences to their non-Vδ2 and conventional CD8+ T cell counterparts. Hierarchical clustering and principle component analysis surface marker expression on Vδ2+ and conventional T cell subsets was performed as before.

While naive CD8+ T cells and CD27hi non-Vδ2 T cells clustered together, as seen previously, the CD27+CD45RA+ Vδ2+ T cell population did not cluster with these naive populations, instead clustering with CD27-CD45RA+ Vδ2+ T cells and the CD27lo/neg effector non-Vδ2 T cells (Fig. 5-3A). The CD27-CD45RA- and CD27+ CD45RA- Vδ2+ T cell subsets clustered closer to the conventional memory CD8+ T cells.

There were differences in surface marker expression between Vδ2+ subsets, with CD27+CD45RA- and CD27-CD45RA+ populations showing distinct phenotypes. CD27-CD45RA+ populations expressed higher levels of CX3CR1, CD16, CD8a, CD11b, and CD56, while CD27+CD45RA- populations expressed higher levels of CD26, CD28, CCR6, and CD161(Fig. 5-3B), consistent with previous work(Ryan et al., 2016).

In summary, the CD27+CD45RA+ population of Vδ2+ T cells did not possess a naive-like pattern of surface marker expression, challenging the traditional naive and memory descriptors of Vδ2+ T cell subsets based on CD27 and CD45RA expression. There were differences in surface markers associated with effector function between the Vδ2+ T cell subsets, with the largest differences between the CD27+CD45RA- and CD27-CD45RA+ populations. Overall, the use of CD27 and CD45RA does not adequately describe the phenotypic heterogeneity of Vδ2+ T cells.

Interim conclusion

In conclusion, Vδ1+ and Vδ1-/2- γδ T cells, which constitute the non-Vδ2 T cell population, show near-identical surface marker phenotype. CD27hi and CD27lo/neg non-Vδ2 T cells form naive and memory populations with similar phenotype to their conventional CD8+ T cell counterparts, albeit with features suggestive of innate-like functionality. In contrast, CD27+CD45RA+ Vδ2+ T cells, often referred to as naive in the literature, do not share the phenotypic features of naive non-Vδ2 and CD8+ T cells. These findings provide an argument for more detailed analysis of transcriptional and functional heterogeneity of γδ T cells, agnostic of pre-existing markers.

The analysis of individual markers from this experiment is necessarily hypothesis-generating, given the large number of surface markers examined, and the low number of study subjects. This is particularly relevant for the analysis of Vδ2+ T cell subsets, as low cell numbers in one donor

required its removal from the analysis. Due to the limitations of staining in these pre-arranged plates, all staining was performed under identical conditions. This is particularly relevant for some chemokine and cytokine receptors, which cycle to the cell membrane and are best stained at higher temperatures, rather than at 4^{o}C. In particular, negative or low staining results cannot be relied on. Similarly, the analysis is limited to particular antibodies and clones available, some of which may not be the ideal reagent for that specific target antigen.

This experiment raised several questions, which determined the direction for my further work in this area:

1. What is the transcriptional variation at the single cell level of peripheral γδ T cells?
2. Can this identify an improved method of identification of Vδ2+ T cell subsets?
3. What are the differences between naive and effector conventional CD8+ T cells and their adaptive, yet unconventional, non-Vδ2- T cell counterparts?
4. Do the γδ T cell populations share similar innate-like functionality to MAIT cells?

To address these questions, I performed single-cell RNA sequencing of circulating γδ and CD8+ T cells.

5.3 Single cell RNA sequencing of human circulating γδ T cells and conventional CD8+ T cells

Description of scRNAseq dataset

Single-cell RNA sequencing (scRNAseq) and TCR sequencing (scTCRseq) were performed on sorted circulating γδ and CD8+ T cells from six paediatric subjects, three with CD(Experiment 1 - Fig. 5-4A). Older adults were not used as prior infection exposure, particularly to CMV, radically narrows the γδ T cell repertoire and alters cell phenotype(Davey et al., 1AD; Ravens et al., 2017). After sequencing and quality filtering, 23,717 cells were analysed. As samples were processed and sequenced at different times, batch correction was required to align the data. After batch correction, clusters aligned by donor, and disease (Supp. Fig. 5-3A).

Unexpectedly, CD8+ and γδ T cells clustered together, with most clusters containing both cell types. Therefore CD8+ and γδ T cells from pooled samples were identified using a random forest model (see methods), based on features identified from one sample where CD8+ and γδ populations were captured separately (Supplementary Fig. 5-3B), with excellent performance (AUROC 0.998 on withheld cells, Supplementary Fig. 5-3C) and expected expression of the population-defining genes CD8A, CD8B, and TRDC (Supplementary Fig. 5-3D).

Fifteen clusters of peripheral CD8+ and γδ T cells were identified (Fig. 5-4B,C). Cluster-defining genes and transcription factors, along with descriptions of each cluster, are listed in Table 5-2. CD8+ and γδ+ T cells were found in most clusters, in varying proportions(Fig. 5-4D, Supplementary Fig. 5-3F). *TRDV2*-expressing γδ T cells were the most common subset of γδ T cell, consistent with published data, and clustered separately from *TRDV1* and *TRDV3*-expressing populations, as expected given their known distinct transcriptional profiles(Fig. 5-4E) (Davey et al., 2017; Gutierrez-Arcelus et al., 2019). I will first discuss the Vδ2+ containing clusters, then those containing non-Vδ2 T cells.

Table 5-1. Cluster annotations, with cluster-defining genes and transcription factors.

Name	Cell types	Genes of note	TFs and TF modules	Comments
GZMK+ Vδ2/MAITs	Vδ2/CD8	*KLRB1(hi), DPP4(hi), GZMK, IL23R, CCR6, CXCR6, AQP3, NCR3, SLC4A10, FURIN*	*ZBTB16, RORC, MYC, CEBPD, RARG, EIF3E, IKZF2*	TRDV2-expressing cells, plus CD8+ cells (CD8A+) expressing typical MAIT cell TCR sequences. Innate-like population with characteristic transcriptional features of MAIT cells.
ADGRG1+ CX3CR1+ Vδ2	Mainly Vδ2	*ADGRG1, KLRB1, GZMH, GZMA, GZMB, GZMM, CX3CR1, FGFBP2, FCGR3A*	*ZNF683, ZEB2, TBX21, NFATC2, STAT1, STAT4, ZBTB16(int)*	Large population of TRDV2-expressing cells with a cytotoxic transcriptional profile. Expresses *FCGR3A* (CD16) and *CX3CR1*, consistent with previously identified Vδ2 phenotypes.
ADGRG1+ HLA-DR+	Vδ2/CD8	*ADGRG1, KLRB1, GZMH, GZMM, HLA-DRA, HLA-DRB1*	*ZNF683, ZEB2, TBX21, NFATC2, STAT1, STAT4, ZBTB16(int)*	Small population of TRDV2-expressing and CD8+ cells with a cytotoxic transcriptional profile. High expression of class I MHC molecules.
Transitional Vδ2	Mainly Vδ2	*KLRB1, GZMK, GZMM*	*JUN, FOS, STAT3, ZBTB16(int)*	TRDV2-expressing cells with an intermediate phenotype to GZMK+ and ADGRG1+ populations.
CTLA4+ Vδ2	Mainly Vδ2	*KLRB1, GZMK, GZMM, CTLA4, IL2RA*	*JUN, FOS, ZBTB16(int)*	Small population of TRDV2-expressing cells highly related to Transitional population, with expression of *CTLA4*, and *IL2RA*.
LEF1+ Vδ2	Mainly Vδ2	*CCR7(int), KLRB1(int), GZMM/GZMK(lo)*	*LEF1(int),*	TRDV2-expressing cells expressing intermediate levels of genes associated with naïve and memory cells. May represent a central memory phenotype.
Activated	Vδ2/CD8	*KLRB1, GZMK, GZMM, IFNG, TNF*		Small population of activated cells expressing *TNF* and *IFNG*.
Cycling	γδ/CD8	*MKI67*		Mixed population of actively dividing cells.
LEF1 #1	Mainly CD8	*CCR7, SELL*	*LEF1, TCF7, MYC, EIF3E*	Naïve, predominantly CD8+ T cell population
LEF1 #2	Mainly CD8	*CCR7, SELL*	*LEF1, TCF7, MYC, EIF3E*	Naïve, predominantly CD8+ T cell population
LEF1 #3	Mainly CD8	*CCR7, SELL*	*LEF1, TCF7, MYC, EIF3E*	Naïve, predominantly CD8+ T cell population
LEF1 Vδ1+	Mainly non-Vδ2	*CCR7, SELL, IFNAR1*	*LEF1, TCF7, MYC, EIF3E*	Naïve, predominantly non-Vδ2 T cell population
LEF1 Vδ1+ SOX4+	Mainly non-Vδ2	*CCR7, SELL, IFNAR1, CCR9, TRDV1*	*LEF1, TCF7, MYC, EIF3E, SOX4*	Naïve, predominantly non-Vδ2 T cell population, expressing the TF *SOX4*, and gut-homing chemokine receptor *CCR9*
CXCR3+ Vδ1+	γδ/CD8	*NCR3, KLRC3, CXCR3, IFITM1, IFNAR1*	*ZNF683*	Predominantly non-Vδ2 T cell population with memory phenotype and expression of NK-associated molecules.
ADGRG1+ CD8+/Vδ1+	γδ/CD8	*GZMH, GZMM, GZMB, ADGRG1, NCR1, TIGIT, TNFRSF9, KIR2DL1, KIR2DL3, CX3CR1, FGFBP2*		Effector population with highly cytotoxic phenotype.

5.3.1 Vδ2+ T cells display a transcriptional spectrum of effector function

Vδ2+ T cell effector states share features with MAIT cells

Vδ2+ T cells formed 4 effector clusters, along with some co-clustered CD8+ T cells (Fig. 5-5A). A *GZMK*+ population with high expression of *KLRB1* (encoding the C-type lectin-like receptor CD161) expressed transcription factors (TFs) *ZBTB16* and *RORC*, and genes *AQP3*, *NCR3*, *CCR6*, *DPP4*, and *SLC4A10* (Fig. 5-4C, Fig. 5-5B), as well as the cytokine receptors IL23R, IL18R1, IL18RAP, IL12RB1, IL15RA (Supplementary Fig. 5-3G). This gene expression pattern is typical of mucosal-associated invariant T (MAIT) cells(Huang et al., 2019), which express a semi-invariant TRAV1-2/TRAJ33/12/20 TCR(Lepore et al., 2014). Along with Vδ2+ T cells, the GZMK+ cluster contained CD8+ T cells, most of which expressed CD8A but not CD8B, and possessed a TRAV1-2/TRAJ33/12/20 TCR, consistent with MAIT cells (Fig. 5-5C). TRAV1-2/TRAJ33+ CD8+ T cells were almost exclusively confined to the GZMK+ cluster (Fig. 5-5D). The TRB V-gene usage and CDR3 length, and the TRA CDR3 sequences of these CD8+ T cells was consistent with prior studies of MAIT cells (Fig. 5-5E-H) (Gherardin et al., 2016; Lepore et al., 2014; Tilloy et al., 1999). In sum, one effector population of Vδ2+ T cells share a transcriptional profile with MAIT cells.

Two closely related ADGRG1+ clusters expressed *GZMH* rather than *GZMK*, lacked *RORC* expression, and demonstrated intermediate *ZBTB16* and *KLRB1* expression. Instead, they expressed the TFs *ZNF683* and *ZEB2*. The two ADGRG1+ clusters differed: one expressed *CX3CR1* and *FCGR3A* (CD16), the other expressed greater levels of *HLA-DRA* and *HLA-DRB1* (Fig. 5-4B, 5-5B, Table 5-1).

Two clusters(Transitional and CTLA4+) formed intermediates between ADGRG1+ and GZMK+ clusters (Fig. 5-4B, 5-5B, Table 5-1). One small cluster of Vδ2 T cells (formed of three highly similar sub-clusters, merged together for analysis; Supplementary Fig. 5-3F,G) possessed mixed naive-like and effector transcriptional characteristics.

In summary, effector Vδ2 T cells can take on a range of different transcriptional states. This is dominated by two phenotypes on a spectrum, with one population sharing multiple transcriptional features with MAIT cells, and the other population possessing genes associated with cytotoxicity, ADCC, and antigen presentation.

Pseudotime analysis reveals a transcriptional spectrum of effector Vδ2+ T cells

In order to examine the relationship between the series of transcriptionally-related Vδ2+ T cell clusters, I performed pseudotime analysis of resting, effector Vδ2+ T cell clusters.

This revealed a transcriptional spectrum, with one major trajectory dominating the pseudotime axis (Fig. 5-6A). The GZMK+ cluster was placed at one pole of the pseudotime axis, ADGRG1+ clusters at the other pole, with transitional and CTLA4+ clusters in between(Fig. 5-6B). RNA velocity (the time derivative of gene expression, estimated via the ratio of unspliced and spliced mRNA) can be used to predict the future transcriptional state of individual cells, providing insight into the direction of developmental lineages(La Manno et al., 2018). This approach indicated the direction of differentiation was from GZMK+ to transitional clusters, then on towards the ADGRG1+ clusters, consistent with *in vitro* differentiation(Barisa et al., 2017) (Fig. 5-6C).

Gene transcripts which showed significant variation along pseudotime were then examined. 3,170 transcripts varied significantly along pseudo time (FDR<0.01). the ADGRG1+ pole was characterised by increased expression of cytotoxic molecules, *FGFBP2*, *CX3CR1* and *FCGR3A*, consistent with a terminally differentiated cytotoxic phenotype(Fig. 5D). The GZMK+ pole demonstrated an expression pattern analogous to MAIT cells, with high expression of *KLRB1* and *DPP4* (CD26), as well as SLC4A10, a gene encoding a sodium-driven chloride and bicarbonate transporter expressed on MAIT and iNKT cells(H. Huang et al., 2019). Two chemokine receptors characteristic of MAIT cells, *CCR6*

and *CXCR6*, were highly expressed, as was *IL23R*, a key cytokine receptor in MAIT cell responses(Fig. 5-6E) (Dusseaux et al., 2011).

Gene set enrichment analysis

To examine the potential relevance of the Vδ2+ T cell spectrum of effector function, I performed gene set enrichment analysis (GSEA) on the ranked differentially expressed genes between ADGRG1+ and GZMK+ Vδ2+ T cells(Subramanian et al., 2005). The ADGRG1+ clusters were associated with Fc receptor signalling pathways and phagocytosis, as well as antigen presentation, consistent with prior descriptions of the functionality of CD16+ Vδ2+ T cells(Barisa et al., 2017; Brandes et al., 2005; Himoudi et al., 2012)(Supplementary Fig. 5-4A). The ADGRG1+ clusters were also associated with leukocyte transendothelial migration and with NK cell cytotoxicity, consistent with a peripheral-homing phenotype expressing of cytotoxic molecules and NK cell receptors.

In contrast, the GZMK+ cluster was associated with protein translation (Supplementary Fig. 5-4B), gene sets that correlate with proliferative capacity(Gutierrez-Arcelus et al., 2019). The GZMK+ cluster was also associated with memory CD8+ phenotype and cytokine receptor activity, suggestive of differential effector potential and response to cytokine stimuli. The GZMK+ cluster did not show enrichment of Th17 gene sets, suggesting this population may lack MAIT cell Tc17 functionality (Supplementary Fig. 5-4C).

TCR analysis of peripheral Vδ2+ T cells

Single-cell TCRD sequences reconstructed from scRNAseq data (the 10x genomics platform does not include a specific TRG/TRD sequencing platform) showed dominance of TRDV2-TRDJ1/TRDJ3 usage, with higher TRDJ3 usage in the GZMK+ cluster, more similar to foetal-derived TCRs (Supplementary Fig. 5-5A) (Davey et al., 2018b; Papadopoulou et al., 2019; Willcox et al., 2018). TRG reconstruction was not successful from scRNAseq data, therefore bulk TCR repertoire sequencing was performed.

TRG repertoires of bulk sorted CD28+ and CX3CR1+ Vδ2+ T cells (corresponding to the ends of the transcriptional spectrum) showed expected dominance TRGV9 and TRGJP usage, similar clonal diversity, and considerable clonal overlap (Supplementary Fig. 5-5B-F). TRD clonotypes overlapped extensively between GZMK+/Transitional clusters, and Transitional/ADGRG1+ clusters, suggestive of a sequence of differentiation (Supplementary Fig. 5-6G-H). Some LEF1+ Vδ2+ clonotypes were expanded and also shared with other clusters, consistent with this population not being an unexpanded 'naive' subset.

In sum, effector Vδ2+ T cells possess several transcriptional states, dominated by two effector phenotypes on a spectrum, one similar to MAIT cells, the other displaying a cytotoxic effector phenotype. Transcriptional changes along this spectrum suggest differences in functional potential.

Transcriptional regulation varies along the Vδ2+ T cell effector spectrum

We characterised the transcription regulation landscape of the Vδ2+ T cell effector spectrum. Differential expression of known TFs (identified from a curated gene list(Lambert et al., 2018)) between ADGRG1+ and GZMK+ clusters, and along the pseudotime axis, was examined, as were TF module expression scores (a metric of the expression of gene sets regulated by particular TFs). Vδ2+ T cell clusters differed in TF expression, mirroring the wider transcriptional changes seen over pseudotime (Fig. 5-7A).

Several TFs were differentially expressed between ADGRG1+ and GZMK+ clusters (Fig. 5-7B). The GZMK+ cluster expressed *RORC*, *MYC*, and eukaryotic initiation factors such as *EIFC3*, as previously discussed. *ZBTB16*, a putative master regulator of innate-like T cell function, was expressed throughout the Vδ2+ effector spectrum, with slightly increased expression in the GZMK+ cluster. *FOS* and *JUN*, transcription factors within the mitogen-activated protein kinase (MAPK) TCR signalling pathway(Gaud et al., 2018), showed enrichment in the GZMK+ cluster, with their gene modules

showing enrichment at an intermediate point along pseudotime, suggesting that TCR-mediated responses may alter, or play a role in differentiation, along the spectrum (Fig. 5-7C).

In contrast, the ADGRG1+ clusters expressed *ZEB2, ZNF683, TBX21*, and *NFATC2*, TFs associated with cytotoxicity and terminal differentiation in virus- and tumour-specific CD8+ T cell responses(Dominguez et al., 2015; Guan et al., 2018; Zander et al., 2019) and cytotoxic γδ+ T cells (Oja et al., 2017b; Wragg et al., 2020)(Fig. 5-7D). The ADGRG1+ clusters were also associated with increased expression of *STAT1, STAT3*, and *STAT4*, which, in combination with increased *JAK1* expression(FC 1.23, FDR=$7x10^{18}$), suggests potential differences in response to IL-6- or IL-10-family cytokines, or interferons(Morris et al., 2018).

Transcription factor module expression analysis highlighted gene sets regulated by TFs that are differentially expressed between clusters. Within the GZMK+ cluster, *RORC, FOS, JUN, FOSB, JUNB*, and *EOMES* gene modules were increased in expression, concordant with TF expression patterns(Fig. 5-7C, Supplementary Fig. 5-5I). *RORA* (encodes RORα) and *NR1D1* (encodes REV-ERBα), TFs with roles in the mammalian circadian cycle, were also associated with the GZMK+ and transitional clusters, along with *CEBPD* and *MEOX1*. The ADGRG1+ clusters were associated with the TBX21 TF module, RUNX2 and RUNX3 modules, and several interferon-regulatory factor modules (IRF1, IRF2, IRF5, and IRF7)(Supplementary Fig. 5-5I). TF modules were not available for ZBTB16, ZEB2, or ZNF683, so these could not be examined.

In sum, there are extensive changes to the transcriptional regulatory landscape across the Vδ2+ T cell effector spectrum, with implications for cell function. The MAIT-like GZMK+ cluster TF profile is indicative of innate-like and Tc17 function, along with increased proliferative capacity and links to circadian rhythms. The cytotoxic ADGRG1+ cluster TF profile is suggestive of a highly cytotoxic, terminally differentiated population, with increased interferon-responsiveness.

The Vδ2+ T cell effector spectrum aligns to previously identified transcriptional heterogeneity

While transcriptional heterogeneity of Vδ2+ γδ T cells has previously been analysed using bulk RNAseq sorted Vδ2+ T cell populations. Ryan and colleagues examined transcriptional differences between four putative Vδ2+ T cell subsets (identified by CD27, CD28, CCR7, CD16) using microarray(Ryan et al., 2016). Similarly, Wragg et al. identified four putative subsets of Vδ2+ T cells using bulk RNAseq, based on the markers CD26 and CD94(Wragg et al., 2020). I sought to compare the transcriptional heterogeneity identified in these studies to that identified through scRNAseq in this study.

I compared genes differentially expressed between CD27+CD28+ and CD16+ subsets from Ryan et al. to DEGs between the ADGRG1+ and GZMK+ Vδ2+ populations(Supplementary Figure 5-6A). The 94 genes differentially expressed in both datasets correlated closely ($R2 = 0.694$, $p<0.0001$), and included a number of potential additional phenotypic markers for these subsets. I then compared DEGs from my work to those identifying CD26+CD94- Vδ2+ T cells from Wragg et al. Again, several similarities emerged, with the CD26+CD94- population characterised by high expression of *CD26, IL23R, CCR6,* and *RORC*, and low expression of *FGFBP2, ADGRG1, CD16, CX3CR1*, and *GZMB*. *KLRD1* (CD94) was not differentially expressed in the Ryan et al. study, and while it did vary along pseudotime in my analysis, it did not mark out other distinct subsets, in contrast to Wragg et al.

In summary, two previous subset identification approaches, both of which split Vδ2+ T cells into 4 populations based on surface marker expression, capture some aspects of the continuum of effector function identified by scRNAseq.

Chronic infection shifts the Vδ2+ T cell transcriptional profile

I sought to identify whether in vivo exposure to pAg-producing infections was associated with a shift in the transcriptional profile of Vδ2+ T cells along the effector spectrum. Malaria is one such infection, in which γδ T cells play a role in the immune response(Dantzler and Jagannathan, 2018; Deroost and Langhorne, 2018).

I performed differential gene expression analysis on published microarray data of Vδ2+ T cells from the blood of children from high- or low- malaria endemicity regions(Jagannathan et al., 2014). I then performed Gene Set Enrichment Analysis (GSEA) using two gene sets derived from differential expression analysis between the GZMK+ and ADGRG1+ Vδ2+ T cell clusters at each end of the Vδ2+ transcriptional spectrum.

GZMK+ and ADGRG1+ cluster gene sets were highly enriched, with ADGRG1+ gene set enriched in samples from high malaria-endemicity areas (Supplementary Fig. 5-6B), and the GZMK+ gene set enriched in low malaria-endemicity samples (Supplementary Fig. 5-6C). This suggests that chronic, repeated malaria exposure alters the Vδ2+ T cell transcriptional profile along the effector spectrum towards a cytotoxic phenotype.

Changes in circulating γδ T cell phenotype have been noted in the context of chronic HIV infection, in particular an increase in TIGIT+ γδ T cells, which were associated with higher granzyme and pro-inflammatory cytokine release ex vivo(Belkina et al., 2018). Therefore, I examined differential expression of stimulatory, inhibitory, and apoptotic receptors between the ADGRG1+ and GZMK+ Vδ2+ T cell clusters. The ADGRG1+ Vδ2+ T cell cluster expressed higher levels of *TIGIT*, as well as the apoptosis-related receptor *TNFRSF1B*. In contrast, *CD28*, *SLAMF1*, and *TNFRSF25* (DR3) were more highly expressed in the GZMK+ cluster (Supplementary Fig. 5-6D). This suggests that chronic HIV infection may also shift the effector spectrum towards an ADGRG1+ phenotype.

In sum, comparison of the transcriptional variation along the identified Vδ2+ effector spectrum with prior studies suggest that recurrent malaria infection and chronic HIV infection may shift the Vδ2+ effector spectrum towards a more cytotoxic, less innate-like phenotype.

5.3.2 Non-Vδ2 γδ T cells

Non-Vδ2 γδ T cells divide into multiple naive and effector populations

Next, I characterised the heterogeneity of circulating non-Vδ2 γδ T cells. These clustered with naive and memory CD8+ T cell populations rather than Vδ2+ and MAIT cells, consistent with an adaptive biology (Fig. 5-4B-C) (Davey et al., 2018a).

Two clusters contained effector populations of non-Vδ2 and CD8+ T cells. The CXCR3+ cluster expressed *NCR3* (NKp30), *KLRC3* (NKG2E), and *GZMK*. The TIGIT+ cluster expressed co-inhibitory receptors (*TIGIT, TNFRSF9*) and KIR molecules (*KIR2DL1, KIR2DL3*). The TIGIT+ cluster expressed a different pattern of cytotoxic molecules, expressing *GZMH* rather than *GZMK*, and expressed *FCGR3A, CX3CR1, FGFBP2*, and *ADGRG1*(Table 5-1).

Several clusters of naive CD8+ and non-Vδ2 T cells were seen (Fig. 5-8A and Table 5-1), with the two non-Vδ2 T cell LEF1+ clusters of particular interest. One LEF1+ non-Vδ2 population expressed the transcription factor *SOX4*, a characteristic not shared by other clusters (Fig. 5-8B). SOX4 is a High Mobility Group TF with roles in iNKT cell differentiation and innate-like T cell Tc17 function(Malhotra et al., 2013; 2018).

Naive non-Vδ2 γδ T cells contain a SOX4+CCR9+ population

Pseudotime analysis demonstrated two potential differentiation trajectories from naive to early memory states, with branch 1 including the SOX4+ cluster (Fig. 5-8C-D). Differential expression

analysis between branches revealed two differences of particular interest: first, branch 2 (SOX4+) expressed higher levels of TRDV1 and reduced expression of *TRGV9*, second, this branch also showed higher expression of the gut-homing chemokine receptor *CCR9* (Fig. 5-8E). The SOX4+ LEF1+ cluster showed differences in gene sets associated with lymphocyte differentiation and adhesion than other LEF1+ clusters (Fig. 5-8F). The SOX4+ cluster showed greater *TRDV1* expression (Fig. 5-8G), while LEF1+ and SOX4+ clusters all showed minimal clonal expansion or overlap with other clusters, consistent with naive populations (Fig. 5-8H).

In summary, the non-Vδ2 γδ T cell populations (dominated by TRDV1 expression) contain sizable naive populations in the circulation, analogous to, although distinct from conventional CD8+ T cells, with SOX4 a potential transcription factor in their development. They can take on two effector transcriptional states, which may differ in their cytotoxic potential, ability to perform ADCC, and their pattern of co-inhibitory receptors.

5.3.3 Interim conclusions

The key conclusions from this single-cell RNAseq experiment were:

- Vδ2+ and non-Vδ2 T cells form transcriptionally distinct populations at the single-cell level
- A subset of Vδ2+ T cells show transcriptional similarity to MAIT Cells
- Vδ2+ T cells form a spectrum of effector phenotype, from an innate-like to cytotoxic profile, with widespread associated changes in transcriptional regulation
- Non-Vδ2 T cells show broad similarities in transcriptional profile to conventional CD8+ T cells
- A subset of naive non-Vδ2 T cells expresses SOX4, CCR9, and TRDV1

To explore these results further, I performed a further single-cell sequencing experiment, this time examining functional heterogeneity, as well as transcriptional heterogeneity at rest. I also performed

flow cytometric work, cell sorting, TCR repertoire sequencing, quantitative PCR, and *in vitro* stimulations to confirm key findings.

5.4 Single-cell functional heterogeneity of γδ T cells

Rationale for experimental design

Based on the finding of striking transcriptional similarity of GZMK+ Vδ2+ T cells and MAIT cells, I hypothesised that this subset of Vδ2+ T cells might share greater functional similarity to MAIT cells than has previously been appreciated. A key characteristic of MAIT cells is their robust IFNγ response to combinatorial cytokine stimulation(Ussher et al., 2013; van Wilgenburg et al., 2016), a characteristic shared by other innate-like T cells, including Vδ2+ T cells(Provine et al., 2018; Tsai et al., 2015; Wragg et al., 2020). Recent studies of MAIT cells have more completely categorised the complex and distinct transcriptional responses of MAIT cells to both cytokine and TCR stimulation, and have highlighted new MAIT cell roles, including IL-26 production (cytokine) and tissue repair (TCR) (Lamichhane et al., 2019; Leng et al., 2019). It remains unclear if Vδ2+ T cells, or a subset thereof, undergo these transcriptional changes, or if they share these newly-described functional roles.

To confirm key findings of transcriptional heterogeneity at rest, and to explore transcriptional responses and heterogeneity to stimulation, I designed an experiment involving simultaneous targeted single-cell RNAseq and surface protein quantification using oligo-conjugated antibodies using the BD Rhapsody platform (Experiment 2; Fig. 5-4A) (Trzupek et al., 2020).

There are several reasons that I used this particular technique for confirmation experiments. While targeted gene expression is limiting for hypothesis-generating experiments compared to scRNAseq, it is helpful for confirmatory experiments as dropout, the failure to detect particular gene transcripts

in single-cell experiments, is less common. As only a small proportion of the total transcriptome is amplified, sequencing costs are vastly reduced. This, plus the ease of capturing large numbers of cells (15,000-20,000 on a chip) and the ability to barcode up to 12 populations on each chip, means multiple samples, sorted populations, and stimulation conditions can be run in parallel, reducing cost and batch effects. Finally, the ability to use oligo-conjugated antibodies allows correlation of protein and transcript expression in one experiment.

I performed simultaneous targeted single-cell RNAseq (565 transcripts) and surface protein quantification (91 oligo-conjugated antibodies) on sorted, oligo-barcoded Vδ2+, Vδ1+, MAIT , and conventional CD4+ and CD8+ T cells from 3 healthy adult donors (chosen to ensure findings were valid beyond childhood). Cells were either unstimulated, or stimulated with combinatorial cytokine (IL-12/IL-18) or TCR-ligation (CD3/CD28)(Experiment 2; Fig. 5-4A). IL-12/IL-18 stimulation was used as this has been shown to provide the most potent combinatorial cytokine stimulus to innate-like T cells(van Wilgenburg et al., 2016). After filtering and batch correction, 36,478 cells were analysed. 15 clusters were identified, with co-clustering of different donor subjects, consistent with appropriate batch correction(Fig. 5-9A-B). Clusters segregated predominantly by cell type and stimulation condition, with cell lineage markers used to confirm cluster annotation(Fig. 5-9B-D).

5.4.1 Vδ2+ T cells form a spectrum of effector function

I analysed the unstimulated Vδ2+ T cells separately, which formed 5 transcriptionally distinct clusters (Fig. 5-10A). The 3 major clusters formed a transcriptomic and phenotypic spectrum analogous to that seen in the first scRNAseq dataset (Fig. 5-10B). Cluster 1 showed a high degree of similarity to the GZMK+ MAIT-like cluster, cluster 2 was similar to the cytotoxic ADGRG1+ clusters, with cluster 0 intermediate (Fig. 5-10C). This spectrum of effector function closely replicated that seen in the 10x genomics dataset. The MAIT-like cluster 1 highly expressed *DPP4, IL7R,* and *GZMK,* and the TFs *RORC,* and *FOS*, with increased surface protein expression of CD26 and CD28 (Fig. 5-10D-

F). In contrast, the ADGRG1-like cluster 2 expressed higher levels of *CX3CR1, FCGR3A, GZMH,* and *GNLY,* and the TFs *ZEB2, TBX21,* and *ZNF683*, as well as protein expression of CD16 (Fig. 5-10D-F).

In summary, targeted single-cell gene and proteomic expression of resting Vδ2+ γδ T cells using BD Rhapsody replicates a transcriptional effector spectrum from an innate-like to a cytotoxic phenotype.

5.4.2 Vδ2+ and MAIT cell responses to cytokine and TCR stimulation

Gene and surface protein expression of γδ+, MAIT and conventional T cell populations stimulated with cytokine (IL-12/IL-18) or TCR ligation (CD3/CD28) for 20 hours was analysed (Fig. 5-11A). Conventional T cells were included as a positive control comparator for functional responses.

Aggregated MAIT and Vδ2+ T cell populations showed analogous responses to cytokine and TCR stimulation (Fig. 5-11B-C). Both stimulation conditions elicited upregulation of co-inhibitory receptors (*HAVCR2*, *CTLA4*, and *LAG3*), *IL2RA*, and cytotoxic molecules. Both cell types responded to cytokine stimulation with robust *IFNG* expression, while *IFNG* expression was much more muted on TCR stimulation, as previously described(Leng et al., 2019). Both MAIT and Vδ2+ T cells showed increased in *IL26* expression on cytokine stimulation, suggesting Vδ2+ T cells share a MAIT-like capacity for production of this anti-microbial molecule (Lamichhane et al., 2019; Larochette et al., 2019; Leng et al., 2019).

MAIT cells contribute to tissue repair, upregulating a genes associated with tissue repair on TCR stimulation, including *CCL3, HIF1A, TNF, CSF2*, and *FURIN*(Constantinides et al., 2019; Leng et al., 2019). While this experiment had not been designed to examine direct tissue repair functionality, the increased FURIN expression seen by resting GZMK+ Vδ2+ T cells in the scRNAseq Experiment 1 (Fig. 5-11D) raised the possibility of shared tissue repair functionality, so I examined expression of

tissue repair-associated genes upregulated in MAIT cells on TCR stimulation. Consistent with prior reports, *CCL3*, *CSF2*, *TNF*, and *HIF1A* were all upregulated in MAIT cells on TCR stimulation(Leng et al., 2019). Vδ2+ T cells also upregulated these genes with a similar fold change, suggesting Vδ2+ T cells may possess analogous tissue repair roles (Fig. 5-11E-F).

There were several notable differences between MAIT and Vδ2+ T cell responses to stimulation. MAIT cell IL-17 production was replicated, with robust induction of *IL17F* expression on TCR stimulation. However, there was no IL-17 expression by Vδ2+ T cells with TCR stimulation (Fig. 5-11B-C).

Vδ2+ T cells showed heterogeneous responses to cytokine stimulation. There were two transcriptionally distinct responses of Vδ2+ T cells to IL-12/IL-18 stimulation, one dominated by IFNG expression which co-clustered with cytokine-stimulated MAIT cells (IFNG-high response), and one with more muted IFNG expression, which clustered separately (IFNG-low response) (Fig. 5-12A). The transcriptional and surface protein phenotype of these clusters aligned to the Vδ2+ T cell transcriptional effector spectrum (Fig. 5-12B). IFNG-high responding cells showed higher expression of *DPP4, CD28, CXCR6*, and *RORC*, and protein expression of CD26 and CD28, similar to the MAIT-like transcriptional cluster at rest. IFNG-low responsive cells showed higher expression of *TBX21, ZEB2, ZNF683, HLA-DPA1* and *HLA-DPB1*, similar to the ADGRG1+ cluster at rest. This indicates that these two discrete responses to cytokine stimulation divide the Vδ2+ T cell transcriptional effector spectrum into two functional subsets.

The IFNG-high and IFNG-low responses of Vδ2+ T cells to cytokine stimulation showed notable similarities and differences (Fig. 5-12C-D). Both responses showed increased expression of cytotoxic molecules (*GZMB, GZMH, PRF1*), as well as modest *TNF* production and expression of *HAVCR2*, *LGALS1*, and *LGALS3*. The IFNG-high response was dominated by strong *IFNG* expression, as well as

IL26 and *CXCL13* production, suggesting that *IL26* production is limited to MAIT-like Vδ2+ T cells. The IFNG-low response showed up-regulation of interferon-stimulated anti-viral genes that were not increased in expression in the IFNG-high response, including *STAT1, IFITM3, OAS1, ISG15, IRF7,* and *IRF1*.

In sum, Vδ2+ T cells show similar transcriptional changes to MAIT cells in response to cytokine and TCR stimulation, including *IFNG* and *IL26* expression with cytokine stimulation, with the key exception of minimal Tc17 functionality with TCR stimulation. Moreover, Vδ2+ T cells show two discrete functional responses to cytokine stimulation, which align to the phenotypes at either end of the Vδ2+ T cell transcriptional effector spectrum. This provides evidence that the transcriptional effector spectrum of Vδ2+ T cells can be split into two subsets based on distinct functional responses to cytokine stimulation.

5.4.3 Non-Vδ2 T cells show transcriptional heterogeneity in CD27hi naive populations

I went on to examine the transcriptional heterogeneity of non-Vδ2 T cells in Experiment 2, with comparison to the findings from scRNAseq Experiment 1. Unstimulated non-Vδ2 T cells formed six transcriptionally distinct clusters, with two CD27hi naive clusters, and four CD27low effector clusters, consistent with prior studies (Fig. 5-13A) (Davey et al., 2018b; 2017). The CD27hi clusters possessed a naive phenotype, with high expression of *LEF1*, *CCR7*, and *SELL*, and higher protein expression of CCR7 (CD197), CD62L, and CD127. These two populations showed analogous transcriptional features to the LEF1+ and SOX4+ populations identified in Experiment 1 (Fig. 5-13C-D). Cluster 4 expressed *SOX4*, *EGR1*, and the gut-homing chemokine receptor *CCR9* (Fig. 5-13A,E). The CD27low effector clusters had high cytotoxic granule expression (*GZMK*, *GZMH*) and expressed

TFs *ZEB2* and *TBX21*. In addition, these populations expressed genes typical of innate lymphoid and NK cells, including KIR molecules (*KIR3DL1* and *KIR2DL1*), and *FCGR3A* (Fig. 5-13E).

5.4.4 Non-Vδ2 T cells show NK-like responses to stimulation

I then compared non-Vδ2 and conventional T cell transcriptional responses to stimulation. Both non-Vδ2 and conventional T cells showed little response to cytokine stimulation, consistent with prior reports (Fig. 5-14A) (Provine et al., 2018). TCR stimulation induced much greater transcriptional change in non-Vδ2 T cells compared to cytokine stimulation (Fig. 5-14B). Comparison of gene expression changes upon TCR-stimulation between non-Vδ2 and CD8+ T cells revealed shared responses, including upregulation of cytotoxic molecules, chemokines, and co-inhibitory receptors (Fig. 5-14C). However, unlike non-Vδ2 T cells, CD8+ T cells showed *IL9* production, and greater upregulation of *CTLA4* and *LAG3*. In contrast, non-Vδ2 T cells upregulated a suite of genes similar to NK cells in response to TCR stimulation, including Fc receptor (FcR) genes *FCER1G* and *FCGR3A*, integrins *ITGAM* and *ITGAX*, *GNLY*, and KIR molecules (*KIR2DL1, KIR2DL4, KIR3DL1*) and *NKG7* (Fig. 5-14C,D).

In sum, non-Vδ2 γδ T cells show transcriptional heterogeneity in CD27hi naive γδ T cell populations, with a SOX4+ population expressing *CCR9*. Effector non-Vδ2 T cells exhibit a phenotype and responses to stimulation suggestive of combined adaptive and NK-like functionality.

5.5 Phenotypic and functional characterisation of Vδ2+ T cells

CD26 and GPR56 expression delineate the Vδ2+ T cell transcriptional spectrum

Single-cell RNA sequencing had delineated a spectrum of Vδ2+ T cell transcriptional heterogeneity, with one end categorised by CD28 and CD26 (*DPP4*), and the other by GPR56 (*ADGRG1*), *CX3CR1*, and *CD16*. CX3CR1 and CD16 are only expressed on a small proportion of Vδ2+ T cells, and were only expressed on one of the two ADGRG1+ clusters in the scRNAseq data, making them potentially less useful subset markers. Both CD26 and CD28 are easily stained surface markers, however CD28 is challenging to stain following *in vitro* CD3/CD28 TCR stimulations. Therefore, I chose to test CD26 and GPR56 as putative flow cytometry markers to identify Vδ2+ T cells at each end of this transcriptional spectrum.

I examined CD26 and GPR56 surface expression on Vδ2+ γδ T cells in frozen PBMCs using flow cytometry. Vδ2+ T cells identified by the B1 clone all expressed Vγ9, consistent with prior work (Davey et al., 2018b)(Supplementary Fig. 5-7A). As expected, CD26 stained clearly, with a CD26-, CD26mid, and CD26bright population clearly seen. GPR56 also stained well, with distinct GPR56- and GPR56+ populations (Supp. Fig. 5-7B). GPR56+ Vδ2+ γδ T cells were predominantly CD26- or CD26mid, while CD26bright populations were almost all GPR56-. Based on the transcriptional data, which suggested that all GPR56+ cells fell within one end of the transcriptional spectrum, I gated GPR56+ cells and CD26bright cells as shown (Fig. 5-15A). CD26bright Vδ2+ γδ T cells made up 33% of the total population, while the GPR56+ subset accounted for 52%. At rest, there was a small population (<4%) of CD26-GPR56- Vδ2+ γδ T cells (Fig. 5-15B). There was no relationship between total Vδ2+ T cell number and the proportions of the two major subsets (Supp. Fig. 5-7C). This practical categorisation splits Vδ2+ γδ T cells in to two dominant effector populations, both frequent in blood.

The phenotype of CD26bright and GPR56+ Vδ2+ T cells

I sought to compare the expression of markers used in previous subset classifications by the proposed GPR56+ and CD26bright Vδ2+ T cell subsets. Therefore, I examined the surface expression of CD45RA, CX3CR1, CD161, CD27, CD28, and CD16, as well as the putative markers CD26 and GPR56, on Vδ2+ γδ T cells from frozen PBMCs from eight healthy donors. tSNE analysis of surface marker expression showed that CD26bright and GPR56+ populations separated based on these markers alone (Fig. 5-15C). CD16 and CX3CR1 expression were almost entirely restricted to the GPR56+ population (Fig. 5-15D).

Almost all (>99.5%) of the CD26bright subset expressed CD28, while 41% of the GPR56+ population expressed CD28 (Fig. 5-15D), supporting the use of CD26 over CD28 as a subset marker. CD161 expression was high on both subsets, consistent with prior work(Provine et al., 2018). However 37% of CD26bright Vδ2+ T cells were also CD161++ (a MAIT-like phenotype previously associated with increased cytokine responsiveness in multiple T cell subsets(Fergusson et al., 2014)), compared to just 4% of GPR56+ Vδ2+ γδ T cells,(Supplementary Fig. 5-7D,E).

MAIT cells demonstrate a characteristic pattern of chemokine receptor expression, which directly relates to their tissue-homing and functional capacity, including expression of CCR6 and CXCR6(Fergusson et al., 2014). CCR6 expression was almost entirely confined to the CD26bright population, with 36% of CD26bright cells expressing CCR6, compared to 4% of GPR56+ cells (Fig. 5-15E). Similarly, 50% of CD26bright cells expressed CXCR6, compared to 20% of GPR56+ cells (Fig. 5-15F).

In summary, CD26 and GPR56 expression can identify 2 dominant subsets of Vδ2+ γδ T cells, with distinct phenotypic profiles. CD26bright Vδ2+ T cells are CD161bright, CD27+ and CD28+, and expressed the chemokine receptors CCR6 and CXCR6. In contrast, GPR56+ Vδ2+ T cells are

predominantly CX3CR1+ and CD45RA+, contain the functionally-relevant CD16+ subset, and lack CCR6 expression.

Transcription factor expression of CD26bright and GPR56+ Vδ2+ T cells

The scRNAseq data indicated that multiple transcription factors (TFs) and TF modules were differentially expressed along the Vδ2+ T cell effector spectrum. I examined TF expression by GPR56+ and CD26bright Vδ2+ T cell populations using intranuclear staining and flow cytometry (Fig. 5-16A-E).

Promyelocytic leukaemia zine finger (PLZF, encoded by *ZBTB16*), is an archetypal innate-like TF, expressed by iNKT and MAIT cells(Savage et al., 2008). *ZBTB16* was expressed throughout the Vδ2+ T cell effector spectrum in the scRNAseq data, with higher expression in GZMK+ cells. PLZF expression of GPR56+ and CD26bright Vδ2+ T cells populations was similar to that of MAIT cells (Fig. 5-16A). RAR-related orphan receptor gamma (RORγt, encoded by *RORC*), is associated with Tc17 function and expressed by MAIT cells(Ivanov et al., 2006; Kurioka et al., 2016). RORγt was more highly expressed in the CD26bright Vδ2+ γδ T cells than in the GPR56+ population, although not to the same intensity as in MAIT cells (Fig. 5-16C). However, Helios, another transcription factor expressed by MAIT cells, was expressed at much lower levels on both CD26bright and GPR56+ Vδ2+ T cells (18% and 6% respectively), compared to MAIT cells (89%)(Fig. 5-16E).

The scRNAseq data highlighted several TFs associated with GPR56+ Vδ2+ T cells, including *ZNF683*, *TBX21*, and *ZEB2*. *ZNF683* (encoding Homolog of Blimp-1 in T cells (Hobit)), is expressed by terminally differentiated effector populations in response to viral infection (Oja et al., 2017b). Hobit expression was higher in the GPR56+ population compared to both CD26bright Vδ2+ and MAIT cells, as was Tbet(Fig. 5-16B,D). I attempted ZEB2 staining with an AF647-conjugated antibody (for immunofluorescence), however it was not successful for intranuclear staining.

I hypothesised that these differences in transcriptional regulation would define shared and distinct functional capacities of MAIT cells and Vδ2+ γδ T cells, and therefore proceeded to evaluate their functional capacity with intracellular staining for cytotoxic granules, and *in vitro* stimulation assays.

Cytotoxic molecule expression of CD26bright and GPR56+ Vδ2+ T cells

The single cell RNAseq data delineated a spectrum of cytotoxic molecule expression, with ADGRG1+ Vδ2+ γδ T cells expressing high levels of the transcripts *GZMB*, *GZMH*, and *GNLY*, while the CD26+ Vδ2+ γδ T cells expressed higher levels of *GZMK* in a manner analogous to MAITs. These differences in cytotoxic molecule expression were replicated by flow cytometry. GPR56+ Vδ2+ γδ T cells had higher expression of granzyme A, granzyme B, and perforin, while CD26bright Vδ2+ γδ T cells had high expression of granzyme K, in a manner directly analogous to MAIT cells (Fig. 5-16F-I).

Functional responses of CD26bright and GPR56+ Vδ2+ T cells

To confirm and extend the functional results from the second single-cell experiment, I examined Vδ2+ T cell subset responses to combinatorial cytokine stimulation.

CD26bright Vδ2+ T cells expressed more surface IL18Rα than GPR56 counterparts. Upon cytokine stimulation (IL-12/IL-18 for 20 hours), 75% of the CD26bright subset produced IFNγ, compared to just 9% of the GPR56+ subset (Fig. 5-17B). CD26bright Vδ2+ T cells also partially responded to IL18/IFN-α stimulation, akin to MAIT cells, but not to IL-18 or IFN-α alone (Fig. 5-17C) (van Wilgenburg et al., 2016). Consistent with the transcriptional data, IL12/IL18 stimulation induced LAG3 expression on CD26bright Vδ2+ T cells, as did IL18/IFN-α and IFN-α (Supplementary Fig. 5-7F). CD56 expression was similar on both subsets, and its expression did not associate with differences in cytokine responsiveness, despite differences in IL18Rα expression, in contrast to MAIT cells(Supplementary Fig. 5-7G-I) (Dias et al., 2017).

MAIT cells can produce IL-26, a secreted anti-microbial cytokine, upon cytokine stimulation(Leng et al., 2019), and the functional single-cell data from Experiment 2 indicated that CD26bright Vδ2+ T cells could produce also IL-26. I tested this using cytokine stimulation and intracellular staining and flow cytometry, using reagents as previously described(Lamichhane et al., 2019). Vδ2+ T cells produced IL-26 on cytokine stimulation, with the greatest responses seen in the CD26bright population, analogous to MAIT cells (Fig. 5-17D,E) (Lamichhane et al., 2019).

The differential expression of genes associated with translation and proliferation, including MYC, EIF3E, and ribosomal proteins, suggested possible differences in proliferative potential. I tested this hypothesis though stimulation of PBMCs with cytokine or TCR stimulation for 7 days. CD26bright Vδ2+ T cells demonstrated greater proliferative capacity following stimulation with cytokine (IL-15 or IL12/IL18) or TCR (HMBPP) (Fig. 5-17G).

In summary, CD26bright Vδ2+ T cells show robust cytokine responsiveness, including production of IFN-γ and IL-26, similar to MAIT cells. CD26bright Vδ2+ T cells also show increased proliferative capacity to GPR56+ counterparts. GPR56+ Vδ2+ T cells demonstrate minimal responses to cytokine stimulation, potentially mediated by lower IL18Rα expression, but express multiple cytotoxic granules.

5.6 Investigation of CCR9 expression on non-Vδ2 T cells

CD27hi non-Vδ2 T cells express CCR9

One unexpected result from the scRNAseq experiments was the expression of *CCR9* on a population of naive SOX4+ non-Vδ2+ γδ T cells. The CCR9-CCL25 axis mediates α4β7-dependent adhesion of circulating memory and effector lymphocytes to endothelial MAdCAM-1, facilitating entry into intestinal mucosa, and expressed on T cells in GALT and the gut(Miles et al., 2008; Papadakis et al., 2000; Wendt et al., 2016).

Naive non-Vδ2+ T cells are characterised by high expression of CD27. I therefore sought to examine CCR9 expression, and other putative gut-homing molecules, on CD27hi and CD27lo/neg non-Vδ2 T cells. A subset of CD27hi non-Vδ2 T cells, expressed CCR9 at appreciable levels by flow cytometry, with 16% of cells CCR9+, while their memory CD27lo/neg counterparts expressed CCR9 at much lower levels, with only (3% CCR9+; Fig. 5-18A). CCR9 staining with the L053E8 clone was validated with multiple fluorophores and a different anti-CCR9 clone (Supplementary Fig. 5-7A,B). CCR9 staining was not altered by Fc receptor blockade, nor did staining temperature abrogate staining. CCR9 transcript expression by CD27hi non-Vδ2+ T cells was validated further using qPCR following whole transcriptome amplification of FACS-sorted CD27hi or CD27lo/neg populations (Fig. 5-18B). CCR9 transcript expression correlated with protein CCR9 expression quantified by flow cytometry (Fig. 5-18C).

Expression of β7-integrin and CD103 was not different between CD27hi and CD27lo/neg populations (Supplementary Fig. 5-8C,D). Putative gut-homing cells co-expressing β7-integrin and CCR9 were more common in the CD27hi subset than in CD27lo/neg cells, or conventional memory or naive CD8+ populations (Fig. 5-18D).

CD27hi non-Vδ2 T cells have phenotypic and functional similarities to naive conventional T cell populations, and a diverse TCR repertoire(Davey et al., 2018a; 1AD). I hypothesised that CCR9+ CD27hi non-Vδ2 γδ T cells also possessed a naive-like phenotype. CCR9+ non-Vδ2 T cells expressed a

surface marker phenotype similar to naive conventional T cells. CCR9+ non-Vδ2 T cells clustered together upon tSNE analysis of co-expressed memory status surface markers, with low CD8 and CD161 expression, and high CD62L, CCR7, and CD27 expression, consistent with a naive population(Fig. 5-18E-G). CCR7 was highly expressed on CD27hi non-Vδ2 γδ T cells, with minimal expression on CD27lo populations (Supplementary Fig. 5-8E). CCR7 expression was present on both CCR9- and CCR9+ CD27hi subsets (Fig. 5-18F, Supplementary Fig. 5-8F). CCR9- and CCR9+ CD27hi Vδ2+ T cells were almost entirely CD8-, while CD27lo/neg subset frequently expressed CD8 (CD8αα or CD8αβ) (Fig. 5-18H-J).

All-trans retinoic acid (ATRA) induces CCR9 expression on conventional T cells(Iwata et al., 2004; Wendt et al., 2016). I examined whether non-Vδ2 T cells responded to ATRA stimulation in a similar manner. *In vitro* stimulation of frozen PBMCs with TCR ligation (plate-bound CD3, soluble CD28) and ATRA, induced robust CCR9 expression, particularly striking on CD27hi non-Vδ2 T cells. (Supplementary Fig. 5-8G-H).

TCR repertoire sequencing of CCR9+ non-Vδ2 T cells

The expression of CCR9, a gut-homing chemokine, on peripheral non-Vδ2 γδ T cells with a naive phenotype raises the possibility that these populations have pre-determined gut-tropic behaviour. An alternative hypothesis is that this population is not truly naive, but represents a memory population with clonal overlap with γδ T cells in the intestine.

To test these hypotheses, TCR repertoire sequencing of sorted γδ T cell populations from stored peripheral blood was performed, and compared to small intestinal γδ T cell TCR repertoires which had previously been sequenced (see chapter 3). Frozen PBMC samples were available for four study subjects for whom intestinal γδ T cell TCR repertoires were available. CD27hi CCR9-, CD27hi CCR9+,

and CD27lo non-Vδ2 γδ T cells were sorted by FACS, then frozen in Trizol. RNA extraction was performed, before TCR repertoire library generation for TRG and TRD.

TCR repertoire diversity was lower in the CD27lo population than the CD27hi populations, consistent with memory and naive phenotypes respectively (Supplementary Fig. 5-8I). The TCR repertoires in the gut showed higher diversity than the CD27lo memory populations in the blood, as shown previously (Eggesbø et al., 2019). CCR9- and CCR9+ CD27hi γδ T cells showed differences in TRGV and TRDV gene usage (Fig. 5-18K,L), with CCR9+ populations showing lower TRGV9 and a trend towards higher TRGV4 gene usage, similar to gut populations (Supplementary Fig. 5-8J,K).

Shared clonotypes between blood and intestine were found in both the TRG and TRD repertoires. Peripheral clonotypes shared with the intestinal repertoire were highest in the CD27lo memory population consistent with a memory phenotype, and lowest for CD27hi populations, consistent with a naive phenotype (Fig. 5-18M,N).

In summary, circulating non-Vδ2 γδ T cells contain a naive, CD27hi LEF1+SOX4+ population which expresses CCR9, and with a different pattern of TRGV gene usage compared to CCR9- populations.

5.7 Discussion

Summary of findings

In this chapter I have examined the single-cell phenotypic, transcriptional, and functional heterogeneity of circulating human γδ T cells. Effector Vδ2+ T cells form a transcriptional and phenotypic spectrum, which can be identified by CD26 and GPR56 expression, and confers differences in function, including response to cytokine stimulation, IL-26 production, and proliferation. While CD27hi and CD27lo/neg non-Vδ2 T cell subsets mirror naive and effector

conventional memory populations respectively, CD27lo/neg effector non-Vδ2 T cells demonstrate NK-like features both in phenotype and response to TCR stimulation, while naive CD27hi non-Vδ2 T cells show previously unappreciated heterogeneity, with a SOX4+ subset expressing the gut-homing chemokine receptor CCR9.

Philosophical considerations of T cell subsets: hair-splitters and lumpers

"*I am got extremely interested in tabulating according to mere size of genera, the species having any varieties marked by greek letters or otherwise: the result (as far as I have yet gone) seems to me one of the most important arguments I have yet met with, that varieties are only small species—or species only strongly marked varieties. The subject is in many ways so very important for me; I wish much you would think of any well-worked Floras with from 1000–2000 species, with the varieties marked. It is good to have hair-splitters & lumpers*."

Charles R Darwin to Joseph D Hooker, August 1857

The proposed classification of Vδ2+ T cells based on their transcriptional variation and certain associated surface markers raises epistemological questions about systems of scientific classification. Some immunological classifications fit into the category of 'natural kinds' - for instance the distinction between a T cell and a B cell(Bird and Tobin, 2008). These have distinct, non-overlapping characteristics, are categorically distinct without intermediates, they contain distinct subtypes within them that do not span between each other, and share key properties within, but not between, these groups. Importantly, the existence of these natural kinds permits inductive reasoning and inferences - a particular function of a T cell may be generalisable to all T cells, but not to B cells.

Within this framework, the categories of Vδ2+ and non-Vδ2 γδ T cells seem to meet the criteria of distinct natural kinds. These populations are defined by distinct TCR gene usage, determined during their development, with no intermediate that spans between them. Key properties are shared within each group; an adaptive non-conventional biology in non-Vδ2 T cells, an innate-like, pAg-

responsive biology in Vδ2+ T cells. My results suggest inductive reasoning can be applied within each group, with Vδ1+ and Vδ1-/2- T cells sharing similar phenotypic and transcriptional profiles.

In contrast, much immunological variation between cell types is not categorical, and would not satisfy the definitions of 'natural kinds'. Instead, these systems are pragmatic methods for describing the variation that we see, irrespective of whether they represent a natural kind or not. Such classifications are tools, providing a common language with which to perform and communicate experiments, but bringing with them biases and flaws inherent in any system that does not represent a natural kind. Given the spectacular breadth of functional, phenotypic, transcriptional, genetic, and epigenetic variation we can examine with modern techniques, on what basis should a particular categorisation be adopted?

First, the system should explain patterns of variation larger than merely the variable itself, i.e. the identifying characteristic should correlate with underlying transcriptional or (epi)genetic variation. Second, the system should correlate with relevant functions of identified populations. Third, the system should allow inference about additional functions, although this can only be tested in retrospect once a system is developed. Fourth, it must be practical; if a system is not describing a 'natural kind', then it should act as a useful tool for the development of further knowledge.

My results make a strong case that no subset classification of Vδ2+ T cells will satisfy the criteria of natural kinds. While there is demonstrable transcriptional and phenotypic heterogeneity which is linked to functional differences, this represents a spectrum, with intermediate populations and the likelihood that cells can transition from one state to the other. On the other hand, the division of the Vδ2+ T cell transcriptional spectrum based on GPR56 and CD26 holds up relatively well against criteria for a useful classification tool. The data show that this classification aligns to underlying transcriptional heterogeneity, while epigenetic variation remains an important area for future

research. GPR56/CD26 subsets differ in their phenotype, TF expression, cytotoxic molecule expression, and proliferative capacity. Importantly, the classification is practical.

In the absence of a 'natural kind', it is unclear what the 'right' number of subsets of a particular cell type is. As Darwin alludes to in this letter, this is inherently subjective; the classification (and its success) is defined by the purpose to which it is put, rather than an inherent philosophical principle(Darwin, 1857). In immunological work, additional subset complexity comes at a cost: cell numbers are reduced, complexity is increased, additional reagents and processes are required. As such, any sub-categorisation should seek to be as simple as possible, collapsing subtler varieties into key distinct subtypes, using as few markers as possible. The identification of two major subtypes based on CD26 and GPR56 is simple, parsimonious, and may represent a step forward over more complex systems.

Findings with reference to the wider literature

Although single-cell approaches have been used to examine γδ T cells before, this work is the most comprehensive to date, both in terms of single-cell methods, and in sample and cell number. In particular, I focused on single-cell functional heterogeneity, which has not been examined before. One prior study used scRNAseq to confirm heterogeneity between innate-like T cell subsets found with bulk RNAseq methods, rather than within the γδ T cell compartment(Gutierrez-Arcelus et al., 2019). However, this study did demonstrate that Vδ2+ T cells clusters localised both with MAIT cells, and with conventional CD8+ T cells. These clusters are likely to represent the two ends of the transcriptional spectrum that I have identified. Another study used a novel method to identify small numbers of γδ T cells in existing datasets, as well as limited novel single-cell work(Pizzolato et al., 2019). While this study did examine potential differentiation trajectories within Vδ2+ T cells, it did not examine transcriptional heterogeneity in detail. Single-cell functional heterogeneity, in terms of stimulation responses, has not been examined in this manner before.

The striking transcriptional, phenotypic, and functional similarity of CD26bright Vδ2+ T cells to MAIT cells indicates that this Vδ2+ subset may share other functions with MAIT and iNKT cells, and may provide overlapping roles in health and disease(Garner et al., 2018; Provine and Klenerman, 2020). MAIT cells can display tissue repair functions in mice and humans(Constantinides et al., 2019; Leng et al., 2019). The up-regulation of genes associated with tissue repair suggests that CD26+ Vδ2+ T cells may share this function, and functional assays to evaluate this possibility are a priority for future research.

This work has examined in detail the transcriptional regulation of human Vδ2+ T cells. Innate-like responses to combinatorial cytokine are thought to be linked to expression of CD161 and the TF PLZF(Fergusson et al., 2014). However, both PLZF and CD161 were expressed across the Vδ2+ T cell effector spectrum despite the differential response to cytokine stimulation. This suggests that PLZF is necessary, but not sufficient, for innate-like cytokine responses. Similarly, despite RORγt expression, CD26 Vδ2+ T cells do not display the same degree of Tc17 function as MAIT cells in response to TCR stimulation. One identified TF difference between CD26bright Vδ2+ T cells and MAIT cells was Helios, which is highly expressed by MAIT cells, and may modulate some differences between the two subsets.

Cytotoxic GPR56+ Vδ2+ T cells express the transcription factors Hobit, ZEB2, Tbet, and NFATC2, with related elevated expression of these TF modules. Hobit and ZEB2 have been linked to cytotoxic and terminally differentiated CD8+ T cell populations(Oja et al., 2017b; Omilusik et al., 2015). However, it remains unclear if these TFs, or others, are involved the initiation of the transition from innate-like to cytotoxic phenotype, and why the transcriptionally similar MAIT cells do not undergo such a transition.

The evidence that recurrent malaria infection shifts the transcriptional profile of Vδ2+ T cells along this effector spectrum demonstrates the relevance to human disease. It also raises the possibility that pAg-producing infection, through alteration in the ratio of two distinct functional Vδ2+ T cell subsets, could alter Vδ2+ T cell functional responses, perhaps permanently. This shift in transcriptional profile may also occur with tuberculosis and HIV infection, as well as *in vitro* with TCR stimulation, combined with IL-23 and CD26 ligation(H. Shen et al., 2016; Wragg et al., 2020). A shift towards a more cytotoxic phenotype may be of benefit for anti-tumour responses (for instance in generating autologous cytotoxic Vδ2+ T cells *ex vivo* for cancer immunotherapy). Conversely, a loss of CD26bright Vδ2+ T cells, in particular their cytokine-dependent responses, could lead to compromised antiviral responses, anti-tuberculous immunity, or adenovirus vector-based vaccine responses (Provine et al., 2019; H. Shen et al., 2016; Tsai et al., 2015; van Wilgenburg et al., 2016). Whether Vδ2+ T cells play non-redundant roles in these settings, and the magnitude of such an effect in the context of human disease, is of considerable translational importance, particularly for infectious disease and vaccination strategies in sub-Saharan Africa.

While we included both children and adults in this study, we did not include foetal and cord blood samples. Foetal Vδ2+ T cells are preprogrammed effectors(Dimova et al., 2015), and recent work has identified that CD26+ Vδ2+ T cells predominate in cord blood, supporting a differentiation from CD26bright to GPR56+ with age(Wragg et al., 2020). Further work is needed to understand how Vδ2+ T cell phenotype and function alters in early life. In addition, this work was largely confined to circulating γδ T cells. However, the transcriptional heterogeneity of γδ T cells in tissue and at mucosal surfaces requires additional study.

The transcription factor *Sox4* has been identified in murine γδ thymocytes and naive T cell populations(Sagar et al., 2020; L. Tan et al., 2019). *Sox4*, together with *Sox13* regulate *Rorc* expression, leading to Tc17 functionality in mice(Malhotra et al., 2013). *SOX4* expression has also

been identified in a naive human γδ T cells, predominantly in cord blood(L. Tan et al., 2020), although not associated with CCR9 expression.

CCR9 expression in humans is thought to be confined to thymocytes, and to conventional memory T cells either resident in the gut, or with gut-homing potential(Miles et al., 2008; Papadakis et al., 2000; Wendt et al., 2016). The carefully-validated findings of CCR9 expression on naive non-Vδ2 T cells are unexpected, but tally with recent murine work. In addition to the expected expression of *Ccr9* and *Sox4* by immature murine γδ thymocytes(L. Tan et al., 2019), a recent study identified a *Ccr9*-expressing population of immature murine γδ T cells in the circulation of adult mice, which are pre-primed for IFN-γ production(Sagar et al., 2020). Murine Vγ5+Vδ1+ dendritic epidermal T cells (DETCs) emerge in utero and are directed by CCR10 expression to colonise the skin epidermis(Jin et al., 2010; Parker and Ciofani, 2020). Similarly, γδ T cell colonisation of the murine gut is partially CCR9-dependent(Wurbel et al., 2001). It is unclear if the human CCR9+ population has pre-programmed gut-homing potential in an analogous manner, and what the implications of this would be for human health and disease. It may be that naïve non-Vδ2 T cells that express particular TCR V-genes associated with BTNL recognition in certain tissues are 'pre-programmed' with gut-specific homing molecules, facilitating targeted surveillance of gut-associated lymphoid tissue.

These data add to the weight of evidence that not all γδ T cells are created equal, and studies in human disease reporting total γδ T cell frequency or functional responses provide limited insight into their biology. Vδ2Vγ9+ and Vδ2- T cell populations must be identified, ideally with frequencies of relevant subsets, to gain understanding of the role of γδ T cells in disease.

Strengths and limitations

There are several strengths to the scRNAseq experimental work. First, the use of both paediatric and adult study samples in the two scRNAseq experiments provides evidence that these findings can be

generalisable throughout life. Additional work on cord blood or neonatal samples would be of particular interest, given findings of recent murine work(Sagar et al., 2020). Second, the confirmation of key findings in two separate experiments, using different scRNAseq approaches and with a large number of cells included in the experiments, provides confidence that these findings are robust. Third, the analysis of how single-cell transcriptional and functional heterogeneity are linked, particularly for Vδ2+ T cells, is of considerable importance when considering the translational relevance of these results.

There are two important weaknesses of the first scRNAseq experiment: samples were run one by one, and samples from coeliac disease subjects were included. Cell capture, library prep, and sequencing were performed one sample at a time, as at this stage the lab was less familiar with the technique, and I had not appreciated the problems that batch effects generated by this approach could generate. This was one of the reasons that a second experiment, with all samples run in parallel, was performed, which broadly confirmed the findings of the first experiment.

Coeliac disease samples were included as a hypothesis-generating tool about the biology of circulating CD8+ and γδ T cells in coeliac disease, and to examine for evidence of clonal sharing with intestinal T cell scRNAseq samples run from the same individuals. However, differences between CD and healthy subject samples were small, consistent with the hypothesis that coeliac disease is predominantly a disease of mucosal immune cell subsets. Moreover, the experimental design, with samples run individually, meant that it was difficult to distinguish disease-related and individual-related effects, and therefore robust conclusions about the role of disease could not be drawn from this comparison.

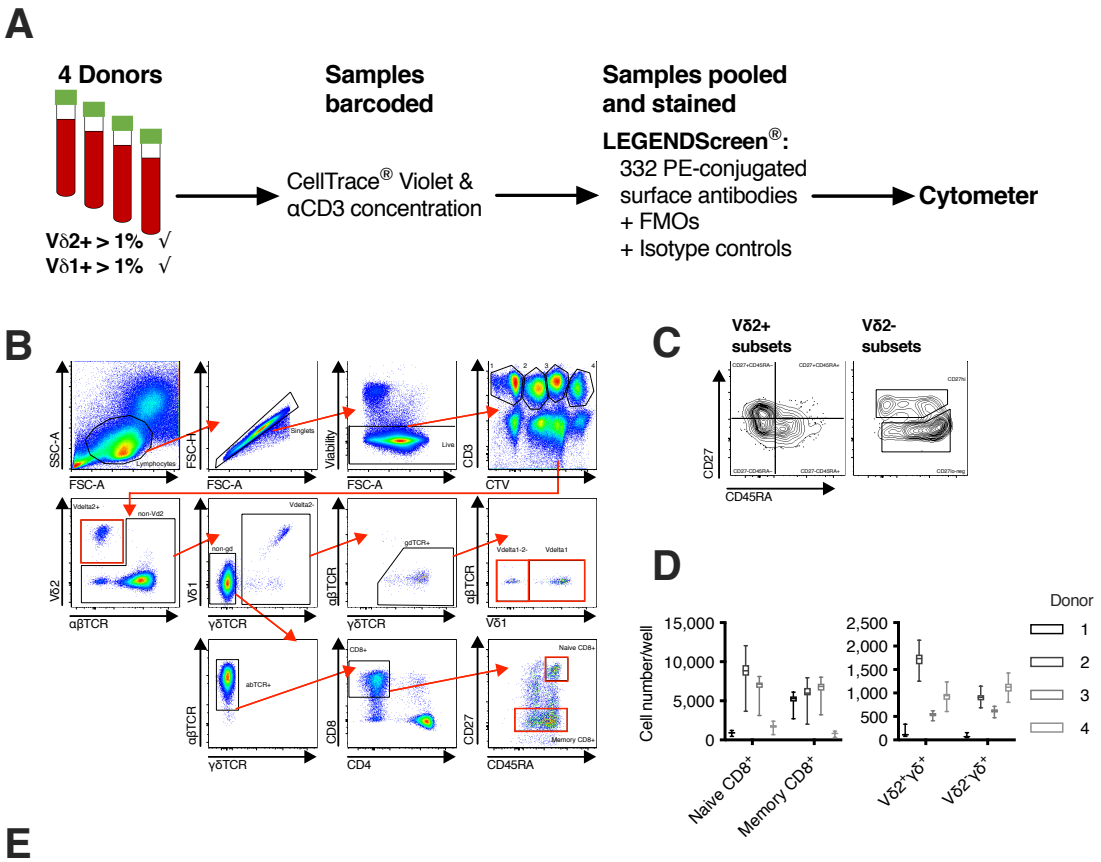
Conclusions and future work

This chapter has described the transcriptional and functional heterogeneity of human γδT cells, identified a transcriptional, phenotypic, and functional spectrum of Vδ2+ T cells, and uncovered previously unappreciated heterogeneity in naive non-Vδ2 T cells, including a CCR9+ population.

I would like to perform further work to examine the translational relevance of the Vδ2+ T cell effector spectrum in humans, in particular the hypothesis that certain chronic or recurring infections, such as malaria or HIV, could permanently shift the phenotype, and potentially the function, of Vδ2+ T cells in affected individuals. There are three aspects to this work. First, I would seek to confirm the shift in phenotypic and transcriptional profile directly, rather than through indirect analyses of published datasets. Second, I would evaluate whether this leads to altered responses to cytokine or TCR stimulation, and cytotoxic function. Third, I would examine whether these γδ T cell responses are redundant or critical; i.e. if total immune responses to biologically relevant stimuli - viral infection, vaccines, tumour cell lysis - are diminished in this setting.

The presence of CCR9+ naive γδ T cells in humans is also interesting, with relevance to mucosal immune responses and autoimmunity, as discussed. I would seek to investigate the functional properties of this CCR9+ population, through *in vitro* stimulation and chemotaxis assays. I would also seek to identify this population in umbilical cord and paediatric blood samples, as well as in GALT. Finally, more definitive analysis of peripheral and intestinal γδ TCR repertoires may shed light on the relevance of this population in the development of mucosal non-Vδ2 T cell populations.

5.8 Figures



E

	Cell subsets			
	CD8+ naïve	CD8+ memory	Vδ2+	Vδ2-
Mean	4584	4713	826.5	675.2
Range	456-12050	335-8017	78-2129	52-1430
Median	2760	5575	619.5	703
IQR	1105-7682	1342-6577	353.8-1250	235.5-981.8

Figure 5-1. Circulating γδ T cell surface marker phenotype - experimental plan, gating strategy, and cell numbers.

(A) Experimental scheme showing sample barcoding and staining.

(B) Representative flow cytometry gating scheme to deconvolute the four barcoded donor samples, and identify γδ T cell subsets and conventional CD8+ T cells.

(C) Representative flow cytometry plot of memory subsets for Vδ2+ T cells (4 populations identified by CD27 and CD45RA expression) and Vδ2- T cells (CD27hi and CD27lo/neg populations).

(D) Box and whiskers plot showing number of naive CD8+, memory CD8+, Vδ2+ γδ, and Vδ2- γδ T cells from each donor subject per well. Median and IQR displayed in box, with min-max range displayed in whiskers.

(E) Table showing number of naive CD8+, memory CD8+, Vδ2+ γδ, and Vδ2- γδ T cells from each donor subject (n=4) per well.

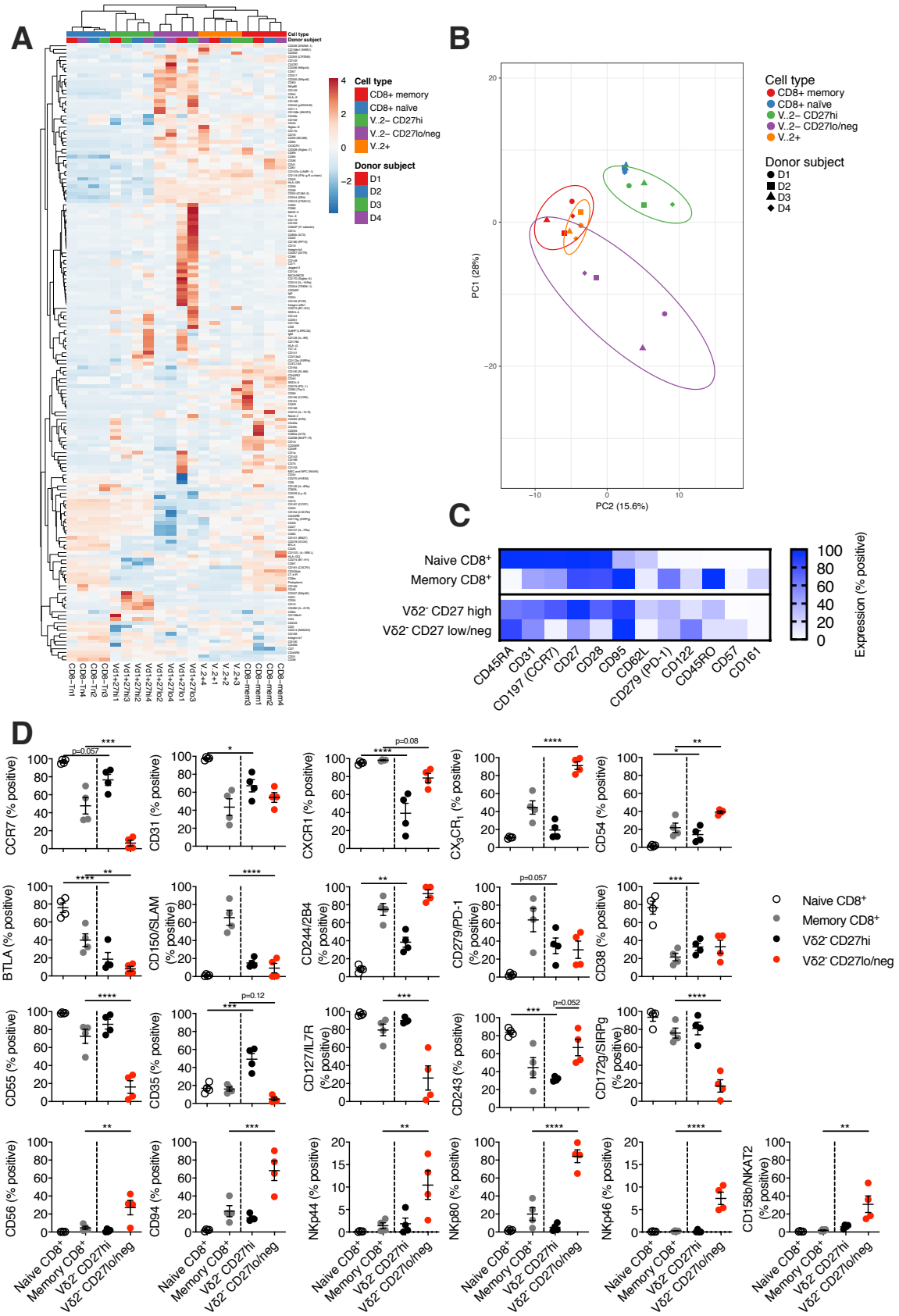

A
Cell type
CD8+ memory
CD8+ naïve
V..2– CD27hi
V..2– CD27lo/neg
V..2+
Donor subject
D1
D2
D3
D4
B
PC1 (28%)
PC2 (15.6%)
C
Naive CD8+
Memory CD8+
Vδ2- CD27 high
Vδ2- CD27 low/neg
CD45RA
CD31
CD197 (CCR7)
CD27
CD28
CD95
CD62L
CD279 (PD-1)
CD122
CD45RO
CD57
CD161
Expression (% positive)
D
CCR7 (% positive)
CD31 (% positive)
CXCR1 (% positive)
CX3CR1 (% positive)
CD54 (% positive)
BTLA (% positive)
CD150/SLAM (% positive)
CD244/2B4 (% positive)
CD279/PD-1 (% positive)
CD38 (% positive)
CD55 (% positive)
CD35 (% positive)
CD127/IL7R (% positive)
CD243 (% positive)
CD172g/SIRPg (% positive)
CD56 (% positive)
CD94 (% positive)
NKp44 (% positive)
NKp80 (% positive)
NKp46 (% positive)
CD158b/NKAT2 (% positive)
Naive CD8+
Memory CD8+
Vδ2- CD27hi
Vδ2- CD27lo/neg

Figure 5-2. CD27hi and CD27lo/neg non-Vδ2 T cells display analogous phenotypic profiles to naive and memory conventional CD8+ T cells respectively

(A) Heatmap and hierarchical clustering of the % of cells expressing 167 surface markers within naive CD8+ (CD8-Tn, blue), memory CD8+ (CD8-Tmem, red), Vδ2+ (Vd2, yellow), Vδ2- CD27hi (green), and Vδ2- CD27lo/neg (purple) T cell subsets (n=4 for all subsets).

(B) PCA plot of PCs 1 and 2 of the % of cells expressing 167 surface markers within naive CD8+ (CD8-Tn, blue), memory CD8+ (CD8-Tmem, red), Vδ2+ (Vd2, yellow), Vδ2- CD27hi (green), and Vδ2- CD27lo/neg (purple) T cell subsets (n=4 for all subsets).

(C) Mean % positive expression of surface markers associated with naive and memory states of conventional T cells on naive and memory CD8+ T cells and CD27hi and CD27lo/neg Vδ2- γδ T cells (n=4).

(D) Mean percentage (+/- SEM) of peripheral CD8+ and γδ T cells expressing CCR7, CD31, CXCR1, CX3CR1, CD54, BTLA, CD150/SLAM, CD244, CD279/PD-1, CD38, CD55, CD35, CD127/IL7R, CD243, CD172g/SIRPg, CD56, CD94, NKp44, NKp80, NKp46, and CD158b/NKAT2 (n=4). Naive CD8+ T cells, black open circles; memory CD8+ T cells, grey; CD27hi Vδ2- T cells, black; CD27lo/neg Vδ2- T cells, red.

Statistical analysis performed with one-way ANOVA with Sidak's multiple comparisons test. *, $P \leq 0.05$; **, $P \leq 0.01$; ***, $P \leq 0.001$; ****, $P \leq 0.0001$.

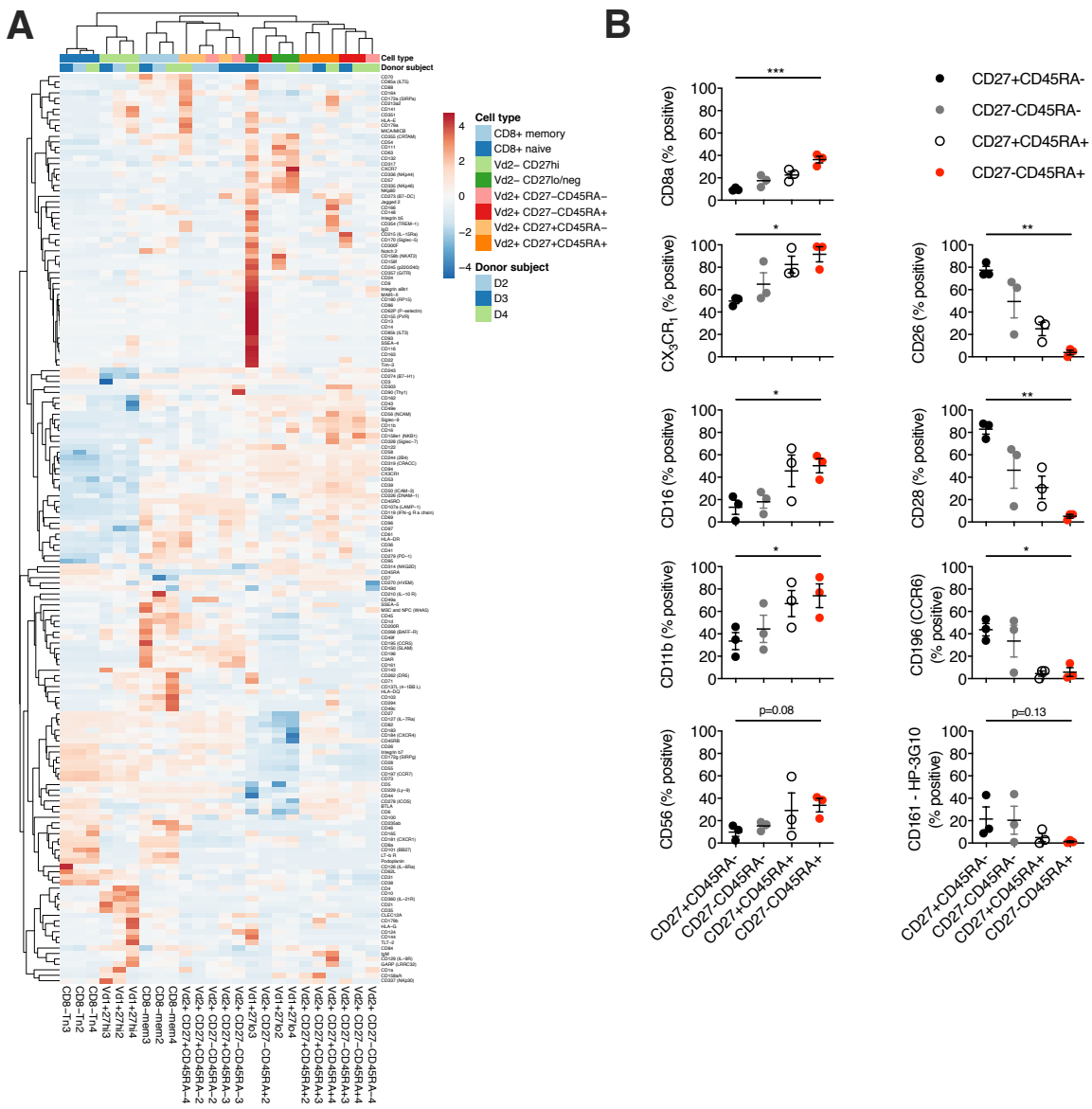


Figure 5-3. CD27/CD45RA Vδ2+ T cell subsets do not separate into naive and memory phenotypic profiles.

(A) Heatmap and hierarchical clustering of the % of cells expressing 167 surface markers within naive CD8+ (dark blue), memory CD8+ (light blue), Vδ2- CD27hi (light green), and Vδ2- CD27lo/neg (dark green) Vδ2+ CD27-CD45RA- (pink), Vδ2+ CD27-CD45RA+ (red), Vδ2+ CD27+CD45RA- (yellow), Vδ2+ CD27+CD45RA+ (orange) T cell subsets (n=3 for all subsets).

(B) Mean percentage (+/- SEM) of peripheral Vδ2+ γδ T cells expressing CD8a, CX3CR1, CD16, CD11b, CD56, CD26, CD28, CD196/CCR6, and CD161 (n=4). CD27+CD45RA-, black circles; CD27-CD45RA-, grey; CD27+CD45RA+, black open circles; CD27-CD45RA+, red.

Statistical analysis performed with multiple t-tests in (C), and one-way ANOVA with Sidak's multiple comparisons test in (D). *, P ≤ 0.05; **, P ≤ 0.01; ***, P ≤ 0.001; ****, P ≤ 0.0001.

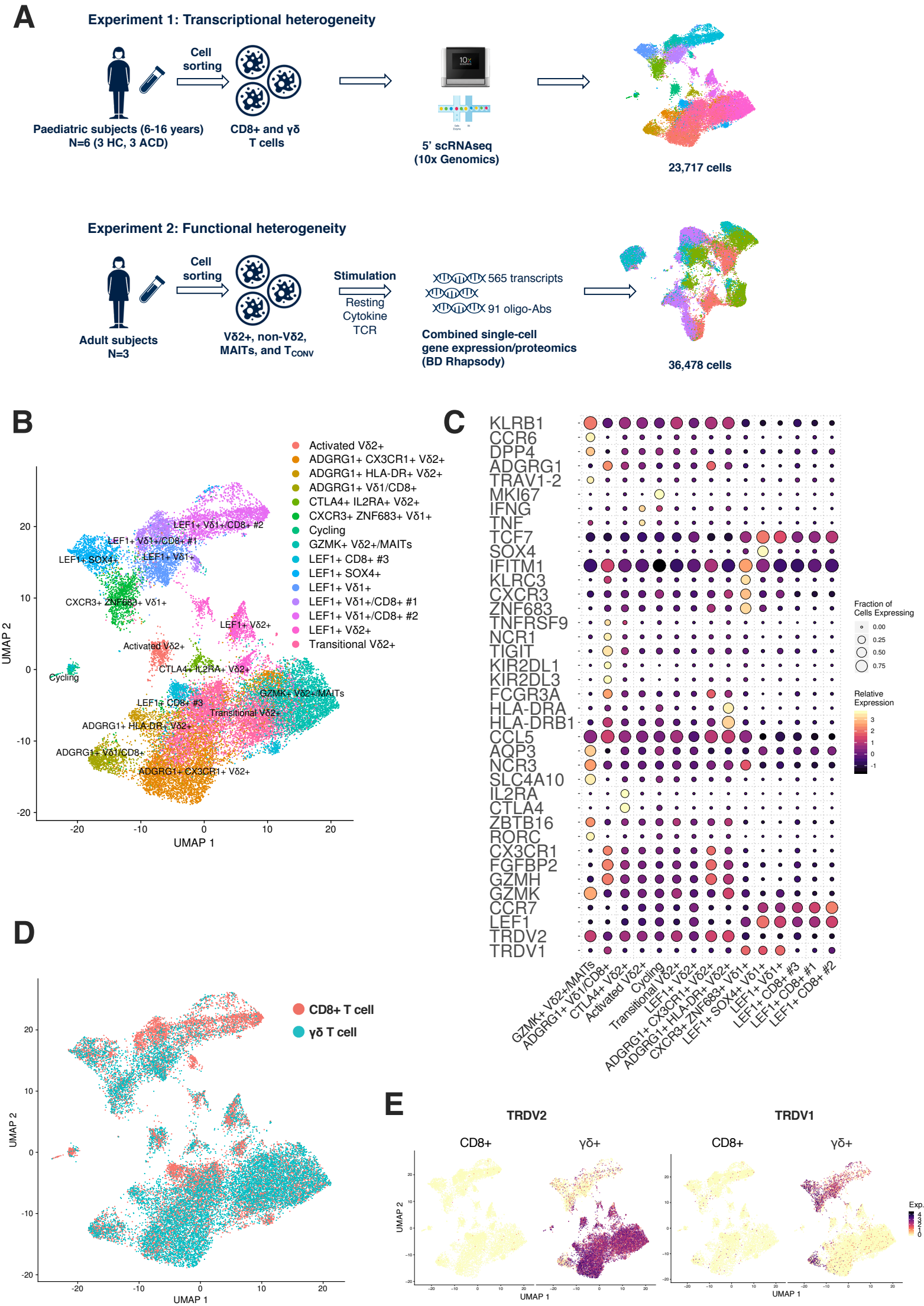

A
Experiment 1: Transcriptional heterogeneity
Cell sorting
Paediatric subjects (6-16 years)
N=6 (3 HC, 3 ACD)
CD8+ and γδ T cells
5' scRNAseq
(10x Genomics)
23,717 cells
Experiment 2: Functional heterogeneity
Cell sorting
Adult subjects
N=3
Vδ2+, non-Vδ2, MAITs, and T_CONV
Stimulation
Resting
Cytokine
TCR
565 transcripts
91 oligo-Abs
Combined single-cell gene expression/proteomics (BD Rhapsody)
36,478 cells
B
Activated Vδ2+
ADGRG1+ CX3CR1+ Vδ2+
ADGRG1+ HLA-DR+ Vδ2+
ADGRG1+ Vδ1/CD8+
CTLA4+ IL2RA+ Vδ2+
CXCR3+ ZNF683+ Vδ1+
Cycling
GZMK+ Vδ2+/MAITs
LEF1+ CD8+ #3
LEF1+ SOX4+
LEF1+ Vδ1+
LEF1+ Vδ1+/CD8+ #1
LEF1+ Vδ1+/CD8+ #2
LEF1+ Vδ2+
Transitional Vδ2+
UMAP 1
UMAP 2
C
KLRB1
CCR6
DPP4
ADGRG1
TRAV1-2
MKI67
IFNG
TNF
TCF7
SOX4
IFITM1
KLRC3
CXCR3
ZNF683
TNFRSF9
NCR1
TIGIT
KIR2DL1
KIR2DL3
FCGR3A
HLA-DRA
HLA-DRB1
CCL5
AQP3
NCR3
SLC4A10
IL2RA
CTLA4
ZBTB16
RORC
CX3CR1
FGFBP2
GZMH
GZMK
CCR7
LEF1
TRDV2
TRDV1
GZMK+ Vδ2+/MAITs
ADGRG1+ Vδ1/CD8+
CTLA4+ Vδ2+
Activated Vδ2+
Cycling
Transitional Vδ2+
LEF1+ Vδ2+
ADGRG1+ CX3CR1+ Vδ2+
ADGRG1+ HLA-DR+ Vδ2+
CXCR3+ ZNF683+ Vδ1+
LEF1+ SOX4+ Vδ1+
LEF1+ Vδ1+
LEF1+ CD8+ #3
LEF1+ CD8+ #1
LEF1+ CD8+ #2
Fraction of Cells Expressing
0.00
0.25
0.50
0.75
Relative Expression
3
2
1
0
-1
D
CD8+ T cell
γδ T cell
UMAP 1
UMAP 2
E
TRDV2
TRDV1
CD8+
γδ+
CD8+
γδ+
UMAP 1
UMAP 2
Exp.
4
3
2
1
0

Figure 5-4. The single-cell transcriptional landscape of circulating CD8+ and γδ+ T cells highlights distinct properties of Vδ1+ and Vδ2+ γδ+ T cells

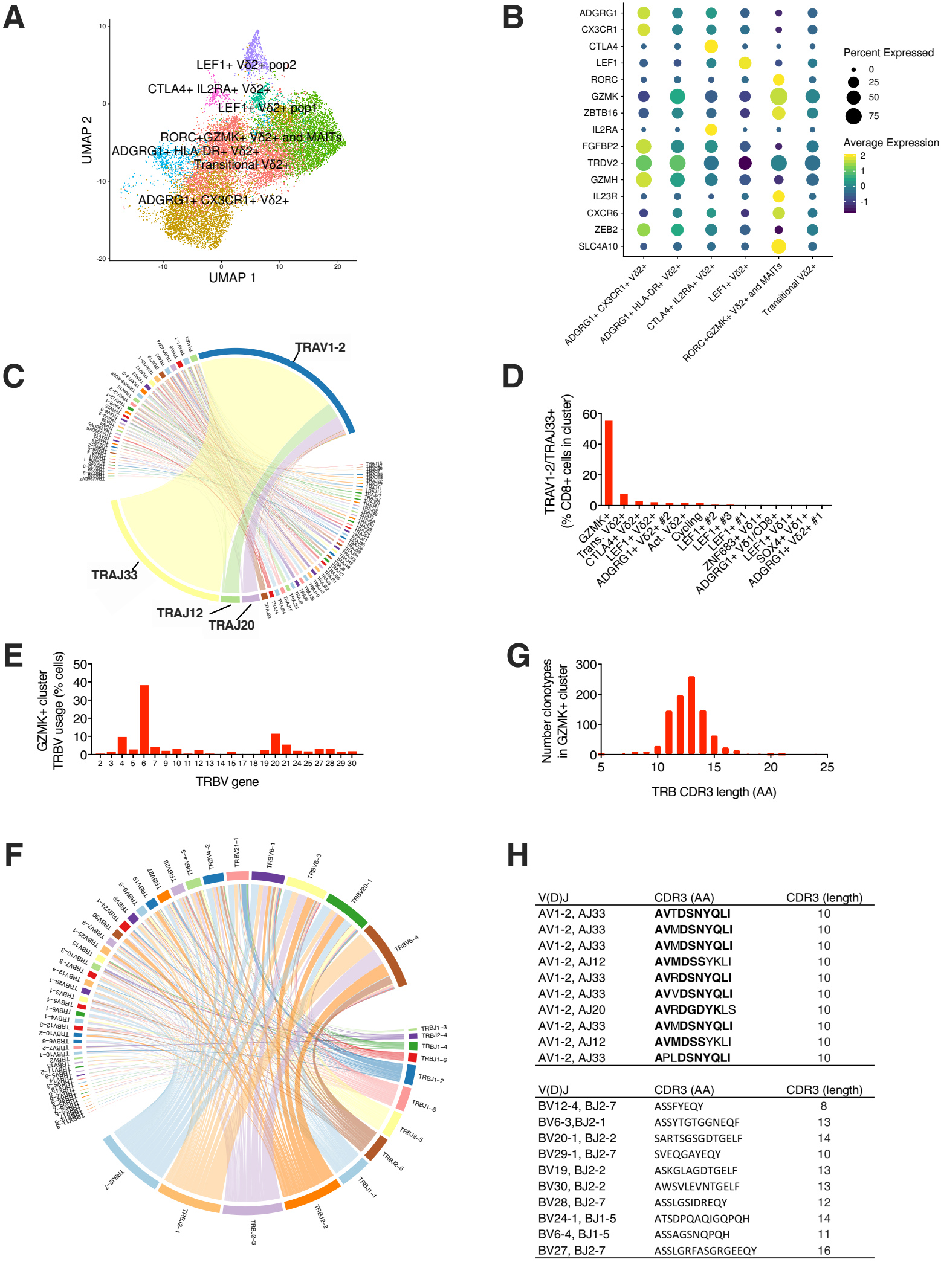
(A) Schematic diagram of two key scRNAseq experiments. Experiment 1 characterised transcriptional heterogeneity at rest of circulating γδ T cells using 5' scRNAseq (10x Genomics). Experiment 2 characterised transcriptional and phenotypic heterogeneity and functional responses in response to stimulation using targeted single-cell gene and protein expression (BD Rhapsody). Study subject and cell numbers are indicated. HC, healthy control; ACD, active coeliac disease.

(B) UMAP plot of 23,717 circulating CD8+ and γδ+ T cells from six donor subjects. 15 transcriptionally distinct clusters are identified.

(C) Bubble plot of key gene identifiers for the 15 clusters identified in the dataset. Bubble size indicates the proportion of cells in which the gene is present. Colour intensity indicates the expression level of the gene in cells in that cluster.

(D) UMAP plot with predicted CD8+ (red) or γδ+ (teal) T cell identity illustrated.

(E) UMAP plots for predicted CD8+ T cells (left) and γδ+ T cells (right) overlaid with the expression of TRDV2 and TRDV1.



V(D)J	CDR3 (AA)	CDR3 (length)
AV1-2, AJ33	**AVTDSNYQLI**	10
AV1-2, AJ33	**AVMDSNYQLI**	10
AV1-2, AJ33	**AVMDSNYQLI**	10
AV1-2, AJ12	**AVMDSS**YKLI	10
AV1-2, AJ33	**AVRDSNYQLI**	10
AV1-2, AJ33	**AVVDSNYQLI**	10
AV1-2, AJ20	**AVRDGDYK**LS	10
AV1-2, AJ33	**AVMDSNYQLI**	10
AV1-2, AJ12	**AVMDSS**YKLI	10
AV1-2, AJ33	**APLDSNYQLI**	10

V(D)J	CDR3 (AA)	CDR3 (length)
BV12-4, BJ2-7	ASSFYEQY	8
BV6-3,BJ2-1	ASSYTGTGGNEQF	13
BV20-1, BJ2-2	SARTSGSGDTGELF	14
BV29-1, BJ2-7	SVEQGAYEQY	10
BV19, BJ2-2	ASKGLAGDTGELF	13
BV30, BJ2-2	AWSVLEVNTGELF	13
BV28, BJ2-7	ASSLGSIDREQY	12
BV24-1, BJ1-5	ATSDPQAQIGQPQH	14
BV6-4, BJ1-5	ASSAGSNQPQH	11
BV27, BJ2-7	ASSLGRFASGRGEEQY	16

Figure 5-5. GZMK+ Vδ2+ and MAIT cells share a transcriptional profile

(A) UMAP plot of circulating Vδ2+ γδ+ T cells from six donor subjects. 6 transcriptionally distinct clusters are identified.

(B) Bubble plot of key gene identifiers for the 6 clusters of Vδ2+ γδ+ T cells . Bubble size indicates the proportion of cells in which the gene is present. Colour intensity indicates the expression level of the gene in cells in that cluster.

(C) Chord diagram of paired TRAV-TRAJ gene usage of CD8+ T cells in the GZMK+ cluster.

(D) Proportion of CD8+ T cell clonotypes expressing the TRAV1-2/TRAJ33 TCRα in each cluster.

(E) Proportion of clonotypes in the GZMK+ cluster containing different TRBV genes.

(F) Chord diagram of paired TRBV-TRBJ gene usage of CD8+ T cells in the GZMK+ cluster.

(G) Histogram of TRB CDR3 length of GZMK+ cluster clonotypes.

(H) V(D)J gene usage, CDR3 amino acid (AA) sequence, and CDR3 AA length of the 10 most common TRA (top) and TRB (bottom) clonotypes in the GZMK+ cluster. TRA CDR3 amino acids consistent with canonical MAIT cell sequences from prior studies are in bold(Lepore et al., 2014; Tilloy et al., 1999).

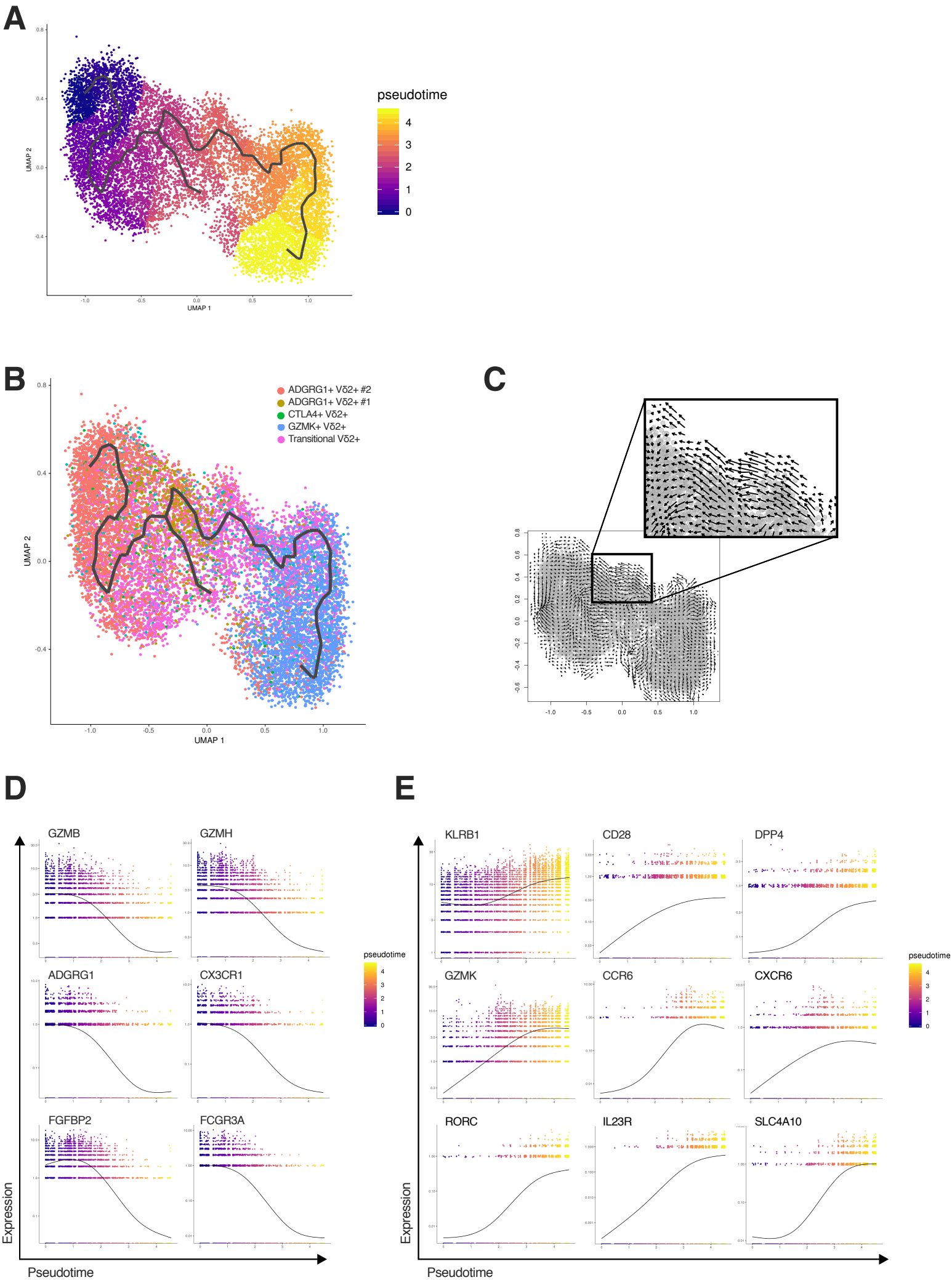

A
pseudotime
4
3
2
1
0
UMAP 2
UMAP 1
B
ADGRG1+ Vδ2+ #2
ADGRG1+ Vδ2+ #1
CTLA4+ Vδ2+
GZMK+ Vδ2+
Transitional Vδ2+
UMAP 2
UMAP 1
C
D
GZMB
GZMH
ADGRG1
CX3CR1
FGFBP2
FCGR3A
pseudotime
Expression
Pseudotime
E
KLRB1
CD28
DPP4
GZMK
CCR6
CXCR6
RORC
IL23R
SLC4A10
pseudotime
Expression
Pseudotime

Figure 5-6. Vδ2+ γδ T cell transcriptional heterogeneity is dominated by a spectrum of effector function.

Pseudotime trajectory of gene expression of Vδ2+ γδ+ T cells, coloured by pseudotime axis (A), and cluster identity (B).

RNA velocity (the time derivative of gene expression, calculated by integration of the ratio of unspliced/spliced mRNA) is overlaid (C), with arrow direction pointing to predicted future transcriptional state. Inset shows RNA direction at the border of GZMK+ and Transitional Vδ2+ clusters.

(D) Single-cell gene expression along pseudotime of selected genes which decrease with pseudotime.

(E) Single-cell gene expression along pseudotime of selected genes which increase with pseudotime.

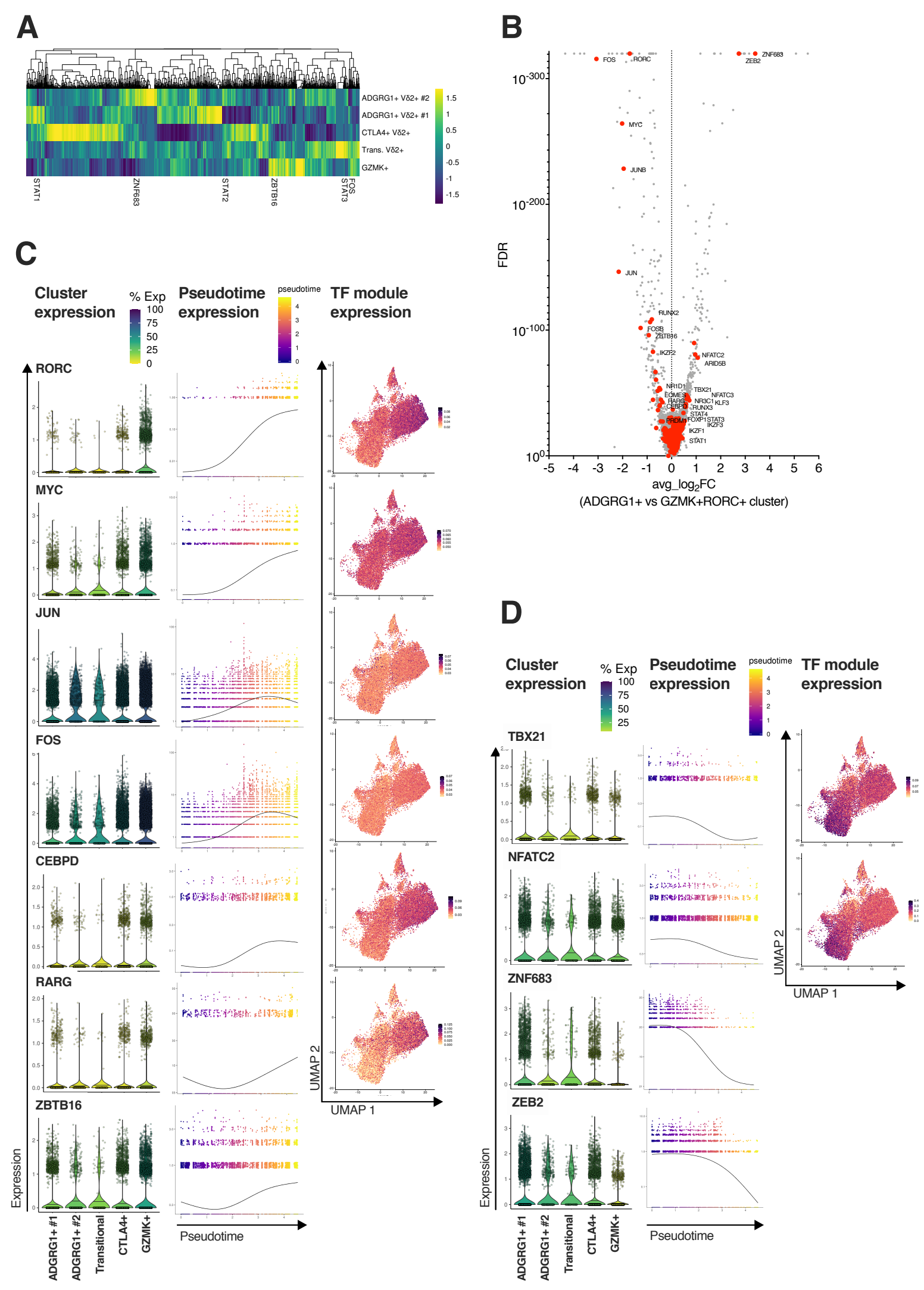

A
ADGRG1+ Vδ2+ #2
ADGRG1+ Vδ2+ #1
CTLA4+ Vδ2+
Trans. Vδ2+
GZMK+
1.5
1
0.5
0
-0.5
-1
-1.5
STAT1
ZNF683
STAT2
ZBTB16
FOS
STAT3
B
FDR
10^{-300}
10^{-200}
10^{-100}
10^{0}
FOS
RORC
ZNF683
ZEB2
MYC
JUNB
JUN
RUNX2
FOSB
ZBTB16
IKZF2
NFATC2
ARID5B
NR1D1
TBX21
NFATC3
EGMES
RARG
NR3C1
KLF3
CEBPD
RUNX3
STAT4
PRDM1
FOXP1
STAT3
IKZF3
IKZF1
STAT1
-5 -4 -3 -2 -1 0 1 2 3 4 5 6
avg_log2FC
(ADGRG1+ vs GZMK+RORC+ cluster)
C
Cluster expression
% Exp
100
75
50
25
0
Pseudotime expression
pseudotime
4
3
2
1
0
TF module expression
RORC
MYC
JUN
FOS
CEBPD
RARG
ZBTB16
Expression
ADGRG1+ #1
ADGRG1+ #2
Transitional
CTLA4+
GZMK+
Pseudotime
UMAP 2
UMAP 1
D
Cluster expression
% Exp
100
75
50
25
Pseudotime expression
pseudotime
4
3
2
1
0
TF module expression
TBX21
NFATC2
ZNF683
ZEB2
Expression
ADGRG1+ #1
ADGRG1+ #2
Transitional
CTLA4+
GZMK+
Pseudotime
UMAP 2
UMAP 1

Figure 5-7: Transcriptional regulation varies along the Vδ2+ T cell spectrum

(A) Heatmap of transcription factor expression within Vδ2+ T cell clusters. Transcription factors identified from Lambert et al., 2018(Lambert et al., 2018).

(B) Volcano plot of differentially expressed genes between ADGRG1+ and GZMK+ clusters of Vδ2+ T cells, transcription factors of interest marked in red.

(C) Expression of transcription factors of interest associated with the GZMK+ effector cluster. Violin plot of TF expression within effector clusters (left), TF expression along pseudotime (centre), and expression of TF gene modules overlaid onto UMAP plots (right, if available) are displayed.

(D) Expression of transcription factors of interest associated with the ADGRG1+ effector clusters. Violin plot of TF expression within effector clusters (left), TF expression along pseudotime (centre), and expression of TF gene modules overlaid onto UMAP plots (right, if available) are displayed.

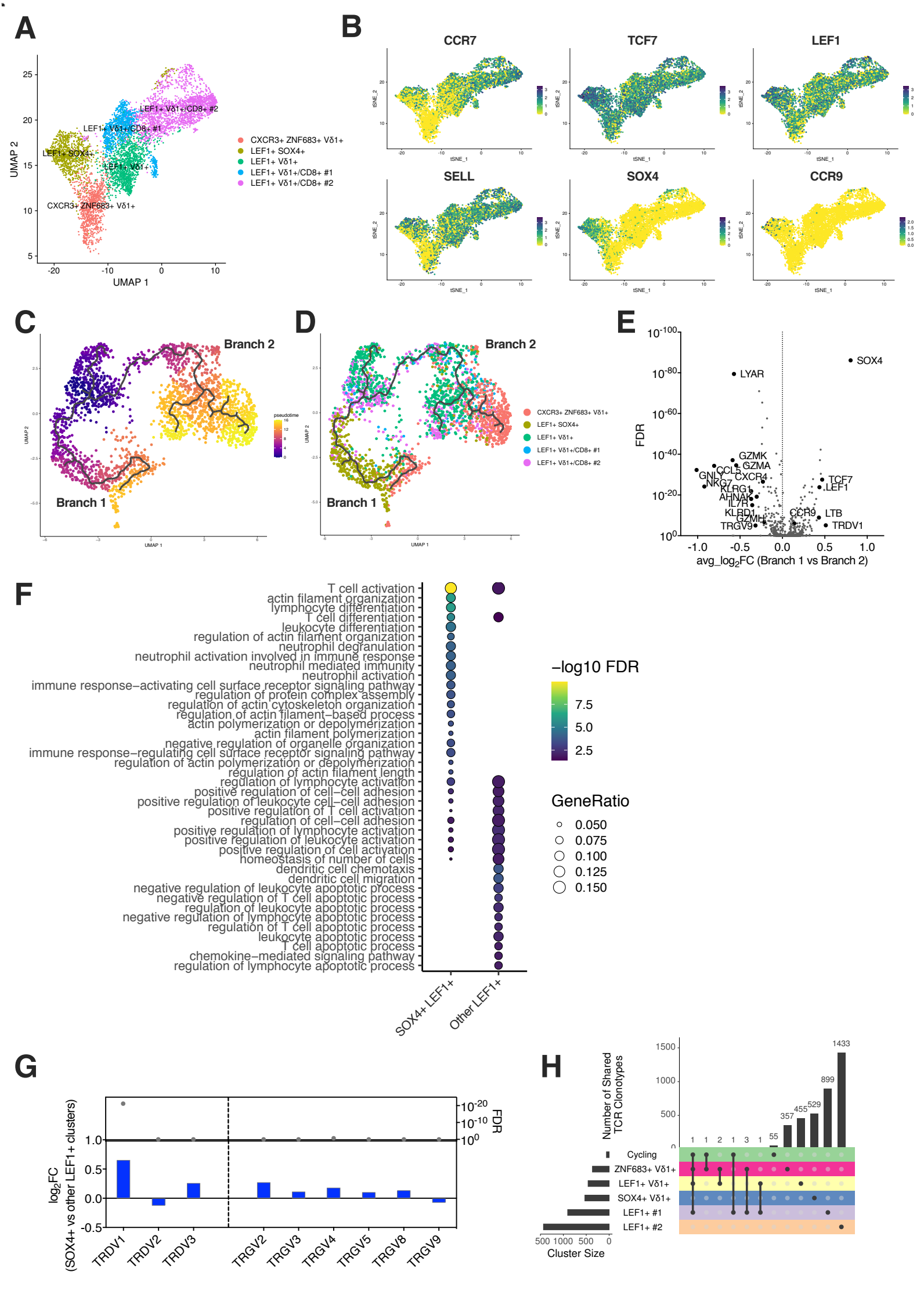

A
UMAP 2
UMAP 1
LEF1+ Vδ1+/CD8+ #2
LEF1+ Vδ1+/CD8+ #1
LEF1+ SOX4+
LEF1+ Vδ1+
CXCR3+ ZNF683+ Vδ1+
CXCR3+ ZNF683+ Vδ1+
LEF1+ SOX4+
LEF1+ Vδ1+
LEF1+ Vδ1+/CD8+ #1
LEF1+ Vδ1+/CD8+ #2
B
CCR7
TCF7
LEF1
SELL
SOX4
CCR9
tSNE_1
tSNE_2
C
Branch 2
Branch 1
pseudotime
UMAP 1
UMAP 2
D
Branch 2
Branch 1
CXCR3+ ZNF683+ Vδ1+
LEF1+ SOX4+
LEF1+ Vδ1+
LEF1+ Vδ1+/CD8+ #1
LEF1+ Vδ1+/CD8+ #2
E
FDR
SOX4
LYAR
GZMK
GZMA
CCL5
GNLY
CXCR4
NKG7
KLRG1
AHNAK
IL7R
KLRD1
GZMH
TRGV9
CCR9
LTB
TRDV1
TCF7
LEF1
avg_log2FC (Branch 1 vs Branch 2)
F
T cell activation
actin filament organization
lymphocyte differentiation
T cell differentiation
leukocyte differentiation
regulation of actin filament organization
neutrophil degranulation
neutrophil activation involved in immune response
neutrophil mediated immunity
neutrophil activation
immune response−activating cell surface receptor signaling pathway
regulation of protein complex assembly
regulation of actin cytoskeleton organization
regulation of actin filament−based process
actin polymerization or depolymerization
actin filament polymerization
negative regulation of organelle organization
immune response−regulating cell surface receptor signaling pathway
regulation of actin polymerization or depolymerization
regulation of actin filament length
regulation of lymphocyte activation
positive regulation of cell−cell adhesion
positive regulation of leukocyte cell−cell adhesion
positive regulation of T cell activation
regulation of cell−cell adhesion
positive regulation of lymphocyte activation
positive regulation of leukocyte activation
positive regulation of cell activation
homeostasis of number of cells
dendritic cell chemotaxis
dendritic cell migration
negative regulation of leukocyte apoptotic process
negative regulation of T cell apoptotic process
regulation of leukocyte apoptotic process
negative regulation of lymphocyte apoptotic process
regulation of T cell apoptotic process
leukocyte apoptotic process
T cell apoptotic process
chemokine−mediated signaling pathway
regulation of lymphocyte apoptotic process
SOX4+ LEF1+
Other LEF1+
−log10 FDR
7.5
5.0
2.5
GeneRatio
0.050
0.075
0.100
0.125
0.150
G
log2FC (SOX4+ vs other LEF1+ clusters)
FDR
TRDV1
TRDV2
TRDV3
TRGV2
TRGV3
TRGV4
TRGV5
TRGV8
TRGV9
H
Number of Shared TCR Clonotypes
Cycling
ZNF683+ Vδ1+
LEF1+ Vδ1+
SOX4+ Vδ1+
LEF1+ #1
LEF1+ #2
Cluster Size

Figure 5-8: Non-Vδ2 γδ T cells show heterogeneity in naive subsets, and NK-like effector features.
(A) UMAP plot of closely related naive and early memory Vδ2- γδ+ T cells from six donor subjects (Experiment 1). 5 transcriptionally distinct clusters are identified.
(B) Gene expression of *CCR7*, *TCF7*, *LEF1* , *SELL*, *SOX4*, and *CCR9* overlaid over Vδ2- γδ+ T cell UMAP plot.
Pseudotime trajectory of gene expression of Vδ2- γδ+ T cells (C) delineates two trajectories within the naive to early memory spectrum. (D) The cluster identity of cells is illustrated.
(E) Volcano plot of differentially expressed genes between pseudotime branch 1 and branch 2 Vδ2- γδ+ T cells, with genes of interest labelled.
(F) GO terms with enriched gene expression in branch 1 (B1) and branch 2 (B2) cell populations. Dot size indicates the gene ratio; dot colour indicates the false discovery rate value.
(G) Fold change (log_2) of *TRDV* and *TRGV* gene expression between SOX4+ cluster cells and other LEF1+ cluster cells.
(H) Upset plot displaying shared TCR clonotypes between naive and early memory Vδ2- T cell clusters, with shared clonotypes visualized as an 'interaction', indicated by a black circle joined by black lines. Bars above indicate the total number of shared TCR clonotypes for that interaction. Bars to left indicate number of clonotypes in the cluster. Cluster intersections with no shared TCR clonotypes are not shown.

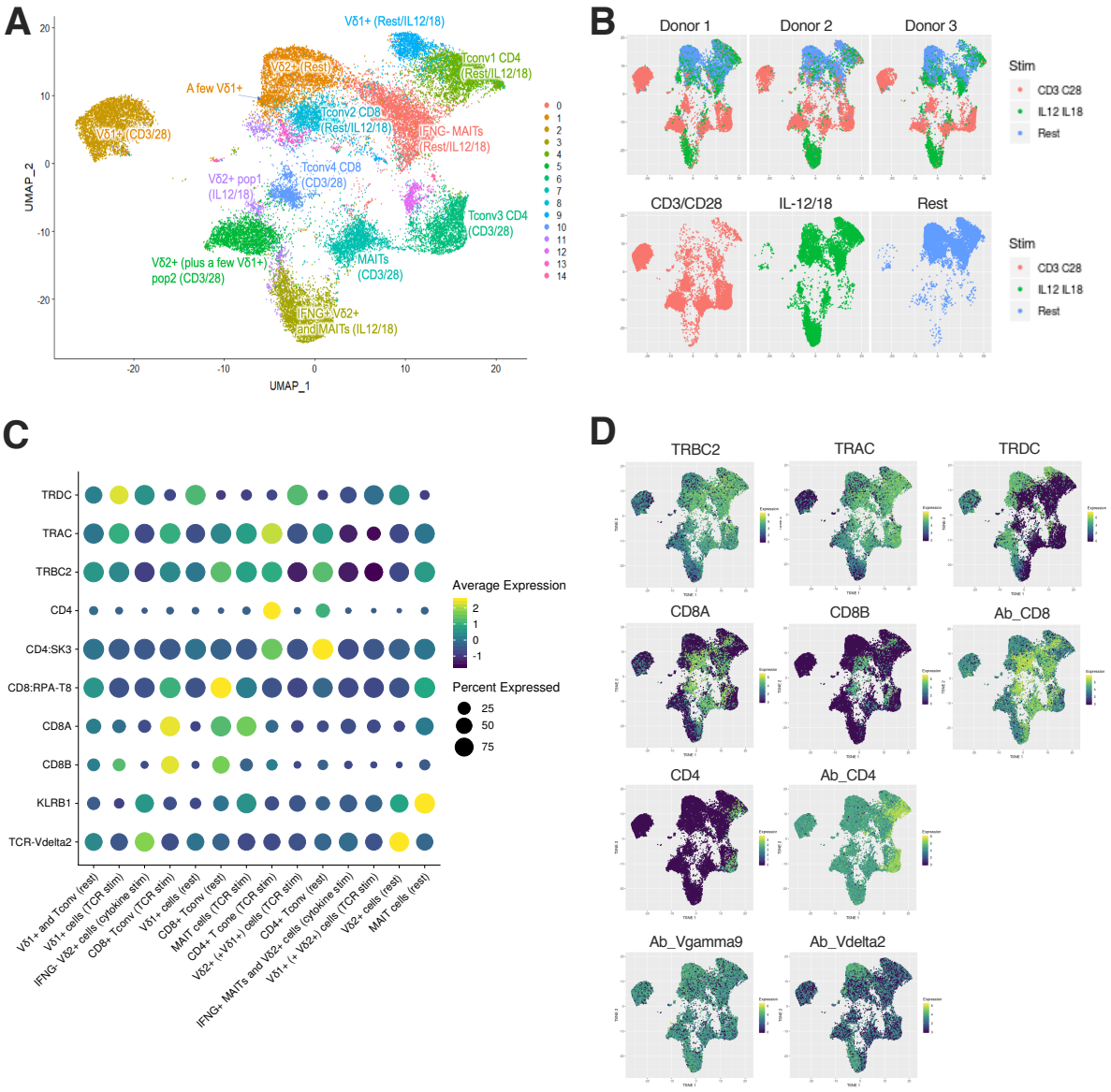


Figure 5-9: Single-cell targeted gene and surface protein expression of stimulated conventional and innate-like T cells.

(A) UMAP plot of sorted Vδ1+, Vδ2+ γδ+ T cells, MAIT cells, and CD4+ and CD8+ conventional T cells from three donors. Cells were either unstimulated, or stimulated with combinatorial cytokine (IL-12/IL-18) or TCR ligation (CD3/CD28) for 20 hours.

(B) Split UMAPs (as above) with panels divided by donor (top) and stimulation condition (bottom) after batch correction.

(C) Bubble plot of lineage and subset gene and protein expression for each cluster. Bubble size indicates the proportion of cells in which the gene is present. Colour intensity indicates the expression level of the gene in cells in that cluster.

(D) UMAP plot overlaid with gene or protein expression of lineage and subset markers.

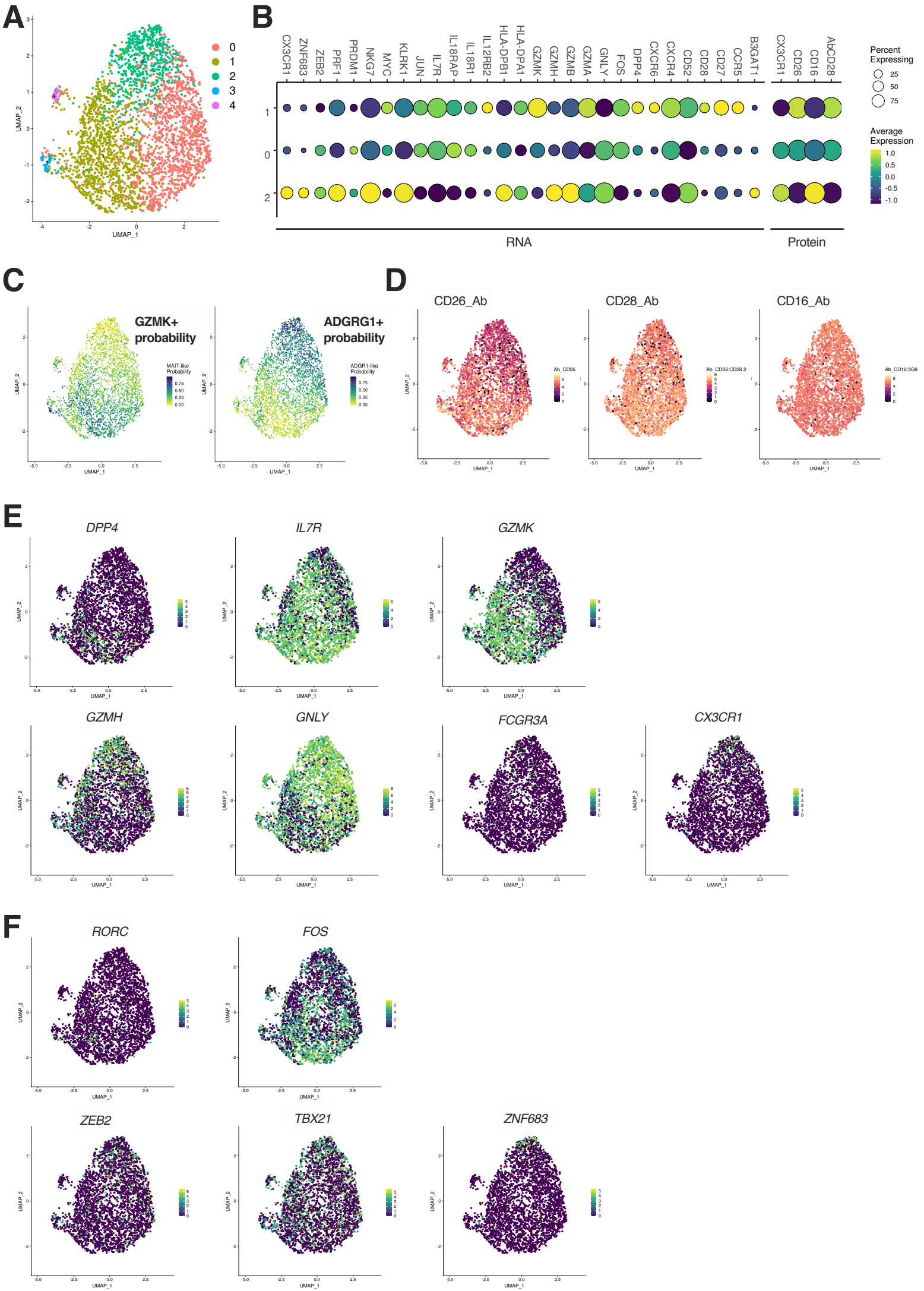

A
B
C
D
E
F
UMAP_1
UMAP_2
0
1
2
3
4
CX3CR1
ZNF683
ZEB2
PRF1
PRDM1
NKG7
MYC
KLRK1
JUN
IL7R
IL18RAP
IL18R1
IL12RB2
HLA-DPB1
HLA-DPA1
GZMK
GZMH
GZMB
GZMA
GNLY
FOS
DPP4
CXCR6
CXCR4
CD52
CD28
CD27
CCR5
B3GAT1
CX3CR1
CD26
CD16
AbCD28
RNA
Protein
Percent Expressing
25
50
75
Average Expression
1.0
0.5
0.0
-0.5
-1.0
GZMK+ probability
MAIT-like Probability
ADGRG1+ probability
ADGR1-like Probability
CD26_Ab
CD28_Ab
CD16_Ab
Ab_CD26
Ab_CD28:CD28.2
Ab_CD16:3G8
DPP4
IL7R
GZMK
GZMH
GNLY
FCGR3A
CX3CR1
RORC
FOS
ZEB2
TBX21
ZNF683

Figure 5-10: Single-cell targeted gene and surface protein expression replicates the transcriptional spectrum of effector Vδ2+ T cells.

(A) UMAP plot of unstimulated Vδ2+ γδ+ T cells from 3 healthy adult donors demonstrate five clusters.

(B) Bubble plot of key genes and proteins of interest for the 3 major clusters of Vδ2+ γδ+ T cells. Bubble size indicates the proportion of cells in which the gene is present. Colour intensity indicates the expression level of the gene in cells in that cluster.

(C) UMAP plot of unstimulated Vδ2+ γδ+ T cells, overlaid with the per-cell probability of belonging to the MAIT-like GZMK+ cluster (left) or ADGRG1+ cluster (right) based on gene expression.

(D) UMAP plot of unstimulated Vδ2+ γδ+ T cells overlaid with the expression of surface marker proteins showing differential expression in the major clusters. The proteins CD26, CD28, and CD16 are displayed.

(E) UMAP plot of unstimulated Vδ2+ γδ+ T cells overlaid with the expression of genes showing differential expression in the major clusters. The genes *DPP4*, *IL7R*, *GZMK*, *CX3CR1*, *GZMH*, *GNLY*, and *FCGR3A* are displayed.

(F) UMAP plot of unstimulated Vδ2+ γδ+ T cells overlaid with the expression of transcription factors showing differential expression in the major clusters. The genes *RORC*, *FOS*, *ZEB2*, *TBX21*, and *ZNF683* are displayed.

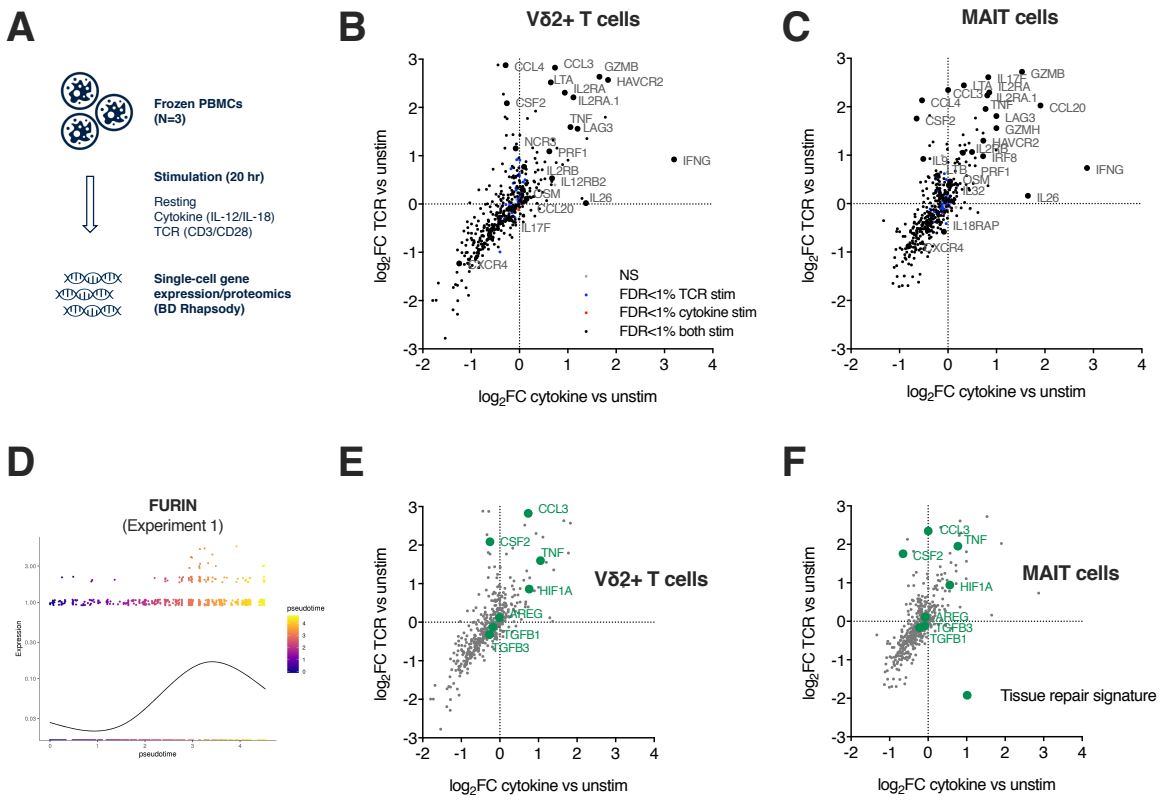


Figure 5-11: Vδ2+ T cells demonstrate MAIT-like responses to stimulation.

(A) Schematic diagram illustrating stimulation conditions for functional single-cell heterogeneity experiment.

Scatter plot of log_2 fold change (log_2FC) of cytokine-stimulated vs unstimulated cells (x-axis) against log_2FC of TCR-stimulated vs unstimulated cells (y-axis) for Vδ2+ T cells (B) and MAIT cells (C). FDR<1% for TCR stimulation, blue; FDR<1% for cytokine stimulation, red; FDR<1% for both conditions, black (with grey labels).

(D) FURIN expression along pseudotime from Experiment 1, showing enrichment of FURIN in the GZMK+ Vδ2+ end of the transcriptional spectrum.

Scatter plot of log_2 fold change (log_2FC) of cytokine-stimulated vs unstimulated cells (x-axis) against log_2FC of TCR-stimulated vs unstimulated cells (y-axis) for Vδ2+ T cells (E) and MAIT cells (F). Genes associated with tissue repair are highlighted in green(Leng et al., 2019; Linehan et al., 2018).

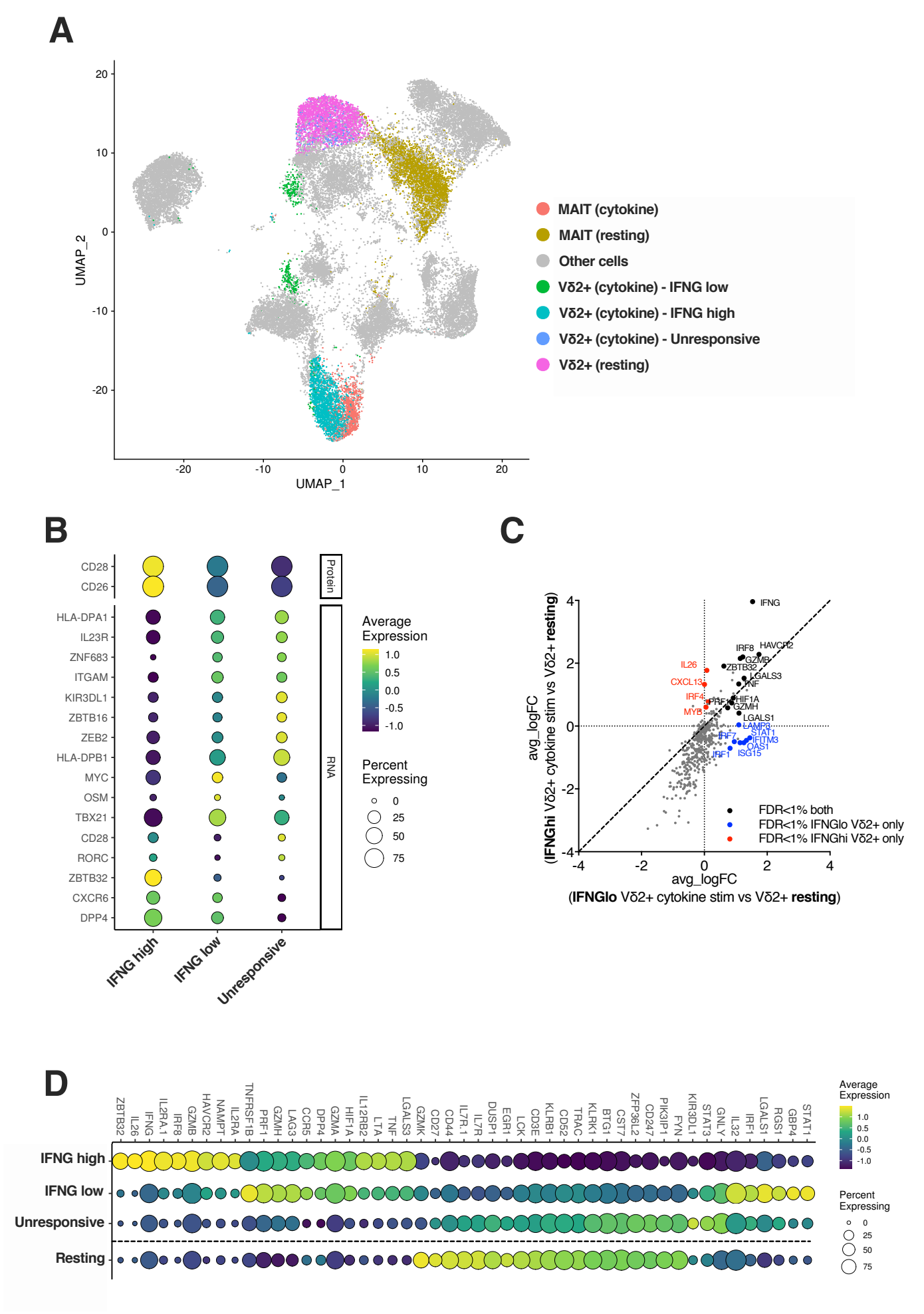

A
UMAP_2
UMAP_1
MAIT (cytokine)
MAIT (resting)
Other cells
Vδ2+ (cytokine) - IFNG low
Vδ2+ (cytokine) - IFNG high
Vδ2+ (cytokine) - Unresponsive
Vδ2+ (resting)
B
CD28
CD26
Protein
HLA-DPA1
IL23R
ZNF683
ITGAM
KIR3DL1
ZBTB16
ZEB2
HLA-DPB1
MYC
OSM
TBX21
CD28
RORC
ZBTB32
CXCR6
DPP4
RNA
IFNG high
IFNG low
Unresponsive
Average Expression
Percent Expressing
C
avg_logFC
(IFNGhi Vδ2+ cytokine stim vs Vδ2+ resting)
(IFNGlo Vδ2+ cytokine stim vs Vδ2+ resting)
FDR<1% both
FDR<1% IFNGlo Vδ2+ only
FDR<1% IFNGhi Vδ2+ only
D
IFNG high
IFNG low
Unresponsive
Resting
Average Expression
Percent Expressing

Figure 5-12: Vδ2+ T cells demonstrate heterogeneity in functional responses to cytokine stimulation.

(A) UMAP plot, with resting and cytokine-stimulated Vδ2+ and MAIT cell clusters highlighted. Resting MAIT cells, gold; Cytokine-stimulated MAIT cells, red; Resting Vδ2+ T cells, pink; Unresponsive cytokine-stimulated Vδ2+ T cells, purple, IFNG-low cytokine-stimulated Vδ2+ T cells, green; IFNG-high cytokine-stimulated Vδ2+ T cells, teal.

(B) Bubble plot of selected phenotypic markers and transcription factors in cytokine-stimulated Vδ2+ γδ+ T cells, categorised by their response to stimulation - unresponsive (remain clustered with the resting cells), IFNG-low cluster (cluster 11), and IFNG-high cluster (cluster 3, co-clustering with cytokine-stimulated MAIT cells). Bubble size indicates the proportion of cells in which the gene is present. Colour intensity indicates the expression level of the gene in cells in that cluster.

(C) Scatter plot of $\log_2$ fold change ($\log_2$FC) of cytokine-stimulated IFNG-low vs unstimulated Vδ2+ γδ+ T cells (x-axis) against $\log_2$FC of cytokine-stimulated IFNG-high vs unstimulated Vδ2+ γδ+ T cells (y-axis). Increased expression and FDR<1% for IFNG-low cluster, blue; Increased expression and FDR<1% for IFNG-high cluster, red; Increased expression and FDR<1% for both clusters, black (with grey labels).

(D) Bubble plot of genes altered by cytokine stimulation in Vδ2+ γδ+ T cells, categorised by their response to stimulation - unresponsive (remain clustered with the resting cells), IFNG-low cluster (cluster 11), and IFNG-high cluster (cluster 3, co-clustering with cytokine-stimulated MAIT cells). Unstimulated Vδ2+ γδ+ T cells (REST) are included for reference. Bubble size indicates the proportion of cells in which the gene is present. Colour intensity indicates the expression level of the gene in cells in that cluster.

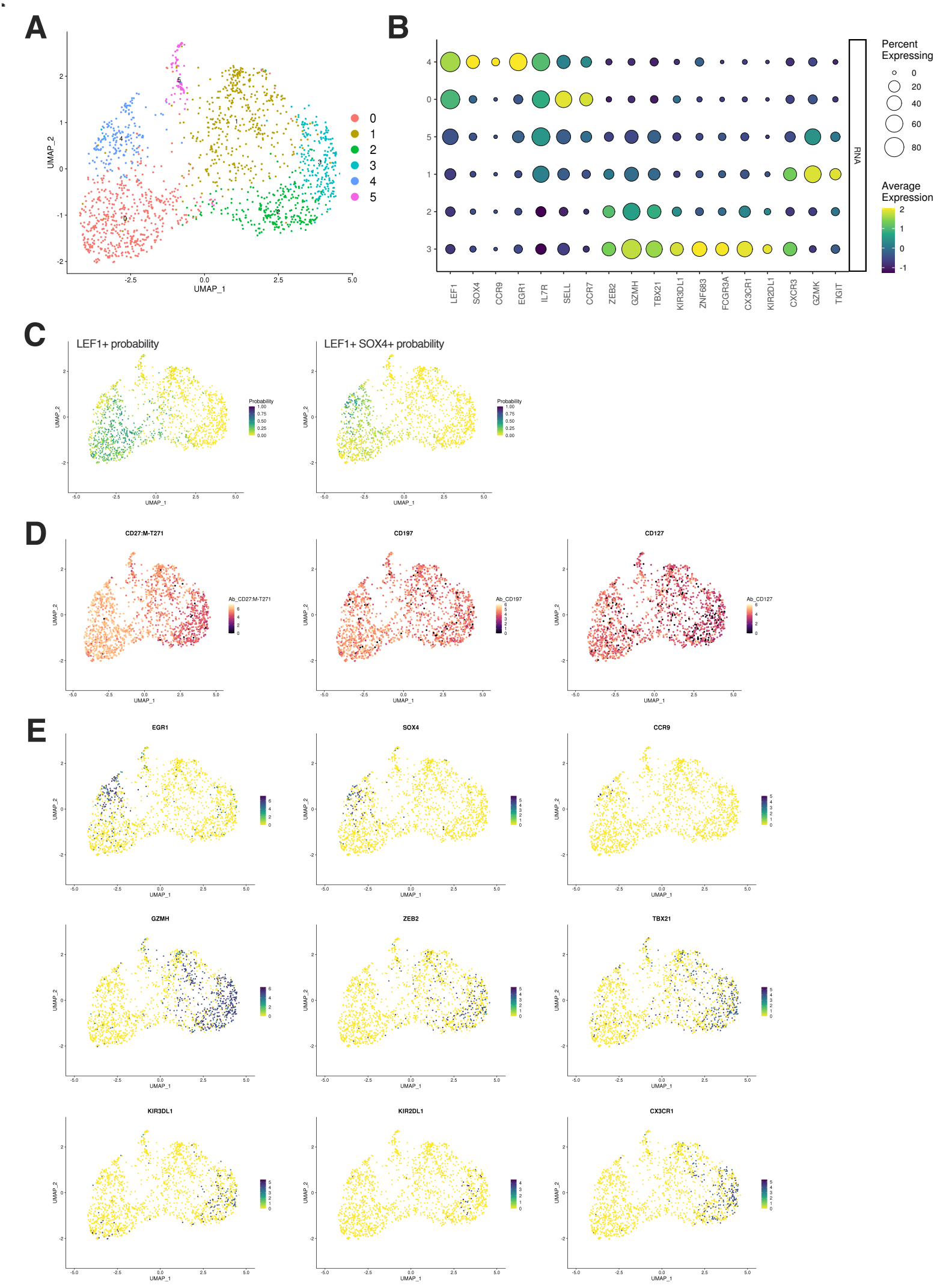

A
UMAP_2
UMAP_1
0
1
2
3
4
5
B
RNA
Percent Expressing
0
20
40
60
80
Average Expression
2
1
0
-1
LEF1
SOX4
CCR9
EGR1
IL7R
SELL
CCR7
ZEB2
GZMH
TBX21
KIR3DL1
ZNF683
FCGR3A
CX3CR1
KIR2DL1
CXCR3
GZMK
TIGIT
C
LEF1+ probability
LEF1+ SOX4+ probability
Probability
D
CD27:M-T271
CD197
CD127
Ab_CD27:M-T271
Ab_CD197
Ab_CD127
E
EGR1
SOX4
CCR9
GZMH
ZEB2
TBX21
KIR3DL1
KIR2DL1
CX3CR1

Figure 5-13: Non-Vδ2 γδ T cells show heterogeneity in naive subsets.

(A) UMAP plot of closely related naive and early memory non-Vδ2 T cells from six donor subjects (10x Genomics). 5 transcriptionally distinct clusters are identified.

(B) Bubble plot of key genes of interest for the clusters of non-Vδ2 T cells. Bubble size indicates the proportion of cells in which the gene is present. Colour intensity indicates the expression level of the gene in cells in that cluster.

(C) UMAP plot of unstimulated non-Vδ2 T cells, overlaid with the per-cell probability of belonging to *LEF1*+ or *LEF1*+*SOX4*+ clusters from Experiment 1 (10x genomics dataset) based on gene expression.

(D) UMAP plot of unstimulated non-Vδ2 T cells overlaid with surface protein expression showing differential expression in the major clusters. CD27, CD197 (CCR7), and CD127 are displayed.

(E) UMAP plot of unstimulated non-Vδ2 T cells overlaid with the expression of genes showing differential expression in the major clusters. The genes *EGR1, SOX4, CCR9, GZMH, ZEB2, TBX21, KIR3DL1, KIR2DL1*, and *CX3CR1* are displayed.

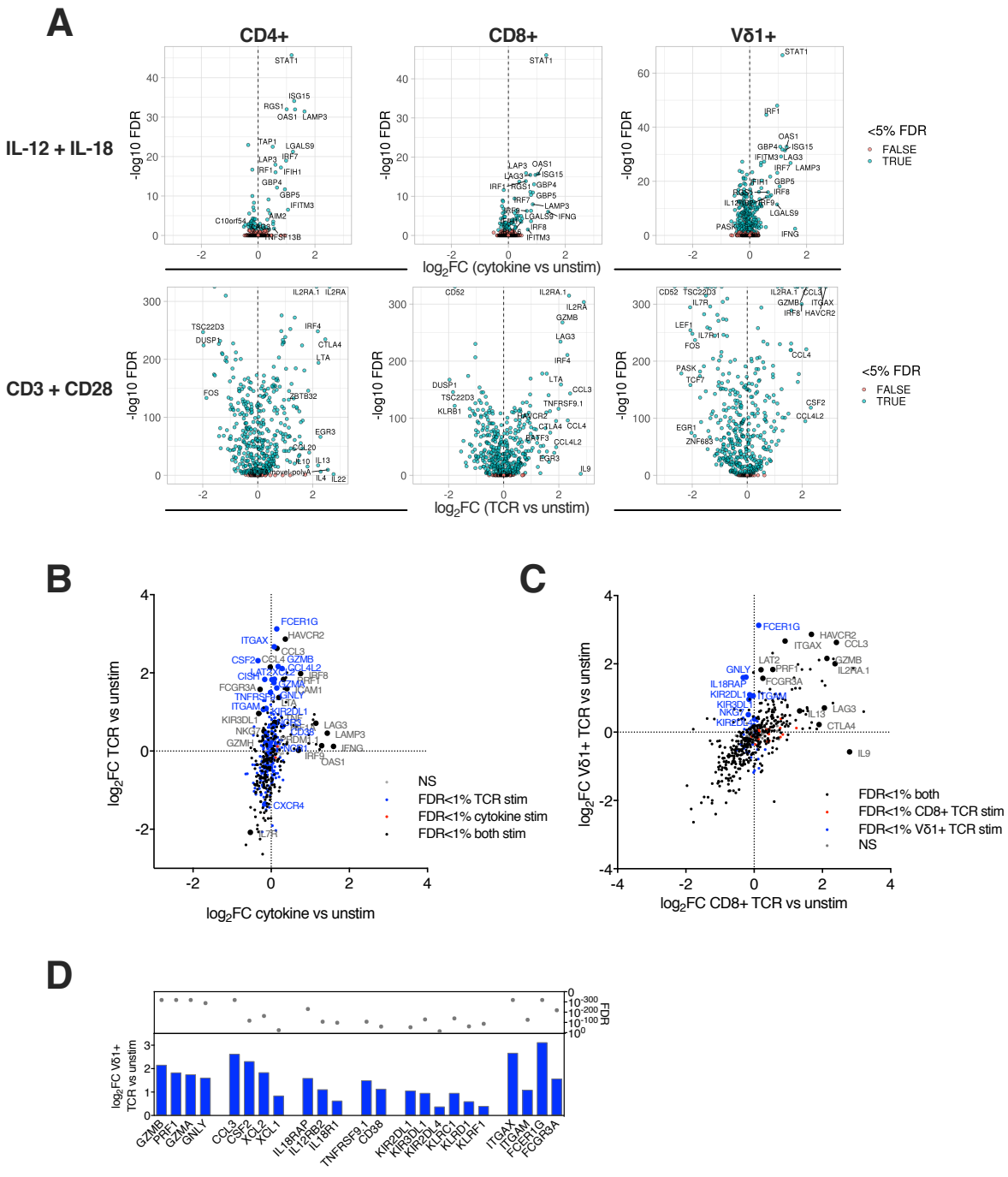

A
CD4+
CD8+
Vδ1+
IL-12 + IL-18
CD3 + CD28
-log10 FDR
log2FC (cytokine vs unstim)
log2FC (TCR vs unstim)
<5% FDR
FALSE
TRUE
B
log2FC TCR vs unstim
log2FC cytokine vs unstim
NS
FDR<1% TCR stim
FDR<1% cytokine stim
FDR<1% both stim
C
log2FC Vδ1+ TCR vs unstim
log2FC CD8+ TCR vs unstim
FDR<1% both
FDR<1% CD8+ TCR stim
FDR<1% Vδ1+ TCR stim
NS
D
log2FC Vδ1+ TCR vs unstim
FDR
GZMB
PRF1
GZMA
GNLY
CCL3
CSF2
XCL2
XCL1
IL18RAP
IL12RB2
IL18R1
TNFRSF9.1
CD38
KIR2DL1
KIR3DL1
KIR2DL4
KLRC1
KLRD1
KLRF1
ITGAX
ITGAM
FCER1G
FCGR3A

Figure 5-14: Non-Vδ2 T cells display an NK-like response profile upon TCR stimulation.

(A) Volcano plots of gene expression by conventional (CD8+ and CD4+) and non-Vδ2 T cells to either cytokine (IL-12/IL-18 - top) or TCR (CD3/CD28 - bottom) stimulation, compared with unstimulated cells.

(B) Scatter plot of log_2 fold change (log_2FC) of cytokine-stimulated vs unstimulated Vδ1+ γδ+ T cells (x-axis) against log_2FC of TCR-stimulated vs unstimulated Vδ1+ γδ+ T cells (y-axis). FDR<1% for TCR stimulation, blue; FDR<1% for cytokine stimulation, red; FDR<1% for both conditions, black (with grey labels).

(C) Scatter plot of log_2 fold change (log_2FC) of TCR-stimulated vs unstimulated CD8+ T cells (x-axis) against log_2FC of TCR-stimulated vs unstimulated Vδ1+ γδ+ T cells (y-axis). FDR<1% for Vδ1+ γδ+ T cells, blue; FDR<1% for CD8+ T cells, red; FDR<1% for both cell types, black (with grey labels).

(D) log_2FC (blue bars, left y-axis) and FDR (grey dots, right y-axis) of cytotoxic and NK-related genes of interest between TCR-stimulated vs unstimulated Vδ1+ γδ+ T cells.

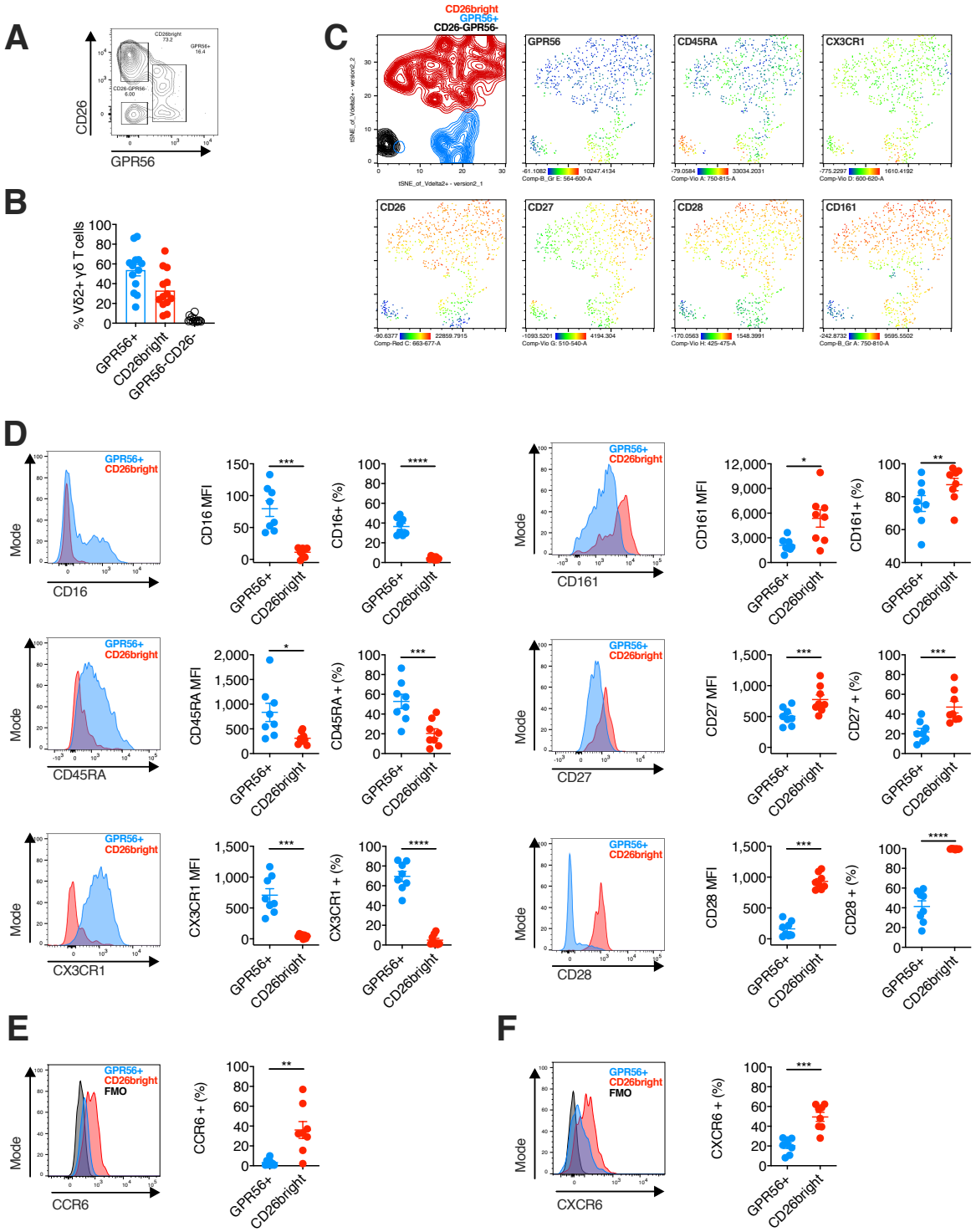

A
CD26
GPR56
B
% Vδ2+ γδ T cells
GPR56+
CD26bright
GPR56-CD26-
C
CD26bright
GPR56+
CD26-GPR56-
GPR56
CD45RA
CX3CR1
CD26
CD27
CD28
CD161
D
GPR56+
CD26bright
Mode
CD16
CD16 MFI
CD16+ (%)
CD161
CD161 MFI
CD161+ (%)
CD45RA
CD45RA MFI
CD45RA + (%)
CD27
CD27 MFI
CD27 + (%)
CX3CR1
CX3CR1 MFI
CX3CR1 + (%)
CD28
CD28 MFI
CD28 + (%)
E
FMO
CCR6
CCR6 + (%)
F
CXCR6
CXCR6 + (%)

Figure 5-15. Phenotype of GPR56+ and CD26bright Vδ2+ T cell populations

(A) Representative plot of GPR56 and CD26 expression on circulating Vδ2+ T cells, with gating for CD26bright, GPR56+, and CD26-GPR56- populations displayed.

(B) Group summary of the proportion of GPR56+ (teal), CD26bright (red), and GPR56-CD26- (black) Vδ2+ T cells in peripheral blood of healthy subjects (n=13).

(C) tSNE representation of Vδ2+ T cell phenotype from flow cytometry concatenated from 6 healthy subjects, with expression of the following markers superimposed: GPR56, CD45RA, and CX3CR1 (first row); CD26, CD27, CD28, and CD161 (second row). The location of GPR56+, CD26bright, and GPR56-CD26- Vδ2+ T cell subsets is indicated. GPR56+, teal; CD26bright, red; GPR56-CD26-, black.

(D) Representative histograms of expression, and group summaries of MFI and proportion of circulating Vδ2+ T cells expressing CD16, CD45RA, CX3CR1, CD161, CD27, and CD28, categorised by GPR56+ and CD26bright subsets, (n=8). GPR56+, teal; CD26bright, red.

Representative histograms of expression, and group summaries proportion of circulating Vδ2+ T cells expressing the chemokine receptors CCR6 **(E)** and CXCR6 **(F)**, categorised by GPR56+ and CD26bright subsets, (n=8). GPR56+, teal; CD26bright, red.

Statistical analysis performed with Wilcoxon signed ranks test (D-F). *, $P \leq 0.05$; **, $P \leq 0.01$; ***, $P \leq 0.001$; ****, $P \leq 0.0001$.

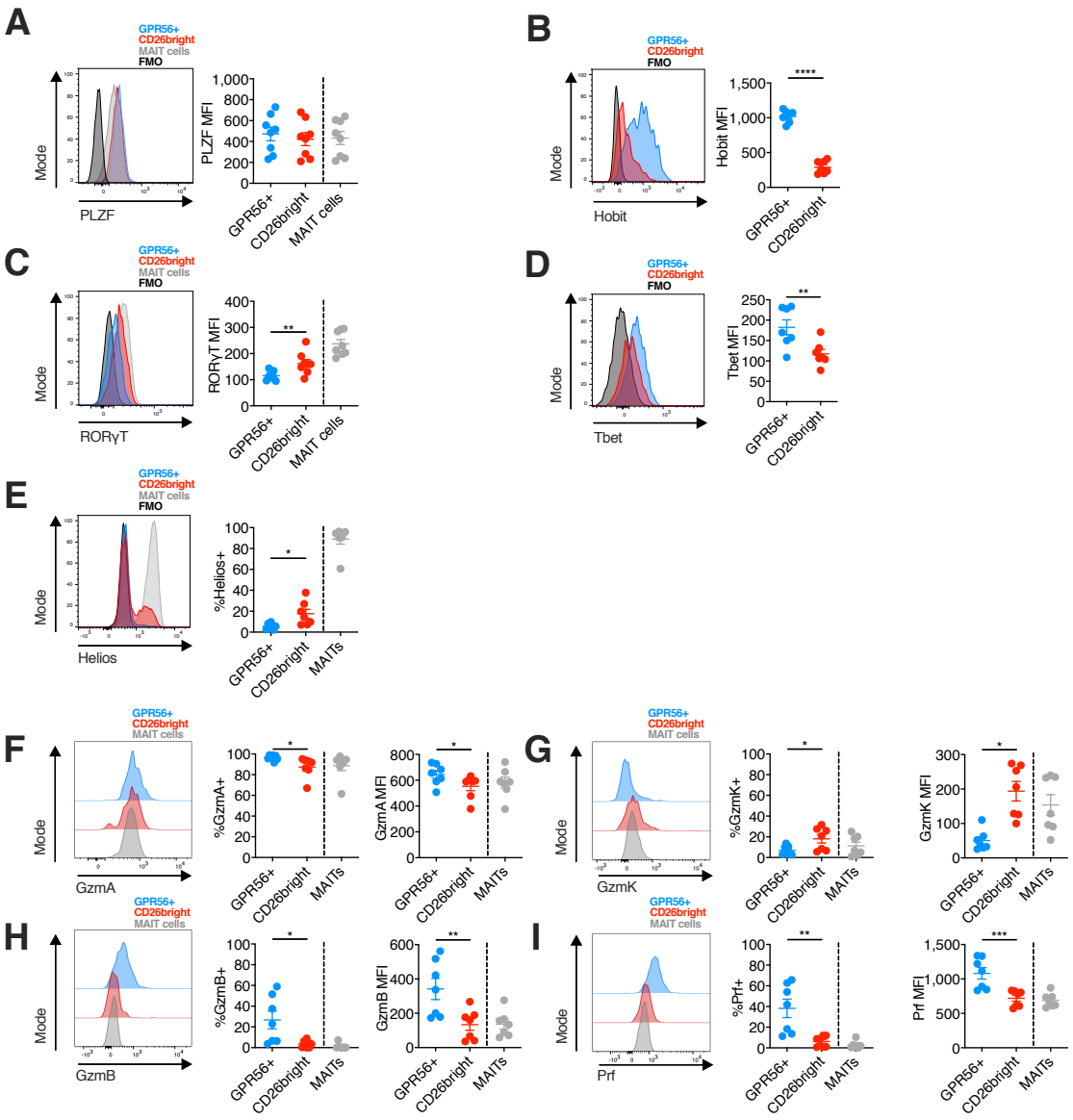


Figure 5-16. Transcription factor and cytotoxic molecule expression of GPR56+ and CD26bright Vδ2+ T cell populations.

Representative histograms of expression, and group summaries of MFI of Vδ2+ T and MAIT cells of PLZF (A), Hobit (B), RORγt (C), Tbet (D), and Helios (E), categorised by GPR56+ and CD26bright subsets, (n=8). GPR56+, teal; CD26bright, red; MAIT cells, grey; fluorescence minus one (FMO) controls on histograms, black.

Representative histograms of expression, and group summaries of MFI and proportion of circulating Vδ2+ T and MAIT cells expressing the cytotoxic molecules granzyme A (F), granzyme K (G), granzyme B (H), and perforin (I) categorised by GPR56+ and CD26bright subsets, (n=8). GPR56+, teal; CD26bright, red; MAIT cells, grey.

Statistical analysis performed with Wilcoxon signed ranks test. *, P ≤ 0.05; **, P ≤ 0.01; ***, P ≤ 0.001; ****, P ≤ 0.0001.

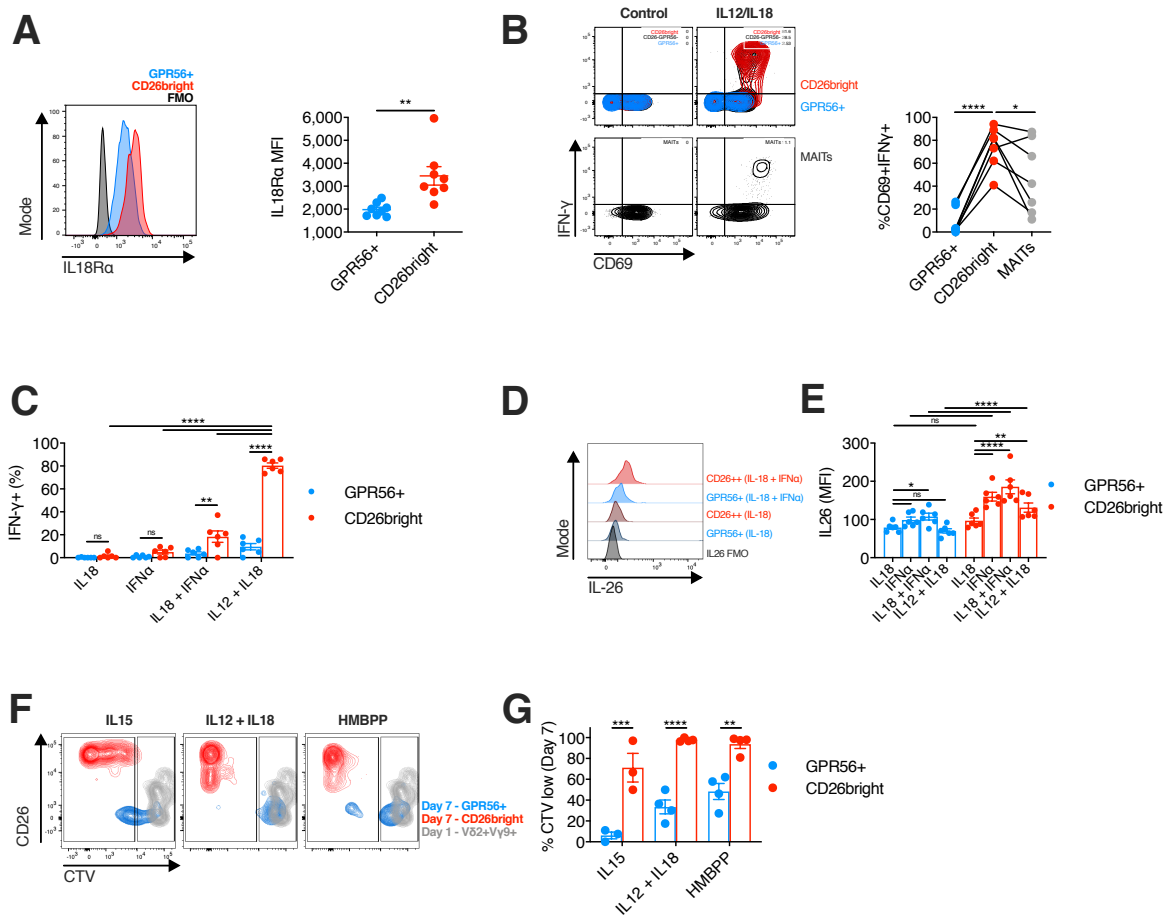

A
GPR56+
CD26bright
FMO
Mode
IL18Rα
IL18Rα MFI
GPR56+
CD26bright
B
Control
IL12/IL18
CD26bright
GPR56+
MAITs
IFN-γ
CD69
%CD69+IFNγ+
GPR56+
CD26bright
MAITs
C
IFN-γ+ (%)
IL18
IFNα
IL18 + IFNα
IL12 + IL18
GPR56+
CD26bright
D
CD26++ (IL-18 + IFNα)
GPR56+ (IL-18 + IFNα)
CD26++ (IL-18)
GPR56+ (IL-18)
IL26 FMO
Mode
IL-26
E
IL26 (MFI)
IL18
IFNα
IL18 + IFNα
IL12 + IL18
GPR56+
CD26bright
F
IL15
IL12 + IL18
HMBPP
CD26
CTV
Day 7 - GPR56+
Day 7 - CD26bright
Day 1 - Vδ2+Vγ9+
G
% CTV low (Day 7)
IL15
IL12 + IL18
HMBPP
GPR56+
CD26bright

Figure 5-17. Functional responses of Vδ2+ T cell subsets by flow cytometry.

(A) Representative histogram of expression, and group summaries of MFI of Vδ2+ T cells of IL18Rα, categorised by GPR56+ and CD26bright subsets, (n=8). GPR56+, teal; CD26bright, red; fluorescence minus one (FMO) controls on histogram, black.

(B) Representative plot of CD69 and IFN-γ expression and group summary of the proportion of Vδ2+ T and MAIT cells expressing CD69 and IFN-γ upon combinatorial IL12 + IL18 stimulation, categorised by GPR56+ and CD26bright subsets, (n=7). GPR56+, teal; CD26bright, red; MAIT cells, grey.

(C) Proportion of Vδ2+ T cells producing IFN-γ upon IL18, IFN-α, IL18 + IFN-α, and IL12 + IL18 stimulation, categorised by GPR56+ and CD26bright subsets, (n=6). GPR56+, teal; CD26bright, red; MAIT cells, grey.

IL26 production by Vδ2+ T cells. Representative histogram of expression **(D)**, and group summaries of MFI of Vδ2+ T cells of IL26 **(E)** upon IL18, IFN-α, IL18 + IFN-α, and IL12 + IL18 stimulation, categorised by GPR56+ and CD26bright subsets, (n=8). GPR56+, teal; CD26bright, red; fluorescence minus one (FMO) controls on histogram, black.

Proliferative capacity of Vδ2+ T cell subsets. Representative plot of CellTrace® Violet (CTV) **(F)**, and group summaries of proportion of CTV low Vδ2+ T cells after 7 days in culture with IL15, IL12 + IL18, and HMBPP stimulation **(G)**, categorised by GPR56+ and CD26bright subsets, (n=3 for IL15, n=4 for IL12 + IL18 and HMBPP). Day 7 GPR56+, teal; Day 7 CD26bright, red, Day 1 Vδ2+Vγ9+ T cells, grey. Statistical analysis performed with Wilcoxon signed ranks test (A), one-way ANOVA with Holm-Sidak's multiple comparisons test (B), and two-way ANOVA with Sidak's multiple comparisons test (C, E, G). *, $P \leq 0.05$; **, $P \leq 0.01$; ***, $P \leq 0.001$; ****, $P \leq 0.0001$.

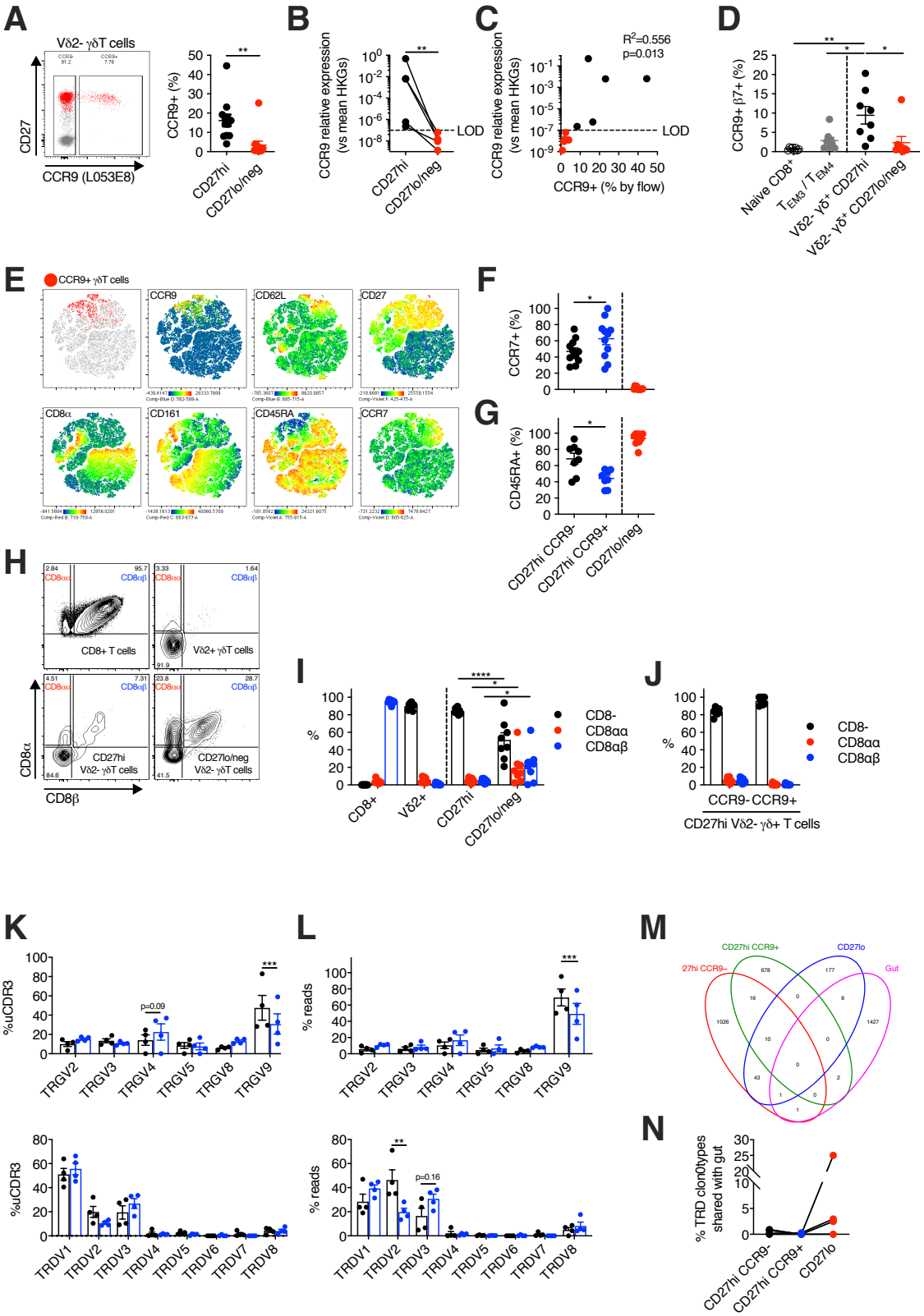

A
Vδ2- γδT cells
CD27
CCR9 (L053E8)
CCR9+ (%)
CD27hi
CD27lo/neg
B
CCR9 relative expression (vs mean HKGs)
LOD
C
R2=0.556
p=0.013
CCR9+ (% by flow)
D
CCR9+ β7+ (%)
Naive CD8+
TEM3 / TEM4
Vδ2- γδ+ CD27hi
Vδ2- γδ+ CD27lo/neg
E
CCR9+ γδT cells
CCR9
CD62L
CD27
CD8α
CD161
CD45RA
CCR7
F
CCR7+ (%)
G
CD45RA+ (%)
CD27hi CCR9-
CD27hi CCR9+
CD27lo/neg
H
CD8+ T cells
Vδ2+ γδT cells
CD27hi Vδ2- γδT cells
CD27lo/neg Vδ2- γδT cells
CD8α
CD8β
I
%
CD8-
CD8αα
CD8αβ
CD8+
Vδ2+
CD27hi
CD27lo/neg
J
CCR9- CCR9+
CD27hi Vδ2- γδ+ T cells
K
%uCDR3
p=0.09
TRGV2
TRGV3
TRGV4
TRGV5
TRGV8
TRGV9
TRDV1
TRDV2
TRDV3
TRDV4
TRDV5
TRDV6
TRDV7
TRDV8
L
% reads
p=0.16
M
CD27hi CCR9+
CD27lo
Gut
N
% TRD clonotypes shared with gut

Figure 5-18: CD27hi non-Vδ2 γδ T cells contain a naive CCR9+ population.

(A) Representative plot of CCR9 expression and group summary of the proportion of circulating Vδ2- γδ T cells expressing CCR9, categorised by CD27hi and CD27lo/neg subsets (n=12). CD27hi, black; CD27lo/neg, red.

(B) CCR9 gene transcript expression relative to the mean of 3 housekeeping genes (HKGs; ACTB, GUSB, GAPDH) by sorted CD27hi and CD27lo/neg Vδ2- γδ T cells by quantitative real-time PCR (qPCR) (n=5). RNA extracted from sorted CD27hi and CD27lo/neg Vδ2- γδ T cells was amplified by whole transcriptome amplification prior to qPCR. In samples where CCR9 transcript was not detected by the final cycle, the maximum number of cycles + 1 was used to calculate relative expression.

(C) Scatter plot of relative CCR9 gene transcript expression and proportion of Vδ2- γδ T cells expressing surface CCR9 as determined by flow cytometry.

(D) Group summary of the proportion of circulating Vδ2- γδ T cells co-expressing CCR9 and β7-integrin, categorised by CD27hi and CD27lo/neg subsets (n=8). CD27hi, black; CD27lo/neg, red.

(E) tSNE representation of Vδ2- γδ T cell phenotype from flow cytometry concatenated from 3 healthy subjects, with expression of the following markers superimposed: CCR9, CD62L, CD27 (first row); CD8α, CD161, CD45RA, and CCR7 (second row). The location of CCR9+ Vδ2- γδ T cells is indicated in red.

Group summaries of the proportion of circulating Vδ2- γδ T cells expressing CCR7 **(F)** and CD45RA **(G)**, categorised by CD27hi CCR9-, CD27hi CCR9+, and CD27lo/neg subsets (n=8). CD27hi CCR9-, black; CD27hi CCR9+, blue; CD27lo/neg, red.

Representative plot of CD8α and CD8β expression **(H)** and group summary **(I)** of the proportion of circulating CD8+ αβ, Vδ2+, CD27hi and CD27lo/neg Vδ2- γδ T cells expressing CD8α and CD8β (n=8). CD8neg, black; CD8αα, red; CD8αβ, blue.

(j) Group summary of the proportion of circulating CCR9- and CCR9+ CD27hi Vδ2- γδ T cells expressing CD8α and CD8β (n=8). CD8neg, black; CD8αα, red; CD8αβ, blue.

Proportion of **(K)** unique CDR3 clonotypes (uCDR3; mean+/-SEM), and proportion of **(l)** reads (mean+/-SEM) of CD27hi Vδ2- γδ T cells using TRGV genes (top) and TRDV genes (bottom), categorised by CCR9 expression (n=4). CCR9-, black; CCR9+, red.

(M) Venn diagram of shared TRD clonotypes between circulating CD27hi CCR9-, CD27hi CCR9+, CD27lo Vδ2- γδ T cells, and intestinal γδ T cells from a representative donor.

(N) Percentage of TRD clonotypes from peripheral Vδ2- γδ T cell populations which are shared with intestinal γδ T cells from the same donor (n=4).

Statistical analysis performed with Wilcoxon signed ranks test **(A)**, Mann-Whitney test **(B)**, Pearson correlation **(C)**, 1-way ANOVA with Sidak multiple comparisons test **(D)**, paired t tests (**F,G**), and 2-way ANOVA with Holm-Sidak multiple comparisons test **(I,K,L)**. *, $P \leq 0.05$; **, $P \leq 0.01$; ***, $P \leq 0.001$; ****, $P \leq 0.0001$.

Chapter 6: Characterisation of tissue resident memory populations using intestinal transplantation as a model system

6.1 Acknowledgement of contributions

The conception and design of the project was in collaboration with Dr Nicholas Provine, Professor Paul Klenerman, and Dr Philip Allan. Clinical support for patient recruitment and biological sample collection was in collaboration with Drs Philip Allan and Timothy Ambrose. Design of the spectral flow cytometry panel, some sample processing and flow cytometry was performed in collaboration with Dr Nicholas Provine. Single cell RNA sequencing data analysis was performed in collaboration with Dr Lucy Garner, who generated plots for Figures 6-2, 6-3A, and Supplemental Figure 6-2. Chip cytometry was performed at the facility at the Peter Medawar Building by Dr Kate Powell. I am grateful for advice concerning tissue resident memory T cell biology from Professor Laura Mackay. This work is currently undergoing revisions after peer-review, in preparation for publication, and is available as a preprint(FitzPatrick et al., 2019).

6.2 Introduction

Overview

As discussed in the introduction, the immune response in coeliac disease is predominantly mucosal, with involvement of CD4+, CD8+, and γδ T cells with characteristics of T_{RM} cells. In chapter 4, my research revealed evidence of altered TCR repertoires in intestinal T cell populations, along with an altered transcriptional profile of cytotoxic IEL populations. In addition, CD8+ populations in CD

possessed a TCR repertoire enriched for TRBV28-containing clonotypes, with clonally expanded TRBV28+ clonotypes expressed by cytotoxic, tissue resident CD8+ T cells on scRNAseq.

This association between CD and tissue residency in the small intestine, along a fortuitous collaboration with Dr Philip Allan and the intestinal transplant service, led to this work examining T_{RM} cell heterogeneity in the human gut.

This work used human intestinal transplantation as a model system to study T_{RM} cells. I identified two transcriptionally distinct populations of *bona fide* human intestinal CD8+ T_{RM} cells, which show phenotypic and functional differences.

Tissue-resident memory T cells

Tissue-resident memory T (T_{RM}) cells are a subset of long-lived T cells that reside in tissue and do not recirculate (Mackay and Kallies, 2017; Szabo et al., 2019). T_{RM} cells can provide rapid, *in situ* adaptive protection against viral, bacterial, and parasitic pathogens (Gebhardt et al., 2011; Schenkel et al., 2014), have a role in cancer immune surveillance (Park et al., 2019), and are increasingly implicated in autoimmunity in murine and human studies, including in inflammatory bowel disease (IBD) and coeliac disease (Mayassi et al., 2019). CD8+ T_{RM} cells have potent cytotoxic capacity and produce pro-inflammatory cytokines which activate wider responses by the innate and adaptive immune system(Ariotti et al., 2014; Schenkel et al., 2014).

6.2.1 Identification of T_{RM} cells

While mouse studies have advanced our understanding of T_{RM} cells substantially, there are clear differences in T_{RM} phenotype, transcriptional profiles, and genetic regulation between mice and humans(Hombrink et al., 2016; Kumar et al., 2017; Oja et al., 2017a). While murine T_{RM} cell studies can use tools such as parabiosis and intravenous antibody labelling to study unequivocal tissue residency, until recently, human studies of T_{RM} biology were limited by the inability to prove long-lived tissue residency, with surface molecules CD69 and CD103 (αE integrin) used as surrogate

markers of T_{RM} cells. Such studies have provided a putative gene signature of human T_{RM} cells(Kumar et al., 2017), however this gene signature was derived from bulk-sorted populations, and it remains unclear if human T_{RM} cells comprise transcriptionally distinct subsets .

Indeed, despite the expression of CD69 on almost all murine and human T_{RM} cells, its use as a residency marker has been questioned. While CD69 restricts lymphocyte exit from tissue via S1P1 inhibition, it is not required for the development of T_{RM} cells in mice (Shiow et al., 2006; Walsh et al., 2019). CD69 can also be induced via cytokine stimulation, while a proportion of CD69+ T cells in tissue are not resident, which makes CD69 a suboptimal residency marker when used alone(Beura et al., 2018; Sancho et al., 2005; Shiow et al., 2006). Therefore, additional markers which can be used to identify CD103- T_{RM} cells are required.

6.2.2 Intestinal transplantation as a model for T_{RM} cell study

Recent studies have used organ transplantation in humans to study long-lived donor-origin T cells, which are definitively resident T_{RM} cells(Bartolomé-Casado et al., 2019; Snyder et al., 2019; Zuber et al., 2016). These studies have demonstrated persistence of intestinal CD8+ T_{RM} cells for up to 1 year in the small intestine (SI) (Bartolomé-Casado et al., 2019), and of donor-origin T_{RM} cells for up to 600 days post-transplant (Zuber et al., 2016). This approach has also identified putative intestinal CD8+ T_{RM} subsets based on CD103 and KLRG1 expression, with functional implications(Bartolomé-Casado et al., 2019). However, it remains unclear whether these cell populations are transcriptionally distinct subsets.

This work sought to examine transcriptional, phenotypic, and functional heterogeneity within definitively-resident donor-derived T cells in the gut following intestinal transplantation. I used flow cytometry in combination with HLA-allele congenic cell tracking, single-cell RNA sequencing

(scRNAseq), fluorescence microscopy chip cytometry, and functional *ex vivo* assays to address these questions.

6.3 Results

Long-lived conventional CD4+ and CD8+ T cells, but not unconventional T cell populations, can persist for at least 5 years in the human intestine

I sought to examine the persistence of resident T cells in the small intestine (SI) following transplantation. To this end, I used HLA allele congenic cell tracking, which allows discrimination of donor- and recipient-derived cells using fluorophore-conjugated antibodies to Class I HLA haplotypes discordant between donor and recipient, previously discussed in the background chapter (Fig. 6-1A, Supplemental Fig. 6-1A) (Bartolomé-Casado et al., 2019; Zuber et al., 2016). Clear discrimination of donor- and recipient-origin T cells was achieved with HLA-A2 and HLA-A3, but could not be achieved with HLA-B7 or HLA-Bw4 (data not shown). Intestinal biopsy samples were collected from a cohort of 18 intestinal transplant recipients, with biopsies from multiple timepoints available from some patients (study subject characteristics are presented in Supplemental Table 6-1). HLA-allele congenic cell tracking was possible for 16 subjects. The presence of intestinal donor- and recipient-origin T cells *in situ* was confirmed by chip cytometry (Fig. 6-1B) (Leng et al., 2019).

The proportion of recipient-origin T cells in the graft increased with time post-transplantation, with great heterogeneity between individuals (Fig. 6-1C). A history of current or previous clinical rejection was associated with a greater proportion of recipient-origin T cells (Fig. 6-1D), consistent with a previous study(Zuber et al., 2016). Two study subjects had persistent donor-origin intestinal T cell populations 4 years 7 months (1684 days) and 5 years 1 month (1865 days) after transplantation

(Fig. 6-1E). This is longer than prior reports of long-term persistence of donor-origin T cells following intestinal transplantation(Bartolomé-Casado et al., 2019; Zuber et al., 2016).

Haematopoietic stem and progenitor cells can persist in the intestinal transplant graft, which can lead to persistent chimerism of donor-origin populations in the circulation (Fu et al., 2019). This could potentially provide a source of donor-origin T cells which could enter from the blood, and confound assessment of *bona fide* tissue residency (Bartolomé-Casado et al., 2019). In contrast with the work of Fu and colleagues, the percentage of circulating donor origin T cells in the blood of transplant recipients (collected synchronously with some biopsy samples) was extremely low beyond 3 months post-transplant (median 0.042%, 95% CI 0-1.22%; Fig. 6-1F). Previous work posited a cut-off for macrochimerism in the blood of 4% (Fu et al., 2019), with these results well below that level. Indeed the proportion of donor-origin T cells in the blood was similar to background non-specific staining in non-transplant recipients (0.01-0.12%; Supplemental Fig. 6-1B). This indicates that continuous replacement from circulating donor-origin macrochimerism is unlikely to be responsible for sustained donor chimerism in this cohort of patients.

The cause for different results around circulating macrochimerism in this study and the prior work are of interest, both from the perspective of future T_{RM} cell studies in intestinal transplant recipients, and from the clinical perspective of GvHD. The discrepancy may result from differences in the transplant procedure (isolated intestinal transplantation in this study; (modified) multi-visceral transplantation in the previous work) and transplant recipient age (adult in this study; paediatric in the previous work) (Fu et al., 2019; Zuber et al., 2015).

Conventional T cell populations were most common in the graft post-transplant (Fig. 6-1G). Both CD4+ and CD8+ T cells demonstrated similar kinetics of increased recipient-origin populations with time (Fig. 6-1H). I also examined unconventional and innate-like T cell subsets and their dynamics

post-transplant, as the residency characteristics of these populations are poorly understood, particularly in humans (Supplemental Fig. 6-1C). Mucosal-associated invariant T (MAIT) cells (identified as CD161+Vα7.2+CD8+ T cells), and Vδ2+ γδ T cells (which share phenotypic and functional features with MAIT cells (Gutierrez-Arcelus et al., 2019; Provine et al., 2018)) were rare in the graft at early timepoints post-transplant, recovering to expected proportions in the tissue at one year (Fig, 6-1I) . Non-Vδ2 γδ T cell subsets demonstrated different dynamics, with this population present at early timepoints, and at particularly high frequencies in one donor. Much like conventional T cells, these unconventional subsets showed replacement with recipient-origin populations over time(Fig. 6-1J). The cause for the different dynamics between unconventional T cells post-transplantation is unclear. The low frequency of MAIT and Vδ2+ T cells post-transplant could be due to differences in residency characteristics, or to a propensity for activation-induced cell death following from ischaemia during surgery or sensitivity to perioperative conditioning regimes. The higher proportion of non-Vδ2 γδ T cells in some individuals could be due to their more adaptive biology, or due to a non-Vδ2 γδ T cell response to a pathogen, such as CMV(Davey et al., 2018a; Willcox et al., 2012).

The expression of canonical markers of tissue residency,CD69 and CD103, were examined on donor- and recipient-origin CD4+ and CD8+ T cell populations in the graft. CD103 expression was restricted to CD69+ T cells, with more CD8+ cells expressing CD103 in comparison to CD4+ cells (Fig. 6-1K), in line with previous work(Bartolomé-Casado et al., 2020; Kumar et al., 2017). Donor-origin T cells showed near-ubiquitous expression of CD69, which is consistent with a lack of recent tissue entry from the circulation, and had fewer CD69- cells than recipient-origin populations for both CD8+ (median 0.03% vs 4.17%, $p < 0.0001$, Wilcoxon signed rank test) and CD4+ cells (median 0.10% vs 5.65%, $p < 0.0001$, Wilcoxon signed rank test) (Fig. 6-1L). Although recent mouse studies show that CD69 is not required for the establishment of tissue residency in the gut(Walsh et al., 2019), these results indicate that a lack of CD69 expression on intestinal T cells is a surrogate for non-resident

populations. Recipient-origin conventional T cell populations showed increasing expression of CD103 with time post-transplant, consistent with the acquisition of a T_{RM} phenotype, as shown previously(Zuber et al., 2016). Higher expression of CD161 (a C-type lectin-like receptor) is seen on intestinal CD103+ CD8+ T cells (Fergusson et al., 2015). In this study, more donor-derived CD8+ T cells expressed CD161, consistent with an association between residency and CD161 expression in the gut (Supplemental Fig. 6-1D,E).

Single-cell RNA sequencing delineates transcriptionally distinct states within CD4+ and CD8+ T_{RM} cell populations

The persistence of CD103- and CD103+ donor-origin T cells in the intestinal graft for up to five years post-transplant, as well as the enrichment of CD103+ recipient-origin T cells at later time points, suggested that CD103- and CD103+ T cells could represent distinct cell states. To test whether donor-origin T cells formed transcriptionally distinct subsets, I performed droplet-based scRNAseq of sorted donor-origin intestinal T_{RM} cells from one subject 12-months post-transplant (Experiment 1, Fig. 6-2A). 1,774 cells were captured and sequenced, with 974 cells remaining after quality control steps and filtering (Supplemental Fig. 6-2A).

Four distinct clusters were identified (Fig. 6-2B): conventional CD4+ T cells, regulatory CD4+ T cells which expressed *IL2RA* (encoding CD25) and the transcription factor *FOXP3*, and two clusters of conventional CD8+ T cells (Fig. 6-2C). The differentially expressed genes (DEGs) between the CD8+ T_{RM} cell clusters (referred to as CD8+ population 1 and 2) were then analysed (Fig. 6-2D). Population 1 expressed *ITGAE* (CD103), as well as higher levels of *KLRB1* (CD161), *IL7R* (CD127), *CD7*, and the chemokine receptor *CCR6* (Fig. 6-2E). IL-7 is a stromal-derived homeostatic cytokine which provides survival and proliferative signals to lymphocytes (Raeber et al., 2018). IL-7 is required for the persistence of epidermal TRM cells (Adachi et al., 2015), with CD127 is expressed by intestinal

memory T cell populations(Thome et al., 2014). This differential expression of *IL7R* suggests that there may be differences in the mechanisms, or nature, of residency and long-term persistence between the two CD8+ populations(Raeber et al., 2018).

CD8+ population 2 expressed low levels of *ITGAE*, but higher levels of *KLRG1*, cytotoxic granzyme molecules, and class II MHC (Fig. 6-2D,E). Surface KLRG1 expression has been used to delineate two putative intestinal CD103- CD8+ T cell subsets(Bartolomé-Casado et al., 2019). However, population 2 did not sub-cluster further based on KLRG1 gene expression, which suggests that these KLRG1-/+ populations are not transcriptionally distinct states. Of interest, the integrin *ITGB2* (β2-integrin, or CD18), was highly expressed by the CD103- CD8+ population 2. β2-integrin forms potential heterodimers with four α-integrins (Fagerholm et al., 2019). Only one heterodimeric partner, *ITGAL* (CD11a), was detected, and was highly expressed on the CD103- CD8+ population 2 (Supplemental Fig. 6-2B,C).

CD8+ CD103+ and CD103-ITGB2hi T_{RM} cell subsets differ in expression of putative residency-associated genes

Previous human studies have defined a core transcriptional signature associated with human tissue residency from bulk RNAseq from tissue-derived T cells sorted based on CD69 expression(Kumar et al., 2017). The expression of this putative T_{RM} cell gene set was examined in the two CD8+ T cell populations. As expected, the genes downregulated in CD69+ T cells in the prior study were either not detected, or found at low levels in both clusters, including genes associated with the control of tissue egress pathways, such as *KLF2* and *S1PR1*(Supplemental Fig. 6-2D,E). Of interest, several genes previously found to be upregulated in CD69+T_{RM} T cells were differentially expressed between the two clusters. Population 1 expressed higher levels of *ITGAE* and *ITGA1* (consistent with prior work on T_{RM} cells in the kidney (de Leur et al., 2019)), while population 2 expressed higher levels of *CRTAM* (Fig. 6-2D, F, Supplemental Fig. 6-2F). T cell receptor (TCR) repertoire analysis identified several

shared clonotypes between the two T_{RM} clusters (Supplemental Fig. 6-2G). These data indicate that previously identified T_{RM} cell gene signatures may represent an amalgamation of several distinct T_{RM} cell transcriptional states.

Single-cell RNA sequencing identifies a core geneset distinguishing two CD8+ T_{RM} cell populations

To confirm this finding of transcriptionally distinct CD8+ T_{RM} cell states, a second scRNAseq experiment was performed on donor-origin intestinal CD8+ T cells from two further transplant recipients (Experiment 2, Fig. 6-3A). Donor-derived CD103- and CD103+ CD8+ T cells were index-sorted into 96-well plates, before scRNAseq using the Smart-Seq2 protocol (Picelli et al., 2013). 267 cells were sorted and sequenced, with 196 cells remaining after quality control and filtering (Supplemental Fig. 6-2H-J). Analysis revealed three transcriptionally distinct clusters. Cluster 1 was predominantly formed of CD103- T cells, while the transcriptionally similar clusters 2 and 3 were predominantly CD103+ T cells (Fig. 6-3A). Clusters 2 and 3 expressed higher levels of *ITGAE*, *CD7*, and *IL7R*, while cluster 1 expressed higher levels of granzymes, class II HLA molecules, and *ITGB2*, concordant with the previous experiment(Fig. 6-3B). *ITGAL*, the putative heterodimeric partner of *ITGB2* identified in the first experiment, was detected in cluster 1 (Supplemental Fig. 6-2K).

Differential expression analysis between cluster 1 and clusters 2 and 3 combined showed a similar pattern of transcriptional differences to those in Experiment 1 (Fig. 6-3C, Supplemental Table 6-2). By comparison of the DEGs identified in the two experiments, a core set of 30 genes that distinguished the two populations in both experiments was identified (Fig. 6-3C,D).

ZNF683 (Hobit), a transcriptional regulator of residency in mice (Mackay et al., 2016), was more highly expressed in population 1 in Experiment 1 (Fig. 6-2E). The expression of a curated list of transcription factors previously associated with residency was examined in the four clusters identified in experiment 1(C. Li et al., 2019; Mackay et al., 2015b; Milner et al., 2017). *ZEB2*, and *JUN*,

transcription factors previously associated with residency in murine studies, were differentially expressed between the two clusters, with higher expression of *ZEB2* in population 2, and of *JUN* and *ZNF683* in population 1(Fig. 6-3E).

Analysis of published intestinal T cell datasets

I sought to confirm if these T_{RM} population gene sets were applicable outside the transplant setting. First, I examined the expression of the two gene sets in conventional resident CD8+ T cell clusters in published scRNAseq data from human colon (Corridoni et al., 2020). Hierarchical clustering of these seven populations on total gene expression, or on the expression of the 30-gene T_{RM} gene set identified in the transplant scRNAseq dataset, showed highly congruent clustering of the populations, indicating that this gene set separated two transcriptionally distinct populations (Supplemental Fig. 6-3A,B). Reassuringly, unbiased hierarchical clustering of the 30 genes in the clusters perfectly separated those associated with the two populations (Supplemental Fig. 6-3C).

Next, I examined the expression of the two gene sets in 3 CD8A+/CD8B+ T cell clusters in published scRNAseq data from human ileum(J. C. Martin et al., 2019). Hierarchical clustering again split genes perfectly into those associated with the two populations, with 2 ileal CD8+ clusters (4 and 47) showing similarities to population 1, and cluster 21 showing similarities to population 2 (Supplemental Fig. 6-3D).

Recent murine work has described transcriptionally distinct subsets of intestinal CD8+ T_{RM} cells in the LCMV model of tissue residency, which highlighted CD28 as a possible marker for these subsets(Kurd et al., 2020). CD28 was increased in the CD103- T_{RM} population in experiment 1, although this difference was not replicated in experiment 2. We examined the expression of murine orthologs of the CD103- population gene set in the published data. CD103- population genes were significantly enriched in one of the clusters at both the Day 60 and 90 timepoint post LCMV infection, providing evidence of analogous T_{RM} subsets in the human and mouse intestine (Supplementary Fig. 6-3E).

CD103+ and CD103- CD8+ T cells display distinct phenotypes in the healthy intestine

To examine whether these transcriptionally distinct populations possessed phenotypic differences, I performed flow cytometry of intestinal T cells, both within and outside the transplant setting. Flow cytometry of donor-origin T cells showed differential expression of CD161, β2-integrin, and granzyme K between CD103+ and CD103- CD8+ T cells, in agreement with the sequencing data (Fig. 6-4A). To validate these phenotypic differences between the intestinal CD8+ T_{RM} cell subsets we performed flow cytometry of intestinal T cells from healthy subjects. CD8+ intestinal T cells expressing both CD69 and CD103 were most common (88.9% (range 81.7-96.0%) of CD8+ T cells) with no difference observed between intestinal CD8+ T cells from the duodenum or ileum(Supplementary Fig. 6-4A).

I examined the expression of markers that differentially expressed between the two T_{RM} subsets in our scRNAseq data. CD103+ CD8+ T cells expressed higher levels of CD161 and CD127 (IL7R) compared with the CD69- or CD69+CD103- cells, as expected (Fig. 6-4B,C). CD7 expression was higher on all CD69+ T cells, with no difference between CD69+CD103- and CD69+CD103+ populations. In contrast, CD69+CD103- CD8+ T cells expressed higher levels of β2-integrin, KLRG1, and granzyme K than either CD69- cells or CD69+CD103+ cells.

Ki-67 expression formed a gradient between the three populations, with higher expression in the CD69- population, and a trend towards increased Ki67 expression in CD69+CD103- CD8+ T cells compared to CD103+ CD8+ T cells (mean 14.88% vs 5.72%, one-way ANOVA and Tukey's multiple comparisons test, P=0.067). This is consistent with prior work indicating that T_{RM} cell persistence is due to longevity rather than *in situ* proliferation (Thome et al., 2014).

Graft-infiltrating, recipient-derived T cells take on a T_{RM} cell phenotype over time, with CD103+ and CD103- CD8+ T cells displaying distinct phenotypes

I examined graft-infiltrating, recipient-derived T cells to explore the acquisition of a T_{RM} cell phenotype. In the early post-transplant period, 52.7% of infiltrating CD8+ T cells lacked CD69 expression, with acquisition of a T_{RM} cell phenotype (CD69+ CD103+) over time (Fig. 6-4D). At later times post-transplant, CD103- and CD103+ populations clearly differed in phenotype, consistent with the two subsets observed previously. CD161 expression was higher on CD103+ CD8+ T cells than CD103- counterparts, while granzyme K expression was higher on CD69+CD103- CD8+ T cells (Fig. 6-4E-I). Recipient-origin CD69+CD103- CD8+ T cells demonstrated higher expression of β2-integrin than either CD69- or CD103+ populations (Fig. 6-4G), while CD69+ populations showed higher Ki-67 expression as before (Fig. 6-4I). Recipient-origin CD8+ T cells infiltrating the graft in the early post-transplant period displayed analogous expression, particularly of β2-integrin, although small sample number precluded further analysis (Supplemental Fig. 6-4B).

Intestinal CD8+ T cells, both intraepithelial lymphocytes (IELs) and lamina propria lymphocytes (LPLs), displayed an effector memory (T_{EM}) phenotype (Supplemental Fig. 6-4C,D). IELs almost exclusively expressed CD103+, as shown previously(Supplemental Fig. 6-4E) (Bartolomé-Casado et al., 2019). β2 integrin expression was high on all memory T cells in peripheral blood, and highest on T_{EM} CD8+ T cells (Supplemental Fig. 6-4F). This pattern of expression was expected, due to the involvement of LFA-1 in tissue entry via ICAM-1, making the lower expression on CD103+ LPLs and IELs, as well as on CD69- T cells in the gut, all the more striking(Fagerholm et al., 2019).

CD103+ and CD103- CD8+ T cells maintain their distinct phenotypes in lamina propria and intra-epithelial compartments

The presence of CD103- and CD103+ donor-origin CD8+ T cells in the intestinal mucosa of the transplant graft was confirmed *in situ* using chip cytometry (Fig. 6-5A). CD103+ T cells were dominant in the epithelium, in concordance with flow cytometric data (Fig. 6-5A; Supplementary Fig. 6-4E). The scRNAseq results indicated that CD8+ CD103+ T cells from the intestinal mucosa formed a single transcriptionally distinct cluster. However a prior study divided CD8+ CD103+ T cells into two populations based on their location (IELs or LPLs) (Bartolomé-Casado et al., 2019). Flow cytometry of CD8+ CD103+ T cells separated from the IEL and LPL compartments of the small intestine from healthy subjects was performed. Phenotypic differences between CD8+ CD103- and CD103+ T cells were again seen, with CD103- cells showing higher expression of β2-integrin and KLRG1, and lower expression of CD161, CD7, and CD127(Fig. 6-5B). The CD8+ CD103+ T cell populations isolated from IEL and LPL compartments showed similar expression of β2-integrin, KLRG1, CD161, CD7, and CD127, indicating that these populations are both transcriptionally and phenotypically similar, and do not represent distinct subsets of T_{RM} cells(Fig. 6-5B).

Additional chip cytometry staining for KLRG1, CD18 (β2-integrin), and granzyme K was performed on a second section of intestinal mucosa from the same transplant donor as Figure 6-5A. Additional samples were not able to be collected due to restrictions on sample collection during the COVID-19 pandemic. Again, donor-origin CD103+ and CD103- CD8+ T_{RM} cells were seen, with CD103+ T cells found in both IEL and LPL compartments, while CD103- T cells were restricted to the lamina propria (Fig. 6-5C). CD103- CD8+ donor-origin T cells showed expression of CD18, KLRG1, and granzyme K, with lower expression on identified CD103+ counterparts (Fig. 6-5D).

CD103+ CD8+ intestinal T cells demonstrate greater capacity for cytokine production

To assess the function of these identified subsets, intestinal T cells from healthy subjects were stimulated with short-term PMA and ionomycin, before intracellular staining and flow cytometry for TNFα, IFNγ, IL-2, CCL4, IL-17A, and IL-10. 77% of CD103+ CD8+ T cells produced one cytokine or

more, more than either CD69+CD103- comparators (47.7% cytokine positive, P < 0.001), or CD69- CD8+ T cells (37% cytokine positive, P < 0.001) (Fig. 6-6A-F). Both CD69+ populations produced more TNFα and IFNγ than CD69- cells, with no difference based on CD103 expression (Fig. 6-6A,B). While scRNAseq data showed higher CCL4 gene expression by CD103- populations, CCL4 production following stimulation was not different between CD69+ populations (Fig. 6-6C). CD103+ CD8+ T cells expressed more IL-2 than both CD69+CD103- and CD69- T cells(Fig. 6-6D), consistent with prior work indicating that hepatic CD103+ CD8+ T_{RM} cells also produce increased IL-2 (Pallett et al., 2017).

There was a spectrum of functional capacity between the three populations. CD69- CD8+ T cells were mainly non- or mono-functional, while CD103+ CD8+ T cells were predominantly polyfunctional, with CD69+CD103- CD8+ T cells intermediate in their function(Fig. 6-6E,F), consistent with previous work(Bartolomé-Casado et al., 2019). Quadruple functional cells were most common in CD103+ CD8+ T cells compared to CD69+CD103- T cells (21.76% vs 10.32%, P<0.0001), and were rare in the CD69- population (0.38%). These results show that the transcriptionally distinct CD8+ T_{RM} cell populations show both functional and phenotypic differences, with CD103+ CD8+ populations more polyfunctional, and showing robust IL-2 production.

CD103+ and CD103- CD4+ T cells display analogous phenotypic and functional differences to their CD8+ counterparts

Non-regulatory CD4+ T_{RM} cells did not form transcriptionally distinct clusters in the single-cell dataset. However, CD4+ intestinal T cells showed phenotypic heterogeneity, dependent on CD69 and CD103 expression. CD69- populations expressed lower levels of CD161 and CD127, while CD69+CD103- CD4+ T cells had higher expression of β2-integrin than either CD69- or CD103+ populations, in a similar manner to CD8+ T cells (Fig. 6-7A). No differences in CD7, KLRG1, and granzyme K expression were seen between CD69+CD103- and CD103+ CD4+ populations, in contrast

to CD8+ T cells. Recipient-origin, CD69+CD103- CD4+ T cells also displayed higher expression of β2-integrin than their CD103+ counterparts (Fig. 6-7B).

A donor-origin CD4+ FOXP3+ T cell population, consistent with a T_{REG} cell subset, was detected in the scRNAseq data (Fig. 6-2C). Donor-origin CD25+CD127- CD4+ T cells, again consistent with a T_{REG} cell phenotype, were detected in some subjects, consistent with long-term residency of intestinal CD4+ T_{REG} cell populations (Supplementary Fig. 6-4G). Low cell number of this population precluded further analysis.

CD69+ CD4+ intestinal T cells were potent producers of multiple cytokines, consistent with a recent study(Bartolomé-Casado et al., 2020), with greater cytokine production potential than CD69- CD4+ T cells (Fig. 6-7C-I). In particular, IL-17A was almost exclusively produced by CD69+ T cells (Fig. 6-7C). CD69+ CD103+ CD4+ T cells production greater levels of TNFα, CCL4, IL-17A, and IL-10 than CD69+ CD103- counterparts. As seen in CD8+ T cell populations, there was a gradient of functionality between CD4+ populations, with CD103+ cells showing greatest polyfunctional cytokine production (Fig. 6-7I). In summary, intestinal CD4+ T cell populations showed some analogous patterns of phenotype and functionality to CD8+ subsets.

6.4 Discussion

Summary of findings

This work identified two transcriptionally distinct subsets of functionally-resident *bona fide* human intestinal CD8+ T_{RM} cells with differences in phenotype and cytokine production, using the human 'model' of intestinal transplantation, which confirms functional tissue residency. Additional evidence for these distinct subsets was also seen within recipient-origin T cells infiltrating the graft (and

therefore establishing residency *de novo*), and in healthy intestine. These CD8+ T_{RM} subsets differ in the expression of genes previously associated with a human T_{RM} cell 'signature'. This suggests that this gene set, which was derived from bulk RNAseq experiments of all CD69+ T cell populations, may be an amalgamation of two transcriptionally distinct T_{RM} cell subsets (Kumar et al., 2017).

Discussion in context with the literature

αE-integrin (CD103) is expressed on all IEL CD8+ T cells and a proportion of LPLs. Prior work considered IELs and LPLs to be distinct subsets (Bartolomé-Casado et al., 2019), however the presence of only a single transcriptionally distinct CD103+ cluster, along with the phenotypic similarity between CD103+ IELs and LPLs, indicates that these populations are likely to represent a single subset found in two spatially distinct but adjacent mucosal compartments. Similarly, KLRG1 was proposed as a marker that distinguished two subsets of LPL CD103- CD8+ T cells(Bartolomé-Casado et al., 2019). However, the CD103- CD8+ T cells did not form transcriptionally distinct subsets using scRNAseq, which does not support the conclusion that KLRG1 marks out transcriptionally distinct subsets.

While this work confirms that the CD103- CD8+ T_{RM} population contains definitively resident cells as demonstrated by persistence after transplantation, CD103- T cells are found at declining frequencies at later times post-transplant. It may be that CD103- T_{RM} cells represent an intermediate state differentiating to a CD103+ population, or that the CD103- T_{RM} cell subset has a reduced capacity for longevity and persistence. The two CD8+ T_{RM} populations do differ in IL7R (CD127) expression, as well as in IL-2 production, which may lead to reduced persistence and proliferation in the CD103- subset. Autocrine IL-2 production is critical to secondary proliferative responses and IFN-γ production in CD8+ T cells (Feau et al., 2011). This may be particularly pertinent to the intra-

The CD8+ T_{RM} populations showed differential expression of chemokine receptors and integrins, which may indicate differences in tissue homing and retention. Of interest, β2-integrin is highly expressed on CD69+CD103- T_{RM} cells, a population which remains difficult to positively distinguish from recent immigrants from the circulation. This is of particular relevance during inflammation or infection, where CD69 expression may represent cellular activation by cytokines rather than residency(Freeman et al., 2012). Despite the constitutively high β2-integrin expression on peripheral effector populations, expression is low on CD69- T cells in intestinal tissue, which could indicate that β2-integrin surface expression is reduced on recent tissue immigrants, before subsequent upregulation on CD69+CD103- T_{RM} cells. β2-integrin, in combination with CD69 expression, could therefore represent an additional positive marker to identify the CD103- T_{RM} population.

β2-integrin forms the heterodimer LFA-1 with αL-integrin. LFA-1 facilitates firm adhesion on blood vessel endothelium via ICAM-1, a key stage in lymphocyte trafficking (Fagerholm et al., 2019). β2-integrin also regulates the immunological synapse and provides a co-stimulatory signal, both when interacting with antigen-presenting cells, and with infected target cells (D. Liu et al., 2009). LFA-1 is upregulated on resident T cells in the liver and facilitates their patrolling of hepatic sinusoids, indicating a role for LFA-1 in T_{RM} cell motility and tissue surveillance (McNamara et al., 2017). β2-integrin has been implicated in IEL development and function in mice (Huleatt and Lefrançois, 1996). Of note, LFA-1/ICAM-1 interaction reduces cell responses to TGFβ, a cytokine that plays a key role in T_{RM} development (Verma et al., 2012), while conversely TGFβ can inhibit LFA-1 expression and function (Boutet et al., 2016). This suggests that β2-integrin may play a role in the development of CD103- CD8+ T_{RM} cells, which may be TGFβ-independent, as in mice (Bergsbaken and Bevan, 2015).

The ITGB2 locus is a differentially methylated region in the blood and mucosa in IBD, and mucosal gene expression is associated with disease activity (Harris et al., 2014; Kennedy et al., 2016; Román

et al., 2013). We hypothesize that this association with IBD, in which T_{RM} cells play a key role (Zundler et al., 2019), could be mediated via altered β2-integrin expression by T_{RM} cells, or suggest that T_{RM} cell subsets play a pathogenic role.

Transcriptional heterogeneity has been examined in lung T_{RM} cells using scRNAseq, with two potential subsets identified, however these populations were characterised by predominantly different gene signatures to those that I have found in the intestine (Snyder et al., 2019). However, the subsets identified in that previous study contained both CD4+ and CD8+ cells co-clustering together, which separated clearly this work. In addition, lung T_{RM} cell subsets did split based on CD103 expression. T_{RM} cell phenotype and behaviour in lung and the gut have been shown to differ (Thome et al., 2014), which suggests that these differences between studies may be driven by tissue-specific T_{RM} properties. It could also be an artifact of the higher cell number in our study, which provides greater power to detect transcriptionally distinct clusters. Therefore remains unclear if T_{RM} subsets analogous to those described in the gut in this study exist in other tissues. Whether these subsets are imbued with differences in residency characteristics and function, and if they play different roles in human disease, remains unclear.

Strengths and limitations

A key strength of this study is the use of the rigorous transplant model to identify donor-origin definitive T_{RM} cells, which provides the clearest evidence in human studies of functional residence. The exclusion of ongoing donor macrochimerism in the blood presented in this study provides reassurance that the continued presence of donor-origin cells is not from recent circulating immigrants.

Even in a centre for intestinal transplantation, intestinal biopsy samples from such patients are challenging to obtain, which limits study subject number and the generalisability of the results.

However, the identification of populations of T cells with similar phenotype and with different functional capacity in healthy control subjects strengthens the work and provides evidence that these results are generalisable beyond intestinal transplantation.

The identification of transcriptionally distinct clusters, particularly within a population of cells that is relatively homogeneous to start with, is a necessarily subjective process, as the balance between lumping similar groups together, or splitting them apart can be altered by the choice of variables in the clustering algorithm. The process of clustering is also dependent on study design (particularly the degree of batch effects) and on cell number also. As such, it is highly reassuring that clusters with similar transcriptional profiles were found in both single-cell sequencing experiments, which used different donors, at different times post-transplantation, and using different sequencing approaches. Moreover, the finding that the identified core gene signature discriminating these clusters also divided transcriptionally distinct clusters found in the gut in health and disease in two previously published datasets is most reassuring. It is unclear to what extent those two subsets can be further divided, however, it strongly suggests that there are at least two distinct subsets of human intestinal T_{RM} cells.

I assumed that the development of recipient-origin T_{RM} cells in the graft was due to de novo T_{RM} development from circulating effector populations, however, another possibility is that lateral spread of recipient T_{RM} cells from recipient-origin gut could be the mechanism. However, in most patients, very little recipient-origin intestine (and some some patients none) was left following transplantation, making this possibility less likely. Moreover, the data presented here showing that at early timepoints recipient-origin T cells lack markers of T_{RM} status suggests that this is not a relevant mechanism in this patient cohort.

In conclusion, I used human intestinal transplantation as a model to study single-cell transcriptional heterogeneity in *bona fide* intestinal T_{RM} cells. CD8+ T_{RM} cells comprise two transcriptionally, phenotypically, and functionally distinct subsets, while CD4+ T cells show some analogous differences in phenotype and function. β2-integrin expression is highly expressed by CD69+CD103- intestinal T_{RM} cells and could provide a useful marker for this population. β2-integrin may also have a role in T_{RM} cell development.

6.5 Figures

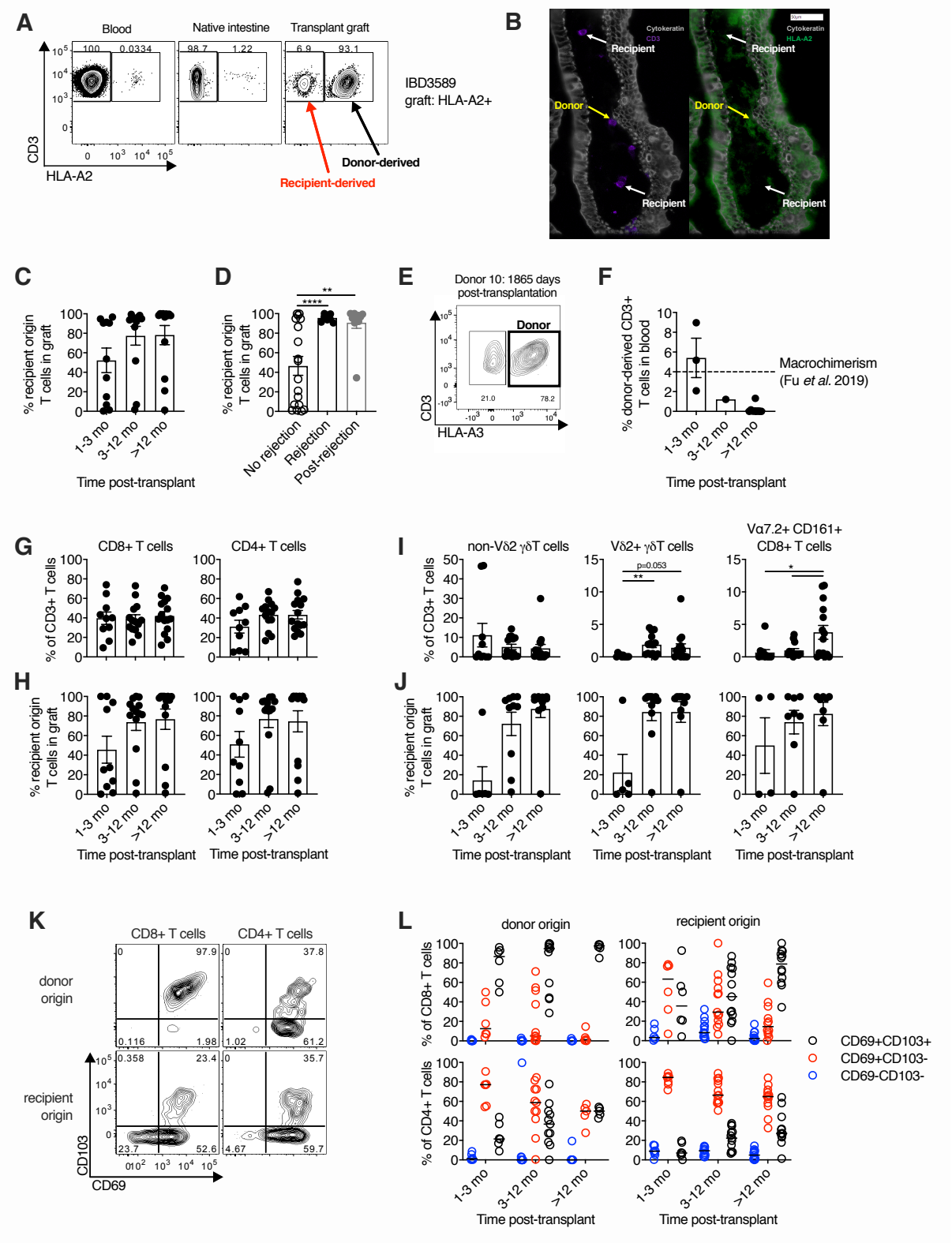

A
Blood
Native intestine
Transplant graft
100
0.0334
98.7
1.22
6.9
93.1
CD3
HLA-A2
IBD3589
graft: HLA-A2+
Donor-derived
Recipient-derived
B
Cytokeratin
CD3
HLA-A2
Recipient
Donor
C
% recipient origin T cells in graft
1-3 mo
3-12 mo
>12 mo
Time post-transplant
D
% recipient origin T cells in graft
No rejection
Rejection
Post-rejection
E
Donor 10: 1865 days post-transplantation
Donor
CD3
HLA-A3
21.0
78.2
F
% donor-derived CD3+ T cells in blood
Macrochimerism
(Fu et al. 2019)
Time post-transplant
G
CD8+ T cells
CD4+ T cells
% of CD3+ T cells
H
% recipient origin T cells in graft
Time post-transplant
I
non-Vδ2 γδT cells
Vδ2+ γδT cells
Vα7.2+ CD161+ CD8+ T cells
p=0.053
J
K
donor origin
recipient origin
CD103
CD69
97.9
37.8
0.116
1.98
1.02
61.2
0.358
23.4
35.7
23.7
52.6
4.67
59.7
L
donor origin
recipient origin
% of CD8+ T cells
% of CD4+ T cells
CD69+CD103+
CD69+CD103-
CD69-CD103-

Figure 6-1. Long-lived conventional CD4+ and CD8+ T cells, but not unconventional T cell populations, can persist for at least 5 years in the human intestine

(A) Representative flow cytometry plot of HLA-A2 expression on T cells from the blood, the recipient native intestinal mucosa, and the intestinal transplant graft, demonstrating identification of donor- and recipient-derived populations by HLA mismatch.

(B) Representative chip cytometry image of intestinal graft mucosa demonstrating the presence of donor-derived (HLA-A2+, yellow arrows) and recipient-derived (HLA-A2-, white arrows) CD3+ T cells in the lamina propria. Cytokeratin (grey); CD3 (purple); HLA-A2 (green).

(C) Percentage of recipient-origin CD3+ T cells in intestinal grafts, categorised by time post-transplant (n=37 (16 subjects); mean +/- SEM).

(D) Percentage of recipient-origin CD3+ T cells in intestinal grafts, categorised by history of graft rejection. Unfilled circles, no rejection; Black, current rejection; Grey, previous (post) rejection. (n=37 (16 subjects); mean +/- SEM).

(E) Flow cytometry plot of HLA-A3 expression on graft-derived T cells in one subject who demonstrated persistent donor chimerism in the intestinal graft 1865 days (5 years and 1 month) post-transplant.

(F) Percentage of donor-origin CD3+ T cells in the blood of intestinal transplant recipients, categorised by time post-transplant (n=13; mean +/- SEM). Dashed line at 4% represents the cut-off for significant macrochimerism from prior studies (Fu et al., 2019; Zuber et al., 2015).

(G) Conventional CD8+ and CD4+ T cell subsets in the small intestinal graft as a proportion of total T cells, categorised by time post-transplant (n=39 (18 subjects); mean +/- SEM).

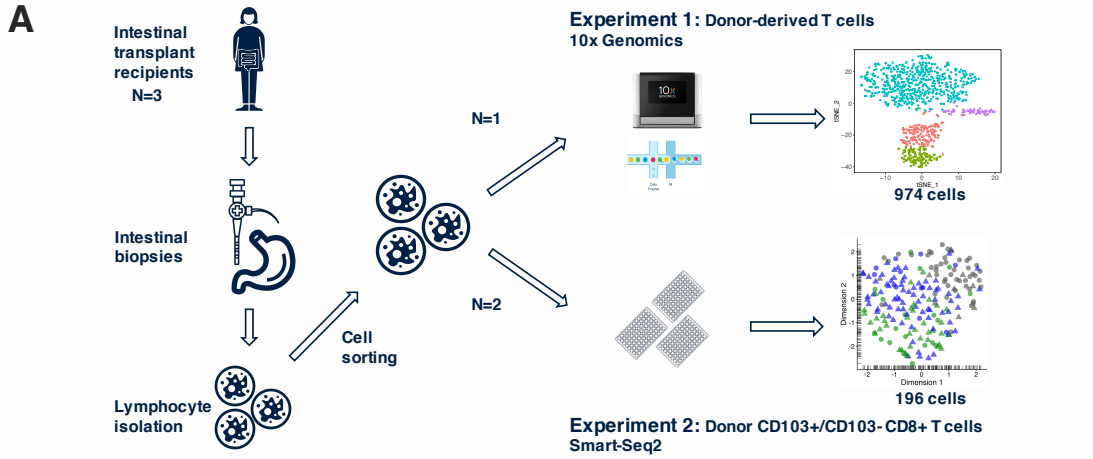
(H) The percentage of recipient-derived T cells infiltrating the intestinal graft within conventional CD8+ and CD4+ T cell subsets, categorised by time post-transplant (n=37 (16 subjects); mean +/- SEM).

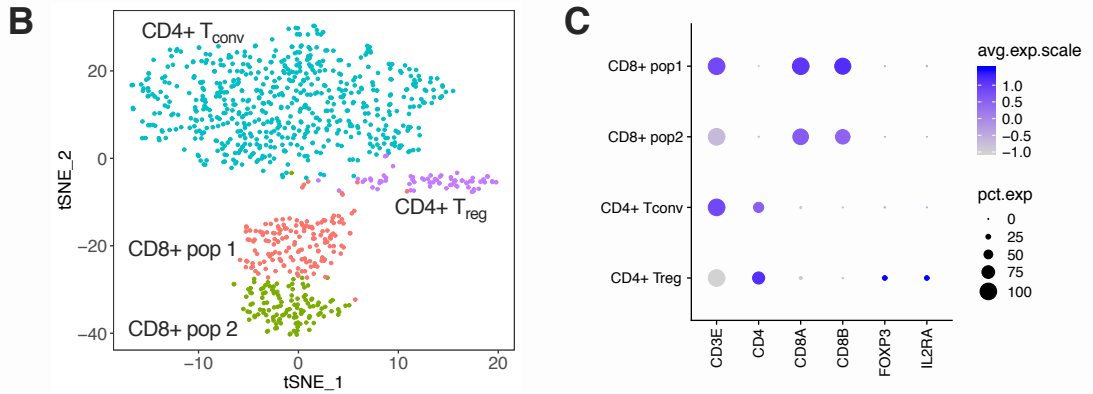
(I) Unconventional non-Vδ2+ γδ T cell, Vδ2+ γδ T cell, and Vα7.2+CD161+ CD8+ T cell (mucosal-associated invariant T cell) subsets in the small intestinal graft as a proportion of total T cells, categorised by time post-transplant (n=39 (18 subjects); mean +/- SEM).

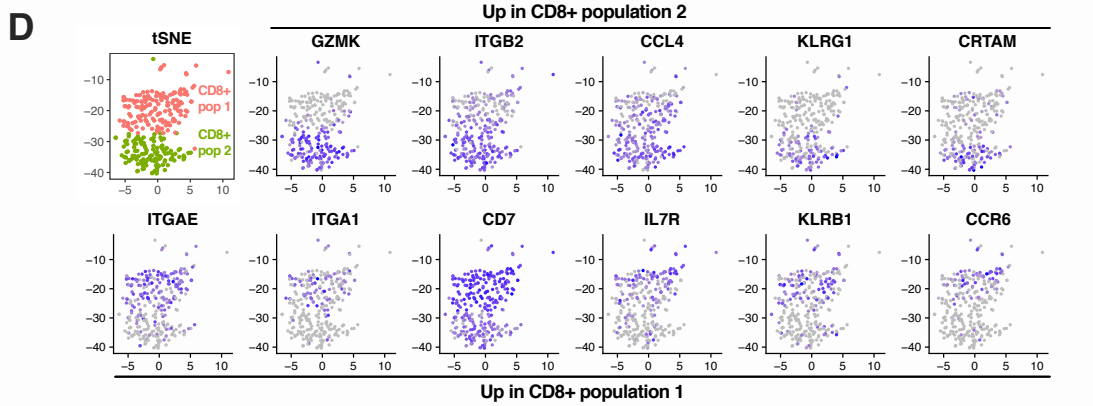
(J) The percentage of recipient-derived T cells infiltrating the intestinal graft within unconventional non-Vδ2+ γδ T cell (n=27; 12 subjects), Vδ2+ γδ T cell (n=25; 12 subjects), and Vα7.2+CD161+ CD8+ T cell subsets (n=20; 12 subjects), categorised by time post-transplant (mean +/- SEM).

(K) Representative flow cytometry plot of CD69 and CD103 expression on donor- and recipient-derived CD8+ and CD4+ T cells in the intestinal graft.

(L) Percentage of donor- and recipient-derived CD8+ and CD4+ T cells in the intestinal graft co-expressing CD69 and CD103 categorised by time post-transplant (n=35 (16 subjects); median marked with black line). Blue, CD69-CD103- cells; Red, CD69+CD103- cells; Black, CD69+CD103+ cells.
For further analysis of surface marker expression, rare populations with fewer than 10 cells were excluded from the analysis (J, L). Statistical analysis performed with one-way ANOVA with Dunnett's multiple comparisons test. *, $P \leq 0.05$; **, $P \leq 0.01$.


A
Intestinal transplant recipients N=3
Intestinal biopsies
Lymphocyte isolation
Cell sorting
N=1
N=2
Experiment 1: Donor-derived T cells
10x Genomics
974 cells
Experiment 2: Donor CD103+/CD103- CD8+ T cells
Smart-Seq2
196 cells


B
CD4+ Tconv
CD4+ Treg
CD8+ pop 1
CD8+ pop 2
tSNE_1
tSNE_2
C
CD8+ pop1
CD8+ pop2
CD4+ Tconv
CD4+ Treg
CD3E
CD4
CD8A
CD8B
FOXP3
IL2RA
avg.exp.scale
pct.exp


D
tSNE
Up in CD8+ population 2
GZMK
ITGB2
CCL4
KLRG1
CRTAM
ITGAE
ITGA1
CD7
IL7R
KLRB1
CCR6
Up in CD8+ population 1

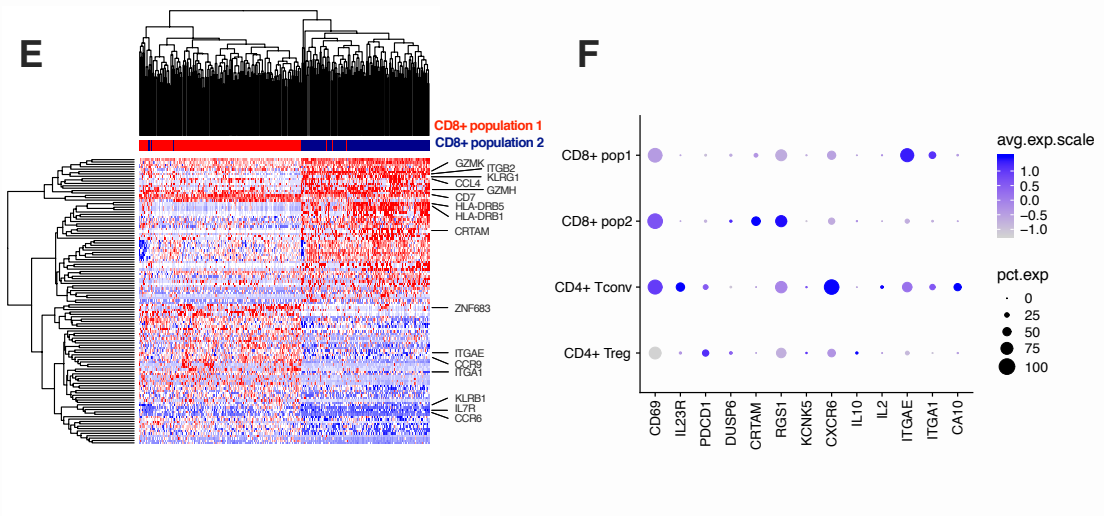

E
CD8+ population 1
CD8+ population 2
GZMK
ITGB2
KLRG1
CCL4
GZMH
CD7
HLA-DRB5
HLA-DRB1
CRTAM
ZNF683
ITGAE
CCR9
ITGA1
KLRB1
IL7R
CCR6
F
CD8+ pop1
CD8+ pop2
CD4+ Tconv
CD4+ Treg
CD69
IL23R
PDCD1
DUSP6
CRTAM
RGS1
KCNK5
CXCR6
IL10
IL2
ITGAE
ITGA1
CA10
avg.exp.scale
pct.exp

Figure 6-2. Single-cell RNA sequencing delineates transcriptionally distinct states within CD4+ and CD8+ T_{RM} cell populations

(A) Schematic of two scRNAseq experiments. Biopsies of small intestinal transplant tissue were collected from subjects at endoscopy, dissociated to isolate intestinal lymphocytes, before cell sorting by FACS. In Experiment 1, all live, donor-derived CD3+ T cells were bulk-sorted. In Experiment 2, live donor-derived CD8+ CD103- and CD103+ T cells were index sorted. scRNAseq library preparation and sequencing was performed using the 10x Genomics platform (Experiment 1) or the Smart-Seq2 protocol (Experiment 2). See p69-70 in Chapter 2 for further method details.

(B) tSNE plot of 974 donor-derived T cells from a single subject showing four transcriptionally distinct populations of conventional CD4+ and CD8+ T cells.

(C) Dot plot of key gene identifiers for the four clusters showing two clusters of CD8+ T cells, and two clusters of CD4+ T cells, including one containing cells expressing IL2RA and FOXP3, consistent with a regulatory T cell phenotype. Dot size indicates the proportion of cells in which the gene is present. Colour intensity indicates the mean expression level of the gene in cells in that cluster.

(D) tSNE plots showing the expression of key genes upregulated in CD8+ population 2 (top row) or upregulated in CD8+ population 1 (bottom row).

(E) Heatmap indicating hierarchical clustering of gene expression of CD8+ donor-derived T cells from population 1 and population 2. Cell labels above indicate cluster: Red, population 1; Blue, population 2. Genes of interest are highlighted.

(F) Dot plot showing the expression of 13 genes previously associated with tissue residency in human CD69+ T cells (Kumar et al., 2017). Dot size indicates the proportion of cells in which the gene is present. Colour intensity indicates the mean level of expression of the gene in cells in that cluster.

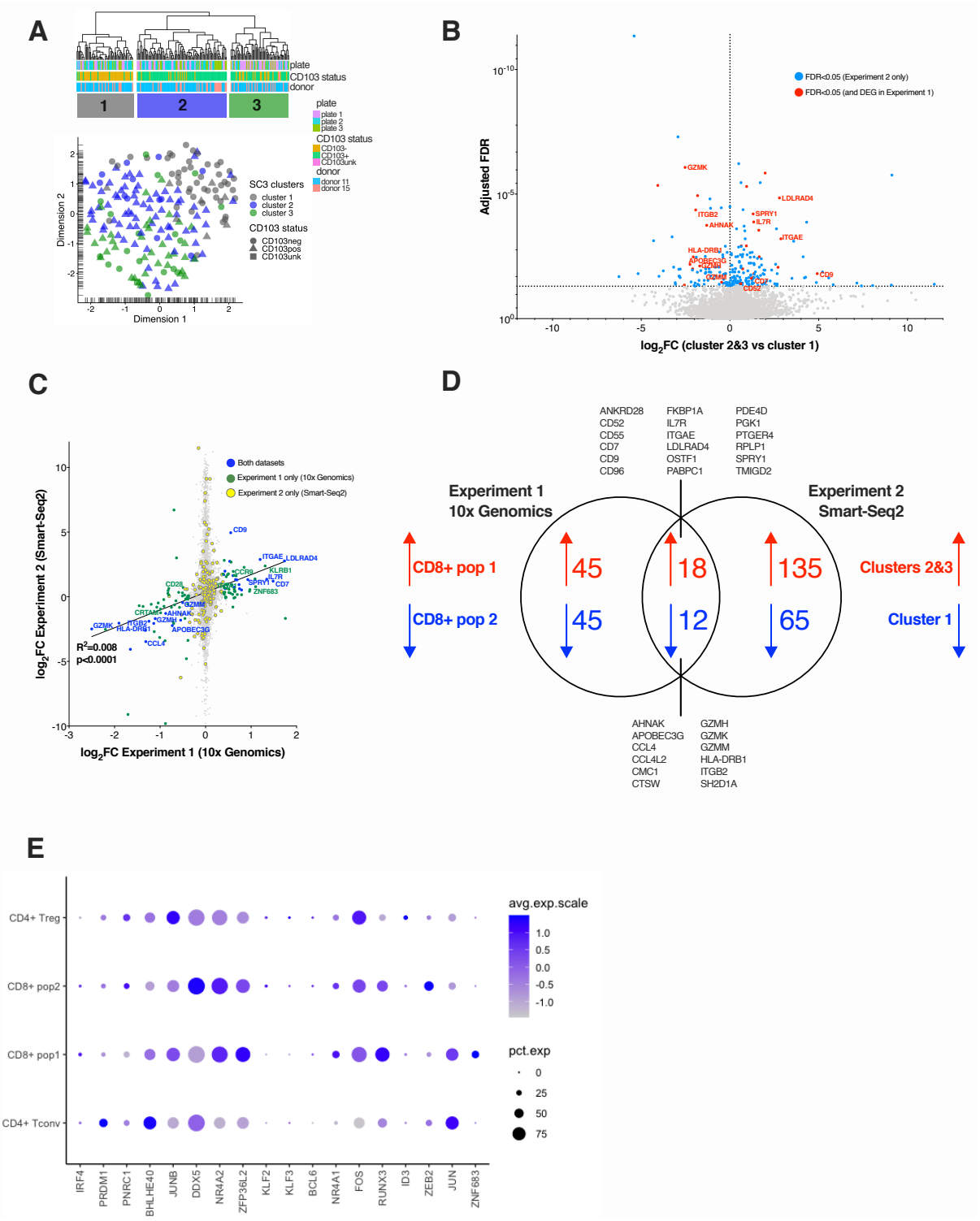

A
plate
CD103 status
donor
1
2
3
plate
plate 1
plate 2
plate 3
CD103 status
CD103-
CD103+
CD103unk
donor
donor 11
donor 15
SC3 clusters
cluster 1
cluster 2
cluster 3
CD103 status
CD103neg
CD103pos
CD103unk
Dimension 1
Dimension 2
B
FDR<0.05 (Experiment 2 only)
FDR<0.05 (and DEG in Experiment 1)
Adjusted FDR
log2FC (cluster 2&3 vs cluster 1)
GZMK
LDLRAD4
ITGB2
SPRY1
IL7R
AHNAK
ITGAE
HLA-DRB1
APOBEC3G
CD9
C
Both datasets
Experiment 1 only (10x Genomics)
Experiment 2 only (Smart-Seq2)
log2FC Experiment 2 (Smart-Seq2)
log2FC Experiment 1 (10x Genomics)
R2=0.008
p<0.0001
D
ANKRD28
CD52
CD55
CD7
CD9
CD96
FKBP1A
IL7R
ITGAE
LDLRAD4
OSTF1
PABPC1
PDE4D
PGK1
PTGER4
RPLP1
SPRY1
TMIGD2
Experiment 1
10x Genomics
Experiment 2
Smart-Seq2
CD8+ pop 1
CD8+ pop 2
45
45
18
12
135
65
Clusters 2&3
Cluster 1
AHNAK
APOBEC3G
CCL4
CCL4L2
CMC1
CTSW
GZMH
GZMK
GZMM
HLA-DRB1
ITGB2
SH2D1A
E
CD4+ Treg
CD8+ pop2
CD8+ pop1
CD4+ Tconv
IRF4
PRDM1
PNRC1
BHLHE40
JUNB
DDX5
NR4A2
ZFP36L2
KLF2
KLF3
BCL6
NR4A1
FOS
RUNX3
ID3
ZEB2
JUN
ZNF683
avg.exp.scale
1.0
0.5
0.0
-0.5
-1.0
pct.exp
0
25
50
75

Figure 6-3. Single-cell RNA sequencing identifies a core gene set distinguishing two CD8+ T_{RM} cell populations

(A) Hierarchical clustering and UMAP plot of 196 index-sorted CD103- and CD103+ CD8+ donor-derived T cells from two subjects in Experiment 2 identified three transcriptionally distinct clusters of conventional CD8+ T cells. Cell labels below the dendrogram indicate the sorting plate, the subject, and CD103 expression determined by index sorting. For UMAP plot: circles, CD103- cells by index-sorting; triangles, CD103+ cells by index-sorting; square, unknown CD103 expression by index-sorting.

(B) Volcano plot of differential gene expression between cluster 1 and clusters 2 & 3 identified in (G), with genes upregulated (right) or downregulated (left) in clusters 2 & 3 compared to cluster 1. Log2(fold change) is plotted against the FDR-adjusted p-value, with horizontal dotted line at FDR=0.05. Differentially expressed genes are marked in blue, with those differentially expressed in both Experiments 1 and 2 marked in red.

(C) Correlation of log2(fold change) in CD8+ population 1 vs 2 in Experiment 1 (10x Genomics, x-axis) and clusters 2 & 3 vs cluster 1 in Experiment 2 (Smart-Seq2, y-axis). Blue, genes differentially expressed in both experiments; green, genes differentially expressed in Experiment 1 only; yellow, genes differentially expressed in Experiment 2 only; grey, genes not differentially expressed.

(D) Venn diagram showing differentially expressed genes upregulated (red) or downregulated (blue) in cluster 1 (CD103-) of Experiment 2 (Smart-Seq2), or CD8+ population 2 of Experiment 1 (10x Genomics). A core gene set of 30 genes that differentiated the two populations in both experiments are listed.

(E) Expression of transcription factors associated with tissue residency from prior studies by the four T_{RM} cell clusters identified in the Experiment 1 (10x Genomics) dataset. Dot size indicates the proportion of cells in which the gene is present. Colour intensity indicates the mean expression level of the gene in cells in that cluster.

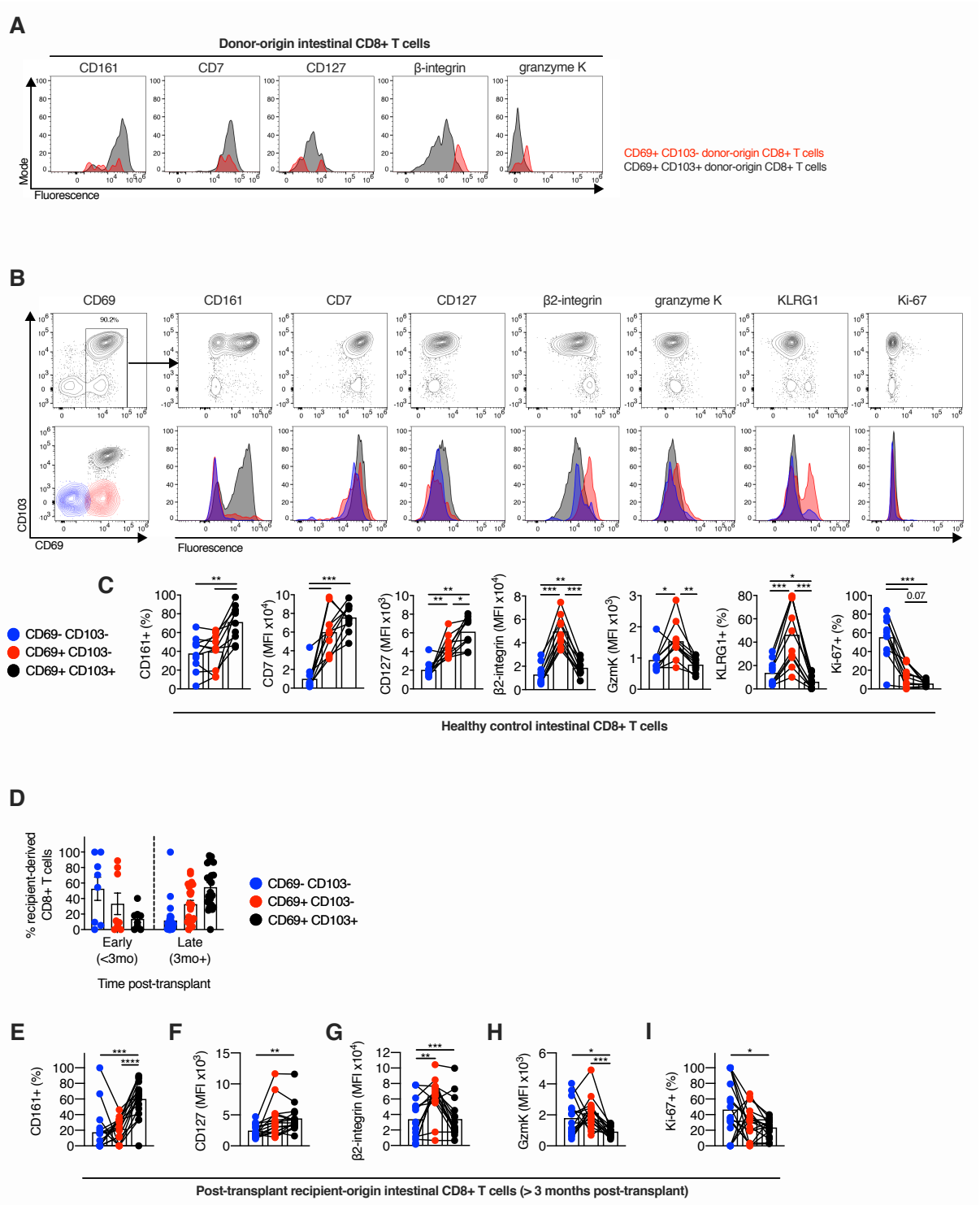

A
Donor-origin intestinal CD8+ T cells
CD161
CD7
CD127
β-integrin
granzyme K
Mode
Fluorescence
CD69+ CD103- donor-origin CD8+ T cells
CD69+ CD103+ donor-origin CD8+ T cells
B
CD69
CD161
CD7
CD127
β2-integrin
granzyme K
KLRG1
Ki-67
90.2%
CD103
CD69
Fluorescence
C
CD69- CD103-
CD69+ CD103-
CD69+ CD103+
CD161+ (%)
CD7 (MFI x10^4)
CD127 (MFI x10^3)
β2-integrin (MFI x10^4)
GzmK (MFI x10^3)
KLRG1+ (%)
Ki-67+ (%)
0.07
Healthy control intestinal CD8+ T cells
D
% recipient-derived CD8+ T cells
Early (<3mo)
Late (3mo+)
Time post-transplant
CD69- CD103-
CD69+ CD103-
CD69+ CD103+
E
CD161+ (%)
F
CD127 (MFI x10^3)
G
β2-integrin (MFI x10^4)
H
GzmK (MFI x10^3)
I
Ki-67+ (%)
Post-transplant recipient-origin intestinal CD8+ T cells (> 3 months post-transplant)

Figure 6-4. CD103+ and CD103- CD8+ T cells display distinct phenotypes in healthy and transplanted intestine

(A) Representative expression of CD161, CD7, CD127 (IL7R), ITGB2, and granzyme K on CD103- (red) and CD103+ (black) donor-derived T cells from the intestinal transplant graft.

(B,C) Phenotypic analysis of CD8+ T cell populations in healthy small intestine.

(B) Representative flow cytometry plots and histograms of CD8+ T cell phenotype from spectral flow cytometry, with expression of the following markers plotted against CD103: CD69, CD161, CD7, CD127, β2-integrin, granzyme K, KLRG1, and Ki-67. Cells co-expressing CD69 and CD103 is indicated. Blue, CD69-CD103- cells; Red, CD69+CD103- cells; Black, CD69+CD103+ cells.

(C) Proportion of positive cells (CD161, KLRG1, Ki-67) or MFI (CD7, CD127, β2-integrin, granzyme K) of CD8+ T cells, categorised by CD69 and CD103 expression, in small intestinal biopsies from healthy control subjects (n=10). Mean percentage or MFI represented by bars. Connecting lines represent populations from the same subject. Blue, CD69-CD103- cells; Red, CD69+CD103- cells; Black, CD69+CD103+ cells.

(D-I) Phenotypic analysis of recipient-derived CD8+ T cell populations infiltrating the intestinal transplant graft.

(D) The proportion of recipient-derived CD8+ T cells co-expressing CD69 and CD103 in intestinal transplant grafts, categorised by time post-transplant (n=35; 16 subjects). Blue, CD69-CD103- cells; Red, CD69+CD103- cells; Black, CD69+CD103+ cells.

(E-I) Proportion of CD161+ cells (E), MFI of CD127 (F), β2 integrin (G), and granzyme K (H), and proportion of Ki-67+ cells (I) of recipient-derived CD8+ T cells, categorised by CD69 and CD103 expression and time post-transplant, in intestinal transplant grafts (n=23; 12 subjects). Mean percentage or MFI represented by bars. Black lines connect populations from the same sample. Blue, CD69-CD103- cells; Red, CD69+CD103- cells; Black, CD69+CD103+ cells.

Statistical analysis performed with one-way ANOVA with Tukey's multiple comparisons test. * $P \leq 0.05$; ** $P \leq 0.01$; *** $P \leq 0.001$; **** $P \leq 0.0001$.

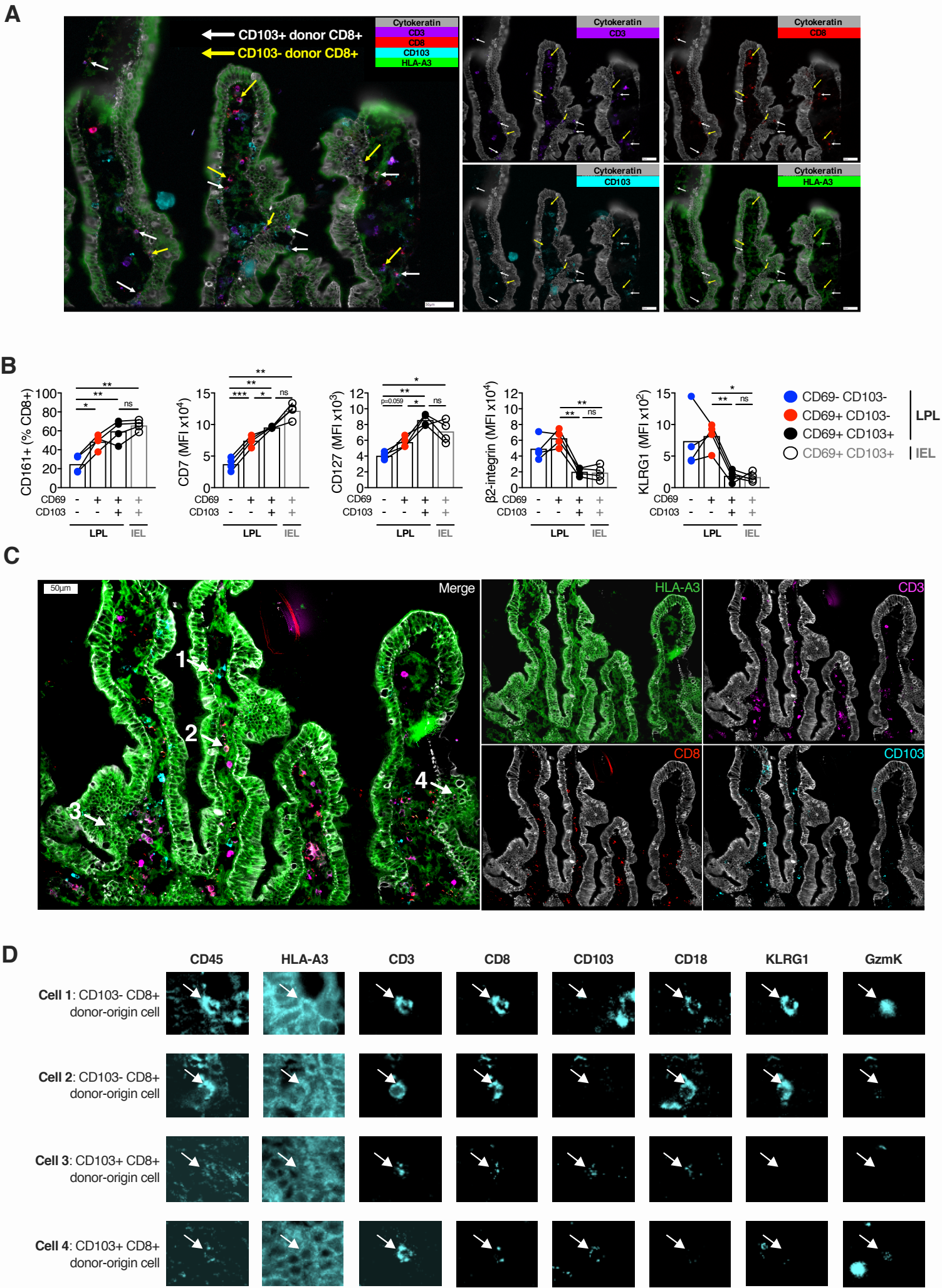

A
CD103+ donor CD8+
CD103- donor CD8+
Cytokeratin
CD3
CD8
CD103
HLA-A3
B
CD161+ (% CD8+)
CD7 (MFI x10^4)
CD127 (MFI x10^3)
β2-integrin (MFI x10^4)
KLRG1 (MFI x10^2)
p=0.059
ns
CD69
CD103
LPL
IEL
CD69- CD103-
CD69+ CD103-
CD69+ CD103+
CD69+ CD103+
C
50µm
Merge
HLA-A3
CD3
CD8
CD103
1
2
3
4
D
CD45
HLA-A3
CD3
CD8
CD103
CD18
KLRG1
GzmK
Cell 1: CD103- CD8+ donor-origin cell
Cell 2: CD103- CD8+ donor-origin cell
Cell 3: CD103+ CD8+ donor-origin cell
Cell 4: CD103+ CD8+ donor-origin cell

Figure 6-5: CD103+ and CD103- CD8+ T cells maintain their distinct phenotypes in lamina propria and intra-epithelial compartments

(A) Fluorescence microscopy chip cytometry image of small intestinal transplant mucosa from a single subject 3 months post-transplant. The donor was HLA-A3+, and recipient was HLA-A3-. False colour fluorescence imaging for cytokeratin (grey), CD3 (purple), CD8 (red), CD103 (blue), and HLA-A3 (green). Donor-derived CD8+ CD103+ and CD103- cells are indicated by white and yellow arrows respectively.

(B) Phenotypic analysis of CD8+ T cell populations in healthy small intestinal epithelium and lamina propria. Proportion of positive cells (CD161) or MFI (CD7, CD127, β2-integrin, KLRG1) of intraepithelial lymphocyte (IEL) or lamina propria lymphocyte (LPL) CD8+ T cells, categorised by CD69 and CD103 expression, in small intestinal biopsies from healthy control subjects (n=4). Mean percentage or MFI represented by bars. Connecting lines represent populations from the same subject. Blue, CD69-CD103- cells (LPL); Red, CD69+CD103- cells (LPL); Black, CD69+CD103+ LPL cells; open circles and grey bars, CD69+CD103+ IEL cells.

(C) Fluorescence microscopy chip cytometry image from a separate section from same donor as (A). False colour fluorescence imaging for cytokeratin (grey), CD3 (purple), CD8 (red), CD103 (blue), and HLA-A3 (green). Representative donor-derived CD8+ CD103+ and CD103- cells for further characterisation are numbered.

(D) Fluorescence microscopy chip cytometry of representative CD103- (cells 1 & 2) and CD103+ (cells 3 & 4) donor-derived CD8+ T cells, showing the expression of CD18 (β2-integrin), KLRG1, and granzyme K.

Statistical analysis performed with one-way ANOVA with Tukey's multiple comparisons test. * $P \leq 0.05$; ** $P \leq 0.01$; *** $P \leq 0.001$; **** $P \leq 0.0001$.

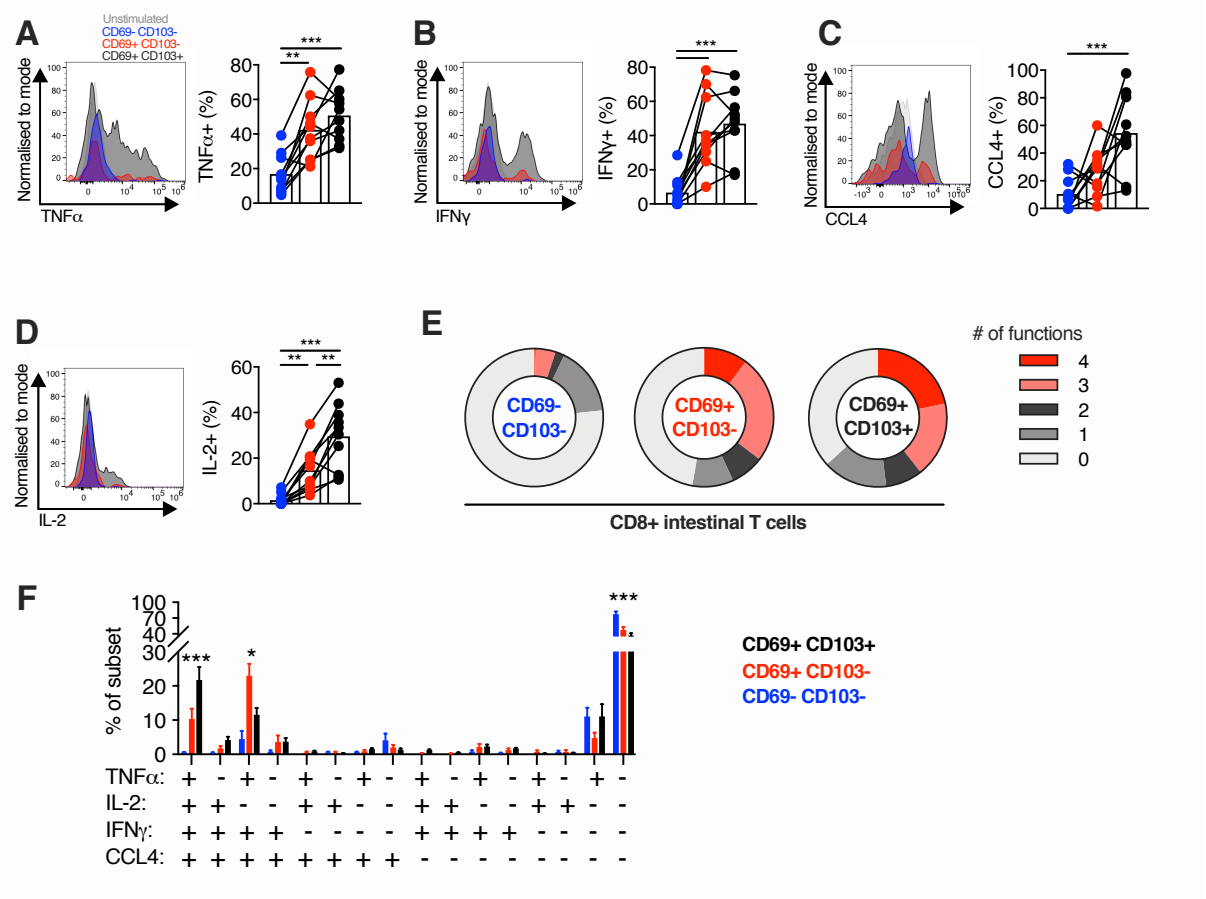


Figure 6-6. CD103+ CD8+ intestinal T cells demonstrate greater capacity for cytokine production

(A-D) Cytokine production by small intestinal CD8+ T cells. Representative histograms of expression, and group summaries of proportion of CD8+ T cells expressing TNFα (A), IFNγ (B), CCL4 (C), and IL-2 (D) after four hour stimulation with PMA and ionomycin in the presence of brefeldin A and monensin, categorised by CD69 and CD103 expression, in small intestinal biopsies from healthy control subjects (n=10). Blue, CD69-CD103- cells; Red, CD69+CD103- cells; Black, CD69+CD103+ cells.

(E) Mean proportion of CD8+ T cells expressing 0, 1, 2, 3, or 4 of the cytokines or chemokines TNFα, IFNγ, CCL4, and IL-2, categorised by CD69 and CD103 co-expression, from small intestinal biopsies from healthy control subjects (n=10).

(F) Mean percentage (+/- SEM) of CD8+ T cells co-expressing TNFα, IFNγ, CCL4, and/or IL-2 after PMA/ionomycin stimulation as described, categorised by CD69 and CD103 expression. Blue, CD69-CD103- cells; Red, CD69+CD103- cells; Black, CD69+CD103+ cells.

Statistical analysis performed with one-way ANOVA with Tukey's multiple comparisons test. * $P \leq 0.05$; ** $P \leq 0.01$; *** $P \leq 0.001$.

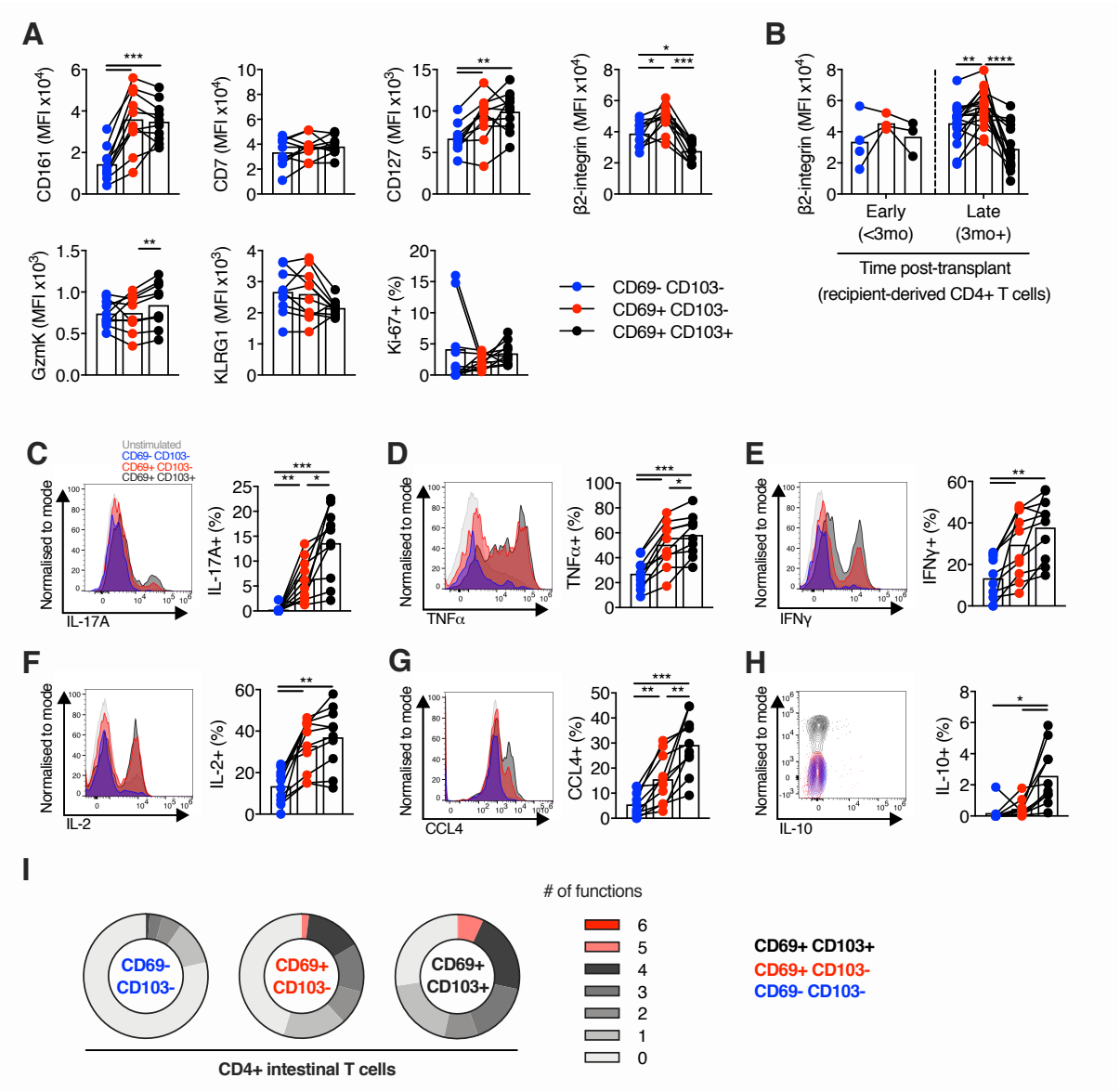

A
CD161 (MFI x10^4)
CD7 (MFI x10^4)
CD127 (MFI x10^3)
β2-integrin (MFI x10^4)
GzmK (MFI x10^3)
KLRG1 (MFI x10^3)
Ki-67+ (%)
CD69- CD103-
CD69+ CD103-
CD69+ CD103+
B
β2-integrin (MFI x10^4)
Early (<3mo)
Late (3mo+)
Time post-transplant
(recipient-derived CD4+ T cells)
C
Unstimulated
CD69- CD103-
CD69+ CD103-
CD69+ CD103+
Normalised to mode
IL-17A
IL-17A+ (%)
D
TNFα
TNFα+ (%)
E
IFNγ
IFNγ+ (%)
F
IL-2
IL-2+ (%)
G
CCL4
CCL4+ (%)
H
IL-10
IL-10+ (%)
I
# of functions
6
5
4
3
2
1
0
CD69- CD103-
CD69+ CD103-
CD69+ CD103+
CD4+ intestinal T cells
CD69+ CD103+
CD69+ CD103-
CD69- CD103-

Figure 6-7. CD103+ and CD103- CD4+ T cells display analogous phenotypic and functional differences to their CD8+ counterparts

(A) MFI (CD161, CD7, CD127, β2-integrin, granzyme K, and KLRG1) or percentage positive (Ki-67) of CD4+ T cells, categorised by CD69 and CD103 expression, in small intestinal biopsies from healthy control subjects (n=10). MFI represented by bars. Connecting lines represent populations from the same subject. Blue, CD69-CD103- cells; Red, CD69+CD103- cells; Black, CD69+CD103+ cells.

(B) MFI of β2-integrin on recipient-derived CD4+ T cells, categorised by CD69 and CD103 expression and time post-transplant, in intestinal transplant grafts (n=21). MFI represented by bars. Blue, CD69-CD103- cells; Red, CD69+CD103- cells; Black, CD69+CD103+ cells.

(C-I) Cytokine production by small intestinal CD4+ T cells.

Representative histograms of expression, and group summaries of proportion of CD4+ T cells expressing IL-17A (C), TNFα (D), IFNγ (E), IL-2 (F), CCL-4 (G), and IL-10 (H) after four hour stimulation with PMA and ionomycin in the presence of brefeldin A and monensin, categorised by CD69 and CD103 expression, in small intestinal biopsies from healthy control subjects (n=10). Blue, CD69-CD103- cells; Red, CD69+CD103- cells; Black, CD69+CD103+ cells.

(I) Mean proportion of CD4+ T cells expressing 0, 1, 2, 3, 4, 5, or 6 of the cytokines or chemokines IL-17A, TNFα, IFNγ, CCL4, IL-2, and IL-10, categorised by CD69 and CD103 co-expression, from small intestinal biopsies from healthy control subjects (n=10).

Statistical analysis performed with one-way ANOVA with Tukey's multiple comparisons test. * $P \leq 0.05$; ** $P \leq 0.01$; *** $P \leq 0.001$.

Chapter 7: Discussion

In this thesis I examined the roles of CD8+ and γδ T cells in coeliac disease, using a number of sequencing approaches. I went onto examine other aspects of γδ T cell biology, in particular the innate-like responses of a proportion of Vδ2+ T cells, and their similarities with MAIT cells. Finally, used clinical intestinal transplantation as a model to study human T_{RM} cells, in particular their transcriptional and functional heterogeneity.

7.1 CD8+ and γδ T cells in CD

In Chapter 4, I examined intestinal CD8+ and γδ T cells in CD using several transcriptomic approaches. Two γδ T cell populations, the Vδ1+ and Vδ1/2- subsets, were increased in CD, and showed highly similar transcriptional profiles, suggesting that they are best considered as a single population. Examination of the γδ T cell TCR repertoire showed a loss of TRGV4-containing clonotypes, and an increase in TRGV2/3-containing clonotypes, as has been recently described(Eggesbø et al., 2019; Mayassi et al., 2019). Moreover, I found evidence that hypothesised CD-specific CDR3δ motifs were increased in the repertoire(Han et al., 2013), in contrast to two recent studies(Eggesbø et al., 2019; Mayassi et al., 2019). These differences between studies may be due to the number of cells included in the TCR repertoires analysed, as antigen-specific T cells are rare, even at the site of inflammation.

The most striking result was an increase in the proportion of the CD8+ T cell TCR repertoire using TRBV28. This TRBV28 gene usage was associated with a population of CD8+ T cells with a highly cytotoxic and pro-inflammatory profile, expressing genes associated with tissue residency, and high expression of co-inhibitory receptors. This unexpected association of a particular V-gene usage with CD was seen in the TCRseq and RNAseq datasets, with additional supportive evidence seen in the

scRNAseq data. In addition, peripheral CD8+ T cells expressing gut-homing integrins showed increased TRBV28 expression in subjects with CD.

These congruent findings from different experimental approaches and patient cohorts provide reassurance that this is a genuine result, and I have made considerable efforts to minimise confounders and bias. It is frustrating that the COVID-19 pandemic has stopped further laboratory work that sought to examine the phenotype and function of TRBV28-expressing cells in the gut.

The finding of TCR repertoire perturbations in the CD8+ T cell population in CD challenges some aspects of the current CD model, which posits no CD8+ TCR-dependent process is required(Jabri and Sollid, 2017). There are several hypotheses about the role of the TCR that could explain this association.

First, TRBV28-expressing cells could represent an innate-like semi-invariant T cell population increased in inflammation. However, the TCR repertoire analysis did not indicate the characteristics of a semi-invariant TCR as displayed by MAIT cells, nor do these cells display the distinctive, shared transcriptional profile of innate-like T cells.

Second, this population could represent an adaptive conventional or unconventional T cell responsive to a non-disease specific antigen, mediated by intestinal inflammation. The cytokine milieu in CD could drive CD8+ T cell clones to low-affinity self-antigens. However, if this hypothesis were true, we would expect to see increased TRBV28 usage in other chronic inflammatory intestinal diseases, and no evidence of enrichment was seen in ulcerative colitis or irAE colitis. Therefore, this antigen would need to be restricted to the proximal small intestine if this were the case.

Third, this population could be an adaptive conventional CD8 T cell responsive to a coeliac disease specific antigen. Class I HLA-restricted CD8+ gluten-specific CD8+ T cells have been described(Gianfrani et al., 2003; Mazzarella et al., 2008; Picascia et al., 2017), and there are Class I MHC associations with CD in recent fine-mapping studies(Gutierrez-Achury et al., 2015).

Fourth, this could represent an adaptive unconventional CD8 T cell responsive to a coeliac disease specific antigen. MHC-like molecules like MICA and HLA-E are increased in expression in CD, and while it is postulated that they stimulated CD8+ T cells via activating NKRs, these ligands are also recognised by unconventional T cell TCRs(Joosten et al., 2016; Walters et al., 2018). A related possibility would be HLA-Class II restriction of these CD8+ T cells, a phenomenon reported in CMV and HIV responses(Hansen et al., 2013; Ranasinghe et al., 2016).

Meticulous in vitro studies using T cell clones will be required to test these hypotheses, indeed much the same approaches that delivered insights into gluten-specific CD4+ T cell responses.

7.2 Insights into γδ T cell and innate-like T cell biology

In chapter 5, I examined transcriptional, phenotypic, and functional heterogeneity within and between the two major populations of γδ T cells: the Vδ2+ and non-Vδ2 T cells. Vδ2+ T cells, along with MAIT and iNKT cells, fall in a group of rebellious innate-like T cells that possess characteristics that bridge innate and adaptive immunity(Garner et al., 2018; Godfrey et al., 2015). However, unlike MAIT cells, Vδ2+ T cells form a spectrum of function, from a cytokine-responsive, innate-like CD26bright population highly similar to MAIT cells, to a cytotoxic, more NK-like GPR56+ population (Fig. 7-1). It is interesting to consider why the mechanisms of differentiation or plasticity that allow this differentiation within Vδ2+ T cells are closed off for MAIT cells. Epigenetic differences might form a block to MAIT cell phenotypic change, or the stimuli that drive differentiation in Vδ2+ T cells

may trigger activation-induced cell death in MAIT cells. Understanding the differences in differentiation potential of innate-like T cells could have relevance to their role in infection, and their potential in oncological cellular therapy.

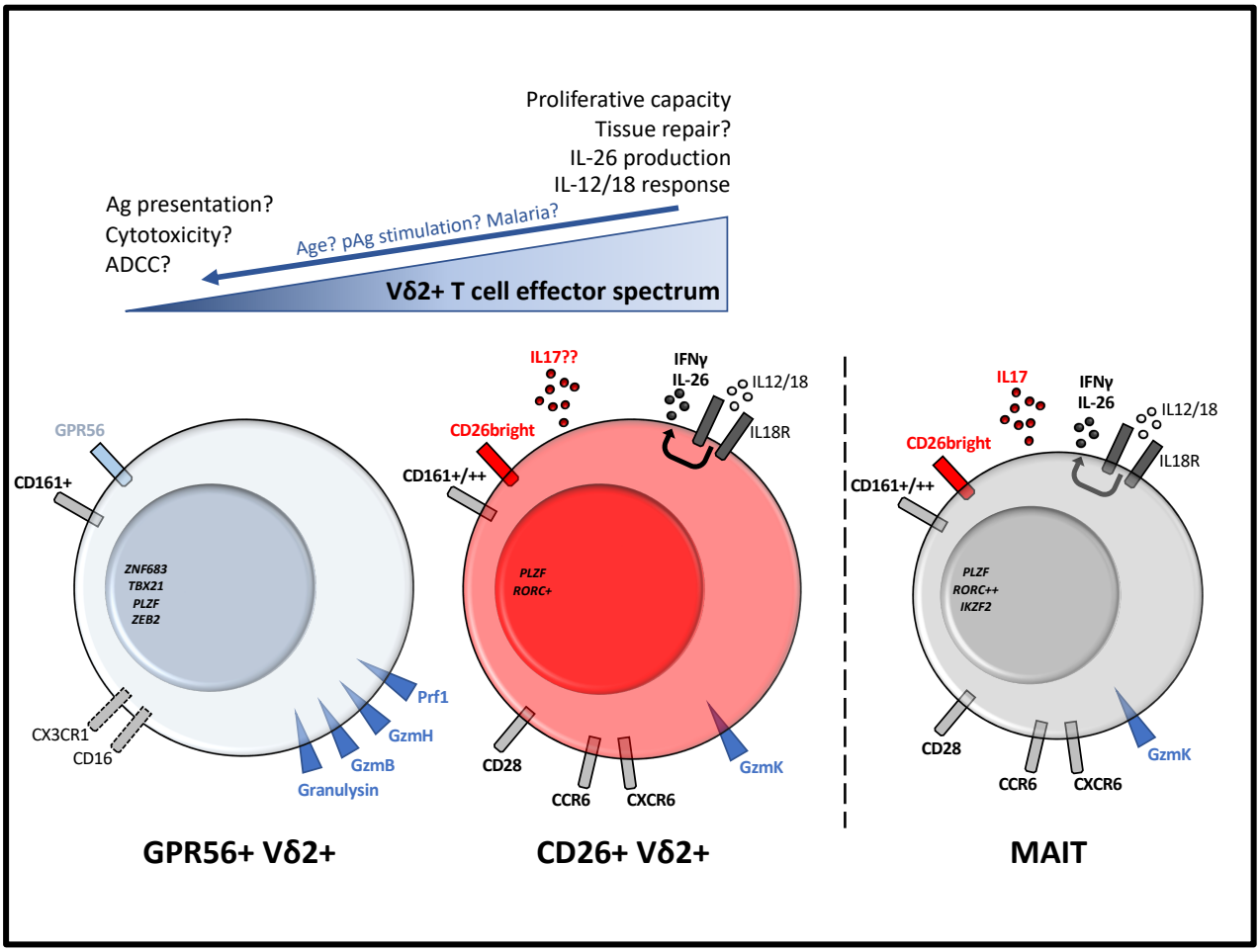


Figure 7-1. Proposed model describing a Vδ2+ T cell effector spectrum.

Vδ2+ T cells from a transcriptional, phenotypic and functional spectrum, from a CD26bright innate-like subset, to a GPR56+ highly cytotoxic subset. CD26bright Vδ2+ T cells demonstrate a highly similar transcriptional and phenotypic profile to MAIT cells, and exhibit similar responses to combinatorial cytokine stimulation, including the production of IFNγ and IL-26. GPR56+ Vδ2+ T cells express high levels of granzymes and perforin, express TFs including Hobit, Tbet, and ZEB2, the surface molecules CD16 and CX3CR1, and do not respond to cytokine stimulation. Vδ2+ T cells may be driven along this transcriptional spectrum with exposure to antigen, and infections including malaria.

The drivers for this differentiation spectrum have particular significance due to the circumstantial data that malarial infection alters the Vδ2+ T cell phenotype. If chronic pAg-producing infection permanently shifts an individual's Vδ2+ T cell population from a innate-like cytokine-responsive phenotype to a cytotoxic one, this has the potential to reshape that individuals' immune responses to infection, vaccination, and cancer, as IL12/18 responses are implicated in responses to viral infection and Ad-vector vaccination(Provine et al., 2019; van Wilgenburg et al., 2016), of particular relevance in the COVID-19 pandemic(Jeyanathan et al., 2020). In particular, if malaria, and other pAg-producing pathogens can drive Vδ2+ T cells down this spectrum, and their impact on these processes is non-redundant, then it could be that populations where such infections are endemic could have compromised responses, with significant public health implications.

To investigate this important hypothesis, further work would need to examine how gd T cell subsets and phenotype are altered in malaria infection, both acute and chronic, and whether such effects are temporary or permanent. Second, the degree of redundancy between these different cytokine responsive innate like T cell subsets would need to be examined. Much of the work on these subsets is carried out by research groups that focus on a single cell population in isolation, however, such research would need to look not at individual cell populations, but on the immunological niche which they fill.

Non-Vδ2 T cells do not respond to cytokine stimulation in the same manner. However, one observation from the functional transcriptomic experiment was that the genetic machinery associated with cytokine responsiveness is induced by TCR stimulation. This raises the possibility that in certain contexts their innate-like characteristics can be induced, an interesting hypothesis given the curious group of antigens that can stimulate non-Vδ2 T cells, and the tissues in which they are found. This link between their adaptive receptor and innate-like functionality could be relevant to γδ T IELs in the gut.

Finally, the unexpected finding of CCR9 expression on naive non-Vδ2 T cells challenges dogma of how T cells enter tissue. This finding, replicated in two single-cell sequencing experiments, at the protein level with flow cytometry, and using qPCR, seems to be genuine. Outside the thymus, CCR9 expression is associated with homing to the intestinal mucosa(Habtezion et al., 2019), and suggests that these naive T cells are pre-programmed for intestinal residency. Indeed, CCR9-deficient mice show a reduction in intestinal IELs, predominantly γδ T cells(Wurbel et al., 2001). One hypothesis is that these naive cells maintain the capacity to patrol intestinal tissue, where, if exposed to antigen or to inflammatory signals, can develop a effector phenotype and take up residence there. A second hypothesis is that these cells can be recruited to the intestine in response to inflammatory signals in a TCR-independent manner. The latter hypothesis might explain the seemingly paradoxical finding of increased TCR repertoire diversity in the intestinal γδ T cell population in coeliac disease(Eggesbø et al., 2019; Mayassi et al., 2019), as inflammatory signals might recruit these naive CCR9+ T cells from the circulation, thereby increasing both cell number and TCR diversity.

7.3 Transcriptional heterogeneity of human CD8+ T_{RM} cells

In Chapter 6, I describe two distinct subsets of functionally-resident CD8+ T_{RM} cells in the human gut, leveraging the unusual situation of intestinal transplantation. These two subsets show differences in phenotype and function, and may differ in proliferative capacity and persistence. It remains unclear whether these subsets represent two states along a differentiation trajectory (Figure 7-2).

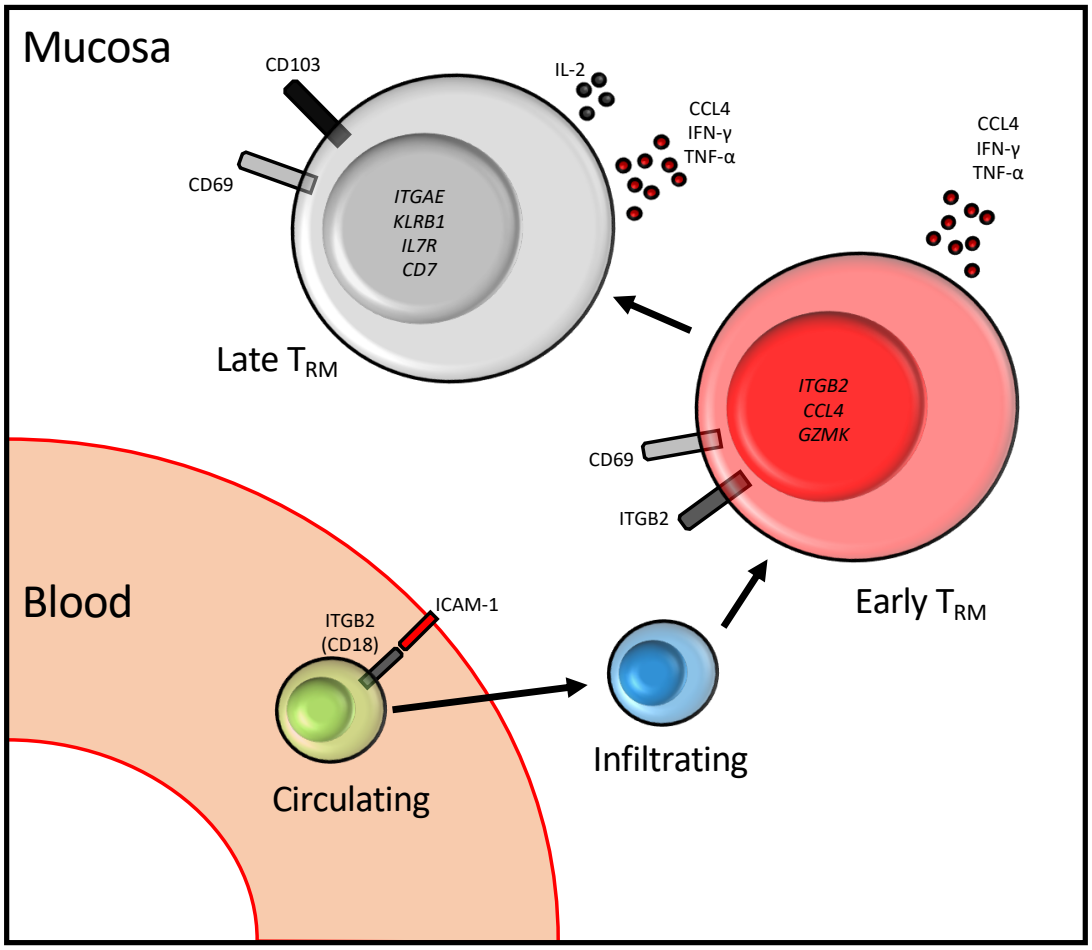


Figure 7-2. A model of intestinal CD8+ T_{RM} cell development.

Circulating effector CD8+ T cells (green) enter tissue, mediated by β2-integrin/ICAM1 interactions, leading to low β2-integrin expression on CD69- T cells in tissue (blue). Induction of early residency programmes upregulate CD69 and β2-integrin on early CD103- T_{RM} cells (red), which possess pro-inflammatory capacity and express granzyme K. Late T_{RM} cells develop from this population, upregulating CD103, CD161, and the IL7R. These cells maintain high pro-inflammatory capacity as well as IL-2 production.

The differential expression between the two subsets of genes previously associated with residency suggests that genetic 'signatures' of residency based on bulk RNAseq may represent amalgamations of two or more distinct subsets(Kumar et al., 2017). This work was in the setting of health and intestinal transplantation, although there was a clear signal for the gene signature discriminating these two populations from reanalysis of single cell data sets from IBD(Corridoni et al., 2020; J. C. Martin et al., 2019). These data provide a frame work for examining T_{RM} cell heterogeneity and function in disease.

I focused on CD8+ T_{RM} cells, however, the characteristics of tissue residency in CD4+ and γδ T cells would be of great interest, as it is not clear if the processes and implications of residency are the same(Sasson et al., 2020). In particular, if we consider gluten-specific CD4+ T cells in CD, which are likely to be resident, what are the implications of their resident status on their response to therapeutic strategies, such as checkpoint inhibitor agonists or tolerance-induction(Christophersen et al., 2019b)?

The second interesting observation is the number of CD8+ T_{RM} cell subsets identified in my work (two main subsets), compared to the other datasets I examined (three and seven subsets) (Corridoni et al., 2020; J. C. Martin et al., 2019). It raises a similar epistemic question as discussed in Chapter 5 about the nature of T cell heterogeneity and natural kinds. The algorithms used to identify clusters in single-cell data will identify transcriptional variation irrespective of whether it represents biologically meaningful subdivisions of cells. My data support the hypothesis that there are *at least* two transcriptionally distinct states within CD8+ T_{RM} cells, and that these two states are also found in the colon in health and disease. However, whether these two populations can, or should, be further subdivided unclear, and will require further work with multiple datasets.

7.4 Common themes: rebellious T cells, and the nature of immune cell heterogeneity

While the impetus for my research stemmed from initial questions about CD8+ and γδ T cells in coeliac disease, the work in chapters 5 and 6 led in distinct directions, examining questions about the heterogeneity of human γδ T cells and tissue-resident populations. However, two overarching themes do occur to me.

First, this research is linked by a common theme of the importance of unconventional and atypical T cell populations that break the 'rules' of conventional adaptive T cell biology. The unusual biology of IELs is well-described(Mayassi and Jabri, 2018), and the work in chapter 4 provided evidence that CD8+ T IELs in CD may possess TCR-dependent roles in coeliac disease, contrary to previous work. The work in chapter 5 uncovered the shared and distinct phenotypic and functional properties of γδ T cells, and their innate-like counterparts, the MAIT cells. Finally, chapter 6 described previously unappreciated transcriptional and functional heterogeneity within human T_{RM} cells, a population that also possess unusual characteristics not displayed by their circulating counterparts.

I believe that these data support the hypothesis that these rebellious T cells, that break many of the 'rules' of adaptive immunity derived from the study of conventional circulating populations, have important roles in human health and disease. For all these subsets, their ability to respond rapidly to pathogens or stress signals, combined with their characteristics that bridge the boundaries of innate and adaptive immunity, make them important populations to study, and the understanding of disease processes will be incomplete without elucidating their role.

Second, this work highlights the epistemic challenge of how we describe heterogeneity in immune cell populations, and in particular what should constitute a subset of T cells. I have already discussed this in some detail in chapter 5, but I wish to draw out some additional themes.

This work highlights the challenge of determining the significance of heterogeneity within a particular population. The decision to label that heterogeneity as a 'subset', which implies a population with at least some of the characteristics of a natural kind, or to attribute that heterogeneity to a spectrum of differentiation, or phenotypic plasticity driven by the local milieu, is a subjective decision imposed by the researcher. In much of this work, a case could be made for any of these possibilities as the underlying 'ground truth' of the heterogeneity described. Understanding of the epigenetic control of this heterogeneity, in particular the degree to which differentiation processes can be reversed, may be important to inform our conceptual understanding of cellular heterogeneity.

A different type of grouping of cells emerges from the data, one not defined by a developmental relationship, but by a shared immunological niche. Chapter 4 described shared features between CD8+ and γδ T cells in the epithelial compartment. These two populations, from fundamentally different lineages, take on shared features in response to the immunological and spatial milieu. Similarly, chapter 5 described the near-identical characteristics of MAIT cells and CD26bright Vδ2+ T cells, a phenotype also associated with iNKT cells(Garner et al., 2018). These populations share features despite their different origins, ligands, and antigens. This is reminiscent of convergent evolutionary processes, where species from distinct phylogenetic lineages take on highly similar phenotypes and behaviours due to their occupation of similar ecological niches; the example of the shared anatomy and eusocial behavioural structure of the ants and termites comes to mind.

This shared immunological niche raises questions about the extent to which these populations fulfil redundant roles. The absence of pAg-sensing Vδ2+ T cells in the majority of vertebrate lineages suggests that they are, to some extent, redundant, but the persistence of Vδ2+ T cells in the Hominidae suggests there have been specific drivers for their positive selection in the relatively recent past, perhaps due to their role in defence from malaria and tuberculosis(Fichtner et al., 2018; Karunakaran et al., 2014). Understanding to what extent their different roles are redundant or not would have implications to our understanding of the role of these different subsets in human disease.

7.5 Future work

First, I intend to look into the potential link between TRBV28-containing CD8+ T cell clonotypes and coeliac disease in more detail. However, any major advance will require the meticulous *in vitro* work with T cell clones that provided the insights into gluten-specific T cells in coeliac disease. This work has additional challenges, as the MHC restriction is not known, indeed Class I restriction cannot be assumed by such rebellious T cell populations.

Second, the overlapping phenotype and function of innate like T cells interests me greatly. This would require careful transcriptional and functional work, both *in vitro* and *in vivo*, to understand the extent of their shared functionality, and the degree to which these populations provide redundant roles in host defence. Related to this, the changes in innate-like T cell populations following malarial infection is an intriguing and potentially important hypothesis that I would like to explore.

Finally, there are additional insights to be gained from the study of resident populations in intestinal transplantation, in particular, understanding the nature of CD4+ and γδ T cell residency in humans would be of particular interest, given their association with coeliac disease.

List of Publications

Publications and submissions related to laboratory work

Provine, N.M., Binder, B., **FitzPatrick, M.E.B.,** Schuch, A., Garner, L.C., Williamson, K.D., van Wilgenburg, B., Thimme, R., Klenerman, P., Hofmann, M., 2018. Unique and Common Features of Innate-Like Human Vδ2+ γδT Cells and Mucosal-Associated Invariant T Cells. Front. Immunol. 9, 120–12. doi:10.3389/fimmu.2018.00756 **(Co-first author)**

FitzPatrick, M.E.B., Provine, N.M., Garner, L.C., Powell, K., Amini, A., Irwin, S., Ferry, H., Ambrose, T., Friend, P., Vrakas, G., Reddy, S., Soilleux, E., Klenerman, P., Allan, P.J., 2019. Human intestinal tissue-resident memory CD8+ T cells comprise transcriptionally and functionally distinct subsets. bioRxiv 869917. **(Under second review following revisions; co-first author)**

Provine, N.M., Amini, A., Garner, L.C., Dold, C., Hutchings, C., **FitzPatrick, M.E.B.,** Reyes, L.S., Chinnakannan, S., Oguti, B., Raymond, M., Capone, S., Folgori, A., Rollier, C.S., Barnes, E., Pollard, A.J., Klenerman, P., 2019. Activation of MAIT cells plays a critical role in viral vector vaccine immunogenicity. bioRxiv 7, 11653–40. doi:10.1101/661397 **(accepted at Science)**

Publications and submissions unrelated to laboratory work, but published during DPhil

Clough, J., FitzPatrick, M., Harvey, P., Morris, L., 2019. Shape of Training Review: an impact assessment for UK gastroenterology trainees. Frontline Gastroenterol 10, 356–8. doi:10.1136/flgastro-2018-101168 **(co-first author)**

Fernandes, L., **FitzPatrick, M.E.B.,** Roycroft, M., 2020. The role of the future physician: building on shifting sands. Clin Med (Lond) 20, 285–289. doi:10.7861/clinmed.2020-0030 **(co-first author)**

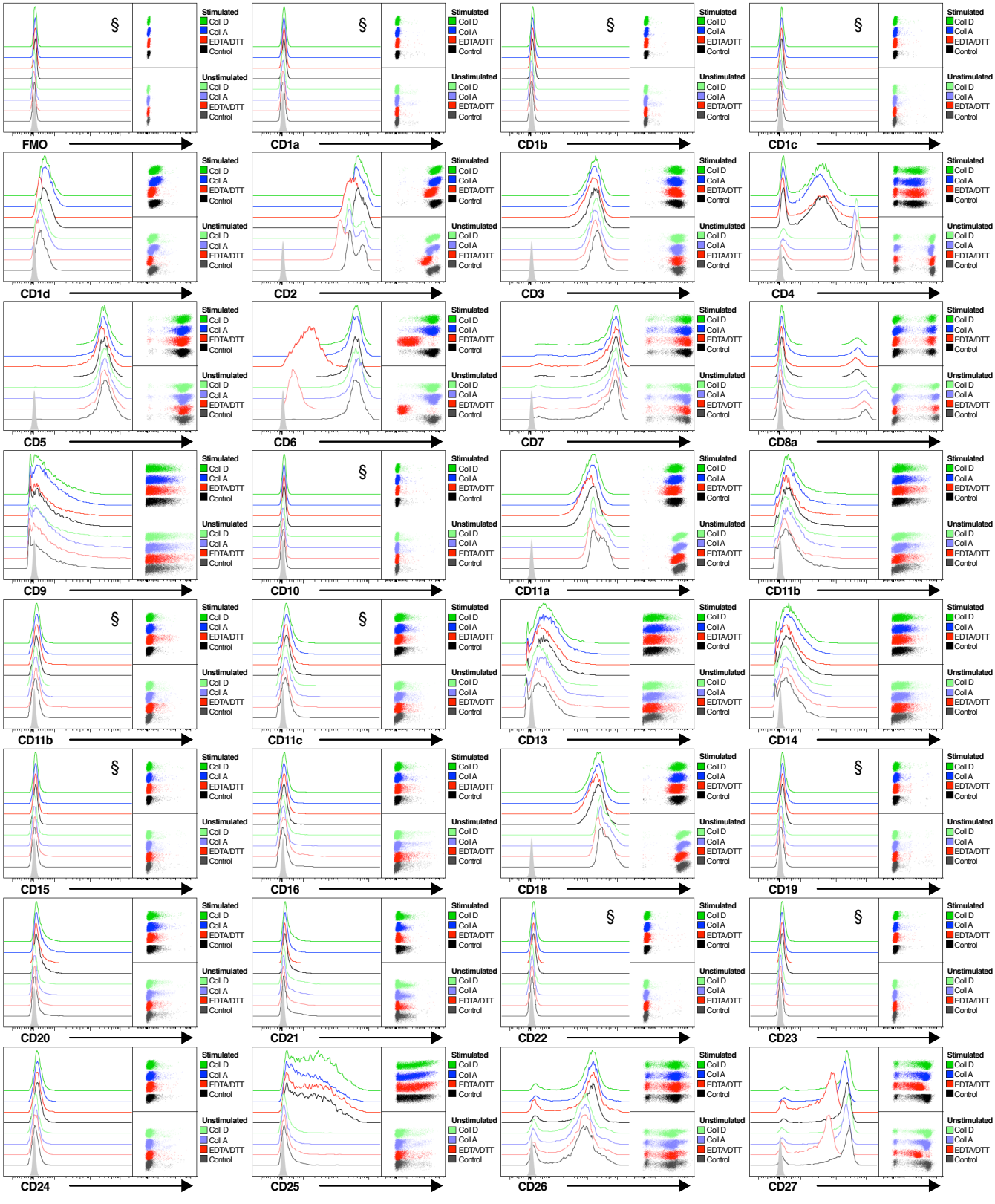
FitzPatrick, M.E.B., Clough, J., Harvey, P., Ratcliffe, E., 2020. How can gastroenterology training thrive in a post-COVID world? Frontline Gastroenterol 0, 1-4. doi: 10.1136/flgastro-2020-101601 **(co-first author)**

Roycroft, M., Abad-Madroñero, J., Cochrane, C., Poots, A., Novak, M., Tallett, A., Burger, S.-A., **FitzPatrick, M.,** 2020. "This is my vocation; is it worth it?" Why do core medical trainees break from training? Future Healthc J 7, s103–s104. doi:10.7861/fhj.7.1.s103

Smith, R., Baldock, J., **FitzPatrick, M.,** Jones, N., Newton, J.L., 2020. Incidence of Undiagnosed Celiac Disease Presenting as Bone Stress Injuries to a Sport and Exercise Medicine Clinic. Clinical Journal of Sport Medicine Publish Ahead of Print. doi:10.1097/JSM.0000000000000820

Vijayakumar, B., Kitt, J., Hynes, G., Millette, S., **FitzPatrick, M.,** 2020. Procedural skills training for medical registrars – is it needed? Future Healthcare Journal 7, s110–s111. doi:10.7861/fhj.7.1.s110

Supplementary Figures and Tables


Stimulated
Coll D
Coll A
EDTA/DTT
Control
Unstimulated
Coll D
Coll A
EDTA/DTT
Control
§
FMO
CD1a
CD1b
CD1c
CD1d
CD2
CD3
CD4
CD5
CD6
CD7
CD8a
CD9
CD10
CD11a
CD11b
CD11b
CD11c
CD13
CD14
CD15
CD16
CD18
CD19
CD20
CD21
CD22
CD23
CD24
CD25
CD26
CD27


Stimulated
Coll D
Coll A
EDTA/DTT
Control
Unstimulated
Coll D
Coll A
EDTA/DTT
Control
CD28
CD29
CD30
CD31
CD32
CD33
CD34
§
CD35
CD36
CD38
CD39
§
CD40
CD41
§
CD42
CD43
CD44
CD45
CD45RA
CD45RB
CD45RO
CD46
CD47
CD48
CD49a
CD49c
CD49d
CD49e
CD49f
CD50 (ICAM-3)
CD51
§
CD51/61
CD52


Stimulated
Coll D
Coll A
EDTA/DTT
Control
Unstimulated
Coll D
Coll A
EDTA/DTT
Control
CD53
CD54
CD55
CD56 (NCAM)
CD57
CD58
CD59
CD61
§
CD62E
CD62L
CD62P (P-selectin)
CD63
CD64
CD66a/c/e
CD66b
CD69
CD70
CD71
CD73
CD74
CD79B
CD80
CD81
CD82
CD83
CD84
CD85a(ILT5)
CD85d(ILT4)
CD85g(ILT7)
CD85h(ILT1)
CD85j(ILT2)
CD85k(ILT3)


Stimulated
Coll D
Coll A
EDTA/DTT
Control
Unstimulated
Coll D
Coll A
EDTA/DTT
Control
§
FMO
CD86
CD87
CD88
CD89
CD90(Thy1)
CD93
CD94
CD95
CD96
CD97
CD99
CD100
CD101(BB27)
CD102
CD103
CD104
CD105
CD106
CD107a(LAMP-1)
CD108
CD109
CD111
CD112(Nectin-2)
CD114
CD115
CD116
CD117(c-kit)
CD119 (IFNγ Ra)
CD122
CD123
CD124


Stimulated
Coll D
Coll A
EDTA/DTT
Control
Unstimulated
Coll D
Coll A
EDTA/DTT
Control
CD126(IL-6Ra)
CD127(IL-7Ra)
CD129(IL-9R)
CD131
CD132
CD134
CD135
CD137(4-1BB)
CD137L(4-1BB L)
CD138
CD140a
CD140b
CD141
CD143
CD144
CD146
CD148
CD150(SLAM)
CD152
CD154
CD155(PVR)
CD156c(ADAM-10)
CD158a/h
CD158b(NKAT2)
CD158d
CD158e1(NKB1)
CD158f
CD161
CD162
CD163
CD164
CD165
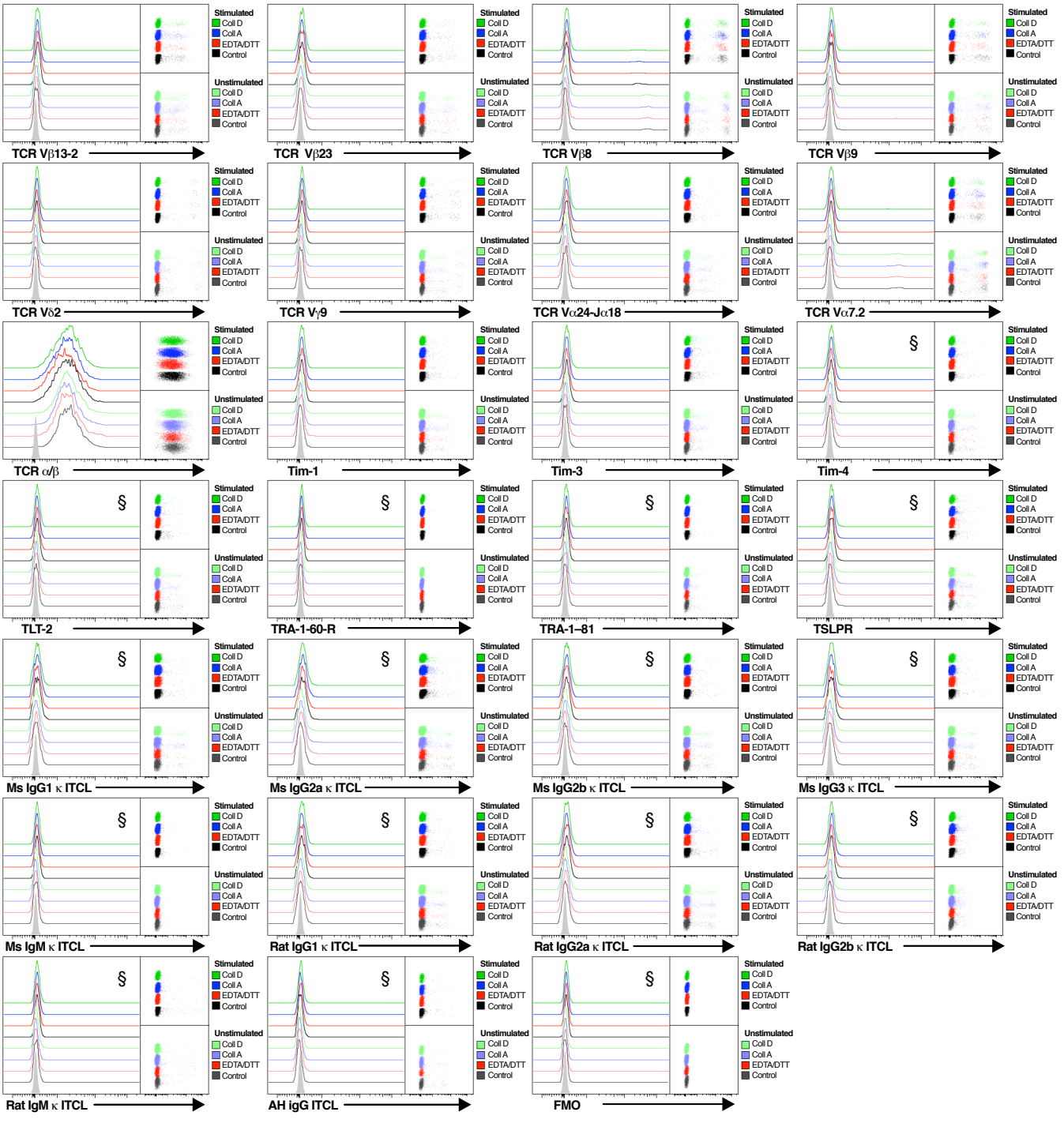

Stimulated
Coll D
Coll A
EDTA/DTT
Control
Unstimulated
Coll D
Coll A
EDTA/DTT
Control
§
CD166
CD167a(DDR1)
CD169
CD170(Siglec-5)
CD172a(SIRPα)
CD172b(SIRPβ)
CD172g(SIRPγ)
CD178(Fas-L)
CD179a
CD179b
CD180(RP105)
CD181(CXCR1)
CD182(CXCR2)
CD183
CD184(CXCR4)
CD193(CCR3)
CD195(CCR5)
CD196
CD197(CCR7)
CD200(OX2)
CD200R
CD201(EPCR)
CD202b(Tie2/TEK)
CD203c(E-NPP3)
CD205(DEC-205)
CD206(MMR)
CD207(Langerin)
CD209(DC-SIGN)
CD210(IL-10R)
CD213a2
CD215(IL-15Ra)
CD218a(IL-18Ra)


Stimulated
Coll D
Coll A
EDTA/DTT
Control
Unstimulated
Coll D
Coll A
EDTA/DTT
Control
§
FMO
CD220
CD221(IGF-1R)
CD226(DNAM-1)
CD229(Ly-9)
CD231(TALLA)
CD235ab
CD243
CD244(2B4)
CD245(p220/240
CD252(OX40L)
CD253(Trail)
CD254
CD255(TWEAK)
CD257(BAFF)
CD258(LIGHT)
CD261(DR4)
CD262(DR5)
CD263(DcR1)
CD266(Fn14)
CD267(TACI)
CD268(BAFF-R)
CD270(HVEM)
CD271
CD273(B7-DC)
CD274(B7-H1)
CD275(B7-H2)
CD276
CD277
CD278(ICOS)
CD279(PD-1)
CD282(TLR2)


Stimulated
Coll D
Coll A
EDTA/DTT
Control
Unstimulated
Coll D
Coll A
EDTA/DTT
Control
CD284(TLR4)
CD286(TLR6)
CD290
CD294
CD298
CD300e(IREM-2)
CD300F
CD301
CD303
CD304
CD307
CD307d(FcRL4)
CD314(NKG2D)
CD317
CD318(CDCP1)
CD319(CRACC)
CD324(E-Cadherin)
CD325
CD326(Ep-CAM)
CD328(Siglec-7)
CD334(FCFR4)
CD335(NKp46)
CD336(NKp44)
CD337(NKp30)
CD338(ABCG2)
CD340(erbB2)
CD344(Frizzled-4)
CD351
CD352(NTB-A)
CD354(TREM-1)
CD355(CRTAM)
CD357(GITR)

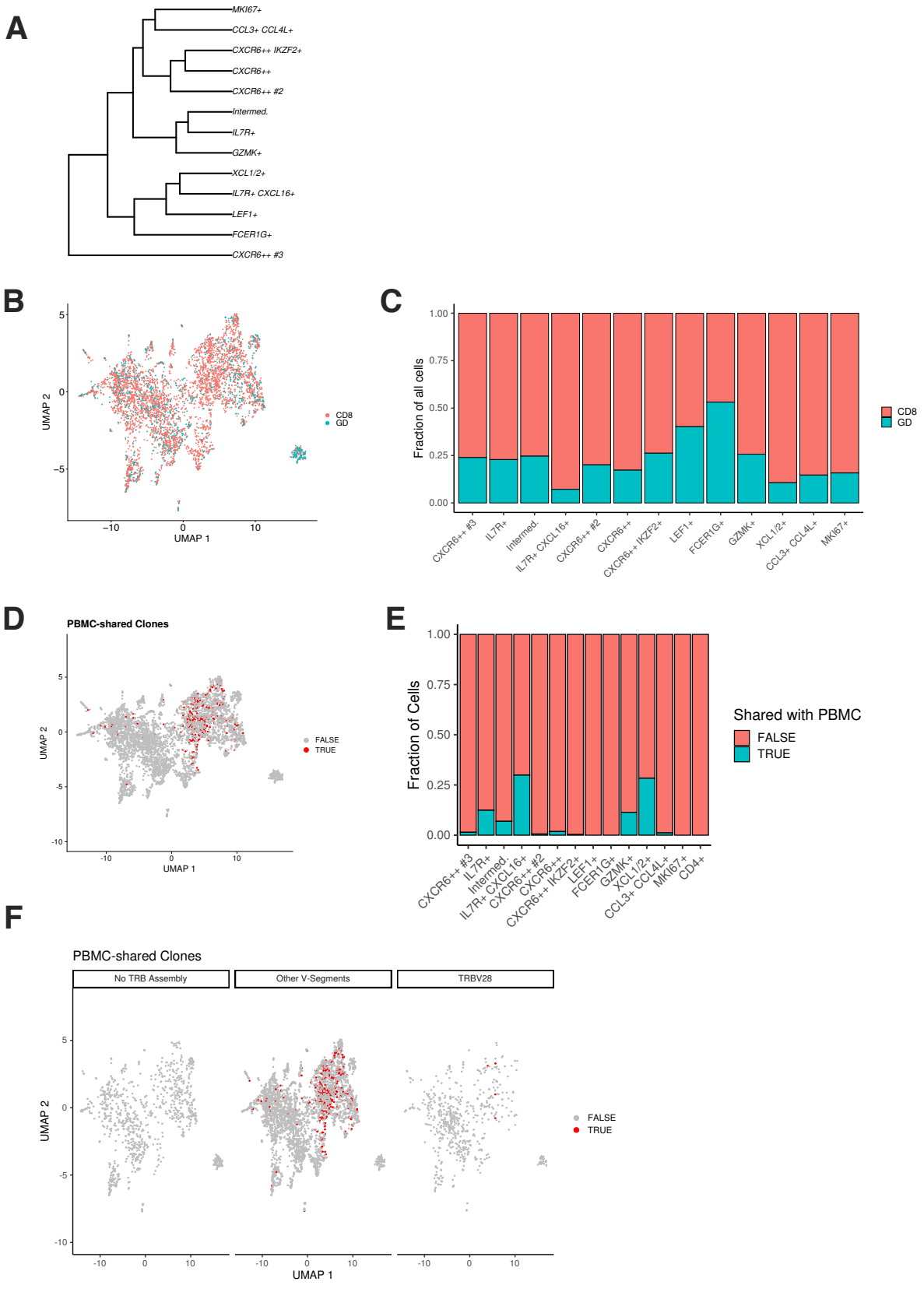

Stimulated
Coll D
Coll A
EDTA/DTT
Control
Unstimulated
Coll D
Coll A
EDTA/DTT
Control
§
CD360(IL-21R)
β2-microglobulin
BTLA
C3AR
C5L2
CCR10
CLEC12A
CLEC9A
CX3CR1
CXCR7
δ-opioid R
DLL1
DLL4
DR3(TRAMP)
EGFR
erbB3/HER-3
FcεRIa
FcRL6
Galectin-9
GARP(LRRC32)
HLA-ABC
HLA-A2
HLA-DQ
HLA-DR
HLA-E
HLA-G
IFNγR β chain
Ig light chain κ
Ig light chain λ
IgD
IgM
IL-28RA


Stimulated
Coll D
Coll A
EDTA/DTT
Control
Unstimulated
Coll D
Coll A
EDTA/DTT
Control
§
FMO
Integrin α9β1
Integrin β5
Integrin β7
Jagged 2
LAP
LT-β R
Mac-2 (Galectin-3)
MAIR-II
MICA-MICB
MSC(W3D5)
MSC(W5C5)
MSC(W7C6)
MSC & NPC (W4A5)
MSCA-1(MSC)
NKp80
Notch 1
Notch 2
Notch 3
Notch 4
NPC (57D2)
Podoplanin
Pre-BCR
PSMA
Siglec-10
Siglec-8
Siglec-9
SSEA-1
SSEA-3
SSEA-4
SSEA-5
TCRγ/δ


Stimulated
Coll D
Coll A
EDTA/DTT
Control
Unstimulated
Coll D
Coll A
EDTA/DTT
Control
TCR Vβ13-2
TCR Vβ23
TCR Vβ8
TCR Vβ9
TCR Vδ2
TCR Vγ9
TCR Vα24-Jα18
TCR Vα7.2
TCR α/β
Tim-1
Tim-3
Tim-4
TLT-2
TRA-1-60-R
TRA-1–81
TSLPR
Ms IgG1 κ ITCL
Ms IgG2a κ ITCL
Ms IgG2b κ ITCL
Ms IgG3 κ ITCL
Ms IgM κ ITCL
Rat IgG1 κ ITCL
Rat IgG2a κ ITCL
Rat IgG2b κ ITCL
Rat IgM κ ITCL
AH igG ITCL
FMO
§

Supplementary Figure 3-1.

Expression of 332 PE-conjugated surface markers on circulating T cells (either unstimulated (below) or stimulated with PMA/Ionomycin(above)) incubated with 1mM EDTA & DTT for 30 minutes (EDTA/DTT, red), DNAse I and Collagenase A for 1 hour (DNAse/Coll A, blue), or DNAse I and Collagenase D for 1 hour (DNAse/Coll D, green), compared to control (complete media, black). Histogram (left) and dot plots (right, plotted against CellTrace Voilet) are displayed for each marker. FMO is displayed on each histogram (grey). Plots are from a single representative donor. Surface markers with minimal expression (indicated by §) were not statistically analysed and were not displayed in the heat maps in Figure 3-2.


A
MKI67+
CCL3+ CCL4L+
CXCR6++ IKZF2+
CXCR6++
CXCR6++ #2
Intermed.
IL7R+
GZMK+
XCL1/2+
IL7R+ CXCL16+
LEF1+
FCER1G+
CXCR6++ #3
B
UMAP 2
UMAP 1
CD8
GD
C
Fraction of all cells
CD8
GD
CXCR6++ #3
IL7R+
Intermed.
IL7R+ CXCL16+
CXCR6++ #2
CXCR6++
CXCR6++ IKZF2+
LEF1+
FCER1G+
GZMK+
XCL1/2+
CCL3+ CCL4L+
MKI67+
D
PBMC-shared Clones
UMAP 2
UMAP 1
FALSE
TRUE
E
Fraction of Cells
Shared with PBMC
FALSE
TRUE
CD4+
F
PBMC-shared Clones
No TRB Assembly
Other V-Segments
TRBV28
UMAP 2
UMAP 1
FALSE
TRUE

Supplementary Figure 4-1.

(A) Phylogenetic dendrogram of the transcriptional profile of intestinal CD8+ and γδ T cell clusters.

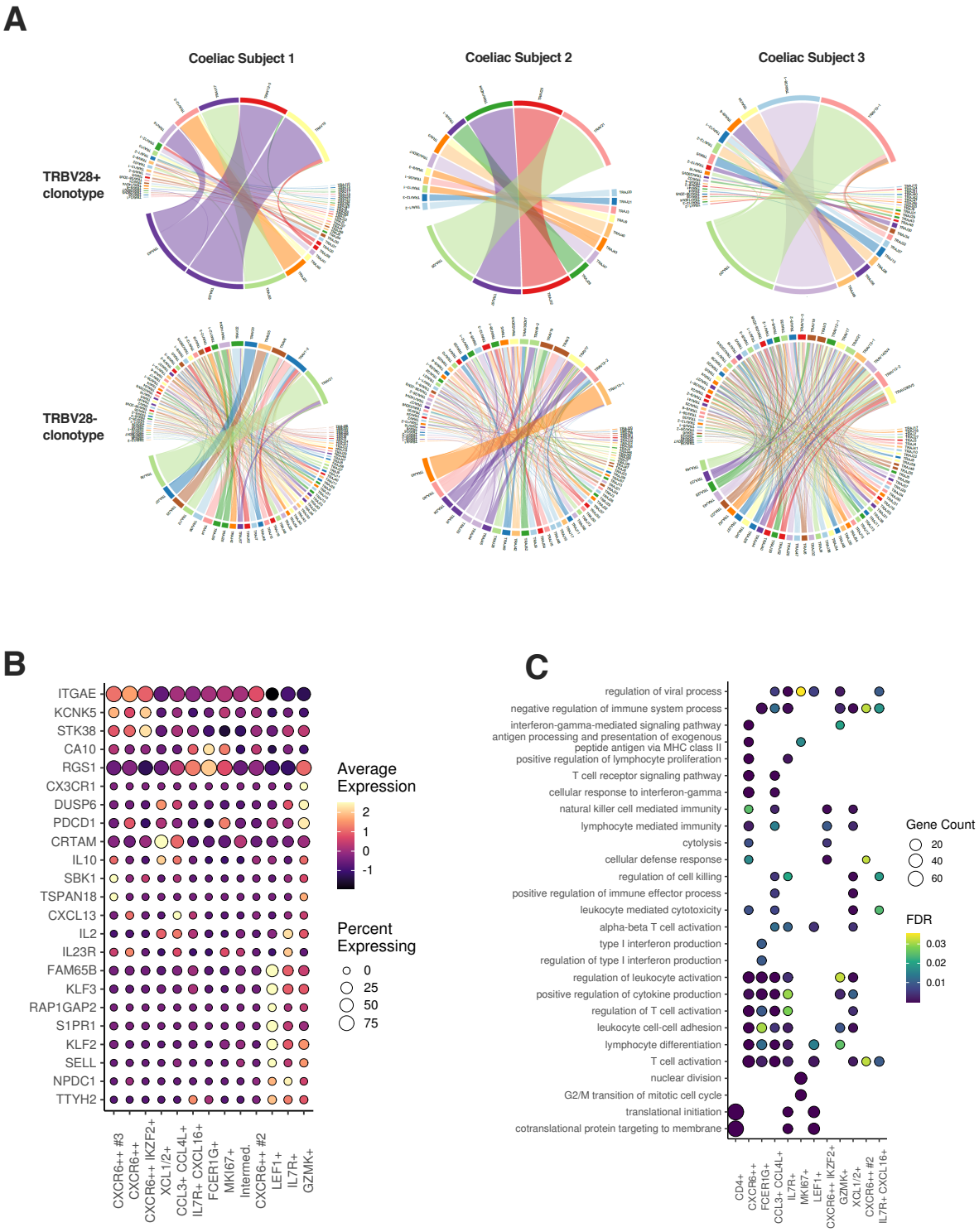
(B) UMAP plot with CD8+ and γδ T cells identified.

(C) Proportion of CD8+ and γδ T cells within each cluster.

(D) UMAP plot with CD8+ T cells with a clonotype shared with peripheral blood CD8+ T cells identified.

(E) Proportion of CD8+ T cells which share a clonotype with peripheral blood CD8+ T cells within each cluster.

(F) UMAP plot with CD8+ T cells with a clonotype shared with peripheral blood CD8+ T cells identified, split by TRBV28 and non-TRBV28 clonotypes.

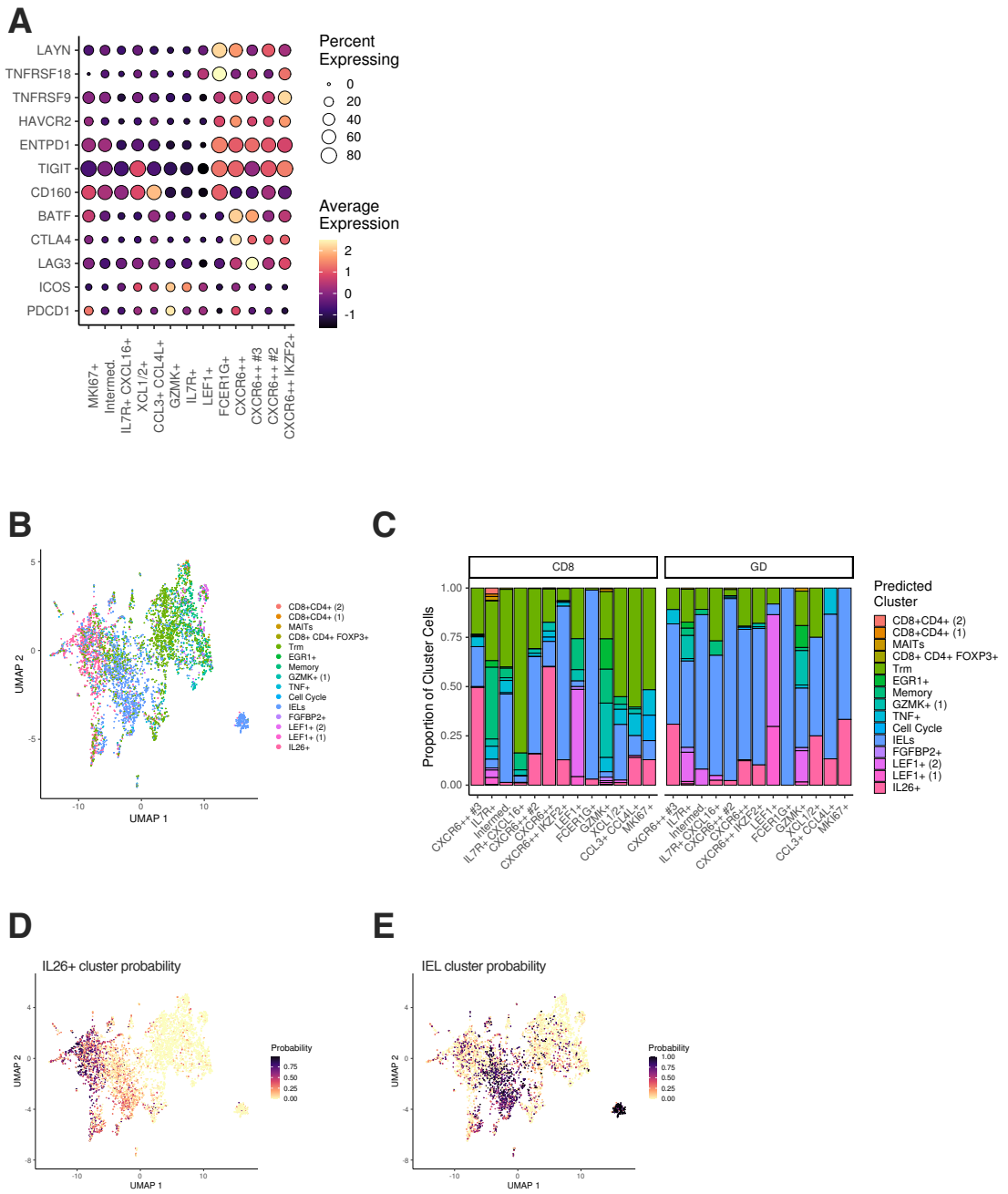

A
Coeliac Subject 1
Coeliac Subject 2
Coeliac Subject 3
TRBV28+ clonotype
TRBV28- clonotype
B
ITGAE
KCNK5
STK38
CA10
RGS1
CX3CR1
DUSP6
PDCD1
CRTAM
IL10
SBK1
TSPAN18
CXCL13
IL2
IL23R
FAM65B
KLF3
RAP1GAP2
S1PR1
KLF2
SELL
NPDC1
TTYH2
CXCR6++ #3
CXCR6++
CXCR6++ IKZF2+
XCL1/2+
CCL3+ CCL4L+
IL7R+ CXCL16+
FCER1G+
MKI67+
Intermed.
CXCR6++ #2
LEF1+
IL7R+
GZMK+
Average Expression
2
1
0
-1
Percent Expressing
0
25
50
75
C
regulation of viral process
negative regulation of immune system process
interferon-gamma-mediated signaling pathway
antigen processing and presentation of exogenous peptide antigen via MHC class II
positive regulation of lymphocyte proliferation
T cell receptor signaling pathway
cellular response to interferon-gamma
natural killer cell mediated immunity
lymphocyte mediated immunity
cytolysis
cellular defense response
regulation of cell killing
positive regulation of immune effector process
leukocyte mediated cytotoxicity
alpha-beta T cell activation
type I interferon production
regulation of type I interferon production
regulation of leukocyte activation
positive regulation of cytokine production
regulation of T cell activation
leukocyte cell-cell adhesion
lymphocyte differentiation
T cell activation
nuclear division
G2/M transition of mitotic cell cycle
translational initiation
cotranslational protein targeting to membrane
CD4+
CXCR6++
FCER1G+
CCL3+ CCL4L+
IL7R+
MKI67+
LEF1+
CXCR6++ IKZF2+
GZMK+
XCL1/2+
CXCR6++ #2
IL7R+ CXCL16+
Gene Count
20
40
60
FDR
0.03
0.02
0.01

Supplementary Figure 4-2

(A) Circos (chord) plots showing TRAV/TRAJ usage of TRBV28 and non-TRBV28 clonotypes in three subjects with coeliac disease.

(B) Bubble plot of expression of a previously reported gene set differentially expressed between resident and non-resident T cells in humans{Kumar:2017el}. Bubble size indicates the proportion of cells in which the gene is present. Colour intensity indicates the expression level of the gene in cells in that cluster.

(C) Cluster-specific GO term expression.



Supplementary Figure 4-3

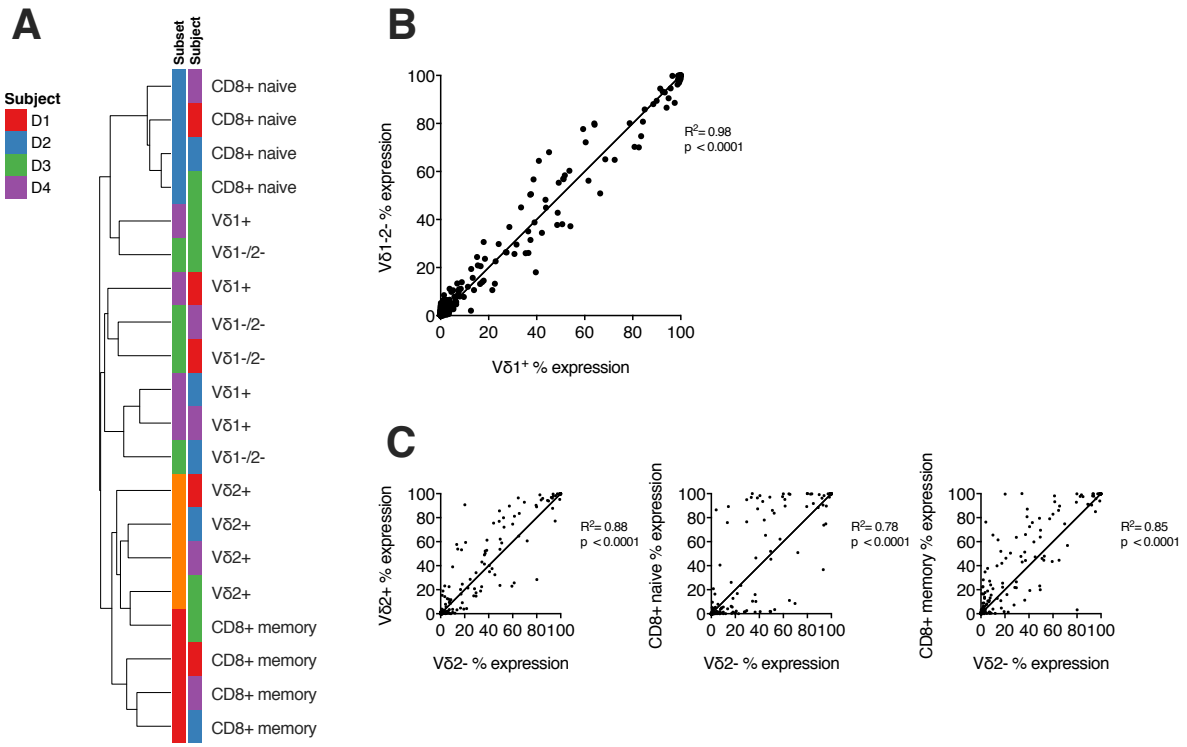
(A) Bubble plot of expression of genes encoding co-inhibitory molecules and associated molecules and transcription factors. Bubble size indicates the proportion of cells in which the gene is present. Colour intensity indicates the expression level of the gene in cells in that cluster.

(B-E) Comparison of scRNAseq dataset to a published dataset of colonic CD8+ T cells in health and ulcerative colitis (Corridoni et al., 2020).

(B) UMAP plot overlaid with the predicted cluster described in Corridoni et al., 2020.

(C) Proportion of each cluster predicted to belong to clusters in Corridoni et al., 2020.

Per cell probability of belonging to IL26+ (D) and IEL (E) clusters described in Corridoni et al., 2020.

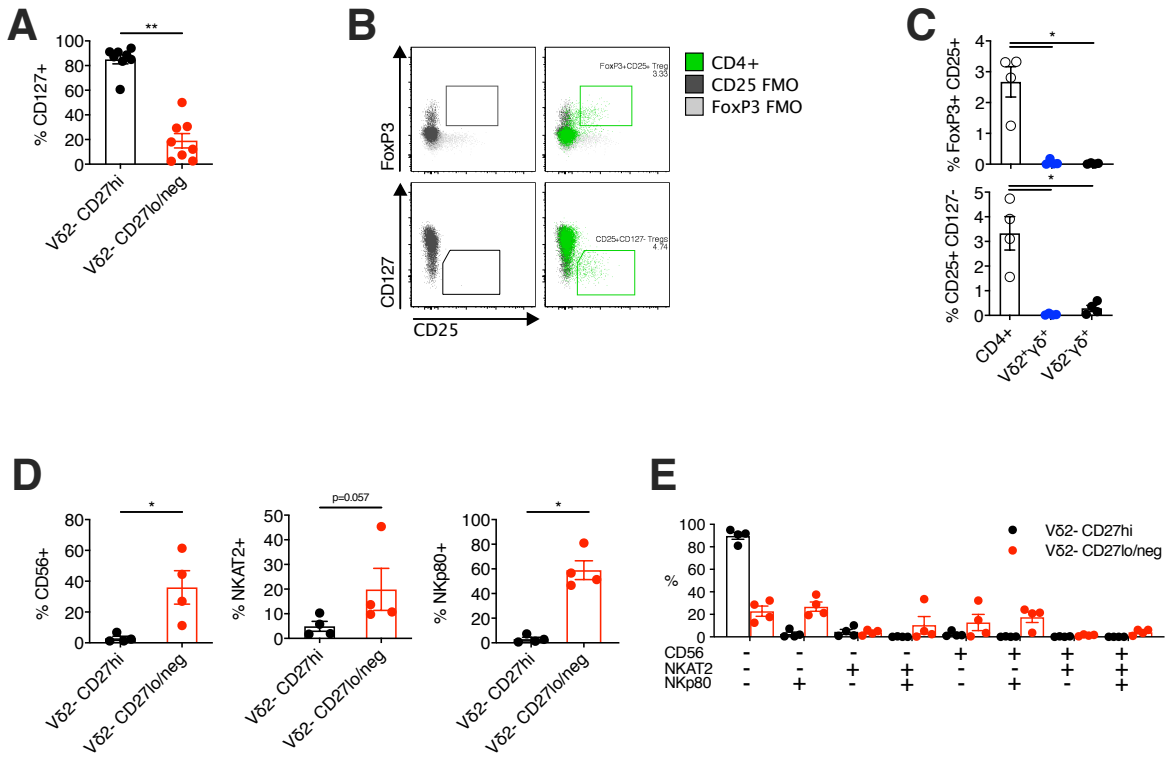


Supplementary Figure 5-1. Vδ1+ and Vδ1-/2- γδ T cells display similar phenotypic profiles.

(A) Hierarchical clustering based on the expression (% positive cells) of 316 surface markers within naive and memory CD8+ , Vδ2+, Vδ1+ , and Vδ1-/2- T cell subsets (n=4).

(B) Scatterplot of the % of Vδ1+ and Vδ1-/2- γδ T cells expressing 316 surface markers (mean of four donors). Line of unity, R^2 and p-value of Pearson correlation are displayed.

(C) Scatterplot of the % of Vδ2+ and Vδ2- γδ T cells (left), Vδ2- and naive CD8+ T cells (centre), and Vδ2- and memory CD8+ T cells (right) expressing 316 surface markers (mean of four donors). Line of unity, R^2 and p-value of Pearson correlation are displayed.



Supplementary Figure 5-2. CD27lo/neg non-Vδ2 T cells express low levels of CD127, but lack a regulatory phenotype, and co-express NK markers and receptors.

(A) Mean percentage (+/- SEM) of peripheral non-Vδ2 γδ T cells expressing CD127 (n=8). CD27hi, black; CD27lo/neg, red.

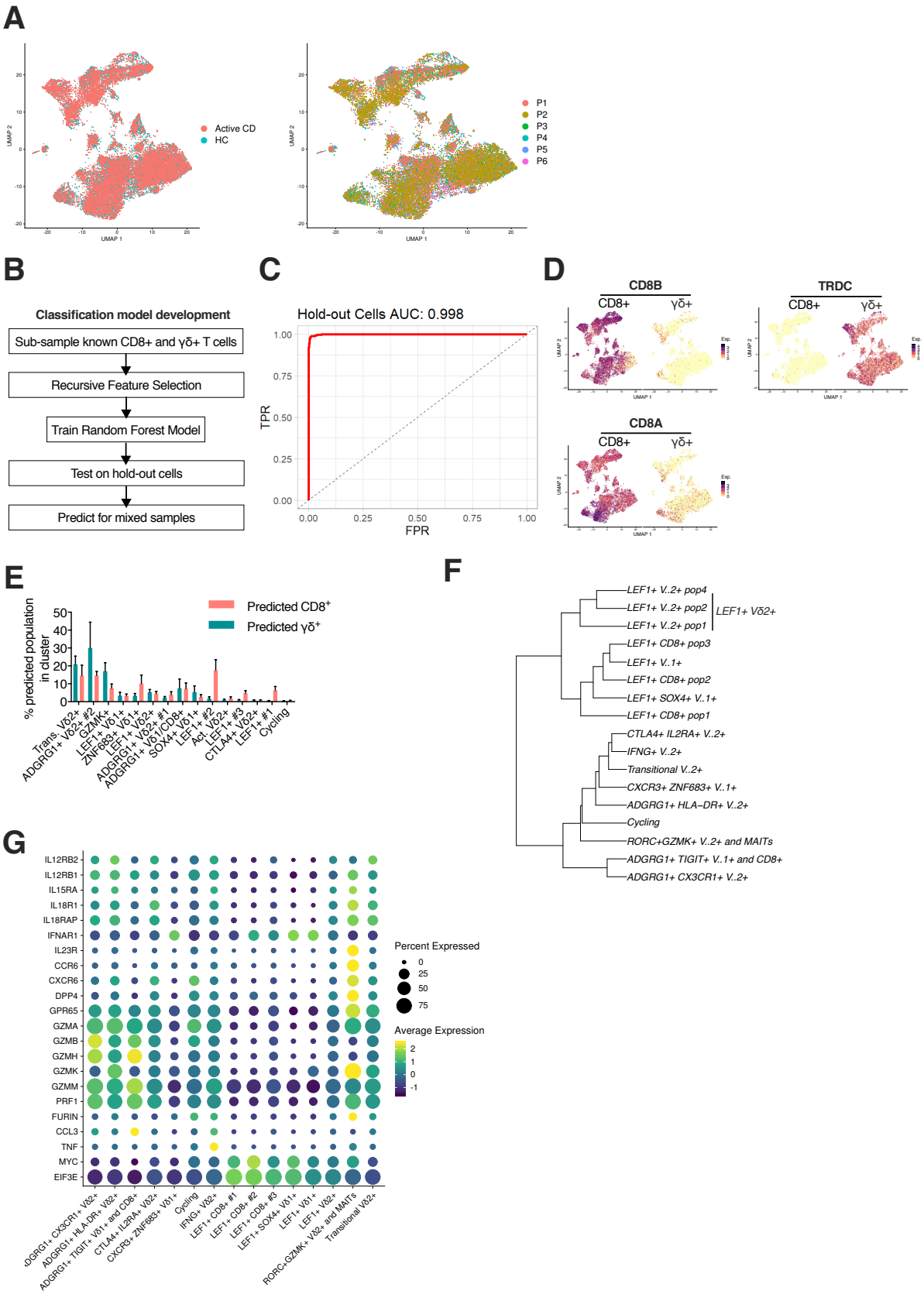
(B) Representative flow cytometry plot of coexpression of CD127, FoxP3, and CD25 on conventional CD4+ T cells (green) to identify regulatory T cell phenotypes. Fluorescence minus one (FMO) controls for CD25 and FoxP3 are displayed in dark and light grey respectively.

(C) Mean percentage (+/- SEM) of peripheral CD4+ T cells and non-Vδ2 γδ T cells co-expressing FoxP3 and CD25, or CD127 and CD25 (n=4). CD4+ T cells, black open circles; Vδ2+ T cells, blue, Vδ2- T cells, black.

(D) Mean percentage (+/- SEM) of peripheral non-Vδ2 γδ T cells expressing CD56, NKAT2, and NKp80 (n=4). CD27hi, black; CD27lo/neg, red.

(E) Mean percentage (+/- SEM) of peripheral non-Vδ2 γδ T cells co-expressing CD56, NKAT2, and NKp80 (n=4). CD27hi, black; CD27lo/neg, red.

Statistical analysis performed with Mann-Whitney test. *, P ≤ 0.05; **, P ≤ 0.01; ***, P ≤ 0.001; ****, P ≤ 0.0001.


A
Active CD
HC
P1
P2
P3
P4
P5
P6
B
Classification model development
Sub-sample known CD8+ and γδ+ T cells
Recursive Feature Selection
Train Random Forest Model
Test on hold-out cells
Predict for mixed samples
C
Hold-out Cells AUC: 0.998
TPR
FPR
D
CD8B
CD8A
TRDC
CD8+
γδ+
E
Predicted CD8+
Predicted γδ+
% predicted population in cluster
F
LEF1+ Vδ2+
G
Percent Expressed
Average Expression

Supplementary Figure 5-3.

(A) UMAP plot of CD8+ and γδ+ T cells, with cluster, disease status, and donor subject marked.

(B) Scheme for the development of the cell classification model to identify CD8+ and γδ+ T cells in mixed samples.

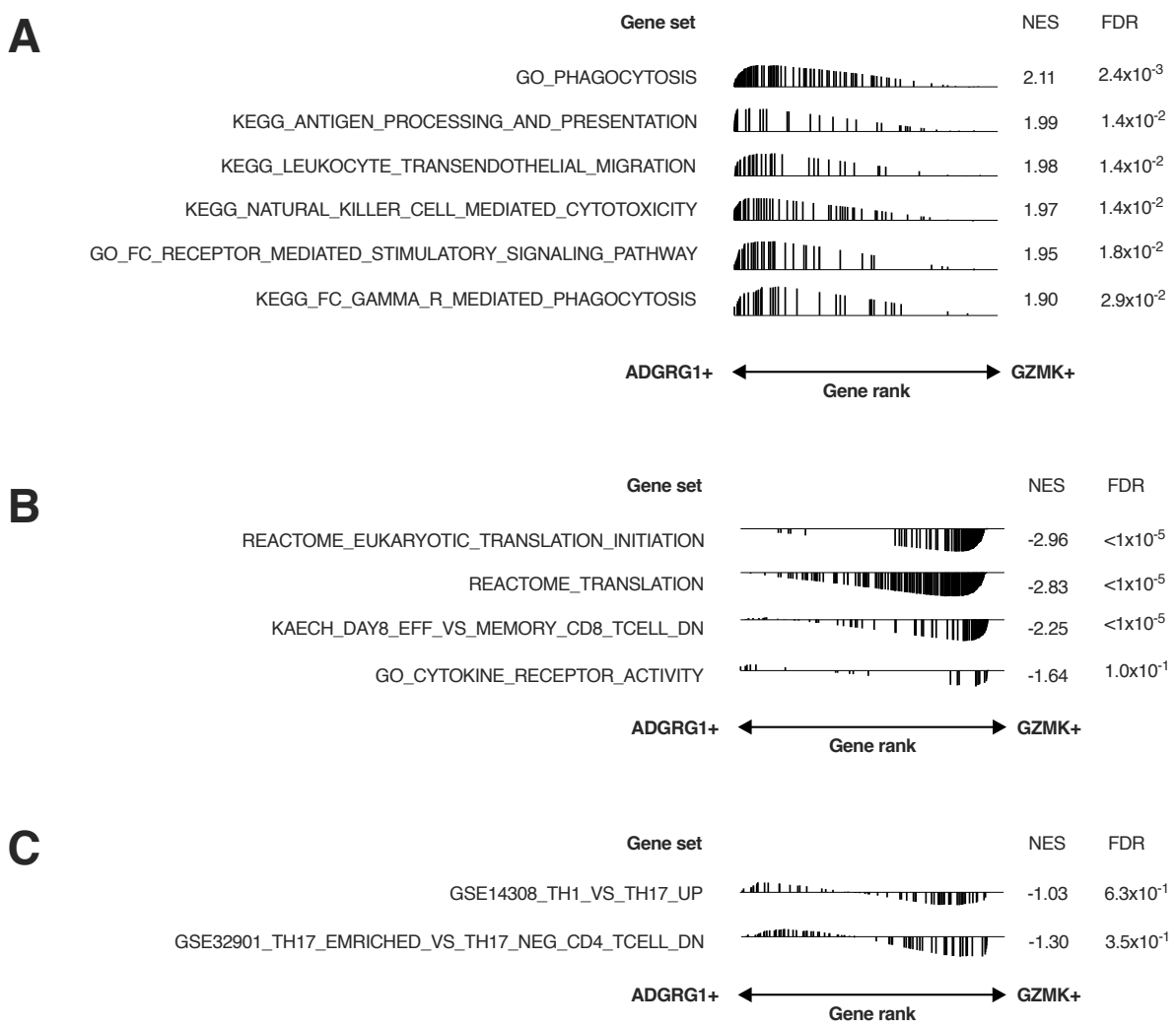
(C) Receiver operator characteristic curve for the cell classification model on hold-out cells not used in the training of the algorithm. TPR, true positive rate; FPR, false positive rate.

(D) UMAP plots for predicted CD8+ T cells (left) and γδ+ T cells (right) overlaid with the expression of CD8B, CD8A, and TRDC.

(E) Percentage (+/- SEM) of predicted CD8+ (red) or γδ+ (teal) T cells found in each cluster.

(F) Phylogenetic tree denoting the similarities and relationships in gene expression of single cell clusters. The merged LEF1+ Vδ2+ T cells are marked.

(G) Bubble plot of per-cluster expression of genes associated with cytokine response, MAIT cell function, cytotoxicity, proliferative potential, and tissue repair. Bubble size indicates the proportion of cells in which the gene is present. Colour intensity indicates the expression level of the gene in cells in that cluster.

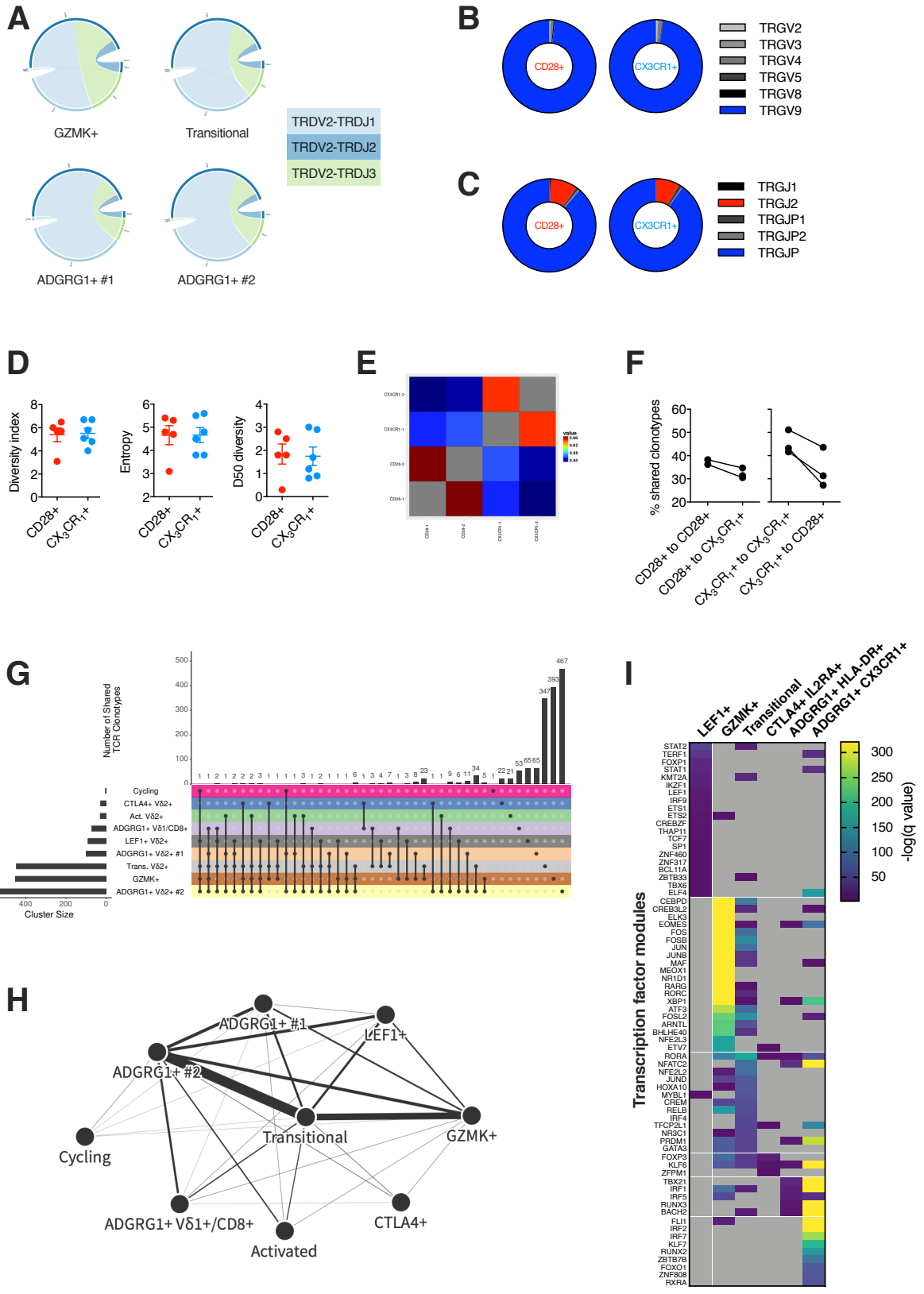


Supplementary Figure 5-4

(A) Gene set enrichment analysis (GSEA) demonstrating the enrichment of listed gene sets in ADGRG1+ Vδ2+ T cell clusters, compared to the GZMK+ Vδ2+ T cell cluster.

(B) GSEA demonstrating the enrichment of the listed gene sets in the GZMK+ Vδ2+ T cell cluster, compared to ADGRG1+ Vδ2+ T cell clusters.

(C) GSEA of Tc17-related gene sets in differential gene expression between the GZMK+ Vδ2+ T cell and ADGRG1+ Vδ2+ T cell clusters. NES, Normalised enrichment score; FDR, False discovery rate.


A
GZMK+
Transitional
ADGRG1+ #1
ADGRG1+ #2
TRDV2-TRDJ1
TRDV2-TRDJ2
TRDV2-TRDJ3
B
CD28+
CX3CR1+
TRGV2
TRGV3
TRGV4
TRGV5
TRGV8
TRGV9
C
CD28+
CX3CR1+
TRGJ1
TRGJ2
TRGJP1
TRGJP2
TRGJP
D
Diversity index
Entropy
D50 diversity
CD28+
CX3CR1+
E
F
% shared clonotypes
CD28+ to CD28+
CD28+ to CX3CR1+
CX3CR1+ to CX3CR1+
CX3CR1+ to CD28+
G
Number of Shared TCR Clonotypes
Cycling
CTLA4+ Vδ2+
Act. Vδ2+
ADGRG1+ Vδ1/CD8+
LEF1+ Vδ2+
ADGRG1+ Vδ2+ #1
Trans. Vδ2+
GZMK+
ADGRG1+ Vδ2+ #2
Cluster Size
H
ADGRG1+ #1
LEF1+
ADGRG1+ #2
Transitional
GZMK+
Cycling
ADGRG1+ Vδ1+/CD8+
CTLA4+
Activated
I
LEF1+
GZMK+
Transitional
CTLA4+ IL2RA+
ADGRG1+ HLA-DR+
ADGRG1+ CX3CR1+
Transcription factor modules
-log(q value)

Supplemental Figure 5-5:

(A) Chord diagram of paired TRDV-TRDJ gene usage of γδ+ T cells in the GZMK+, Transitional, ADGRG1+ #1, and ADGRG1+ #2 effector clusters.

TRGV gene (B) and TRGJ gene (C) usage of bulk FACS-sorted CD28+ and CX3CR1+ Vδ2+ T cells (mean; n=3).

(D) Diversity metrics (diversity index, Shannon entropy, D50 diversity) of bulk FACS-sorted CD28+ and CX3CR1+ Vδ2+ T cells (mean; n=3 with duplicates of each donor).

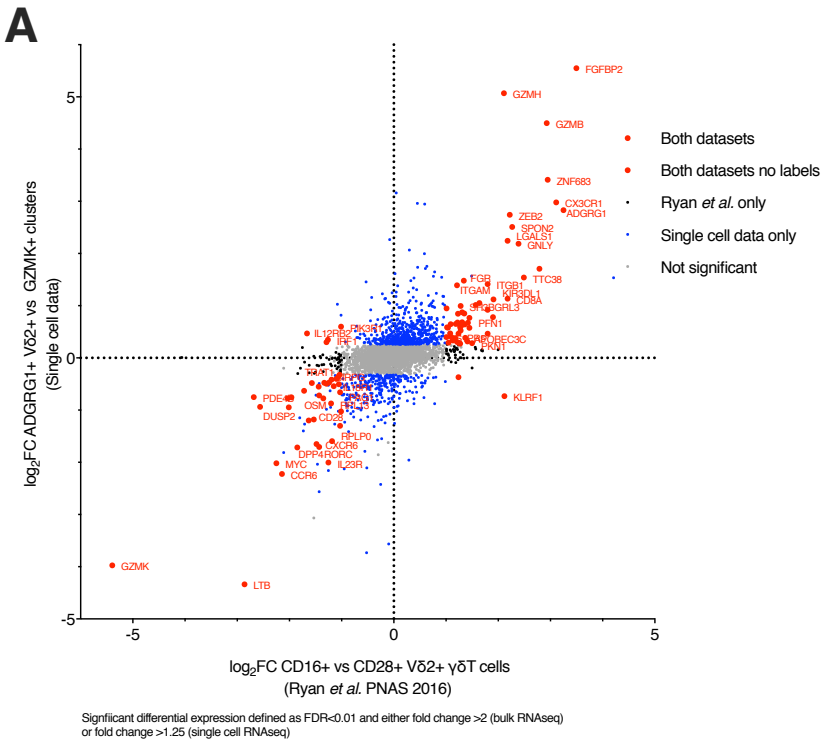
(E) Jaccard similarity index of TRD clonotypes of duplicate CD28+ and CX3CR1+ Vδ2+ T cells from a single donor.

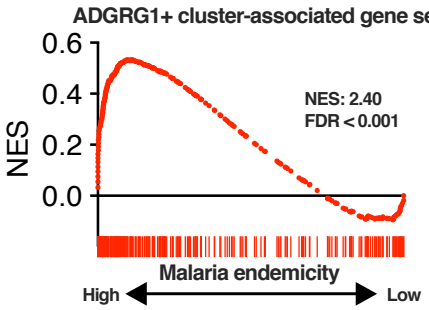
(F) Percentage of shared TRD clonotypes between duplicate CD28+ and CX3CR1+ Vδ2+ T cell populations of equal cell number (n=3).

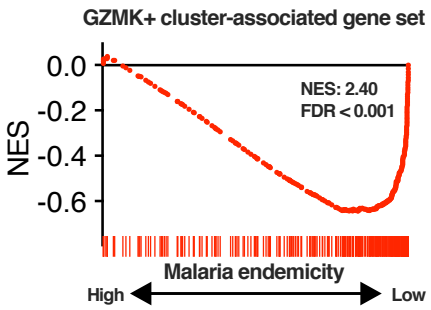
(G) Upset plot displaying shared TCR clonotypes between Vδ2+ T cell clusters, with shared clonotypes visualized as an 'interaction', indicated by a black circle joined by black lines. Bars above indicate the total number of shared TCR clonotypes for that interaction. Bars to left indicate number of clonotypes in the cluster. Cluster intersections with no shared TCR clonotypes are not shown.

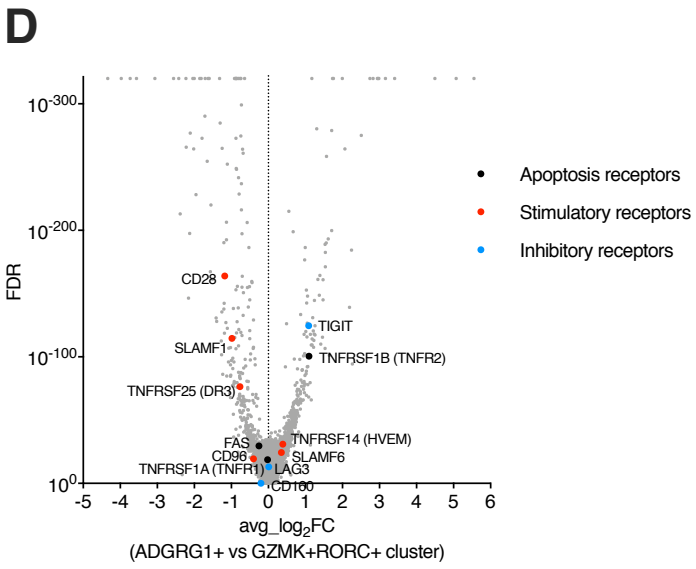
(H) Network plot showing shared clonotypes between Vδ2+ T cell clusters. The thickness of connecting lines is proportional to the number of shared clonotypes between the two clusters.

(I) Heatmap showing -log(adjusted p values) for enrichment tests of transcription factor modules which are differentially expressed in Vδ2+ T cell clusters when compared to all cells in the dataset (FDR <0.01). The top 20 enriched transcription factor modules for each cluster are indicated. Non-significant enrichment, grey.


A
FGFBP2
GZMH
GZMB
ZNF683
CX3CR1
ADGRG1
ZEB2
SPON2
LGALS1
GNLY
TTC38
ITGB1
ITGAM
CD84
PFN1
KLRF1
PDE4D
DUSP2
CD22
DPP4
RORC
MYC
CCR6
IL23R
GZMK
LTB
Both datasets
Both datasets no labels
Ryan et al. only
Single cell data only
Not significant
log2FC ADGRG1+ Vδ2+ vs GZMK+ clusters
(Single cell data)
log2FC CD16+ vs CD28+ Vδ2+ γδT cells
(Ryan et al. PNAS 2016)
Signficant differential expression defined as FDR<0.01 and either fold change >2 (bulk RNAseq)
or fold change >1.25 (single cell RNAseq)


B
ADGRG1+ cluster-associated gene set
NES
NES: 2.40
FDR < 0.001
Malaria endemicity
High
Low


C
GZMK+ cluster-associated gene set
NES
NES: 2.40
FDR < 0.001
Malaria endemicity
High
Low

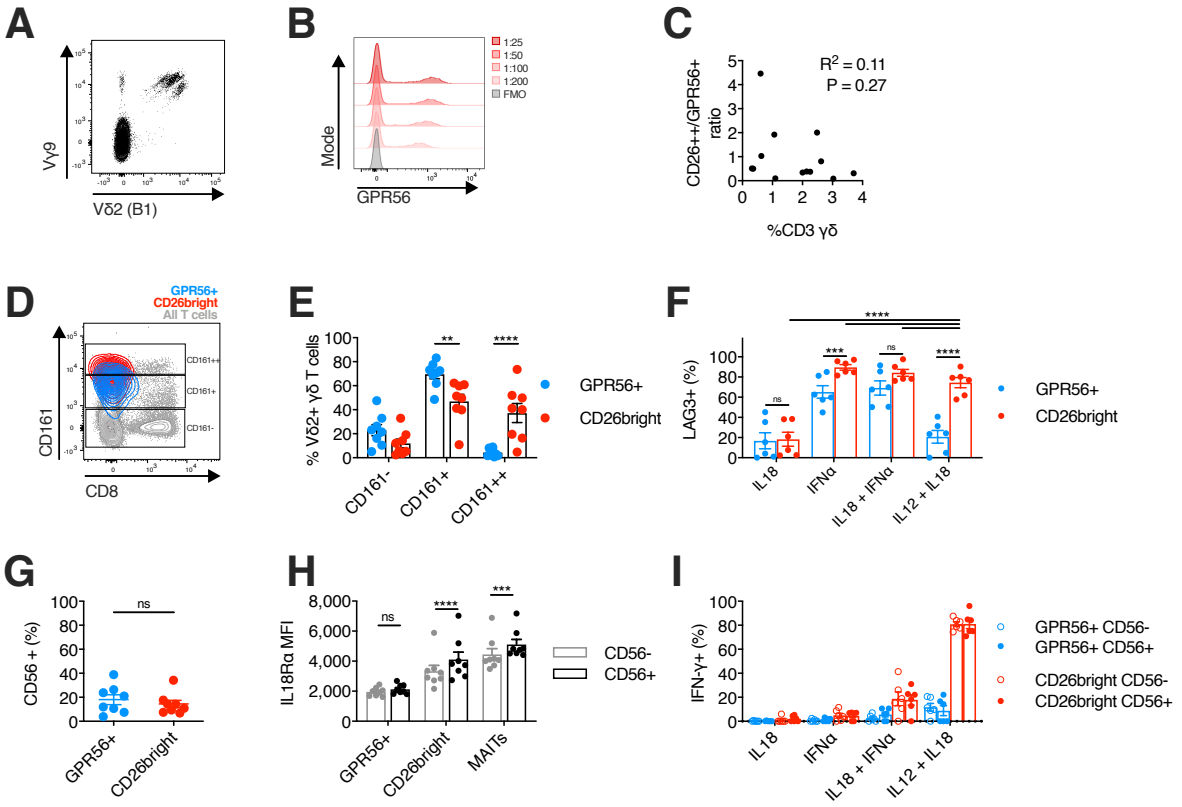

D
FDR
CD28
SLAMF1
TIGIT
TNFRSF1B (TNFR2)
TNFRSF25 (DR3)
FAS
CD96
TNFRSF1A (TNFR1)
TNFRSF14 (HVEM)
SLAMF6
LAG3
CD160
Apoptosis receptors
Stimulatory receptors
Inhibitory receptors
avg_log2FC
(ADGRG1+ vs GZMK+RORC+ cluster)

Supplemental Figure 5-6:

(A) Comparison of log_2(Fold Change) of differentially expressed genes between CD16+ and CD28+ Vδ2+ T cells in a published dataset (Ryan et al., 2016), and log_2(Fold Change) of differentially expressed genes between ADGRG1+ and GZMK+ clusters from scRNAseq Experiment 1.

Gene set enrichment analysis (GSEA) demonstrating the enrichment of a ADGRG1+ Vδ2+ cluster gene signature in Vδ2+ T cells from children from high malaria endemicity areas (B), and enrichment of a GZMK+ Vδ2+ cluster gene signature in Vδ2+ T cells from children from low malaria endemicity areas (C) (Jagannathan et al., 2014).

(D) Volcano plot of differentially expressed genes between ADGRG1+ and GZMK+ clusters of Vδ2+ T cells, with receptors with inhibitory (blue), stimulatory (red) and apoptotic (black) roles indicated.


A
Vγ9
Vδ2 (B1)
B
Mode
GPR56
1:25
1:50
1:100
1:200
FMO
C
R² = 0.11
P = 0.27
CD26++/GPR56+ ratio
%CD3 γδ
D
GPR56+
CD26bright
All T cells
CD161
CD8
CD161++
CD161+
CD161-
E
% Vδ2+ γδ T cells
CD161-
CD161+
CD161++
GPR56+
CD26bright
F
LAG3+ (%)
IL18
IFNα
IL18 + IFNα
IL12 + IL18
GPR56+
CD26bright
G
CD56 + (%)
GPR56+
CD26bright
H
IL18Rα MFI
GPR56+
CD26bright
MAITs
CD56-
CD56+
I
IFN-γ+ (%)
IL18
IFNα
IL18 + IFNα
IL12 + IL18
GPR56+ CD56-
GPR56+ CD56+
CD26bright CD56-
CD26bright CD56+

Supplementary Figure 5-7

(A) Representative plot of co-expression of Vδ2+ (B6 clone) and Vγ9+ (B3 clone).

(B) Representative histogram of GPR56 expression with titration of GPR56 antibody (REA467 clone).

(C) Scatter plot showing proportion of Vδ2+ T cells as a proportion of total CD3+ T cells (x-axis) and the ratio of the proportion of CD26bright and GPR56+ Vδ2+ T cells (n=13).

(D) Representative plot of CD161 expression on circulating T cells, with CD161-, CD161+, and CD161++ gates marked. The expression of GPR56+ (teal) and CD26bright (red) Vδ2+ T cells is indicated.

(E) Proportion of CD161-, CD161+, and CD161++ Vδ2+ T cells, categorised by GPR56+ and CD26bright subsets, (n=8). GPR56+, teal; CD26bright, red.

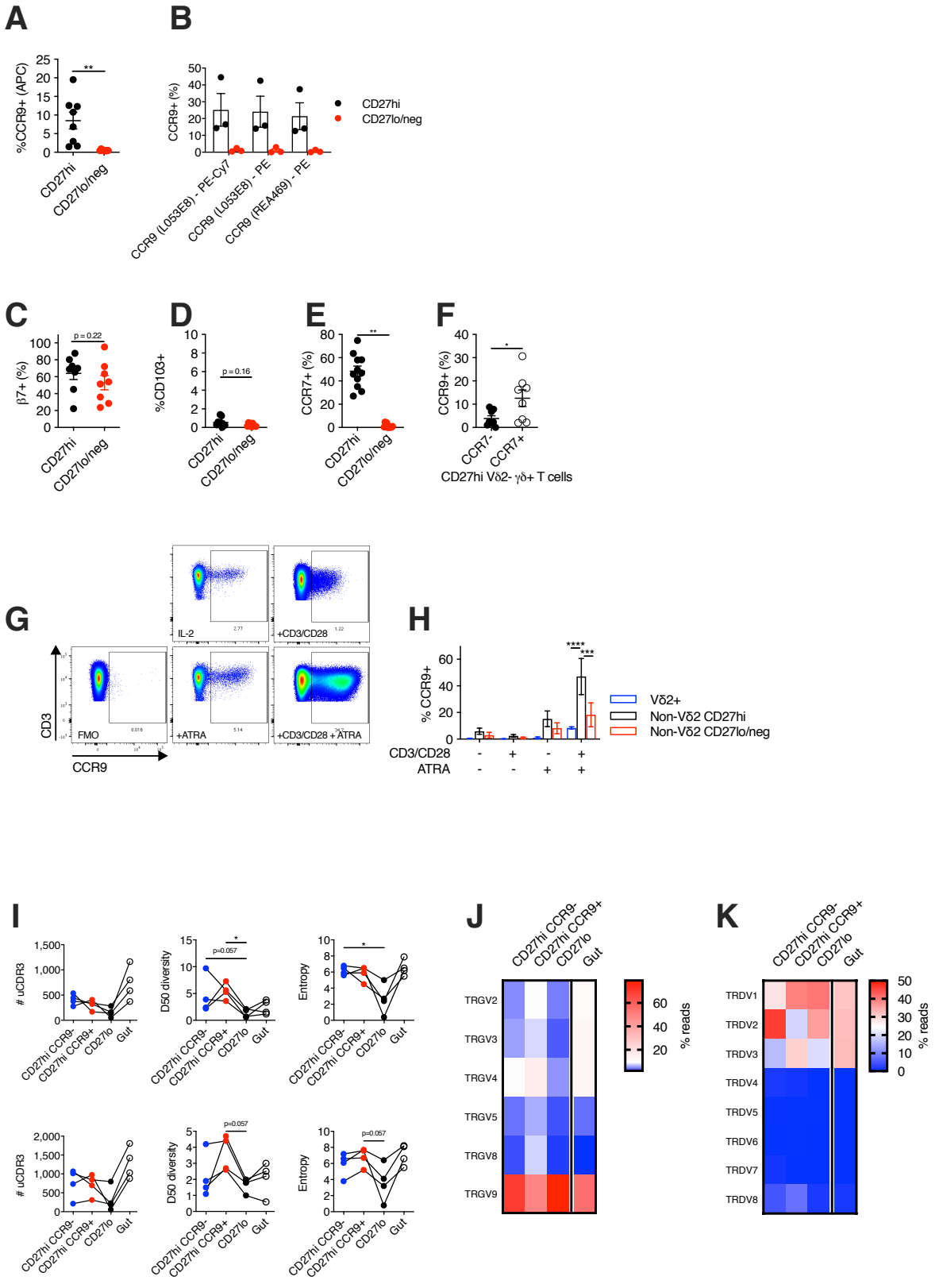
(F) Proportion of Vδ2+ T expressing LAG3 upon IL18, IFN-α, IL18 + IFN-α, and IL12 + IL18 stimulation, categorised by GPR56+ and CD26bright subsets, (n=6). GPR56+, teal; CD26bright, red.

(G) Proportion of CD56+ Vδ2+ T cells, categorised by GPR56+ and CD26bright subsets, (n=8). GPR56+, teal; CD26bright, red.

(H) MFI of IL18Rα of GPR56+ Vδ2+, CD26bright Vδ2+ T, and MAIT cells, categorised by CD56 expression, (n=6). CD56-, grey; CD56+, black.

(I) Proportion of Vδ2+ T producing IFN-γ upon IL18, IFN-α, IL18 + IFN-α, and IL12 + IL18 stimulation, categorised by GPR56+ and CD26bright subsets, and by CD56 expression (n=6). GPR56+, teal; CD26bright, red, CD56-, open circles; CD56+, filled circles.

Statistical analysis performed with Spearman's correlation (C), Wilcoxon signed ranks test (G), and two-way ANOVA with Sidak's multiple comparisons test (E, F, H, I). *, $P \leq 0.05$; **, $P \leq 0.01$; ***, $P \leq 0.001$; ****, $P \leq 0.0001$.


A
%CCR9+ (APC)
CD27hi
CD27lo/neg
B
CCR9+ (%)
CCR9 (L053E8) - PE-Cy7
CCR9 (L053E8) - PE
CCR9 (REA469) - PE
CD27hi
CD27lo/neg
C
β7+ (%)
p = 0.22
D
%CD103+
p = 0.16
E
CCR7+ (%)
F
CCR9+ (%)
CCR7-
CCR7+
CD27hi Vδ2- γδ+ T cells
G
IL-2
+CD3/CD28
FMO
+ATRA
+CD3/CD28 + ATRA
CD3
CCR9
H
% CCR9+
Vδ2+
Non-Vδ2 CD27hi
Non-Vδ2 CD27lo/neg
CD3/CD28
ATRA
I
uCDR3
D50 diversity
Entropy
p=0.057
CD27hi CCR9-
CD27hi CCR9+
CD27lo
Gut
J
TRGV2
TRGV3
TRGV4
TRGV5
TRGV8
TRGV9
% reads
K
TRDV1
TRDV2
TRDV3
TRDV4
TRDV5
TRDV6
TRDV7
TRDV8
% reads

Supplementary Figure 5-8

(A) Group summary of the proportion of circulating Vδ2- γδ T cells staining positive for CCR9 using the L053E8 APC-conjugated clone, categorised by CD27hi and CD27lo/neg subsets (n=8). CD27hi, black; CD27lo/neg, red.

(B) Group summary of the proportion of circulating Vδ2- γδ T cells staining positive for CCR9 using either the L053E8 PE- or PE-Cy7-conjugated clone, or the REA469 PE-conjugated clone, categorised by CD27hi and CD27lo/neg subsets (n=3). CD27hi, black; CD27lo/neg, red.

Group summaries of the proportion of circulating Vδ2- γδ T cells expressing β7-integrin **(C),** CD103 **(D)**, categorised by CD27hi and CD27lo/neg subsets (n=8). CD27hi, black; CD27lo/neg, red.

(E) Group summaries of the proportion of circulating Vδ2- γδ T cells expressing CCR7 , categorised by CD27hi, and CD27lo/neg subsets (n=12). CD27hi, black; CD27lo/neg, red.

(F) Group summaries of the proportion of circulating Vδ2- γδ T cells expressing CCR9, categorised by CCR7- and CCR7+ subsets (n=8). CCR7-, black closed circles; CCR7+, open circles.

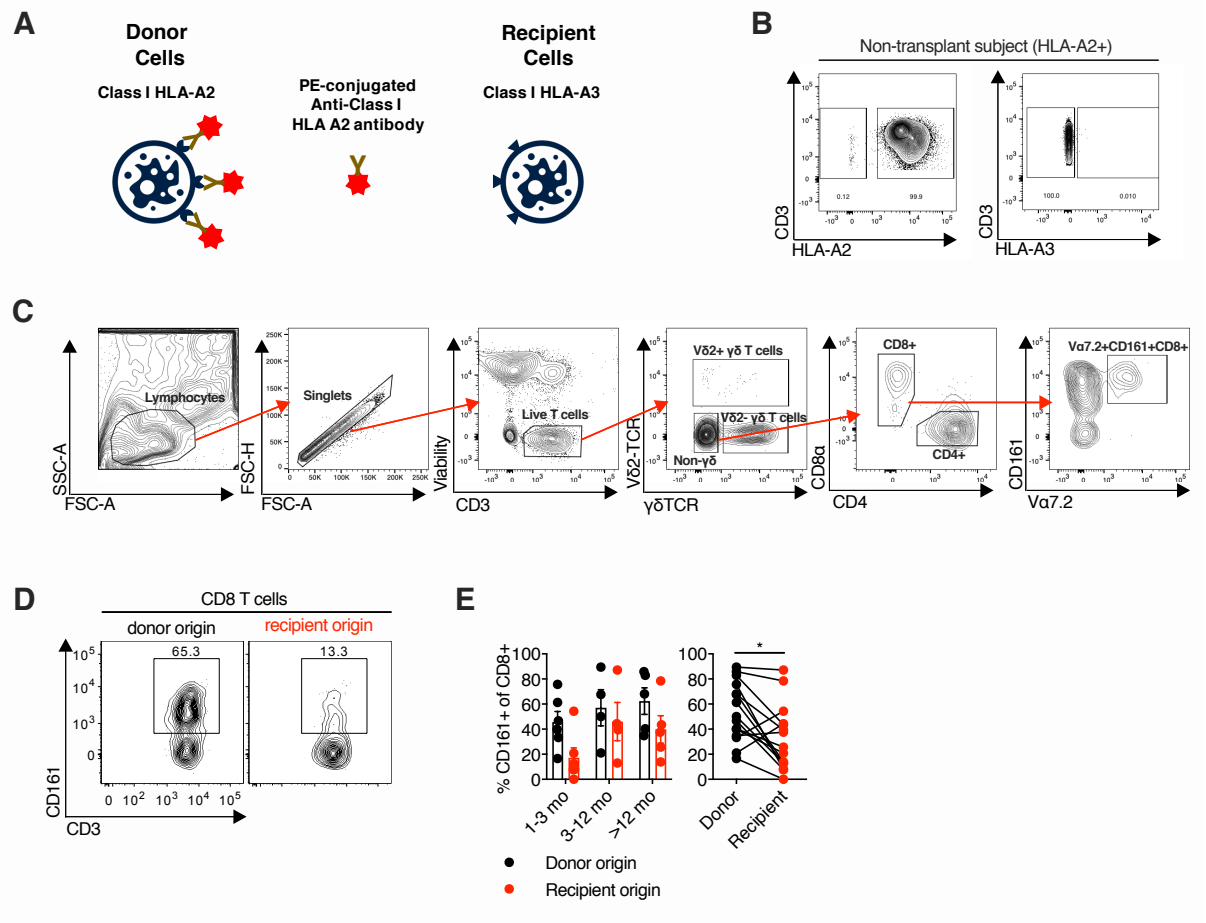
(G) Representative plots of CCR9 expression on CD3+ T cells stimulated for 7 days with combinations of IL-2, ATRA, and CD3/CD28.

(H) Proportion of Vδ2+, CD27hi, and CD27lo/neg non-Vδ2 γδ T cells expressing CCR9 after stimulation for seven days with IL-2 +/- ATRA and CD3/CD28 (n=4). Vδ2+ T cells, blue; CD27hi non-Vδ2 T cells, black; CD27lo/neg non-Vδ2 T cells, red.

(I) Diversity metrics (number of unique clonotypes (uCDR3), D50 diversity, Shannon entropy) for TRG (top) and TRD (bottom) repertoires of bulk FACS-sorted circulating CD27hi CCR9-, CD27hi CCR9+, CD27lo Vδ2- γδ T cells, and intestinal γδ T cells (n=4; lines connect samples from each donor).

Heatmaps showing the proportion of reads using TRGV genes **(J)** and TRDV genes **(K)** from bulk FACS-sorted circulating CD27hi CCR9-, CD27hi CCR9+, CD27lo Vδ2- γδ T cells, and intestinal γδ T cells (n=4).

Statistical analysis performed with Wilcoxon signed ranks test **(A,E)**, paired t tests **(C,D,F)**, Friedman test with Dunn's multiple comparisons **(I)** *, $P \leq 0.05$; **, $P \leq 0.01$; ***, $P \leq 0.001$; ****, $P \leq 0.0001$.



Supplemental Figure 6-1

(A) Illustration demonstrating the principle of HLA allele congenic cell tracking to identify donor- and recipient-derived T cell populations in the transplanted small intestinal graft using fluorophore-conjugated antibodies to Class I HLA haplotypes discordant between donor and recipient.

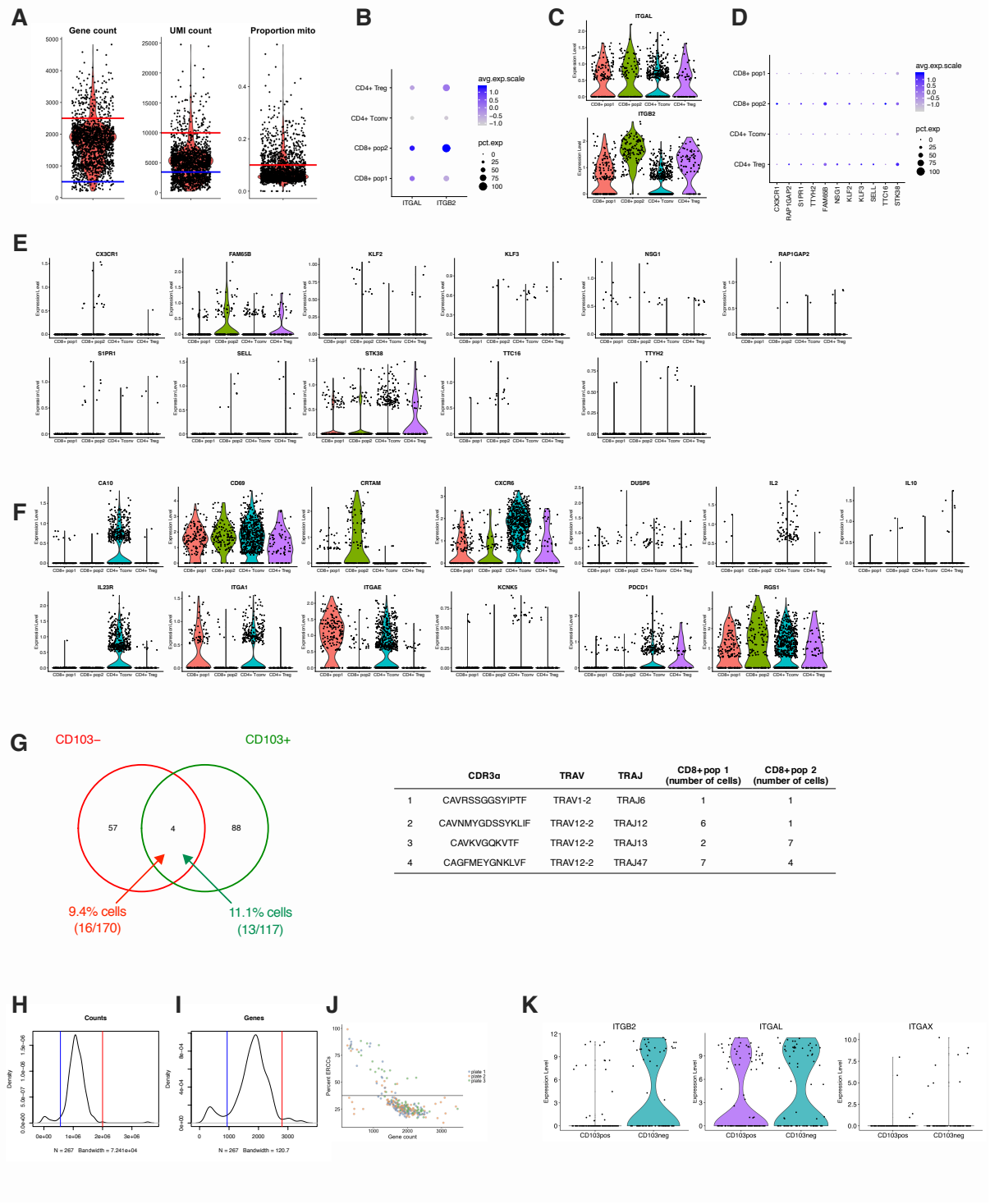
(B) Representative flow cytometry plot of Class I HLA non-specific staining (0.01-0.12%) from a non-transplant PBMC sample. Gated on live CD3+ T cells.

(C) Representative flow cytometry gating scheme for identification of T cell subsets.

(D) Representative histogram of CD161 expression on paired donor- and recipient-derived CD8+ intestinal T cells.

(E) Percentage of CD161+ donor- and recipient-derived CD8+ intestinal T cells categorised by time post-transplant (left), or grouped, with paired samples connected by black lines (right) (n=15 (8 subjects); mean +/- SEM).

Statistical analysis performed with Wilcoxon matched-pairs signed rank test. * $P \leq 0.05$.



	CDR3α	TRAV	TRAJ	CD8+pop 1 (number of cells)	CD8+pop 2 (number of cells)
1	CAVRSSGGSYIPTF	TRAV1-2	TRAJ6	1	1
2	CAVNMYGDSSYKLIF	TRAV12-2	TRAJ12	6	1
3	CAVKVGQKVTF	TRAV12-2	TRAJ13	2	7
4	CAGFMEYGNKLVF	TRAV12-2	TRAJ47	7	4

Supplemental Figure 6-2:

(A) Quality control parameters and thresholds for 10x Genomics scRNAseq Experiment 1. Number of genes per cell (left), number of unique molecular identifiers (UMIs) per cell (centre), and percentage of mitochondrial reads per cell (right) are displayed. Each dot represents a single cell, with red and blue lines indicating maximum and minimum thresholds, respectively.

(B) Dot plot showing expression of ITGB2 and its potential heterodimeric partner, ITGAL in Experiment 1. Other potential heterodimeric alpha integrin partners, ITGAD, ITGAM, and ITGAX were not detected. Dot size indicates the proportion of cells in which the gene is present. Colour intensity indicates the mean expression level of the gene.

(C) Violin plots showing expression of ITGB2 and its potential heterodimeric partner ITGAL in Experiment 1. Other potential heterodimeric alpha integrin partners, ITGAD, ITGAM, and ITGAX were not detected.

(D) Dot plot showing expression in Experiment 1 of 11 genes previously negatively associated with tissue residency (downregulated in human CD69+ cells in comparison to CD69- T cells; (Kumar et al., 2017)). Dot size indicates the proportion of cells in which the gene is present. Colour intensity indicates the mean expression level of the gene. Other genes in the geneset were not detected in the data (SBK1, NPDC1, KRT72, SOX13, KRT73, TSPAN18, PTGDS).

(E) Violin plots showing expression in Experiment 1 of 11 genes previously negatively associated with tissue residency (downregulated in human CD69+ cells in comparison to CD69- T cells; (Kumar et al., 2017)).

(F) Violin plots showing expression in Experiment 1 of 13 genes previously associated with tissue residency in human CD69+ T cells (Kumar et al., 2017), demonstrating discordant expression in conventional T cell clusters.

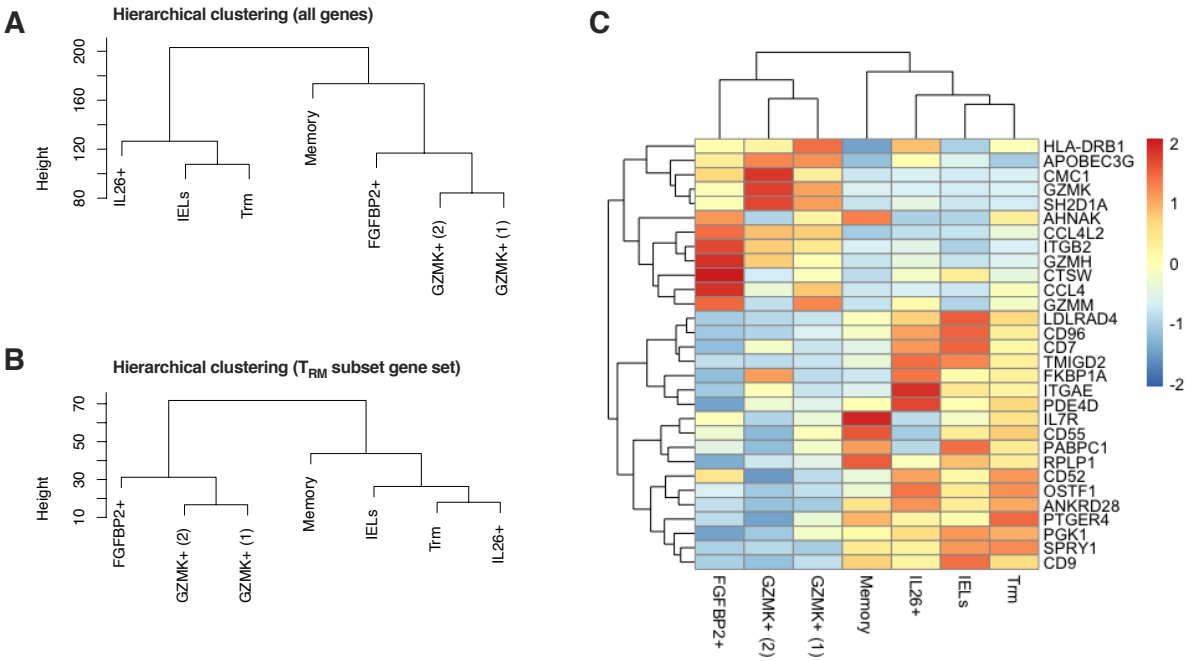
(G) Clonal sharing of TRA sequences from single-cell T cell receptor (TCR) repertoire sequencing of CD8+ T_{RM} cells from populations 1 and 2 from experiment 1. Shared TRA clonotypes, with the cell frequency in each cluster using each clonotype, are listed.

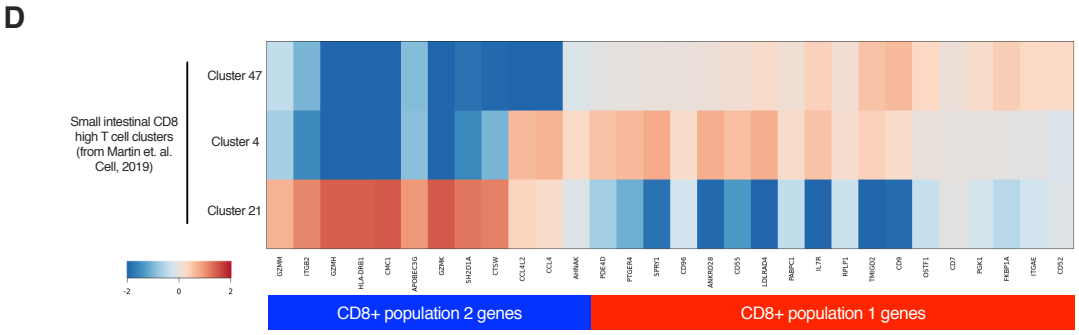
(H-J) Quality control parameters and thresholds for Smart-Seq2 scRNAseq Experiment 2.

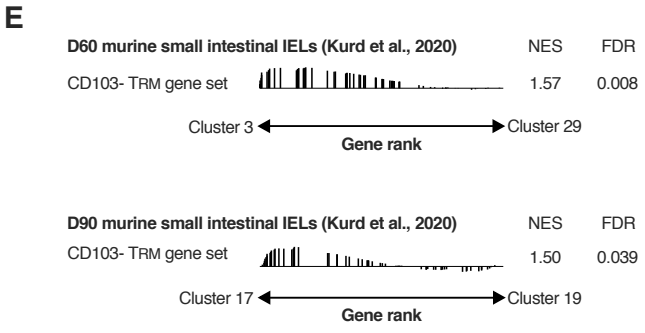
(H) Histogram of number of reads per cell and (I) number of genes per cell. Red and blue lines indicate maximum and minimum thresholds, respectively.

(J) Plot showing the percentage of External RNA Controls Consortium (ERCC) spike-ins per cell against the number of genes per cell. Black line indicates upper threshold.

(K) Violin plots showing expression of ITGB2 and its potential heterodimeric partners ITGAL and ITGAX in Experiment 2. ITGAD and ITGAM were not detected in the data.


A
Hierarchical clustering (all genes)
Height
200
160
120
80
IL26+
IELs
Trm
Memory
FGFBP2+
GZMK+ (2)
GZMK+ (1)
B
Hierarchical clustering (T$_{RM}$ subset gene set)
Height
70
50
30
10
FGFBP2+
GZMK+ (2)
GZMK+ (1)
Memory
IELs
Trm
IL26+
C
HLA-DRB1
APOBEC3G
CMC1
GZMK
SH2D1A
AHNAK
CCL4L2
ITGB2
GZMH
CTSW
CCL4
GZMM
LDLRAD4
CD96
CD7
TMIGD2
FKBP1A
ITGAE
PDE4D
IL7R
CD55
PABPC1
RPLP1
CD52
OSTF1
ANKRD28
PTGER4
PGK1
SPRY1
CD9
2
1
0
-1
-2
FGFBP2+
GZMK+ (2)
GZMK+ (1)
Memory
IL26+
IELs
Trm


D
Small intestinal CD8 high T cell clusters (from Martin et. al. Cell, 2019)
Cluster 47
Cluster 4
Cluster 21
CD8+ population 2 genes
CD8+ population 1 genes

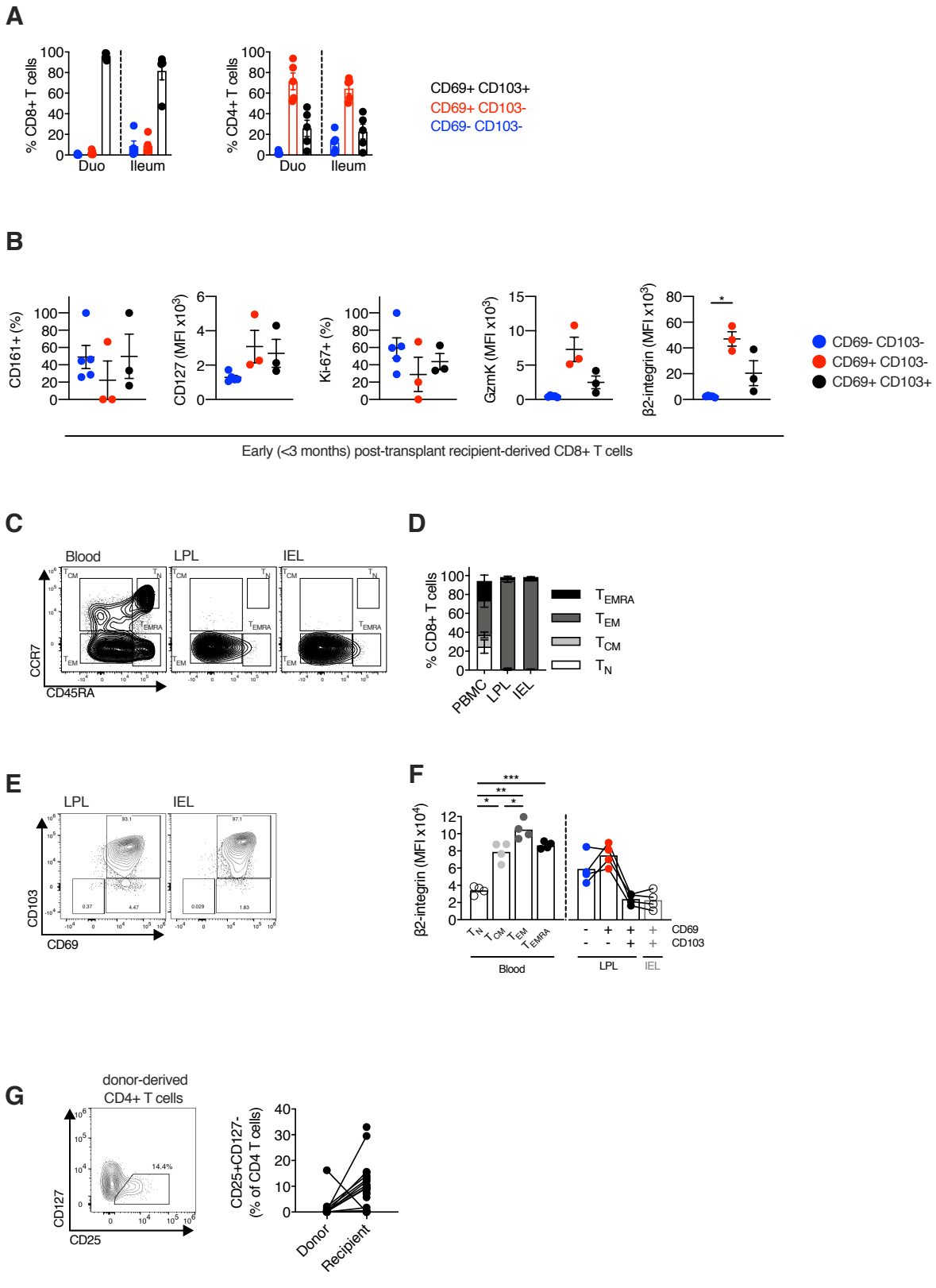

E
D60 murine small intestinal IELs (Kurd et al., 2020)
NES
FDR
CD103- TRM gene set
1.57
0.008
Cluster 3
Cluster 29
Gene rank
D90 murine small intestinal IELs (Kurd et al., 2020)
NES
FDR
CD103- TRM gene set
1.50
0.039
Cluster 17
Cluster 19
Gene rank

Supplemental Figure 6-3:

Comparison of identified T_{RM} subset gene sets with published studies of tissue-derived CD8+ T cells. (A-C) Examination of core T_{RM} gene set in conventional CD8+ intestinal T cells from human colon samples (published previously (Corridoni et al., 2020)). (A) Hierarchical clustering of colonic CD8+ T cell clusters based on total gene expression. (B) Hierarchical clustering of colonic CD8+ T cell clusters based on expression of 30 genes of the core T_{RM} geneset. (C) Heatmap of expression of the core gene set differentiating T_{RM} subsets within CD8+ colonic T cells.

(D) Normalised expression of the core gene set differentiating T_{RM} subsets within CD8A/CD8Bhi, CD4lo intestinal T cell clusters from human ileum samples (published previously (J. C. Martin et al., 2019)).

(E) Gene Set Enrichment Analysis showing the enrichment of a gene set associated with human CD103- T_{RM} cells from this study in clusters of murine intestinal T cells at Day 60 (D60) and Day 90 (D90) post-LCMV infection. NES, normalised enrichment score. FDR, False discovery rate (<0.25 considered significant).


A
% CD8+ T cells
% CD4+ T cells
Duo
Ileum
CD69+ CD103+
CD69+ CD103-
CD69- CD103-
B
CD161+ (%)
CD127 (MFI x10³)
Ki-67+ (%)
GzmK (MFI x10³)
β2-integrin (MFI x10³)
CD69- CD103-
CD69+ CD103-
CD69+ CD103+
Early (<3 months) post-transplant recipient-derived CD8+ T cells
C
Blood
LPL
IEL
CCR7
CD45RA
D
% CD8+ T cells
PBMC
LPL
IEL
E
CD103
CD69
F
β2-integrin (MFI x10⁴)
CD69
CD103
Blood
LPL
IEL
G
donor-derived
CD4+ T cells
CD127
CD25
CD25+CD127- (% of CD4 T cells)
Donor
Recipient

Supplemental Figure 6-4:

(A) The proportion of CD8+ T cells co-expressing CD69 and CD103 in small intestinal biopsies from the duodenum (duo) or ileum from healthy control subjects (n=5 for both duodenum and ileum). Blue, CD69-CD103- cells; Red, CD69+CD103- cells; Black, CD69+CD103+ cells.

(B) Phenotypic analysis of recipient-derived CD8+ T cell populations infiltrating the intestinal graft in the early post-transplant period (<3 months). Proportion of CD161+ cells, Ki-67+ cells or MFI of CD127, granzyme K, and β2 integrin of recipient-derived CD8+ T cells, categorised by CD69 and CD103 expression, in intestinal transplant grafts at early (<3 months) timepoints post-transplantation (n=5; 2 subjects). Mean percentage or MFI represented by bars. Black lines connect populations from the same sample. Blue, CD69-CD103- cells; Red, CD69+CD103- cells; Black, CD69+CD103+ cells.

(C-F) CD8+ T cell memory status and phenotype in intestinal epithelium and peripheral blood.

(C) Representative plot of CCR7 and CD45RA expression of circulating, lamina propria lymphocyte (LPL), and intra-epithelial lymphocyte (IEL) CD8+ T cells, identifying naïve (TN), central memory (TCM), effector memory (TEM), and terminally differentiated (TEMRA) populations.

(D) Stacked plots showing mean percentage (+/- SEM) of CD8+ T cells comprising naïve (TN; white), central memory (TCM; light grey), effector memory (TEM; dark grey), and terminally differentiated (TEMRA; black) populations (n=4).

(E) Representative flow cytometry plot of CD69 and CD103 expression on LPL and IEL T cells.

(F) MFI of β2-integrin expression on circulating, LPL, and IEL CD8+ T cells (n=4). Mean percentage or MFI represented by bars. Connecting lines represent populations from the same subject. Unfilled circles, circulating TN; light grey, circulating TCM; dark grey, circulating TEM; black, circulating TEMRA; Blue, CD69-CD103- cells (LPL); Red, CD69+CD103- cells (LPL); Black, CD69+CD103+ LPL cells; open circles and grey bars, CD69+CD103+ IEL cells.

(G) Representative flow cytometry gating of CD4+ CD25+CD127lo T cells. Percentage of donor- or recipient-derived intestinal CD4+ CD25+CD127lo T cells. Connecting lines represent populations from the same subject (n=23).

Statistical analysis performed with one-way ANOVA with Tukey's multiple comparisons test. * $P \leq 0.05$; ** $P \leq 0.01$; *** $P \leq 0.001$; **** $P \leq 0.0001$.

Supplementary table 6-1. Subject characteristics

Subject	Age	Transplant type	Indication	HLA mismatch	No. samples	Timepoints (days post-Tx)	Notes
1	32	Isolated small bowel transplant	Crohn's Disease	A2	1	1747	
2	28	Isolated small bowel transplant	Ischaemia	A2	2	23, 184	
3	54	Isolated small bowel transplant	Pseudomyxoma peritonii	A2	3	32, 67, 184, 362	10x Genomics Experiment 1
4	52	Modified multivisceral transplant	Neuroendocrine tumour	A3	2	1684, 1831	
5	65	Isolated small bowel transplant	Crohn's Disease	A3	1	1861	
6	35	Isolated small bowel transplant	Desmoid	Bw4	1	1306	
7	42	Isolated small bowel transplant	Crohn's Disease	A2	1	180	
8	23	Isolated small bowel transplant	Neuropathy	A3	4	63, 269, 333, 486	
9	39	Isolated small bowel transplant	Pseudomyxoma peritonii	Bw4	1	1097	
10	29	Isolated small bowel transplant	Crohn's Disease	A3	1	1865	
11	62	Isolated small bowel transplant	Ischaemia	A2	2	21, 109, 190	Smart-Seq2 Experiment 2
12	56	Isolated small bowel transplant	Crohn's Disease	A2	4	625, 632, 684, 694	
13	63	Isolated small bowel transplant	Desmoid tumour	A2	1	2710	
14	36	Isolated small bowel transplant	Pseudomyxoma peritonii	A2	6	28, 49, 53, 59, 73, 193	
15	46	Isolated small bowel transplant	Pseudomyxoma peritonii	A3	4	86, 115, 122, 128,	Smart-Seq2 Experiment 2
16	42	Isolated small bowel transplant	Crohn's Disease	A2	1	559	
17	35	Isolated small bowel transplant	Gastroschisis	A3	4	227, 267, 295, 420	
18	46	Isolated small bowel transplant	Pseudomyxoma peritonii	A3	4	31, 115, 122, 128,	
19	55	Healthy control		N/A	1		
20	36	Healthy control		N/A	1		
21	68	Healthy control		N/A	1		
22	50	Healthy control		N/A	1		
23	24	Healthy control		N/A	1		
24	20	Healthy control		N/A	1		
25	41	Healthy control		N/A	1		
26	42	Healthy control		N/A	1		
27	47	Healthy control		N/A	1		
28	24	Healthy control		N/A	1		

Supplementary Table 6-2.

Differentially expressed genes between populations 1 and 2 in Experiment 1 (10x Genomics)

Gene symbol	Fold change	Gene symbol	Fold change	Gene symbol	Fold change
GZMK	-2.501345	HLA-DRA	-1.0092579	LITAF	-0.5713577
HLA-DRB1	-1.9032128	CD3D	0.63180289	CD8B	0.51581868
CD7	1.48385649	LAIR1	0.67342934	LTB	0.41118937
ITGB2	-1.2437265	ZNF683	0.96676928	SLAMF1	0.44134281
ITGAE	1.19951285	CKLF	0.79227144	PRMT9	0.46603604
LDLRAD4	1.73351151	VCAM1	-0.8219136	CDKN1A	0.62148137
SH2D1A	-1.1374149	TPT1	0.40929927	ITPRIP	-0.3880301
CD52	0.74797565	SAMD3	-0.700187	TPI1	0.42349402
PABPC1	0.73705122	CCR6	0.84724376	MAP4	0.43787537
SPRY1	0.9303036	SMIM3	0.56167447	CCR9	0.61017079
IL7R	1.34481813	SPINK2	0.50402145	PDCD4	0.44948314
PGK1	0.79257215	RPL30	-0.3730415	LINC00861	-0.4195145
AHNAK	-0.876956	CRTAM	-1.3724953	OXNAD1	0.39920062
CMC1	-1.3192418	RPS14	-0.3788703	FKBP11	0.38427509
TMIGD2	0.68991807	CD3G	0.64595697	ZFP36	0.62970645
GZMH	-1.1050793	RPS24	-0.387526		
CD9	0.55368567	RNF19A	-0.7496581		
RPLP1	0.4282613	ITM2B	0.59690503		
APOBEC3G	-0.7309281	CLEC2B	-0.8280459		
CCL4	-1.3123288	XCL1	1.75589881		
PDE4D	0.63353535	TMEM14C	0.48467903		
OSTF1	0.53179707	KLRB1	1.30975133		
CD55	0.65990607	RPL13A	-0.437385		
CD96	0.57087561	HCST	-0.4606218		
ANKRD28	0.40022644	ITGA1	0.48548115		
CTSW	-0.5474394	HOPX	0.62806382		
PTGER4	0.60308641	RPL23A	-0.3806241		
CCL4L2	-1.6508848	FABP5	-0.7106752		
FKBP1A	0.42749359	JUN	0.60082064		
GZMM	-0.5022827	CD28	-0.4927376		
HLA-DRB5	-2.1991275	ZEB2	-0.808163		
CST7	-1.4573335	EVL	0.54871541		
HLA-DQA1	-1.7042636	RPL24	-0.3818548		
RPS27	-0.6506229	CD226	0.44742877		
HLA-DPA1	-1.0716559	SH3BGRL3	0.40232621		
KLRG1	-1.1274998	CD160	0.64576779		
NKG7	-1.0399565	LAIR2	-0.6368599		
ENC1	-0.8801076	SH3KBP1	-0.5087312		
CD74	-1.192491	CXCR4	-0.6801581		
HLA-DPB1	-0.9908018	TRAT1	-0.5912528		
HLA-DQB1	-0.6927867	PDLIM1	-0.3859111		
CAPG	0.97392191	TAGAP	-0.9127364		
FTH1	1.10114114	COMMD5	0.41014245		
RPS15A	-0.5058964	TIMP1	0.45474042		
LYST	-0.9865243	MAP3K8	0.58197509		
GAPDH	0.69849345	ID2	0.64836505		
TMSB4X	0.510761	ALOX5AP	0.48517352		
PLEK	-0.8902106	DTHD1	-0.4536788		
CD44	-0.9174022	SLA	-0.8089673		
PFKFB3	1.08819635	RPL27A	-0.4020863		

Supplementary Table 6-3.

Differentially expressed genes between cluster 1 and clusters 2&3 combined in Experiment 2 (Smart-Seq2)

Gene symbol	Fold change	Gene symbol	Fold change	Gene symbol	Fold change
GZMK	-2.4888605	UBE3C	5.2313709	NUP153	2.31096277
HLA-DRB1	-2.0431357	ITGB1	-1.3633559	ASCC3	1.85768036
CD7	1.21268476	STAT4	0.78418968	ZSWIM6	-0.7504253
ITGB2	-1.8966904	CHP1	0.95190763	GZMA	-0.7929903
ITGAE	2.8877346	ATF7IP	1.06165122	ATP6V1D	0.01987679
LDLRAD4	2.77432825	SDF2L1	0.74842709	UCP2	1.93435613
SH2D1A	-2.0611032	GZMB	-1.4251506	EDF1	0.1202781
CD52	0.61893486	VAMP5	-1.9934766	COQ10A	-1.1541223
PABPC1	0.9416013	RNPS1	0.23814185	SRSF6	1.24898564
SPRY1	1.32615241	HCLS1	-0.2202737	RASD1	-3.9726588
IL7R	1.3542543	BRMS1	-0.5865974	STARD4	3.51763804
PGK1	0.53349289	COX7A2L	1.94239004	AHR	0.41364731
AHNAK	-1.2889017	ISCA1	2.58889455	NUDT1	-0.3432213
CMC1	-2.6012175	LY6E	-0.472669	RBX1	1.28855552
TMIGD2	1.30539513	SDCBP	0.92135488	EIF1B	-0.3878083
GZMH	-1.6871916	POLR1C	-0.3707589	COMMD10	2.59651199
CD9	4.95711777	SMIM12	0.48612281	COX6A1	0.17349949
RPLP1	0.64570391	RNASET2	0.72544584	GDI1	-1.0806586
APOBEC3G	-2.2231416	PELP1	-0.2276727	DXO	-3.1643877
CCL4	-3.4679825	RPS17	-0.5845798	HMGXB3	0.07236803
PDE4D	0.74015486	CYB5B	0.70754338	ARPC5	-0.2847239
OSTF1	2.74846367	TMEM50B	0.92517793	ZNHIT3	0.29856703
CD55	1.32975007	DHPS	-2.8289555	LRRFIP1	0.71302823
CD96	0.94728627	COLGALT1	0.2608009	BCAP31	0.34779105
ANKRD28	1.70833104	CHMP7	1.28157543	LAPTM4A	2.08223603
CTSW	-1.8110573	OASL	-3.0670331	RHOT2	9.13076422
PTGER4	1.64204096	SNAP23	-1.7083304	H2AFJ	-0.1094574
CCL4L2	-4.0641239	BFAR	0.11442989	IL10RB	-1.7446667
FKBP1A	1.98412568	CNIH4	0.67342978	MRPL47	1.19218921
GZMM	-0.4529084	WDR33	0.78169715	COPS6	-0.2454435
MT-CO2	0.43060049	WASF2	1.29187241	NPIPB11	2.73167279
CD8A	0.3292585	ADGRE2	-1.9270807	MTA2	2.31905074
LAPTM5	0.42161804	TNFAIP3	0.50195345	TMEM11	0.63901975
FCRL6	-1.9790072	EIF3L	0.07488526	PRPS2	0.18294087
BPGM	-1.3405387	ZNHIT1	-0.3960895	DPM1	-0.363315
DBI	0.96374381	SNRPB	0.3379266	RGS16	-2.8067409
ELF1	0.58539678	SCUBE1	5.56752609	TSPYL4	-2.8947736
PDE4A	1.44173293	RBMXL1	4.83120846	CKS2	-1.3908241
RPL38	0.54690651	ORMDL3	0.04314544	UFC1	-0.1620345
NINJ1	3.58656358	DRAP1	0.88257478	RNF181	1.56968325
TUBA4A	-1.3822773	H2AFX	-1.6408146	HLA-G	0.56341326
PPP1CB	1.72494403	CUTA	1.34258293	TM9SF4	-0.2363756
G3BP2	1.15575984	EID1	0.78705529	EEF1A1	0.49492314
TSC22D3	0.60204593	FKBP1C	1.94576457	LRRC37A2	0.22425688
CD48	-1.3357992	KLRD1	1.74137385	LRRC41	-0.1101467
LAX1	-1.7914115	DGCR6	1.9599831	NDUFAF3	0.66898557
CCL3	-6.2555671	SURF4	1.15366685	C16orf91	0.63780564
P2RY10	2.64470668	DEAF1	4.30096052	PPM1D	-1.0310353
ORAI2	1.26753113	SURF2	0.00150165	MLLT3	-0.579627
PLXDC1	4.11637547	CYTIP	1.20002671	TAZ	-1.1187608
JMJD1C	1.36278728	C19orf53	0.10940959	DEK	0.33230631
RGS1	0.04563271	TTC19	0.34527743	COX4I1	0.01005021
GADD45B	-1.0870114	RNASEK	-3.0387158	FYN	0.258808
WDR54	11.4997687	BBS4	1.95869773	RAB1A	0.16395737
IFNG	-3.2463092	IDS	0.21631512	YPEL5	0.37647654
IRF7	1.34808867	AKAP13	1.02327788	DRG1	0.53958839
CREM	0.84673061	GGNBP2	1.26691024	DYNLT1	1.57135207
PRDX5	0.43885095	PPIG	2.70982832	TOR1A	-1.0982579
CIB1	0.50307938	EEF1B2	1.16120212	TSPYL2	1.35716956
AURKAIP1	-0.1352131	CLEC2D	0.55375509	TRPV2	-1.2449248
SGF29	1.74533498	PSMB5	0.62951398	RYBP	5.75573391
ZFP36L1	-0.8814822	ARHGEF6	1.06483481	PSMC4	0.70890947
PTPRC	0.16832684	CISD2	8.03280242	INPP4A	1.0896515
UNC45A	9.11541005	C9orf16	2.57617609	PLEKHO2	-5.1979144
AGAP2	1.78442623	PDCD6	1.12217913	PREB	-0.5531378
ADK	0.68289186	NDUFA10	-0.1346382	SLC9A1	7.41571202
ADRB2	-1.8195956	AP3M1	0.7250827	TBCB	-0.6083622
MIR155HG	-2.8386827	ATF5	0.24650205	INTS1	0.14964409
		MED15	0.58231477	OSTC	0.11881291

References

Abadie, V., Jabri, B., 2014. IL-15: a central regulator of celiac disease immunopathology. Immunol Rev 260, 221–234. doi:10.1111/imr.12191

Abadie, V., Kim, S.M., Lejeune, T., Palanski, B.A., Ernest, J.D., Tastet, O., Voisine, J., Discepolo, V., Marietta, E.V., Hawash, M.B.F., Ciszewski, C., Bouziat, R., Panigrahi, K., Horwath, I., Zurenski, M.A., Lawrence, I., Dumaine, A., Yotova, V., Grenier, J.-C., Murray, J.A., Khosla, C., Barreiro, L.B., Jabri, B., 2020. IL-15, gluten and HLA-DQ8 drive tissue destruction in coeliac disease. Nature 1–28. doi:10.1038/s41586-020-2003-8

Abadie, V., Sollid, L.M., Barreiro, L.B., Jabri, B., 2011. Integration of Genetic and Immunological Insights into a Model of Celiac Disease Pathogenesis. Annu. Rev. Immunol. 29, 493–525. doi:10.1146/annurev-immunol-040210-092915

Abuzakouk, M., Feighery, C., O'Farrelly, C., 1996. Collagenase and Dispase enzymes disrupt lymphocyte surface molecules. Journal of Immunological Methods 194, 211–216.

Adachi, T., Kobayashi, T., Sugihara, E., Yamada, T., Ikuta, K., Pittaluga, S., Saya, H., Amagai, M., Nagao, K., 2015. Hair follicle–derived IL-7 and IL-15 mediate skin-resident memory T cell homeostasis and lymphoma. Nature Medicine 21, 1272–1279. doi:10.1038/nm.3962

Afrache, H., Pontarotti, P., Abi-Rached, L., Olive, D., 2017. Evolutionary and polymorphism analyses reveal the central role of BTN3A2 in the concerted evolution of the BTN3 gene family 1–12. doi:10.1007/s00251-017-0980-z

Aibar, S., González-Blas, C.B., Moerman, T., Huynh-Thu, V.A., Imrichova, H., Hulselmans, G., Rambow, F., Marine, J.-C., Geurts, P., Aerts, J., van den Oord, J., Atak, Z.K., Wouters, J., Aerts, S., 2017. SCENIC: single-cell regulatory network inference and clustering. Nat Meth 14, 1083–1086. doi:10.1038/nmeth.4463

AKOBENG, A.K., THOMAS, A.G., 2008. Systematic review: tolerable amount of gluten for people with coeliac disease. Aliment Pharmacol Ther 27, 1044–1052. doi:10.1111/j.1365-2036.2008.03669.x

Al-Toma, A., Goerres, M.S., Meijer, J.W.R., Blomberg, von, B.M.E., Wahab, P.J., Kerckhaert, J.A.M., Mulder, C.J.J., 2006. Cladribine Therapy in Refractory Celiac Disease With Aberrant T Cells. Clinical Gastroenterology and Hepatology 4, 1322–1327. doi:10.1016/j.cgh.2006.07.007

Anderson, R.P., 2005. T cells in peripheral blood after gluten challenge in coeliac disease. Gut 54, 1217–1223. doi:10.1136/gut.2004.059998

Anderson, R.P., Degano, P., Godkin, A.J., Jewell, D.P., Hill, A.V.S., 2000. In vivo antigen challenge in celiac disease identifies a single transglutaminase-modified peptide as the dominant A- gliadin T-cell epitope. Nature Medicine 6, 337–342. doi:10.1038/73200

Andrews, T.S., Andrews, T.S., Hemberg, M., 2018. M3Drop: dropout-based feature selection for scRNASeq. Bioinformatics 35, 2865–2867. doi:10.1093/bioinformatics/bty1044

Angelini, D.F., Borsellino, G., Poupot, M., Diamantini, A., Poupot, R., Bernardi, G., Poccia, F., Fournié, J.-J., Battistini, L., 2004. FcγRIII discriminates between 2 subsets of Vγ9Vδ2 effector cells with different responses and activation pathways. Blood 104, 1801–1807. doi:10.1182/blood-2004-01-0331

Arentz Hansen, H., Fleckenstein, B., Molberg, Ø., Scott, H., Koning, F., Jung, G., Roepstorff, P., Lundin, K.E.A., Sollid, L.M., 2004. The Molecular Basis for Oat Intolerance in Patients with Celiac Disease. PLoS Med 1, e1–9. doi:10.1371/journal.pmed.0010001

Arguelles-Grande, C., Tennyson, C.A., Lewis, S.K., Green, P.H.R., Bhagat, G., 2012. Variability in small bowel histopathology reporting between different pathology practice settings: impact on the diagnosis of coeliac disease. Journal of Clinical Pathology 65, 242–247. doi:10.1136/jclinpath-2011-200372

Arike, L., Seiman, A., van der Post, S., Piñeiro, A.M.R., Ermund, A., Schütte, A., Bäckhed, F., Johansson, M.E.V., Hansson, G.C., 2020. Protein Turnover in Epithelial Cells and Mucus along the Gastrointestinal Tract Is Coordinated by the Spatial Location and Microbiota. CellReports 30, 1077–1087.e3. doi:10.1016/j.celrep.2019.12.068

Ariotti, S., Hogenbirk, M.A., Dijkgraaf, F.E., Visser, L.L., Hoekstra, M.E., Song, J.-Y., Jacobs, H., Haanen, J.B., Schumacher, T.N., 2014. T cell memory. Skin-resident memory $CD8^+$ T cells trigger a state of tissue-wide pathogen alert. Science 346, 101–105. doi:10.1126/science.1254803

Arranz, E., Bode, J., Kingstone, K., Ferguson, A., 1994. Intestinal antibody pattern of coeliac disease: association with gamma/delta T cell receptor expression by intraepithelial lymphocytes, and other indices of potential coeliac disease. Gut 35, 476–482.

Autengruber, A., Gereke, M., Hansen, G., Hennig, C., Bruder, D., 2012. Impact of enzymatic tissue disintegration on the level of surface molecule expression and immune cell function. European Journal of Microbiology and Immunology 2, 112–120. doi:10.1556/EuJMI.2.2012.2.3

Aziz, I., Peerally, M.F., Barnes, J.-H., Kandasamy, V., Whiteley, J.C., Partridge, D., Vergani, P., Cross, S.S., Green, P.H., Sanders, D.S., 2017. The clinical and phenotypical assessment of seronegative villous atrophy; a prospective UK centre experience evaluating 200 adult cases over a 15-year period (2000–2015). Gut 66, 1563–1572. doi:10.1136/gutjnl-2016-312271

Babicki, S., Arndt, D., Marcu, A., Liang, Y., Grant, J.R., Maciejewski, A., Wishart, D.S., 2016. Heatmapper: web-enabled heat mapping for all. Nucleic Acids Res 44, W147–W153. doi:10.1093/nar/gkw419

Bai, L., Picard, D., Anderson, B., Chaudhary, V., Luoma, A., Jabri, B., Adams, E.J., Savage, P.B., Bendelac, A., 2012. The majority of CD1d-sulfatide-specific T cells in human blood use a semiinvariant Vδ1 TCR. Eur. J. Immunol. 42, 2505–2510. doi:10.1002/eji.201242531

Barisa, M., Kramer, A.M., Majani, Y., Moulding, D., Saraiva, L., Bajaj-Elliott, M., Anderson, J., Gustafsson, K., 2017. E. coli promotes human Vγ9Vδ2 T cell transition from cytokine-producing bactericidal effectors to professional phagocytic killers in a TCR-dependent manner. Sci Rep 7, 15–12. doi:10.1038/s41598-017-02886-8

Barnitz, R.A., Imam, S., Yates, K., Haining, W.N., 2013. Isolation of RNA and the Synthesis and Amplification of cDNA from Antigen-Specific T Cells for Genome-Wide Expression Analysis, in: Snow, A.L., Lenardo, M.J. (Eds.), Immune Homeostasis, Methods in Molecular Biology. Humana Press, Totowa, NJ, pp. 161–173. doi:10.1007/978-1-62703-290-2_13

Bartolomé-Casado, R., Landsverk, O.J.B., Chauhan, S.K., Richter, L., Phung, D., Greiff, V., Risnes, L.F., Yao, Y., Neumann, R.S., Yaqub, S., Øyen, O., Horneland, R., Aandahl, E.M., Paulsen, V., Sollid, L.M., Qiao, S.-W., Bækkevold, E.S., Jahnsen, F.L., 2019. Resident memory CD8 T cells persist for years in human small intestine. J Exp Med 157, jem.20190414–23. doi:10.1084/jem.20190414

Bartolomé-Casado, R., Landsverk, O.J.B., Chauhan, S.K., Sætre, F., Hagen, K.T., Yaqub, S., Øyen, O., Horneland, R., Aandahl, E.M., Aabakken, L., Bækkevold, E.S., Jahnsen, F.L., 2020. CD4 + T cells persist for years in the human small intestine and display a T H 1 cytokine profile. Mucosal Immunology 291, 1–9. doi:10.1038/s41385-020-0315-5

Behr, F.M., Kragten, N.A.M., Wesselink, T.H., Nota, B., van Lier, R.A.W., Amsen, D., Stark, R., Hombrink, P., van Gisbergen, K.P.J.M., 2019. Blimp-1 Rather Than Hobit Drives the Formation of Tissue-Resident Memory CD8+ T Cells in the Lungs. Front. Immunol. 10, 79–14. doi:10.3389/fimmu.2019.00400

Behr, F.M., Parga-Vidal, L., Kragten, N.A.M., Dam, T.J.P., Wesselink, T.H., Sheridan, B.S., Arens, R., Lier, R.A.W., Stark, R., Gisbergen, K.P.J.M., 2020. Tissue-resident memory CD8+ T cells shape local and systemic secondary T cell responses. Nat Immunol 1–28. doi:10.1038/s41590-020-0723-4

Belkina, A.C., Starchenko, A., Drake, K.A., Proctor, E.A., Pihl, R.M.F., Olson, A., Lauffenburger, D.A., Lin, N., Snyder-Cappione, J.E., 2018. Multivariate Computational Analysis of Gamma Delta T Cell Inhibitory Receptor Signatures Reveals the Divergence of Healthy and ART-Suppressed HIV+ Aging. Front. Immunol. 9, 116–17. doi:10.3389/fimmu.2018.02783

Bergsbaken, T., Bevan, M.J., 2015. Proinflammatory microenvironments within the intestine regulate the differentiation of tissue-resident CD8+ T cells responding to infection. Nat Immunol 16, 406–414. doi:10.1038/ni.3108

Berlin, C., Berg, E.L., Briskin, M.J., Andrew, D.P., Kilshaw, P.J., Holzmann, B., Weissman, I.L., Hamann, A., Butcher, E.C., 1993. Alpha 4 beta 7 integrin mediates lymphocyte binding to the mucosal vascular addressin MAdCAM-1. Cell 74, 185–195. doi:10.1007/978-4-431-67895-3_37.pdf

Bernardo, D., van Hoogstraten, I.M.W., Verbeek, W.H.M., Peña, A.S., Mearin, M.L., Arranz, E., Garrote, J.A., Scheper, R.J., Schreurs, M.W.J., Bontkes, H.J., Mulder, C.J.J., Blomberg, von, B.M.E., 2008. Decreased circulating iNKT cell numbers in refractory coeliac disease. Clinical Immunology 126, 172–179. doi:10.1016/j.clim.2007.09.005

Beura, L.K., Wijeyesinghe, S., Thompson, E.A., Macchietto, M.G., Rosato, P.C., Pierson, M.J., Schenkel, J.M., Mitchell, J.S., Vezys, V., Fife, B.T., Shen, S., Masopust, D., 2018. T Cells in Nonlymphoid Tissues Give Rise to Lymph- Node-Resident Memory T Cells. Immunity 48, 327–338.e5. doi:10.1016/j.immuni.2018.01.015

Bhagat, G., Naiyer, A.J., Shah, J.G., Harper, J., Jabri, B., Wang, T.C., Green, P.H.R., Manavalan, J.S., 2008. Small intestinal CD8+TCRγδ+NKG2A+ intraepithelial lymphocytes have attributes of regulatory cells in patients with celiac disease. J. Clin. Invest. 118, 281–293. doi:10.1172/JCI30989

Bird, A., Tobin, E., 2008. Natural Kinds.

Black, K.E., Murray, J.A., David, C.S., 2002. HLA-DQ Determines the Response to Exogenous Wheat Proteins: A Model of Gluten Sensitivity in Transgenic Knockout Mice. J.I. 169, 5595–5600. doi:10.4049/jimmunol.169.10.5595

Bodd, M., ki, M.R.A., Tollefsen, S., Fallang, L.E., Bergseng, E., Lundin, K.E.A., Sollid, L.M., 2010. HLA-DQ2-restricted gluten-reactive T cells produce IL-21 but not IL-17 or IL-22. Mucosal Immunology 3, 594–601. doi:10.1038/mi.2010.36

Bolger, A.M., Lohse, M., Usadel, B., 2014. Trimmomatic: a flexible trimmer for Illumina sequence data. Bioinformatics 30, 2114–2120. doi:10.1093/bioinformatics/btu170

Bourlière, M., Oulés, V., Perrier, H., Mengotti, C., 2001. Onset of coeliac disease and interferon treatment. The Lancet 357, 803–804. doi:10.1016/S0140-6736(05)71230-7

Boutet, M., Gauthier, L., Leclerc, M., Gros, G., de Montpreville, V., Théret, N., Donnadieu, E., Mami-Chouaib, F., 2016. TGFβ Signaling Intersects with CD103 Integrin Signaling to Promote T-Lymphocyte Accumulation and Antitumor Activity in the Lung Tumor Microenvironment. Cancer Res 76, 1757–1769. doi:10.1158/0008-5472.CAN-15-1545

Bouziat, R., Biering, S.B., Kouame, E., Sangani, K.A., Kang, S., Ernest, J.D., Varma, M., Brown, J.J., Urbanek, K., Dermody, T.S., Ng, A., Hinterleitner, R., Hwang, S., Jabri, B., 2018. Murine Norovirus Infection Induces TH1 Inflammatory Responses to Dietary Antigens. Cell Host and Microbe 24, 677–688.e5. doi:10.1016/j.chom.2018.10.004

Bouziat, R., Hinterleitner, R., Brown, J.J., Stencel-Baerenwald, J.E., Ikizler, M., Mayassi, T., Meisel, M., Kim, S.M., Discepolo, V., Pruijssers, A.J., Ernest, J.D., Iskarpatyoti, J.A., Costes, L.M.M., Lawrence, I., Palanski, B.A., Varma, M., Zurenski, M.A., Khomandiak, S., McAllister, N., Aravamudhan, P., Boehme, K.W., Hu, F., Samsom, J.N., Reinecker, H.-C., Kupfer, S.S., Guandalini, S., Semrad, C.E., Abadie, V., Khosla, C., Barreiro, L.B., Xavier, R.J., Ng, A., Dermody, T.S., Jabri, B., 2017. Reovirus infection triggers inflammatory responses to dietary antigens and development of celiac disease. Science 356, 44–50. doi:10.1126/science.aah5298

Boyd, S.D., Liu, Y., Wang, C., Martin, V., Dunn-Walters, D.K., 2013. ScienceDirect Human lymphocyte repertoires in ageing. Current Opinion in Immunology 25, 511–515. doi:10.1016/j.coi.2013.07.007

Boyman, O., Hefti, H.P., Conrad, C., Nickoloff, B.J., Suter, M., Nestle, F.O., 2004. Spontaneous Development of Psoriasis in a New Animal Model Shows an Essential Role for Resident T Cells and Tumor Necrosis Factor-α. J Exp Med 199, 731–736. doi:10.1084/jem.20031482

Brandes, M., Willimann, K., Moser, B., 2005. Professional Antigen-Presentation Function by Human γδ T Cells. Science 309, 264–268. doi:10.1126/science.1110267

British Society of Gastroenterology, 2005. COVID-19 Specific Interim Guidance on Biopsy in Adult Coeliac Disease. www.bsg.org.uk/covid-19-advice/covid-19-specific-non-biopsy-protocol-guidance-for-those-with-suspected-coeliac-disease/ [accessed September 2020]

Broughton, S.E., Petersen, J., Theodossis, A., Scally, S.W., Loh, K.L., Thompson, A., van Bergen, J., Kooy-Winkelaar, Y., Henderson, K.N., Beddoe, T., Tye-Din, J.A., Mannering, S.I., Purcell, A.W., McCluskey, J., Anderson, R.P., Koning, F., Reid, H.H., Rossjohn, J., 2012. Biased T Cell Receptor Usage Directed against Human Leukocyte Antigen DQ8-Restricted Gliadin Peptides Is Associated with Celiac Disease. Immunity 37, 611–621. doi:10.1016/j.immuni.2012.07.013

Butler, A., Hoffman, P., Smibert, P., Papalexi, E., Satija, R., 2018. Integrating single-cell transcriptomic data across different conditions, technologies, and species. Nat Biotechnol 36, 411–420. doi:10.1038/nbt.4096

Caccamo, N., La Mendola, C., Orlando, V., Meraviglia, S., Todaro, M., Stassi, G., Sireci, G., Fournié, J.-J., Dieli, F., 2011. Differentiation, phenotype, and function of interleukin-17–producing human Vγ9Vδ2 T cells. Blood 118, 129–138. doi:10.1182/blood-2011-01-331298

Caio, G., Ciccocioppo, R., Zoli, G., De Giorgio, R., Volta, U., 2020. Therapeutic options for coeliac disease: What else beyond gluten-free diet? Digestive and Liver Disease 52, 130–137. doi:10.1016/j.dld.2019.11.010

Cairo, C., Longinaker, N., Cappelli, G., Leke, R.G.F., Ondo, M.M., Djokam, R., Fogako, J., Leke, R.J., Sagnia, B., Sosso, S., Colizzi, V., Pauza, C.D., 2013. Cord Blood Vγ2Vδ2 T Cells Provide a Molecular Marker for the Influence of Pregnancy-Associated Malaria on Neonatal Immunity. Journal of Infectious Diseases 209, 1653–1662. doi:10.1093/infdis/jit802

Calleja, S., Vivas, S., Santiuste, M., Arias, L., Hernando, M., Nistal, E., Casqueiro, J., Ruiz de Morales, J.G., 2011. Dynamics of Non-conventional Intraepithelial Lymphocytes—NK, NKT, and γδ T—in Celiac Disease: Relationship with Age, Diet, and Histopathology. Dig Dis Sci 56, 2042–2049. doi:10.1007/s10620-010-1534-5

Camarero, C., Eiras, P., Asensio, A., Leon, F., Olivares, F., Escobar, H., Roy, G., 2000. Intraepithelial lymphocytes and coeliac disease: permanent changes in CD3−/CD7+ and T cell receptor γβ subsets studied by flow cytometry. Acta Paediatrica 89, 1–6. doi:10.1111/j.1651-2227.2000.tb01330.x

Cammarota, G., Cuoco, L., Cianci, R., Pandolfi, F., Gasbarrini, G., 2000. Onset of coeliac disease during treatment with interferon for chronic hepatitis C. The Lancet 356, 1494–1495. doi:10.1016/S0140-6736(00)02880-4

Catalan-Serra, I., Sandvik, A.K., Bruland, T., Andreu-Ballester, J.C., 2017. Gammadelta T Cells in Crohn's Disease: A New Player in the Disease Pathogenesis? J Crohns Colitis 11, 1135–1145. doi:10.1093/ecco-jcc/jjx039

Catassi, C., Kryszak, D., Bhatti, B., Sturgeon, C., Helzlsouer, K., Clipp, S.L., Gelfond, D., Puppa, E., Sferruzza, A., Fasano, A., 2010. Natural history of celiac disease autoimmunity in a USA cohort followed since 1974. Ann Med 42, 530–538. doi:10.3109/07853890.2010.514285

Celli, R., Hui, P., Triscott, H., Bogardus, S., Gibson, J., Hwang, M., Robert, M.E., 2019. Clinical Insignficance of Monoclonal T-Cell Populations and Duodenal Intraepithelial T-Cell Phenotypes in Celiac and Nonceliac Patients. Am J Surg Pathol 43, 151–160. doi:10.1097/PAS.0000000000001172

Cellier, C., Bouma, G., van Gils, T., Khater, S., Malamut, G., Crespo, L., Collin, P., Green, P.H.R., Crowe, S.E., Tsuji, W., Butz, E., Cerf-Bensussan, N., Macintyre, E., Parnes, J.R., Leon, F., Hermine, O., Mulder, C.J., Jabri, B., Murray, J., DiMarino, A., Kelly, C.P., Byrnes, V., Sanders, D., Lundin, K.E., Schumann, M., Bontkes, H., Meresse, B., Roy Ariño, G., Bhagat, G., Viiri, K., Rounioja, S., Bui, J., Perez Maseda, R., García-Hoz, C., Trinquand, A., Vlad, G., Hadjivassiliou, M., Azizi, M., Blanchard, A., Llewellyn, B., Palmer, A., Raymond, R., 2019. Safety and efficacy of AMG 714 in patients with type 2 refractory coeliac disease: a phase 2a, randomised, double-blind, placebo-controlled, parallel-group study. The Lancet Gastroenterology & Hepatology 4, 960–970. doi:10.1016/S2468-1253(19)30265-1

Cellier, C., Patey, N., Mauvieux, L., Jabri, B., Delabesse, E., Cervoni, J.P., Burtin, M.L., Guy-Grand, D., Bouhnik, Y., Modigliani, R., Barbier, J.P., Macintyre, E., Brousse, N., Cerf-Bensussan, N., 1998. Abnormal intestinal intraepithelial lymphocytes in refractory sprue. Gastroenterology 114, 471–481. doi:10.1016/S0016-5085(98)70530-X

Cheminant, M., Bruneau, J., Malamut, G., Sibon, D., Guegan, N., van Gils, T., Cording, S., Trinquand, A., Verkarre, V., Lhermitte, L., Brousse, N., Jannot, A.-S., Khater, S., Frenzel, L., Delarue, R., Suarez, F., Marçais, A., Mulder, C.J., Macintyre, E., Asnafi, V., Pouyet, L., Bonnafous, C., Lhospice, F., Molina, T.J., Meresse, B., Cellier, C., Cerf-Bensussan, N., Hermine, O., 2019. NKp46 is a diagnostic biomarker and may be a therapeutic target in gastrointestinal T-cell lymphoproliferative diseases: a CELAC study. Gut 68, 1396–1405. doi:10.1136/gutjnl-2018-317371

Chen, X., Teichmann, S.A., Meyer, K.B., 2018. From Tissues to Cell Types and Back: Single-Cell Gene Expression Analysis of Tissue Architecture. Annu. Rev. Biomed. Data Sci. 1, 29–51. doi:10.1146/annurev-biodatasci-080917-013452

Cheuk, S., Schlums, H., Sérézal, I.G., Martini, E., Chiang, S.C., Marquardt, N., Gibbs, A., Detlofsson, E., Introini, A., Forkel, M., Höög, C., Tjernlund, A., Michaëlsson, J., Folkersen, L., Mjösberg, J., Blomqvist, L., Ehrström, M., Ståhle, M., Bryceson, Y.T., Eidsmo, L., 2017. CD49a Expression Defines Tissue-Resident CD8+ T Cells Poised for Cytotoxic Function in Human Skin. Immunity 46, 287–300. doi:10.1016/j.immuni.2017.01.009

Cheuk, S., Wikén, M., Blomqvist, L., Nylén, S., Talme, T., Ståhle, M., Eidsmo, L., 2014. Epidermal Th22 and Tc17 Cells Form a Localized Disease Memory in Clinically Healed Psoriasis. J.I. 192, 3111–3120. doi:10.4049/jimmunol.1302313

Chowers, Y., Holtmeier, W., Harwood, J., Morzycka-Wroblewska, E., Kagnoff, M.F., 1994. The V delta 1 T cell receptor repertoire in human small intestine and colon. J Exp Med 180, 183–190. doi:10.1084/jem.180.1.183

Christophersen, A., Lund, E.G., Snir, O., Solà, E., Kanduri, C., Dahal-Koirala, S., Zühlke, S., Molberg, Ø., Utz, P.J., Rohani-Pichavant, M., Simard, J.F., Dekker, C.L., Lundin, K.E.A., Sollid, L.M., Davis, M.M., 2019a. Distinct phenotype of CD4+ T cells driving celiac disease identified in multiple autoimmune conditions. Nature Medicine 1–21. doi:10.1038/s41591-019-0403-9

Christophersen, A., Raki, M., Bergseng, E., Lundin, K.E., Jahnsen, J., Sollid, L.M., Qiao, S.W., 2014. Tetramer-visualized gluten-specific CD4+ T cells in blood as a potential diagnostic marker for coeliac disease without oral gluten challenge. United European Gastroenterology Journal 2, 268–278. doi:10.1177/2050640614540154

Christophersen, A., Risnes, L.F., Bergseng, E., Lundin, K.E.A., Sollid, L.M., Qiao, S.-W., 2016. Healthy HLA-DQ2.5 +Subjects Lack Regulatory and Memory T Cells Specific for Immunodominant Gluten Epitopes of Celiac Disease. J.I. 196, 2819–2826. doi:10.4049/jimmunol.1501152

Christophersen, A., Risnes, L.F., Dahal-Koirala, S., Sollid, L.M., 2019b. Therapeutic and Diagnostic Implications of T Cell Scarring in Celiac Disease and Beyond. Trends in Molecular Medicine 1–17. doi:10.1016/j.molmed.2019.05.009

Colaert, N., Helsens, K., Martens, L., Vandekerckhove, J., Gevaert, K., 2009. Improved visualization of protein consensus sequences by iceLogo. Nat Meth 1–2. doi:10.1038/nmeth1109-786

Constantinides, M.G., Link, V.M., Tamoutounour, S., Wong, A.C., Perez-Chaparro, P.J., Han, S.-J., Chen, Y.E., Li, K., Farhat, S., Weckel, A., Krishnamurthy, S.R., Vujkovic-Cvijin, I., Linehan, J.L., Bouladoux, N., Merrill, E.D., Roy, S., Cua, D.J., Adams, E.J., Bhandoola, A., Scharschmidt, T.C., Aubé, J., Fischbach, M.A., Belkaid, Y., 2019. MAIT cells are imprinted by the microbiota in early life and promote tissue repair. Science 366, eaax6624–15. doi:10.1126/science.aax6624

Conway, J.R., Lex, A., Gehlenborg, N., 2017. UpSetR: an R package for the visualization of intersecting sets and their properties. Bioinformatics 33, 2938–2940. doi:10.1093/bioinformatics/btx364

Corgnac, S., Boutet, M., Kfoury, M., Naltet, C., Mami-Chouaib, F., 2018. The Emerging Role of CD8+ Tissue Resident Memory T (TRM) Cells in Antitumor Immunity: A Unique Functional Contribution of the CD103 Integrin. Front. Immunol. 9, 269–9. doi:10.3389/fimmu.2018.01904

Corridoni, D., Antanaviciute, A., Gupta, T., Fawkner-Corbett, D., Aulicino, A., Jagielowicz, M., Parikh, K., Repapi, E., Taylor, S., Ishikawa, D., Hatano, R., Yamada, T., Xin, W., Slawinski, H., Bowden, R., Napolitani, G., Brain, O., Morimoto, C., Koohy, H., Simmons, A., 2020. Single-cell atlas of colonic CD8+ T cells in ulcerative colitis. Nature Medicine 1–32. doi:10.1038/s41591-020-1003-4

Cosnes, J., Cellier, C., VIOLA, S., COLOMBEL, J., MICHAUD, L., SARLES, J., HUGOT, J., GINIES, J., Dabadie, A., MOUTERDE, O., 2008. Incidence of Autoimmune Diseases in Celiac Disease: Protective Effect of the Gluten-Free Diet. Clinical Gastroenterology and Hepatology 6, 753–758. doi:10.1016/j.cgh.2007.12.022

Costantino, G., Torre, della, A., Presti, Lo, M.A., Caruso, R., Mazzon, E., Fries, W., 2008. Treatment of life-threatening type I refractory coeliac disease with long-term infliximab. Digestive and Liver Disease 40, 74–77. doi:10.1016/j.dld.2006.10.017

Dantzler, K.W., Jagannathan, P., 2018. γδ T Cells in Antimalarial Immunity: New Insights Into Their Diverse Functions in Protection and Tolerance. Front. Immunol. 9, 467–14. doi:10.3389/fimmu.2018.02445

Daveson, A.J.M., Ee, H.C., Andrews, J.M., King, T., Goldstein, K.E., Dzuris, J.L., MacDougall, J.A., Williams, L.J., Treohan, A., Cooreman, M.P., Anderson, R.P., 2017. Epitope-Specific Immunotherapy Targeting CD4-Positive T Cells in Celiac Disease: Safety, Pharmacokinetics, and Effects on Intestinal Histology and Plasma Cytokines with Escalating Dose Regimens of Nexvax2 in a Randomized, Double-Blind, Placebo-Controlled Phase 1 Study. EBIOM 26, 78–90. doi:10.1016/j.ebiom.2017.11.018

Daveson, A.J.M., Popp, A., Taavela, J., Goldstein, K.E., Isola, J., Truitt, K.E., Mäki, M., Anderson, R.P., the RESET CeD Study Group, Adams, A., Andrews, J., Behrend, C., Brown, G., Chen Yi Mei, S., Coates, A., Daveson, A.J., DiMarino, A., Elliott, D., Epstein, R., Feyen, B., Fogel, R., Friedenberg, K., Gearry, R., Gerdis, M., Goldstein, M., Gupta, V., Holmes, R., Holtmann, G., Idarraga, S., James, G., King, T., Klein, T., Kupfer, S., Lebwohl, B., Lowe, J., Murray, J., Newton, E., Quinn, D., Radin, D., Ritter, T., Stacey, H., Strout, C., Stubbs, R., Thackwray, S., Trivedi, V., Tye Din, J., Weber, J., Wilson, S., 2020. Baseline quantitative histology in therapeutics trials reveals villus atrophy in most patients with coeliac disease who appear well controlled on gluten-free diet. GastroHep 2, 22–30. doi:10.1002/ygh2.380

Daveson, A.J.M., Tye-Din, J.A., Goel, G., Goldstein, K.E., Hand, H.L., Neff, K.M., Williams, L.J., Truitt, K.E., Anderson, R.P., the RESET CeD Study Group, 2019. Masked bolus gluten challenge low in FODMAPs implicates nausea and vomiting as key symptoms associated with immune activation in treated coeliac disease. Aliment Pharmacol Ther 51, 244–252. doi:10.1111/apt.15551

Davey, M.S., Willcox, C.R., Baker, A.T., Hunter, S., Willcox, B.E., 2018a. Recasting Human Vδ1 Lymphocytes in an Adaptive Role. Trends in Immunology 1–14. doi:10.1016/j.it.2018.03.003

Davey, M.S., Willcox, C.R., Hunter, S., Kasatskaya, S.A., Remmerswaal, E.B.M., Salim, M., Mohammed, F., Bemelman, F.J., Chudakov, D.M., Oo, Y.H., Willcox, B.E., 2018b. The human Vδ2+ T-cell compartment comprises distinct innate-like Vγ9+ and adaptive Vγ9- subsets. Nature Communications 1–14. doi:10.1038/s41467-018-04076-0

Davey, M.S., Willcox, C.R., Joyce, S.P., Ladell, K., Kasatskaya, S.A., McLaren, J.E., Hunter, S., Salim, M., Mohammed, F., Price, D.A., Chudakov, D.M., Willcox, B.E., 2017. Clonal selection in the human Vδ1 T cell repertoire indicates γδ TCR-dependent adaptive immune surveillance. Nature Communications 8, 1–15. doi:10.1038/ncomms14760

Davey, M.S., Willcox, C.R., Joyce, S.P., Ladell, K., Kasatskaya, S.A., McLaren, J.E., Hunter, S., Salim, M., Mohammed, F., Price, D.A., Chudakov, D.M., Willcox, B.E., 1AD. Clonal selection in the human Vδ1 T cell repertoire indicates γδ TCR-dependent adaptive immune surveillance. Nature Communications 8, 1–15. doi:10.1038/ncomms14760

de Hoog, M.L.A., Vesikari, T., Giaquinto, C., Huppertz, H.-I., Martinon-Torres, F., Bruijning-Verhagen, P., 2018. Report of the 5th European expert meeting on rotavirus vaccination \(EEROVAC\) 1–9. doi:10.1080/21645515.2017.1412019

de Kauwe, A.L., Chen, Z., Anderson, R.P., Keech, C.L., Price, J.D., Wijburg, O., Jackson, D.C., Ladhams, J., Allison, J., McCluskey, J., 2009. Resistance to Celiac Disease in Humanized HLA-DR3-DQ2-Transgenic Mice Expressing Specific Anti-Gliadin CD4 +T Cells. J.I. 182, 7440–7450. doi:10.4049/jimmunol.0900233

de Leur, K., Dieterich, M., Hesselink, D.A., Corneth, O.B.J., Dor, F.J.M.F., de Graav, G.N., Peeters, A.M.A., Mulder, A., Kimenai, H.J.A.N., Claas, F.H.J., Groningen, M.C.C.-V., van der Laan, L.J.W., Hendriks, R.W., Baan, C.C., 2019. Characterization of donor and recipient CD8+ tissue-resident memory T cells in transplant nephrectomies. Sci Rep 9, 1–12. doi:10.1038/s41598-019-42401-9

De Rosa, S.C., Andrus, J.P., Perfetto, S.P., Mantovani, J.J., Herzenberg, L.A., Herzenberg, L.A., Roederer, M., 2004. Ontogeny of T Cells in Humans. J.I. 172, 1637–1645. doi:10.4049/jimmunol.172.3.1637

De Simone, M., Rossetti, G., Pagani, M., 2018. Single Cell T Cell Receptor Sequencing: Techniques and Future Challenges. Front. Immunol. 9, 15–7. doi:10.3389/fimmu.2018.01638

Deroost, K., Langhorne, J., 2018. Gamma/Delta T Cells and Their Role in Protection Against Malaria. Front. Immunol. 9, 1359–9. doi:10.3389/fimmu.2018.02973

Deusch, K., Lüling, F., Reich, K., Classen, M., Wagner, H., Pfeffer, K., 1991. A major fraction of human intraepithelial lymphocytes simultaneously expresses the γ/δ T cell receptor, the CD8 accessory molecule and preferentially uses the Vδ1 gene segment. Eur. J. Immunol. 21, 1053–1059. doi:10.1002/eji.1830210429

Déchanet, J., Merville, P., Lim, A., Retière, C., Pitard, V., Lafarge, X., Michelson, S., Méric, C., Hallet, M.-M., Kourilsky, P., Potaux, L., Bonneville, M., Moreau, J.-F., 1999. Implication of γδ T cells in the human immune response to cytomegalovirus. J. Clin. Invest. 103, 1437–1449. doi:10.1172/JCI5409

Di Marco Barros, R., Roberts, N.A., Dart, R.J., Vantourout, P., Jandke, A., Nussbaumer, O., Deban, L., Cipolat, S., Hart, R., Iannitto, M.L., Laing, A., Spencer-Dene, B., East, P., Gibbons, D., Irving, P.M., Pereira, P., Steinhoff, U., Hayday, A., 2016. Epithelia Use Butyrophilin-like Molecules to Shape Organ-Specific γδ T Cell Compartments. Cell 167, 203–209.e17. doi:10.1016/j.cell.2016.08.030

Di Niro, R., Mesin, L., Zheng, N.-Y., Stamnaes, J., Morrissey, M., Lee, J.-H., Huang, M., Iversen, R., Pr eacute, du, M.F., Qiao, S.-W., Lundin, K.E.A., Wilson, P.C., Sollid, L.M., 2012. High abundance of plasma cells secreting transglutaminase 2–specific IgA autoantibodies with limited somatic hypermutation in celiac disease intestinal lesions. Nature Medicine 18, 441–445. doi:10.1038/nm.2656

Di Sabatino, A., Pickard, K.M., Gordon, J.N., Salvati, V., Mazzarella, G., Beattie, R.M., Vossenkaemper, A., Rovedatti, L., Leakey, N.A.B., Croft, N.M., Troncone, R., Corazza, G.R., Stagg, A.J., Monteleone, G., MacDonald, T.T., 2007. Evidence for the Role of Interferon-alfa Production by Dendritic Cells in the Th1 Response in Celiac Disease. Gastroenterology 133, 1175–1187. doi:10.1053/j.gastro.2007.08.018

Dias, J., Leeansyah, E., Sandberg, J.K., 2017. Multiple layers of heterogeneity and subset diversity in human MAIT cell responses to distinct microorganisms and to innate cytokines. Proc Natl Acad Sci USA 114, E5434–E5443. doi:10.1073/pnas.1705759114

Dieli, F., Poccia, F., Lipp, M., Sireci, G., Caccamo, N., Di Sano, C., Salerno, A., 2003. Differentiation of Effector/Memory Vδ2 T Cells and Migratory Routes in Lymph Nodes or Inflammatory Sites. J Exp Med 198, 391–397. doi:10.1084/jem.20030235

Dimova, T., Brouwer, M., Gosselin, F., Tassignon, J., Leo, O., Donner, C., Marchant, A., Vermijlen, D., 2015. Effector Vγ9Vδ2 T cells dominate the human fetal γδ T-cell repertoire. Proc Natl Acad Sci USA 112, E556–E565. doi:10.1073/pnas.1412058112

Djenidi, F., Adam, J., Goubar, A., Durgeau, A., Meurice, G., de Montpreville, V., Validire, P., Besse, B., Mami-Chouaib, F., 2015. CD8 +CD103 +Tumor–Infiltrating Lymphocytes Are Tumor-Specific Tissue-Resident Memory T Cells and a Prognostic Factor for Survival in Lung Cancer Patients. J.I. 194, 3475–3486. doi:10.4049/jimmunol.1402711

Dobin, A., Davis, C.A., Schlesinger, F., Drenkow, J., Zaleski, C., Jha, S., Batut, P., Chaisson, M., Gingeras, T.R., 2012. STAR: ultrafast universal RNA-seq aligner. Bioinformatics 29, 15–21. doi:10.1093/bioinformatics/bts635

Dominguez, C.X., Amezquita, R.A., Guan, T., Marshall, H.D., Joshi, N.S., Kleinstein, S.H., Kaech, S.M., 2015. The transcription factors ZEB2 and T-bet cooperate to program cytotoxic T cell terminal differentiation in response to LCMV viral infection. J Exp Med 212, 2041–2056. doi:10.1084/jem.20150186

Dubois, P.C.A., Trynka, G., Franke, L., Hunt, K.A., Romanos, J., Curtotti, A., Zhernakova, A., Heap, G.A.R., Ádány, R., Aromaa, A., Bardella, M.T., van den Berg, L.H., Bockett, N.A., la Concha, de, E.G., Dema, B., Fehrmann, R.S.N., Fernández-Arquero, M., Fiatal, S., Grandone, E., Green, P.M., Groen, H.J.M., Gwilliam, R., Houwen,

R.H.J., Hunt, S.E., Kaukinen, K., Kelleher, D., Korponay-Szabo, I., Kurppa, K., MacMathuna, P., Mäki, M., Mazzilli, M.C., McCann, O.T., Mearin, M.L., Mein, C.A., Mirza, M.M., Mistry, V., Mora, B., Morley, K.I., Mulder, C.J., Murray, J.A., Núñez, C., Oosterom, E., Ophoff, R.A., Polanco, I., Peltonen, L., Platteel, M., Rybak, A., Salomaa, V., Schweizer, J.J., Sperandeo, M.P., Tack, G.J., Turner, G., Veldink, J.H., Verbeek, W.H.M., Weersma, R.K., Wolters, V.M., Urcelay, E., Cukrowska, B., Greco, L., Neuhausen, S.L., McManus, R., Barisani, D., Deloukas, P., Barrett, J.C., Saavalainen, P., Wijmenga, C., van Heel, D.A., 2010. Multiple common variants for celiac disease influencing immune gene expression. Nature Publishing Group 42, 295–302. doi:10.1038/ng.543

Dunne, M.R., Elliott, L., Hussey, S., Mahmud, N., Kelly, J., Doherty, D.G., Feighery, C.F., 2013. Persistent Changes in Circulating and Intestinal γδ T Cell Subsets, Invariant Natural Killer T Cells and Mucosal-Associated Invariant T Cells in Children and Adults with Coeliac Disease. PLoS ONE 8, e76008–10. doi:10.1371/journal.pone.0076008

Dusseaux, M., Martin, E., Serriari, N., Péguillet, I., Premel, V., Louis, D., Milder, M., Le Bourhis, L., Soudais, C., Treiner, E., Lantz, O., 2011. Human MAIT cells are xenobiotic-resistant, tissue-targeted, CD161hi IL-17–secreting T cells. Blood 117, 1250–1259. doi:10.1182/blood-2010-08-303339

Dydensborg, S., Toftedal, P., Biaggi, M., Lillevang, S.T., Hansen, D.G., Husby, S., 2011. Increasing prevalence of coeliac disease in Denmark: a linkage study combining national registries. Acta Paediatrica 101, 179–184. doi:10.1111/j.1651-2227.2011.02392.x

Edwards, J., Wilmitt, j.s., Madore J., Gide T.N., Quek C., Tasker A., Ferguson A., Chen J., Hewavisenti R., Hersey P., Gebhardt T., Weninger W., Britton W.J., Saw R.P.M., RThompson J.F., Menzies A.M., Long G.V., Scolyer R.A., Palendira U., 2018. CD103+ Tumor-Resident CD8+ T Cells Are Associated with Improved Survival in Immunotherapy-Naïve Melanoma Patients and Expand Significantly During Anti–PD-1 Treatment. Clinical Cancer Research 24(13). doi: 10.1158/1078-0432.CCR-17-2257

Eggesbø, L.M., Risnes, L.F., Neumann, R.S., Lundin, K.E.A., Christophersen, A., Sollid, L.M., 2019. Single-cell TCR sequencing of gut intraepithelial γδ T cells reveals a vast and diverse repertoire in celiac disease. Mucosal Immunology 1–9. doi:10.1038/s41385-019-0222-9

Egner, W., Shrimpton, A., Sargur, R., Patel, D., Swallow, K., 2012. ESPGHAN Guidance on Coeliac Disease 2012. Journal of Pediatric Gastroenterology and Nutrition 55, 733–735. doi:10.1097/MPG.0b013e31826531f6

Eigner, W., Bashir, K., Primas, C., Kazemi-Shirazi, L., Wrba, F., Trauner, M., Vogelsang, H., 2016. Dynamics of occurrence of refractory coeliac disease and associated complications over 25 years. Aliment Pharmacol Ther 45, 364–372. doi:10.1111/apt.13867

Ewels, P., Magnusson, M., Lundin, S., Käller, M., 2016. MultiQC: summarize analysis results for multiple tools and samples in a single report. Bioinformatics 32, 3047–3048. doi:10.1093/bioinformatics/btw354

Fagerholm, S.C., Guenther, C., Llort Asens, M., Savinko, T., Uotila, L.M., 2019. Beta2-Integrins and Interacting Proteins in Leukocyte Trafficking, Immune Suppression, and Immunodeficiency Disease. Front. Immunol. 10, 549–10. doi:10.3389/fimmu.2019.00254

FALK, M.C., NG, G., ZHANG, G.Y., FANNING, G.C., KAMATH, K.R., KNIGHT, J.F., 2008. Predominance of T cell receptor Vδ3 in small bowel biopsies from celiac disease patients. Clinical & Experimental Immunology 98, 78–82. doi:10.1111/j.1365-2249.1994.tb06610.x

Farh, K.K.-H., Marson, A., Zhu, J., Kleinewietfeld, M., Housley, W.J., Beik, S., Shoresh, N., Whitton, H., Ryan, R.J.H., Shishkin, A.A., Hatan, M., Carrasco-Alfonso, M.J., Mayer, D., Luckey, C.J., Patsopoulos, N.A., De Jager, P.L., Kuchroo, V.K., Epstein, C.B., Daly, M.J., Hafler, D.A., Bernstein, B.E., 2015. Genetic and epigenetic fine mapping of causal autoimmune disease variants. Nature 518, 337–343. doi:10.1038/nature13835

Feau, S., Arens, R., Togher, S., Schoenberger, S.P., 2011. Autocrine IL-2 is required for secondary population expansion of CD8+ memory T cells. Nat Immunol 12, 908–913. doi:10.1038/ni.2079

Fenoglio, D., Poggi, A., Catellani, S., Battaglia, F., Ferrera, A., Setti, M., Murdaca, G., Zocchi, M.R., 2009. V 1 T lymphocytes producing IFN- and IL-17 are expanded in HIV-1-infected patients and respond to Candida albicans. Blood 113, 6611–6618. doi:10.1182/blood-2009-01-198028

Fergusson, J.R., hn, M.H.H.U., Swadling, L., Walker, L.J., Kurioka, A., Llibre, A., Bertoletti, A., nder, G.H.A., Newell, E.W., Davis, M.M., m, E.S.-E.O., Powrie, F., Capone, S., Folgori, A., Barnes, E., Willberg, C.B., Ussher, J.E., Klenerman, P., 2015. CD161intCD8+ T cells: a novel population of highly functional, memory CD8+ T cells enriched within the gut 1–13. doi:10.1038/mi.2015.69

Fergusson, J.R., Smith, K.E., Fleming, V.M., Rajoriya, N., Newell, E.W., Simmons, R., Marchi, E., Björkander, S., Kang, Y.-H., Swadling, L., Kurioka, A., Sahgal, N., Lockstone, H., Baban, D., Freeman, G.J., Sverremark-Ekström, E., Davis, M.M., Davenport, M.P., Venturi, V., Ussher, J.E., Willberg, C.B., Klenerman, P., 2014.

CD161 Defines a Transcriptional and Functional Phenotype across Distinct Human T Cell Lineages. CellReports 9, 1075–1088. doi:10.1016/j.celrep.2014.09.045
Fernández-Bañares, F., Carrasco, A., García-Puig, R., Rosinach, M., González, C., Alsina, M., Loras, C., Salas, A., Viver, J.M., Esteve, M., 2014. Intestinal Intraepithelial Lymphocyte Cytometric Pattern Is More Accurate than Subepithelial Deposits of Anti-Tissue Transglutaminase IgA for the Diagnosis of Celiac Disease in Lymphocytic Enteritis. PLoS ONE 9, e101249–11. doi:10.1371/journal.pone.0101249
Fichtner, A.S., Bubke, A., Rampoldi, F., Wilharm, A., Tan, L., Steinbrück, L., Schultze-Florey, C., Kaisenberg, C., Prinz, I., Herrmann, T., Ravens, S., 2020a. TCR repertoire analysis reveals phosphoantigen-induced polyclonal proliferation of Vγ9Vδ2 T cells in neonates and adults. J Leukoc Biol 107, 1023–1032. doi:10.1002/JLB.1MA0120-427RR
Fichtner, A.S., Karunakaran, M.M., Gu, S., Boughter, C.T., Borowska, M.T., Starick, L., Nöhren, A., Göbel, T.W., Adams, E.J., Herrmann, T., 2020b. Alpaca (Vicugna pacos), the first nonprimate species with a phosphoantigen-reactive Vγ9Vδ2 T cell subset. Proc Natl Acad Sci USA 117, 6697–6707. doi:10.1073/pnas.1909474117
Fichtner, A.S., Karunakaran, M.M., Starick, L., Truman, R.W., Herrmann, T., 2018. The Armadillo (Dasypus novemcinctus): A Witness but Not a Functional Example for the Emergence of the Butyrophilin 3/Vγ9Vδ2 System in Placental Mammals. Front. Immunol. 9, 59–12. doi:10.3389/fimmu.2018.00265
Fichtner, A.S., Ravens, S., Prinz, I., 2020c. Human γδ TCR Repertoires in Health and Disease. Cells 9, 800–14. doi:10.3390/cells9040800
Finak, G., McDavid, A., Yajima, M., Deng, J., Gersuk, V., Shalek, A.K., Slichter, C.K., Miller, H.W., McElrath, M.J., Prlic, M., Linsley, P.S., Gottardo, R., 2015. MAST: a flexible statistical framework for assessing transcriptional changes and characterizing heterogeneity in single-cell RNA sequencing data. Genome Biol. 1–13. doi:10.1186/s13059-015-0844-5
Fisher, J., Anderson, J., 2018. Engineering Approaches in Human Gamma Delta T Cells for Cancer Immunotherapy. Front. Immunol. 9, 4099–10. doi:10.3389/fimmu.2018.01409
FitzPatrick, M.E.B., Provine, N.M., Garner, L.C., Powell, K., Amini, A., Irwin, S., Ferry, H., Ambrose, T., Friend, P., Vrakas, G., Reddy, S., Soilleux, E., Klenerman, P., Allan, P.J., 2019. Human intestinal tissue-resident memory CD8+ T cells comprise transcriptionally and functionally distinct subsets. bioRxiv 869917.
Flajnik, M.F., Kasahara, M., 2009. Origin and evolution of the adaptive immune system: genetic events and selective pressures. Nature Reviews Genetics 1–13. doi:10.1038/nrg2703
Fonseca, R., Beura, L.K., Quarnstrom, C.F., Ghoneim, H.E., Fan, Y., Zebley, C.C., Scott, M.C., Fares-Frederickson, N.J., Wijeyesinghe, S., Thompson, E.A., da Silva, H.B., Vezys, V., Youngblood, B., Masopust, D., 2020. Developmental plasticity allows outside-in immune responses by resident memory T cells. Nat Immunol 1–12. doi:10.1038/s41590-020-0607-7
Ford, A.L., Foulcher, E., Goodsall, A.L., Sedgwick, J.D., 1996. Tissue digestion with dispase substantially reduces lymphocyte and macrophage cell-surface antigen expression. Journal of Immunological Methods 1, 71–75.
Fox, E.J., Reid-Bayliss, K.S., Emond, M.J., Loeb, L.A., 2014. Accuracy of Next Generation Sequencing Platforms. Next Gener Seq Appl 1, 1–5. doi:10.4172/jngsa.1000106
Freeman, B.E., Hammarlund, E., Raue, H.P., Slifka, M.K., 2012. Regulation of innate CD8+ T-cell activation mediated by cytokines. Proc Natl Acad Sci USA 109, 9971–9976. doi:10.1073/pnas.1203543109
Fu, J., Zuber, J., Martinez, M., Shonts, B., Obradovic, A., Wang, H., Lau, S.-P., Xia, A., Waffarn, E.E., Frangaj, K., Savage, T.M., Simpson, M.T., Yang, S., Guo, X.V., Miron, M., Senda, T., Rogers, K., Rahman, A., Ho, S.-H., Shen, Y., Griesemer, A., Farber, D.L., Kato, T., Sykes, M., 2019. Human Intestinal Allografts Contain Functional Hematopoietic Stem and Progenitor Cells that Are Maintained by a Circulating Pool. Stem Cell 24, 227–239.e8. doi:10.1016/j.stem.2018.11.007
Gale, J., Simmonds, P.D., Mead, G.M., Sweetenham, J.W., Wright, D.H., 2000. Enteropathy-Type Intestinal T-Cell Lymphoma: Clinical Features and Treatment of 31 Patients in a Single Center. J Clin Oncol 18, 795–795. doi:10.1200/JCO.2000.18.4.795
Garner, L.C., Klenerman, P., Provine, N.M., 2018. Insights Into Mucosal-Associated Invariant T Cell Biology From Studies of Invariant Natural Killer T Cells. Front. Immunol. 9, 911–25. doi:10.3389/fimmu.2018.01478
Gaud, G., Lesourne, R., Love, P.E., 2018. Regulatory mechanisms in T cell receptor signalling. Nat Rev Immunol 1–13. doi:10.1038/s41577-018-0020-8
Gebhardt, T., Wakim, L.M., Eidsmo, L., Reading, P.C., Heath, W.R., Carbone, F.R., 2009. Memory T cells in nonlymphoid tissue that provide enhanced local immunity during infection with herpes simplex virus. Nat Immunol 10, 524–530. doi:10.1038/ni.1718

Gebhardt, T., Whitney, P.G., Zaid, A., Mackay, L.K., Brooks, A.G., Heath, W.R., Carbone, F.R., Mueller, S.N., 2011. Different patterns of peripheral migration by memory CD4+ and CD8+ T cells. Nature 477, 216–219. doi:10.1038/nature10339

Gentles, A.J., Newman, A.M., Liu, C.L., Bratman, S.V., Feng, W., Kim, D., Nair, V.S., Xu, Y., Khuong, A., Hoang, C.D., Diehn, M., West, R.B., Plevritis, S.K., Alizadeh, A.A., 2015. The prognostic landscape of genes and infiltrating immune cells across human cancers. Nature Medicine 1–12. doi:10.1038/nm.3909

Gherardin, N.A., Keller, A.N., Woolley, R.E., Le Nours, J., Ritchie, D.S., Neeson, P.J., Birkinshaw, R.W., Eckle, S.B.G., Waddington, J.N., Liu, L., Fairlie, D.P., Uldrich, A.P., Pellicci, D.G., McCluskey, J., Godfrey, D.I., Rossjohn, J., 2016. Diversity of T Cells Restricted by the MHC Class I- Related Molecule MR1 Facilitates Differential Antigen Recognition. Immunity 44, 32–45. doi:10.1016/j.immuni.2015.12.005

Gianfrani, C., Troncone, R., Mugione, P., Cosentini, E., De Pascale, M., Faruolo, C., Senger, S., Terrazzano, G., Southwood, S., Auricchio, S., Sette, A., 2003. Celiac Disease Association with CD8+ T Cell Responses: Identification of a Novel Gliadin-Derived HLA-A2-Restricted Epitope. J.I. 170, 2719–2726. doi:10.4049/jimmunol.170.5.2719

Gober, H.-J., Kistowska, M., Angman, L., Jenö, P., Mori, L., De Libero, G., 2003. Human T Cell Receptor γδ Cells Recognize Endogenous Mevalonate Metabolites in Tumor Cells. J Exp Med 197, 163–168. doi:10.1084/jem.20021500

Godfrey, D.I., Uldrich, A.P., McCluskey, J., Rossjohn, J., Moody, D.B., 2015. The burgeoning family of unconventional T cells. Nat Immunol 16, 1114–1123. doi:10.1038/ni.3298

Goel, G., Tye-Din, J.A., Qiao, S.-W., Russell, A.K., Mayassi, T., Ciszewski, C., Sarna, V.K., Wang, S., Goldstein, K.E., Dzuris, J.L., Williams, L.J., Xavier, R.J., Lundin, K.E.A., Jabri, B., Sollid, L.M., Anderson, R.P., 2019. Cytokine release and gastrointestinal symptoms after gluten challenge in celiac disease. Sci. Adv. 5, eaaw7756–15. doi:10.1126/sciadv.aaw7756

Goerres, M.S., Meijer, J.W.R., Wahab, P.J., Kerckhaert, J.A.M., Groenen, P.J.T.A., Van Krieken, J.H.J.M., Mulder, C.J.J., 2003. Azathioprine and prednisone combination therapy in refractory coeliac disease. Aliment Pharmacol Ther 18, 487–494. doi:10.1046/j.1365-2036.2003.01687.x

Gordon, C.L., Miron, M., Thome, J.J.C., Matsuoka, N., Weiner, J., Rak, M.A., Igarashi, S., Granot, T., Lerner, H., Goodrum, F., Farber, D.L., 2017. Tissue reservoirs of antiviral T cell immunity in persistent human CMV infection. J Exp Med 214, 651–667. doi:10.1084/jem.20160758

Grange, C., Létourneau, J., Forget, M.-A., Godin-Ethier, J., Martin, J., Liberman, M., Latour, M., Widmer, H., Lattouf, J.-B., Piccirillo, C.A., Cailhier, J.-F., Lapointe, R., 2011. Phenotypic characterization and functional analysis of human tumor immune infiltration after mechanical and enzymatic disaggregation. Journal of Immunological Methods 372, 119–126. doi:10.1016/j.jim.2011.07.002

Grant, D., Abu-Elmagd, K., Mazariegos, G., Vianna, R., Langnas, A., Mangus, R., Farmer, D.G., Lacaille, F., Iyer, K., Fishbein, T., 2014. Intestinal Transplant Registry Report: Global Activity and Trends. American Journal of Transplantation 15, 210–219. doi:10.1111/ajt.12979

Gratz, I.K., Campbell, D.J., 2020. Resident memory T cells show that it is never too late to change your ways. Nat Immunol 1–2. doi:10.1038/s41590-020-0637-1

Gu, S., Sachleben, J.R., Boughter, C.T., Nawrocka, W.I., Borowska, M.T., Tarrasch, J.T., Skiniotis, G., Roux, B., Adams, E.J., 2017. Phosphoantigen-induced conformational change of butyrophilin 3A1 (BTN3A1) and its implication on Vγ9Vδ2 T cell activation. Proc Natl Acad Sci USA 114, E7311–E7320. doi:10.1073/pnas.1707547114

Guan, T., Dominguez, C.X., Amezquita, R.A., Laidlaw, B.J., Cheng, J., Henao-Mejia, J., Williams, A., Flavell, R.A., LU, J., Kaech, S.M., 2018. ZEB1, ZEB2, and the miR-200 family form a counterregulatory network to regulate CD8+ T cell fates. J Exp Med 215, 1153–1168. doi:10.1084/jem.20171352

Gutierrez-Achury, J., Zhernakova, A., Pulit, S.L., Trynka, G., Hunt, K.A., Romanos, J., Raychaudhuri, S., van Heel, D.A., Wijmenga, C., de Bakker, P.I.W., 2015. Fine mapping in the MHC region accounts for 18% additional genetic risk for celiac disease. Nature Publishing Group 47, 577–578. doi:10.1038/ng.3268

Gutierrez-Arcelus, M., Teslovich, N., Mola, A.R., Polidoro, R.B., Nathan, A., Kim, H., Hannes, S., Slowikowski, K., Watts, G.F.M., Korsunsky, I., Brenner, M.B., Raychaudhuri, S., Brennan, P.J., 2019. Lymphocyte innateness defined by transcriptional states reflects a balance between proliferation and effector functions. Nature Communications 1–15. doi:10.1038/s41467-019-08604-4

HAAS, S.V., 1924. THE VALUE OF THE BANANA IN THE TREATMENT OF CELIAC DISEASE. Am J Dis Child 28, 421–437.

Habtezion, A., Nguyen, L.P., Hadeiba, H., Butcher, E.C., 2019. Leukocyte Trafficking to the Small Intestine and Colon 1–15. doi:10.1053/j.gastro.2015.10.046

Hadjivassiliou, M., Sanders, D.D., Aeschlimann, D.P., 2015. Gluten-related disorders: gluten ataxia. Dig Dis 33, 264–268. doi:10.1159/000369509
Halstensen, T.S., Scott, H., Brandtzaeg, P., 1989. Intraepithelial T Cells of the TcRγ/δ+CD8− and Vδ1/Jδ1+ Phenotypes are Increased in Coeliac Disease. Scand J Immunol 30, 665–672. doi:10.1111/j.1365-3083.1989.tb02474.x
Han, A., Newell, E.W., Glanville, J., Fernandez-Becker, N., Khosla, C., Chien, Y.-H., Davis, M.M., 2013. Dietary gluten triggers concomitant activation of CD4+ and CD8+ αβ T cells and γδ T cells in celiac disease. Proc. Natl. Acad. Sci. U.S.A. 110, 13073–13078. doi:10.1073/pnas.1311861110
Hansen, S.G., Sacha, J.B., Hughes, C.M., Ford, J.C., Burwitz, B.J., Scholz, I., Gilbride, R.M., Lewis, M.S., Gilliam, A.N., Ventura, A.B., Malouli, D., Xu, G., Richards, R., Whizin, N., Reed, J.S., Hammond, K.B., Fischer, M., Turner, J.M., Legasse, A.W., Axthelm, M.K., Edlefsen, P.T., Nelson, J.A., Lifson, J.D., Fruh, K., Picker, L.J., 2013. Cytomegalovirus Vectors Violate CD8+ T Cell Epitope Recognition Paradigms. Science 340, 1237874–1237874. doi:10.1126/science.1237874
Hansen, S.G., Zak, D.E., Xu, G., Ford, J.C., Marshall, E.E., Malouli, D., Gilbride, R.M., Hughes, C.M., Ventura, A.B., Ainslie, E., Randall, K.T., Selseth, A.N., Rundstrom, P., Herlache, L., Lewis, M.S., Park, H., Planer, S.L., Turner, J.M., Fischer, M., Armstrong, C., Zweig, R.C., Valvo, J., Braun, J.M., Shankar, S., Lu, L., Sylwester, A.W., Legasse, A.W., Messerle, M., Jarvis, M.A., Amon, L.M., Aderem, A., Alter, G., Laddy, D.J., Stone, M., Bonavia, A., Evans, T.G., Axthelm, M.K., Früh, K., Edlefsen, P.T., Picker, L.J., 2018. Prevention of tuberculosis in rhesus macaques by a cytomegalovirus-based vaccine. Nature Medicine 24, 130–143. doi:10.1038/nm.4473
Harly, C., Guillaume, Y., Nedellec, S., Peigné, C.-M., Mönkkönen, H., Mönkkönen, J., Li, J., Kuball, J., Adams, E.J., Netzer, S., Déchanet-Merville, J., Léger, A., Herrmann, T., Breathnach, R., Olive, D., Bonneville, M., Scotet, E., 2012. Key implication of CD277/butyrophilin-3 (BTN3A) in cellular stress sensing by a major human γδ T-cell subset. Blood 120, 2269–2279. doi:10.1182/blood-2012-05-430470
Harris, R.A., Nagy-Szakal, D., Mir, S.A., Frank, E., Szigeti, R., Kaplan, J.L., Bronsky, J., Opekun, A., Ferry, G.D., Winter, H., Kellermayer, R., 2014. DNA methylation-associated colonic mucosal immune and defense responses in treatment-naïve pediatric ulcerative colitis. Epigenetics 9, 1131–1137. doi:10.4161/epi.29446
Hartwig, T., Pantelyushin, S., Croxford, A.L., Kulig, P., Becher, B., 2015. Dermal IL-17-producing γδ T cells establish long-lived memory in the skin. Eur. J. Immunol. 45, 3022–3033. doi:10.1002/eji.201545883
Heikkilä, K., Pearce, J., Mäki, M., Kaukinen, K., 2015. Celiac Disease and Bone Fractures: A Systematic Review and Meta-Analysis. J Clin Endocrinol Metab 100, 25–34. doi:10.1210/jc.2014-1858
Hennig, C., Adams, N., Hansen, G., 2009. A versatile platform for comprehensive chip-based explorative cytometry. Cytometry 75A, 362–370. doi:10.1002/cyto.a.20668
Himoudi, N., Morgenstern, D.A., Yan, M., Vernay, B., Saraiva, L., Wu, Y., Cohen, C.J., Gustafsson, K., Anderson, J., 2012. Human T Lymphocytes Are Licensed for Professional Antigen Presentation by Interaction with Opsonized Target Cells. J.I. 188, 1708–1716. doi:10.4049/jimmunol.1102654
Hirano, M., Guo, P., McCurley, N., Schorpp, M., Das, S., Boehm, T., Cooper, M.D., 2013. Evolutionary implications of a third lymphocyte lineage in lampreys. Nature 501, 435–438. doi:10.1038/nature12467
Hirokawa, M., Horiuchi, T., Kawabata, Y., Kitabayashi, A., Miura, A.B., 2000. Reconstitution of γδ T cell repertoire diversity after human allogeneic hematopoietic cell transplantation and the role of peripheral expansion of mature T cell population in the graft. Bone Marrow Transplantation 26, 177–185. doi:10.1038/sj.bmt.1702478
Ho, A.W., Kupper, T.S., 2019. T cells and the skin: from protective immunity to inflammatory skin disorders. Nat Rev Immunol 1–13. doi:10.1038/s41577-019-0162-3
Hoeres, T., Smetak, M., Pretscher, D., Wilhelm, M., 2018. Improving the Efficiency of Vγ9Vδ2 T-Cell Immunotherapy in Cancer. Front. Immunol. 9, 605–18. doi:10.3389/fimmu.2018.00800
Holtmeier, W., Chowers, Y., Lumeng, A., Morzycka-Wroblewska, E., Kagnoff, M.F., 1995. The delta T cell receptor repertoire in human colon and peripheral blood is oligoclonal irrespective of V region usage. J. Clin. Invest. 96, 1108–1117. doi:10.1172/JCI118097
Hombrink, P., Helbig, C., Backer, R.A., Piet, B., Oja, A.E., Stark, R., Brasser, G., Jongejan, A., Jonkers, R.E., Nota, B., Basak, O., Clevers, H.C., Moerland, P.D., Amsen, D., van Lier, R.A.W., 2016. Programs for the persistence, vigilance and control of human CD8+ lung-resident memory T cells. Nat Immunol 17, 1467–1478. doi:10.1038/ni.3589
Howard, J., Zaidi, I., Loizon, S., Mercereau-Puijalon, O., Déchanet-Merville, J., Mamani-Matsuda, M., 2018. Human Vγ9Vδ2 T Lymphocytes in the Immune Response to P. falciparum Infection. Front. Immunol. 9, 59–7. doi:10.3389/fimmu.2018.02760

Howie, B., Sherwood, A.M., Berkebile, A.D., Berka, J., Emerson, R.O., Williamson, D.W., Kirsch, I., Vignali, M., Rieder, M.J., Carlson, C.S., Robins, H.S., 2015. High-throughput pairing of T cell receptor α and β sequences. Science Translational Medicine 7, 301ra131–301ra131. doi:10.1126/scitranslmed.aac5624

Howson, L.J., Awad, W., Borstel, von, A., Lim, H.J., McWilliam, H.E.G., Sandoval-Romero, M.L., Majumdar, S., Hamzeh, A.R., Andrews, T.D., McDermott, D.H., Murphy, P.M., Le Nours, J., Mak, J.Y.W., Liu, L., Fairlie, D.P., McCluskey, J., Villadangos, J.A., Cook, M.C., Turner, S.J., Davey, M.S., Ojaimi, S., Rossjohn, J., 2020. Absence of mucosal-associated invariant T cells in a person with a homozygous point mutation in MR1. Science Immunology 5, eabc9492–14. doi:10.1126/sciimmunol.abc9492

Huang, D.W., Sherman, B.T., Lempicki, R.A., 2008. Systematic and integrative analysis of large gene lists using DAVID bioinformatics resources. Nat Protoc 4, 44–57. doi:10.1038/nprot.2008.211

Huang, H., Sikora, M.J., Islam, S., Chowdhury, R.R., Chien, Y.-H., Scriba, T.J., Davis, M.M., Steinmetz, L.M., 2019. Select sequencing of clonally expanded CD8+T cells reveals limits to clonal expansion. Proc. Natl. Acad. Sci. U.S.A. 116, 8995–9001. doi:10.1073/pnas.1902649116

Hughes, S.M., Shu, Z., Levy, C.N., Ferre, A.L., Hartig, H., Fang, C., Lentz, G., Fialkow, M., Kirby, A.C., Adams Waldorf, K.M., Veazey, R.S., Germann, A., Briesen, von, H., McElrath, M.J., Dezzutti, C.S., Sinclair, E., Baker, C.A.R., Shacklett, B.L., Gao, D., Hladik, F., 2016. Cryopreservation of Human Mucosal Leukocytes. PLoS ONE 11, e0156293–17. doi:10.1371/journal.pone.0156293

Huleatt, J.W., Lefrançois, L., 1996. β2 Integrins and ICAM-1 Are Involved in Establishment of the Intestinal Mucosal T Cell Compartment. Immunity 5, 263–273. doi:10.1016/S1074-7613(00)80321-0

Hunter, S., Willcox, C.R., Davey, M.S., Kasatskaya, S.A., Jeffery, H.C., Chudakov, D.M., Oo, Y.H., Willcox, B.E., 2018. Human liver infiltrating Î³Î´ T cells are composed of clonally expanded circulating and tissue-resident populations. Journal of Hepatology 1–13. doi:10.1016/j.jhep.2018.05.007

Husby, S., Koletzko, S., Korponay-Szabo, I.R., Mearin, M.L., Phillips, A., Shamir, R., Troncone, R., Giersiepen, K., Branski, D., Catassi, C., Lelgeman, M., Mäki, M., Ribes-Koninckx, C., Ventura, A., Zimmer, K.P., 2012. European Society for Pediatric Gastroenterology, Hepatology, and Nutrition Guidelines for the Diagnosis of Coeliac Disease. Journal of Pediatric Gastroenterology and Nutrition 54, 136–160. doi:10.1097/MPG.0b013e31821a23d0

Huynh-Thu, V.A., Irrthum, A., Wehenkel, L., Geurts, P., 2010. Inferring Regulatory Networks from Expression Data Using Tree-Based Methods. PLoS ONE 5, e12776–10. doi:10.1371/journal.pone.0012776

Hüe, S., Mention, J.-J., Monteiro, R.C., Zhang, S., Cellier, C., Schmitz, J., Verkarre, V., Fodil, N., Bahram, S., Cerf-Bensussan, N., Caillat-Zucman, S., 2004. A Direct Role for NKG2D/MICA Interaction in Villous Atrophy during Celiac Disease. Immunity 21, 367–377. doi:10.1016/j.immuni.2004.06.018

Hviid, L., Smith-Togobo, C., Willcox, B.E., 2019. Human Vδ1+ T Cells in the Immune Response to Plasmodium falciparum Infection. Front. Immunol. 10, 17050–5. doi:10.3389/fimmu.2019.00259

Høydahl, L.S., Richter, L., Frick, R., Snir, O., Gunnarsen, K.S., Landsverk, O.J.B., Iversen, R., Jeliazkov, J.R., Gray, J.J., Bergseng, E., Foss, S., Qiao, S.-W., Lundin, K.E.A., Jahnsen, J., Jahnsen, F.L., Sandlie, I., Sollid, L.M., Løset, G.-Å., 2019. Plasma Cells Are the Most Abundant Gluten Peptide MHC-expressing Cells in Inflamed Intestinal Tissues From Patients With Celiac Disease. Gastroenterology 156, 1428–1439.e10. doi:10.1053/j.gastro.2018.12.013

Ivanov, I.I., McKenzie, B.S., Zhou, L., Tadokoro, C.E., Lepelley, A., Lafaille, J.J., Cua, D.J., Littman, D.R., 2006. The Orphan Nuclear Receptor RORγt Directs the Differentiation Program of Proinflammatory IL-17+ T Helper Cells. Cell 126, 1121–1133. doi:10.1016/j.cell.2006.07.035

Iversen, R., Amundsen, S.F., Kleppa, L., Fleur du Pré, M., Stamnaes, J., Sollid, L.M., 2020. Evidence that pathogenic transglutaminase 2 in celiac disease derives from enterocytes. Gastroenterology 1–6. doi:10.1053/j.gastro.2020.04.018

Iwata, M., Hirakiyama, A., Eshima, Y., Kagechika, H., Kato, C., Song, S.-Y., 2004. Retinoic Acid Imprints Gut-Homing Specificity on T Cells. Immunity 21, 527–538. doi:10.1016/j.immuni.2004.08.011

Jabri, B., Abadie, V., 2015. IL-15 functions as a danger signal to regulate tissue-resident T cells and tissue destruction. Nature Publishing Group 15, 771–783. doi:10.1038/nri3919

Jabri, B., Selby, J.M., Negulescu, H., Lee, L., Roberts, A.I., Beavis, A., Lopez-Botet, M., Ebert, E.C., Winchester, R.J., 2002. TCR Specificity Dictates CD94/NKG2A Expression by Human CTL. Immunity 17, 487–499. doi:10.1016/S1074-7613(02)00427-2

Jabri, B., Sollid, L.M., 2017. T Cells in Celiac Disease. J.I. 198, 3005–3014. doi:10.4049/jimmunol.1601693

Jagannathan, P., Kim, C.C., Greenhouse, B., Nankya, F., Bowen, K., Eccles-James, I., Muhindo, M.K., Arinaitwe, E., Tappero, J.W., Kamya, M.R., Dorsey, G., Feeney, M.E., 2014. Loss and dysfunction of Vδ2+ γδ T cells are associated with clinical tolerance to malaria. Science Translational Medicine 6, 251ra117–251ra117. doi:10.1126/scitranslmed.3009793

Jameson, J.M., Cruz, J., Costanzo, A., Terajima, M., Ennis, F.A., 2010. A role for the mevalonate pathway in the induction of subtype cross-reactive immunity to influenza A virus by human γδ T lymphocytes. Cellular Immunology 264, 71–77. doi:10.1016/j.cellimm.2010.04.013

Janatuinen, E.K., Kemppainen, T.A., Pikkarainen, P.H., Holm, K.H., Kosma, V.M., Uusitupa, M.I., Mäki, M., Julkunen, R.J., 2000. Lack of cellular and humoral immunological responses to oats in adults with coeliac disease. Gut 46, 327–331. doi:10.1136/gut.46.3.327

Jeyanathan, M., Afkhami, S., Smaill, F., Miller, M.S., Lichty, B.D., Xing, Z., 2020. Immunological considerations for COVID-19 vaccine strategies. Nat Rev Immunol 1–18. doi:10.1038/s41577-020-00434-6

Jiang, X., Clark, R.A., Liu, L., Wagers, A.J., Fuhlbrigge, R.C., Kupper, T.S., 2012. Skin infection generates non-migratory memory CD8+ TRM cells providing global skin immunity. Nature 1–6. doi:10.1038/nature10851

Jin, Y., Xia, M., Saylor, C.M., Narayan, K., Kang, J., Wiest, D.L., Wang, Y., Xiong, N., 2010. Cutting Edge: Intrinsic Programming of Thymic γδT Cells for Specific Peripheral Tissue Localization. J.I. 185, 7156–7160. doi:10.4049/jimmunol.1002781

Joosten, S.A., Sullivan, L.C., Ottenhoff, T.H.M., 2016. Characteristics of HLA-E Restricted T-Cell Responses and Their Role in Infectious Diseases. Journal of Immunology Research 2016, 1–11. doi:10.1155/2016/2695396

Jozwik, A., Habibi, M.S., Paras, A., Zhu, J., Guvenel, A., Dhariwal, J., Almond, M., Wong, E.H.C., Sykes, A., Maybeno, M., Del Rosario, J., Trujillo-Torralbo, M.-B., Mallia, P., Sidney, J., Peters, B., Kon, O.M., Sette, A., Johnston, S.L., Openshaw, P.J., Chiu, C., 2019. RSV-specific airway resident memory CD8+ T cells and differential disease severity after experimental human infection. Nature Communications 1–17. doi:10.1038/ncomms10224

Juno, J.A., Kent, S.J., 2020. What Can Gamma Delta T Cells Contribute to an HIV Cure? Front. Cell. Infect. Microbiol. 10, 895–9. doi:10.3389/fcimb.2020.00233

Kabelitz, D., Bender, A., Prospero, T., Wesselborg, S., Janssen, O., Pechhold, K., 1991. The primary response of human gamma/delta + T cells to Mycobacterium tuberculosis is restricted to V gamma 9-bearing cells. J Exp Med 173, 1331–1338. doi:10.1084/jem.173.6.1331

Kabelitz, D., He, W., 2012. The Multifunctionality of Human Vγ9Vδ2 γδ T Cells: Clonal Plasticity or Distinct Subsets? Scand J Immunol 76, 213–222. doi:10.1111/j.1365-3083.2012.02727.x

Kagnoff, M.F., 1984. Possible role for a human adenovirus in the pathogenesis of celiac disease. J Exp Med 160, 1544–1557. doi:10.1084/jem.160.5.1544

Kahrs, C.R., Chuda, K., Tapia, G., Stene, L.C., Mårild, K., Rasmussen, T., Rønningen, K.S., Lundin, K.E.A., Kramna, L., Cinek, O., Størdal, K., 2019. Enterovirus as trigger of coeliac disease: nested case-control study within prospective birth cohort. BMJ 34, l231–8. doi:10.1136/bmj.l231

Kallemeijn, M.J., Boots, A.M.H., le Y Klift, M.X., Brouwer, E., Abdulahad, W.H., Verhaar, J.A.N., Dongen, J.J.M., Langerak, A.W., 2017. Ageing and latent CMV infection impact on maturation, differentiation and exhaustion profiles of T-cell receptor gammadelta T-cells. Sci Rep 1–14. doi:10.1038/s41598-017-05849-1

KAMER, J.H.V.D., WEIJERS, H.A., DICKE, W.K., 1953. Coeliac Disease: An Investigation into the Injurious Constituents of Wheat in Connection with their Action on Patients with Coeliac Disease. Acta Paediatrica 42, 223–231. doi:10.1111/j.1651-2227.1953.tb05586.x

Karolchik, D., 2004. The UCSC Table Browser data retrieval tool. Nucleic Acids Res 32, 493D–496. doi:10.1093/nar/gkh103

Karunakaran, M.M., Göbel, T.W., Starick, L., Walter, L., Herrmann, T., 2014. Vγ9 and Vδ2 T cell antigen receptor genes and butyrophilin 3 (BTN3) emerged with placental mammals and are concomitantly preserved in selected species like alpaca (Vicugna pacos). Immunogenetics 66, 243–254. doi:10.1007/s00251-014-0763-8

Karunakaran, M.M., Willcox, C.R., Salim, M., Paletta, D., Fichtner, A.S., Noll, A., Starick, L., Nöhren, A., Begley, C.R., Berwick, K.A., Chaleil, R.A.G., Pitard, V., Déchanet-Merville, J., Bates, P.A., Kimmel, B., Knowles, T.J., Kunzmann, V., Walter, L., Jeeves, M., Mohammed, F., Willcox, B.E., Herrmann, T., 2020. Butyrophilin-2A1 Directly Binds Germline-Encoded Regions of the Vγ9Vδ2 TCR and Is Essential for Phosphoantigen Sensing. Immunity 52, 487–498.e6. doi:10.1016/j.immuni.2020.02.014

Kasaian, M.T., Whitters, M.J., Carter, L.L., Lowe, L.D., Jussif, J.M., Deng, B., Johnson, K.A., Witek, J.S., Senices, M., Konz, R.F., Wurster, A.L., Donaldson, D.D., Collins, M., Young, D.A., Grusby, M.J., 2002. IL-21 Limits NK Cell Responses and Promotes Antigen-Specific T Cell Activation. Immunity 16, 559–569. doi:10.1016/S1074-7613(02)00295-9

Kemppainen, K.M., Vehik, K., Lynch, K.F., Larsson, H.E., Canepa, R.J., Simell, V., Koletzko, S., Liu, E., Simell, O.G., Toppari, J., Ziegler, A.-G., Rewers, M.J., Lernmark, Å., Hagopian, W.A., She, J.-X., Akolkar, B., Schatz, D.A., Atkinson, M.A., Blaser, M.J., Krischer, J.P., Hyöty, H., Agardh, D., Triplett, E.W., for The Environmental

Determinants of Diabetes in the Young (TEDDY) Study Group, 2017. Association Between Early-Life Antibiotic Use and the Risk of Islet or Celiac Disease Autoimmunity. JAMA Pediatr 171, 1217–9. doi:10.1001/jamapediatrics.2017.2905

Kenna, T.J., Davidson, S.I., Duan, R., Bradbury, L.A., McFarlane, J., Smith, M., Weedon, H., Street, S., Thomas, R., Thomas, G.P., Brown, M.A., 2012. Enrichment of circulating interleukin-17-secreting interleukin-23 receptor-positive γ/δ T cells in patients with active ankylosing spondylitis. Arthritis Rheum 64, 1420–1429. doi:10.1002/art.33507

Kennedy, N.A., Adams, A.T., Kalla, R., Heath, S., Leary, K.R.O.A., Drummond, H., Wilson, D.C., Gut, I.G., Nimmo, E.R., Satsangi, J., Lauc, G., Campbell, H., McGovern, D.P.B., Annese, V., scaron, V.Z., Permberton, I.K., Wuhrer, M., Kolarich, D., Fernandes, D.L., Theorodorou, E., Merrick, V., Spencer, D.I., Gardner, R.A., Doran, R., Shubhakar, A., Boyapati, R., Rudan, I., Lionetti, P., cacute, I.T.C.A.C.I., cacute, J.K.S.T., cacute, F.V.C.K., tambuk, J.S., Novokmet, M., cacute, M.P.C.I.C.B., Gornik, O., Andriulli, A., Cantoro, L., Sturniolo, G., Fiorino, G., Manetti, N., Latiano, A., Kohn, A., agrave, R.D.R.I., Danese, S., Arnott, I.D., Noble, C.L., Lees, C.W., Shand, A.G., Ho, G.-T., Dunlop, M.G., Murphy, L., Gibson, J., Evenden, L., Wrobel, N., Gilchrist, T., Fawkes, A., Kammeijer, G.S.M., Clerc, F., de Haan, N., Vojta, A., ija, I.S.Z., Markulin, D., cacute, M.K., cacute, P.D., Aulchenko, Y., van den Heuve, T., Jonkers, D., Pierik, M., Vatn, S., Ricanek, P., Jahnsen, J.O.R., You, P., lvernes, J.S.O., Frengen, A.B., s, T.M.T.A., Moen, A.E.F., Dahl, F.A., m, J.C.L.O., Ekeland, G.S., Detlie, T.E., Keita, A.S.V., derholm, J.D.S.O., Hjortswang, H., Halfvarson, J., Bergemalm, D., n, F.G.O., Amato, M.D.A., rkvist, L.T.O., Hjelm, F., Gullberg, M., Nordberg, N., Ocklind, A., Pettersson, E., Ekman, D., Sundell, M., Modig, E., Veillard, A.C.E.M., Schoemans, R., Poncelet, D., Sabatel, C.E.L., Gut, M., Bayes, M., n, C.C.E., Lindahl, T.O.R., Ciemniejewska, E., Vatn, M.H., Ventham, N.T., 2016. Integrative epigenome-wide analysis demonstrates that DNA methylation may mediate genetic risk in inflammatory bowel disease. Nature Communications 7, 1–14. doi:10.1038/ncomms13507

Khairallah, C., Déchanet-Merville, J., Capone, M., 2017. γδ T Cell-Mediated Immunity to Cytomegalovirus Infection. Front. Immunol. 8, 8833–13. doi:10.3389/fimmu.2017.00105

King, J.A., Jeong, J., Underwood, F.E., Quan, J., Panaccione, N., Windsor, J.W., Coward, S., deBruyn, J., Ronksley, P.E., Shaheen, A.-A., Quan, H., Godley, J., Veldhuyzen van Zanten, S., Lebwohl, B., Ng, S.C., Ludvigsson, J.F., Kaplan, G.G., 2020. Incidence of Celiac Disease Is Increasing Over Time. The American Journal of Gastroenterology 115, 507–525. doi:10.14309/ajg.0000000000000523

Kiniry, B.E., Li, S., Ganesh, A., Hunt, P.W., Somsouk, M., Skinner, P.J., Deeks, S.G., Shacklett, B.L., 2017. Detection of HIV-1-specific gastrointestinal tissue resident CD8+ T-cells in chronic infection. Mucosal Immunology 11, 909–920. doi:10.1038/mi.2017.96

Kiselev, V.Y., Kirschner, K., Schaub, M.T., Andrews, T., Yiu, A., Chandra, T., Natarajan, K.N., Reik, W., Barahona, M., Green, A.R., Hemberg, M., 2017. SC3: consensus clustering of single-cell RNA-seq data. Nat Meth 14, 483–486. doi:10.1038/nmeth.4236

Kivelä, L., Kaukinen, K., Lähdeaho, M.-L., Huhtala, H., Ashorn, M., Ruuska, T., Hiltunen, P., Visakorpi, J., Mäki, M., Kurppa, K., 2015. Presentation of Celiac Disease in Finnish Children Is No Longer Changing: A 50-Year Perspective. The Journal of Pediatrics 167, 1109–1115.e1. doi:10.1016/j.jpeds.2015.07.057

Klenerman, P., 2018. The (gradual) rise of memory inflation. Immunol Rev 283, 99–112. doi:10.1111/imr.12653

Koletzko, S., Lee, H.-S., Beyerlein, A., Aronsson, C.A., Hummel, M., Liu, E., Simell, V., Kurppa, K., Lernmark, Å., Hagopian, W., Rewers, M., She, J.-X., Simell, O., Toppari, J., Ziegler, A.-G., Krischer, J., Agardh, D., 2018. Cesarean Section on the Risk of Celiac Disease in the Offspring. Journal of Pediatric Gastroenterology and Nutrition 66, 417–424. doi:10.1097/MPG.0000000000001682

Kondrashova, A., Mustalahti, K., Kaukinen, K., Viskari, H., Volodicheva, V., Haapala, A.M., Ilonen, J., Knip, M., Mäki, M., Hyöty, H., the EPIVIR Study Group, 2009. Lower economic status and inferior hygienic environment may protect against celiac disease. Ann Med 40, 223–231. doi:10.1080/07853890701678689

Konnikova, L., Boschetti, G., Rahman, A., Mitsialis, V., Lord, J., Richmond, C., Tomov, V.T., Gordon, W., Jelinsky, S., Canavan, J., Liss, A., Wall, S., Field, M., Zhou, F., Goldsmith, J.D., Bewtra, M., Breault, D.T., Merad, M., Snapper, S.B., 2018. High-dimensional immune phenotyping and transcriptional analyses reveal robust recovery of viable human immune and epithelial cells from frozen gastrointestinal tissue. Mucosal Immunology 11, 1684–1693. doi:10.1038/s41385-018-0047-y

Koutsakos, M., Illing, P.T., Nguyen, T.H.O., Mifsud, N.A., Crawford, J.C., Rizzetto, S., Eltahla, A.A., Clemens, E.B., Sant, S., Chua, B.Y., Wong, C.Y., Allen, E.K., Teng, D., Dash, P., Boyd, D.F., Grzelak, L., Zeng, W., Hurt, A.C., Barr, I., Rockman, S., Jackson, D.C., Kotsimbos, T.C., Cheng, A.C., Richards, M., Westall, G.P., Loudovaris, T., Mannering, S.I., Elliott, M., Tangye, S.G., Wakim, L.M., Rossjohn, J., Vijaykrishna, D., Luciani, F.,

Thomas, P.G., Gras, S., Purcell, A.W., Kedzierska, K., 2019. Human CD8+ T cell cross-reactivity across influenza A, B and C viruses. Nat Immunol 1–19. doi:10.1038/s41590-019-0320-6
Krutzik, P.O., Clutter, M.R., Trejo, A., Nolan, G.P., 2001. Fluorescent Cell Barcoding for Multiplex Flow Cytometry. John Wiley & Sons, Inc., Hoboken, NJ, USA. doi:10.1002/0471142956.cy0631s55
Krutzik, P.O., Nolan, G.P., 2006. Fluorescent cell barcoding in flow cytometry allows high-throughput drug screening and signaling profiling. Nat Meth 3, 361–368. doi:10.1038/nmeth872
Kuhn, M., 2008. Building Predictive Models in R Using the caret Package. Journal of Statistical Software 28, 1–26.
Kuhn, R.M., Haussler, D., Kent, W.J., 2013. The UCSC genome browser and associated tools. Brief Bioinform 14, 144–161. doi:10.1093/bib/bbs038
Kumar, B.V., Kratchmarov, R., Miron, M., Carpenter, D.J., Senda, T., Lerner, H., Friedman, A., Reiner, S.L., Farber, D.L., 2018. Functional heterogeneity of human tissue-resident memory T cells based on dye efflux capacities. JCI Insight 3, 1561–17. doi:10.1172/jci.insight.123568
Kumar, B.V., Ma, W., Miron, M., Granot, T., Guyer, R.S., Carpenter, D.J., Senda, T., Sun, X., Ho, S.-H., Lerner, H., Friedman, A.L., Shen, Y., Farber, D.L., 2017. Human Tissue-Resident Memory T Cells Are Defined by Core Transcriptional and Functional Signatures in Lymphoid and Mucosal Sites. CellReports 20, 2921–2934. doi:10.1016/j.celrep.2017.08.078
Kurd, N.S., He, Z., Louis, T.L., Milner, J.J., Omilusik, K.D., Jin, W., Tsai, M.S., Widjaja, C.E., Kanbar, J.N., Olvera, J.G., Tysl, T., Quezada, L.K., Boland, B.S., Huang, W.J., Murre, C., Goldrath, A.W., Yeo, G.W., Chang, J.T., 2020. Early precursors and molecular determinants of tissue-resident memory CD8 +T lymphocytes revealed by single-cell RNA sequencing. Science Immunology 5, eaaz6894–17. doi:10.1126/sciimmunol.aaz6894
Kuric, E., Seiron, P., Krogvold, L., Edwin, B., Buanes, T., Hanssen, K.F., Skog, O., Dahl-Jørgensen, K., Korsgren, O., 2017. Demonstration of Tissue Resident Memory CD8 T Cells in Insulitic Lesions in Adult Patients with Recent-Onset Type 1 Diabetes. The American Journal of Pathology 187, 581–588. doi:10.1016/j.ajpath.2016.11.002
Kurien, M., Evans, K.E., Hopper, A.D., Hale, M.F., Cross, S.S., Sanders, D.S., 2012. Duodenal bulb biopsies for diagnosing adult celiac disease: is there an optimal biopsy site? YMGE 75, 1190–1196. doi:10.1016/j.gie.2012.02.025
Kurioka, A., Walker, L.J., Klenerman, P., Willberg, C.B., 2016. MAIT cells: new guardians of the liver. Clin Transl Immunol 5, e98–11. doi:10.1038/cti.2016.51
Kutlu, T., Brousse, N., Rambaud, C., Le Deist, F., Schmitz, J., Cerf-Bensussan, N., 1993. Numbers of T cell receptor (TCR) alpha beta+ but not of TcR gamma delta+ intraepithelial lymphocytes correlate with the grade of villous atrophy in coeliac patients on a long term normal diet. Gut 34, 208–214. doi:10.1136/gut.34.2.208
La Manno, G., Soldatov, R., Zeisel, A., Braun, E., Hochgerner, H., Petukhov, V., Lidschreiber, K., Kastriti, M.E., Lönnerberg, P., Furlan, A., Fan, J., Borm, L.E., Liu, Z., Bruggen, D., Guo, J., He, X., Barker, R., Sundström, E., Castelo-Branco, G., Cramer, P., Adameyko, I., Linnarsson, S., Kharchenko, P.V., 2018. RNA velocity of single cells. Nature 1–25. doi:10.1038/s41586-018-0414-6
Lambert, S.A., Jolma, A., Campitelli, L.F., Das, P.K., Yin, Y., Albu, M., Chen, X., Taipale, J., Hughes, T.R., Weirauch, M.T., 2018. The Human Transcription Factors. Cell 172, 650–665. doi:10.1016/j.cell.2018.01.029
Lamichhane, R., Schneider, M., la Harpe, de, S.M., Harrop, T.W.R., Hannaway, R.F., Dearden, P.K., Kirman, J.R., Tyndall, J.D.A., Vernall, A.J., Ussher, J.E., 2019. TCR- or Cytokine-Activated CD8+ Mucosal-Associated Invariant T Cells Are Rapid Polyfunctional Effectors That Can Coordinate Immune Responses. CellReports 28, 3061–3076.e5. doi:10.1016/j.celrep.2019.08.054
Langfelder, P., Horvath, S., 2008. WGCNA: an R package for weighted correlation network analysis. BMC Bioinformatics 9, 559–13. doi:10.1186/1471-2105-9-559
Larochette, V., Miot, C., Poli, C., Beaumont, E., Roingeard, P., Fickenscher, H., Jeannin, P., Delneste, Y., 2019. IL-26, a Cytokine With Roles in Extracellular DNA-Induced Inflammation and Microbial Defense. Front. Immunol. 10, 25–11. doi:10.3389/fimmu.2019.00204
Laydon, D.J., Bangham, C.R.M., Asquith, B., 2015. Estimating T-cell repertoire diversity: limitations of classical estimators and a new approach. Phil. Trans. R. Soc. B 370, 20140291–11. doi:10.1098/rstb.2014.0291
Lähdeaho, M.-L., Scheinin, M., Vuotikka, P., Taavela, J., Popp, A., Laukkarinen, J., Koffert, J., Koivurova, O.-P., Pesu, M., Kivelä, L., Lovró, Z., Keisala, J., Isola, J., Parnes, J.R., Leon, F., Mäki, M., 2019. Safety and efficacy of AMG 714 in adults with coeliac disease exposed to gluten challenge: a phase 2a, randomised, double-

blind, placebo-controlled study. The Lancet Gastroenterology & Hepatology 4, 948–959. doi:10.1016/S2468-1253(19)30264-X
Leffler, D., Schuppan, D., Pallav, K., Najarian, R., Goldsmith, J.D., Hansen, J., Kabbani, T., Dennis, M., Kelly, C.P., 2013. Kinetics of the histological, serological and symptomatic responses to gluten challenge in adults with coeliac disease. Gut 62, 996–1004. doi:10.1136/gutjnl-2012-302196
Leffler, D.A., Green, P.H.R., Fasano, A., 2015. Extraintestinal manifestations of coeliac disease. Nature Publishing Group 12, 561–571. doi:10.1038/nrgastro.2015.131
LeFranc, M.P., 2011. IMGT, the International ImMunoGeneTics Information System. Cold Spring Harbor Protocols 2011, pdb.top115–pdb.top115. doi:10.1101/pdb.top115
LeFranc, M.P., Forster, A., Baer, R., Stinson, M.A., Rabbitts, T.H., 1986. Diversity and rearrangement of the human T cell rearranging γ genes: Nine germ-line variable genes belonging to two subgroups. Cell 45, 237–246. doi:10.1016/0092-8674(86)90388-0
Leng, T., Akther, H.D., Hackstein, C.-P., Powell, K., King, T., Friedrich, M., Christoforidou, Z., McCuaig, S., Neyazi, M., Arancibia-Cárcamo, C.V., Hagel, J., Powrie, F., Peres, R.S., Millar, V., Ebner, D., Lamichhane, R., Ussher, J., Hinks, T.S.C., Marchi, E., Willberg, C., Klenerman, P., Investigators3, O.I., 2019. TCR and Inflammatory Signals Tune Human MAIT Cells to Exert Specific Tissue Repair and Effector Functions. CellReports 28, 3077–3091.e5. doi:10.1016/j.celrep.2019.08.050
Leonard, W.J., Spolski, R., 2005. Interleukin-21: a modulator of lymphoid proliferation, apoptosis and differentiation. Nat Rev Immunol 5, 688–698. doi:10.1038/nri1688
Lepore, M., Kalinichenko, A., Colone, A., Paleja, B., Singhal, A., Tschumi, A., Lee, B., Poidinger, M., Zolezzi, F., Quagliata, L., Sander, P., Newell, E., Bertoletti, A., Terracciano, L., De Libero, G., Mori, L., 2014. Parallel T-cell cloning and deep sequencing of human MAIT cells reveal stable oligoclonal TCRβ repertoire. Nature Communications 5, 1–15. doi:10.1038/ncomms4866
Lerner, A., Arleevskaya, M., Schmiedl, A., Matthias, T., 2017. Microbes and Viruses Are Bugging the Gut in Celiac Disease. Are They Friends or Foes? Front. Microbiol. 8, 158–16. doi:10.3389/fmicb.2017.01392
Li, C., Zhu, B., Son, Y.M., Wang, Z., Jiang, L., Xiang, M., Ye, Z., Beckermann, K.E., Wu, Y., Jenkins, J.W., Siska, P.J., Vincent, B.G., Prakash, Y.S., Peikert, T., Edelson, B.T., Taneja, R., Kaplan, M.H., Rathmell, J.C., Dong, H., Hitosugi, T., Sun, J., 2019. The Transcription Factor Bhlhe40 Programs Mitochondrial Regulation of Resident CD8+ T Cell Fitness and Functionality. Immunity 51, 491–507.e7. doi:10.1016/j.immuni.2019.08.013
Li, H., Li, H., Handsaker, B., Handsaker, B., Wysoker, A., Wysoker, A., Fennell, T., Fennell, T., Ruan, J., Ruan, J., Homer, N., Homer, N., Marth, G., Marth, G., Abecasis, G., Abecasis, G., Durbin, R., Durbin, R., 1000 Genome Project Data Processing Subgroup, 2009. The Sequence Alignment/Map format and SAMtools. Bioinformatics 25, 2078–2079. doi:10.1093/bioinformatics/btp352
Li, W.V., Li, J.J., 2018. An accurate and robust imputation method scImpute for single-cell RNA-seq data. Nature Communications 9, 1–9. doi:10.1038/s41467-018-03405-7
Li, Y., Wang, X., Teng, D., Chen, H., Wang, M., Wang, J., Zhang, J., He, W., 2019. Identification of the Ligands of TCRγδ by Screening the Immune Repertoire of γδT Cells From Patients With Tuberculosis. Front. Immunol. 10, 180–15. doi:10.3389/fimmu.2019.02282
Lian, C.G., Bueno, E.M., Granter, S.R., Laga, A.C., Saavedra, A.P., Lin, W.M., Susa, J.S., Zhan, Q., Chandraker, A.K., Tullius, S.G., Pomahac, B., Murphy, G.F., 2014. Biomarker evaluation of face transplant rejection: association of donor T cells with target cell injury. Modern Pathology 27, 788–799. doi:10.1038/modpathol.2013.249
Liao, Y., Liao, Y., Smyth, G.K., Smyth, G.K., Shi, W., Shi, W., 2014. featureCounts: an efficient general purpose program for assigning sequence reads to genomic features. Bioinformatics 30, 923–930. doi:10.1093/bioinformatics/btt656
Liao, Y., Smyth, G.K., Shi, W., 2013. The Subread aligner: fast, accurate and scalable read mapping by seed-and-vote. Nucleic Acids Res 41, e108–e108. doi:10.1093/nar/gkt214
Lindfors, K., Ciacci, C., Kurppa, K., Lundin, K.E.A., Makharia, G.K., Mearin, M.L., Murray, J.A., Verdu, E.F., Kaukinen, K., 2019. Coeliac disease. Nat. Rev. Dis. Primers 1–18. doi:10.1038/s41572-018-0054-z
Lindfors, K., Lin, J., Lee, H.-S., Hyöty, H., Nykter, M., Kurppa, K., Liu, E., Koletzko, S., Rewers, M., Hagopian, W., Toppari, J., Ziegler, A.-G., Akolkar, B., Krischer, J.P., Petrosino, J.F., Lloyd, R.E., Agardh, D., 2020. Metagenomics of the faecal virome indicate a cumulative effect of enterovirus and gluten amount on the risk of coeliac disease autoimmunity in genetically at risk children: the TEDDY study. Gut 69, 1416–1422. doi:10.1136/gutjnl-2019-319809
Linehan, J.L., Harrison, O.J., Han, S.-J., Byrd, A.L., Vujkovic-Cvijin, I., Villarino, A.V., Sen, S.K., Shaik, J., Smelkinson, M., Tamoutounour, S., Collins, N., Bouladoux, N., Dzutsev, A., Rosshart, S.P., Arbuckle, J.H.,

Wang, C.-R., Kristie, T.M., Rehermann, B., Trinchieri, G., Brenchley, J.M., O'Shea, J.J., Belkaid, Y., 2018. Non-classical Immunity Controls Microbiota Impact on Skin Immunity and Tissue Repair. Cell 172, 784–796.e18. doi:10.1016/j.cell.2017.12.033

Liu, D., Bryceson, Y.T., Meckel, T., Vasiliver-Shamis, G., Dustin, M.L., Long, E.O., 2009. Integrin-Dependent Organization and Bidirectional Vesicular Traffic at Cytotoxic Immune Synapses. Immunity 31, 99–109. doi:10.1016/j.immuni.2009.05.009

Liu, H., Brais, R., Lavergne-Slove, A., Jeng, Q., Payne, K., Ye, H., Liu, Z., Carreras, J., Huang, Y., Bacon, C.M., Hamoudi, R.A., Save, V., Venkatraman, L., Isaacson, P.G., Woodward, J., Du, M.-Q., 2010. Continual monitoring of intraepithelial lymphocyte immunophenotype and clonality is more important than snapshot analysis in the surveillance of refractory coeliac disease. Gut 59, 452–460. doi:10.1136/gut.2009.186007

Livak, K.J., Schmittgen, T.D., 2001. Analysis of Relative Gene Expression Data Using Real-Time Quantitative PCR and the 2−ΔΔCT Method. Methods 25, 402–408. doi:10.1006/meth.2001.1262

Loo, L., Vrakas, G., Reddy, S., Allan, P., 2017. Intestinal transplantation. Current Opinion in Gastroenterology 33, 203–211. doi:10.1097/MOG.0000000000000358

Loppow, D., Böttcher, M., Gercken, G., Magnussen, H., Jörres, R.A., 2000. Flow cytometric analysis of the effect of dithiothreitol on leukocyte surface markers. Eur. Respir. J. 16, 324–329.

Losowsky, M.S., 2008. A History of Coeliac Disease. Dig Dis 26, 112–120. doi:10.1159/000116768

Love, M.I., Huber, W., Anders, S., 2014. Moderated estimation of fold change and dispersion for RNA-seq data with DESeq2. Genome Biol. 15, 31–21. doi:10.1186/s13059-014-0550-8

Ludvigsson, J.F., Bai, J.C., Biagi, F., Card, T.R., Ciacci, C., Ciclitira, P.J., Green, P.H.R., Hadjivassiliou, M., Holdoway, A., van Heel, D.A., Kaukinen, K., Leffler, D.A., Leonard, J.N., Lundin, K.E.A., McGough, N., Davidson, M., Murray, J.A., Swift, G.L., Walker, M.M., Zingone, F., Sanders, D.S., Authors of the BSG Coeliac Disease Guidelines Development Group, 2014. Diagnosis and management of adult coeliac disease: guidelines from the British Society of Gastroenterology. Gut 63, 1210–1228. doi:10.1136/gutjnl-2013-306578

Ludvigsson, J.F., Leffler, D.A., Bai, J.C., Biagi, F., Fasano, A., Green, P.H.R., Hadjivassiliou, M., Kaukinen, K., Kelly, C.P., Leonard, J.N., Lundin, K.E.A., Murray, J.A., Sanders, D.S., Walker, M.M., Zingone, F., Ciacci, C., 2012. The Oslo definitions for coeliac disease and related terms. Gut 62, 43–52. doi:10.1136/gutjnl-2011-301346

Lun, A.T.L., McCarthy, D.J., Marioni, J.C., 2016. A step-by-step workflow for low-level analysis of single-cell RNA-seq data with Bioconductor. F1000Res 5, 2122. doi:10.12688/f1000research.9501.2

Lundin, K.E., 1993. Gliadin-specific, HLA-DQ(alpha 1*0501,beta 1*0201) restricted T cells isolated from the small intestinal mucosa of celiac disease patients. J Exp Med 178, 187–196. doi:10.1084/jem.178.1.187

Lundin, K.E.A., Nilsen, E.M., Scott, H.G., Løberg, E.M., Gjøen, A., Bratlie, J., Skar, V., Mendez, E., Løvik, A., Kett, K., 2003. Oats induced villous atrophy in coeliac disease. Gut 52, 1649–1652. doi:10.1136/gut.52.11.1649

Luoma, A.M., Castro, C.D., Mayassi, T., Bembinster, L.A., Bai, L., Picard, D., Anderson, B., Scharf, L., Kung, J.E., Sibener, L.V., Savage, P.B., Jabri, B., Bendelac, A., Adams, E.J., 2013. Crystal Structure of Vδ1 T Cell Receptor in Complex with CD1d-Sulfatide Shows MHC-like Recognition of a Self-Lipid by Human γδ T Cells. Immunity 39, 1032–1042. doi:10.1016/j.immuni.2013.11.001

Luoma, A.M., Suo, S., Williams, H.L., Sharova, T., Sullivan, K., Manos, M., Bowling, P., Hodi, F.S., Rahma, O., Sullivan, R.J., Boland, G.M., Nowak, J.A., Dougan, S.K., Dougan, M., Yuan, G.-C., Wucherpfennig, K.W., 2020. Molecular Pathways of Colon Inflammation Induced by Cancer Immunotherapy. Cell 182, 655–671.e22. doi:10.1016/j.cell.2020.06.001

Machado-Santos, J., Saji, E., Tröscher, A.R., Paunovic, M., Liblau, R., Gabriely, G., Bien, C.G., Bauer, J., Lassmann, H., 2018. The compartmentalized inflammatory response in the multiple sclerosis brain is composed of tissue-resident CD8+ T lymphocytes and B cells. Brain 141, 2066–2082. doi:10.1093/brain/awy151

Mackay, L.K., Braun, A., Macleod, B.L., Collins, N., Tebartz, C., Bedoui, S., Carbone, F.R., Gebhardt, T., 2015a. Cutting Edge: CD69 Interference with Sphingosine-1-Phosphate Receptor Function Regulates Peripheral T Cell Retention. J.I. 194, 2059–2063. doi:10.4049/jimmunol.1402256

Mackay, L.K., Kallies, A., 2017. Transcriptional Regulation of Tissue-Resident Lymphocytes. Trends in Immunology 38, 94–103. doi:10.1016/j.it.2016.11.004

Mackay, L.K., Minnich, M., Kragten, N.A.M., Liao, Y., Nota, B., Seillet, C., Zaid, A., Man, K., Preston, S., Freestone, D., Braun, A., Wynne-Jones, E., Behr, F.M., Stark, R., Pellicci, D.G., Godfrey, D.I., Belz, G.T., Pellegrini, M., Gebhardt, T., Busslinger, M., Shi, W., Carbone, F.R., van Lier, R.A.W., Kallies, A., van

Gisbergen, K.P.J.M., 2016. Hobit and Blimp1 instruct a universal transcriptional program of tissue residency in lymphocytes. Science 352, 459–459. doi:10.1126/science.aad2035
Mackay, L.K., Rahimpour, A., Ma, J.Z., Collins, N., Stock, A.T., Hafon, M.-L., Vega-Ramos, J., Lauzurica, P., Mueller, S.N., Stefanovic, T., Tscharke, D.C., Heath, W.R., Inouye, M., Carbone, F.R., Gebhardt, T., 2013. The developmental pathway for CD103+CD8+ tissue-resident memory T cells of skin. Nat Immunol 14, 1294–1301. doi:10.1038/ni.2744
Mackay, L.K., Wynne-Jones, E., Freestone, D., Pellicci, D.G., Mielke, L.A., Newman, D.M., Braun, A., Masson, F., Kallies, A., Belz, G.T., Carbone, F.R., 2015b. T-box Transcription Factors Combine with the Cytokines TGF-β and IL-15 to Control Tissue-Resident Memory T Cell Fate. Immunity 43, 1101–1111. doi:10.1016/j.immuni.2015.11.008
Madrigal, L., Lynch, S., Feighery, C., Weir, D., Kelleher, D., O'Farelly, C., 1993. Flow cytometric analysis of surface major histocompatibility complex class II expression on human epithelial cells prepared from small intestinal biopsies. Journal of Immunological Methods 158, 207–214. doi:10.1016/0022-1759(93)90216-T
Mahnke, Y.D., Brodie, T.M., Sallusto, F., Roederer, M., Lugli, E., 2013. The who's who of T-cell differentiation: Human memory T-cell subsets. Eur. J. Immunol. 43, 2797–2809. doi:10.1002/eji.201343751
Mahuron, K.M., Moreau, J.M., Glasgow, J.E., Boda, D.P., Pauli, M.L., Gouirand, V., Panjabi, L., Grewal, R., Luber, J.M., Mathur, A.N., Feldman, R.M., Shifrut, E., Mehta, P., Lowe, M.M., Alvarado, M.D., Marson, A., Singer, M., Wells, J., Jupp, R., Daud, A.I., Rosenblum, M.D., 2020. Layilin augments integrin activation to promote antitumor immunity. J Exp Med 217, 339–17. doi:10.1084/jem.20192080
Maiuri, L., Ciacci, C., Auricchio, S., Brown, V., Quaratino, S., Londei, M., 2000. Interleukin 15 mediates epithelial changes in celiac disease. Gastroenterology 119, 996–1006. doi:10.1053/gast.2000.18149
Malamut, G., Afchain, P., Verkarre, V., Lecomte, T., Amiot, A., Damotte, D., Bouhnik, Y., Colombel, J.F., Delchier, J.C., Allez, M., Cosnes, J., Slove, A.L., Meresse, B., Trinquart, L., Macintyre, E., Weiss, I.R., Hermine, O., Brousse, N., Bensussan, N.C., Cellier, C., 2009. Presentation and Long-Term Follow-up of Refractory Celiac Disease: Comparison of Type I With Type II. Gastroenterology 136, 81–90. doi:10.1053/j.gastro.2008.09.069
Malhotra, N., Narayan, K., Cho, O.H., Sylvia, K.E., Yin, C., Melichar, H., Rashighi, M., Lefebvre, V., Harris, J.E., Berg, L.J., Kang, J., Consortium5, T.I.G.P., 2013. A Network of High-Mobility Group Box Transcription Factors Programs Innate Interleukin-17 Production. Immunity 38, 681–693. doi:10.1016/j.immuni.2013.01.010
Malhotra, N., Qi, Y., Spidale, N.A., Frascoli, M., Miu, B., Cho, O., Sylvia, K., Kang, J., 2018. SOX4 controls invariant NKT cell differentiation by tuning TCR signaling. J Exp Med 215, 2887–2900. doi:10.1084/jem.20172021
Mandala, S., 2002. Alteration of Lymphocyte Trafficking by Sphingosine-1-Phosphate Receptor Agonists. Science 296, 346–349. doi:10.1126/science.1070238
Marchi, E., Lee, L.N., Klenerman, P., 2019. Inflation vs. Exhaustion of Antiviral CD8+ T-Cell Populations in Persistent Infections: Two Sides of the Same Coin? Front. Immunol. 10, 758–11. doi:10.3389/fimmu.2019.00197
Marlin, R., Pappalardo, A., Kaminski, H., Willcox, C.R., Pitard, V., Netzer, S., Khairallah, C., Lomenech, A.-M., Harly, C., Bonneville, M., Moreau, J.-F., Scotet, E., Willcox, B.E., Faustin, B., Déchanet-Merville, J., 2017. Sensing of cell stress by human γδ TCR-dependent recognition of annexin A2. Proc Natl Acad Sci USA 114, 3163–3168. doi:10.1073/pnas.1621052114
Marsh, M.N., 1992. Gluten, major histocompatibility complex, and the small intestine: A molecular and immunobiologic approach to the spectrum of gluten sensitivity (“celiac sprue”). Gastroenterology 102, 330–354.
Martin, J.C., Chang, C., Boschetti, G., Ungaro, R., Giri, M., Grout, J.A., Gettler, K., Chuang, L.-S., Nayar, S., Greenstein, A.J., Dubinsky, M., Walker, L., Leader, A., Fine, J.S., Whitehurst, C.E., Mbow, M.L., Kugathasan, S., Denson, L.A., Hyams, J.S., Friedman, J.R., Desai, P.T., Ko, H.M., Laface, I., Akturk, G., Schadt, E.E., Salmon, H., Gnjatic, S., Rahman, A.H., Merad, M., Cho, J.H., Kenigsberg, E., 2019. Single-Cell Analysis of Crohn’s Disease Lesions Identifies a Pathogenic Cellular Module Associated with Resistance to Anti-TNF Therapy. Cell 178, 1493–1508.e20. doi:10.1016/j.cell.2019.08.008
Martin, M., 2011. Cutadapt removes adapter sequences from high-throughput sequencing reads. EMBnet.journal; Vol 17, No 1: Next Generation Sequencing Data Analysis 33, 2938–2940. doi:10.14806/ej.17.1.200
Mayassi, T., Jabri, B., 2018. Human intraepithelial lymphocytes. Mucosal Immunology 1–9. doi:10.1038/s41385-018-0016-5

Mayassi, T., Ladell, K., Gudjonson, H., McLaren, J.E., Shaw, D.G., Tran, M.T., Rokicka, J.J., Lawrence, I., Grenier, J.-C., van Unen, V., Ciszewski, C., Dimaano, M., Sayegh, H.E., Kumar, V., Wijmenga, C., Green, P.H.R., Gokhale, R., Jericho, H., Semrad, C.E., Guandalini, S., Dinner, A.R., Kupfer, S.S., Reid, H.H., Barreiro, L.B., Rossjohn, J., Price, D.A., Jabri, B., 2019. Chronic Inflammation Permanently Reshapes Tissue-Resident Immunity in Celiac Disease. Cell 1–35. doi:10.1016/j.cell.2018.12.039

Mazzarella, G., Stefanile, R., Camarca, A., Giliberti, P., Cosentini, E., Marano, C., Iaquinto, G., Giardullo, N., Auricchio, S., Sette, A., Troncone, R., Gianfrani, C., 2008. Gliadin Activates HLA Class I-Restricted CD8+ T Cells in Celiac Disease Intestinal Mucosa and Induces the Enterocyte Apoptosis. Gastroenterology 134, 1017–1027. doi:10.1053/j.gastro.2008.01.008

Mårild, K., Stephansson, O., Montgomery, S., Murray, J.A., LUDVIGSSON, J.F., 2012. Pregnancy Outcome and Risk of Celiac Disease in Offspring: A Nationwide Case-Control Study. Gastroenterology 142, 39–45.e3. doi:10.1053/j.gastro.2011.09.047

Mårild, K., Ye, W., Lebwohl, B., Green, P.H., Blaser, M.J., Card, T., Ludvigsson, J.F., 2013. Antibiotic exposure and the development of coeliac disease: a nationwide case–control study. BMC Gastroenterol 13, 1–9. doi:10.1186/1471-230X-13-109

McCarthy, D.J., Campbell, K.R., Lun, A.T.L., Wills, Q.F., 2017. Scater: pre-processing, quality control, normalization and visualization of single-cell RNA-seq data in R. Bioinformatics 247, btw777–1186. doi:10.1093/bioinformatics/btw777

McCarthy, N.E., Eberl, M., 2018. Human γδ T-Cell Control of Mucosal Immunity and Inflammation. Front. Immunol. 9, 938–8. doi:10.3389/fimmu.2018.00985

McInnes, L., Healy, J., Melville, J., 2018. UMAP: Uniform Manifold Approximation and Projection for Dimension Reduction. doi:arxiv.org/abs/1802.03426v2

McNamara, H.A., Cai, Y., Wagle, M.V., Sontani, Y., Roots, C.M., Miosge, L.A., O'Connor, J.H., Sutton, H.J., Ganusov, V.V., Heath, W.R., Bertolino, P., Goodnow, C.G., Parish, I.A., Enders, A., Cockburn, I.A., 2017. Up-regulation of LFA-1 allows liver-resident memory T cells to patrol and remain in the hepatic sinusoids. Science Immunology 2, 1–11. doi:10.1126/sciimmunol.aaj1996

Meresse, B., Chen, Z., Ciszewski, C., Tretiakova, M., Bhagat, G., Krausz, T.N., Raulet, D.H., Lanier, L.L., Groh, V., Spies, T., Ebert, E.C., Green, P.H., Jabri, B., 2004. Coordinated Induction by IL15 of a TCR-Independent NKG2D Signaling Pathway Converts CTL into Lymphokine-Activated Killer Cells in Celiac Disease. Immunity 21, 357–366. doi:10.1016/j.immuni.2004.06.020

Meresse, B., Curran, S.A., Ciszewski, C., Orbelyan, G., Setty, M., Bhagat, G., Lee, L., Tretiakova, M., Semrad, C., Kistner, E., Winchester, R.J., Braud, V., Lanier, L.L., Geraghty, D.E., Green, P.H., Guandalini, S., Jabri, B., 2006. Reprogramming of CTLs into natural killer–like cells in celiac disease. J Exp Med 203, 1343–1355. doi:10.1084/jem.20060028

Metsalu, T., Vilo, J., 2015. ClustVis: a web tool for visualizing clustering of multivariate data using Principal Component Analysis and heatmap. Nucleic Acids Res 43, W566–W570. doi:10.1093/nar/gkv468

Miao, Z., Deng, K., Wang, X., Zhang, X., 2018. DEsingle for detecting three types of differential expression in single-cell RNA-seq data. Bioinformatics 34, 3223–3224. doi:10.1093/bioinformatics/bty332

Mikulak, J., Oriolo, F., Bruni, E., Roberto, A., Colombo, F.S., Villa, A., Bosticardo, M., Bortolomai, I., Presti, Lo, E., Meraviglia, S., Dieli, F., Vetrano, S., Danese, S., Bella, Della, S., Carvello, M.M., Sacchi, M., Cugini, G., Colombo, G., Klinger, M., Spaggiari, P., Roncalli, M., Prinz, I., Ravens, S., Di Lorenzo, B., Marcenaro, E., Silva-Santos, B., Spinelli, A., Mavilio, D., 2019. NKp46-expressing human gut-resident intraepithelial Vδ1 T cell subpopulation exhibits high antitumor activity against colorectal cancer. JCI Insight 4, 8900–42. doi:10.1172/jci.insight.125884

Miles, A., Liaskou, E., Eksteen, B., Lalor, P.F., Adams, D.H., 2008. CCL25 and CCL28 promote α 4β 7-integrin-dependent adhesion of lymphocytes to MAdCAM-1 under shear flow. AJP: Gastrointestinal and Liver Physiology 294, G1257–G1267. doi:10.1152/ajpgi.00266.2007

Milner, J.J., Toma, C., He, Z., Kurd, N.S., Nguyen, Q.P., McDonald, B., Quezada, L., Widjaja, C.E., Witherden, D.A., Crowl, J.T., Shaw, L.A., Yeo, G.W., Chang, J.T., Omilusik, K.D., Goldrath, A.W., 2020. Heterogenous Populations of Tissue-Resident CD8+ T Cells Are Generated in Response to Infection and Malignancy. Immunity 52, 808–824.e7. doi:10.1016/j.immuni.2020.04.007

Milner, J.J., Toma, C., Yu, B., Zhang, K., Omilusik, K., Phan, A.T., Wang, D., Getzler, A.J., Nguyen, T., Crotty, S., Wang, W., Pipkin, M.E., Goldrath, A.W., 2017. Runx3 programs CD8+ T cell residency in non-lymphoid tissues and tumours. Nature 552, 253–257. doi:10.1038/nature24993

Mitchell, H., Garg, M., 2019. Editorial: a non-dietary treatment for coeliac disease-two steps forward, one step back? Aliment Pharmacol Ther 50, 955–956. doi:10.1111/apt.15470

Molberg, O., Kett, K., Scott, H., Thorsby, E., Sollid, L.M., Lundin, K.E.A., 2003. Gliadin Specific, HLA DQ2-Restricted T Cells are Commonly Found in Small Intestinal Biopsies from Coeliac Disease Patients, but not from Controls. Scand J Immunol 46, 103–109. doi:10.1046/j.1365-3083.1996.d01-17.x

Monod, M.Y., Giudicelli, V., Chaume, D., LeFranc, M.P., 2004. IMGT/JunctionAnalysis: the first tool for the analysis of the immunoglobulin and T cell receptor complex V-J and V-D-J JUNCTIONs. Bioinformatics 20, i379–i385. doi:10.1093/bioinformatics/bth945

Montalvillo, E., Bernardo, D., Martínez-Abad, B., Allegretti, Y., Fernández-Salazar, L., Calvo, C., Chirdo, F., Garrote, J., Arranz, E., 2015. Increased Intraepithelial Vα24 Invariant NKT Cells in the Celiac Duodenum. Nutrients 7, 8960–8976. doi:10.3390/nu7115444

Monteleone, G., 2001. Role of interferon alpha in promoting T helper cell type 1 responses in the small intestine in coeliac disease. Gut 48, 425–429. doi:10.1136/gut.48.3.425

Mooney, P.D., Kurien, M., Evans, K.E., Rosario, E., Cross, S.S., Vergani, P., Hadjivassiliou, M., Murray, J.A., Sanders, D.S., 2016. Clinical and Immunologic Features of Ultra-Short Celiac Disease. Gastroenterology 150, 1125–1134. doi:10.1053/j.gastro.2016.01.029

Morris, R., Kershaw, N.J., Babon, J.J., 2018. The molecular details of cytokine signaling via the JAK/STAT pathway. Protein Science 27, 1984–2009. doi:10.1002/pro.3519

Mubarak, A., Nikkels, P., Houwen, R., Kate, Ten, F., 2011. Reproducibility of the histological diagnosis of celiac disease. Scandinavian Journal of Gastroenterology 46, 1065–1073. doi:10.3109/00365521.2011.589471

Mukewar, S.S., Sharma, A., Rubio Tapia, A., Wu, T.-T., Jabri, B., Murray, J.A., 2017. Open-Capsule Budesonide for Refractory Celiac Disease 1–9. doi:10.1038/ajg.2017.71

Mulder, W.M.C., Koenen, H., van de Muysenberg, A.J.C., Bloemena, E., Wagsfaff, J., Scheper, R.J., 1994. Reduced expression of distinct T-cell CD molecules by collagenase/DNase treatment. Cancer Immunol Immunother 38, 253–258. doi:10.1007/BF01533516

Murphy, A.G., O'Keeffe, K.M., Lalor, S.J., Maher, B.M., Mills, K.H.G., McLoughlin, R.M., 2014. Staphylococcus aureus infection of mice expands a population of memory γδ T cells that are protective against subsequent infection. J. Immunol. 192, 3697–3708. doi:10.4049/jimmunol.1303420

Murray, J.A., Kelly, C.P., Green, P.H.R., Marcantonio, A., Wu, T.-T., Mäki, M., Adelman, D.C., Investigators, C.S.G.O., Ansari, S., Ayub, K., Basile, A., Behrend, C., Bercik, P., Bressler, B., Byrnes, V., Chandan, V.S., Cheekati, V., Chipps, B., Coates, A., Collatrella, A., Condemi, J., Corder, C., Corren, J., Curtis, C., DeMeo, M., Desta, T., Devereaux, C., DiMarino, A., DuPree, M., Ennis, C., Fedorak, R., Fogel, R., Freeman, S., Freilich, B., Friedenberg, K., Geenen, D., Gill, K., Goldsobel, A., Goldstein, J., Goldstein, M., Gordon, G., Hardi, R., Harris, L., Holmes, R., Jagarlamundi, K., James, G., Kaplan, M., Kirstein, J., Knoll, A., Kotfila, R., Krause, R., Kravitz, A., Kreines, M., Lähdeaho, M.L., Lamet, M., Laskin, K., Lebwohl, B., Leffler, D., Lewis, S., Liakos, S., Lundin, K., Marks, K., Merkes, K., Minton, S., Moussa, S., Narayen, V., Nehra, V., Newton, E., Nyberg, A., Oosthuizen, J., Otrok, T., Patel, D., Pepin, C., Phillips, R., Pyle, G., Reichelderfer, M., Reid, B., Ritter, T., Saini, S., Sanders, D., Schulman, M., Semrad, C., Shah, S., Stockwell, D., Strout, C., Suez, D., Tatum, H., Torbenson, M.S., Turner, M., Varunok, P., Vazquez-Roque, M., Vento, A., Welton, T., Wohlman, R., Wood, M., Woods, S., Yousef, K., 2017. No Difference Between Latiglutenase and Placebo in Reducing Villous Atrophy or Improving Symptoms in Patients With Symptomatic Celiac Disease. Gastroenterology 152, 787–798.e2. doi:10.1053/j.gastro.2016.11.004

Muruganandah, V., Sathkumara, H.D., Navarro, S., Kupz, A., 2018. A Systematic Review: The Role of Resident Memory T Cells in Infectious Diseases and Their Relevance for Vaccine Development. Front. Immunol. 9, 79–21. doi:10.3389/fimmu.2018.01574

Myléus, A., Hernell, O., Gothefors, L., Hammarström, M.-L., Persson, L.-Å., Stenlund, H., Ivarsson, A., 2012. Early infections are associated with increased risk for celiac disease: an incident case-referent study. BMC Pediatr 12, 1–8. doi:10.1186/1471-2431-12-194

Myléus, A., Ivarsson, A., Webb, C., Danielsson, L., Hernell, O., Högberg, L., Karlsson, E., Lagerqvist, C., Norström, F., Rosén, A., Sandström, O., Stenhammar, L., Stenlund, H., Wall, S., Carlsson, A., 2009. Celiac Disease Revealed in 3% of Swedish 12-year-olds Born During an Epidemic. Journal of Pediatric Gastroenterology and Nutrition 49, 170–176. doi:10.1097/MPG.0b013e31818c52cc

Namatovu, F., m, O.S., Olsson, C., Lindkvist, M., Ivarsson, A., 2014. Celiac disease risk varies between birth cohorts, generating hypotheses about causality: evidence from 36 years of population-based follow-up. BMC Gastroenterol 14, 1–8. doi:10.1186/1471-230X-14-59

Nasr, I., Nasr, I., Beyers, C., Chang, F., Donnelly, S., Ciclitira, P., 2015. Recognising and Managing Refractory Coeliac Disease: A Tertiary Centre Experience. Nutrients 7, 9896–9907. doi:10.3390/nu7125506

Ng, S.C., Shi, H.Y., Hamidi, N., Underwood, F.E., Tang, W., Benchimol, E.I., Panaccione, R., Ghosh, S., Wu, J.C.Y., Chan, F.K.L., Sung, J.J.Y., Kaplan, G.G., 2017. Worldwide incidence and prevalence of inflammatory bowel

disease in the 21st century: a systematic review of population-based studies. The Lancet 390, 2769–2778. doi:10.1016/S0140-6736(17)32448-0
Nguyen, C.T., Maverakis, E., Eberl, M., Adamopoulos, I.E., 2019. γδ T cells in rheumatic diseases: from fundamental mechanisms to autoimmunity 1–11. doi:10.1007/s00281-019-00752-5
Nguyen, P., Ma, J., Pei, D., Obert, C., Cheng, C., Geiger, T.L., 2011. Identification of errors introduced during high throughput sequencing of the T cell receptor repertoire. BMC Genomics 12, 1–13. doi:10.1186/1471-2164-12-106
Nicoud, I.B., Clarke, D.M., Taber, G., Stolowski, K.M., Roberge, S.E., Song, M.K., Mathew, A.J., Reems, J.-A., 2012. Cryopreservation of umbilical cord blood with a novel freezing solution that mimics intracellular ionic composition. Transfusion 52, 2055–2062. doi:10.1111/j.1537-2995.2011.03547.x
Oberhuber, G., Granditsch, G., Vogelsang, H., 1999. The histopathology of coeliac disease: time for a standardized report scheme for pathologists. European Journal of Gastroenterology & Hepatology 11.
Oja, A.E., Piet, B., Helbig, C., Stark, R., van der Zwan, D., Blaauwgeers, H., Remmerswaal, E.B.M., Amsen, D., Jonkers, R.E., Moerland, P.D., Nolte, M.A., van Lier, R.A.W., Hombrink, P., 2017a. Trigger-happy resident memory CD4+ T cells inhabit the human lungs. Mucosal Immunology 11, 654–667. doi:10.1038/mi.2017.94
Oja, A.E., Vieira Braga, F.A., Remmerswaal, E.B.M., Kragten, N.A.M., Hertoghs, K.M.L., Zuo, J., Moss, P.A., van Lier, R.A.W., van Gisbergen, K.P.J.M., Hombrink, P., 2017b. The Transcription Factor Hobit Identifies Human Cytotoxic CD4+ T Cells. Front. Immunol. 8, 1276–11. doi:10.3389/fimmu.2017.00325
Olaussen, R.W., Johansen, F.E., Lundin, K.E.A., Jahnsen, J., Brandtzaeg, P., Farstad, I.N., 2002. Interferon-γ-Secreting T Cells Localize to the Epithelium in Coeliac Disease. Scand J Immunol 56, 652–664. doi:10.1046/j.1365-3083.2002.01195.x
Omilusik, K.D., Best, J.A., Yu, B., Goossens, S., Weidemann, A., Nguyen, J.V., Seuntjens, E., Stryjewska, A., Zweier, C., Roychoudhuri, R., Gattinoni, L., Bird, L.M., Higashi, Y., Kondoh, H., Huylebroeck, D., Haigh, J., Goldrath, A.W., 2015. Transcriptional repressor ZEB2 promotes terminal differentiation of CD8+ effector and memory T cell populations during infection. J Exp Med 212, 2027–2039. doi:10.1084/jem.20150194
Pallett, L.J., Davies, J., Colbeck, E.J., Robertson, F., Hansi, N., Easom, N.J.W., Burton, A.R., Stegmann, K.A., Schurich, A., Swadling, L., Gill, U.S., Male, V., Luong, T., Gander, A., Davidson, B.R., Kennedy, P.T.F., Maini, M.K., 2017. IL-2high tissue-resident T cells in the human liver: Sentinels for hepatotropic infection. J Exp Med 214, 1567–1580. doi:10.1084/jem.20162115
Papadakis, K.A., Prehn, J., Nelson, V., Cheng, L., Binder, S.W., Ponath, P.D., Andrew, D.P., Targan, S.R., 2000. The Role of Thymus-Expressed Chemokine and Its Receptor CCR9 on Lymphocytes in the Regional Specialization of the Mucosal Immune System. J.I. 165, 5069–5076. doi:10.4049/jimmunol.165.9.5069
Papadopoulou, M., Tieppo, P., McGovern, N., Gosselin, F., Chan, J.K.Y., Goetgeluk, G., Dauby, N., Cogan, A., Donner, C., Ginhoux, F., Vandekerckhove, B., Vermijlen, D., 2019. TCR Sequencing Reveals the Distinct Development of Fetal and Adult Human Vγ9Vδ2 T Cells. J. Immunol. ji1900592–16. doi:10.4049/jimmunol.1900592
Park, S.L., Gebhardt, T., Mackay, L.K., 2019. Tissue-Resident Memory T Cells in Cancer Immunosurveillance. Trends in Immunology 40, 735–747. doi:10.1016/j.it.2019.06.002
Parker, M.E., Ciofani, M., 2020. Regulation of γδ T Cell Effector Diversification in the Thymus. Front. Immunol. 11, 435–11. doi:10.3389/fimmu.2020.00042
Patey-Mariaud de Serre, N., Cellier, C., Jabri, B., Delabesse, E., Verkarre, V., Roche, B., Lavergne, A., Brière, J., Mauvieux, L., Leborgne, M., Barbier, J.P., Modigliani, R., Matuchansky, C., Macintyre, E., Cerf-Bensussan, N., Brousse, N., 2001. Distinction between coeliac disease and refractory sprue: a simple immunohistochemical method. Histopathology 37, 70–77. doi:10.1046/j.1365-2559.2000.00926.x
Patil, R.S., Shah, S.U., Shrikhande, S.V., Goel, M., Dikshit, R.P., Chiplunkar, S.V., 2016. IL17 producing γδT cells induce angiogenesis and are associated with poor survival in gallbladder cancer patients. Int. J. Cancer 139, 869–881. doi:10.1002/ijc.30134
Pauza, C.D., Liou, M.-L., Lahusen, T., Xiao, L., Lapidus, R.G., Cairo, C., Li, H., 2018. Gamma Delta T Cell Therapy for Cancer: It Is Good to be Local. Front. Immunol. 9, D208–11. doi:10.3389/fimmu.2018.01305
Penny, H.A., Raju, S.A., Sanders, D.S., 2020. Progress in the serology-based diagnosis and management of adult celiac disease. Expert Review of Gastroenterology & Hepatology 14, 147–154. doi:10.1080/17474124.2020.1725472
Perdomo, C., Zedler, U., Kühl, A.A., Lozza, L., Saikali, P., Sander, L.E., Vogelzang, A., Kaufmann, S.H.E., Kupz, A., 2016. Mucosal BCG Vaccination Induces Protective Lung-Resident Memory T Cell Populations against Tuberculosis. mBio 7, 1173–11. doi:10.1128/mBio.01686-16

Perera, L., Shao, L., Patel, A., Evans, K., Meresse, B., Blumberg, R., Geraghty, D., Groh, V., Spies, T., Jabri, B., Mayer, L., 2007. Expression of nonclassical class I molecules by intestinal epithelial cells. Inflamm Bowel Dis 13, 298–307. doi:10.1002/ibd.20026

Petersen, J., Montserrat, V., Mujico, J.R., Loh, K.L., Beringer, D.X., van Lummel, M., Thompson, A., Mearin, M.L., Schweizer, J., Kooy-Winkelaar, Y., van Bergen, J., Drijfhout, J.W., Kan, W.-T., La Gruta, N.L., Anderson, R.P., Reid, H.H., Koning, F., Rossjohn, J., 2014. T-cell receptor recognition of HLA-DQ2–gliadin complexes associated with celiac disease. Nature Publishing Group 21, 480–488. doi:10.1038/nsmb.2817

Philip, M., Schietinger, A., 2019. ScienceDirect Heterogeneity and fate choice: T cell exhaustion in cancer and chronic infections. Current Opinion in Immunology 58, 98–103. doi:10.1016/j.coi.2019.04.014

Picascia, S., Sidney, J., Camarca, A., Mazzarella, G., Giardullo, N., Greco, L., Auricchio, R., Auricchio, S., Troncone, R., Sette, A., Gianfrani, C., 2017. Gliadin-Specific CD8 +T Cell Responses Restricted by HLA Class I A*0101 and B*0801 Molecules in Celiac Disease Patients. J.I. 1601208–14. doi:10.4049/jimmunol.1601208

Picelli, S., Björklund, Å.K., Faridani, O.R., Sagasser, S., Winberg, G., Sandberg, R., 2013. Smart-seq2 for sensitive full-length transcriptome profiling in single cells. Nat Meth 10, 1096–1098. doi:10.1038/nmeth.2639

Picelli, S., Faridani, O.R., rklund, A.S.K.B.O., Winberg, G.O.S., Sagasser, S., Sandberg, R., 2014. Full-length RNA-seq from single cells using Smart-seq2. Nat Protoc 9, 171–181. doi:10.1038/nprot.2014.006

Pizzolato, G., Kaminski, H., Tosolini, M., Franchini, D.-M., Pont, F., Martins, F., Valle, C., Labourdette, D., Cadot, S., Quillet-Mary, A., Poupot, M., Laurent, C., Ysebaert, L., Meraviglia, S., Dieli, F., Merville, P., Milpied, P., Déchanet-Merville, J., Fournié, J.-J., 2019. Single-cell RNA sequencing unveils the shared and the distinct cytotoxic hallmarks of human TCRVδ1 and TCRVδ2 γδ T lymphocytes. Proc Natl Acad Sci USA 18, 201818488–10. doi:10.1073/pnas.1818488116

Posavad, C.M., Zhao, L., Dong, L., Jin, L., Stevens, C.E., Magaret, A.S., Johnston, C., Wald, A., Zhu, J., Corey, L., Koelle, D.M., 2017. Enrichment of herpes simplex virus type 2 (HSV-2) reactive mucosal T cells in the human female genital tract 10, 1259–1269. doi:10.1038/mi.2016.118

Pré, Du, M F, Kozijn, A.E., van Berkel, L.A., Borg, ter, M.N.D., Kortleve, D.L., Jensen, L.T., Winkelaar, Y.K., Koning, F., Boon, L., Nieuwenhuis, E.E.S., Sollid, L.M., Fugger, L., Samsom, J.N., 2011. Tolerance to Ingested Deamidated Gliadin in Mice is Maintained by Splenic, Type 1 Regulatory T Cells. Gastroenterology 141, 610–620.e2. doi:10.1053/j.gastro.2011.04.048

Pré, du, M Fleur, Blazevski, J., Dewan, A.E., Stamnaes, J., Kanduri, C., Sandve, G.K., Johannesen, M.K., Lindstad, C.B., Hnida, K., Fugger, L., Melino, G., Qiao, S.-W., Sollid, L.M., 2019. B cell tolerance and antibody production to the celiac disease autoantigen transglutaminase 2. J Exp Med 217, 1223–14. doi:10.1084/jem.20190860

Provine, N.M., Amini, A., Garner, L.C., Dold, C., Hutchings, C., FitzPatrick, M.E.B., Reyes, L.S., Chinnakannan, S., Oguti, B., Raymond, M., Capone, S., Folgori, A., Rollier, C.S., Barnes, E., Pollard, A.J., Klenerman, P., 2019. Activation of MAIT cells plays a critical role in viral vector vaccine immunogenicity. bioRxiv 7, 11653–40. doi:10.1101/661397

Provine, N.M., Binder, B., FitzPatrick, M.E.B., Schuch, A., Garner, L.C., Williamson, K.D., van Wilgenburg, B., Thimme, R., Klenerman, P., Hofmann, M., 2018. Unique and Common Features of Innate-Like Human Vδ2+ γδT Cells and Mucosal-Associated Invariant T Cells. Front. Immunol. 9, 120–12. doi:10.3389/fimmu.2018.00756

Provine, N.M., Klenerman, P., 2020. MAIT Cells in Health and Disease. Annu. Rev. Immunol. 38, 203–228. doi:10.1146/annurev-immunol-080719-015428

Qiao, S.-W., Ráki, M., Gunnarsen, K.S., Løset, G.-Å., Lundin, K.E.A., Sandlie, I., Sollid, L.M., 2011. Posttranslational modification of gluten shapes TCR usage in celiac disease. J. Immunol. 187, 3064–3071. doi:10.4049/jimmunol.1101526

Qiao, S.W., Christophersen, A., Lundin, K.E.A., Sollid, L.M., 2014. Biased usage and preferred pairing of - and - chains of TCRs specific for an immunodominant gluten epitope in coeliac disease. Int. Immunol. 26, 13–19. doi:10.1093/intimm/dxt037

Qin, G., Liu, Y., Zheng, J., Xiang, Z., Ng, I.H.Y., Malik Peiris, J.S., Lau, Y.L., Tu, W., 2012. Phenotypic and Functional Characterization of Human T-Cell Subsets in Response to Influenza A Viruses. Journal of Infectious Diseases 205, 1646–1653. doi:10.1093/infdis/jis253

Qiu, D., Tan, W.C., 1999. Dithiothreitol has a dose-response effect on cell surface antigen expression. Journal of Allergy and Clinical Immunology 103, 873–876. doi:10.1385/1-59259-151-5:77.pdf

Qiu, X., Mao, Q., Tang, Y., Wang, L., Chawla, R., Pliner, H.A., Trapnell, C., 2017. Reversed graph embedding resolves complex single-cell trajectories. Nat Meth 14, 979–982. doi:10.1038/nmeth.4402

Quigley, M., Pereyra, F., Nilsson, B., Porichis, F., Fonseca, C., Eichbaum, Q., Julg, B., Jesneck, J.L., Brosnahan, K., Imam, S., Russell, K., Toth, I., Piechocka-Trocha, A., Dolfi, D., Angelosanto, J., Crawford, A., Shin, H., Kwon, D.S., Zupkosky, J., Francisco, L., Freeman, G.J., Wherry, E.J., Kaufmann, D.E., Walker, B.D., Ebert, B., Haining, W.N., 2010. Transcriptional analysis of HIV-specific CD8+ T cells shows that PD-1 inhibits T cell function by upregulating BATF. Nature Medicine 16, 1147–1151. doi:10.1038/nm.2232

Raeber, M.E., Zurbuchen, Y., Impellizzieri, D., Boyman, O., 2018. The role of cytokines in T-cell memory in health and disease. Immunol Rev 283, 176–193. doi:10.1111/imr.12644

Raki, M., Fallang, L.E., Brottveit, M., Bergseng, E., Quarsten, H., Lundin, K.E.A., Sollid, L.M., 2007. Tetramer visualization of gut-homing gluten-specific T cells in the peripheral blood of celiac disease patients. Proc Natl Acad Sci USA 104, 2831–2836. doi:10.1073/pnas.0608610104

Ramírez-Valle, F., Gray, E.E., Cyster, J.G., 2015. Inflammation induces dermal Vγ4 +γδT17 memory-like cells that travel to distant skin and accelerate secondary IL-17–driven responses. Proc Natl Acad Sci USA 112, 8046–8051. doi:10.1073/pnas.1508990112

Ranasinghe, S., Lamothe, P.A., Soghoian, D.Z., Kazer, S.W., Cole, M.B., Shalek, A.K., Yosef, N., Jones, R.B., Donaghey, F., Nwonu, C., Jani, P., Clayton, G.M., Crawford, F., White, J., Montoya, A., Power, K., Allen, T.M., Streeck, H., Kaufmann, D.E., Picker, L.J., Kappler, J.W., Walker, B.D., 2016. Antiviral CD8+ T Cells Restricted by Human Leukocyte Antigen Class II Exist during Natural HIV Infection and Exhibit Clonal Expansion. Immunity 45, 917–930. doi:10.1016/j.immuni.2016.09.015

Rao, U.N.M., Lee, S.J., Luo, W., Mihm, M.C., Jr, Kirkwood, J.M., 2010. Presence of Tumor-Infiltrating Lymphocytes and a Dominant Nodule Within Primary Melanoma Are Prognostic Factors for Relapse-Free Survival of Patients With Thick (T4) Primary Melanoma. Am J Clin Pathol 133, 646–653. doi:10.1309/AJCPTXMEFOVYWDA6

Rast, J.P., Anderson, M.K., Strong, S.J., Luer, C., Litman, R.T., Litman, G.W., 1997. alpha, beta, gamma, and delta T cell antigen receptor genes arose early in vertebrate phylogeny. Immunity 6, 1–11. doi:10.1016/s1074-7613(00)80237-x

Ravens, S., Schultze-Florey, C., Raha, S., Sandrock, I., Drenker, M., Oberdörfer, L., Reinhardt, A., Ravens, I., Beck, M., Geffers, R., Kaisenberg, von, C., Heuser, M., Thol, F., Ganser, A., Förster, R., Koenecke, C., Prinz, I., 2017. Human γδ T cells are quickly reconstituted after stem-cell transplantation and show adaptive clonal expansion in response to viral infection. Nat Immunol 18, 393–401. doi:10.1038/ni.3686

Raverdeau, M., Cunningham, S.P., Harmon, C., Lynch, L., 2019. γδ T cells in cancer: a small population of lymphocytes with big implications. Clin Transl Immunol 8, 10–15. doi:10.1002/cti2.1080

Remes-Troche, J.M., Adames, K., Castillo-Rodal, A.I., Ram rez, T., Barreto-Zu iga, R., L pez-Vidal, Y., Uscanga, L.F., 2007. Intraepithelial gd+ Lymphocytes. journal of clinical gastroenterology 41, 1–6. doi:10.1097/01.mcg.0000247994.34957.ae

Ribas, A., Wolchok, J.D., 2018. Cancer immunotherapy using checkpoint blockade. Science 359, 1350–1355. doi:10.1126/science.aar4060

Ricaño-Ponce, I., Gutierrez-Achury, J., Costa, A.F., Deelen, P., Kurilshikov, A., Zorro, M.M., Platteel, M., Graaf, A., Sugai, E., Moreno, M.L., Vázquez, H., Barrientos, E., Mauriño, E., Talamo, M., Villarruel, A., Sanna, S., Daffra, O., Zhernakova, A., Fu, J., Trynka, G., Smecuol, E., Niveloni, S.I., Bai, J.C., Kumar, V., Wijmenga, C., 2019. Immunochip meta-analysis in European and Argentinian populations identifies two novel genetic loci associated with celiac disease. European Journal of Human Genetics 1–11. doi:10.1038/s41431-019-0520-4

Riddle, M.S., Murray, J.A., Porter, C.K., 2012. The Incidence and Risk of Celiac Disease in a Healthy US Adult Population. The American Journal of Gastroenterology 107, 1248–1255. doi:10.1038/ajg.2012.130

Rigau, M., Ostrouska, S., Fulford, T.S., Johnson, D.N., Woods, K., Ruan, Z., McWilliam, H.E.G., Hudson, C., Tutuka, C., Wheatley, A.K., Kent, S.J., Villadangos, J.A., Pal, B., Kurts, C., Simmonds, J., Pelzing, M., Nash, A.D., Hammet, A., Verhagen, A.M., Vairo, G., Maraskovsky, E., Panousis, C., Gherardin, N.A., Cebon, J., Godfrey, D.I., Behren, A., Uldrich, A.P., 2020. Butyrophilin 2A1 is essential for phosphoantigen reactivity by γδ T cells. Science 367, eaay5516–15. doi:10.1126/science.aay5516

Rincon-Orozco, B., Kunzmann, V., Wrobel, P., Kabelitz, D., Steinle, A., Herrmann, T., 2005. Activation of Vγ9Vδ2 T Cells by NKG2D. J.I. 175, 2144–2151. doi:10.4049/jimmunol.175.4.2144

Risnes, L.F., Christophersen, A., Dahal-Koirala, S., Neumann, R.S., Sandve, G.K., Sarna, V.K., Lundin, K.E.A., Qiao, S.-W., Sollid, L.M., 2018. Disease-driving CD4+ T cell clonotypes persist for decades in celiac disease. J. Clin. Invest. 128, 2642–2650. doi:10.1172/JCI98819

Román, J., Planell, N., Lozano, J.J., Aceituno, M., Esteller, M., Pontes, C., Balsa, D., Merlos, M., Panés, J., Salas, A., 2013. Evaluation of Responsive Gene Expression as a Sensitive and Specific Biomarker in Patients with Ulcerative Colitis. Inflamm Bowel Dis 19, 221–229. doi:10.1002/ibd.23020

Rosati, E., Dowds, C.M., Liaskou, E., Henriksen, E.K.K., Karlsen, T.H., Franke, A., 2017. Overview of methodologies for T-cell receptor repertoire analysis 1–16. doi:10.1186/s12896-017-0379-9

Roy, S., Ly, D., Castro, C.D., Li, N.-S., Hawk, A.J., Altman, J.D., Meredith, S.C., Piccirilli, J.A., Moody, D.B., Adams, E.J., 2016. Molecular Analysis of Lipid-Reactive Vδ1 γδ T Cells Identified by CD1c Tetramers. J.I. 196, 1933–1942. doi:10.4049/jimmunol.1502202

Rubio Tapia, A., Kyle, R.A., Kaplan, E.L., Johnson, D.R., Page, W., Erdtmann, F., Brantner, T.L., Kim, W.R., Phelps, T.K., Lahr, B.D., Zinsmeister, A.R., Melton, L.J., III, Murray, J.A., 2009. Increased Prevalence and Mortality in Undiagnosed Celiac Disease. Gastroenterology 137, 88–93. doi:10.1053/j.gastro.2009.03.059

Ryan, P.L., Sumaria, N., Holland, C.J., Bradford, C.M., Izotova, N., Grandjean, C.L., Jawad, A.S., Bergmeier, L.A., Pennington, D.J., 2016. Heterogeneous yet stable Vδ2 (+)T-cell profiles define distinct cytotoxic effector potentials in healthy human individuals. Proc Natl Acad Sci USA 113, 14378–14383. doi:10.1073/pnas.1611098113

Safaee, M., Clark, A.J., Ivan, M.E., Oh, M.C., Bloch, O., Sun, M.Z., Oh, T., Parsa, A.T., 2013. CD97 is a multifunctional leukocyte receptor with distinct roles in human cancers. International Journal of Oncology 43, 1343–1350. doi:10.3892/ijo.2013.2075

Sagar, Pokrovskii, M., Herman, J.S., Naik, S., Sock, E., Zeis, P., Lausch, U., Wegner, M., Tanriver, Y., Littman, D.R., Grün, D., 2020. Deciphering the regulatory landscape of fetal and adult γδ T-cell development at single-cell resolution. EMBO J 39, 4244–20. doi:10.15252/embj.2019104159

Salmi, T.T., Collin, P., Korponay-Szabo, I.R., Laurila, K., Partanen, J., Huhtala, H., Kiraly, R., Lorand, L., Reunala, T., Mäki, M., Kaukinen, K., 2006. Endomysial antibody-negative coeliac disease: clinical characteristics and intestinal autoantibody deposits. Gut 55, 1746–1753. doi:10.1136/gut.2005.071514

Salvati, V.M., MacDonald, T.T., Del Vecchio Blanco, G., Mazzarella, G., Monteleone, I., Vavassori, P., Auricchio, S., Pallone, F., Troncone, R., Monteleone, G., 2003. Enhanced Expression of Interferon Regulatory Factor-1 in the Mucosa of Children with Celiac Disease. Pediatr Res 54, 312–318. doi:10.1203/01.PDR.0000079184.70237.9C

Sancho, D., Gómez, M., Sánchez-Madrid, F., 2005. CD69 is an immunoregulatory molecule induced following activation. Trends in Immunology 26, 136–140. doi:10.1016/j.it.2004.12.006

Sant, S., Jenkins, M.R., Dash, P., Watson, K.A., Wang, Z., Pizzolla, A., Koutsakos, M., Nguyen, T.H., Lappas, M., Crowe, J., Loudovaris, T., Mannering, S.I., Westall, G.P., Kotsimbos, T.C., Cheng, A.C., Wakim, L., Doherty, P.C., Thomas, P.G., Loh, L., Kedzierska, K., 2019. Human γδ T-cell receptor repertoire is shaped by influenza viruses, age and tissue compartmentalisation. Clin Transl Immunol 8, 1–17. doi:10.1002/cti2.1079

Sarna, V.K., Lundin, K.E.A., Mørkrid, L., Qiao, S.-W., Sollid, L.M., Christophersen, A., 2018a. HLA-DQ-Gluten Tetramer Blood Test Accurately Identifies Patients With and Without Celiac Disease in Absence of Gluten Consumption. Gastroenterology 154, 886–896.e6. doi:10.1053/j.gastro.2017.11.006

Sarna, V.K., Skodje, G.I., Reims, H.M., Risnes, L.F., Dahal-Koirala, S., Sollid, L.M., Lundin, K.E.A., 2018b. HLA-DQ:gluten tetramer test in blood gives better detection of coeliac patients than biopsy after 14-day gluten challenge. Gut 67, 1606–1613. doi:10.1136/gutjnl-2017-314461

Sasson, S.C., Gordon, C.L., Christo, S.N., Klenerman, P., Mackay, L.K., 2020. Local heroes or villains: tissue-resident memory T cells in human health and disease. Cell Mol Immunol 1–10. doi:10.1038/s41423-019-0359-1

Satija, R., Farrell, J.A., Gennert, D., Schier, A.F., Regev, A., 2015. Spatial reconstruction of single-cell gene expression data. Nat Biotechnol 33, 495–502. doi:10.1038/nbt.3192

Sattler, A., Dang-Heine, C., Reinke, P., Babel, N., 2015. IL-15 dependent induction of IL-18 secretion as a feedback mechanism controlling human MAIT-cell effector functions. Eur. J. Immunol. 45, 2286–2298. doi:10.1002/eji.201445313

Savage, A.K., Constantinides, M.G., Han, J., Picard, D., Martin, E., Li, B., Lantz, O., Bendelac, A., 2008. The Transcription Factor PLZF Directs the Effector Program of the NKT Cell Lineage. Immunity 29, 391–403. doi:10.1016/j.immuni.2008.07.011

Sánchez-Castañon, M., Castro, B.G., Toca, M., Santacruz, C., Arias-Loste, M., Iruzubieta, P., Crespo, J., López-Hoyos, M., 2016. Intraepithelial lymphocytes subsets in different forms of celiac disease. Autoimmunity Highlights 1–7. doi:10.1007/s13317-016-0085-y

Schenkel, J.M., Fraser, K.A., Beura, L.K., Pauken, K.E., Vezys, V., Masopust, D., 2014. Resident memory CD8 T cells trigger protective innate and adaptive immune responses. Science 346, 98–101. doi:10.1126/science.1254536

Schiepatti, A., Savioli, J., Vernero, M., Borrelli de Andreis, F., Perfetti, L., Meriggi, A., Biagi, F., 2020. Pitfalls in the Diagnosis of Coeliac Disease and Gluten-Related Disorders. Nutrients 12, 1711–18. doi:10.3390/nu12061711

Schreurs, R.R.C.E., Drewniak, A., Bakx, R., Corpeleijn, W.E., Geijtenbeek, T.H.B., van Goudoever, J.B., Bunders, M.J., 2017. Quantitative comparison of human intestinal mononuclear leukocyte isolation techniques for flow cytometric analyses. Journal of Immunological Methods 445, 45–52. doi:10.1016/j.jim.2017.03.006

Selby, W.S., Janossy, G., Bofill, M., Jewell, D.P., 1983. Lymphocyte subpopulations in the human small intestine. The findings in normal mucosa and in the mucosa of patients with adult coeliac disease. Clinical & Experimental Immunology 52, 219–228.

Setty, M., Discepolo, V., Abadie, V., Kamhawi, S., Mayassi, T., Kent, A., Ciszewski, C., Maglio, M., Kistner, E., Bhagat, G., Semrad, C., Kupfer, S.S., Green, P.H., Guandalini, S., Troncone, R., Murray, J.A., Turner, J.R., Jabri, B., 2015. Distinct and Synergistic Contributions of Epithelial Stress and Adaptive Immunity to Functions of Intraepithelial Killer Cells and Active Celiac Disease. Gastroenterology 149, 681–691.e10. doi:10.1053/j.gastro.2015.05.013

Shan, L., Molberg, Ø., Parrot, I., Hausch, F., Filiz, F., Gray, G.M., Sollid, L.M., Khosla, C., 2002. Structural Basis for Gluten Intolerance in Celiac Sprue. Science 297, 2275–6. doi:10.1126/science.1074129

Shen, C., Xu, H., Alvarez, X., Lackner, A.A., Veazey, R.S., Wang, X., 2015. Reduced Expression of CD27 by Collagenase Treatment: Implications for Interpreting B Cell Data in Tissues. PLoS ONE 10, e0116667–11. doi:10.1371/journal.pone.0116667

Shen, H., Gu, J., Xiao, H., Liang, S., Yang, E., Yang, R., Huang, D., Chen, C., Wang, F., Shen, L., Chen, Z.W., 2016. Selective Destruction of Interleukin 23–Induced Expansion of a Major Antigen–Specific γδ T-Cell Subset in Patients With Tuberculosis. Journal of Infectious Diseases 296, jiw511–11. doi:10.1093/infdis/jiw511

Sheridan, B.S., Pham, Q.-M., Lee, Y.-T., Cauley, L.S., Puddington, L., Lefrançois, L., 2014. Oral Infection Drives a Distinct Population of Intestinal Resident Memory CD8+ T Cells with Enhanced Protective Function. Immunity 40, 747–757. doi:10.1016/j.immuni.2014.03.007

Sheridan, B.S., Romagnoli, P.A., Pham, Q.-M., Fu, H.-H., Alonzo, F., III, Schubert, W.-D., Freitag, N.E., Lefrançois, L., 2013. γδ T Cells Exhibit Multifunctional and Protective Memory in Intestinal Tissues. Immunity 39, 184–195. doi:10.1016/j.immuni.2013.06.015

Shiow, L.R., Rosen, D.B., Brdičková, N., Xu, Y., An, J., Lanier, L.L., Cyster, J.G., Matloubian, M., 2006. CD69 acts downstream of interferon-α/β to inhibit S1P1 and lymphocyte egress from lymphoid organs. Nature 440, 540–544. doi:10.1038/nature04606

Shugay, M., Bagaev, D.V., Turchaninova, M.A., Bolotin, D.A., Britanova, O.V., Putintseva, E.V., Pogorelyy, M.V., Nazarov, V.I., Zvyagin, I.V., Kirgizova, V.I., Kirgizov, K.I., Skorobogatova, E.V., Chudakov, D.M., 2015. VDJtools: Unifying Post-analysis of T Cell Receptor Repertoires. PLoS Comput Biol 11, e1004503–16. doi:10.1371/journal.pcbi.1004503

Sing, T., Sander, O., Beerenwinkel, N., Lengauer, T., 2005. ROCR: visualizing classifier performance in R. Bioinformatics 21, 3940–3941. doi:10.1093/bioinformatics/bti623

Singh, P., Arora, A., Strand, T.A., Leffler, D.A., Catassi, C., Green, P.H., Kelly, C.P., Ahuja, V., Makharia, G.K., 2018. Global Prevalence of Celiac Disease: Systematic Review and Meta-analysis. Clinical Gastroenterology and Hepatology 16, 823–836.e2. doi:10.1016/j.cgh.2017.06.037

Skon, C.N., Lee, J.-Y., Anderson, K.G., Masopust, D., Hogquist, K.A., Jameson, S.C., 2013. Transcriptional downregulation of S1pr1 is required for the establishment of resident memory CD8+ T cells. Nat Immunol 1–11. doi:10.1038/ni.2745

Slütter, B., Van Braeckel-Budimir, N., Abboud, G., Varga, S.M., Salek-Ardakani, S., Harty, J.T., 2017. Dynamics of influenza-induced lung-resident memory T cells underlie waning heterosubtypic immunity. Science Immunology 2, eaag2031–12. doi:10.1126/sciimmunol.aag2031

Smith, N.M., Wasserman, G.A., Coleman, F.T., Hilliard, K.L., Yamamoto, K., Lipsitz, E., Malley, R., Dooms, H., Jones, M.R., Quinton, L.J., Mizgerd, J.P., 2017. Regionally compartmentalized resident memory T cells mediate naturally acquired protection against pneumococcal pneumonia. Mucosal Immunology 11, 220–235. doi:10.1038/mi.2017.43

Snir, O., Kanduri, C., Lundin, K.E.A., Sandve, G.K., Sollid, L.M., 2019. Transcriptional profiling of human intestinal plasma cells reveals effector functions beyond antibody production. United European Gastroenterology Journal 7, 1399–1407. doi:10.1177/2050640619862461

Snyder, M.E., Finlayson, M.O., Connors, T.J., Dogra, P., Senda, T., Bush, E., Carpenter, D., Marboe, C., Benvenuto, L., Shah, L., Robbins, H., Hook, J.L., Sykes, M., D'Ovidio, F., Bacchetta, M., Sonett, J.R., Lederer, D.J., Arcasoy, S., Sims, P.A., Farber, D.L., 2019. Generation and persistence of human tissue-resident memory T cells in lung transplantation. Sci. Immunol. 4, eaav5581–17. doi:10.1126/sciimmunol.aav5581

Sollid, L.M., Markussen, G., Ek, J., Gjerde, H., Vartdal, F., Thorsby, E., 1989. Evidence for a primary association of celiac disease to a particular HLA-DQ alpha/beta heterodimer. J Exp Med 169, 345–350. doi:10.1084/jem.169.1.345

Sollid, L.M., Qiao, S.-W., Anderson, R.P., Gianfrani, C., Koning, F., 2012. Nomenclature and listing of celiac disease relevant gluten T-cell epitopes restricted by HLA-DQ molecules. Immunogenetics 64, 455–460. doi:10.1007/s00251-012-0599-z

Spitzer, M.H., Nolan, G.P., 2016. Mass Cytometry: Single Cells, Many Features. Cell 165, 780–791. doi:10.1016/j.cell.2016.04.019

Sridhar, S., Begom, S., Bermingham, A., Hoschler, K., Adamson, W., Carman, W., Bean, T., Barclay, W., Deeks, J.J., Lalvani, A., 2019. Cellular immune correlates of protection against symptomatic pandemic influenza. Nature Medicine 1–9. doi:10.1038/nm.3350

Steenholt, J.V., Nielsen, C., Baudewijn, L., Staal, A., Rasmussen, K.S., Sabir, H.J., Barington, T., Husby, S., Toft-Hansen, H., 2017. The composition of T cell subtypes in duodenal biopsies are altered in coeliac disease patients. PLoS ONE 12, e0170270–17. doi:10.1371/journal.pone.0170270

Steinert, E.M., Schenkel, J.M., Fraser, K.A., Beura, L.K., Manlove, L.S., Igyártó, B.Z., Southern, P.J., Masopust, D., 2015. Quantifying Memory CD8 T Cells Reveals Regionalization of Immunosurveillance. Cell 161, 737–749. doi:10.1016/j.cell.2015.03.031

Stelma, F., de Niet, A., Sinnige, M.J., van Dort, K.A., van Gisbergen, K.P.J.M., Verheij, J., van Leeuwen, E.M.M., Kootstra, N.A., Reesink, H.W., 2017. Human intrahepatic CD69 + CD8+ T cells have a tissue resident memory T cell phenotype with reduced cytolytic capacity. Sci Rep 1–10. doi:10.1038/s41598-017-06352-3

Stene, L.C., Honeyman, M.C., Hoffenberg, E.J., Haas, J.E., Sokol, R.J., Emery, L., Taki, I., Norris, J.M., Erlich, H.A., Eisenbarth, G.S., Rewers, M., 2006. Rotavirus Infection Frequency and Risk of Celiac Disease Autoimmunity in Early Childhood: A Longitudinal Study. The American Journal of Gastroenterology 101, 2333–2340. doi:10.1111/j.1572-0241.2006.00741.x

Stoeckius, M., Hafemeister, C., Stephenson, W., Houck-Loomis, B., Chattopadhyay, P.K., Swerdlow, H., Satija, R., Smibert, P., 2017. Simultaneous epitope and transcriptome measurement in single cells. Nat Meth 14, 865–868. doi:10.1038/nmeth.4380

Strauss, W., Quertermous, T., Seidman, J., 1987. Measuring the human T cell receptor gamma-chain locus. Science 237, 1217–1219. doi:10.1126/science.3498213

Stuart, T., Butler, A., Hoffman, P., Hafemeister, C., Papalexi, E., Mauck, W.M., Mauck, W.M., III, Hao, Y., Stoeckius, M., Smibert, P., Satija, R., 2019. Comprehensive Integration of Single-Cell Data. Cell 177, 1888–1902.e21. doi:10.1016/j.cell.2019.05.031

Stubbington, M.J.T., Lönnberg, T., Proserpio, V., Clare, S., Speak, A.O., Dougan, G., Teichmann, S.A., 2016. T cell fate and clonality inference from single-cell transcriptomes. Nat Meth 13, 329–332. doi:10.1038/nmeth.3800

Subramanian, A., Tamayo, P., Mootha, V.K., Mukherjee, S., Ebert, B.L., Gillette, M.A., Paulovich, A., Pomeroy, S.L., Golub, T.R., Lander, E.S., Mesirov, J.P., 2005. Gene set enrichment analysis: A knowledge-based approach for interpreting genome-wide expression profiles. Proc Natl Acad Sci USA 102, 15545–15550. doi:10.1073/pnas.0506580102

Szabo, P.A., Miron, M., Farber, D.L., 2019. Location, location, location: Tissue resident memory T cells in mice and humans. Science Immunology 4, 1–12. doi:10.1126/sciimmunol.aas9673

Taavela, J., Koskinen, O., Huhtala, H., Lähdeaho, M.-L., Popp, A., Laurila, K., Collin, P., Kaukinen, K., Kurppa, K., Mäki, M., 2013. Validation of Morphometric Analyses of Small-Intestinal Biopsy Readouts in Celiac Disease. PLoS ONE 8, e76163–8. doi:10.1371/journal.pone.0076163

Tack, G.J., 2011. Evaluation of Cladribine treatment in refractory celiac disease type II. WJG 17, 506–8. doi:10.3748/wjg.v17.i4.506

Tack, G.J., Wondergem, M.J., Al-Toma, A., Verbeek, W.H.M., Schmittel, A., Machado, M.V., Perri, F., Ossenkoppele, G.J., Huijgens, P.C., Schreurs, M.W.J., Mulder, C.J.J., Visser, O.J., 2011. Auto-SCT in refractory celiac disease type II patients unresponsive to cladribine therapy. Bone Marrow Transplantation 46, 840–846. doi:10.1038/bmt.2010.199

Tai, J.H., Williams, J.V., Edwards, K.M., Wright, P.F., Crowe, J.E., Jr, Dermody, T.S., 2005. Prevalence of Reovirus-Specific Antibodies in Young Children in Nashville, Tennessee. Journal of Infectious Diseases 191, 1221–1224. doi:10.1086/428911

Tan, L., Fichtner, A.S., Bubke, A., Odak, I., Schultze-Florey, C., Koenecke, C., Förster, R., Jarek, M., Kaisenberg, von, C., Borchers, A., Panzer, U., Krebs, C., Ravens, S., Prinz, I., 2020. A fetal wave of human type-3 γδ T cells with restricted TCR diversity persists into adulthood 19, 169–29. doi:10.1101/2020.08.14.248146

Tan, L., Sandrock, I., Odak, I., Aizenbud, Y., Wilharm, A., Barros-Martins, J., Tabib, Y., Borchers, A., Amado, T., Gangoda, L., Herold, M.J., Schmidt-Supprian, M., Kisielow, J., Silva-Santos, B., Koenecke, C., Hovav, A.-H., Krebs, C., Prinz, I., Ravens, S., 2019. Single-Cell Transcriptomics Identifies the Adaptation of Scart1+ Vγ6+ T Cells to Skin Residency as Activated Effector Cells. CellReports 27, 3657–3671.e4. doi:10.1016/j.celrep.2019.05.064

Thome, J.J.C., Yudanin, N., Ohmura, Y., Kubota, M., Grinshpun, B., Sathaliyawala, T., Kato, T., Lerner, H., Shen, Y., Farber, D.L., 2014. Spatial Map of Human T Cell Compartmentalization and Maintenance over Decades of Life. Cell 159, 814–828. doi:10.1016/j.cell.2014.10.026

Thompson, K., Rojas-Navea, J., Rogers, M.J., 2006. Alkylamines cause Vγ9Vδ2 T-cell activation and proliferation by inhibiting the mevalonate pathway. Blood 107, 651–654. doi:10.1182/blood-2005-03-1025

Tilloy, F., Treiner, E., Park, S.-H., Garcia, C., Lemonnier, F., la Salle, de, H., Bendelac, A., Bonneville, M., Lantz, O., 1999. An Invariant T Cell Receptor α Chain Defines a Novel TAP-independent Major Histocompatibility Complex Class Ib–restricted α/β T Cell Subpopulation in Mammals. J Exp Med 189, 1907–15. doi:10.1084/jem.189.12.1907

Truitt, K.E., Anderson, R.P., 2019. Editorial: a non-dietary treatment for coeliac disease-two steps forward, one step back? Authors' reply. Aliment Pharmacol Ther 50, 956–957. doi:10.1111/apt.15494

Truitt, K.E., Daveson, A.J.M., Ee, H.C., Goel, G., MacDougall, J., Neff, K., Anderson, R.P., 2019. Randomised clinical trial: a placebo-controlled study of subcutaneous or intradermal NEXVAX2, an investigational immunomodulatory peptide therapy for coeliac disease. Aliment Pharmacol Ther 50, 547–555. doi:10.1111/apt.15435

Trynka, G., Hunt, K.A., Bockett, N.A., Romanos, J., Mistry, V., Szperl, A., Bakker, S.F., Bardella, M.T., Bhaw-Rosun, L., Castillejo, G., la Concha, de, E.G., de Almeida, R.C., Dias, K.-R.M., van Diemen, C.C., Dubois, P.C.A., Duerr, R.H., Edkins, S., Franke, L., Fransen, K., Gutierrez, J., Heap, G.A.R., Hrdlickova, B., Hunt, S., Izurieta, L.P., Izzo, V., Joosten, L.A.B., Langford, C., Mazzilli, M.C., Mein, C.A., Midah, V., Mitrovic, M., Mora, B., Morelli, M., Nutland, S., Núñez, C., Onengut-Gumuscu, S., Pearce, K., Platteel, M., Polanco, I., Potter, S., Ribes-Koninckx, C., Ricaño-Ponce, I., Rich, S.S., Rybak, A., Santiago, J.L., Senapati, S., Sood, A., Szajewska, H., Troncone, R., Varadé, J., Wallace, C., Wolters, V.M., Zhernakova, A., Thelma, B.K., Cukrowska, B., Urcelay, E., Bilbao, J.R., Mearin, M.L., Barisani, D., Barrett, J.C., Plagnol, V., Deloukas, P., Wijmenga, C., van Heel, D.A., 2011. Dense genotyping identifies and localizes multiple common and rare variant association signals in celiac disease. Nature Publishing Group 43, 1193–1201. doi:10.1038/ng.998

Trzupek, D., Dunstan, M., Cutler, A.J., Lee, M., Godfrey, L., Jarvis, L., Rainbow, D.B., Aschenbrenner, D., Jones, J.L., Uhlig, H.H., Wicker, L.S., Todd, J.A., Ferreira, R.C., 2020. Discovery of CD80 and CD86 as recent activation markers on regulatory T cells by protein-RNA single-cell analysis 1–22. doi:10.1186/s13073-020-00756-z

Tsai, C.-Y., Liong, K.H., Gunalan, M.G., Li, N., Lim, D.S.L., Fisher, D.A., MacAry, P.A., Leo, Y.S., Wong, S.-C., Puan, K.J., Wong, S.B.J., 2015. Type I IFNs and IL-18 Regulate the Antiviral Response of Primary Human γδ T Cells against Dendritic Cells Infected with Dengue Virus. J.I. 194, 3890–3900. doi:10.4049/jimmunol.1303343

Tung, P.-Y., Blischak, J.D., Hsiao, C.J., Knowles, D.A., Burnett, J.E., Pritchard, J.K., Gilad, Y., 2016. Batch effects and the effective design of single-cell gene expression studies. Sci Rep 1–15. doi:10.1038/srep39921

Turner, D.L., Bickham, K.L., Thome, J.J., Kim, C.Y., Ovidio, F.D.A., Wherry, E.J., Farber, D.L., 2019. Lung niches for the generation and maintenance of tissue-resident memory T cells 1–10. doi:10.1038/mi.2013.67

Tye-Din, J.A., Daveson, A.J.M., Ee, H.C., Goel, G., MacDougall, J., Acaster, S., Goldstein, K.E., Dzuris, J.L., Neff, K.M., Truitt, K.E., Anderson, R.P., 2019. Elevated serum interleukin-2 after gluten correlates with symptoms and is a potential diagnostic biomarker for coeliac disease. Aliment Pharmacol Ther 50, 901–910. doi:10.1111/apt.15477

Tyler, C.J., McCarthy, N.E., Lindsay, J.O., Stagg, A.J., Moser, B., Eberl, M., 2017. Antigen-Presenting Human γδ T Cells Promote Intestinal CD4 +T Cell Expression of IL-22 and Mucosal Release of Calprotectin. J.I. 1700003–15. doi:10.4049/jimmunol.1700003

Unalp-Arida, A., Ruhl, C.E., Choung, R.S., Brantner, T.L., Murray, J.A., 2017. Lower Prevalence of Celiac Disease and Gluten-Related Disorders in Persons Living in Southern vs Northern Latitudes of the United States. Gastroenterology 152, 1922–1932.e2. doi:10.1053/j.gastro.2017.02.012

Ussher, J.E., Bilton, M., Attwod, E., Shadwell, J., Richardson, R., de Lara, C., Mettke, E., Kurioka, A., Hansen, T.H., Klenerman, P., Willberg, C.B., 2013. CD161 ++CD8 +T cells, including the MAIT cell subset, are specifically activated by IL-12+IL-18 in a TCR-independent manner. Eur. J. Immunol. 44, 195–203. doi:10.1002/eji.201343509

Uusitalo, U., Andren Aronsson, C., Liu, X., Kurppa, K., Yang, J., Liu, E., Skidmore, J., Winkler, C., Rewers, M., Hagopian, W., She, J.-X., Toppari, J., Ziegler, A.-G., Akolkar, B., Norris, J., Virtanen, S., Krischer, J., Agardh,

D., on behalf of the TEDDY Study Group, 2019. Early Probiotic Supplementation and the Risk of Celiac Disease in Children at Genetic Risk. Nutrients 11, 1790–14. doi:10.3390/nu11081790
van Berge Henegouwen, G.P., Mulder, C.J., 1993. Pioneer in the gluten free diet: Willem-Karel Dicke 1905-1962, over 50 years of gluten free diet. Gut 34, 1473–1475. doi:10.1136/gut.34.11.1473
Van Damme, N., Baeten, D., De Vos, M., Demetter, P., Elewaut, D., Mielants, H., Verbruggen, G., Cuvelier, C., Veys, E.M., De Keyser, F., 2000. Chemical agents and enzymes used for the extraction of gut lymphocytes influence flow cytometric detection of T cell surface markers. Journal of Immunological Methods 236, 27–35.
Van de Sande, B., Flerin, C., Davie, K., De Waegeneer, M., Hulselmans, G., Aibar, S., Seurinck, R., Saelens, W., Cannoodt, R., Rouchon, Q., Verbeiren, T., De Maeyer, D., Reumers, J., Saeys, Y., Aerts, S., 2020. A scalable SCENIC workflow for single-cell gene regulatory network analysis. Nat Protoc 1–32. doi:10.1038/s41596-020-0336-2
van de Water, J.M.W., Cillessen, S.A.G.M., Visser, O.J., Verbeek, W.H.M., Meijer, C.J.L.M., Mulder, C.J.J., 2010. Enteropathy associated T-cell lymphoma and its precursor lesions. Best Practice & Research Clinical Gastroenterology 24, 43–56. doi:10.1016/j.bpg.2009.11.002
van den Broek, T., Borghans, J.A.M., van Wijk, F., 2018. The full spectrum of human naive T cells. Nat Rev Immunol 1–11. doi:10.1038/s41577-018-0001-y
van Gils, T., Nijeboer, P., van Wanrooij, R.L., Bouma, G., Mulder, C.J.J., 2015. Mechanisms and management of refractory coeliac disease. Nature Publishing Group 12, 572–579. doi:10.1038/nrgastro.2015.155
van Wanrooij, R.L.J., Schreurs, M.W.J., Bouma, G., Blomberg, von, B.M.E., Tack, G.J., Verbeek, W.H.M., Mulder, C.J.J., 2010. Accurate classification of RCD requires flow cytometry. Gut 59, 1732–1732. doi:10.1136/gut.2010.223438
van Wilgenburg, B., Scherwitzl, I., Hutchinson, E.C., Leng, T., Kurioka, A., Kulicke, C., de Lara, C., Cole, S., Vasanawathana, S., Limpitikul, W., Malasit, P., Young, D., Denney, L., Moore, M.D., Fabris, P., Giordani, M.T., Oo, Y.H., Laidlaw, S.M., Dustin, L.B., Ho, L.-P., Thompson, F.M., Ramamurthy, N., Willberg, C.B., Screaton, G.R., Barnes, E., Ball, J., Burgess, G., Cooke, G., Dillon, J., Gore, C., Foster, G., Guha, N., Halford, R., Herath, C., Holmes, C., Howe, A., Hudson, E., Irving, W., Khakoo, S., Koletzki, D., Martin, N., Mbisa, T., McKeating, J., McLauchlan, J., Miners, A., Murray, A., Shaw, P., Simmonds, P., Spencer, C., Targett-Adams, P., Thomson, E., Vickerman, P., Zitzmann, N., Mongkolsapaya, J., Klenerman, P., 2016. MAIT cells are activated during human viral infections. Nature Communications 7, 1–11. doi:10.1038/ncomms11653
Vantourout, P., Laing, A., Woodward, M.J., Zlatareva, I., Apolonia, L., Jones, A.W., Snijders, A.P., Malim, M.H., Hayday, A.C., 2018. Heteromeric interactions regulate butyrophilin (BTN) and BTN-like molecules governing γδ T cell biology. Proc Natl Acad Sci USA 115, 1039–1044. doi:10.1073/pnas.1701237115
Venken, K., Jacques, P., Mortier, C., Labadia, M.E., Decruy, T., Coudenys, J., Hoyt, K., Wayne, A.L., Hughes, R., Turner, M., Van Gassen, S., Martens, L., Smith, D., Harcken, C., Wahle, J., Wang, C.-T., Verheugen, E., Schryvers, N., Varkas, G., Cypers, H., Wittoek, R., Piette, Y., Gyselbrecht, L., Van Calenbergh, S., Van den Bosch, F., Saeys, Y., Nabozny, G., Elewaut, D., 2018. RORÎ³t inhibition selectively targets IL-17 producing iNKT and Î³Î´-T cells enriched in Spondyloarthritis patients. Nature Communications 1–15. doi:10.1038/s41467-018-07911-6
Verbeek, W.H.M., Goerres, M.S., Blomberg, von, B.M.E., Oudejans, J.J., Scholten, P.E.T., Hadithi, M., Al-Toma, A., Schreurs, M.W.J., Mulder, C.J.J., 2008. Flow cytometric determination of aberrant intra-epithelial lymphocytes predicts T-cell lymphoma development more accurately than T-cell clonality analysis in Refractory Celiac Disease. Clinical Immunology 126, 48–56. doi:10.1016/j.clim.2007.09.002
Verma, N.K., Dempsey, E., Long, A., Davies, A., Barry, S.P., Fallon, P.G., Volkov, Y., Kelleher, D., 2012. Leukocyte Function-associated Antigen-1/Intercellular Adhesion Molecule-1 Interaction Induces a Novel Genetic Signature Resulting in T-cells Refractory to Transforming Growth Factor-β Signaling. Journal of Biological Chemistry 287, 27204–27216. doi:10.1074/jbc.M112.376616
Vermijlen, D., Ellis, P., Langford, C., Klein, A., Engel, R., Willimann, K., Jomaa, H., Hayday, A.C., Eberl, M., 2007. Distinct cytokine-driven responses of activated blood gammadelta T cells: insights into unconventional T cell pleiotropy. J.I. 178, 4304–4314. doi:10.4049/jimmunol.178.7.4304
Vermijlen, D., Gatti, D., Kouzeli, A., Rus, T., Eberl, M., 2018. γδ T cell responses: How many ligands will it take till we know? Seminars in Cell and Developmental Biology 1–12. doi:10.1016/j.semcdb.2017.10.009
Walrath, J., Zukowski, L., Krywiak, A., Silver, R.F., 2005. Resident Th1-Like Effector Memory Cells in Pulmonary Recall Responses to Mycobacterium tuberculosis. Am J Respir Cell Mol Biol 33, 48–55. doi:10.1165/rcmb.2005-0060OC

Walsh, D.A., Borges da Silva, H., Beura, L.K., Peng, C., Hamilton, S.E., Masopust, D., Jameson, S.C., 2019. The Functional Requirement for CD69 in Establishment of Resident Memory CD8 +T Cells Varies with Tissue Location. J.I. 203, 946–955. doi:10.4049/jimmunol.1900052

Walters, L.C., Harlos, K., Brackenridge, S., Rozbesky, D., Barrett, J.R., Jain, V., Walter, T.S., O'Callaghan, C.A., Borrow, P., Toebes, M., Hansen, S.G., Sacha, J.B., Abdulhaqq, S., Greene, J.M., Früh, K., Marshall, E., Picker, L.J., Jones, E.Y., McMichael, A.J., Gillespie, G.M., 2018. Pathogen-derived HLA-E bound epitopes reveal broad primary anchor pocket tolerability and conformationally malleable peptide binding. Nature Communications 1–13. doi:10.1038/s41467-018-05459-z

Wang, Chuanwu, Thangamani, S., Kim, M., Gu, B.-H., Lee, J.H., Taparowsky, E.J., Kim, C.H., 2013. BATF is required for normal expression of gut-homing receptors by T helper cells in response to retinoic acid. J Exp Med 210, 475–489. doi:10.1084/jem.20121088

Wang, Chunlin, Sanders, C.M., Yang, Q., Schroeder, H.W., Wang, E., Babrzadeh, F., Gharizadeh, B., Myers, R.M., Hudson, J.R., Davis, R.W., Han, J., 2010. High throughput sequencing reveals a complex pattern of dynamic interrelationships among human T cell subsets. Proc. Natl. Acad. Sci. U.S.A. 107, 1518–1523. doi:10.1073/pnas.0913939107

Watanabe, N., Gavrieli, M., Sedy, J.R., Yang, J., Fallarino, F., Loftin, S.K., Hurchla, M.A., Zimmerman, N., Sim, J., Zang, X., Murphy, T.L., Russell, J.H., Allison, J.P., Murphy, K.M., 2003. BTLA is a lymphocyte inhibitory receptor with similarities to CTLA-4 and PD-1. Nat Immunol 4, 670–679. doi:10.1038/ni944

Watanabe, R., Gehad, A., Yang, C., Scott, L.L., Teague, J.E., Schlapbach, C., Elco, C.P., Huang, V., Matos, T.R., Kupper, T.S., Clark, R.A., 2015. Human skin is protected by four functionally and phenotypically discrete populations of resident and recirculating memory T cells. Science Translational Medicine 7, 279ra39–279ra39. doi:10.1126/scitranslmed.3010302

Webb, J.R., Milne, K., Watson, P., deLeeuw, R.J., Nelson, B.H., 2014. Tumor-Infiltrating Lymphocytes Expressing the Tissue Resident Memory Marker CD103 Are Associated with Increased Survival in High-Grade Serous Ovarian Cancer. Clin Cancer Res 20, 434.

Wei, C., Jung, J., Sanz, I., 2011. OMIP-003: Phenotypic analysis of human memory B cells. Cytometry 79A, 894–896. doi:10.1002/cyto.a.21112

Weisberg, S.P., Carpenter, D.J., Chait, M., Dogra, P., Gartrell-Corrado, R.D., Chen, A.X., Campbell, S., Liu, W., Saraf, P., Snyder, M.E., Kubota, M., Danzl, N.M., Schrope, B.A., Rabadan, R., Saenger, Y., Chen, X., Farber, D.L., 2019. Tissue-Resident Memory T Cells Mediate Immune Homeostasis in the Human Pancreas through the PD-1/PD-L1 Pathway. Cell Reports 29, 3916–3932.e5. doi:10.1016/j.celrep.2019.11.056

Welch, J.D., Kozareva, V., Ferreira, A., Vanderburg, C., Martin, C., Macosko, E.Z., 2019. Single-Cell Multi-omic Integration Compares and Contrasts Features of Brain Cell Identity. Cell 177, 1873–1887.e17. doi:10.1016/j.cell.2019.05.006

Wendt, E., White, G.E., Ferry, H., Huhn, M., Greaves, D.R., Keshav, S., 2016. Glucocorticoids Suppress CCR9-Mediated Chemotaxis, Calcium Flux, and Adhesion to MAdCAM-1 in Human T Cells. J.I. 196, 3910–3919. doi:10.4049/jimmunol.1500619

West, J., Fleming, K.M., Tata, L.J., Card, T.R., Crooks, C.J., 2014. Incidence and Prevalence of Celiac Disease and Dermatitis Herpetiformis in the UK Over Two Decades: Population-Based Study. The American Journal of Gastroenterology 109, 757–768. doi:10.1038/ajg.2014.55

Wilk, M.M., Misiak, A., McManus, R.M., Allen, A.C., Lynch, M.A., Mills, K.H.G., 2017. Lung CD4 Tissue-Resident Memory T Cells Mediate Adaptive Immunity Induced by Previous Infection of Mice with Bordetella pertussis. J. Immunol. 199, 233–243. doi:10.4049/jimmunol.1602051

Willcox, C.R., Davey, M.S., Willcox, B.E., 2018. Development and Selection of the Human Vγ9Vδ2+ T-Cell Repertoire. Front. Immunol. 9, 59–7. doi:10.3389/fimmu.2018.01501

Willcox, C.R., Pitard, V., Netzer, S., Couzi, L., Salim, M., Silberzahn, T., Moreau, J.-F., Hayday, A.C., Willcox, B.E., Déchanet-Merville, J., 2012. Cytomegalovirus and tumor stress surveillance by binding of a human γδ T cell antigen receptor to endothelial protein C receptor. Nat Immunol 13, 872–879. doi:10.1038/ni.2394

Willcox, C.R., Vantourout, P., Salim, M., Zlatareva, I., Melandri, D., Zanardo, L., George, R., Kjaer, S., Jeeves, M., Mohammed, F., Hayday, A.C., Willcox, B.E., 2019. Butyrophilin-like 3 Directly Binds a Human Vγ4 T Cell Receptor Using a Modality Distinct from Clonally-Restricted Antigen. Immunity 51, 813–825.e4. doi:10.1016/j.immuni.2019.09.006

Wistuba-Hamprecht, K., Haehnel, K., Janssen, N., Demuth, I., Pawelec, G., 2015. Peripheral blood T-cell signatures from high-resolution immune phenotyping of γδ and αβ T-cells in younger and older subjects in the Berlin Aging Study II. Immunity & Ageing 1–12. doi:10.1186/s12979-015-0052-x

Wistuba-Hamprecht, K., Pawelec, G., Derhovanessian, E., 2014. OMIP-020: Phenotypic characterization of human γδ T-cells by multicolor flow cytometry. Cytometry 85, 522–524. doi:10.1002/cyto.a.22470

Withoff, S., Li, Y., Jonkers, I., Wijmenga, C., 2016. Understanding Celiac Disease by Genomics. Trends in Genetics 32, 295–308. doi:10.1016/j.tig.2016.02.003
Wolf, J., Petroff, D., Richter, T., Auth, M.K.H., Uhlig, H.H., Laass, M.W., Lauenstein, P., Krahl, A., Händel, N., de Laffolie, J., Hauer, A.C., Kehler, T., Flemming, G., Schmidt, F., Rodrigues, A., Hasenclever, D., Mothes, T., 2017. Validation of Antibody-Based Strategies for Diagnosis of Pediatric Celiac Disease Without Biopsy. Gastroenterology 153, 410–419.e17. doi:10.1053/j.gastro.2017.04.023
Woodberry, T., Suscovich, T.J., Henry, L.M., August, M., Waring, M.T., Kaur, A., Hess, C., Kutok, J.L., Aster, J.C., Wang, F., Scadden, D.T., Brander, C., 2005. Alpha E beta 7 (CD103) expression identifies a highly active, tonsil-resident effector-memory CTL population. J.I. 175, 4355–4362. doi:10.4049/jimmunol.175.7.4355
Woodsworth, D.J., Castellarin, M., Holt, R.A., 2013. Sequence analysis of T-cell repertoires in health and disease 5, 1–1. doi:10.1186/gm502
Wragg, K.M., Tan, H.-X., Kristensen, A.B., Nguyen-Robertson, C.V., Kelleher, A.D., Parsons, M.S., Wheatley, A.K., Berzins, S.P., Pellicci, D.G., Kent, S.J., Juno, J.A., 2020. High CD26 and Low CD94 Expression Identifies an IL-23 Responsive Vδ2+ T Cell Subset with a MAIT Cell-like Transcriptional Profile. CellReports 31, 107773. doi:10.1016/j.celrep.2020.107773
Wu, D., Wu, P., Qiu, F., Wei, Q., Huang, J., 2017. Human γδT-cell subsets and their involvement in tumor immunity. Nature Publishing Group 1–9. doi:10.1038/cmi.2016.55
Wu, J., Pendegraft, A.H., Byrne-Steele, M., Yang, Q., Wang, C., Pan, W., Lucious, T., Seay, T., Cui, X., Elson, C.O., Han, J., Mannon, P.J., 2018. Expanded TCRÎ² CDR3 clonotypes distinguish Crohnâ€™s disease and ulcerative colitis patients. Mucosal Immunology 1–9. doi:10.1038/s41385-018-0046-z
Wu, P., Wu, D., Ni, C., Ye, J., Chen, W., Hu, G., Wang, Z., Wang, C., Zhang, Z., Xia, W., Chen, Z., Wang, K., Zhang, T., Xu, J., Han, Y., Zhang, T., Wu, X., Wang, J., Gong, W., Zheng, S., Qiu, F., Yan, J., Huang, J., 2014. γδT17 Cells Promote the Accumulation and Expansion of Myeloid-Derived Suppressor Cells in Human Colorectal Cancer. Immunity 40, 785–800. doi:10.1016/j.immuni.2014.03.013
Wu, Y., Wu, W., Wong, W.M., Ward, E., Thrasher, A.J., Goldblatt, D., Osman, M., Digard, P., Canaday, D.H., Gustafsson, K., 2009. Human gamma delta T cells: a lymphoid lineage cell capable of professional phagocytosis. J. Immunol. 183, 5622–5629. doi:10.4049/jimmunol.0901772
Wurbel, M.-A., Malissen, M., Guy-Grand, D., Meffre, E., Nussenzweig, M.C., Richelme, M., Carrier, A., Malissen, B., 2001. Mice lacking the CCR9 CC-chemokine receptor show a mild impairment of early T- and B-cell development and a reduction in T-cell receptor γδ +gut intraepithelial lymphocytes. Blood 98, 2626–2632. doi:10.1182/blood.V98.9.2626
Xu, B., Pizarro, J.C., Holmes, M.A., McBeth, C., Groh, V., Spies, T., Strong, R.K., 2011. Crystal structure of a gammadelta T-cell receptor specific for the human MHC class I homolog MICA. Proc. Natl. Acad. Sci. U.S.A. 108, 2414–2419. doi:10.1073/pnas.1015433108
Xu, W., Monaco, G., Wong, E.H., Tan, W.L.W., Kared, H., Simoni, Y., Tan, S.W., How, W.Z.Y., Tan, C.T.Y., Lee, B.T.K., Carbajo, D., G, S.K., Low, I.C.H., Mok, E.W.H., Foo, S., Lum, J., Tey, H.L., Tan, W.P., Poidinger, M., Newell, E., Ng, T.P., Foo, R., Akbar, A.N., Fülöp, T., Larbi, A., 2019. Mapping of γ/δ T cells reveals Vδ2+ T cells resistance to senescence. EBIOM 39, 44–58. doi:10.1016/j.ebiom.2018.11.053
Xue, C., Wen, M., Bao, L., Li, H., Li, F., Liu, M., Lv, Q., An, Y., Zhang, X., Cao, B., 2017. Vγ4+γδT Cells Aggravate Severe H1N1 Influenza Virus Infection-Induced Acute Pulmonary Immunopathological Injury via Secreting Interleukin-17A. Front. Immunol. 8, 2605–18. doi:10.3389/fimmu.2017.01054
Yu, G., Wang, L.-G., Han, Y., He, Q.-Y., 2012. clusterProfiler: an R Package for Comparing Biological Themes Among Gene Clusters. OMICS: A Journal of Integrative Biology 16, 284–287. doi:10.1089/omi.2011.0118
Zaid, A., Mackay, L.K., Rahimpour, A., Braun, A., Veldhoen, M., Carbone, F.R., Manton, J.H., Heath, W.R., Mueller, S.N., 2014. Persistence of skin-resident memory T cells within an epidermal niche. Proc. Natl. Acad. Sci. U.S.A. 111, 5307–5312. doi:10.1073/pnas.1322292111
Zander, R., Schauder, D., Xin, G., Nguyen, C., Wu, X., Zajac, A., Cui, W., 2019. CD4+ T Cell Help Is Required for the Formation of a Cytolytic CD8+ T Cell Subset that Protects against Chronic Infection and Cancer. Immunity 51, 1028–1042.e4. doi:10.1016/j.immuni.2019.10.009
Zens, K.D., Chen, J.K., Farber, D.L., 2016. Vaccine-generated lung tissue–resident memory T cells provide heterosubtypic protection to influenza infection. JCI Insight 1, 1–13. doi:10.1172/jci.insight.85832
Zhang, R., Zheng, X., Li, B., Wei, H., Tian, Z., 2006. Human NK Cells Positively Regulate γδ T Cells in Response to Mycobacterium tuberculosis. J.I. 176, 2610–2616. doi:10.4049/jimmunol.176.4.2610
Zhu, J., Koelle, D.M., Cao, J., Vazquez, J., Huang, M.L., Hladik, F., Wald, A., Corey, L., 2007. Virus-specific CD8+ T cells accumulate near sensory nerve endings in genital skin during subclinical HSV-2 reactivation. J Exp Med 204, 595–603. doi:10.1084/jem.20061792

Zimmerli, S.C., Harari, A., Cellerai, C., Vallelian, F., Bart, P.-A., Pantaleo, G., 2005. HIV-1-specific IFN-γ/IL-2-secreting CD8 T cells support CD4-independent proliferation of HIV-1-specific CD8 T cells. Proc. Natl. Acad. Sci. U.S.A. 102, 7239–6. doi:10.1073/pnas.0502393102

Zorro, M.M., Aguirre-Gamboa, R., Mayassi, T., Ciszewski, C., Barisani, D., Hu, S., Weersma, R.K., Withoff, S., Li, Y., Wijmenga, C., Jabri, B., Jonkers, I.H., 2020. Tissue alarmins and adaptive cytokine induce dynamic and distinct transcriptional responses in tissue-resident intraepithelial cytotoxic T lymphocytes. Journal of Autoimmunity 108, 102422. doi:10.1016/j.jaut.2020.102422

Zuber, J., Rosen, S., Shonts, B., Sprangers, B., Savage, T.M., Richman, S., Yang, S., Lau, S.P., DeWolf, S., Farber, D., Vlad, G., Zorn, E., Wong, W., Emond, J., Levin, B., Martinez, M., Kato, T., Sykes, M., 2015. Macrochimerism in Intestinal Transplantation: Association With Lower Rejection Rates and Multivisceral Transplants, Without GVHD. American Journal of Transplantation 15, 2691–2703. doi:10.1111/ajt.13325

Zuber, J., Shonts, B., Lau, S.P., Obradovic, A., Fu, J., Yang, S., Lambert, M., Coley, S., Weiner, J., Thome, J., DeWolf, S., Farber, D.L., Shen, Y., Caillat-Zucman, S., Bhagat, G., Griesemer, A., Martinez, M., Kato, T., Sykes, M., 2016. Bidirectional intragraft alloreactivity drives the repopulation of human intestinal allografts and correlates with clinical outcome. Science Immunology 1, eaah3732–eaah3732. doi:10.1126/sciimmunol.aah3732

Zundler, S., Becker, E., Spocinska, M., Slawik, M., Parga-Vidal, L., Stark, R., Wiendl, M., Atreya, R., Rath, T., Leppkes, M., Hildner, K., López-Posadas, R., Lukassen, S., Ekici, A.B., Neufert, C., Atreya, I., van Gisbergen, K.P.J.M., Neurath, M.F., 2019. Hobit- and Blimp-1-driven CD4 + tissue-resident memory T cells control chronic intestinal inflammation. Nat Immunol 20, 288–300. doi:10.1038/s41590-018-0298-5

Zundler, S., Schillinger, D., Fischer, A., Atreya, R., López-Posadas, R., Watson, A., Neufert, C., Atreya, I., Neurath, M.F., 2017. Blockade of αEβ7 integrin suppresses accumulation of CD8 +and Th9 lymphocytes from patients with IBD in the inflamed gut in vivo. Gut 66, 1936–1948. doi:10.1136/gutjnl-2016-312439